National Research
Council Canada

Conseil national
de recherches Canada

NRC · CNRC

Canadian Journal of Fisheries and Aquatic Sciences

Journal canadien des sciences halieutiques et aquatiques

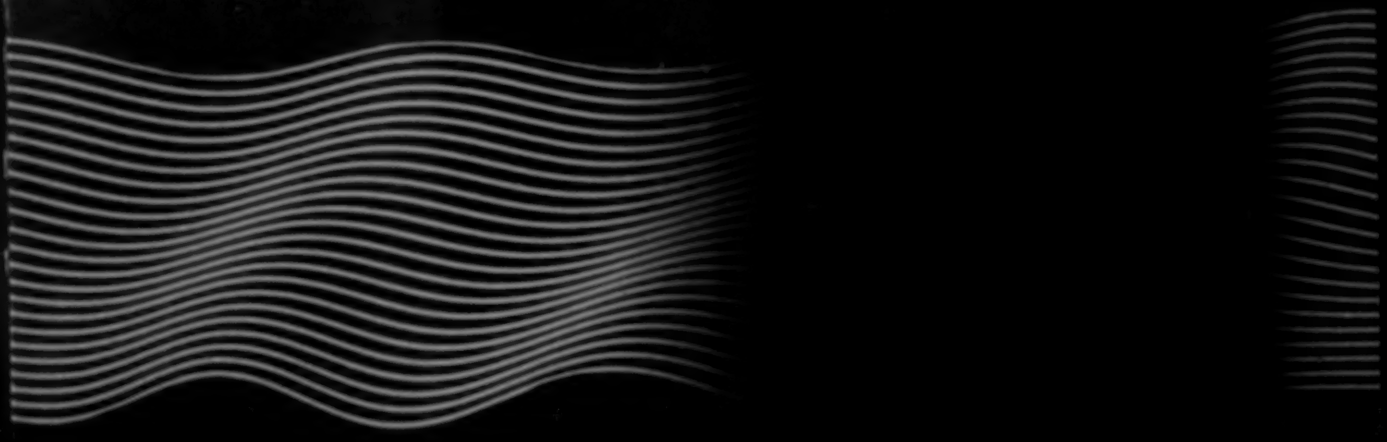

http://cjfas.nrc.ca

http://jcsha.cnrc.ca

ISSN 0706-652X / CJFSDX 63(6) 1193–1438 (2006)

The *Canadian Journal of Fisheries and Aquatic Sciences*, previously published as *Contributions to Canadian Biology* 1901–1925, *Contributions to Canadian Biology and Fisheries* 1926–1934, *Journal of the Biological Board of Canada* 1934–1937, and *Journal of the Fisheries Research Board of Canada* 1938–1979, is issued monthly to form annual volumes of 12 numbers plus supplements.

Editorial policy. The Journal publishes original research articles, perspectives (syntheses, critiques, re-evaluations), discussions (comment and reply), and rapid communications. Manuscripts may concern cells, organisms, populations, communities, ecosystems, or processes that affect aquatic systems. They may cover a range of disciplines including biology and ecology of marine and freshwater organisms, limnology, oceanography, physiology, toxicology, genetics, economics, disease, and management. Preference will be given to manuscripts that emphasize understanding of observed phenomena and interpretation of experimental results. The Journal encourages papers that lead from clearly stated purpose or rationale and from testable hypotheses, concepts, or questions to identifiable conclusions or syntheses. Such papers may amplify, modify, question, or redirect accumulated knowledge embodied in contemporary perceptions of a particular state of aquatic sciences. The Journal discourages papers that are essentially descriptive, except in emerging disciplines; have only site-specific or local applications (a certain year, place, taxon, chemical compound, etc.); only confirm previously established principles; or apply standard techniques without breaking new methodological ground.

Manuscripts for publication should be submitted to the Editorial Office via NRC Research Press' online submission and peer review system (**OSPR**EY) at http://pubs.nrc-cnrc.gc.ca/cjfas/osprey. Alternatively, manuscripts may be submitted to the Senior Editor, *Canadian Journal of Fisheries and Aquatic Sciences*, Department of Integrative Biology, Building #006, Room 118, University of Guelph, Guelph, ON N1G 2W1, Canada (519-824-4120 ext. 52646; fax: 519-767-9798; e-mail: cjfas@uoguelph.ca).

Submissions in either English or French are acceptable. The information must be original, that is, not copyrighted, published, or submitted elsewhere except in abstract form or unless by written consent of the Editor.

Correspondence concerning accepted manuscripts and corrected proofs should be sent to NRC Research Press, National Research Council of Canada, Ottawa, ON K1A 0R6, Canada (fax: 613-952-7656; e-mail: pubs@nrc-cnrc.gc.ca).

Instructions to Authors are published once a year in the first issue of each volume. Copies are available from NRC Research Press or at http://cjfas.nrc.ca. The **Publication Policy** of NRC Research Press is available at http://pubs.nrc-cnrc.gc.ca.

Microfilm. Issues from 1934 through the current volume can be purchased on 16- or 35-mm microfilm. Photocopies of individual articles or issues can be purchased from University Microfilms International, 330 North Zeeb Road, Ann Arbor, MI 48106, USA.

US periodical postage paid at Champlain, NY 12919, USA, and at additional mailing offices. Attention US POSTMASTER: Send address changes to **Canadian Journal of Fisheries and Aquatic Sciences**, c/o USACAN Media Distribution Center, P.O. Box 2888, Plattsburgh, NY 12901, USA.

Publié sans interruption depuis 1901, le *Journal canadien des sciences halieutiques et aquatiques* a paru sous plusieurs titres : *Contributions to Canadian Biology* 1901–1925, *Contributions to Canadian Biology and Fisheries* 1926–1934, *Journal of the Biological Board of Canada* 1934–1937, et *Journal of the Fisheries Research Board of Canada* 1938–1979. Le Journal paraît tous les mois, formant ainsi un volume de 12 numéros, et offre en plus jusqu'à deux suppléments par année.

Politique éditoriale. On publie, dans le Journal, des articles rendant compte de recherche originale, des perspectives (synthèses, critiques et réévaluations), des discussions (commentaires et réponses) et des communications rapides. Les documents peuvent porter sur les cellules, organismes, populations, communautés, écosystèmes ou processus qui affectent les systèmes aquatiques. Ils peuvent relever de divers domaines y compris la biologie et l'écologie des organismes marins et d'eau douce, la limnologie, l'océanographie, la physiologie, la toxicologie, la génétique, l'économie, la pathologie et la gestion. On accorde la préséance aux articles qui contribuent à la compréhension de phénomènes observés et à l'interprétation de résultats expérimentaux. On invite les auteurs à soumettre des articles ayant des objectifs précis ou relevant d'hypothèses, de concepts ou de questions vérifiables et se terminant par de solides conclusions ou d'utiles synthèses. Ces articles enrichissent, changent, mettent en question ou réorientent les connaissances acquises sur divers aspects des sciences aquatiques. On décourage toutefois la soumission d'articles simplement descriptifs (à moins qu'il ne s'agisse de nouvelles disciplines), d'application très limitée (applicables à une seule année, une seule région ou un seul taxon, portant sur un unique composé chimique, etc.); d'articles qui ne font que reprendre les principes énoncés dans des articles précédents; et d'articles rendant compte de l'application de normes sans gain de méthodologie.

Les auteurs sont invités à soumettre leur **manuscrit** au Bureau de la rédaction par le truchement du Système de soumission et d'examen en direct des articles (**OSPR**EY) des Presses scientifique du CNRC à http://pubs.nrc-cnrc.gc.ca/jcsha/osprey. Sinon, ils peuvent transmettre leur manuscrit par la poste à la directrice scientifique principale, *Journal canadien des sciences halieutiques et aquatiques*, Département de biologie intégrative, édifice 006, bureau 118, University of Guelph, Guelph, ON N1G 2W1, Canada (519-824-4120 poste 52646; télécopieur : 519-767-9798; courriel : cjfas@uoguelph.ca).

Les contributions peuvent être en anglais ou en français. Elles doivent être originales, c.-à.-d. qu'elles ne doivent pas avoir fait l'objet d'un copyright, avoir été publiées ou soumises ailleurs, sauf sous forme abrégée ou avec le consentement du rédacteur. Le CNRC ne se tient en aucune façon responsable des opinions exprimées par un collaborateur ou des déclarations qui pourrait faire ce dernier.

La correspondance ayant trait aux manuscrits acceptés et les **épreuves corrigés** doivent être envoyées aux Presses scientifiques du CNRC, Conseil national de recherches du Canada, Ottawa, ON K1A 0R6, Canada (télécopieur : 613-952-7656; courriel : pubs@nrc-cnrc.gc.ca).

Les Recommandations aux auteurs sont publiées une fois par année dans le premier numéro de chaque volume. Des copies sont disponibles auprès du Bureau de la rédaction aux Presses scientifiques du CNRC ou au http://jcsha.cnrc.ca. **La Politique de publication** est disponible auprès des Presses scientifiques du CNRC ou au http://pubs.nrc-cnrc.gc.ca.

Microfilms. On peut acheter sur microfilms de 16 ou 35 mm tous les numéros depuis 1934. Des photocopies d'articles ou de numéros individuels sont aussi en vente auprès de University Microfilms International, 330 North Zeeb Road, Ann Arbor, MI 48106, É.-U.

This Journal is indexed or abstracted in / Cette revue est signalée ou résumée dans
ABSEARCH, Applied Science and Technology Index and Abstracts, Aquatic Sciences and Fisheries Abstracts, Biological Abstracts, Biological and Agricultural Abstracts, CAB Abstracts, Chemical Abstracts, Current Contents, Elsevier BIOBASE, Environmental Abstracts, ETDE Energy Database, General Science Index and Abstracts, GEOBASE, GeoRef, Life Sciences Collection, Meteorological and Geoastrophysical Abstracts, Oceanic Abstracts, PASCAL Database, and Science Citation Index.

Volume 63, Number 6, June 2006

Canadian Journal of Fisheries and Aquatic Sciences

Published by the National Research Council of Canada

Volume 63, numéro 6, juin 2006

Journal canadien des sciences halieutiques et aquatiques

Publié par le Conseil national de recherches du Canada

Senior Editor / Directrice scientifique principale Moira M. Ferguson

Editors / Directeurs

Jeffrey A. Hutchings, *Dalhousie University, Halifax*
Pierre Pepin, *Northwest Atlantic Fisheries Centre, DFO/MPO, St. John's, Newfoundland*
W. Gary Sprules, *University of Toronto at Mississauga*
Assistant to the Editors / Adjointe aux directeurs scientifiques **Holly Foster**

Associate Editors / Directeurs scientifiques associés

D. Boisclair, *Université de Montréal*
U. Borgmann, *Environment Canada, Burlington*
M.J. Bradford, *DFO/MPO and Simon Fraser University*
S.E. Campana, *DFO/MPO, Dartmouth*
R. Carignan, *Université de Montréal*
G.T. Evans, *DFO/MPO, St. John's, Newfoundland*
K.T. Frank, *DFO/MPO, Dartmouth*
J.W.A. Grant, *Concordia University*
M.M. Hansen, *Danish Institute for Fisheries Research, Silkeborg, Denmark*
R. Hilborn, *University of Washington*
D.F. Houlihan, *University of Aberdeen*
F.A. Huntingford, *University of Glasgow*
J.M. Jech, *NFSC/NOAA, Woods Hole, Mass.*
B. Jonsson, *Norwegian Institute for Nature Research, Oslo, Norway*
K.A. Kidd, *University of New Brunswick*
D.L. MacLatchy, *University of New Brunswick, Saint John*
P. Magnan, *Université du Québec à Trois Rivières*
C.T. Marshall, *University of Aberdeen*
R.B. Millar, *University of Auckland, New Zealand*
W.P. Patterson, *University of Saskatchewan*
Y.T. Prairie, *Université du Québec à Montréal*
T.J. Quinn II, *University of Alaska–Fairbanks, Juneau, Alaska*
T.P. Quinn, *University of Washington*
C.W. Ramcharan, *Laurentian University*
J.S. Richardson, *The University of British Columbia*
B. Sainte-Marie, *DFO/MPO, Mont-Joli*
R.E.H. Smith, *University of Waterloo*
S.J. Smith, *DFO/MPO, Dartmouth*
E.B. Taylor, *The University of British Columbia*
W.F. Vincent, *Université Laval*
R.D. Vinebrooke, *University of Alberta*
C.J. Walters, *The University of British Columbia*
B. de Young, *Memorial University of Newfoundland*

NRC Research Press / Presses scientifiques du CNRC

Editor-in-Chief / Directeur scientifique en chef **Bruce P. Dancik**
Assistant Editor-in-Chief / Adjoint au directeur scientifique en chef **Iain E.P. Taylor**

Journals Program / Programme des revues

Fax / Télécopieur : 613-952-7656; e-mail / courriel : pubs@nrc-cnrc.gc.ca; URL / URL : pubs.nrc-cnrc.gc.ca
Director / Directeur **Cameron D. Macdonald**
Business Manager / Gestionnaire des affaires **Jason Charron**
Manager, Journals Program / Gestionnaire, Programme des revues **Carolyn Brown**
Managing Editor / Rédactrice administrative **Cecily M. Pearson** (613-993-9099)
Publication Officers / Agents de publication **Jennifer McColl, Thad Costigan**
Advertising and reprints / Annonces publicitaires et tirés à part **Roxanne Landriault** (613-990-2254)
Subscriptions / Abonnements **Eileen Evans-Nantais** (613-990-7873)

The National Research Council of Canada accepts no responsibility for statements or opinions expressed by a contributor. Acceptance of an advertisement, announcement, or other material does not imply endorsement by either the Journal's Senior Editor or the National Research Council.

© National Research Council of Canada 2006. All rights reserved.

No part of this publication may be reproduced, stored, or transmitted in any form or by any means, without the written permission of the publisher, except as stated below.

The National Research Council of Canada grants **permission*** to individuals to make single copies of articles for personal use. Any person may reproduce short excerpts from articles in the journal for any purpose that respects the moral rights of authors, provided that the source is fully acknowledged. As a courtesy, the consent of authors of such material should be obtained directly from the author.

Authorization to reproduce items for other than personal use, as stated above, is granted by the National Research Council of Canada provided that the copyright fee of $7.00 per copy is paid directly to CANCOPY, One Yonge Street, Suite 1900, Toronto, ON M5E 1E5, Canada.

*The above permission does not extend to other kinds of copying, such as copying for general distribution, for advertising, or promotional purposes, for creating new collective works, or for resale. For such copying, arrangements must be made with the publisher, National Research Council of Canada, Ottawa, ON K1A 0R6, Canada.

Subscription information

The *Canadian Journal of Fisheries and Aquatic Sciences* (ISSN 0706-652X) is published monthly by the National Research Council of Canada. The 2006 annual subscription rates (second class postage) for Canada are $954CAN institutional and $295CAN personal, for US & foreign $954US institutional and $295US personal. For air mail add $150US to foreign rate. Canadian customers please include 7% GST (business no. 12149 1807 RT 0275). Subscriptions are entered for the calendar year. Remittances should be made payable to the Receiver General for Canada, credit NRC. Price for regular single issues: institutional, $110.00; personal, $35.00. Supplements will be priced separately. Special rates apply to members of Canadian scientific and engineering societies if they subscribe through their respective societies.

There are no refunds on cancelled subscriptions once delivery has begun. Claims for missing issues should be made within four months (N. America) or six months (outside N. America) following the date of publication. The publisher expects to supply missing issues only when losses have occurred in transit and when the reserve stock will permit. For change of address and subscription enquiries: Subscription Office, NRC Research Press, National Research Council of Canada, Ottawa, ON K1A 0R6, Canada; tel.: 613-993-9084; fax: 613-952-7656; e-mail: pubs@nrc-cnrc.gc.ca.

Microform backfiles are available from UMI, P.O. Box 1346, Ann Arbor, MI 48106-1346, USA, and Micromedia Ltd., 20 Victoria St., Toronto, ON M5C 2N8, Canada.

All issues of the *Canadian Journal of Fisheries and Aquatic Sciences* since 1996 are available on the Web. Pricing information can be found at http://pubs.nrc-cnrc.gc.ca.

Le Conseil national de recherches du Canada ne se tient en aucune façon responsable des opinions exprimées par un collaborateur ou des déclarations que pourrait faire ce dernier. La publication d'annonces publicitaires, d'avis et autres n'implique pas l'endossement de leur contenu par la directrice principale de la Revue ou le CNRC.

© Conseil national de recherches du Canada 2006. Tous droits réservés.

Il est interdit de reproduire, de sauvegarder ou de transmettre quelque partie de la présente publication dans quelque format ou de quelque façon sans le consentement écrit de l'éditeur, à l'exception des conditions suivantes.

Le Conseil national de recherches du Canada accorde aux particuliers le droit de faire des copies individuelles pour leur usage personnel. Toute personne peut reproduire de courts extraits des articles de la Revue pour autant que les droits moraux de l'auteur soient respectés et que la mention de provenance soit clairement indiquée. Il est de convenance de demander le consentement de l'auteur avant de faire mention de son travail.

On obtiendra l'autorisation de reproduire des articles à d'autres fins que l'usage personnel (tel qu'on l'a décrit ci-dessus) auprès du Conseil national de recherches du Canada pour autant que des redevances de droits d'auteurs de 7,00 $/copie soient versées au CANCOPY, 1, rue Yonge, bureau 1900, Toronto, ON M5E 1E5, Canada.

*La permission ci-dessus ne s'applique pas à la reproduction à grande échelle, telle que la reproduction aux fins de distribution générale, publicitaire ou promotionnelle, de compilation de nouveaux ouvrages collectifs ou de revente. Dans de tels cas, il faudra ratifier une entente particulière avec l'éditeur, le Conseil national de recherches du Canada, Ottawa, ON K1A 0R6, Canada.

Renseignements sur l'abonnement

Journal canadien des sciences halieutiques et aquatiques (ISSN 0706-652X) est une publication mensuelle du Conseil national de recherches du Canada. Le prix de l'abonnement annuel en 2006 au Canada (courrier de deuxième classe) est de 954 $CAN pour les organismes et de 295 $CAN pour les particuliers. À l'étranger (y compris les É.-U.), le prix de l'abonnement est de 954 $US pour les organismes et de 295 $US pour les particuliers. L'expédition par avion exige des frais de 150 $US en sus du prix d'abonnement à l'étranger. Les clients du Canada doivent ajouter la TPS de 7 % (numéro d'entreprise 12149 1807 RT 0275). Les abonnements sont pour l'année civile. Tout paiement doit être adressé au Receveur général du Canada, crédit du CNRC. Le prix par numéro est de 110 $ pour les organismes et de 35 $ pour les particuliers. Le prix des hors-série varie. Les membres des sociétés canadiennes de sciences et de génie bénéficient de taux préférentiels en s'abonnant via leurs sociétés respectives.

Aucun remboursement ne sera accordé ni aucune annulation acceptée une fois que les livraisons auront commencé. Les réclamations de numéros manquants devront être soumises dans les quatre mois (Amérique du Nord) ou dans les six mois (à l'extérieur de l'Amérique du Nord) suivant la date de publication. L'éditeur ne fournira de numéros manquants que si le document a été perdu pendant l'expédition et que si le stock le permet. Adressez tout changement d'adresse ou toute question quant à l'abonnement au : Bureau des abonnements, Presses scientifiques du CNRC, Conseil national de recherches Canada, Ottawa, ON K1A 0R6, Canada; téléphone : 613-993-9084; télécopieur : 613-952-7656; courriel : pubs@nrc-cnrc.gc.ca.

On peut obtenir les fichiers rétrospectifs sur **microforme** auprès de UMI, P.O. Box 1346, Ann Arbor, MI 48106-1346, É.-U., et auprès de Micromedia Ltée, 20, rue Victoria, Toronto, ON M5C 2N8, Canada.

À partir de 1996, tous les numéros de *Journal canadien des sciences halieutiques et aquatiques* sont accessibles sur le Web. On trouvera des renseignements sur les tarifs à http://pubs.nrc-cnrc.gc.ca.

RAPID COMMUNICATION / COMMUNICATION RAPIDE

Transgenerational marking of embryonic otoliths in marine fishes using barium stable isotopes

Simon R. Thorrold, Geoffrey P. Jones, Serge Planes, and Jonathan A. Hare

Abstract: We describe a new technique for transgenerational marking of embryonic otoliths that promises significant advancements in the study of larval dispersal and population connectivity in marine fishes. The approach is based on maternal transmission of ^{137}Ba from spawning females to egg material that is ultimately incorporated into the otoliths of embryos produced by an individual after exposure to the isotope. We injected females of a benthic-spawning clownfish (*Amphiprion melanopus*) and a pelagic-spawning serranid (*Centropristis striata*) with enriched $^{137}BaCl_2$ and then reared the resulting progeny through to settlement. Barium isotope ratios in the cores of larval otoliths were quantified using laser ablation inductively coupled plasma mass spectrometry. Larval otoliths from both species contained unequivocal Ba isotope signatures over a wide range of doses (0.8–23 μg ^{137}Ba·g female^{-1}). Female *A. melanopus* continued to produce marked larvae over multiple clutches and for at least 90 days after a single injection. The ability to administer different combinations of stable Ba isotopes provides a new means of mass-marking larvae of benthic- and pelagic-spawning fishes from multiple populations over extended spawning periods.

Résumé : Nous décrivons une nouvelle méthode pour marquer d'une génération à l'autre les otolithes des embryons chez les poissons marins qui laisse entrevoir des progrès significatifs dans l'étude de la dispersion des larves et de la connectivité des populations. Le principe de la méthode repose sur la transmission maternelle de la femelle reproductrice à la substance des oeufs de ^{137}Ba qui est éventuellement incorporé dans les otolithes des embryons produits par les individus exposés à l'isotope. Nous avons injecté du $^{137}BaCl_2$ enrichi à des femelles de poissons-clowns (*Amphiprion melanopus*) à reproduction benthique et de mérous (*Centropristis striata*) à reproduction pélagique et nous avons ensuite élevé les rejetons produits jusqu'au moment de leur établissement. Les rapports des isotopes de baryum dans les noyaux des otolithes des larves ont été mesurés par spectrométrie de masse couplée à un plasma induit avec ablation laser. Les otolithes des larves des deux espèces contiennent des signatures isotopiques de baryum claires sur une gamme étendue de doses (0,8–23 μg ^{137}Ba·g de masse femelle^{-1}). Les femelles d'*A. melanopus* continuent de produire des larves marquées pendant plusieurs pontes successives, durant au moins 90 jours après une seule injection. La possibilité d'administrer des combinaisons différentes d'ions stables de baryum fournit une nouvelle méthode pour faire des marquages massifs de larves de poissons à reproduction benthique ou pélagique dans plusieurs populations sur des périodes de reproduction prolongées.

[Traduit par la Rédaction]

Received 20 January 2006. Accepted 22 March 2006. Published on the NRC Research Press Web site at http://cjfas.nrc.ca on 13 April 2006.
J19119

S.R. Thorrold.[1] Biology Department MS 50, Woods Hole Oceanographic Institution, Woods Hole, MA 02543, USA.
G.P. Jones. School of Marine Biology and Aquaculture and ARC Centre of Excellence for Coral Reef Studies, James Cook University, Townsville, Queensland 4811, Australia.
Serge Planes. Ecole Pratique des Hautes Etudes (EPHE), Unité Mixte de Recherche (UMR), Centre national de la recherche scientifique (CNRS) 8046, Universite de Perpignan, 66860, Perpignan cedex, France.
J.A. Hare.[2] National Oceanic and Atmospheric Administration (NOAA), National Ocean Service (NOS), National Centers for Coastal Ocean Science (NCCOS), Center for Coastal Fisheries and Habitat Research, 101 Pivers Island Road, Beaufort, NC 28516, USA.

[1] Corresponding author (e-mail: sthorrold@whoi.edu).

[2] Present address: NOAA National Marine Fisheries Service (NMFS), Northeast Fisheries Science Center (NEFSC) Narragansett Laboratory, 28 Tarzwell Drive, Narragansett, RI 02882, USA.

Can. J. Fish. Aquat. Sci. **63**: 1193–1197 (2006)

doi:10.1139/F06-048

Introduction

Quantifying larval dispersal and connectivity remains a major challenge when applying spatially explicit models to the management of marine fish populations (Sale et al. 2005). Coupled biophysical models are providing insights into potential connectivity among reef fish populations (Cowen et al. 2006), but there are remarkably few direct estimates of larval dispersal. Our current lack of knowledge is primarily due to the difficulty of conducting mark–recapture studies for species characterized by the production of large numbers of small pelagic offspring that are quickly diluted in large volumes of water while suffering high mortality rates. Thorrold et al. (2002) recently reviewed a range of chemical markers that have been used to mark marine fish larvae. They noted that only fluorescent compounds have been successfully applied in situ to label fish embryos (Jones et al. 1999, 2005).

We describe a new technique for mass marking fish larvae that relies on transgenerational transfer of a Ba isotope spike from gravid females to the embryonic otoliths of their offspring. To test the effectiveness of the new approach, we addressed the following specific questions. Can Ba isotope labels be detected in otoliths from larvae of both demersal- and pelagic-spawning fishes? Are departures from natural isotope ratios in larval otoliths correlated with maternal dose rates? Will females continue to transfer Ba isotopes to the offspring of subsequent clutches after the initial exposure? And finally, is the mark restricted to the core of the otolith, providing unequivocal evidence that the chemical mark is maternally transmitted? If successful, isotope labeling via maternal transmission will provide fish ecologists with a powerful new method for empirical tests of larval dispersal in aquatic environments.

Materials and methods

We examined transgenerational marking of embryonic otoliths in the fire clownfish (*Amphiprion melanopus*), a benthic-spawning coral reef fish that broods eggs for 8–10 days before hatching, and in black seabass (*Centropristis striata*), a pelagic-spawning temperate reef fish. Adult spawning pairs of *A. melanopus* were maintained in 100 L plastic tanks at James Cook University's Marine Aquarium Facility (Townsville, Queensland, Australia). The feeding regime consisted of ad libitum feeding once daily with tropical marine flakes and an occasional feeding of frozen squid and pilchards. Water temperature and salinity in the tanks ranged between 22.8 and 31.0 °C and between 32‰ and 36‰, respectively. Terracotta pot plant holders were provided as a suitable artificial surface for egg laying.

A solution of 0.55 mg $BaCl_2 \cdot g$ water^{-1}, containing 81.9% ^{137}Ba and 17.4% ^{138}Ba obtained from Oak Ridge National Laboratory (Oak Ridge, Tennessee), was injected into the abdominal cavity of female *A. melanopus*. We injected females with ^{137}Ba at dose rates of 0.45 (n = 3), 2.3 (n = 2), 4.5 (n = 2), and 23 (n = 2) μg $^{137}Ba \cdot g$ female^{-1}, along with two controls in which females were injected with the same volume of a 0.9% NaCl solution as that administered to the highest ^{137}Ba dose treatment. Females were first anaesthetized in a bucket containing 10 mL of clove oil mixed with 50 mL ethanol and diluted with 500 mL seawater and then electronically weighed to determine the injection volume of $BaCl_2$ for each fish. The Ba solution was administered using a hypodermic needle, and each fish was then revived in aerated salt water and returned to its initial tank. Females were maintained for up to 87 days after injection, and all clutches spawned following the injections were reared to settlement. Unfortunately spawning behaviour of females after the injection was inconsistent, leading to a lack of replication for the 4.5 and 23 μg·g female^{-1} treatments.

At the end of an 8–10 day gestation period, pre-hatch egg clutches were removed from the brooding adults at dusk and taken to an indoor, controlled environment hatchery. Larvae were reared in the same hatching tank until settlement at approximately 14 days using standard greenwater methods (reviewed by Wilkerson 1998). Sampling of larvae occurred approximately 14 days after hatching, when all surviving larvae were removed from the rearing tubs. The saggital otolith pairs were extracted from the larvae and stored dry in 1.5 mL plastic centrifuge vials.

Adult *C. striata* were collected in the Newport River estuary and held at the National Marine Fisheries Service's laboratory in Beaufort, North Carolina. Three females and two males were conditioned for 1 year on artificial diet and then allocated to a separate tank where the temperature was maintained with a flow-through, filtered seawater system at approximately 20 °C and 32‰ salinity. Females were injected with human chorionic gonadotropin to induce spawning. The fish were also injected subcutaneously with a 0.55 mg $BaCl_2 \cdot g$ water^{-1} solution at a dosage rate of 0.8 μg $^{137}Ba \cdot g$ female^{-1} at the same time. Eggs were collected 8 days later, and viable eggs were distributed to two tanks and incubated at a density of 100 eggs·L^{-1}. Larvae from one of the tanks experienced high mortality, and therefore all individuals used subsequently came from a single tank. We also obtained *C. striata* larvae from Great Bay Aquaculture in Portsmouth, New Hampshire, that were spawned and reared for approximately 60 days using standard procedures at the facility. Otoliths from these larvae were used as analytical controls for the Ba isotope analyses.

In preparation for laser ablation inductively coupled plasma mass spectrometry (ICP-MS) analysis, larval otoliths from *A. melanopus* and *C. striata* were scraped clean with acid-washed glass probes, ultrasonically cleaned in ultrapure water for 5–7 min, rinsed with ultrapure H_2O_2, and then rinsed three times with ultrapure water. After drying, otoliths were mounted singly on clean petrographic slides with cyanoacrylic glue. One randomly chosen otolith was ground to the midplane on 3 μm lapping film and then sonicated for 5 min to remove surface contamination. After triple rinsing with ultrapure water, otoliths were left to dry in a class 100 laminar flow hood for 24 h. Once dry, otoliths were remounted on petrographic slides using double-sided tape for Ba isotopic analyses

We analysed Ba isotope ratios in otolith cores using a New Wave Research UP213 laser ablation system coupled to a Thermo Finnigan Element2 ICP-MS located at the Woods Hole Oceanographic Institution (Woods Hole, Massachusetts). Instrument setup incorporated the use of a wet aerosol for both laser and solution analyses as outlined by Thorrold et al. (2001). We measured ^{137}Ba and ^{138}Ba in otolith samples,

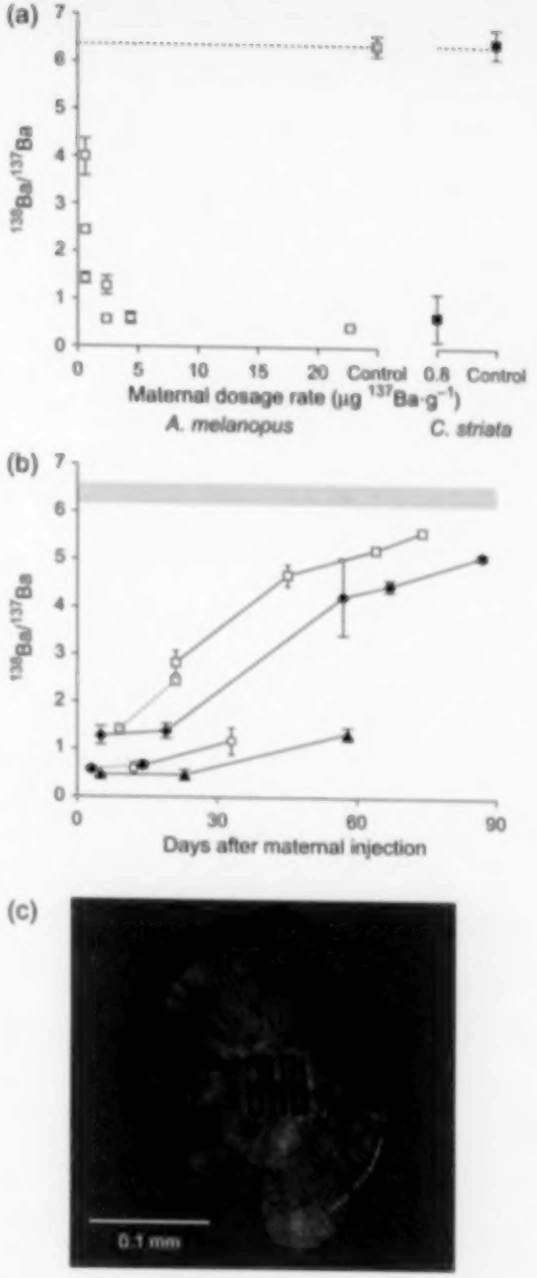

Fig 1. (*a*) Mean (± standard deviation, SD) $^{138}Ba/^{137}Ba$ ratios in larval otolith cores from individual clutches of *Amphiprion melanopus* (open squares) and from otoliths in *Centropristis striata* larvae (solid squares), spawned by females injected with enriched $^{137}BaCl_2$ at several dosage rates and control otoliths (±3 SD; dashed line indicates the natural $^{138}Ba/^{137}Ba$ ratio). (*b*) Mean (±SD) $^{138}Ba/^{137}Ba$ ratios in larval otolith cores from clutches produced by of *A. melanopus* females initially injected with $^{137}BaCl_2$ at dosage rates of 0.45 µg $^{137}Ba \cdot g$ female^{-1} (open squares), 2.3 µg $^{137}Ba \cdot g$ female^{-1} (solid diamonds), 4.5 µg $^{137}Ba \cdot g$ female^{-1} (open circles), and 23 µg $^{137}Ba \cdot g$ female^{-1} (solid triangles) and then left to spawn at natural intervals. The shaded box represents mean (±3 SD) $^{138}Ba/^{137}Ba$ ratios in control otoliths ($n = 20$). (*c*) Laser ablation inductively coupled plasma mass spectrometry was used to analyze Ba isotope ratios from a 50 µm × 50 µm raster centered on the nucleus of otoliths from *A. melanopus* (shown in the photomicrograph) and *C. striata*.

a dissolved otolith reference material (Yoshinaga et al. 2000), and a 2% HNO_3 instrument blank. Ba isotope ratios, expressed as $^{138}Ba/^{137}Ba$, were then calculated from blank-corrected abundances following correction for instrument mass bias. The mass bias correction was calculated from the otolith reference material, dissolved in 2% HNO_3, and diluted to a final Ca concentration of 40 µg·g^{-1}, that was run after every three otoliths. We assumed that the otolith reference material contained the natural isotope ratio for $^{138}Ba/^{137}Ba$ of 6.385. Isotopic analysis of a single otolith using our method takes approximately 2 min, and over 100 otoliths can be processed in a single day.

Results and discussion

Barium isotope ratios in otolith nuclei of larvae ($n = 5$) from the first egg clutch spawned by *A. melanopus* females between 3 and 21 days after injection with enriched ^{137}Ba differed considerably from $^{138}Ba/^{137}Ba$ ratios in otoliths of control larvae (Fig. 1*a*). $^{138}Ba/^{137}Ba$ ratios in otoliths ($n = 20$) from control larvae (mean ± standard deviation, 6.37 ± 0.07) were, in turn, indistinguishable from natural $^{138}Ba/^{137}Ba$ ratios of 6.385. Enriched ^{137}Ba was clearly transmitted from females to their offspring, presumably via incorporation of Ba from maternal yolk. We also found considerable variability among clutches within treatments, suggesting that either there were individual differences in the movement of Ba ions among different tissues of the spawning females or that dosages were unevenly administered. Nonetheless, $^{138}Ba/^{137}Ba$ ratios (2.6 ± 1.3) at the lowest dosage rate of 0.45 µg $^{137}Ba \cdot g$ female^{-1} were still clearly distinct from the natural ratios (Fig. 1*a*).

Turnover rates of Ba in *A. melanopus* tissues will presumably determine the usefulness of Ba isotope labeling in field applications where it is necessary to release labeled larvae over a period of weeks to months. We therefore reared clutches that were spawned up to 87 days after initial ^{137}Ba injections to estimate the length of time over which females continue to produce marked individuals. Spawning durations after injections differed among females; nonetheless, Ba isotope ratios in larval otoliths remained clearly distinguishable from controls for at least 3 months after initial injections (Fig. 1*b*). Females injected with lower amounts of ^{137}Ba approached isotopic equilibrium with the environment more quickly than those females given higher doses, even though initial $^{138}Ba/^{137}Ba$ ratios in larval otoliths were quite similar.

Maternal transmission of enriched isotopes to embryonic otoliths is more likely to occur in benthic-spawning fishes than in species that produce pelagic eggs with smaller amounts of yolk. We found, however, that ^{137}Ba was successfully transmitted from spawning females to embryonic otoliths of a pelagic-spawning serranid, *C. striata* (Fig. 1*a*).

^{138}Ba/^{137}Ba ratios (n = 20) in otoliths from larvae (0.6 ± 0.5) reared from females injected with enriched ^{137}Ba at a dosage rate of 0.8 μg ^{137}Ba·g female^{-1} were substantially different from control larvae (6.4 ± 0.1, n = 10). Barium isotopes in the control larvae were again indistinguishable from natural ^{138}Ba/^{137}Ba ratios (Fig. 1*a*). The ^{138}Ba/^{137}Ba ratios were, therefore, lower in otoliths of *C. striata* larvae than in otoliths from larvae spawned by *A. melanopus* females given a similar ^{137}Ba dose. However, we cannot say if the difference in effectiveness of the ^{137}Ba injections was due to interspecific variability in Ba metabolism or because injections were administered in different body tissues. Finally, we examined Ba isotope profiles across several otoliths from control and treatment groups to determine if the enriched ^{137}Ba signature was restricted to the pre-hatch region of otoliths. Isotope ratio profiles showed that the isotopic label was confined to an area no more than ~50 μm from the center of treatment otoliths (Fig. 2). The profiles were, however, not symmetrical, presumably because of the time required to wash out the enriched ^{137}Ba signal from the sample introduction system of the ICP-MS. As expected, the control otolith showed little variation in ^{138}Ba/^{137}Ba ratios at any point along the profile.

Ba is found naturally in otoliths at concentrations typically ranging from 1 to 10 μg·g^{-1} (Campana and Thorrold 2001). The element is, however, toxic and likely to be poisonous to fishes at high concentrations. Although there are no data available for fishes, researchers have noted increased mortality of juvenile and adult rats to a single acute exposure of $BaCl_2$ at doses of 100–200 μg Ba·g body mass^{-1} (Borzelleca at al. 1988). None of the adult females in the treatment or control groups died during our experiment, and most of the females continued to spawn after we administered the injections, indicating that the dosages (0.2–23 μg ^{137}Ba·g female^{-1}) were below lethal levels for *A. melanopus*. To examine if Ba exposure had an effect on larval development, we tracked embryo development times and measured the diameter of larval otoliths to quantify otolith precipitation rates. Embryos from treatment females took the same amount of time to hatch (mean ± SD = 8 ± 0.9 days) as those from control groups (mean = 8 days). Mean precipitation rates of larval otoliths in treatment groups (17.2 ± 1.3 μm·day^{-1}) were also similar to those from control groups (18.6 ± 1.2 μg·day^{-1}). Otolith precipitation rates are typically correlated with somatic growth (Campana and Thorrold 2001), suggesting that growth rates were similarly unaffected by maternal effects of Ba exposure.

The use of enriched isotopes to label embryonic otoliths via maternal transmission is a promising new in situ method of marking larvae from benthic- and pelagic-spawning fish species. Once captured and injected with an isotope, a single female will potentially produce millions of marked larvae during a spawning season. The isotopic label then remains indelibly locked in the core of otoliths for the life of the tagged individual. The commercial availability of four stable isotopes of Ba (^{135}Ba, ^{136}Ba, ^{137}Ba, and ^{138}Ba), used individually or in combination, allows for 13 unique tags that can be applied to different individuals or subpopulations. Alternative methods for chemical marking of marine fishes and invertebrates require exposure of the embryos or early stage larvae to fluorescent compounds that are incorporated into calcified tissues (Levin et al. 1993; Thorrold et al. 2002). This, in turn, means that the eggs have to be easily handled in the field, as in the case of some damselfishes (Jones et al. 1999, 2005), or alternatively that the species of interest is in culture and larvae can be marked in the lab before release (Moran and Marko 2005). Transgenerational marking of embryos using enriched isotopes provides a new mechanism for

Fig. 2. (*a*) ^{138}Ba/^{137}Ba profiles across a control otolith from a *Centropristis striata* larva (dashed line indicates the natural ^{138}Ba/^{137}Ba ratio) and (*b*) otoliths from two larvae (open and solid squares) spawned by treatment females injected with enriched $^{137}BaCl_2$. Arrow shows direction of laser movement along the profile. (*c*) Laser ablation inductively coupled plasma mass spectrometry was used to analyze Ba isotope ratios from profiles (a line is shown in the photomicrograph of a sectioned otolith from a *C. striata* larva) through the otolith nucleus.

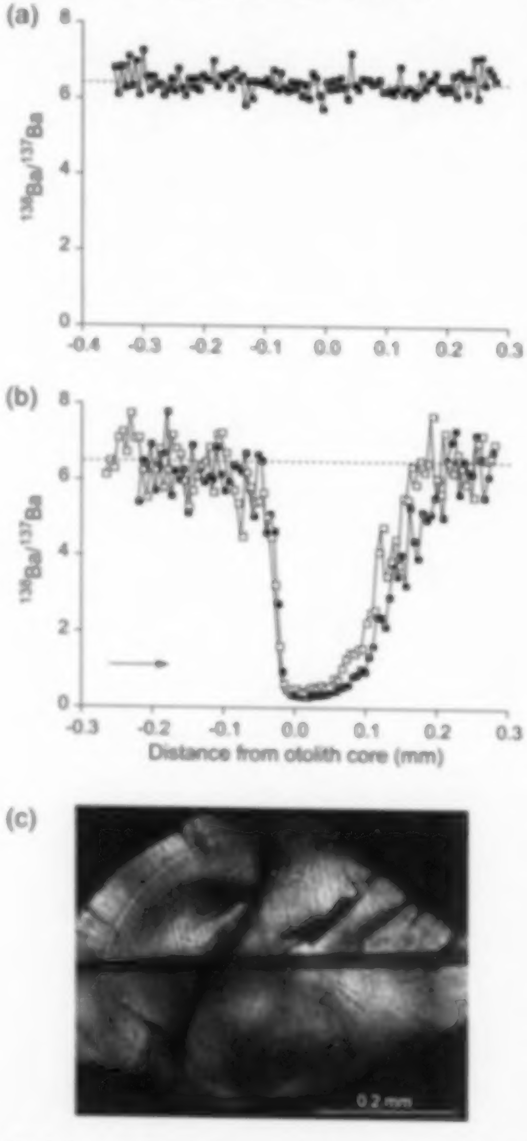

generating large numbers of known origin larvae that are released in situ and under natural conditions by spawning females. Information from these releases will, in turn, generate empirical estimates of larval dispersal that can be used to test the ability of coupled biophysical models to accurately capture connectivity patterns in fish populations.

Acknowledgements

Funding for this study was provided by the National Science Foundation through grants OCE-0215905 and OCE-0424688, Discovery Grant DP 0208120 from the Australian Research Council, and the Oak Foundation. We thank Amy Forrest, Brian Degan, Andrew Kaus, Bridgid Green, James Morris, and Peter Wruck for assistance with larval rearing; Gretchen Martin and Jennifer FitzGerald for help with preparation and analysis of otoliths; and Travis Elsdon, Benjamin Walther, and two anonymous reviewers for helpful comments on the manuscript.

References

Borzelleca, J.F., Condie, L.W., Jr, and Egle, J.L., Jr. 1988. Short-term toxicity (one- and ten-day gavage) of barium chloride in male and female rats. J. Am. Coll. Toxicol. **7**: 675–685.

Campana, S.E., and Thorrold, S.R. 2001. Otoliths, increments, and elements: keys to a comprehensive understanding of fish populations? Can. J. Fish. Aquat. Sci. **58**: 30–38.

Cowen, R.K., Paris, C.B., and Srinivasan, A. 2006. Scaling of connectivity in marine populations. Science (Washington, D.C.), **311**: 522–527.

Jones, G.P., Milicich, M.J., Emslie, M.J., and Lunow, C. 1999. Self-recruitment in a coral reef fish population. Nature (London), **402**: 802–804.

Jones, G.P., Planes, S., and Thorrold, S.R. 2005. Coral reef fish larvae settle close to home. Curr. Biol. **15**: 1314–1318.

Levin, L.A., Huggett, D., Myers, P., and Bridges, T. 1993. Rare-earth tagging methods for the study of larval dispersal by marine invertebrates. Limnol. Oceanogr. **38**: 346–360.

Moran, A.L., and Marko, P.B. 2005. A simple technique for physical marking of larvae or marine bivalves. J. Shellfish Res. **24**: 567–571.

Sale, P.F., Cowen, R.K., Danilowicz, B.S., Jones, G.P., Kritzer, J.P., Lindeman, K.C., Planes, S., Polunin, N.V.C., Russ, G.R., Sadovy, Y.J., and Steneck, R.S. 2005. Critical science gaps impede use of no-take fishery reserves. Trends Ecol. Evol. **20**: 74–80.

Thorrold, S.R., Latkoczy, C., Swart, P.K., and Jones, C.M. 2001. Natal homing in a marine fish metapopulation. Science (Washington, D.C.), **291**: 297–299.

Thorrold, S.R., Jones, G.P., Hellberg, M.E., Burton, R.S., Swearer, S.E., Neigel, J.E., Morgan, S.G., and Warner, R.R. 2002. Quantifying larval retention and connectivity in marine populations with artificial and natural markers. Bull. Mar. Sci. **70**: 291–308.

Wilkerson, J.D. 1998. Clownfishes: a guide to their captive care, breeding and natural history. Microcosm Ltd., Charlotte, Vt.

Yoshinaga, J., Nakama, A., Morita, M., and Edmonds, J.S. 2000. Fish otolith reference material for quality assurance of chemical analyses. Mar. Chem. **69**: 91–97.

Influence of suspended mussel lines on the biogeochemical fluxes in adjacent water in the Îles-de-la-Madeleine (Quebec, Canada)

Marion Richard, Philippe Archambault, Gérard Thouzeau, and Gaston Desrosiers

Abstract: Oxygen consumption and nutrient fluxes were measured in 80 L enclosures containing water, 1- or 2-year-old mussels, or 1- or 2-year-old line sections (mussels plus associated fauna – organic matter complex: AFOM) in August and September 2003 in the Îles-de-la-Madeleine. Mussel lines acted as nutrient sources and oxygen sinks in adjacent water. The magnitude of fluxes at the mussel line interface depended on the nutrient (NH_4 >> $Si(OH)_4$, PO_4 > NO_3 > NO_2). Mussel metabolism contributed greatly to O_2 consumption and NH_4 and PO_4 releases. Mussel influence was greater in stressful periods. The AFOM complex mainly contributed to NO_3, NO_2, and $Si(OH)_4$ fluxes. These fluxes could originate from organic matter decomposition rather than from associated faunal metabolism. The influence of AFOM depended on its composition and thus on line immersion time. Mussel lines by ammonia releases could be a factor of reduction of N limitation in the water column. Mussel line should be integrated as a new interface of biogeochemical exchanges in environmental carrying capacity studies.

Résumé : Des flux d'oxygène et de nutriments ont été mesurés dans des enceintes de 80 L contenant de l'eau, des moules de 1 ou 2 ans, ou des sections de filières de 1 ou 2 ans (moules plus complexe faune associée – matière organique : AFOM) en août et en septembre 2003 aux Îles-de-la-Madeleine. Les filières agissent comme une source de nutriments et comme un puit d'oxygène dans l'eau adjacente. L'importance des flux à l'interface de la filière dépend du nutriment (NH_4 >> $Si(OH)_4$, PO_4 > NO_3 > NO_2). Le métabolisme des moules contribue largement à la consommation d'O_2 et à la libération de NH_4 et de PO_4. L'influence des moules est plus importante en période de stress. Le complexe AFOM contribue principalement aux flux de NO_3, de NO_2 et de $Si(OH)_4$. Ces flux proviennent probablement davantage de la dégradation de la matière organique que du métabolisme de la faune associée. L'influence du complexe AFOM dépend de sa composition et donc du temps d'immersion des lignes. Grâce à leur production d'ammonium, les filières de moules pourraient être un facteur de réduction de la limitation en azote du milieu. Les filières de moules devraient être intégrées comme une nouvelle interface d'échanges biogéochimiques dans les études de capacité de charge.

Introduction

Natural, cultivated, or invasive bivalve populations can play a predominant role in nutrient turnover (Murphy and Kremer 1985; Dame and Libes 1993; Dankers and Zuidema 1995) and strongly modify the functioning of shallow coastal ecosystems (Cloern 2001; Chauvaud et al. 2003). In the case of suspended bivalve cultures, studies have focussed more on the influence of bivalve biodeposition on biogeochemical fluxes at the water–sediment interface (Baudinet et al. 1990; Hatcher et al. 1994; Christensen et al. 2003) than on the effect of the bivalve culture devices on biogeochemical fluxes in the water column (Mazouni et al. 1998; LeBlanc et al. 2003; Mazouni 2004). Nevertheless, in agreement with Mazouni et al. (1998, 2001), it is possible that suspended aquaculture structures can act as a new interface for solute exchanges by macrofaunal (bivalves + epibionts) metabolism and by the mineralization of organic matter trapped between shells. This new interface could play a central role in nutrient recycling. In addition to the influence of mussel lines on nutrient pools, various nutrient releases can change the nutrient ratios in water (Redfield et al. 1963) and enhance the probability of modifying phytoplankton species composition (Smayda 1990).

Blue mussels (*Mytilus edulis* Linneus) have been cultivated on suspended longlines since the 1980s in Grande-Entrée la-

Received 1 August 2005. Accepted 20 February 2006. Published on the NRC Research Press Web site at http://cjfas.nrc.ca on 26 April 2006.
J18818

M. Richard and P. Archambault.[1] Sciences de l'Habitat, Institut Maurice Lamontagne, Pêches et Océans Canada, 850 route de la mer, P.O. Box 1000, Mont Joli, QC G5H 3Z4, Canada.
G. Thouzeau. Centre national de la recherche scientifique (CNRS), Unité mixte de recherche (UMR) 6539, Institut Universitaire Européen de le Mer, Technopôle Brest-Iroise, Place Nicolas Copernic, 29280 Plouzané, France.
G. Desrosiers. Institut des Sciences de la Mer, Université du Québec à Rimouski, 310 allée des Ursulines, C.P. 3300, Rimouski, QC G5L 3A1, Canada.

[1] Corresponding author (e-mail: archambaultp@dfo-mpo.gc.ca).

Can. J. Fish. Aquat. Sci. 63: 1198–1213 (2006)   doi:10.1139/F06-030

goon, Îles-de-la-Madeleine (Quebec, Canada; 47°37′N, 61°31′W). Commercial size is obtained after 18 months of culture. Thus, 2-year-old and 1-year-old mussel lines are deployed in the farm. The principal aim of this study was to test the influence of these two types of mussel lines on O_2 and nutrient (NH_4, PO_4, NO_3, NO_2, and $Si(OH)_4$) fluxes in surrounding waters and to evaluate the relative contributions of mussels and of the associated fauna – organic matter complex (hereafter AFOM) on biogeochemical fluxes during the summer (ice-free period), which is the productive season and is when suspended mussel line influence on biogeochemical fluxes is probably greater. Since the magnitude of the mussel line influence probably depends on various factors related to macrofaunal metabolism and organic matter mineralization, such as the water temperature, mussel condition, and AFOM composition, experiments were carried out during two contrasted periods: (*i*) in August, when water temperature is high and mass mussel mortality events are regularly observed in the Îles-de-la-Madeleine (Tremblay et al. 1998), and (*ii*) in September, when temperature is lower and mussel condition and the associated faunal biomass are probably greater.

More specifically, three hypotheses were tested: (*i*) mussel metabolism contributes to biogeochemical fluxes, and its influence depends on water temperature and mussel stress, (*ii*) the AFOM complex also contributes to biogeochemical fluxes, and its influence depends on its composition and thus on mussel line immersion time, and (*iii*) mussel lines have a significant influence on nutrient pools and ratios. The results of this study should help us to highlight the necessity to integrate the total influence of this new suspended interface on the biogeochemical cycle in benthic–pelagic coupling in future environmental carrying capacity studies.

Materials and methods

Experimental system

Tank experiments were performed using the facilities of the Ministère de l'Agriculture de la Pêche et de l'Alimentation du Québec, Îles-de-la-Madeleine. The tank (180 cm length × 110 cm width × 64 cm height) was filled with unfiltered seawater to avoid disturbance in organism metabolism and biogeochemical fluxes in the incubation chambers (e.g., metabolic stress due to starvation; Hatcher et al. 1997). Two benthic chambers (Boucher and Boucher-Rodoni 1988; Boucher and Clavier 1990; Thouzeau et al., in press[2]) were placed in the tank's circulating water to avoid water warming during the experiments. Water warming is known to modify biogeochemical fluxes (e.g., by increasing the O_2 consumption of benthic communities; Hargrave 1969; Grant et al. 1991; Nakamura 2003). The original opened-bottom benthic chambers were modified for this study and will be referred to hereafter as the "Aquamoule". The Aquamoule is a closed chamber made of opaque polyacrylate that is 50 cm in diameter and 80 L in volume. This large volume allowed us to evaluate the influence of large mussel biomasses (up to 500 g dry weight of mussels) on the biogeochemical fluxes in water without provoking confinement (see Incubation protocol), thus decreasing the small-scale flux variability within treatments. Opaque chambers were used to prevent photosynthesis activity. Thus, only the processes linked to respiration activity of the whole community were studied (Hargrave 1969; Boucher and Clavier 1990; Plante-Cuny et al. 1998).

Experimental design

In summer 2003, two sets of experiments were performed. The experiments were carried out (*i*) between 5 and 11 August (hereafter August) when temperature was high, mussels were in poor conditions (Tremblay et al. 1998), and dead and dying mussels were observed in situ in suspended mussel lines, and (*ii*) between 31 August and 2 September (hereafter September) when temperature was lower, mussels were probably in better condition, and mussel spat recruitment was observed.

Two types of suspended mussel lines were randomly collected by SCUBA divers in the mussel farm of the Grande-Entrée lagoon. The differences between both lines were (*i*) mussel age (1-year-old mussels were 13 and 14 months old in August and September, respectively, whereas 2-year-old mussels were 25 and 26 months old) and (*ii*) line deployment in the water column (1-year-old mussel lines were deployed vertically (traditional line), whereas 2-year-old mussel lines were deployed in loops (continuous sleeve) along a horizontal axis). Both structures were deployed on ~2 m height in the water column.

Mussel line handling was performed carefully to avoid the loss of the associated fauna and organic matter trapped between the mussel shells. Dying and dead mussels observed in August were not removed before the experiments to preserve the original composition of the lines. Lines were cut into 12 sections of 20–25 cm in length. Twelve sections of each type of line were randomly kept along mussel line to integrate the vertical variability of line composition (mussels, associated fauna, and organic matter amount) on the whole measures.

Six sections of 1- and 2-year-old mussel lines were cleaned of associated fauna and sediment to keep only mussels (referred to hereafter as M1 and M2, respectively). The six others sections were replicates of the original 1- (L1) or 2- (L2) year-old lines. These sections were not cleaned and corresponded to the whole assemblage of a mussel line (mussels + associated fauna + organic matter mats). The last treatment (control) consisted of water from the lagoon (referred to hereafter as W; six replicates). A total of 60 incubations were performed during this study.

Incubation protocol

The Aquamoules could contain W, M1, M2, L1, or L2. The treatment inside the chambers was chosen randomly each time to integrate variability due to changing experimental conditions (e.g., possible water temperature variations during a day) within each treatment to exclusively test the effect of treatment on biogeochemical fluxes. Two independent Aquamoules were used at the same time. The incubation time was selected to be 1.5 h (T_{1h30}) after a pilot study was conducted to identify the ideal incubation time, allowing NH_4 fluxes to be measured and final O_2 concentrations no more than 20% below the initial O_2 concentrations. The aim was to prevent hypoxic conditions to develop, which could modify bivalve metabolism (Mazouni et al. 1998). The short incubation time also prevented mussel starvation, since the latter would occur 24 h later after the guts were completely empty (Khalil 1994). Moreover, starvation is known to modify bivalve metabolism only after several days (Bayne and Scullard 1977; Khalil 1994). During the experiments, no modification of mussel metabolic activity was thus presumed.

---

[2] Thouzeau, G., Grall, J., Clavier, J., Chauvaud, L., Jean, F., Leynaert, A., Longphuirt, S., Amice, E., and Amouroux, D. In press. Spatial and temporal variability in benthic biogeochemical fluxes in the Thau lagoon associated with macrophytic and macrofaunal distribution. Estuar. Coast. Shelf. Sci.

Physico-chemical measurements and sample collections

Each Aquamoule was linked to a submersible pump and YSI 6600 probe. Adjustable submersible pumps connected to waterproof batteries provided homogenization of the water inside the enclosures without noticeable particulate matter resuspension. Water flow in each enclosure was adjusted to 2 $L \cdot min^{-1}$, allowing stable measurements to be recorded by the probes (Thouzeau et al., in press[2]). The YSI probes recorded O_2 concentration ($mg \cdot L^{-1} \pm 0.01$), temperature (°C ± 0.01), and salinity (±0.01) in the chambers each minute. This monitoring allowed us to check if there was any change in the experimental conditions that could modify the biogeochemical processes in the enclosures (e.g., an increase in water temperature).

Water samples were collected using 60 mL syringes every 30 min (start, middle, and end of incubation) for nutrient (NH_4, $Si(OH)_4$, PO_4, NO_3, and NO_2) analyses. Three syringes were filled at each sampling time to minimize the variability of measured nutrient concentrations. At the end of each incubation, each Aquamoule was emptied. Water contained in Aquamoules was removed from the tank to avoid modifying the reference water for the next experiment. Mussels or line sections were frozen at −20 °C for biomass measurements in the laboratory. The faeces and pseudofaeces sedimented on bottom of the Aquamoules were collected and removed from the tank. Finally, for the subsequent experiments, the Aquamoules were refilled with reference water contained in the tank, which was from the adjacent lagoon.

Laboratory processing

Mussel and AFOM complex

Line sections were washed over a 0.5 mm sieve to separate mussels from the associated fauna. Mussels were counted and measured with a calliper (±0.01 mm) in each replicate. The associated fauna was sorted, counted, and identified to the genus level and separated into two groups (infauna and epifauna) and two subgroups (sedentary and errant) (Table 1). For counting purpose, epibionts ≤1 mm (e.g., mussel spat) were subsampled with a Folsom splitter (Van Guelpen et al. 1982). As mussel spat settled after the installation of the commercial mussel lines and was not harvested later on, its influence on biogeochemical fluxes was considered with the associated fauna and not with the commercial mussels.

The mussels and the associated fauna were dried separately at 60 °C for 48–72 h, weighed, and burned for 4 h at 450 °C to calculate the ash-free dry weight (AFDW) (Thouzeau et al., in press[2]). Mussel AFDW was measured to the nearest 0.1 g and the associated faunal AFDW to the nearest 0.01 mg with PG 5001-S and AG285 Mettler Toledo balances, repsectively.

Since the extraction of organic matter from washing water and byssus fragments was not possible, the organic matter biomass could not be measured. The hypothetic contribution of processes linked to organic matter on biogeochemical fluxes would be deduced by subtracting the associated faunal contribution to the total AFOM complex contribution.

Nutrient analyses

Ten millilitres per syringe were immediately sampled to measure NH_4 concentration according to the orthophtaldialdhehyde method (Holmes et al. 1999) with an Aquafluor handheld Turner Designs fluorimeter. The remaining water samples were stored in three cryovials and frozen (−80 °C) after filtering on 0.2 µm cellulose acetate Target syringe filters. Analyses for dissolved NO_3, NO_2, PO_4, and $Si(OH)_4$ were performed on a II PAA II Brann and Luebbe Technicon auto-analyser according to Tréguer and Lecorre (1975).

Data standardization

Whereas the dry weight (with shells) of 2-year-old mussels of 20–25 cm length line sections was greater than that of 1-year-old mussels, analysis of variance (ANOVA), which tested the effect of treatment (M and L), age (1 and 2), and date (August and September) on AFDW mussel biomass, revealed that date was the only significant source of variation for mussel AFDW biomass ($p = 0.002$). Mussel biomass increased between August and September (49.43 ± 1.46 g AFDW in August vs. 56.99 ± 1.97 g AFDW in September). There was no significant ($p = 0.074$) difference in mussel biomass among treatments (M, L), allowing a good comparison of treatments for each age at each date. Gross data were reported to a standardized 50 g AFDW mussel biomass, since this biomass was nearly equivalent to the mean mussel biomass (± standard error, SE) of 20–25 cm length sections (53.21 ± 1.33 g AFDW). Standardization in biomass was preferred to standardization in length, since the influence of mussel lines is more easily associated with mussel biomass (production) for modelling purposes than with culture line length.

Flux and Redfield ratio calculations

O_2 and nutrient fluxes were determined from the slopes of the linear regressions established between concentration and incubation time. Fluxes were reported to the chamber volume and standardized to 50 g AFDW mussel biomass. NH_4, NO_3, and NO_2 concentrations were summed to calculate total nitrogen (N) concentrations for each treatment and date at the beginning (T_0) and at the end (T_{1h30}) of each incubation. Initial and final N/P, Si/N, and Si/P ratios were calculated in atomic equivalents.

Mussel metabolic rates and condition index

To compare mussel metabolism between age and date, use of individual metabolic rate was preferred to metabolic rate expressed by grams AFDW, since for a given biomass, mean density of M1 was almost three times greater than those of

Table 1. Macrofaunal community associated with 1- and 2-year-old mussel lines (L1 and L2) in August and September 2003.

	L1		L2	
	August	September	August	September
Sedentary infauna				
Total biomass (mg)	0	0.05±0.02	11.73±3.1[a]	13.67±3.15[a]
Abundance of each genus				
Polychaeta, *Amphitrite*	0	0	22.64[b]	24.06[b]
Amphipoda, *Corophium*	0.15	14.67	0.11	3.52
Total abundance	0.15±0.15	14.67±6.25	22.74±3.06	27.58±4.58
Total number of genera	0.17±0.17	1	1.17±0.17	2
Sedentary epifauna				
Total biomass (mg)	0.92±0.14[a]	55.71±16.41[a]	1.37±0.36	6.18±1.28
Abundance of each genus				
Anthozoa, *Metridium*	0.18	3.13	0.12	4.29
Gastropoda, *Crepidula*	8.42	12.98	1.39	3.86
Bivalva, *Anomia*	0.17	0.18	1.73	0.63
Bivalva, *Mytilus*	152.53[b]	11 259.24[b]	24.77[b]	418.57[b]
Cirripedia, *Balanus*	0.48	0	0.79	1.26
Amphipoda, *Caprella*	4.80	10.52	0.37	4.31
Total abundance	161.78±36.25	11 275.23±5 069.34	28.80±6.49	428.61±65.46
Total number of genera	3.5±0.22	4.17±0.17	3.5±0.43	4.67±0.33
Errant epifauna				
Total biomass (mg)	1.35±0.41	1.24±0.32	1.38±0.24	5.03±0.62
Abundance of each genus				
Polychaeta, *Harmathoe*	19.01[b]	20.14[b]	7.74[b]	20.49[b]
Gasteropoda, *Odostomia*	0	0.74	0	5.64
Gasteropoda, *Hydrobia*	0	0	0	2.12
Asteroida, *Asterias*	0.29	6.27	2.03	14.95
Total abundance	19.3±4.54	27.15±4.75	9.78±1.5	43.2±2.95
Total number of genera	1.17±0.17	2.67±0.21	2±0.26	3.83±0.17
Total biomass of associated fauna (mg)[c]	2.28±0.45	57.00±16.35	14.48±3.12	24.88±3.29
Total abundance of associated fauna[c]	235.17±39.69	11 379.19±5 076.31	128.16±9.44	557.98±67.93
Total number of associated fauna genera	4.83±0.48	7.83±0.31	6.67±0.42	10.50±0.43
Associated fauna biomass/total biomass (%)[d]	0.005±0.001	0.114±0.033	0.029±0.006	0.050±0.006

Note: Biomass is given in mg ash free dry weight (AFDW) ± standard error.

[a] Values correspond to the community's main components in terms of biomass for each treatment.

[b] Values represent the dominant genus in abundance in each faunal group.

[c] $n = 6$; values standardized to 50 g AFDW of mussels.

[d] $n = 6$.

M2. Individual mussel respiration and excretion (NH_4 and PO_4) rates of M1 and M2 were calculated from the ratios of O_2, NH_4, and PO_4 fluxes to mussel density of the corresponding replicate. Allometric relationships were ignored, since only one mussel cohort was present on each mussel line. The stressful condition index, O/N ratio (Schlüter and Josefsen 1994; Hatcher et al. 1997; Tremblay et al. 1998), was calculated for each mussel treatment (M1, M2) in atomic equivalents according to the formula: $O/N = (mg\ O_2{\cdot}h^{-1}/16)/(mg\ NH_4{\cdot}h^{-1}/14)$ (Widdows and Johnson 1998).

Statistical analyses

The mussel lines used for this study originated from two different suspended culture techniques (traditional line vs. continuous sleeves). This change in mussel culture technique had one consequence on the data interpretation: to avoid adding confounding factors because of the techniques used and the mussel age, we made no comparisons of the absolute values between the two types of lines. The fact that data were standardized to a mussel biomass led us to separately analyze the two sets of data (August and September).

ANOVAs were performed to compare (*i*) O_2 consumption and nutrient fluxes among the three treatments (W, M, L) for each type of line (1 and 2) at each date (August and September) (Table 2); (*ii*) respiration, excretion (PO_4 and NH_4) rates, and O/N ratios among the two mussel treatments (M1 and M2) and the two dates (Table 3); and (*iii*) nutrient ratios (N/P, Si/N, and Si/P) among the five treatments (W, M1, M2, L1, and L2), two dates, and two incubation times (T_0 and T_{1h30}; Table 4). Cochran's test was used to verify homogeneity of the variances (Underwood 1997). When required, data were transformed to achieve homogeneity of variances (see Tables 2 and 4). As more than one ANOVA was done for the same hypothesis, the p values were adjusted with a Bonferroni correction for each of the three models (see Tables 2–4). When a source of variation was significant

Table 2. Results of the one-way analyses of variance (ANOVAs) testing the effect of treatment (TR) on the oxygen demand (O_2) and nutrient fluxes (ammonium, NH_4; phosphates, PO_4; nitrates, NO_3; nitrites, NO_2; silicates, $Si(OH)_4$) in August and in September 2003.

			W, M1, L1						W, M2, L2					
			August			September			August			September		
Flux	Source	df	MS	*F*	*p*	MS	*F*	*p*	MS	*F*	*p*	MS	*F*	*p*
O_2	TR	2	3 418.76	57.04	<0.0001	24.8843[*]	41.92	<0.0001	4.32[†]	58.09	<0.0001	6171.07	31.11	<0.0001
	Error	15	59.93			0.5936			0.07			198.36		
NH_4	TR	2	710 658.75	70.21	<0.0001	24 096.59	22.51	<0.0001	1 087 597.03	97.31	<0.0001	2.08[†]	60.16	<0.0001
	Error	15	10 122.24			1 070.52			11 176.93			0.03		
PO_4	TR	2	1.68[‡]	53.81	<0.0001	278.01	17.86	0.0001	1.35[§]	34.75	<0.0001	116.02	10.49	0.0014
	Error	15	0.03			15.57			0.04			11.06		
NO_3	TR	2	32.71	13.91	0.0004	9.77	23.05	<0.0001	1.43[∥]	19.07	0.0001	73.33	71.4	<0.0001
	Error	15	2.35			0.42			0.07			1.03		
NO_2	TR	2	1.57[¶]	42.59	<0.0001	0.13	4.86	0.0236	2.52[¶]	88.25	<0.0001	5.77	62.71	<0.0001
	Error	15	0.03			0.03			0.03			0.09		
$Si(OH)_4$	TR	2	52.79	4.40	0.0313	229.61	4.08	0.0385	130.57	5.29	0.0183	2594.67[†]	22.76	<0.0001
	Error	15	11.99			56.27			24.69			114.02		

Note: W, control; M1 and M2, 1- and 2-year-old mussel lines, respectively, that were cleaned of associated fauna and sediment to keep only mussels; L1 and L2, replicates of the original 1- or 2-year-old lines, respectively; *df*, degrees of freedom; MS, mean square. Adjusted *p* value is 0.0042.

[*] $(x + 1)^2$.

[†] ln (x).

[‡] ln (x + 80).

[§] ln (x + 10).

[∥] ln (x + 3).

[¶] ln (x +1).

Table 3. Results of the analysis of variance (ANOVA) testing the effect of treatment (TR: M1, M2), date (Da: August, September), and their interaction on individual respiration rates, excretion (PO_4 and NH_4) rates, and O/N ratios.

Variable	Source of variation	df	MS	*F*	*p*
O_2 rate	TR	1	4.0381	46.77	<0.0001
	Da	1	0.0002	<0.01	0.9619
	TR × Da	1	0.1623	1.88	0.1855
	Error	20	0.0863		
PO_4 rate	TR	1	0.0532	7.86	0.0110
	Da	1	0.0044	0.65	0.4290
	TR × Da	1	0.0024	0.36	0.5544
	Error	20	0.0068		
NH_4 rate	TR	1	7.3297	161.24	<0.0001
	Da	1	10.2925	226.42	<0.0001
	TR × Da	1	0.4179	9.19	0.0066
	Error	20	0.0455		
O/N ratio	TR	1	32.2133	1.43	0.2456
	Da	1	2227.3	98.95	<0.0001
	TR × Da	1	6.7181	0.3	0.5909
	Error	20	22.5087		

Note: *df*, degrees of freedom; MS, mean square; M1 and M2, 1- and 2-year-old mussel lines, respectively, that were cleaned of associated fauna and sediment to keep only mussels. Adjusted *p* value is 0.0127.

($p < 0.05$), Student–Newman–Keuls (SNK) pairwise multiple comparison tests were carried out to identify the differences.

Results

Environmental conditions

According to the YSI measurements, the mean (± SE) salinity during the incubations was 30.5 ± 0.15 in August vs. 31.14 ± 0.1 in September. The mean water temperature in August (19.33 ± 0.83 °C) was significantly higher than water temperature in September (15.7 ± 0.48 °C). The mean O_2 saturation in water was 90.44% ± 1.56% in August; it was significantly higher in September (101.42% ± 3.42%).

Associated fauna with mussels

The biomass (AFDW) of the associated fauna with 50 g AFDW of 1-year-old mussels varied from 1.47 to 4.45 mg in August and from 22.71 to 135.24 mg in September (Table 1). In a standardized 2-year-old mussel sample of 50 g AFDW, there was 5.60–26.87 mg of epibionts in August and 14.21–36.63 mg in September. The epibiont biomass in L1 made up 0.005% of the total biomass of macrofaunal organisms (epibionts + mussels) fixed on the mussel lines in August. This proportion was significantly higher in September (0.114%; Table 1). Accordingly, the percent biomass of the epibionts in L2 was significantly higher in September (0.05%) than in August (0.029%). The total abundance of the associated fauna in L1 was 235 in August and 11 379 in September, while in L2 it was 128 in August and 558 in September (Table 1). The specific composition of the associated fauna is reported in Table 1; a total of 12 genera were identified on the lines, which included both infaunal and epifaunal taxa. The mean number (±SE) of genera observed in L1 was 4.83 ± 0.48 in August vs. 7.83 ± 0.31 in September. In L2, there were 6.67 ± 0.42 genera of epibionts in August vs. 10.50 ± 0.43 in September.

Infauna

Infaunal biomass was scarce in L1 in August (<0.01 mg per 50 g AFDW mussel) and September (0.07 mg per 50 g AFDW mussel), with the only organism being the amphipod *Corophium* sp. (Table 1). Infauna in L2 was almost exclusively (>99%) represented by a sedentary polychaete (*Amphitrite* sp.). Infauna accounted for 80.98% of the total associated faunal biomass in L2 in August vs. 54.94% in September (Fig. 1).

Epifauna

Epifauna (sedentary and errant forms) accounted for most genera (10 of 12) of the faunal community associated with mussels (Table 1). In L1, sedentary organisms represented 40.35% of the total epifaunal biomass in August, but 97.82% in September. In L2, the variations between dates were less marked (49.81% in August vs. 55.12% in September). The biomass of sedentary epifauna in L1 and L2 was composed mainly of mussel spat (L1: 76.32% in August vs. 95.96% in September; L2: 64.47% in August vs. 59.02% in September), with a mean spat abundance reaching 11 259 individuals on L1 in September. Mussel spat size ranged from 0.5 to 1 cm. The relative biomass of sedentary epifauna among the epibionts was much higher in L1 than in L2 (43.63%–97.73% vs. 9.48%–24.86% from August to September, respectively; Fig. 1). In both L1 and L2, the most abundant errant epifauna was a carnivorous scale worm (*Harmathoe* sp.) (Table 1). The errant epifauna found in L1 accounted for only 2.18% of the total biomass of the macrofauna associated with cultivated mussels in August vs. 59.37% in September (Fig. 1). In L2, the errant epifauna represented 9.53% and 20.20% of the total epibiont biomass in August and September, respectively.

Table 4. Results of the analyses of variance (ANOVAs) testing the effect of treatment (TR: W, M1, M2, L1, L2), date (Da: August, September), incubation time (*T*: T_0, beginnig; T_{18h}, end), and their interactions on N/P, Si/N, and Si/P ratios.

Ratio	Source of variation	df	MS	*F*	*p*
N/P	TR	4	116.54	23.11	<0.0001
	Da	1	3523.94	698.69	<0.0001
	T	1	730.32	144.8	<0.0001
	TR × Da	4	67.96	13.47	<0.0001
	TR × *T*	4	73.01	14.48	<0.0001
	Da × *T*	1	320.13	63.47	<0.0001
	TR × Da × *T*	4	26.95	5.34	0.0006
	Error	100	5.04		
Si/N	TR	4	2.31*	36.68	<0.0001
	Da	1	41.74	663.23	<0.0001
	T	1	11.72	186.3	<0.0001
	TR × Da	4	0.14	2.26	0.0684
	TR × *T*	4	1.02	16.14	<0.0001
	Da × *T*	1	0.01	0.23	0.6332
	TR × Da × *T*	4	0.09	0.09	0.2165
	Error	100	0.06		
Si/P	TR	4	10.27	20.61	<0.0001
	Da	1	23.25	46.62	<0.0001
	T	1	28.24	56.63	<0.0001
	TR × Da	4	1.16	2.33	0.0612
	TR × *T*	4	2.34	4.69	0.0016
	Da × *T*	1	5.78	11.59	0.0010
	TR × Da × *T*	4	0.78	1.56	0.1914
	Error	100	0.5		

Note: df, degrees of freedom; MS, mean square; W, control; M1 and M2, 1- and 2-year-old mussel lines, respectively, that were cleaned of associated fauna and sediment to keep only mussels; L1 and L2, replicates of the original 1- or 2- year-old lines, respectively. Ajusted *p* value is 0.0169.

*ln (*x*).

O_2 consumption

According to the ANOVAs, treatment was a significant source of variation for O_2 demand in August and September (Table 2). Oxygen fluxes were always negative during this study, showing O_2 consumption in all cases (Fig. 2*a*). O_2 consumption rates were not significantly different in L and M treatments for either 1- or 2-year-old mussels in August (SNK a posteriori tests). O_2 consumptions measured in L and M were about four times higher than those measured in W (Fig. 2*a*). In September, (*i*) O_2 consumption in W (control) was significantly lower than O_2 consumption of M and L, and (*ii*) O_2 consumption in L1 and L2 was significantly higher than O_2 consumption in M1 and M2 (Fig. 2*a*). Mussel respiration accounted for 73.8% of the total O_2 demand for the 1-year-old lines vs. 55.4% for the 2-year-old lines.

Nutrient fluxes

The majority of the nutrient fluxes measured in the Aquamoules containing M1, M2, L1, or L2 were positive and corresponded to nutrient releases into the water (Figs. 2 and 3). Fluxes measured in the controls (W) were generally low and were positive or negative (uptake) depending on the particular nutrient and the date. The ANOVAs showed that treatment was a significant source of variation for the majority of nutrient fluxes in August and September (Table 2).

NH_4

NH_4 fluxes were the highest nutrient fluxes recorded in this study (Fig. 2*b*), reaching 837.49 μmol $NH_4 \cdot L^{-1} \cdot h^{-1}$. NH_4 fluxes in water were always significantly lower than those measured in the mussel and line treatments for both age and date (Fig. 2*b*; multiple pairwise tests). Moreover, NH_4 fluxes in M were not significantly different from those in L for both ages and dates. NH_4 fluxes measured in M and L for a standardized 50 g AFDW mussel biomass in August were almost six times higher from those measured in September.

PO_4

PO_4 fluxes in the water were significantly smaller than the fluxes measured in all other treatments (Fig. 2*c*; SNK tests). In August, no significant difference was observed for PO_4 release between M1 and L1 and between M2 and L2. In September, no significant difference was observed for PO_4 release between M2 and L2, but the mean PO_4 flux in L1 was twice the mean flux in M1 (significant difference; Fig. 2*c*).

$Si(OH)_4$

$Si(OH)_4$ fluxes were either negative (uptake) or positive (release) depending on the treatment and date (Fig. 3*a*). The mean $Si(OH)_4$ flux in W was not significantly different from those measured in M1 and L1 in August and in September (Table 2, Fig. 3*a*). The same pattern was observed in August for 2-year-old treatments (Table 2, Fig. 3*a*). In September, no difference was observed for $Si(OH)_4$ flux between W and M2 (uptakes), while L2 exhibited high $Si(OH)_4$ release (Fig. 3*a*).

NO_3

The mean NO_3 flux in W was close to nil for both experimental periods and was significantly lower than fluxes in all other treatments (SNK tests; Fig. 3*b*). NO_3 fluxes in L were significantly higher than fluxes in M for both experimental dates. The mean contribution of the AFOM complex to NO_3 release was estimated by subtracting the mussel contribution from the line contribution (L minus M); it reached 57.76% in August and 52.71% in September for the 1-year-old mussel lines and 71.83% in August and 82.59% in September for 2-year-old lines.

NO_2

NO_2 fluxes were the lowest nutrient fluxes recorded in this study and ranged from –0.18 to 3.70 μmol $NO_2 \cdot L^{-1} \cdot h^{-1}$ (Fig. 3*c*). NO_2 fluxes exhibited the same patterns as NO_3 fluxes in August for both ages (L > M > W; Fig. 3*c*). By contrast, in September the mean NO_2 flux measured in W was not significantly different from those in M1 and L1 (Fig. 3*c*). Nevertheless, at the same date, the mean NO_2 flux measured at L2 was significantly greater than those measured in M2 and W (Fig. 3*c*). The contribution of the AFOM complex of the 1-year-old lines to NO_2 fluxes was 75.35% in August; the contribution of the AFOM complex of the 2-year-old lines was still higher (86.68% in August and 95.15% in September).

Mussel metabolic rates and condition index

Treatment was a source of variation for mussel respiration rate and PO_4 excretion (Table 3). O_2 consumption and PO_4 excretion rates of 2-year-old mussels (1.34 ± 0.13 mg $O_2 \cdot individual^{-1} \cdot h^{-1}$ and 0.2 ± 0.03 μmol $PO_4 \cdot individual^{-1} \cdot h^{-1}$, respectively) were significantly greater than those of 1-year-old mussels (0.52 ± 0.03 mg $O_2 \cdot individual^{-1} \cdot h^{-1}$ and 0.1 ± 0.004 μmol $PO_4 \cdot individual^{-1} \cdot h^{-1}$, respectively). The interaction of treatment and date was a source of variation for NH_4 excretion rates (Table 3); rates of M1 (4.15 ± 0.3 μmol $NH_4 \cdot individual^{-1} \cdot h^{-1}$) and M2 (16.5 ± 1.7 μmol $NH_4 \cdot individual^{-1} \cdot h^{-1}$) in August were significantly greater than those in September (M1: 1.46 ± 0.1 μmol $NH_4 \cdot individual^{-1} \cdot h^{-1}$; M2: 3.4 ± 0.3 μmol $NH_4 \cdot individual^{-1} \cdot h^{-1}$).

Mean O/N ratios (±SE) were 6.76 ± 0.48 and 5.51 ± 0.6 for M1 and M2, respectively, in August vs. respective values of 27.09 ± 2.66 and 23.71 ± 2.71 in September. M1 and M2 values were not significantly different between dates, allowing us to calculate mean condition indices of 1- and 2-year-old mussels in August and September (Fig. 4). According to the ANOVA results, date was a significant source of variation (Table 3) for mussel bioenergetic status. According to a posteriori tests, the mussel O/N ratio increased significantly from August to September (Fig. 4).

Variations of nutrient ratios

N/P ratio

According to the ANOVA results, the interaction of treatment, date, and time was significant for N/P ratios (Table 4). In August, N/P ratios measured in W were not significantly different at T_0 and T_{1h30} (SNK tests; Fig. 5), in contrast with M1, M2, L1, and L2 where the mean N/P ratio at T_{1h30} was always higher than the value at T_0: 1.75 times higher in M1, 1.5 times higher in L1, 2 times higher in M2, and more than 2 times higher in L2. In September, N/P ratios were significantly lower than those observed in August, whatever the incubation time and treatment (Fig. 5; SNK tests). The N/P ratios in W and L1 did not vary significantly during the incubations, whereas they increased significantly with incubation time in M1, M2, and L2 (Fig. 5). Increases in the N/P ratios in September were less marked than in August (1.5 times in M1, 1.8 times in M2, and 1.6 times in L2).

Fig. 1. Mean biomass percentage of each faunal group of the macrofauna associated with mussels (sedentary epifauna, shaded bars; errant epifauna, open bars; sedentary infauna, solid bars) on 1- (L1) and 2- (L2) year-old lines in August and September 2003.

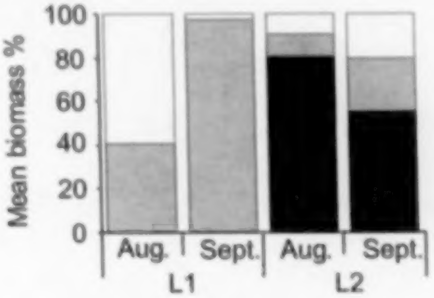

Si/N ratio

The interaction of treatment and time was a significant source of variation for Si/N ratios (Table 4). The Si/N ratios measured in W were not significantly different at T_0 and T_{1h30}, while significant decreases were observed with time in M1, M2, L1, and L2 (Fig. 6*a*; SNK tests). A mean decrease of 49% ± 3% was recorded in M1, vs. 39% ± 3% in M2, 48% ± 3% in L1, and 48% ± 5% in L2. Even though the evolution of the Si/N ratios with incubation time exhibited the same pattern in August and September, date was also a source of variation for Si/N ratios (Table 4); the August values (0.09–0.70) were significantly smaller than the values of September (0.36–1.61; SNK tests).

Si/P ratio

The interaction of date and time was significant for the Si/P ratios (Table 4). The September ratios were significantly greater than the August values at the beginning (5.64 ± 0.14 vs. 4.32 ± 0.1, respectively) and at the end (4.23 ± 0.26 vs. 3.79 ± 0.16, respectively) of the incubations. The interaction of treatment and time was also significant for Si/P ratios (Table 4). Ratios were not significantly different at T_0 and T_{1h30} in W in contrast with all other treatments (greater values at T_0 than at T_{1h30}; Fig. 6*b*, SNK tests), where we observed a mean decrease of 76% ± 3% in M1, 76% ± 5% in M2, and 64% ± 6% in L1 vs. 85% ± 4% in L2.

Fig. 2. Mean (± standard error) oxygen (*a*), ammonium (*b*), and phosphate (*c*) fluxes measured in the *Aquamoule* experiments for each treatment (control (water, W), open bars; 1-year-old mussels (M1), shaded bars; 1-year-old lines (L1), grey hatched bars; 2-year-old mussels (M2), solid bars; 2-year-old lines (L2), black hatched bars) in August and September 2003. Except for W, flux values were standardized to 50 g ash free dry weight (AFDW) mussel biomass. Different letters indicate a significant difference between treatments at a given date; Student–Newman–Keuls (SNK) tests, $p < 0.05$.

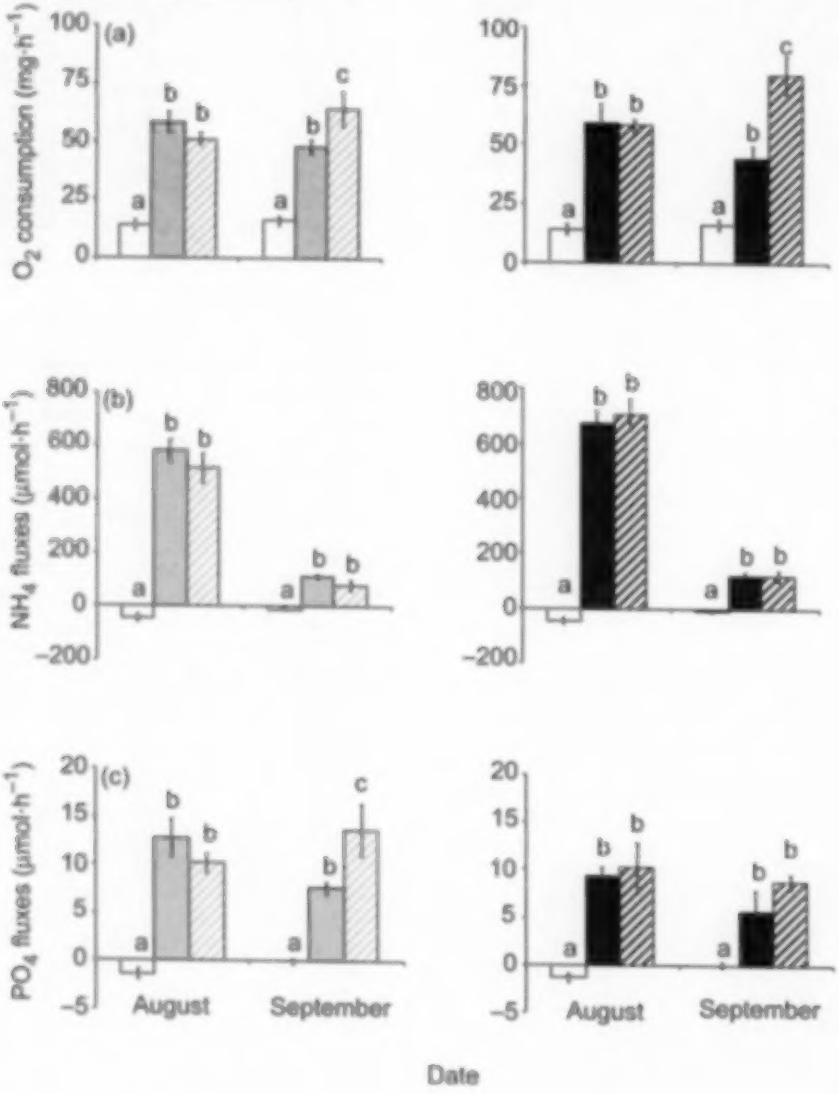

Discussion

This study clearly shows the influence of mussel lines on the biogeochemical fluxes in adjacent waters. Biogeochemical fluxes at the line interfaces (L treatments) were mainly superior to fluxes measured in water. Mussel lines act as oxygen sinks and nutrient sources (with $NH_4 >> Si(OH)_4$, $PO_4 > NO_3 > NO_2$). Biogeochemical fluxes at the water–line interfaces result from the metabolic activities of the macrofauna (mussels and associated fauna) and from organic matter degradation by bacteria. In this study, the relative influence of these processes varied according to type of flux and the date.

Influence of mussel metabolism on biogeochemical fluxes in water

In this study, NH_4, PO_4, and NO_3 releases were greater in the mussel treatments (M1 and M2) than in controls (W). LeBlanc et al. (2003) also observed N and P productions by mussels. These fluxes were considered to be the result of mussel metabolic activities, since the inorganic products of

Fig. 3. Mean (± standard error) silicate (*a*), nitrate (*b*), and nitrite (*c*) fluxes measured in the Aquamoule experiments for each treatment (control (water, W), open bars; 1-year-old mussels (M1), shaded bars; 1-year-old lines (L1), grey hatched bars; 2-year-old mussels (M2), solid bars; 2-year-old lines (L2), black hatched bars) in August and September 2003. Except for W, flux values were standardized to 50 g ash free dry weight (AFDW) mussel biomass. Different letters indicate a significant difference between treatments at a given date; Student–Newman–Keuls (SNK) tests, $p < 0.05$.

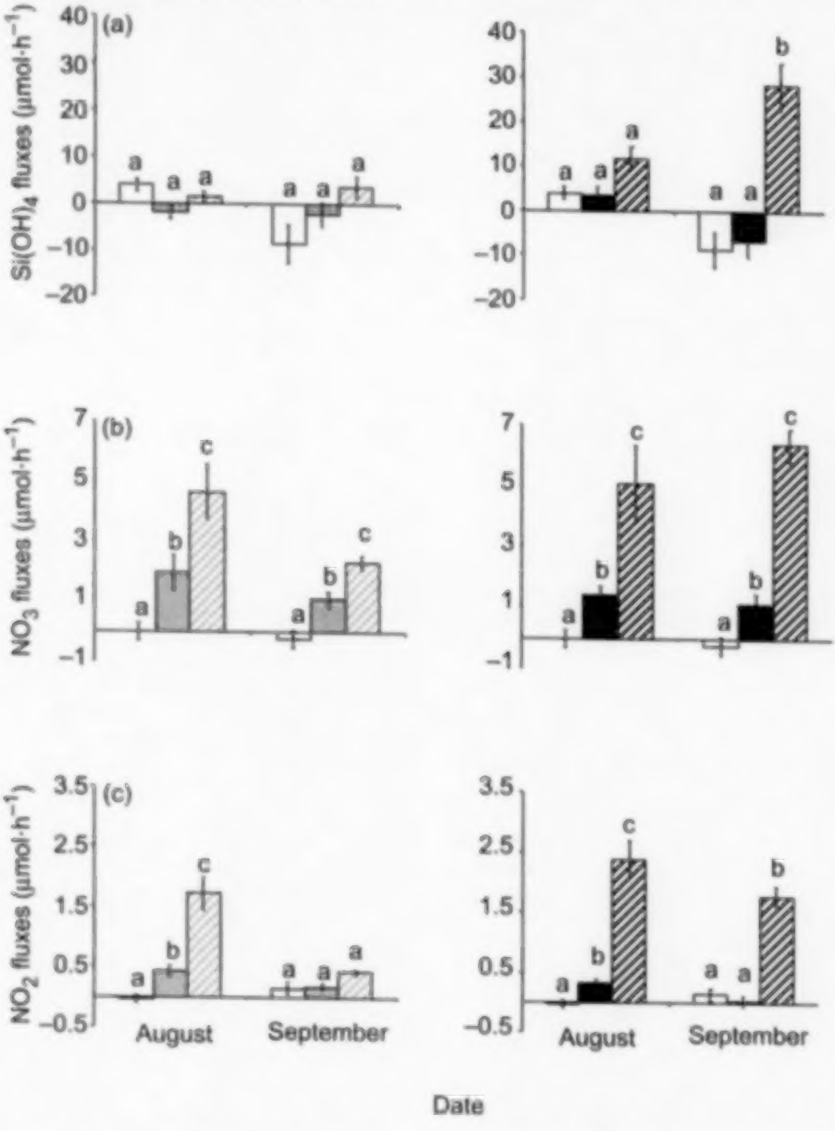

bivalve excretion are mainly NH_4 (Dame et al. 1984; Boucher and Boucher-Rodoni 1988) and PO_4 (Dame and Libes 1993; Schlüter and Josefsen 1994; Asmus et al. 1995), while bivalve faeces and pseudofaeces are sources of P (Sornin et al. 1986; Grenz et al. 1992; Asmus et al. 1995) and N (Kautsky and Evans 1987; Smaal and Zurburg 1997). NO_3 excretion would be the result of enhanced natural nitrification processes by bacteria occurring in some parts of the bivalve digestive glands (Boucher and Boucher-Rodoni 1988). In addition, NH_4 release by the mussels would have stimulated the nitrification process, as has been observed in oysters (Gilbert et al. 1997). This would explain why NO_2, which is an intermediate product of the nitrification process, displayed significantly higher fluxes in August in the mussel treatments than in water. $Si(OH)_4$ fluxes measured in the mussel treatments were similar to Si fluxes measured in water. $Si(OH)_4$ uptakes could originate from the consumption of silicates by siliceous phytoplankton (diatoms). $Si(OH)_4$ release originates from the dissolution of siliceous phytoplankton tests (Balzer et al. 1983; Lerat et al. 1990). It

Fig. 4. Mean (± standard error) values of the mussel O/N ratios (M1 and M2 were combined) in August and September 2003. Different letters indicate a significant difference between dates; Student–Newman–Keuls (SNK) tests, $p < 0.05$.

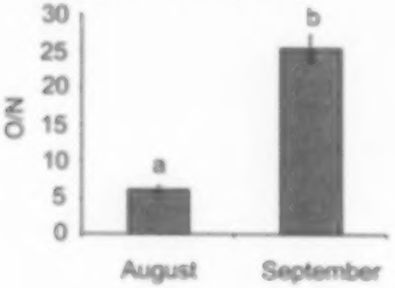

is not surprising that mussels alone do not modify $Si(OH)_4$ release into the water. Indeed, during the experiment, mussels synthesized fresh biodeposits probably containing siliceous phytoplankton tests. A 1.5 h incubation time would be too short to observe biogenic silica dissolution in water, since Baudinet et al. (1990) considered that $Si(OH)_4$ regeneration taking place within 2 months was rapid.

The influence of 50 g AFDW of 1-year-old mussels on O_2 consumption and NH_4 and PO_4 releases seemed to be equivalent to that of 50 g AFDW of 2-year-old mussels. Nevertheless, as Bayne and Scullard (1977) and Sukhotin et al. (2003) related, mussel size had a significant influence on individual metabolic rates, since individual respiration and excretion rates of 2-year-old mussels were greater than those of 1-year-old mussels.

Influence of mussel metabolism on biogeochemical fluxes varied between the two dates of experimentation; it is shown by the individual NH_4 excretion rates decreasing significantly from August to September. These results could be explained by the decrease in water temperature between August (19.33 ± 0.83 °C) and September (15.70 ± 0.48 °C), since temperature influences bivalve metabolic activities such as NH_4 excretion (Khalil 1994; Schlüter and Josefsen 1994; Mazouni et al. 2001). Nevertheless, the decrease of individual NH_4 excretion rate was important compared with the temperature decrease; the Q_{10} for NH_4 excretion in *Mytilus edulis* for the temperature interval 16–21 °C is known to be 1.3 (Bayne and Scullard 1977). Thus, temperature was not the only source of variation for NH_4 excretion.

By contrast, individual mussel respiration and PO_4 excretion rates did not decrease between dates. O_2 consumption (Kautsky and Wallentinus 1980; Murphy and Kremer 1985; Boucher and Boucher-Rodoni 1988) and PO_4 release (Schlüter and Josefen 1994) are known to be influenced by water temperature. Bayne and Scullard (1977) also found that bivalve O_2 consumption and NH_4 excretion do not always vary in the same direction, or to the same extent, in response to changes in the environment.

Fig. 5. Mean (± standard error) values of the N/P ratios measured at the beginning (T_0) and at the end (T_{1h30}) of the incubation experiments for each treatment (control (water, W), open bars; 1-year-old mussels (M1), shaded bars; 1-year-old lines (L1), grey hatched bars; 2-year-old mussels (M2), solid bars; 2-year-old lines (L2), black hatched bars) and each date (August and September 2003). N = total nitrogen. Asterisks indicate that N/P ratios were significantly different between T_0 and T_{1h30}; Student–Newman–Keuls (SNK) tests, $p < 0.05$.

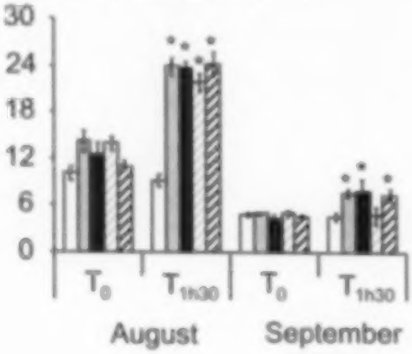

Variations in the individual O/N ratios integrate the changes in O_2 consumption and NH_4 excretion and give information on the physiological status of the organisms (Schlüter and Josefen 1994; Hatcher et al. 1997; Tremblay et al. 1998). An O/N ratio under 25–30 indicates that a high proportion of proteins is being catabolized (Widdows 1978). In this study, there was no significant difference between the O/N ratios of M1 and M2, on either date, implying a similar physiological condition for all mussels. The ratio values exhibited significant differences between the two dates of experimentation, from 5–7 August to 24–27 September. A maximum value of 30 was found for *Mytilus edulis* in Upper South Cove, Nova Scotia (Canada; Hatcher et al. 1997). In the Îles-de-la-Madeleine, Tremblay et al. (1998) also found low O/N ratios (14 ± 3) at the beginning of August and attributed these values to unfavourable environmental and mussel physiological conditions. Hatcher et al. (1997) stated that O_2 consumption and NH_4 excretion could be linked to mussel reproductive status. Similarly, Bayne and Scullard (1977) assumed that high NH_4 excretion rates could be due to the catabolism of short-term reserves used to support reproduction requirements. In the Îles-de-la-Madeleine, mussels spawn twice during summer: in late June (Myrand 1991) and late July (Myrand and Gaudreault 1995). Thus, mussels could be in a weak post-spawning state in early August. Tremblay et al. (1998) related the decrease in the O/N ratios in August to reproduction because the mantle undergoes autolysis, reorganization, and regeneration following spawning. This period also includes frequent but sporadic mass mortality events (Myrand and Gaudreault 1995; Tremblay et al. 1998). Summer mortality would be the result of a synergistic interaction involving high temperature, a possible post-spawning stress, and the genetic characteristics of the stock (Tremblay et al. 1998). The decomposition of dead organisms (Balzer et al. 1983), as dead and dying mussels observed in mussel lines in August, and protein catabolism by mussels in poor condition could explain the great NH_4 excretion and consequent low O/N ratios in August. Mussel condition probably improved rapidly between early August and late August – early September, since mean daily mussel shell growth rates in this period (220 μm·day^{-1} for 1-year-olds and 83 μm·day^{-1} for 2-year-olds; M. Richard, unpublished data) were among the highest ever recorded in the Îles-de-la-Madeleine. Indeed, mean daily mussel shell growth rates in the range of 125–224 μm·day^{-1} were recorded in pearl nets for 1-year-olds between late July and late August 1990 vs. 46–72 μm·day^{-1} for 2-year-olds held in cages between June and November 1991 (Myrand and Gaudreault 1995). The variability of the influence of mussel metabolism on N fluxes in adjacent water between August and September could depend mainly on mussel physiological state.

Influence of the AFOM complex on biogeochemical fluxes

Mussel lines provide a new substrate for the settlement of marine benthic invertebrates, thus leading to the creation of a new ecological niche (Lesser et al. 1992; Dalby and Young 1993; Claereboudt et al. 1994; this study). Indeed, 12 invertebrate genera were observed on mussel lines in our experiment. Most of these biofoulers have already been observed on mussel lines in Tracadie Bay, Prince Edward Island (PEI), Canada (LeBlanc et al. 2003). In our study, the total biomass of the associated macrofauna was very low (≤0.16%) compared with the mussel biomass of the standardized samples. In comparison, Mazouni (1995) found that the associated fauna could represent up to 80% of the total faunal biomass on oyster lines in the Thau lagoon (France) in summer. The biomass of the associated fauna in this study was also much lower than that found on mussel lines in PEI (681 mg for 10 g AFDW of mussels in September; LeBlanc et al. 2003).

The dominant species of associated fauna depended on line age. The faunal community of L1 was mainly composed of epifauna (mostly mussel spat), whereas that of L2 was dominated by infauna. This result would signify that the thickness of the organic matter biodeposit was sufficient to sustain an infaunal community at the 2-year-old mussel line interface. Indeed, biofouling organisms and cultivated bivalves are known to generate organic matter accumulation within aquaculture structures, leading to the creation of a new "soft-bottom" interface suspended in the water column (Arakawa 1990; Mazouni et al. 2001). The associated fauna of L2 was more diverse than that of L1, which agrees with Taylor et al. (1997), who observed that the number and composition of fouling species associated with the pearl oyster varied considerably with immersion time. Pearson and Rosenberg (1978) found that food availability was the most fundamental variable underlying the structure (diversity) of marine communities. The faeces and pseudofaeces trapped between mussel shells on lines could be a supplementary food source for the associated fauna and even the main food source for deposit-feeding species. Organic matter increase with immersion time could explain the greater abundance of deposit-feeding infauna (*Amphitrite* sp. and *Corophium* sp.) on L2 compared with L1. The increasing complexity with age of the line microhabitat would partly explain higher faunal diversity on L2 compared with L1.

The AFOM complex was a major contributor to NO_3 and NO_2 fluxes in this study (e.g., 52%–83% of total NO_3 fluxes and 75%–95% of total NO_2 fluxes, depending on the date and line age) and to $Si(OH)_4$ fluxes in the case of L2 in September. This contribution, which could not mainly originate from the metabolism of the low associated faunal biomass, was likely to result from biodeposit mineralization. Indeed, the decomposition of biodeposits (faeces and pseudofaeces) trapped between bivalve shells is a great N source (Sornin et al. 1983; Boucher and Boucher-Rodoni 1988; Grenz et al. 1992), explaining the NO_2–NO_3 releases after nitrification processes (Henricksen and Kemp 1988; Gilbert et al. 1997; Christensen et al. 2003). In the same way, dissolution of siliceous phytoplankton tests contained in mussel biodeposits trapped between shells could explain the great $Si(OH)_4$ releases on L2. Greater contribution of the L2 AFOM complex to $Si(OH)_4$, NO_3, and NO_2 fluxes, compared with L1, could originate from the mineralization of a probably greater organic matter amount in L2.

Fig. 6. Mean (± standard error) values of the Si/N (*a*) and Si/P (*b*) ratios measured at the beginning (T_0) and at the end (T_{1h30}) of the incubation experiments for each treatment (control (water, W), open bars; 1-year-old mussels (M1), shaded bars; 1-year-old lines (L1), grey hatched bars; 2-year-old mussels (M2), solid bars; 2-year-old lines (L2), black hatched bars). Values were combined within dates according to analysis of variance results. N = total nitrogen. Asterisks indicate that the ratios were significantly different between T_0 and T_{1h30}: Student–Newman–Keuls (SNK) tests, $p < 0.05$.

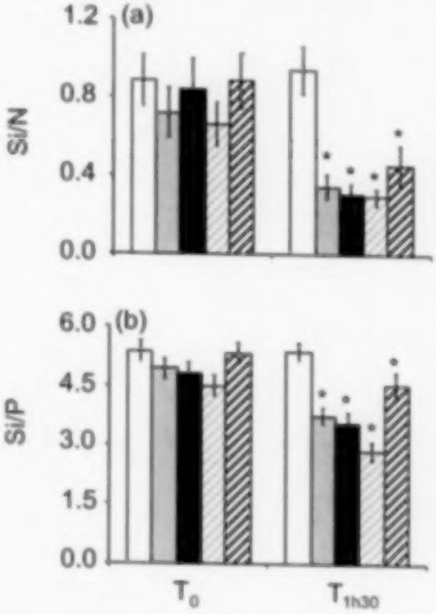

By contrast, the contribution of the AFOM complex to NH_4 fluxes was not significant compared with mussel metabolism, which disagrees with previous studies on bivalve culture devices and beds (Boucher and Boucher-Rodoni 1988; Grenz et al. 1992; LeBlanc et al. 2003). Moreover, bioturbation activities by infaunal organisms (deposit feeding, sediment reworking and irrigation, construction of burrows and tubes; Rosenberg 2001), such as *Amphitrite* sp. and *Corophium* sp. in our study, are known to increase NH_4 releases (Lerat et al. 1985; Kristensen and Blackburn 1987; Biles et al. 2003). The nonsignificant contribution of the AFOM complex to NH_4 fluxes could probably originate from higher intra-treatment than inter-treatment variability of NH_4 releases, but also from the low associated faunal biomass compared with mussel biomass.

Our study also emphasizes the variability of the AFOM complex's contribution to the biogeochemical fluxes between the two dates of experimentation. The O_2 and PO_4 fluxes at the L1 interface were significantly different from those measured at the M1 interface in September but not in August. The higher contribution of the AFOM complex to the O_2 and PO_4 fluxes in September (despite the temperature decrease) could be associated with higher epifaunal biomass (mainly mussel spat). The increase in the epifaunal biomass on L1 would be due to the growth of juvenile mussels recruited in August according to the duration of the mussel larval stage in the Îles-de-la-Madeleine (3–4 weeks; Poirier and Myrand 1982). The metabolic activities of growing mussel spat largely explained why the contribution of the L1 AFOM complex to O_2 and PO_4 fluxes increased with time. In contrast, the significant decreases in the NO_3 and NO_2 fluxes between August and September (in both the M1 and L1 treatments) could emphasize the decrease of mussel NH_4 excretion.

A different pattern was observed on the 2-year-old mussel lines; a probable increase, with immersion time, of the amount of mussel biodeposits trapped on the line sections could have stimulated microbial activity (Dahlbäck and Gunnarson 1981) and induced higher O_2 demand and nutrient (NO_3 and $Si(OH)_4$) fluxes in September compared with August. The increase of infaunal taxa between August and September would have promoted bioturbation activities within the biodeposit mat and thus increased the microbial activity, O_2 demand (Murphy and Kremer 1985; Kristensen and Blackburn 1987; Nickell et al. 2003), and nitrification process (Jenkins and Kemp 1984; Kristensen and Blackburn 1987; Aller 1988). Excretion products (NH_4 and fecal pellets) are transformed by nitrifying bacteria and induce NO_3–NO_2 fluxes at the interface. As well, bioturbation can also enhance $Si(OH)_4$ release (Baudinet et al. 1990; Caffrey et al. 1996).

Influence of mussel lines on nutrient pools and ratios

Mussel lines acted as nutrient sources to the adjacent water. In particular, large amounts of NH_4 and PO_4 releases, mainly by-products of mussel metabolism, were observed at the water–line interfaces, while small NH_4 uptakes occurred in water. Biodeposition and nutrient excretion by filter feeders can play a large role in controlling the amounts of nutrients regenerated in coastal ecosystems. High abundances of bivalves can enhance N (Dame et al. 1989; Smaal and Zurburg 1997; Smaal et al. 2001) and P (Dame et al. 1989; Asmus et al. 1995) turnover. The ecological importance of nutrient regeneration is the reduction of nutrient limitation for phytoplankton, which could result in increased primary production (Smaal 1991). Disequilibria in nutrient release kinetics can change the original nutrient ratios and the specific composition of phytoplankton communities (Baudinet et al. 1990; Chauvaud et al. 2000; Ragueneau et al. 2002). According to Redfield et al.'s theories (1963), normal nutrient ratios for phytoplankton growth are 16:16:1 for Si:N:P. Any variation of this ratio results in nutrient limitation (Ragueneau 1994).

In this study, the initial N/P ratios were <16, indicating potential N limitation (Howarth 1988; Dame and Libes 1993) in lagoon water, especially in September. Souchu et al. (1991) have mentioned that N could be limiting for phytoplankton production in the Îles-de-la-Madeleine. The higher N/P ratios observed at the M and L interfaces compared with the controls (W) at T_{18h30} suggest that mussel lines could reduce the probability or amplitude of N deficiency in adjacent water. A 1.6- to 2.2-fold increase in the N/P ratios was measured in the M and L treatments during the incubations in August vs. a 1.5- to 1.8-fold increase in September. The large decreases in the initial N/P ratios from August to September in the M and L treatments would mostly result from variability of NH_4 excretion by mussels between August and September and thus from mussel condition. Similar NH_4 releases in the M and L treatments at both dates demonstrate that NH_4 out-flux was totally driven by mussel excretion in this study. It is likely that NH_4 excretion by mussels among other NH_4 sources, as benthic interface or atmospheric inputs, could play an important role in N recycling in the Îles-de-la-Madeleine lagoon. This N source could favour the growth of small-sized phytoplankton (flagellates and dinoflagellates; Officer et al. 1982).

The N source at the line interfaces was greater than the $Si(OH)_4$ source. The Si/N ratios calculated in water were ~2 times greater than those calculated for mussels or lines at the end of the incubations, whatever the date. There was no apparent $Si(OH)_4$ limitation in water at T_0 (Si/N ~ 1) in contrast with the mussel or line treatments at T_{18h30} (Si/N $\leq$ 0.4). When considering the Redfield ratios, mussel metabolism (NH_4 excretion) could be a factor of $Si(OH)_4$ limitation that could favour the development of nonsiliceous microalgae (Smayda 1990). However, diatom growth may depend more on $Si(OH)_4$ concentration than on nutrient ratios. For example, Egge and Asknes (1992) observed in Norway that diatom dominance occurred when $Si(OH)_4$ concentration was $>2\ \mu mol \cdot L^{-1}$, while flagellates were dominant with lower Si concentrations. Kennington et al. (1999) also showed that the specific composition of phytoplankton blooms in the northeast Irish Sea varied according to nutrient concentrations and nutrient ratios. $Si(OH)_4$ concentrations were always $>2\ \mu mol \cdot L^{-1}$ in this study and increased with incubation time in the L treatments. The final $Si(OH)_4$ concentration was maximal in L2 (up to $3.96\ \mu mol \cdot L^{-1}$). Since mussel lines increased $Si(OH)_4$ concentration in adjacent water but decreased the Si/N ratio, their potential effect on phytoplankton specific composition is not clear. Further studies in situ are required to investigate the possible effect on phytoplankton composition.

This study illustrates the influence of two types of suspended mussel lines on biogeochemical fluxes (oxygen and nutrients) in the surrounding water. Results showed that (*i*) mussel metabolism contributed mainly to O_2 demand, NH_4, and PO_4 fluxes. Mussel influence was greater in stressful conditions (high temperature and post-spawning state) that lead to high NH_4 releases. (*ii*) The associated fauna – organic matter complex could greatly contribute to NO_3, NO_2, and $Si(OH)_4$ fluxes. In regard to low associated faunal biomass, this contribution could originate from mineralization of organic matter trapped between shells rather than from associated faunal metabolism. The magnitude of the contribution of the AFOM complex on these nutrient sources could depend on the AFOM complex composition and thus on line immersion time. (*iii*) The mussel lines could lead to an increase in nutrient availability, particularly for NH_4 in adjacent water. At the lagoon level, this supplied source among others, such as benthic and atmospheric sources, could be a factor of reduction of the N limitation in water column.

This experimental study shows that mussel lines act as a new "benthic-suspended" interface for biogeochemical exchanges in the water column. Introduction of this new interface in the cultivated ecosystem changes the biogeochemical cycles from a benthic–pelagic system to a benthic–pelagic–aquaculture structure system and should be considered in environmental carrying capacity models.

Acknowledgements

We thank J. Clavier for precious advice during benthic chamber construction; P. Robichaud and B. Chenard for their help on the waterproof systems; and Y. Samson, S. Chartrand, and J.-S. Ouellet for their help on electronic systems. We also thank B. Myrand and G. Tita for providing the facilities (experimental tank) of the Ministère de l'Agriculture de la Pêche et de l'Alimentation du Québec, Îles-de-la-Madeleine, and S. Roy and A. Trottet for lending the fluorometer. We are grateful to Fisheries and Oceans Canada (Mont-Joli) for boat facilities and to G. Arseneault and R. Lavallée for boat piloting. Thanks go to the BECCS team (Bivalve Environmental Carrying Capacity Studies: M. Callier, F. Hartog, C. McKindsey, J. Tomac, A. Weise) and to O. Pitre and B. Remond for their precious help in the field. We are grateful to C. Eloquin, who provided the mussel lines. L. MacLaughlin performed the nutrient analyses on A. Gagné's equipment, while M. Fréchette, L. Girard, P. Goudreau, and R. Larocque provided furnaces. We thank L. Devine for criticizing the manuscript and for linguistic improvements. This study was funded by an Aquaculture Collaborative Research and Development Program (ACRDP) grant to P. Archambault, by ISMER (Institut des Sciences de la Mer), by RAQ (Réseau Aquaculture Québec), and by SODIM (Société de développement de l'industrie maricole).

References

Aller, R.C. 1988. Benthic fauna and biogeochemical processes in marine sediments: the role of burrow structures. *In* Nitrogen cycling in coastal marine environments. *Edited by* T.H. Blackburn and J. Sorensen. J. Wiley & Sons, Chichester, N.Y. pp. 301–341.

Arakawa, K.Y. 1990. Competitors and fouling organisms in the hanging culture of the Pacific oyster, *Crassostrea gigas* (Thunberg). Mar. Behav. Physiol. **17**: 67–94.

Asmus, H., Asmus, R.M., and Zubillaga, G.F. 1995. Do mussel beds intensify the phosphorus exchange between sediment and tidal waters? Ophelia, **41**: 37–55.

Balzer, W., Grasshoff, K., Dieckmann, P., Haardt, H., and Petersohn, U. 1983. Redox-turnover at the sediment–water interface studied in a large bell jar system. Oceanol. Acta, **6**(4): 337–344.

Baudinet, D., Alliot, E., Berland, B., Grenz, C., Plante-Cuny, M., Plante, R., and Salen-Picard, C. 1990. Incidence of mussel culture on biogeochemical fluxes at the sediment–water interface. Hydrobiologia, **207**: 187–196.

Bayne, B.L., and Scullard, C. 1977. Rates of nitrogen excretion by species of *Mytilus* (Bivalvia: Mollusca). J. Mar. Biol. Assoc. U.K. **57**: 355–369.

Biles, C.L., Solan, M., Isaksson, I., Paterson, D.M., Emes, C., and Raffaeilli, D.G. 2003. Flow modifies the effect of biodiversity on ecosystem functioning: an in situ study of estuarine sediments. J. Exp. Mar. Biol. Ecol. **285–286**: 165–177.

Boucher, G., and Boucher-Rodoni, R. 1988. In situ measurement of respiratory metabolism and nitrogen fluxes at the interface of oyster beds. Mar. Ecol. Prog. Ser. **44**: 229–238.

Boucher, G., and Clavier J. 1990. Contribution of benthic biomass to overall metabolism in New Caledonia lagoon sediments. Mar. Ecol. Prog. Ser. **64**: 271–280.

Caffrey, J.M., Hammond, D.E., Kuwabara, J.S., Miller, L.G., and Twilley, R.R. 1996. Benthic process in San Francisco Bay: the role of organic inputs and bioturbation. *In* San Francisco Bay — The Ecosystem. *Edited by* J.T. Hollibaugh. American Association for the Advancement of Science, Pacific Division, San Francisco. pp. 425–439.

Chauvaud, L., Jean, F., Ragueneau, O., and Thouzeau, G. 2000. Long-term variation of the Bay of Brest ecosystem: benthicpelagic coupling revisited. Mar. Ecol. Prog. Ser. **200**(6): 35–48.

Chauvaud, L., Thompson, J.K., Cloern, J.E., and Thouzeau, G. 2003. Clams as CO_2 generators: the *Potamocorbula amurensis* example in San Fransisco Bay. Limnol. Oceanogr. **48**: 2086–2092.

Christensen, P.B., Glud, R.N., Dalsgaard, T., and Gillespie, P. 2003. Impacts of longline mussel farming on oxygen and nitrogen dynamics and biological communities of coastal sediments. Aquaculture, **218**: 567–588.

Claereboudt, M.R., Bureau, D., Côté, J., and Himmelman, J.H. 1994. Fouling development and its effect on the growth of juvenile giant scallops (*Placopecten magellanicus*) in suspended culture. Aquaculture, **121**: 327–342.

Cloern, J.E. 2001. Our evolving conceptual model of the coastal eutrophication problem. Mar. Ecol. Prog. Ser. **210**: 235–265.

Dahlbäck, B., and Gunnarson, L.A.H. 1981. Sediment and sulfate reduction under mussel culture. Mar. Biol. **63**: 269–275.

Dalby, J.E., and Young, C.M. 1993. Variable effects of ascidian competitors on oysters in a Florida epifaunal community. J. Exp. Mar. Biol. Ecol. **167**: 47–57.

Dame, R., and Libes, S. 1993. Oyster reefs and nutrient retention in tidal creeks. J. Exp. Mar. Biol. Ecol. **171**: 251–258.

Dame, R.F., Zingmark, R.G., and Haskin, E. 1984. Oyster reefs as processors of estuarine materials. J. Exp. Mar. Biol. Ecol. **83**: 239–247.

Dame, R.F., Spurrier, J.D., and Wolaver, T.G. 1989. Carbon, nitrogen and phosphorus processing by an oyster reef. Mar. Ecol. Prog. Ser. **54**: 249–256.

Dankers, N., and Zuidema, D.R. 1995. The role of the mussel (*Mytilus edulis* L.) and mussel culture in the Dutch Wadden Sea. Estuaries, **18**: 71–80.

Egge, J.K., and Asknes, D.L. 1992. Silicate as regulating nutrient in phytoplankton competition. Mar. Ecol. Prog. Ser. **83**: 281–289.

Gilbert, F., Souchu, P., Bianchi, M., and Bonin, P. 1997. Influence of shellfish farming activities on nitrification, nitrate reduction to ammonium and denitrification at the water–sediment interface of the Thau lagoon, France. Mar. Ecol. Prog. Ser. **151**: 143–153.

Grant, J., Emerson, C.W., Hargrave, B.T., and Shortle, J.L. 1991. Benthic oxygen consumption on continental shelves of Eastern Canada. Cont. Shelf Res. **11**(8–10): 1083–1097.

Grenz, C., Alliot, E., Baudinet, D., Helis, L., and Masse, H. 1992. Influence des opérations de dévasage sur les flux de nutriments à l'interface eau-sédiment (Bassin de Thau-France). Vie Milieu, **42**(2): 157–164.

Hargrave, B.T. 1969. Similarity of oxygen uptake by benthic communities. Limnol. Oceanogr. **14**(5): 801–805.

Hatcher, A., Grant, J., and Schofield, B. 1994. Effects of suspended mussel culture (*Mytilus* spp.) on sedimentation, benthic respiration and sediment nutrient dynamics in a coastal bay. Mar. Ecol. Prog. Ser. **115**: 219–235.

Hatcher, A., Grant, J., and Schofield, B. 1997. Seasonal changes in the metabolism of cultured mussels (*Mytilus edulis* L.) from a Nova Scotian inlet: the effects of winter cover and nutritive stress. J. Exp. Mar. Biol. Ecol. **217**: 63–78.

Henricksen, K., and Kemp, W.M. 1988. Nitrification in estuarine and coastal marine sediments. *In* Nitrogen cycling in coastal marine environments. *Edited by* T.H. Blackburn and J. Sorensen. J. Wiley & Sons, Chichester, N.Y. pp. 207–250.

Holmes, R.M., Aminot, A., Kérouel, R., Hooker, B.A., and Peterson, B.J. 1999. A simple and precise method for measuring ammonium in marine and freshwater ecosystems. Can. J. Fish. Aquat. Sci. **56**: 1801–1808.

Howarth, R. 1988. Nutrient limitation of net primary production in marine ecosystems. Annu. Rev. Ecol. Syst. **19**: 89–110.

Jenkins, M.C., and Kemp, M. 1984. The coupling of nitrification and denitrification in two estuarine sediments. Limnol. Oceanogr. **29**(3): 609–619.

Kautsky, N., and Evans, S. 1987. Role of biodeposition by *Mytilus edulis* in the circulation of matter and nutrients in a Baltic coastal ecosystem. Mar. Ecol. Prog. Ser. **38**: 201–212.

Kautsky, N., and Wallentinus, I. 1980. Nutrient release from Baltic *Mytilus*-red algal community and its role in benthic and pelagic production. Ophelia, **1**: 17–30.

Kennington, K., Allen, J.R., Wither, A., Shammon, T.M., and Hartnoll, R.G. 1999. Phytoplankton and nutrient dynamics in the north-east Irish Sea. Hydrobiologia, **393**: 57–67.

Khalil, A.M. 1994. Influence of starvation, body size and temperature on ammonia excretion in the marine bivalve *Tapes decussatus* (L.). Aquat. Fish. Manag. **25**: 839–847.

Kristensen, E., and Blackburn, T.H. 1987. The fate of organic carbon and nitrogen in experimental marine sediment systems: influence of bioturbation and anoxia. J. Mar. Res. **45**: 231–257.

LeBlanc, A.R., Landry, T., and Miron, G. 2003. Fouling organisms of the blue mussel *Mytilus edulis*: their effect on nutrient uptake and release. J. Shellfish Res. **22**(3): 633–638.

Lerat, Y., Boucher, G., and Le Corre, P. 1985. Echanges à l'interface eau-sédiment dans un secteur côtier à forte déposition (Parc ostréicole): cas de l'ammonium et des nitrates. Cah. Biol. Mar. **26**: 393–408.

Lerat, Y., Lasserre, P., and Le Corre, P. 1990. Seasonal changes in pore water concentrations of nutrients and their diffusive fluxes at the sediment–water interface. J. Exp. Mar. Biol. Ecol. **135**: 135–160.

Lesser, M.P., Shumway, S.E., Cucci, T., and Smith, J. 1992. Impact of fouling organisms on mussel rope culture: interspecific competition for food among suspension-feeding invertebrates. J. Exp. Mar. Biol. Ecol. **165**: 91–102.

Mazouni, N. 1995. Influence des élevages ostréicoles sur le fonctionnement d'un écosystème lagunaire méditerranéen : étude in situ de l'influence des filtreurs (coquillages et épibiontes) sur les flux de matière particulaire et dissoute. Thèse doctorat, Université d'Aix-Marseille II, Marseille, France.

Mazouni, N. 2004. Influence of suspended oyster cultures on nitrogen regeneration in a coastal lagoon (Thau Lagoon). Mar. Ecol. Prog. Ser. **276**: 103–113.

Mazouni, N., Deslous-Paoli, J.M., and Landrein, S. 1998. Influence d'un élevage ostréicole sur les flux de nutriments et d'oxygène dans un écosystème lagunaire. Oceanol. Acta, **21**(6): 845–857.

Mazouni, N., Gaertner, J.C., and Deslous-Paoli, J.M. 2001. Composition of biofouling communities on suspended oyster cultures: an in situ study of their interactions with the water column. Mar. Ecol. Prog. Ser. **214**: 93–102.

Murphy, R.C., and Kremer, J.N. 1985. Bivalve contribution to benthic metabolism in a California lagoon. Estuaries, **8**(4): 330–341.

Myrand, B. 1991. Conditions environnementales dans les lagunes des Îles-de-la-Madeleine et paramètres biologiques de la moule bleue. *In* Atelier de travail sur la mortalité estivale des moules aux Îles-de-la-Madeleine. Conseil de l'aquaculture et des Pêches du Québec, Québec. pp. 47–58.

Myrand, B., and Gaudreault, J. 1995. Summer mortality of blue mussels (*Mytilus edulis* Linneaus, 1758) in the Magdalen Islands (southern Gulf of St. Lawrence, Canada). J. Shellfish Res. **14**(2): 395–404.

Nakamura, Y. 2003. Sediment oxygen consumption and vertical flux of organic matter in the Seto Inland Sea, Japan. Estuar. Coast. Shelf Sci. **56**: 213–220.

Nickell, L.A., Black, K.D., Hughes, D.J., Overnell, J., Brand, T., Nickell, T.D., Breuer, E., and Harvey, S.M. 2003. Bioturbation, sediment fluxes and benthic community structure around a salmon cage farm in Loch Creran, Scotland. J. Exp. Mar. Biol. Ecol. **285–286**: 221–233.

Officer, C.B., Smayda, T.J., and Mann, R. 1982. Benthic filter feeding: a natural eutrophication control. Mar. Ecol. Prog. Ser. **36**: 225–236.

Pearson, T.H., and Rosenberg, R. 1978. Macrobenthic succession in relation to organic enrichment and pollution of the marine environment. Oceanogr. Mar. Biol. Annu. Rev. **16**: 229–311.

Plante-Cuny, M.-R., Plante, R., Mazouni, N., Fontaine, M.-F., Souchu, P., Deslous-Paoli, J.-M., and Grenz, C. 1998. Oxygen fluxes involving the benthic micro- and macrophytic components in the Thau Lagoon under pre-anoxic conditions. Oceanol. Acta, **21**(6): 1–11.

Poirier, L., and Myrand, B. 1982. Élevage de la moule bleue, *Mytilus edulis*, dans les lagunes des Îles-de-la-Madeleine (Québec). Travaux sur les Pêcheries du Québec MAPAQ, Direction générale des pêches maritimes, MAPAQ, Îles-de-la-Madeleine, Que. Rep. No. 49.

Ragueneau, O. 1994. La dynamique du phytoplancton en écosystèmes macrotidaux: couplage avec l'hydrodynamique et le cycle biogéochimique du Silicium. Thèse doctorat, Université Bretagne Occidentale, Brest, France.

Ragueneau, O., Chauvaud, L., Leynaert, A., Thouzeau, G., Paulet, Y.-M., Bonnet, S., Lorrain, A., Grall, J., Corvaisier, R., Le Hir, M., Jean, F., and Clavier, J. 2002. Direct evidence of a biologically active coastal silicate pump: ecological implications. Limnol. Oceanogr. **47**(6): 1849–1854.

Redfield, A.C., Ketchum, P.H., and Richards, F.A. 1963. The influence of organisms on the composition of seawater. *In* The sea.

Vol. 2. *Edited by* M.N. Hill. Wiley (Interscience), New York. pp. 25–77.

Rosenberg, R. 2001. Marine benthic faunal successional stages and related sedimentary activity. *In* A Marine science odyssey into the 21st century. *Edited by* J.M. Gili, J.L. Pretus, and T.T. Packard. Sci. Mar. **65**(2): 107–119.

Schlüter, L., and Josefsen, S.B. 1994. Annual variation in condition, respiration, and remineralisation of *Mytilus edulis* L. in the Sound, Denmark. Helgol. Meeresunters. **48**: 419–430.

Smaal, A.C. 1991. The ecology and cultivation of mussels: new advances. Aquaculture, **94**: 245–261.

Smaal, A.C., and Zurburg, W. 1997. The uptake and release of suspended and dissolved material by oysters and mussels in Marennes-Oléron Bay. Aquat. Living Resour. **10**: 23–30.

Smaal, A.C., Stralen, M.V., and Schuiling, E. 2001. The interaction between shellfish culture and ecosystem processes. Can. J. Fish. Aquat. Sci. **58**: 991–1002.

Smayda, T.J. 1990. Novel and nuisance phytoplankton blooms in the sea: evidence for a global epidemia. *In* Toxic marine phytoplankton. *Edited by* E. Granéli, B. Sundström, and L. Edler. Elsevier Science Publishing Co., New York. pp. 29–40.

Sornin, J.-M., Feuillet, M., Héral, M., and Deslous-Paoli, J.-M. 1983. Effet des biodépôts de l'huître *Crassostrea gigas* sur l'accumulation de matière organique dans les parcs du bassin de Marennes-Oléron. J. Molluscan Stud. **12**(Suppl. A): 185–197.

Sornin, J.-M., Feuillet, M., Héral, M., and Fardeau, J.-C. 1986. Influence des cultures d'huîtres *Crassostrea gigas* sur le cycle du phosphore en zone intertidale : rôle de la biodéposition. Oceanol. Acta, **9**(3): 313–322.

Souchu, P., Mayzaud, P., and Roy, S. 1991. Environnement physico-chimique et trophique d'un site mytilicole, Îles-de-la-Madeleine (Québec): 1. Evolution estivale des composés de l'azote, du phosphore et du silicium. Publ. Spec. Can. Sci. Halieut. Aquat. **113**: 209–218.

Sukhotin, A.A., Lajus, D.L., and Lesin, P.A. 2003. Influence of age and size on pumping activity and stress resistance in the marine bivalve *Mytilus edulis* L. J. Exp. Mar. Biol. Ecol. **284**: 129–144.

Taylor, J.J., Southgate, P.C., and Rose, R.A. 1997. Fouling animals and their effect on the growth of silver-lip pearl oysters, *Pinctada maxima* (Jameson) in suspended culture. Aquaculture, **153**: 31–40.

Tréguer, P., and Lecorre, P. 1975. Manuel d'analyse des sels nutritifs dans l'eau de mer. Université de Bretagne Occidentale, Laboratoire de chimie marine, Brest, France.

Tremblay, R., Myrand, B., Sevigny, J.-M., Blier, P., and Guderley, H. 1998. Bioenergetic and genetic parameters in relation to susceptibility of blue mussels, *Mytilus edulis* (L.) to summer mortality. J. Exp. Mar. Biol. Ecol. **221**: 27–58.

Underwood, A.J. 1997. Experiments in ecology: their logical design and interpretation using analysis of variance. Cambridge University Press, Cambridge, UK.

Van Guelpen, L., Markle, D.F., and Duggan., D.J. 1982. An evaluation of accuracy, precision, and speed of several zooplankton subsampling techniques. J. Cons. Int. Explor. Mer, **40**: 226–236.

Widdows, J. 1978. Combined effects of body size, food concentration and season on the physiology of *Mytilus edulis*. J. Mar. Biol. Assoc. U.K. **58**: 109–124.

Widdows, J., and Johnson, D. 1988. Physiological energetics of *Mytilus edulis*: scope for growth. Mar. Ecol. Prog. Ser. **46**: 113–121.

Predation, competition, and the recovery of overexploited fish stocks in marine reserves

Marissa L. Baskett, Mary Yoklavich, and Milton S. Love

Abstract: Community interactions alter the management actions necessary to recover overfished species using marine reserves. For example, in communities where a larger species preys on their juveniles' competitors, overfishing of the larger species may cause prey population expansion; subsequent increased competition for the juveniles of the overfished species may impede its recovery within reserves. We explore the implications of such community interactions for reserve design with a model of a subtidal rockfish (genus *Sebastes*) system from the Northeast Pacific Ocean within a no-take reserve. Ignoring community interactions, the model predicts that a reserve large enough for internal recruitment to counterbalance mortality will allow recovery of the overfished species. However, after incorporating community interactions, the model predicts that two alternative stable states exist: one where the overfished species dominates and one where the prey dominates. In the community model, the ability of an overfished system to recover to the equilibrium where the overfished species dominates after reserve establishment depends on the initial densities of both species, and a larger reserve is required for recovery to be possible.

Résumé : Les interactions au sein de la communauté modifient les actions requises pour rétablir les espèces surexploitées à l'aide de réserves marines. Par exemple, dans les communautés où une espèce plus grande fait de la prédation sur les compétiteurs de ses petits, une surpêche de l'espèce plus grande peut causer une expansion de la population de proies; la compétition subséquente qui en résulte pour les jeunes de l'espèce surexploitée peut alors nuire à son rétablissement au sein des réserves. Nous examinons les implications de telles interactions communautaires pour la planification de réserves à l'aide d'un modèle d'un système sublittoral de sébastes (genre *Sebastes*) dans une réserve sans capture. Si l'on ne tient pas compte des interactions de la communauté, le modèle prédit qu'une réserve assez grande pour que le recrutement interne contrebalance la mortalité permet le rétablissement de l'espèce surexploitée. Cependant, une fois les interactions communautaires incorporées, le modèle indique qu'il existe deux états stables de rechange, l'un où c'est l'espèce surexploitée qui prédomine et l'autre où c'est la proie. Dans le modèle communautaire, lorsque l'espèce surexploitée domine après l'établissement de la réserve, la capacité du système surexploité à atteindre de nouveau l'équilibre dépend des densités initiales des deux espèces; une réserve de plus grande taille est alors requise pour permettre le rétablissement de l'espèce.

[Traduit par la Rédaction]

Introduction

In intensively fished ecosystems, abundance of species at the top of the food web often declines, and as a result, fisheries shift to target species at lower trophic levels (Pauly et al. 1998). In addition, fisheries have a greater long-term negative impact on species with lower population growth rates, later maturation, larger organism size, and greater longevity than on species with faster production (Jennings et al. 1998; Heino and Godø 2002). The bias in fisheries' effects on trophic level and reproductive strategies may significantly alter ecosystem structure and function, in which case community dynamics may influence the recovery of depleted stocks.

For example, with intense fishing, marine communities may shift to new stable states in which trophic interactions, lower production rates, or a combination of the two prevent overfished species from recovering (Heino and Godø 2002). In general, alternative stable states involve multiple possible dominating species or groups of species in an ecosystem, and in this paper, we focus on the case in which multiple stable states exist for a particular set of conditions rather than a new stable state arising as conditions (e.g., temperature regime, fishing effort) change. Empirical evidence suggests that the existence of alternative stable states is possible, although unproven, in many marine ecosystems (Petraitis and Dudgeon 2004). Anthropogenic disturbances to ecosystems, such as the dominating influence of fisheries in marine

Received 8 June 2005. Accepted 23 November 2005. Published on the NRC Research Press Web site at http://cjfas.nrc.ca on 25 April 2006.
J18733

M.L. Baskett.[1] Department of Ecology and Evolutionary Biology, Princeton University, Princeton, NJ 08544, USA.
M. Yoklavich. Southwest Fisheries Science Center (NOAA Fisheries), National Marine Fisheries Service, Fisheries Ecology Division, 110 Shaffer Road, Santa Cruz, CA 95060, USA.
M.S. Love. Marine Science Institute, University of California at Santa Barbara, Santa Barbara, CA 93106, USA.

[1] Corresponding author (e-mail: mbaskett@princeton.edu).

Can. J. Fish. Aquat. Sci. **63**: 1214–1229 (2006) doi:10.1139/F06-013

ecosystems, alter the local stability of the alternative states and, therefore, the resilience to a shift between states (Scheffer et al. 2001; McClanahan et al. 2002; Collie et al. 2004).

Alternative stable states are theoretically feasible in a variety of simple models of ecological systems (May 1977), including models of intraguild predation (Holt and Polis 1997; Mylius et al. 2001) in which predator and prey species compete for a common resource. Intraguild predation occurs frequently in marine and terrestrial ecosystems (Polis et al. 1989). The existence of alternative states in communities with intraguild predation, including the specific case in which competition and predation occur during different life history stages, means that the final state of the communities depends on which species dominates initially (Polis and Holt 1992). Therefore, dominance of an intraguild prey may cause recovery efforts of the large predator species to fail in fisheries (Polis and Holt 1992). For example, one possible explanation for the lack of recovery of Newfoundland Atlantic cod (*Gadus morhua*) is the "cultivation effect" suggested by Walters and Kitchell (2001): with fewer adult cod to prey on smaller species that compete with or prey on juvenile cod, increased abundance of the smaller species has reduced the recruitment rate of juvenile cod (Swain and Sinclair 2000). Analogously, Barkai and McQuaid (1988) demonstrated that predation reversal between rock lobsters (*Jasus lalandii*) and whelks (*Burnupena* spp.) prevented the reintroduction of rock lobsters to a whelk-dominated community.

Cultivation effects may also influence rockfish (*Sebastes* spp.) communities in the rocky subtidal zone of the Northeast Pacific Ocean. In rockfish communities, as in many marine communities, fishing efforts disproportionately affect larger, slow-growing, late-maturing species such as the yelloweye rockfish (*Sebastes ruberrimus*) compared with smaller, fast-growing, early-maturing, nonfished species such as pygmy rockfish (*Sebastes wilsoni*). These co-occurring species can interact when the juveniles of the larger species compete with the smaller species, as well as when the adults of the larger species prey on the smaller species. The smaller rockfish species represents one component of the larger species' varied diet; for example, yelloweye rockfish prey on Pacific herring (*Clupea pallasii*), Pacific sand lance (*Ammodytes hexapterus*), flatfishes, shrimps, and crabs, as well as smaller rockfishes (Love et al. 2002).

Before anthropogenic disturbance dominated the system, predation and competition pressure from the larger species likely kept the smaller species at low population densities, except in suboptimal habitats not occupied by larger species. Now overfishing has substantially reduced population densities of the larger species, thereby releasing predation and competition pressures and likely causing a subsequent explosion in the smaller species' populations in the higher quality habitat previously dominated by the larger species. From surveys of rock habitats in deep water off California and Oregon, larger individuals of several overfished species of rockfishes, such as canary (*Sebastes pinniger*) and bocaccio (*Sebastes paucispinis*), as well as yelloweye rockfish, are in low numbers or almost absent, whereas dwarf species such as halfbanded (*Sebastes semicinctus*) and squarespot (*Sebastes hopkinsi*) rockfishes, as well as pygmy rockfishes, dominate the fish assemblages in these areas (Stein et al. 1992; Yoklavich et al. 2000, 2002). Though fisheries closures are implemented in response to overfishing, competition between expanded populations of the smaller species and juveniles of the larger species may slow or prevent the overfished larger species from recovering (MacCall 2002; Mangel and Levin 2005). Stock assessments and rebuilding plans for overfished populations currently use single-species models (Punt 2003), which ignore the interactions described above. Regardless of whether species interactions cause shifts to alternative stable states or simply slow recovery following anthropogenic disturbance, the outcome is a reason for concern (Knowlton 2004), and management decisions may need to account for community interactions.

Permanent spatial closures, or no-take marine reserves, provide an alternative form of fisheries management that may reduce the likelihood of overfishing (e.g., Lauck et al. 1998; Mangel 2000; Apostolaki et al. 2002) and the chance of shifts in coastal marine community structure following anthropogenic disturbance. Generally, marine reserves serve to protect biodiversity and ecosystem function within protected areas by reducing anthropogenic impact (Allison et al. 1998), and reserves may benefit fisheries outside reserves for intensively harvested fisheries (Man et al. 1995; Holland and Brazee 1996; Sladek Nowlis and Roberts 1999), depending on movement and reproductive rates (Hilborn et al. 2004). In systems with alternative stable states, marine reserves may increase the yield of depleted stocks (Steele and Beet 2003).

Although the general response of marine communities to reserve establishment can be an increase in numbers and biomass (Halpern and Warner 2002), the combination of historical overfishing and community interactions may impede recovery of specific species with reserve establishment. In addition, accounting for community interactions may influence the reserve size necessary for recovery to be possible (Walters 2000). Because the collapse of previously dominant species such as Atlantic cod has contributed to systemic changes in community composition and interactions (Choi et al. 2004), recovery of such species is necessary to achieve the goals of marine reserves to protect ecosystem structure and function (Murray et al. 1999).

By exploring the feasibility of alternative stable states, simple mathematical models help inform empirical studies and large simulations (Scheffer and Carpenter 2003). Furthermore, theoretical knowledge of thresholds between alternative stable states can educate conservation decisions and planning (Huggett 2005). Here we propose a model to determine how reserve area affects the recovery of overfished species while accounting for "cultivation effect" community interactions. We use the above-described competition–predation interactions between rockfish species as our model system. As a simplified treatment of a complex system, the community model presented here allows a qualitative assessment of the importance of various processes and parameters that could influence expectations to recover ecosystem structure and function via marine reserves (Essington 2004).

Materials and methods

Model summary

The model represents a community of interacting rockfish species with three groups (Fig. 1): smaller rockfish species

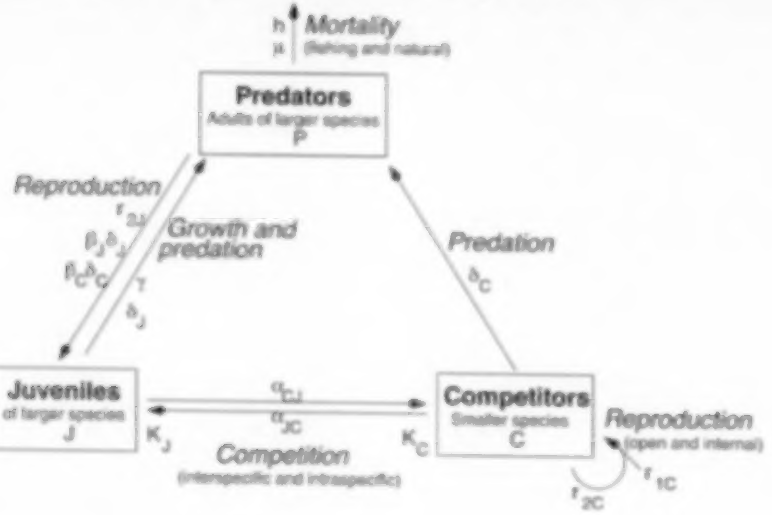

Fig. 1. Schematic of the model. See Appendix A for explanation of parameter symbols.

(competitors), juveniles of larger rockfish species (juveniles), and adults of larger rockfish species (predators). Juveniles and competitors experience both interspecific and intraspecific competition for space. We assume that competitors have partially open population dynamics: their reproduction depends on both an internal recruitment rate and a constant external recruitment rate from populations in the suboptimal habitat. Predators prey primarily on competitors, but also on juveniles of their own species. For the predation dynamics, we use the simplest functional response possible whereby predation increases directly with prey density (see below for test of the importance of this assumption). Juveniles grow (mature) into predators. Predators produce more juveniles based on conversion of energy, gained from predation, into reproductive potential; prey include competitors, juveniles, and other species assumed to be constantly available. The closed predator–juvenile dynamics reflect the "scorched earth" assumption that populations of larger rockfish species are depleted outside the reserve (see below for test of the importance of this assumption). Predators experience natural mortality, as well as fishing mortality resulting from edge effects on the border of the reserve.

The model follows population densities (fish per unit area) over time within a no-take reserve. To determine the effect of reserve area on the rockfish community dynamics, we define the parameters as functions of reserve area. Given competition for space, carrying capacities are proportional to area. Predation rates, which depend on prey encounter rates and therefore prey per unit area, are inversely proportional to area. External recruitment for competitors is proportional to area and reflects increased probability of larvae settling in the reserve with increased area. Internal recruitment rates for competitors and predators vary with reserve width and length according to the percent retention of larvae given a dispersal kernel for each species (Appendix A, Fig. A1). Finally, fishing mortality for predators depends on the probability of predators crossing the reserve boundaries and therefore varies with the perimeter-to-area ratio of the reserve (Appendix A, Fig. A2), as well as on the amount of fishing effort outside the reserve.

For a detailed mathematical formulation of the model, see Appendix A. To analyze the model, we determine the possible equilibria states (i.e., population densities where there is no change over time) and local stability of each equilibrium (i.e., whether a system starting near the equilibrium will go toward it (locally stable) or away from it (locally unstable)) for a range of reserve lengths. Where parameter values are uncertain, we test a range of values. In addition, we test the effect of relaxing some assumptions made in developing the model. First, we compare the Laplace dispersal kernel, used for mathematical simplicity, with a normal dispersal kernel, which may be more a realistic representation of larval dispersal. Second, we try a more realistic predation function that includes handling time and thus predation saturation at high prey densities (type II predation, as opposed to the linear type I predation in the main model). Third, we relax the scorched earth assumption by modeling the exchange between protected and fished areas in a reserve network (Appendix A, Fig. A3).

Parameters

In the model analysis, we base the parameter values for the larger species on yelloweye rockfish (*S. ruberrimus*) and the parameter values for the smaller species on pygmy rockfish (*S. wilsoni*; Table 1). In general, rockfish have a diversity of life histories from which to choose representative species for parameter values (Love et al. 2002). Yelloweye rockfish are large (maximum total length of 91 cm), slow-growing, late-maturing (age at 50% maturity around 20 years), long-lived (maximum age of at least 118 years), and heavily fished. This species extends from northern Baja California to the Aleutian Islands, commonly inhabiting depths of 91–180 m (Love et al. 2002). On the US west coast, spawner abundance fell below the target level in 1991 and was estimated at 24.1% of the unfished level in 2002 (Methot et al. 2002). Pygmy rockfish are small (maximum

Table 1. Parameter values used to develop the model for community interactions inside marine reserves, including ranges tested and alternate values for relaxing assumptions.

Parameter		Default value	Alternate value(s)	Units	Reference(s)
Open recruitment	r_{A1C}	0.001	0.00067–0.0015	$C{\cdot}m^{-2}{\cdot}year^{-1}$	
Internal recruitment	r_{A2C}	0.0271	0.0194–0.0379	$year^{-1}$	Love et al. 2002; Ralston et al. 2003
	r_{A2J}	0.3486	0.249–0.488	$year^{-1}$	Love et al. 2002; Anderson 1984
Prey conversion	β_{AC}	0.003		$J{\cdot}C^{-1}$	Charnov et al. 2001
	β_{AJ}	0.003		$J{\cdot}J^{-1}$	Charnov et al. 2001
Mean dispersal distance	$\overline{D}_C$	30 000	20 000 – 60 000	m	Shanks et al. 2003; Kinlan and Gaines 2003
	$\overline{D}_J$	30 000	20 000 – 60 000	m	Shanks et al. 2003; Kinlan and Gaines 2003
Carrying capacities	K_{AC}	0.213	0.213–0.89	$C{\cdot}m^{-2}$	Yoklavich et al. 2000; Stein et al. 1992
	K_{AJ}	0.028	0.019–0.028	$J{\cdot}m^{-2}$	Yoklavich et al. 2000
Competition coefficients	α_{JC}	1		$C{\cdot}J^{-1}$	
	α_{CJ}	1		$J{\cdot}C^{-1}$	
Predation attack rates	δ_{AC}	912.5	547.5–2555	$(P{\cdot}m^{-2})^{-1}{\cdot}year^{-1}$	Johnson 2004
	δ_{AJ}	547.5	54.75–912.5	$(P{\cdot}m^{-2})^{-1}{\cdot}year^{-1}$	
Predation handling times	τ_C	0	$2.74{\times}10^{-8}$	year	Mylius et al. 2001
	τ_J	0	$2.74{\times}10^{-8}$	year	Mylius et al. 2001
Growth	γ	0.05		$year^{-1}$	Love et al. 2002
Natural mortality	μ	0.05		$year^{-1}$	Methot et al. 2002
Fishing mortality	h_A	0.2	0.1–0.7	$year^{-1}$	
Habitat width	ω	4828.03	4828.03–6759.24	m	
Reserve width	W	4828.03		m	
Reserve length	L (or L_R)	50 000	1000 – 100 000	m	
Region length	L_T	L	200 000	m	
Number of reserves	N_R	1	1–5	Reserves	

Note: For units: m, metres; *C*, competitors; *J*, juveniles; *P* = predators (number of fish).

total length of 23 cm), relatively short-lived (maximum age of 26 years), and unfished and extend from southern California to the Gulf of Alaska at depths of 44–200 m (Love et al. 2002). Yelloweye and pygmy rockfishes are two species with overlapping ranges but divergent life histories with which to represent the general groups of large, longer-lived and small, shorter-lived species, respectively, in our community model.

Although pygmy rockfish have the most representative life history of the dwarf rockfish species that have increased after overfishing of larger species, not all parameter values are available for this unfished species; therefore, we use a slightly larger (maximum total length of 35 cm), longer-lived (maximum age of 32 years) species, shortbelly rockfish (*S. jordani*), to determine internal recruitment values for the smaller species (Love et al. 2002). To calculate internal recruitment, we solve the continuous-time Euler equation for intrinsic growth rate (i.e., r in $1 = \int l(x)m(x)\exp(-rx)dx$, where $l(x)$ is survivorship and $m(x)$ is fecundity at age x). We base survivorship on the mortality rate in Methot et al. (2002) for yelloweye rockfish (which also provides the model parameter value for adult yelloweye rockfish natural mortality) and in Ralston et al. (2003) for shortbelly rockfish. To calculate fecundity, Love et al. (2002) provide age at maturity (the inverse of which also provides the parameter value for growth from juveniles into adult yelloweye rockfish), maximum age, age–length relationships, and length–weight relationships for both rockfish species. We convert weight to egg production based on maximum size and egg production for yelloweye rockfish (Love et al. 2002) and using the weight–fecundity relationship for shortbelly rockfish (Ralston et al. 2003). Finally, we convert egg production to fecundity in terms of larval recruitment using larval survivorship estimates: Ralston et al. (2003) provide larval survivorship estimates for shortbelly rockfish, and we use the general *Sebastes* spp. larval survivorship in Anderson (1984) for yelloweye rockfish.

For external recruitment in the smaller species, we test the range of values for which coexistence between the two species is possible. In the reserve network model, we reduce the smaller species' external recruitment by a factor of 10, because larval dispersal from regions outside the reserve are now accounted for, but larval dispersal from shallow, suboptimal habitat is still possible. For predation–reproduction conversion in the larger species, we assume 10% of the prey eaten contributes to maintenance, growth, and reproduction. The proportion of the 10% energetic gain that contributes to reproduction is the gonadosomatic index, estimated from the allometric relationships described by Charnov et al. (2001; the analogous approach specific to viviparous fish by Gunderson (1997) yields similar parameter values). We test larval dispersal distances for which coexistence between the two species was possible within a range of feasible values (20–500 km; Kinlan and Gaines 2003; Shanks et al. 2003). To convert average dispersal distance to dispersal kernel parameters, we use the formulas from Lockwood et al. (2002).

To determine carrying capacities, we use estimates from the coasts of central California (Yoklavich et al. 2000) and

Oregon (Stein et al. 1992) for pygmy rockfish and from the central California coast for yelloweye rockfish (Yoklavich et al. 2000). In determining competition coefficients, given the absence of quantitative measures of competitive interactions between our model species, we make the baseline assumption that juveniles of the larger species and the smaller species are equally aggressive. Competitive superiority of the smaller species arises from the greater carrying capacity and, therefore, ability to use the same resource (space, which provides a refuge from predation; note that this ignores competition for food) more efficiently. For predation attack rates, we generally assume that cannibalism is less frequent than predation on the smaller species (although we test a range of values that includes equal attack rates for juveniles and competitors), within the range of feasible values reported by Johnson (2004). We base predation handling time on Mylius et al. (2001).

We assume that reserve width (perpendicular to the coastline) is equal to California's jurisdictional boundary (3 nautical miles offshore (1 nautical mile = 1852 m)). In addition, we assume that the habitat width ends the same distance from the coast as the reserve width, again testing a range of values. We tested a range of values (1–100 km) for reserve length based on expected adult movement (Love et al. 2002) and larval dispersal distances (Kinlan and Gaines 2003; Shanks et al. 2003).

Results

There are up to three biologically relevant (i.e., real and nonnegative) equilibria for the system described above. The first equilibrium, where the juvenile and predator densities are zero and competitor density is at its carrying capacity, is always locally stable when competitors outcompete juveniles (see Appendix A for analytic proof). It is possible for equilibrium densities of the larger species to be exactly zero because, with the conservative assumption of scorched earth, the dynamics are closed for the larger species: there is no input from outside the reserve for the larger species. Given the open nature of marine systems, a stable equilibrium with exactly zero density is unlikely (low densities would be more realistic). Therefore, this result emphasizes the fact that our model is not appropriate for quantitative predictions, but rather is useful for qualitative assessment of relevant processes.

Numerically, within all of the parameter values tested, the second equilibrium, with intermediate juvenile, predator, and competitor densities, is always locally unstable; the third equilibrium, with high juvenile and predator densities and low competitor densities, is always locally stable. The interior equilibria, where the larger species density is nonzero, do not exist unless the reserve is large enough for internal recruitment (recruitment after the loss from spillover beyond reserve boundaries) to outweigh competition and mortality for the larger species (Fig. 2; note that for all figures in which we present equilibrium densities for varying reserve length, solid lines represent locally stable equilibria and broken lines represent locally unstable equilibria). This result parallels the classic result of critical patch size from spatially explicit diffusion models in which a patch (in this case, the reserve) must be large enough for within-patch reproduction to outweigh loss over patch edges in order for a population to persist (Skellam 1951; Kierstead and Slobodkin 1953).

Fig. 2. (*a*) Juvenile, (*b*) predator, and (*c*) competitor equilibria densities dependent on reserve length scaled by mean juvenile dispersal distance ($L/\bar{D}_J$). The solid black lines represent the equilibrium with no larger species and the smaller species at its carrying capacity (smaller species dominated equilibrium), which is locally stable. The broken black lines represent the equilibrium with intermediate larger and smaller species densities (threshold equilibrium), which is locally unstable. The shaded lines represent the equilibrium with high larger species density and low smaller species density (larger species dominated equilibrium), which is locally stable.

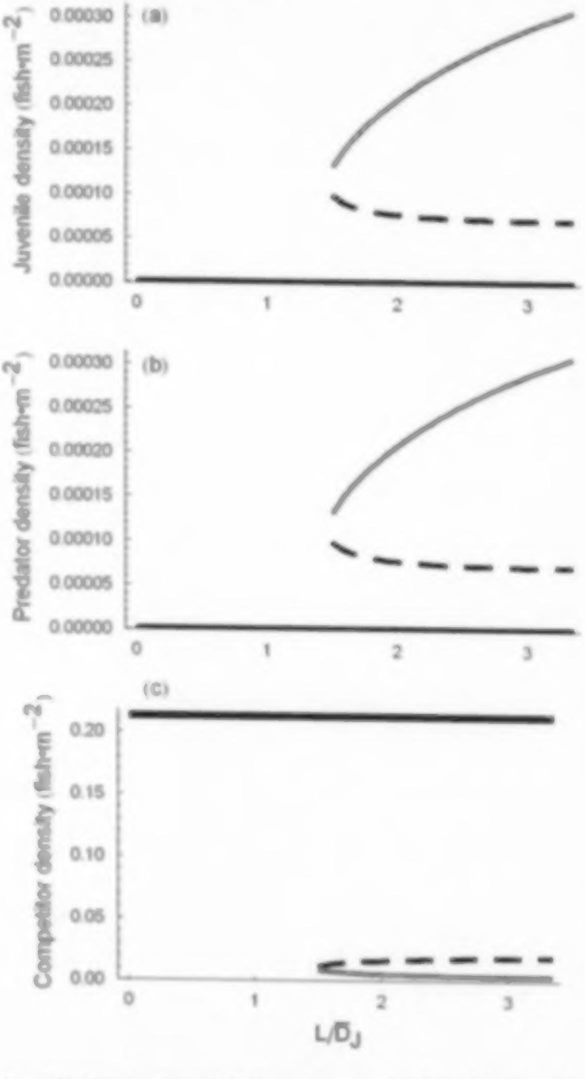

Therefore, in reserves larger than a critical reserve size, two alternative stable states exist. The additional unstable equilibrium sets a threshold as an upper limit for the smaller species and lower limit for the larger species. If the smaller species density is below and the larger species density is

Fig. 3. Time trajectories for the smaller (competitors) and larger (juveniles + predators) species densities (fish·m^{-2}) with varying initial conditions. (*a*–*b*) Simulations in which one species starts above and the other below the threshold equilibrium (solid lines for smaller species above and larger species below, broken lines for smaller species below and larger species above; dotted lines represent equilibrium values; different grayscale for each simulation). (*c*–*d*) Simulations in which the smaller and larger species start both below or both above the threshold (solid lines for both below and broken lines for both above; dotted lines represent equilibrium values; different grayscale for each simulation).

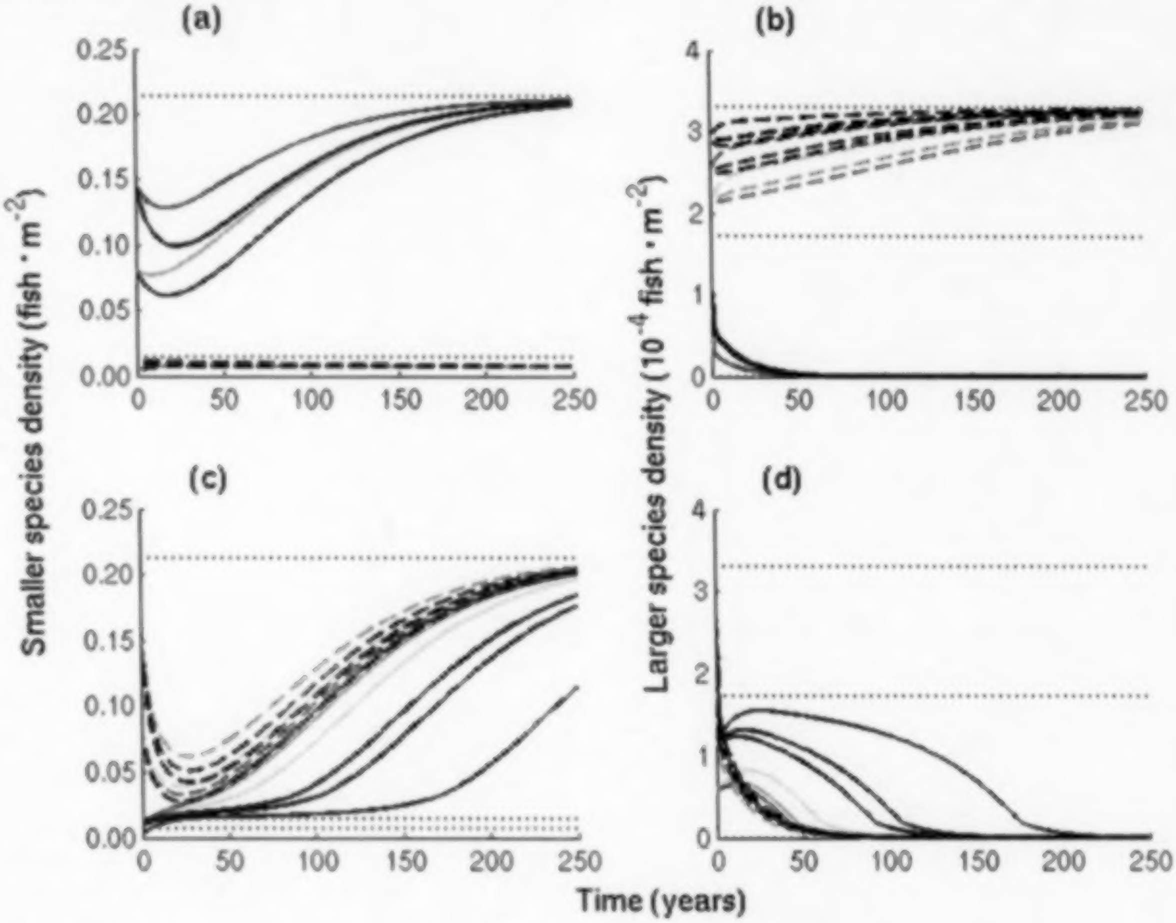

above this "threshold equilibrium" (broken lines in Fig. 2), then the smaller species will decline and the larger species will increase to the "larger species dominated equilibrium" densities (high larger species density and low smaller species density; solid shaded lines in Fig. 2), which is presumably representative of the state before overfishing. Alternately, if the smaller species density is above and the larger species density is below the threshold equilibrium, then the smaller species will increase and the larger species will decline to the "smaller species dominated equilibrium" (no larger species and high smaller species density; solid black lines in Fig. 2). The larger species dominated equilibrium density for the larger species increases with reserve length (Figs. 2*a*, 2*b*).

Impact of initial conditions

To determine the relative importance of smaller and larger species' initial densities, we numerically integrated the model to explore predicted time trajectories with varying initial conditions. As expected, simulations that begin near locally stable equilibria tend toward those equilibria: if the smaller species starts above the threshold equilibrium and the larger species starts below the threshold equilibrium, the system goes to the smaller species dominated equilibrium (solid lines in Figs. 3*a* and 3*b*); if the smaller species starts below the threshold equilibrium and the larger species starts above the threshold equilibrium, the system goes to the larger species dominated equilibrium (broken lines in Figs. 3*a* and 3*b*). In addition, within the initial values and parameters tested, if both the larger species and the smaller species start below the threshold equilibrium or both start above the threshold equilibrium, then the system goes to the smaller species dominated equilibrium (solid lines for both below and broken lines for both above in Figs. 3*c* and 3*d*). In other words, in simulations that did not begin near a locally stable equilibrium and in which one species would need to cross the threshold equilibrium in order for the system to reach a locally stable equilibrium, the system went to the smaller species dominated equilibrium in all of the simulations explored here. Thus, recovery to the desired state of the larger species dominated equilibrium within a reserve depends not only on the larger species starting with a high enough density, but also on the smaller species starting with a low enough density.

Impact of predation and competition

When predation and competition are not included in the model, there are two biologically relevant equilibria: with zero or with nonzero predator and juvenile densities. The nonzero equilibrium exists and is locally stable only when the zero equilibrium is locally unstable (see Appendix A for analytic proof); therefore, alternative stable states do not exist, as in the case with community interactions (where the smaller species dominated and the larger species dominated equilibria are both locally stable). Without interspecific interactions, the model predicts that larger species will recover as long as the reserve is large enough for reproduction within the reserve to counteract mortality, regardless of initial conditions (Fig. 4), whereas the model with interspecific interactions predicts that initial conditions determine the potential for the larger species to recover (Figs. 2–3). Furthermore, the model with interspecific interactions requires a larger reserve for equilibria with nonzero larger species density to exist and therefore for recovery to be possible (Fig. 2 versus Fig. 4).

Equilibria dependence on uncertain parameter values and assumptions

In this section we summarize the key results for varying uncertain parameter values and relaxing assumptions made in developing the basic model (for detailed results, see Appendix B).

Parameters important for estimating threshold equilibrium density for the smaller species are predation on the smaller species, predation on juveniles of the larger species, and juvenile carrying capacity. Parameters important for estimating threshold equilibrium density for the larger species are predation on the smaller species, juvenile carrying capacity, and the smaller species external recruitment. Finally, parameters important for estimating both the reserve size necessary for recovery to be possible and the larger species density at the recovered state are predation on the smaller species, predation on juveniles of the larger species, juvenile carrying capacity, habitat width compared with reserve width, the smaller species external recruitment, the larger species internal recruitment, and the larger species dispersal distance (Appendix B, Figs. B1–B6).

Although uncertain parameter values can substantially change quantitative predictions of our model, the model predictions do not depend greatly on the predatory dynamics assumed or the shape of the dispersal kernel (as has been found in other marine reserve models; Lockwood et al. 2002). However, the scorched earth assumption that larger species outside the reserve do not contribute to the reserve population does substantially impact the quantitative outcome, particularly the threshold equilibrium densities within the reserve (Fig. 5). Furthermore, fragmenting a single reserve into a network of reserves alters the within-reserve equilibrium density for the larger species (Appendix B, Fig. B7).

Fig. 4. Equilibrium (*a*) juvenile and (*b*) predator densities dependent on reserve length scaled to mean juvenile dispersal distance ($L/\bar{D}_J$) when ignoring predation and competition. Solid and broken lines indicate stable and unstable equilibria, respectively.

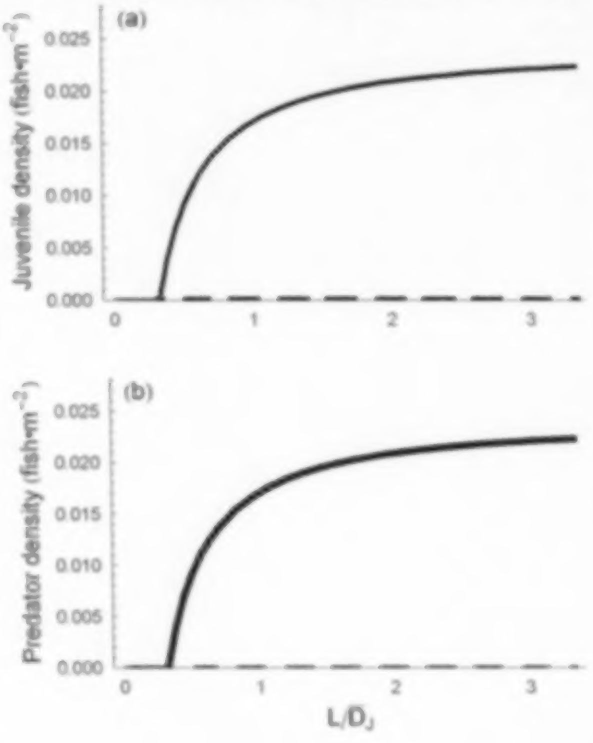

Discussion

Negative community interactions such as predation and competition may impede the recovery of overfished species in marine reserves. To explore one scenario where this is a concern, we presented a model of a rockfish community in which species are identified as overfished "larger species" and unfished "smaller species". The larger species competes with the smaller species as juveniles and preys on the smaller species as adults. As with other models in which the predator and prey compete for common resource (e.g., Polis and Holt 1992; Mylius et al. 2001), numerical analysis of our model indicates that two alternative stable states exist, one in which the larger species dominates and one in which the smaller species dominates, with an unstable threshold equilibrium between the two. In contrast, the equivalent model without predation and competitive community interactions has only one stable state. Therefore, the model without community interactions predicts that any overfished rockfish will recover within a marine reserve as long as the reserve is large enough for recruitment to outweigh mortality, whereas the model with community interactions predicts that recovery depends on both reserve size and the initial densities of the interacting species in the rockfish community.

Fig. 5. Equilibria densities (fish·m^{-2}) for (*a*–*b*) larger and (*c*–*d*) smaller species, dependent on reserve length scaled to mean juvenile dispersal distance ($L/\bar{D}_J$), inside and outside reserves (black lines); shaded lines indicate basic model with "scorched earth" assumption (i.e., areas outside reserve not modeled). Solid and broken lines indicate stable and unstable equilibria, respectively.

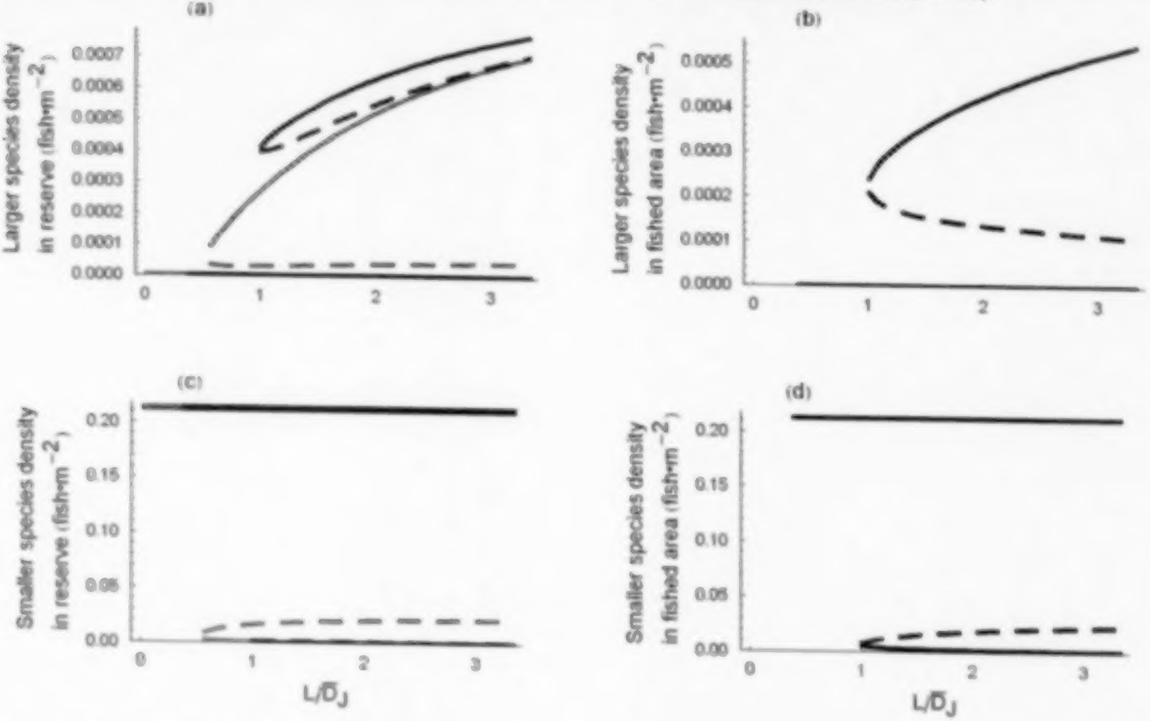

Specifically, both the initial density of the larger species must be large enough and that of the smaller species must be small enough for recovery to take place within a marine reserve. Similarly, Walters and Kitchell (2001) hypothesize that community interactions such as the ones modeled here can explain unexpected recruitment depensation in Ecosim simulations, in which case recovery does not necessarily follow reduced take. Because initial community composition may be vital for the successful restoration of ecosystem structure and function, choosing areas with high abundance of overfished species, and possibly low abundance of interacting species such as competitors, may be more important than choosing areas with generally high biomass and diversity when making reserve placement decisions. Further actions to enhance densities of larger species and (or) reduce densities of smaller species within a reserve may be necessary as well. However, such measures may be difficult to implement in the rockfish system modeled here. In addition, given that we intend this model for qualitative assessment, further research is needed to make more specific recommendations on management actions required to promote recovery of overfished stocks given community interactions. In particular, our model ignores countless aspects of reality, such as environmentally driven fluctuations in recruitment, that could alter theoretical predictions.

Along with altering the initial conditions necessary for recovery, consideration of community interactions increases the reserve size necessary for the larger species to persist within the reserve and for recovery to be possible regardless of initial conditions. Analogously, in models and simulations without marine reserves but with varying fishing mortality, scenarios that incorporate community interactions require a lower fishing rate to maintain sustainable yield compared with scenarios without community interactions (Walters and Kitchell 2001; MacCall 2002). Both the larger reserve and lower fishing mortality requirements arise from the need for recruitment by the overfished species to outweigh negative interactions with unfished species. The increase in reserve size necessary for protection of ecosystem structure in this and other models of community interactions (Walters 2000) indicates the importance of such interactions in designing reserves to achieve biodiversity goals.

For both the reserve size necessary for recovery and the various equilibria densities, the quantitative predictions of our model vary substantially with values for poorly known parameters such as predation and recruitment, as well as with the scorched earth assumption of no input from unprotected areas. Therefore, future models or simulations that are designed for quantitative rather than qualitative predictions will require a better understanding of parameter values and will likely need to incorporate contributions from both protected and unprotected areas to ensure accuracy. Another outcome of the version of our model that incorporates unprotected areas is that the recovered state in which the larger species has high density within the reserve corresponds to higher density for the larger species outside the reserve as well, even at a fishing rate outside the reserve that would lead to population collapse if the reserve were not there. In other words, if the larger species can recover from overfishing within the reserve, it will lead to an increase in larger species density outside the reserve and prevent stock collapse from overfishing. This result parallels Steele and Beet's (2003) outcome from a single-species model that the establishment of reserves can increase the yield of depleted stocks with alternative stable states, as well as reinforces the role, suggested from single-species models (e.g., Guénette and Pitcher 1999; Apostolaki et al. 2002), that reserves may play in enhancing resilience to overfishing.

In addition to the predation and competitive interactions modeled here, incorporating community interactions in marine reserve models generally alters reserve design recommendations and expectations after reserve establishment. For example, in Mangel and Levin's (2005) model of a target species with offshore adults and inshore juveniles, when ignoring community interactions, establishing an inshore reserve is more effective in terms of recovery rate and recovered-state biomass than establishing an offshore reserve or stopping all take. However, when they incorporated an inshore predator, establishing an inshore reserve is the least effective policy in their model. Furthermore, Micheli et al. (2004) show that the counterintuitive outcome of population declines after marine reserve establishment is feasible in a predator–prey model with exchange between protected and unprotected areas, dependent on fishing mortality outside the reserve. Finally, Ecospace simulations indicate that incorporating community interactions can reduce the potential for small reserves to protect target species (Walters 2000). In general, predictions from community models such as the ones described above and the one presented here are preferable to the traditional single-species approach to fisheries modeling when they include key interactions (Hollowed et al. 2000).

In summary, even with its simplified representation of rockfish communities, our model indicates that community interactions substantially alter the conditions necessary for recovery of overfished species within marine reserves. Given the additional initial density requirements and increased reserve size necessary for recovery when incorporating community interactions, the model results suggest that recovery from overfishing within reserves may require management action beyond the elimination of fishing mortality. Regardless of whether the community interactions result in prevented recovery, as is possible in models with alternative stable states, or slowed recovery, these theoretical predictions indicate the importance of considering community interactions in conservation planning (Knowlton 2004). In the variety of systems in which relevant community interactions occur, from the rockfish system explored here to Atlantic cod to rock lobsters (Barkai and McQuaid 1988; Swain and Sinclair 2000; MacCall 2002), a better understanding of such interactions is vital to policy decisions such as reserve design and expectations after reserve establishment.

Acknowledgments

Discussions with Simon Levin, Steve Pacala, Alec MacCall, Steve Ralston, Mark Carr, and Dave Fluharty were extremely helpful in developing the ideas and model. This paper benefited from comments on an earlier version by John Field, Heather Leslie, Simon Levin, and two anonymous reviewers. M.L.B. received support for this research from the National Science Foundation Graduate Research Fellowship Program and the Burroughs Wellcome Fund Training Program in Biological Dynamics (No. 1001781). This work was conducted as part of the Development of Tools for the Practical Design of Marine Reserves Working Group supported by the National Center for Ecological Analysis and Synthesis, a Center funded by NSF (Grant No. DEB-00-72909), the University of California at Santa Barbara, and the State of California.

References

Allison, G.W., Lubchenco, J., and Carr, M.H. 1998. Marine reserves are necessary but not sufficient for marine conservation. Ecol. Appl. **8**: S79–S92.

Anderson, J.T. 1984. Early life-history of redfish (*Sebastes* spp.) on Flemish Cap. Can. J. Fish. Aquat. Sci. **41**(7): 1106–1116.

Apostolaki, P., Milner-Gulland, E.J., McAllister, M.K., and Kirkwood, G.P. 2002. Modelling the effects of establishing a marine reserve for mobile fish species. Can. J. Fish. Aquat. Sci. **59**: 405–415.

Barkai, A., and McQuaid, C. 1988. Predator–prey role reversal in a marine benthic ecosystem. Science (Washington, D.C.), **242**(4875): 62–64.

Charnov, E.L., Turner, T.F., and Winemiller, K.O. 2001. Reproductive constraints and the evolution of life histories with indeterminate growth. Proc. Natl. Acad. Sci. U.S.A. **98**(16): 9460–9464.

Choi, J.S., Frank, K.T., Leggett, W.C., and Drinkwater, K. 2004. Transition to an alternate state in a continental shelf ecosystem. Can. J. Fish. Aquat. Sci. **61**: 505–510.

Collie, J.S., Richardson, K., and Steele, J.H. 2004. Regime shifts: can ecological theory illuminate the mechanisms? Prog. Oceanogr. **60**(2–4): 281–302.

Essington, T.E. 2004. Getting the right answer from the wrong model: evaluating the sensitivity of multispecies fisheries advice to uncertain species interactions. Bull. Mar. Sci. **74**(3): 563–581.

Guénette, S., and Pitcher, T.J. 1999. An age-structured model showing the benefits of marine reserves in controlling overexploitation. Fish. Res. **39**: 295–303.

Gunderson, D.R. 1997. Trade-off between reproductive effort and adult survival in oviparous and vivparous fishes. Can. J. Fish. Aquat. Sci. **54**: 990–998.

Halpern, B.S., and Warner, R.R. 2002. Marine reserves have rapid and lasting effects. Ecol. Lett. **5**: 361–366.

Heino, M., and Godø, O.R. 2002. Fisheries-induced selection pressures in the context of sustainable fisheries. Bull. Mar. Sci. **70**: 639–656.

Hilborn, R., Stokes, K., Maguire, J.J., Smith, T., Botsford, L.W., Mangel, M., Orensanz, J., Parma, A., Rice, J., Bell, J., Cochrane, K.L., Garcia, S., Hall, S.J., Kirkwood, G.P., Sainsbury, K., Stefansson, G., and Walters, C. 2004. When can marine reserves improve fisheries management? Ocean Coast. Manag. **47**(3–4): 197–205.

Holland, D.S., and Brazee, R.J. 1996. Marine reserves for fisheries management. Mar. Resour. Econ. **11**: 157–71.

Hollowed, A.B., Bax, N., Beamish, R., Collie, J., Fogarty, M., Livingston, P., Pope, J., and Rice, J.C. 2000. Are multispecies models an improvement on single-species models for measuring fishing impacts on marine ecosystems? ICES J. Mar. Sci. **57**(3): 707–719.

Holt, R.D., and Polis, G.A. 1997. A theoretical framework for intraguild predation. Am. Nat. **149**(4): 745–764.

Huggett, A.J. 2005. The concept and utility of 'ecological thresholds' in biodiversity conservation. Biol. Conserv. **124**: 301–310.

Jennings, S., Reynolds, J.D., and Mills, S.C. 1998. Life history correlates of responses to fisheries exploitation. Proc. R. Soc. Lond. Ser. B Biol. Sci. **265**: 333–339.

Johnson, D. 2004. Early, post-settlement mortality and the population dynamics of nearshore rockfish. Ph.D. dissertation, University of California at Santa Cruz, Santa Cruz, California.

Kierstead, H., and Slobodkin, L.B. 1953. The size of water masses containing plankton blooms. J. Mar. Res. **12**: 141–147.

Kinlan, B.P., and Gaines, S.D. 2003. Propagule dispersal in marine and terrestrial environments: a community perspective. Ecology, **84**(8): 2007–2020.

Knowlton, N. 2004. Multiple "stable" states and the conservation of marine ecosystems. Prog. Oceanogr. **60**(2–4): 387–396.

Lauck, T., Clark, C.W., Mangel, M., and Munro, G.R. 1998. Implementing the precautionary principle in fisheries management through marine reserves. Ecol. Appl. **8**: S72–S78.

Lockwood, D.R., Hastings, A., and Botsford, L.W. 2002. The effects of dispersal patterns on marine reserves: does the tail wag the dog? Theor. Popul. Biol. **61**: 297–309.

Love, M.S., Yoklavich, M., and Thorsteinson, L. 2002. The rockfishes of the Northeast Pacific. The University of California Press, Berkeley, California.

MacCall, A.D. 2002. Fishery-management and stock-rebuilding prospects under conditions of low-frequency environmental variability and species interactions. Bull. Mar. Sci. **70**: 613–628.

Man, A., Law, R., and Polunin, N.V.C. 1995. Role of marine reserves in recruitment to reef fisheries: a metapopulation model. Biol. Conserv. **71**: 197–204.

Mangel, M. 2000. Irreducible uncertainties, sustainable fisheries and marine reserves. Evol. Ecol. Res. **2**: 547–557.

Mangel, M., and Levin, P.S. 2005. Regime, phase and paradigm shifts: making community ecology the basic science for fisheries. Philos. Trans. R. Soc. Lond. Ser. B Biol. Sci. **360**: 95–105.

May, R.M. 1977. Thresholds and breakpoints in ecosystems with a multiplicity of stable states. Nature (London), **269**(5628): 471–477.

McClanahan, T., Polunin, N., and Done, T. 2002. Ecological states and the resilience of coral reefs. Conserv. Ecol. **6**(2): 18.

Methot, R., Wallace, R., and Piner, K. 2002. Status of yelloweye rockfish off the U.S. west coast in 2002. National Marine Fisheries Service, Portland, Oregon.

Micheli, F., Amarasekare, P., Bascompte, J., and Gerber, L.R. 2004. Including species interactions in the design and evaluation of marine reserves: some insights from a predator–prey model. Bull. Mar. Sci. **74**(3): 653–669.

Murray, S.N., Ambrose, R.F., Bohnsack, J.A., Botsford, L.W., Carr, M.H., Davis, G.E., Dayton, P.K., Gotshall, D., Gunderson, D.R., Hixon, M.A., Lubchenco, J., Mangel, M., MacCall, A., McArdle, D.A., Ogden, J.C., Roughgarden, J., Starr, R.M., Tegner, M.J., and Yoklavich, M.M. 1999. No-take reserve networks: sustaining fishery populations and marine ecosystems. Fisheries, **24**: 11–25.

Mylius, S.D., Klumpers, K., de Roos, A.M., and Persson, L. 2001. Impact of intraguild predation and stage structure on simple communities along a productivity gradient. Am. Nat. **158**: 259–276.

Pauly, D., Christensen, V., Dalsgaard, J., Froese, R., and Torres, F., Jr. 1998. Fishing down marine food webs. Science (Washington, D.C.), **279**: 860–863.

Petraitis, P.S., and Dudgeon, S.R. 2004. Detection of alternative stable states in marine communities. J. Exp. Mar. Biol. Ecol. **300**(1–2): 343–371.

Polis, G.A., and Holt, R.D. 1992. Intraguild predation: the dynamics of complex trophic interactions. Trends Ecol. Evol. **7**(5): 151–154.

Polis, G.A., Myers, C.A., and Holt, R.D. 1989. The ecology and evolution of intraguild predation — potential competitors that eat each other. Annu. Rev. Ecol. Syst. **20**: 297–330.

Punt, A.E. 2003. Evaluating the efficacy of managing West Coast groundfish resources through simulations. Fish. Bull. **101**: 860–873.

Ralston, S., Bence, J.R., Eldridge, M.B., and Lenarz, W.H. 2003. An approach to estimating rockfish biomass based on larval production, with application to *Sebastes jordani*. Fish. Bull. **101**(1): 129–146.

Scheffer, M., and Carpenter, S.R. 2003. Catastrophic regime shifts in ecosystems: linking theory to observation. Trends Ecol. Evol. **18**(12): 648–656.

Scheffer, M., Carpenter, S., Foley, J.A., Folke, C., and Walker, B. 2001. Catastrophic shifts in ecosystems. Nature (London), **413**(6856): 591–596.

Shanks, A.L., Grantham, B.A., and Carr, M.H. 2003. Propagule dispersal distance and the size and spacing of marine reserves. Ecol. Appl. **13**: S159–S169.

Skellam, J.G. 1951. Random dispersal in theoretical populations. Biometrika, **38**(1–2): 196–218.

Sladek Nowlis, J., and Roberts, C.M. 1999. Fisheries benefits and optimal design of marine reserves. Fish. Bull. **97**: 604–616.

Steele, J.H., and Beet, A.R. 2003. Marine protected areas in 'nonlinear' ecosystems. Proc. R. Soc. Lond. Ser. B Biol. Sci. **270**: S230–S233.

Stein, D.L., Tissot, B.N., Hixon, M.A., and Barss, W. 1992. Fish–habitat associations on a deep reef at the edge of the Oregon continental shelf. Fish. Bull. **90**: 540–551.

Swain, D.P., and Sinclair, A.F. 2000. Pelagic fishes and the cod recruitment dilemma in the Northwest Atlantic. Can. J. Fish. Aquat. Sci. **57**: 1321–1325.

Walters, C. 2000. Impacts of dispersal, ecological interactions, and fishing effort dynamics on efficacy of marine protected areas: how large should protected areas be? Bull. Mar. Sci. **66**: 745–757.

Walters, C., and Kitchell, J.F. 2001. Cultivation/depensation effects on juvenile survival and recruitment: implications for the theory of fishing. Can. J. Fish. Aquat. Sci. **58**: 39–50.

Whipple, S.J., Link, J.S., Garrison, L.P., and Fogarty, M.J. 2000. Models of predation and fishing mortality in aquatic ecosystems. Fish Fish. **1**: 22–40.

Yoklavich, M., Greene, H.G., Cailliet, G., Sullivan, D., Lea, R., and Love, M. 2000. Habitat associations of deep-water rockfishes in a submarine canyon: an example of a natural refuge. Fish. Bull. **98**: 625–641.

Yoklavich, M.M., Cailliet, G.M., Lea, R.N., Greene, H.G., Starr, R., deMarignac, J., and Field, J. 2002. Deepwater habitat and fish resources associated with the Big Creek Ecological Reserve. CalCOFI (California Cooperative Oceanic Fisheries Investigations), Rep. **43**: 120–140. Available at http://www.calcofi.org/newhome/publications/CalCOFI_Reports/V43/V43_toc.htm.

Appendix A. Model details

The smaller rockfish species, represented by C (competitors), have open recruitment at rate r_{1C} from the suboptimal habitat, as well as internal recruitment at rate r_{2C}. Assuming depletion of the larger, fished rockfish species outside the reserve (scorched earth), juveniles of the larger species, represented by J, only have internal recruitment at a rate of r_{2J}.

Table A1. Variables, parameters, and relation to reserve area.

Number	Density	
Variables		
C	$\rho_C A$	Competitors (smaller species)
J	$\rho_J A$	Juveniles (of larger species)
P	$\rho_P A$	Predators (adults of larger species)
Parameters		
r_{1X}	$r_{A1X} A$	Open recruitment rate for X (C or J)
r_{2X}	$r_{A2X} \frac{W}{\omega} \int_0^L \int_0^L \frac{\kappa_X(y-x)}{L} \mathrm{d}y \mathrm{d}x$	Internal recruitment rate for X (see Fig. A1)
V_X	$\overline{D}_X$ or $\frac{\pi}{2} \overline{D_X^2}$	Variance in dispersal distance for kernel $\kappa_X(y-x)$ (Laplace or normal, respectively)[a]
K_X	$K_{AX} A$	Carrying capacity of X
α_{XY}		Competitive effect of X on Y
δ_X	δ_{AX}/A	Predation rate of predators on X
τ_X		Handling time for X in type II predation
β_X	$\beta_{AX} \frac{W}{\omega} \int_0^L \int_0^L \frac{\kappa_X(y-x)}{L} \mathrm{d}y\, \mathrm{d}x$	Conversion factor of predation on X into reproductive capacity
γ		Growth rate from juveniles to predators
μ		Natural mortality for predators
h	$h_0 \left(\frac{2W + L}{LW} \right)$	Fishing mortality in predators (see Fig. A2)
A	LW	Reserve area = length × width
N_R		Number of reserves in a reserve network

[a] Lockwood et al. 2002.

Fig. A1. Length L parallel to the coast and width W perpendicular to the coast characterize a theoretical reserve. The dispersal kernel $\kappa(y-x)$ (either normal or Laplace) represents the settlement distribution along the coast (each point y) of offspring originating at point x. At each settlement point y, individuals are equally likely to settle at any distance perpendicular to coast within the suitable habitat width, ω.

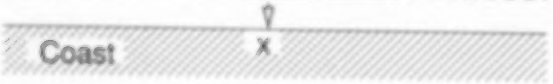

Fig. A2. The checked area represents a reserve of length L and width W, each check of size $a \times a$ represents an adult territory, and the solid checks on the perimeter of the reserve are vulnerable to fishing edge effects.

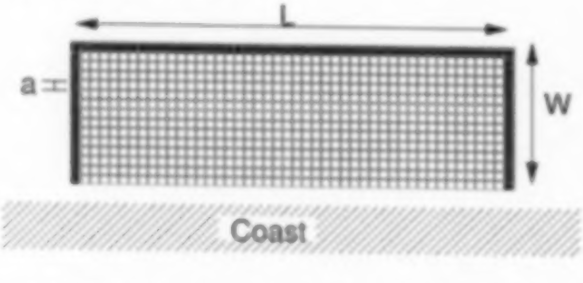

The reserve has carrying capacities K_C for the competitors and K_J for the juveniles, and the juveniles and competitors compete according to constants α_{JC} and α_{CJ}. The adults of the larger species, represented by P (predators), prey on the competitors and juveniles at rates δ_C and δ_J, respectively. This predation is converted into reproductive capacity according to β_C and β_J; r_{2J} represents additional reproductive capacity due to constant predation on other prey not included in the dynamics below. The growth rate of juveniles into adult predators is γ, the natural adult mortality rate is μ, and the fishing mortality rate as a result of edge effects on the border of the reserve is h. Then competitor, juvenile, and predator populations vary over time (t) according to :

$$\text{(A1)} \quad \frac{\mathrm{d}C}{\mathrm{d}t} = \frac{r_{1C} + r_{2C} C}{K_C} (K_C - C - \alpha_{JC} J) - \delta_C PC$$

$$\text{(A2)} \quad \frac{\mathrm{d}J}{\mathrm{d}t} = \frac{P(r_{2J} + \beta_J \delta_J J + \beta_C \delta_C C)}{K_J} (K_J - J - \alpha_{CJ} C) - (\delta_J P + \gamma) J$$

$$\text{(A3)} \quad \frac{\mathrm{d}P}{\mathrm{d}t} = \gamma J - (\mu + h) P$$

(Fig. 1). Here we use Lotka–Volterra dynamics based on their frequent and historical use in ecological dynamics, in-

Fig. A3. Integrating and summing the dispersal kernel ($\kappa(y-x)$) over reserves and (or) fished areas in a reserve network (with width W equal to habitat width ω and total reserve network length L_R out of region length L_T divided into N_R reserves) yields the movement rates ($m_{X,YZ}$) within and between reserves and fished areas for each species.

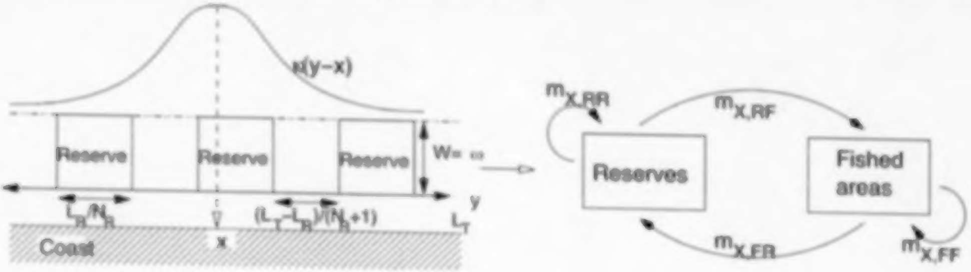

cluding multispecies fisheries dynamics, as well as for mathematical simplicity and the use of relatively few (albeit difficult to estimate) parameters (Whipple et al. 2000).

Density dynamics

To redefine the model in terms of population density (fish per unit area) rather than number of individuals, let $\rho_C = C/A$, $\rho_J = J/A$, and $\rho_P = P/A$. Given the area relationships in Table A1, eqs. A1–A3 become

$$\text{(A4)}\quad \frac{\mathrm{d}\rho_C}{\mathrm{d}t} = \frac{r_{AC} + r_{2C}[L,W]\rho_C}{K_{AC}}(K_{AC} - \rho_C - \alpha_{JC}\rho_J) - \delta_{AC}\rho_P\rho_C$$

$$\text{(A5)}\quad \frac{\mathrm{d}\rho_J}{\mathrm{d}t} = \frac{\rho_P(r_{2J}[L,W] + \beta_J[L,W]\delta_{AJ}\rho_J + \beta_C[L,W]\delta_{AC}\rho_C)}{K_{AJ}} \times (K_{AJ} - \rho_J - \alpha_{CJ}\rho_C) - (\delta_{AJ}\rho_P + \gamma)\rho_J$$

$$\text{(A6)}\quad \frac{\mathrm{d}\rho_P}{\mathrm{d}t} = \gamma\rho_J - (\mu + h[L,W])\rho_P$$

Analysis

We primarily use local stability analysis of our community model. The leading eigenvalue λ of the Jacobian matrix of eqs. A4–A6 evaluated at an equilibrium ($\hat{\rho}_C$, $\hat{\rho}_J$, $\hat{\rho}_P$ such that $\frac{\mathrm{d}\rho_C}{\mathrm{d}t} = \frac{\mathrm{d}\rho_J}{\mathrm{d}t} = \frac{\mathrm{d}\rho_P}{\mathrm{d}t} = 0$) indicates the local stability of that equilibrium: if $\lambda < 0$, then the above equilibrium is locally stable; if $\lambda > 0$, then the above equilibrium is locally unstable.

One biologically relevant equilibrium for system A4–A6 is $\hat{\rho}_C = K_{AC}$, $\hat{\rho}_J = \hat{\rho}_P = 0$, or with competitors at their carrying capacity and juveniles and predators not present. The three eigenvalues of system A4–A6 evaluated at this equilibrium are

$$\text{(A7)}\quad \lambda_1 = -\frac{r_{AC} + r_{2C}K_{AC}}{K_{AC}}$$

$$\text{(A8)}\quad \lambda_2 = -\frac{1}{2}(\gamma + \mu + h) - \frac{1}{2}\sqrt{(\gamma - (\mu + h))^2 + 4\gamma(r_{2J} + \beta_C\delta_{AC}K_{AC})\left(1 - \alpha_{CJ}\frac{K_{AC}}{K_{AJ}}\right)}$$

$$\text{(A9)}\quad \lambda_3 = -\frac{1}{2}(\gamma + \mu + h) + \frac{1}{2}\sqrt{(\gamma - (\mu + h))^2 + 4\gamma(r_{2J} + \beta_C\delta_{AC}K_{AC})\left(1 - \alpha_{CJ}\frac{K_{AC}}{K_{AJ}}\right)}$$

Given that all parameter values are positive, λ_1 and λ_2 have a negative real part. λ_3 has a negative real part if

$$\text{(A10)}\quad \mu + h > (r_{2J} + \beta_C\delta_{AC}K_{AC})\left(1 - \alpha_{CJ}\frac{K_{AC}}{K_{AJ}}\right)$$

or the larger species mortality outweighs its recruitment reduced by a factor based on competition with the smaller species. Note that inequality A10 is always true if $\alpha_{CJ} < K_{AJ}/K_{AC}$, or the smaller species is a superior competitor to the juveniles of the larger species, which is true for all parameter values used here. Therefore, when the smaller species is the superior competitor (and, more generally, when inequality A10 holds), all eigenvalues are negative and the equilibrium is locally stable.

For analysis of additional equilibria, we numerically solve for the equilibria and calculate the leading eigenvalue of the Jacobian matrix evaluated at those equilibria using the parameter values in Table 1. An analytical exploration of the generality of the numerical results shown here is worth future theoretical investigation.

Equivalent system without predation and competition

Without the competition and predation ($\alpha_{CJ} = \alpha_{JC} = \delta_{AJ} = \delta_{AC} = 0$; i.e., removing the smaller species from the system), there are two biologically relevant equilibria. Based on local stability analysis as described above, the trivial equilibrium, $\hat{\rho}_J = \hat{\rho}_P = 0$, is locally stable if $\mu + h[L,W] > r_{2J}[L,W]$ (mortality outweighs reproduction). For the nontrivial equilibrium, $\hat{\rho}_J = \gamma\frac{K_{AJ}}{r_{2J}}\left(\frac{r_{2J}}{\mu + h} - 1\right)$, $\hat{\rho}_P = K_{AJ}\left(1 - \frac{\mu + h}{r_{2J}}\right)$, the condition for its biological existence (nonnegative densities) and local stability are identical: $r_{2J}[L,W] > \mu + h[L,W]$ (reproduction outweighs mortality), exactly the reverse of the stability condition for the trivial equilibrium. Therefore, if reproduction outweighs mortality, the system will go to positive equilibrium densities; otherwise, the juveniles and predators will decline to zero.

Relaxing assumptions

Type I predation

For mathematical simplicity, the above model uses a linear (type I) functional response of predators to prey density; however, a saturating (type II) functional response is more biologically realistic. To determine whether incorporating type II functional response significantly impacts the results, system A4–A6 with type II predation is

$$\text{(A11)}\quad \frac{d\rho_C}{dt} = \frac{r_{AC} + r_{2C}[L,W]\rho_C}{K_{AC}}(K_{AC} - \rho_C - \alpha_{JC}\rho_J) - \frac{\delta_{AC}\rho_P\rho_C}{1 + \tau_C\delta_{AC}\rho_C + \tau_J\delta_{AJ}\rho_J}$$

$$\text{(A12)}\quad \frac{d\rho_J}{dt} = \frac{\rho_P}{K_{AJ}}\left(r_{2J}[L,W] + \frac{\beta_J[L,W]\delta_{AJ}\rho_J + \beta_C[L,W]\delta_{AC}\rho_C}{1 + \tau_C\delta_{AC}\rho_C + \tau_J\delta_{AJ}\rho_J}\right)(K_{AJ} - \rho_J - \alpha_{CJ}\rho_C) - \rho_J\left(\frac{\delta_{AJ}\rho_P}{1 + \tau_C\delta_{AC}\rho_C + \tau_J\delta_{AJ}\rho_J} + \gamma\right)$$

$$\text{(A13)}\quad \frac{d\rho_P}{dt} = \gamma\rho_J - (\mu + h[L,W])\rho_P$$

We numerically compare equilibria densities and local stabilities for the system with type I and type II predation over a range of reserve lengths with the default parameters listed in Table 1.

Scorched earth

To relax the scorched earth assumption that overfishing negates any contribution of predator populations outside the reserve to juvenile populations inside the reserve, we model the dynamics within and exchange between reserves (with competitor, juvenile, and predator populations C_R, J_R, and P_R, respectively) and fished areas (with competitor, juvenile, and predator populations C_H, J_H, and P_H, respectively) according to

$$\text{(A14)}\quad \frac{dC_R}{dt} = \frac{r_{AC}A_R + r_{AX}(m_{C,RR}C_R + m_{C,FR}C_H)}{K_{AC}A_R}(K_{AC}A_R - C_R - \alpha_{JC}J_R) - \delta_{AC}A_RP_RC_R$$

$$\text{(A15)}\quad \frac{dC_H}{dt} = \frac{r_{AC}A_H + r_{AX}(m_{C,FF}C_H + m_{C,RF}C_R)}{K_{AC}A_H}(K_{AC}A_H - C_H - \alpha_{JC}J_H) - \delta_{AC}A_HP_HC_H$$

$$\text{(A16)}\quad \frac{dJ_R}{dt} = \frac{1}{K_{AJ}A_R}(m_{J,RR}P_R(r_{A2J} + \delta_{AJ}A_R\beta_{AJ}J_R + \delta_{AC}A_R\beta_{AC}C_R) + m_{J,FR}P_H(r_{A2J} + \delta_{AJ}A_H\beta_{AJ}J_H + \delta_{AC}A_H\beta_{AC}C_H))$$
$$\times (K_{AJ}A_R - J_R - \alpha_{CJ}C_R) - (\delta_{AJ}A_RP_R + \gamma)J_R$$

$$\text{(A17)}\quad \frac{dJ_H}{dt} = \frac{1}{K_{AJ}A_H}(m_{J,FF}P_H(r_{A2J} + \delta_{AJ}A_H\beta_{AJ}J_H + \delta_{AC}A_H\beta_{AC}C_H) + m_{J,RF}P_R(r_{A2J} + \delta_{AJ}A_R\beta_{AJ}J_R + \delta_{AC}A_R\beta_{AC}C_R))$$
$$\times (K_{AJ}A_H - J_H - \alpha_{CJ}C_H) - (\delta_{AJ}A_HP_H + \gamma)J_H$$

$$\text{(A18)}\quad \frac{dP_R}{dt} = \gamma J_R - \left(\mu + h_A\frac{L_R + N_RW}{L_RW}\right)P_R \qquad \text{(A19)}\quad \frac{dP_H}{dt} = \gamma J_H - (\mu + h_A)P_H$$

In the above system, there is no adult movement, and all movement occurs as a result of larval dispersal. Movement parameters $m_{X,RR}$ and $m_{X,FF}$ represent the portion of larvae retained within reserves and fished areas, respectively, whereas $m_{X,FR}$ is the proportion of larvae that move from fished to reserve areas and $m_{X,RF}$ is the proportion of larvae that move from reserve to fished areas. Integrating and summing the dispersal kernel over reserves or fished areas yields the retention and exchange rates for each species X (C or J; Fig. A3). Because we do not explicitly account for adult movement, predators in reserves still experience edge-effects fishing. Again, we numerically analyze the equilibria values and local stabilities of system A14–A19 with the parameter values in Table 1.

Reference

Lockwood, D.R., Hastings, A., and Botsford, L.W. 2002. The effects of dispersal patterns on marine reserves: does the tail wag the dog? Theor. Popul. Biol. **61**: 297–309.

Appendix B. Exploration of uncertain parameter values and assumptions

Here we determine the impact of changing uncertain parameter values on our results. Rather than a formal sensitivity analysis, we explore biologically feasible ranges to determine which parameters may require more precise values in order to make quantitative predictions. In the following graphs, shaded lines represent lower limits and black lines represent upper limits of uncertain parameter ranges.

Fig. B1. Equilibria densities (fish·m^{-2}) for larger species dependent on reserve length scaled to mean juvenile dispersal distance ($L/\bar{D}_J$) for ranges of recruitment rate values with (*a*) juvenile internal recruitment ranges, (*b*) competitor internal recruitment ranges, and (*c*) competitor external recruitment ranges. Solid and broken lines indicate stable and unstable equilibria, respectively; shaded and black lines indicate lower and upper bounds for value ranges, respectively.

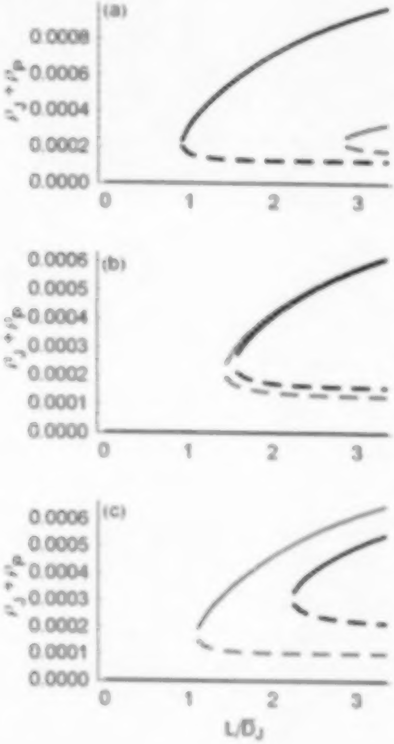

Decreasing recruitment rates, increasing dispersal distances, and increasing habitat width all have the similar affect of decreasing within-reserve recruitment, by decreasing reproduction, decreasing retention, and decreasing the proportion of the habitat covered by the reserve, respectively. Therefore, changes in these parameters have similar effects on equilibrium values. Specifically, because of decreased within-reserve recruitment, decreasing the juvenile internal recruitment rate, increasing the juvenile dispersal distance, and increasing habitat width all substantially increase the reserve size necessary for the threshold and larger species dominated equilibria to exist and decrease the larger species dominated equilibrium density for the larger species (Figs. B1*a*, B2*a*, and B3, respectively). Analogous changes in parameter values for the smaller species have less of an impact on equilibrium values. Qualitatively, decreasing the competitor internal recruitment rate, decreasing the competitor external recruitment rate, and increasing the competitor dispersal distance all decrease the reserve size necessary for the threshold and larger species dominated equilibria to exist and decrease the threshold equilibrium density for the larger species (decreasing the smaller species' external recruitment increases the larger species density at the larger species dominated equilibrium as well), presumably because of decreased competition for the larger species' juveniles with the decreased recruitment for the smaller species (Figs. B1*b*, B1*c*, and B2*b*, respectively). Beyond affecting the reserve lengths for which the equilibria exist, changes in these parameters have little affect on the smaller species equilibria densities (results not shown). In addition, choosing a Laplace or normal dispersal kernel does not impact the qualitative results of the model (Fig. B4).

Fig. B2. Equilibria densities (fish·m^{-2}) for larger species dependent on reserve length (L, m) for ranges of values for dispersal distance for (*a*) juveniles and (*b*) competitors. Solid and broken lines indicate stable and unstable equilibria, respectively; shaded and black lines indicate lower and upper bounds for value ranges, respectively.

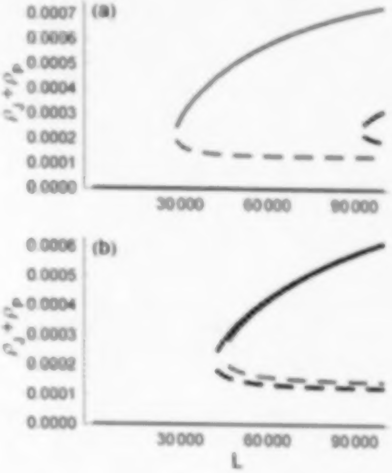

Altering carrying capacities tests the effect of altering competition between the juveniles and the competitors. Decreasing the juvenile carrying capacity increases the reserve size necessary for the threshold and larger species dominated equilibria to exist, increases the threshold equilibrium density for the larger species, decreases the threshold equilibrium density for the smaller species, and decreases the larger species dominated equilibrium density for the larger species, all presumably because of the greater competitive disadvantage (Figs. B5*a*, B5*b*). The primary effect of increasing the smaller species carrying capacity is to increase its density at the smaller species dominated equilibrium to the new carrying capacity (Figs. B5*c*, B5*d*).

Within the parameter ranges tested, changing the fishing mortality outside the reserve has virtually no impact on the smaller or larger species equilibria densities (results not shown).

Altering predation parameter values has a substantial impact on equilibrium predictions. Both increasing predation on juveniles and decreasing predation on competitors increase the reserve size necessary for the threshold and larger species dominated equilibria to exist, decrease the threshold equilibrium density for the smaller species, and decrease the larger species dominated equilibrium density for the larger species (Fig. B6). Furthermore, decreasing predation on competitors increases the threshold equilibrium density for the larger species (Fig. B6*c*). A likely ex-

Fig. B3. Equilibria densities (fish·m^{-2}) for larger species dependent on reserve length scaled to mean juvenile dispersal distance ($L/\bar{D}_J$), for a range of habitat widths (impacting percent of habitat that the reserve covers). Solid and broken lines indicate stable and unstable equilibria, respectively; shaded and black lines indicate lower and upper bounds for value ranges, respectively.

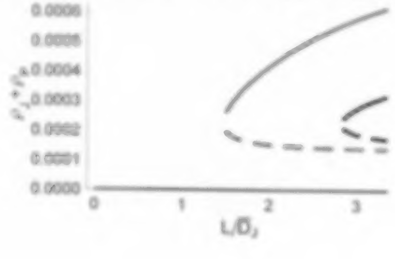

Fig. B4. Equilibria densities (fish·m^{-2}) for larger species dependent on reserve length scaled to mean juvenile dispersal distance ($L/\bar{D}_J$) using the Laplace dispersal kernel (shaded lines) and the normal dispersal kernel (black lines). Solid and broken lines indicate stable and unstable equilibria, respectively.

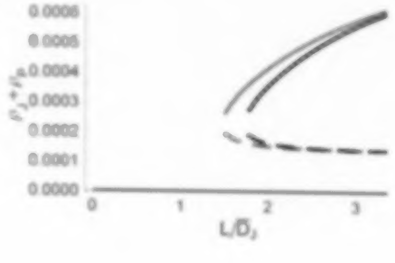

Fig. B5. Equilibria densities (fish·m^{-2}) for larger and smaller species dependent on reserve length scaled to mean juvenile dispersal distance ($L/\bar{D}_J$) for ranges of values for carrying capacity for (*a–b*) juveniles and (*c–d*) competitors. Solid and broken lines indicate stable and unstable equilibria, respectively; shaded and black lines indicate lower and upper bounds for value ranges, respectively.

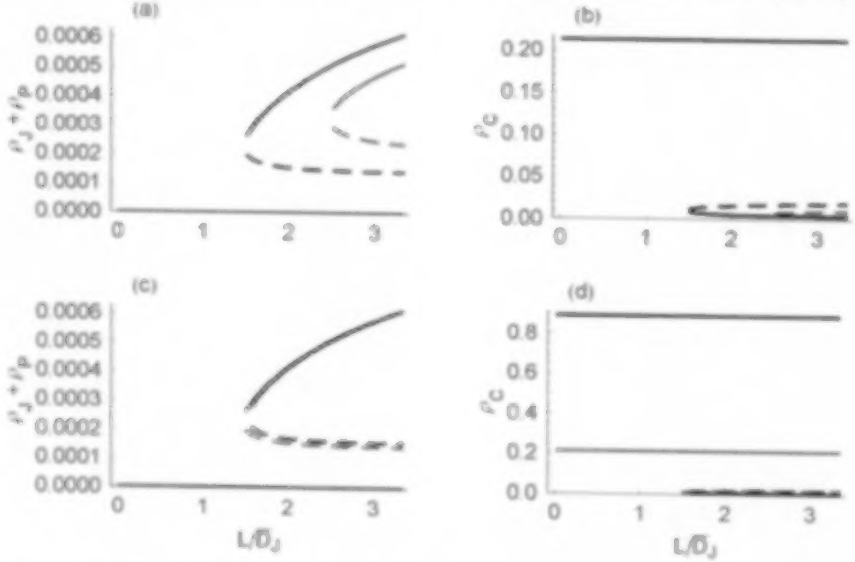

planation for these trends is increased juvenile mortality and decreased predation pressure offsetting competition with increased juvenile predation and decreased competitor predation, respectively. Incorporating handling time and prey saturation in the predation dynamics has little impact on equilibrium predictions (results not shown).

We explore the effect of relaxing the scorched earth assumption and explicitly modeling exchange between protected and fished areas with numerical analysis. With the parameter values tested, the protected-fished exchange model has the same qualitative equilibrium outcome as the scorched earth model: two alternative stable states (smaller species dominated and larger species dominated equilibria) and an unstable threshold in between, both in the reserve and in the fished areas (Fig. 5). However, incorporating exchange between protected and unprotected areas substantially increases the threshold equilibrium density for the larger species inside the reserve and decreases the threshold equilibrium density for the small species inside the reserve (Figs. 5*a*, 5*c*). Increasing the number of reserves in a reserve network primarily decreases the threshold and larger species dominated equilibria densities for the larger species (Fig. B7).

Fig. B6. Equilibria densities (fish·m^{-2}) for larger and smaller species dependent on reserve length scaled to mean juvenile dispersal distance ($L/\bar{D}_J$) for ranges of values for predation rate on (*a*–*b*) juveniles and (*c*–*d*) competitors. Solid and broken lines indicate stable and unstable equilibria, respectively; shaded and black lines indicate lower and upper bounds for value ranges, respectively.

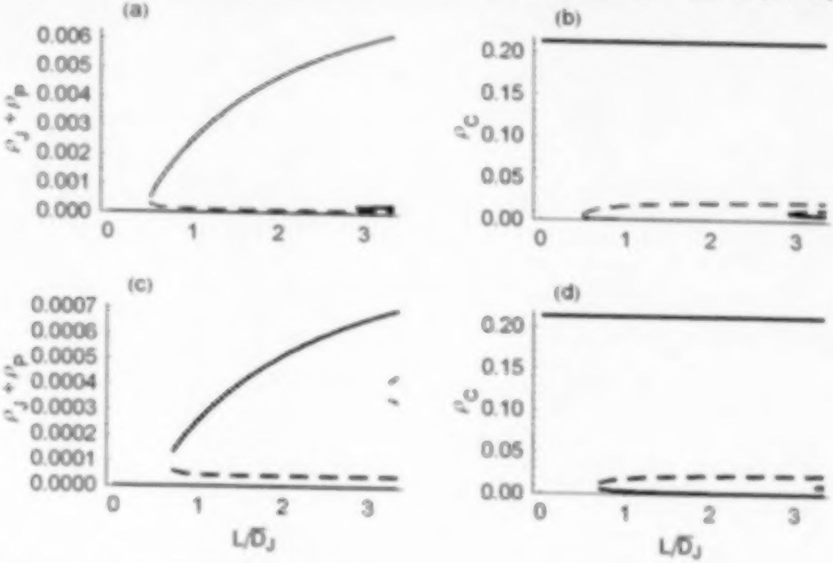

Fig. B7. Equilibria densities (fish·m^{-2}) for larger species in (*a*) reserves and (*b*) fished areas dependent on reserve length scaled to mean juvenile dispersal distance ($L/\bar{D}_J$) for a range of number of reserves in a reserve network. Solid and broken lines indicate stable and unstable equilibria, respectively; shaded and black lines indicate lower and upper bounds for value ranges, respectively.

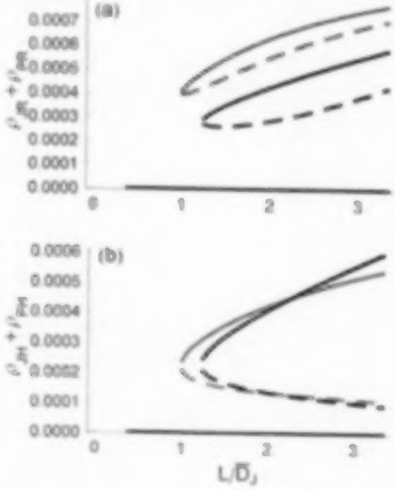

Response of nutrients, biofilm, and benthic insects to salmon carcass addition

Shannon M. Claeson, Judith L. Li, Jana E. Compton, and Peter A. Bisson

Abstract: Salmon carcass addition to streams is expected to increase stream productivity at multiple trophic levels. This study examined stream nutrient (nitrogen, phosphorus, and carbon), epilithic biofilm (ash-free dry mass and chlorophyll *a*), leaf-litter decomposition, and macroinvertebrate (density and biomass) responses to carcass addition in three headwater streams of southwestern Washington State, USA. We used stable isotopes ($\delta^{13}C$ and $\delta^{15}N$) to trace incorporation of salmon-derived (SD) nutrients into stream food webs. SD nutrients were assimilated by biofilm, benthic insects (Perlidae and Limnephilidae spp.), and age-1 steelhead (*Oncorhynchus mykiss gairdneri*). SD nutrients peaked ~2 weeks after carcass addition for insects and fish feeding on carcasses, but indirect uptake of SD nutrients by biofilm and insects was delayed by ~2 months. A strong stable isotope signal did not always correspond with measurable biological change. At reaches 10–50 m downstream from carcasses, ammonium concentration, leaf-litter decomposition, and benthic insect density all increased relative to upstream control sites. The strongest responses and greatest SD-nutrient uptake were observed 10 m from decomposing carcasses, with effects generally decreasing to undetectable levels 250 m downstream. Carcass addition to headwater streams can have a transient effect on primary and secondary trophic levels, but responses may be limited to specific taxa near carcass locations.

Résumé : L'addition de carcasses de saumons dans les cours d'eau doit augmenter, croit-on, la productivité du milieu à plusieurs niveaux trophiques. Notre étude examine les réactions des nutriments du cours d'eau (azote, phosphore et carbone), du biofilm épilithique (masse sèche sans les cendres et chlorophylle *a*), de la décomposition de la litière de feuilles et des macroinvertébrés (densité et biomasse) à l'addition de carcasses dans trois cours d'eau d'amont du sud-ouest de l'état de Washington, É.-U. Nous utilisons les isotopes stables ($\delta^{13}C$ et $\delta^{15}N$) pour suivre l'incorporation des nutriments dérivés des saumons (nutriments SD) dans les réseaux alimentaires des cours d'eau. Les nutriments SD sont assimilés par le biofilm, les insectes benthiques (des espèces de Perlidae et de Limnephilidae) et les truites arc-en-ciel anadromes (*Oncorhynchus mykiss gairdneri*) d'âge 1. Les nutriments SD atteignent un sommet ~2 semaines après l'addition des carcasses chez les insectes et les poissons qui se nourrissent de carcasses, mais l'incorporation indirecte des nutriments SD par le biofilm et les insectes est retardée de ~2 mois. Un fort signal d'isotopes stables ne correspond pas toujours à un changement biologique mesurable. Dans des secteurs 10–50 m en aval des carcasses, les concentrations d'ammonium, la décomposition de la litière de feuilles et la densité des insectes benthiques augmentent toutes par rapport aux sites témoins d'amont. Les réactions les plus fortes et l'incorporation la plus importante de nutriments SD s'observent à 10 m des carcasses en décomposition et les effets décroissent généralement à des niveaux non décelables 250 m en aval. L'addition de carcasses dans les cours d'eau d'amont peut avoir un effet transitoire sur les niveaux trophiques primaire et secondaire, mais les effets peuvent se limiter à des taxons particuliers près de l'emplacement des carcasses.

[Traduit par la Rédaction]

Introduction

Restoration techniques in human-disturbed Pacific streams may include salmon carcass addition to increase nutrient supply and productivity. Pacific salmon (*Oncorhynchus* spp.) migrating from the ocean to freshwater to spawn subsidize streams with salmon-derived (SD) nutrients during gamete release, waste excretion, and carcass decomposition (Cederholm et al. 2001). Spawning salmon can increase dissolved nutrient concentrations in stream water columns (Richey et al. 1975; Mitchell and Lamberti 2005) and can be important sources of nitrogen and carbon for freshwater aquatic organisms (Kline et al. 1990; Johnston et al. 1997). In the Pacific Northwest, where freshwater ecosystems are

Received 19 July 2005. Accepted 22 December 2005. Published on the NRC Research Press Web site at http://cjfas.nrc.ca on 26 April 2006.
J18800

S.M. Claeson[1] and P.A. Bisson. US Department of Agriculture Forest Service, Pacific Northwest Research Station, 3625 93rd Avenue SW, Olympia, WA 98512, USA.
J.L. Li. Department of Fisheries and Wildlife, Oregon State University, Corvallis, OR 97331, USA.
J.E. Compton. US Environmental Protection Agency, Western Ecology Division, Corvallis, OR 97333, USA.

[1]Corresponding author (e-mail: sclaeson@fs.fed.us).

Can. J. Fish. Aquat. Sci. 63: 1230–1241 (2006) doi:10.1139/F06-029

generally oligotrophic (Gregory et al. 1987), SD nutrient enrichment may enhance ecological processes and biota.

The consistency, timing, and magnitude of response to SD nutrients vary considerably among studies. Epilithic biofilm, measured as ash-free dry mass (AFDM) or chlorophyll *a*, can increase in response to salmon presence (Mathisen 1972; Chaloner et al. 2004; Johnston et al. 2004). However, other studies observed no change in chlorophyll *a* (Minshall et al. 1991) or gross primary production (Ambrose et al. 2004). Moreover, variable chlorophyll response can occur among streams and between years (Mitchell and Lamberti 2005). Dissolved nutrients from salmon carcasses may stimulate microbial and invertebrate shredder activity leading to faster leaf decomposition. High nutrient levels can increase microbial biomass and leaf processing by microbes (Meyer and Johnson 1983) and, subsequently, the abundance or size of invertebrate shredders (Robinson and Gessner 2000). Macroinvertebrate abundance can increase in response to salmon presence (Wipfli et al. 1998, 1999), whereas total biomass may show little difference in areas with and without salmon (Chaloner et al. 2004). Positive response by chironomid larvae (Diptera) to carcass addition may reflect their dispersal ability, rapid growth and reproduction, and broad food and habitat preferences (Wipfli et al. 1999; Chaloner et al. 2004). Grazing insects may respond positively to increased biofilm production, although a change in biofilm composition could negatively impact specialized grazers (Wipfli et al. 1999). Increased secondary production should, in turn, provide more food resources to juvenile salmonids, thereby increasing their growth and abundance (Groot and Margolis 1991). Response variability is likely caused by system-specific factors, such as nutrient concentrations, organic matter retention, light levels, water temperature, and flow regimes (Wipfli et al. 1999).

Some macroinvertebrates and juvenile salmonids consume salmon tissue or eggs (Bilby et al. 1998; Chaloner et al. 2002; Minakawa et al. 2002). Salmon carcasses can provide consumers with a high-quality organic food resource (Cederholm et al. 2001). However, colonization of salmon carcasses by invertebrates is not ubiquitous (Minshall et al. 1991; Johnston et al. 2004), suggesting that insect colonization may be influenced by local community composition or by the availability, timing, and quality of other food resources.

Although carcass addition is a current restoration technique in the Pacific Northwest, the effects of this practice are little studied and few in situ studies have been documented. In this study, we experimentally added salmon carcasses to three streams in Washington State, USA, to determine if SD nutrients resulted in increased density and biomass standing stock in the primary and secondary trophic levels. We used stable isotope analysis of nitrogen ($^{15}N:^{14}N$) and carbon ($^{13}C:^{12}C$) to determine which food web components assimilate SD nutrients. Before and after carcasses were added, we measured benthic biofilm and macroinvertebrate density and biomass and monitored dissolved organic and inorganic nutrient concentrations in the water column. Our objectives were (*i*) to quantify changes in nutrient concentrations, epilithic biofilm, leaf-litter decomposition, and benthic macroinvertebrates, (*ii*) to determine the incorporation of SD nutrients by different trophic levels, and (*iii*) to measure spatial and temporal dynamics in measured responses relative to carcass locations. We hypothesized that (*i*) adding salmon carcasses to streams would increase nutrient concentrations in the water column and SD nutrients in the food web and (*ii*) these additional nutrients would stimulate biofilm and macroinvertebrate density and biomass and speed leaf decomposition. Lastly, responses were expected to decrease with distance downstream from carcasses and also decrease in magnitude through time.

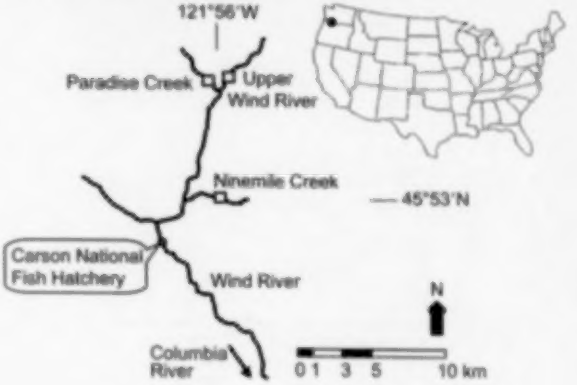

Fig. 1. Location of study reaches (☐) in the Wind River basin of southwest Washington State, USA.

Materials and methods

Study area

The study took place in the Wind River basin (Gifford Pinchot National Forest) in southwestern Washington State, USA (Fig. 1). The maritime climate is characterized by cool, wet winters and warm, dry summers. Currently, steelhead and spring Chinook salmon (*Oncorhynchus tshawytscha*) spawn in the Wind River basin; however, steelhead populations were federally listed as threatened in 1998 and are quite small. The study was replicated in three forested, second-order streams: Upper Wind River (UW), Paradise Creek (PR), and Ninemile Creek (NM) (Fig. 1). Douglas fir (*Pseudotsuga menziesii*) was the dominant overstory vegetation, with some vine maple (*Acer circinatum*) and N_2-fixing red alder (*Alnus rubra*) also present in the riparian. Chinook spawn in the mainstem of the Wind River beginning in mid-July. Our experiment spanned 21 July 2003 through 15 October 2003, ending with the onset of winter rains.

A 300 m reach was chosen within each stream. Stream reaches differed somewhat in size and discharge but were otherwise physically similar and largely undisturbed (Table 1). Drainage area (hectares) for each reach was estimated from 30 m digital elevation maps using ArcInfo® (ESRI, Redlands, California). Instantaneous discharge ($L \cdot s^{-1}$) was calculated bimonthly by multiplying depth- and time-averaged water velocity flow (measured with a Marsh-McBirney® meter, Frederick, Maryland) with stream depths and widths (measured over at least 10 equal increments across stream width). Discharge was high in July from snowmelt and in October from rain and was lowest in early September. Stream gradient (%) was estimated with a cli-

Table 1. Physical characteristics of the three study reaches from July to October 2003.

	Upper Wind	Paradise	Ninemile
Drainage area (ha)	37.4	19.9	10.6
Discharge ($L \cdot s^{-1}$)	119 (83–154)	40 (20–72)	14 (4–33)
Bankfull width (m)	14	12	8
Gradient (%)	4	4	5
Gravel–cobble (%)	79	84	77
Water temperature (°C)	12.8 (8.9–15.4)	11.9 (9.1–14.0)	11.4 (9.3–13.0)
Solar flux ($mJ \cdot m^{-2} \cdot day^{-1}$)	4.6 (2.1–7.8)	2.5 (0.5–3.6)	2.3 (0.2–5.5)
Riparian vegetation[a]	Psme/Thpl	Psme/Thpl	Psme/Alru
Background SRP ($\mu g \cdot L^{-1}$)	17 (15–19)	8 (7–9)	24 (22–30)
Background TDN ($mg \cdot L^{-1}$)	0.07 (0.05–0.08)	0.07 (0.03–0.11)	0.10 (0.06–0.21)
Bedrock	Andesite	Andesite	Lapilli/Breccia
Elevation (m)	457	466	427

Note: Discharge, water temperature, solar flux, soluble reactive phosphorus (SRP), and total dissolved nitrogen (TDN) values are means with their range in parentheses (minimum to maximum).

[a] Dominant overstory vegetation: *Pseudotsuga menziesii* (Psme, Douglas fir), *Thuja plicata* (Thpl, western red cedar), *Alnus rubra* (Alru, red alder).

nometer. To characterize substrates, we used a modified Wolman pebble count consisting of 500 randomly stratified points classified as sand, gravel, cobble, boulder, bedrock, or wood. During the study period, daily mean temperatures were averaged from temperatures recorded each hour by submerged iButtons® (Maxim Integrated Products, Sunnyvale, California). Solar flux ($mJ \cdot m^{-2} \cdot day^{-1}$) at the study areas was estimated with a Solar Pathfinder™ (Linden, Tennessee). Water temperature and solar flux decreased from July through October.

Experimental design

Frozen hatchery Chinook carcasses, adult male and female (some with eggs), were obtained from a local hatchery and tested for diseases (a slit was made in each ripe carcass to remove a small section of skein for disease testing). Carcasses were added to each stream on 30–31 July 2003 and were evenly distributed among streams by sex and presence of eggs. Carcasses were retained within a 5 m long reach, centered at the 0 m site, using chicken wire and rebar to group carcasses and keep them submerged and from floating downstream. Each stream received approximately the same amount of wet carcass tissue per streambed surface area ($1.5\ kg \cdot m^{-2}$ within a 5 m long reach × bankfull width): 104 kg of carcasses in Upper Wind, 88 kg of carcasses in Paradise, and 58 kg of carcasses in Ninemile. Within each stream, four sampling sites were located downstream from the carcasses. Each site was 10 m long and centered at 10, 50, 150, and 250 m from the carcasses, respectively. Effective loading rates at the downstream sites were $0.75\ kg \cdot m^{-2}$ at the 10 m site, $0.15\ kg \cdot m^{-2}$ at the 50 m site, $0.05\ kg \cdot m^{-2}$ at the 150 m site, and $0.03\ kg \cdot m^{-2}$ at the 250 m site. A control site was located 50 m upstream of the carcasses (–50 m site). We assumed that carcasses did not affect trophic processes upstream of the treatments. Responses measured from each downstream site were compared with the corresponding stream's control site.

Water chemistry

Stream water chemistry was sampled on 28 July, 6 August, 2 September, and 15 October 2003. One water sample was collected from each of the five sites per stream, in addition to collecting a sample 1 m downstream from the carcasses. Total dissolved nitrogen (TDN) was determined using persulfate digestion (Cabrera and Beare 1993), followed by measurement of nitrate. Ammonium (NH_4-N), nitrate (NO_3-N), nitrite (NO_2-N), and soluble reactive phosphorus (SRP) levels were determined with an automated colorimetric continuous flow autoanalyzer (Lachat Instruments Flow Injection Autoanalyzer, Hach Instruments, Loveland, Colorado). Dissolved organic nitrogen (DON) was calculated as TDN minus ammonium-N, nitrate-N, and nitrite-N. Dissolved organic carbon (DOC) was determined by automated UV-persulfate oxidation followed by infrared spectrophotometry (Dohrmann TOC analyzer, Teledyne Tekmar, Mason, Ohio). Detection limits for these analyses were determined within the laboratory and are $0.001\ mg\ NO_3\text{-}N \cdot L^{-1}$, $0.002\ mg\ NH_4\text{-}N \cdot L^{-1}$, $1\ \mu g\ PO_4\text{-}P \cdot L^{-1}$, and $0.1\ mg\ DOC \cdot L^{-1}$ (Erway et al. 2001).

Epilithon and leaf decomposition

Epilithic biofilm was collected from streambed rocks at each site for AFDM and chlorophyll *a* measurements. Epilithon appeared to be primarily diatoms with little green algae observed. Each sample was a composite of biofilm scraped, with a metal brush, from three randomly collected, cobble-sized rocks ($20\ cm^2$ area of biofilm per rock). Three composite samples were collected at each site on 21–23 July, 19–21 August, 16–18 September, and 13–15 October 2003. Each composite sample was mixed, split in half, and filtered through glass-fiber filters (Whatman® GF/F, Clifton, New Jersey) for analysis of AFDM ($mg \cdot cm^{-2}$) and chlorophyll *a* ($mg \cdot cm^{-2}$). Prewashed and preweighed filters for AFDM were oven-dried, weighed, ashed at 500 °C, and reweighed (Steinman and Lamberti 1996). The difference in weights was an estimate of AFDM. Chlorophyll *a* was extracted from the filter in 90% buffered acetone for 24 h, measured spectrophotometrically, and corrected for phaeopigments (Steinman and Lamberti 1996).

Leaf decomposition rates were measured by calculating the average dry mass lost per day from preweighed leaf packs (Benfield 1996). Leaf packs were composed of red alder (3.0 ± 0.1 g dry mass) and vine maple (2.0 ± 0.1 g dry mass) leaves that had recently fallen from riparian trees. Oven-dried leaves were weighed and secured together in large-mesh bags (10 mm × 4 mm mesh). In each stream, six leaf packs were randomly spaced within each site, excluding the 250 m site. Leaf packs were accessible to microbes, aquatic macroinvertebrates, and some physical abrasion by flowing water. Leaf packs were removed after 1 month, on 25 September 2003, with a 500 µm net. Leaves and remaining leaf fragments were removed from mesh bags, swirled in water, and visually inspected to remove macroinvertebrates. Oven-dried leaves and fragments were weighed, their weights were subtracted from predecomposed weights, and the difference was divided by the number of days in the stream.

Benthic macroinvertebrates

Six macroinvertebrate samples were randomly collected at each site in each stream on the same dates as biofilm collections. Macroinvertebrates were collected with a Surber sampler (250 µm mesh, 0.09 m^2) and stored in 70% ethyl alcohol. In the laboratory, the six samples per site were pooled together and subsampled with a zooplankton splitter for a minimum of 500 individuals, usually one-eighth of the total sample. Aquatic insects were counted and identified generally to genus, except Chironomidae, which were identified to subfamily or tribe (Merritt and Cummins 1996). Non-insects were identified to order. To estimate insect biomass (mg·m^{-2}), length – dry mass regressions at the family or order level (Smock 1980; Benke et al. 1999) were used after the body length of each insect was measured with a microscope micrometer. Subsample counts and biomass were divided by the fraction subsampled to obtain full-sample estimates.

Stable isotopes

Riparian litterfall, epilithic biofilm, benthic macroinvertebrates, fish, and carcass tissue were sampled for analysis of $\delta^{15}N$ and $\delta^{13}C$. Five riparian litterfall baskets (0.6 m^2) were placed in the riparian along each stream in August and September 2003 to collect material entering the stream (generally red alder leaves, vine maple leaves, cedar twigs, and hemlock or fir needles). Baskets were combined to form one sample per stream per month. We assumed that the added carcasses did not affect riparian vegetation during the short duration of this study. Litterfall was collected to represent the riparian input of $\delta^{15}N$ and $\delta^{13}C$ into each stream.

Epilithic biofilm was scraped from streambed rocks as described above. Three biofilm samples were collected per site and stream, excluding the 250 m site, on 24 July, 12 August, and 21 September 2003. Biofilm samples were freeze-dried and homogenized before analysis. Benthic macroinvertebrates were collected with a 500 µm dip net from the same sites and dates. We targeted common macroinvertebrates representing three functional feeding groups (FFG): scraper–collectors *Ecclisomyia* (Trichoptera: Limnephilidae), shredders *Pteronarcys* (Plecoptera: Pteronarcyidae), and predators Perlidae spp. (Plecoptera) (Merritt and Cummins 1996). Multiple individuals of the same taxa were combined into one sample to provide sufficient mass for isotopic analysis. Macroinvertebrates were oven-dried at 50 °C, were not acid-washed, and were homogenized before analysis.

Juvenile steelhead (age-0 and age-1+) and sculpins were collected from each stream on 12 August and 21 September 2003 via electroshocking. Three fish per taxa and age group were collected at least 150 m upstream from the carcasses (0 m site), above summertime natural fish blockages (i.e., above debris dams or places of intermittent surface flow), and 1–25 m downstream of the carcasses. For analysis, upstream fish were placed in the −50 m sites and downstream fish were grouped in the 10 m sites. All fish were killed by a quick blow to the head and stomach contents were removed. Whole bodies were used for isotopic analysis because their small size (fork length: 36–157 mm) made it difficult to separate muscle from other tissues. One sample of Chinook carcass tissue was collected per stream on 12 August 2003 for isotope analyses. Fish samples were oven-dried at 50 °C and homogenized before analysis.

Samples were analyzed for $\delta^{15}N$ and $\delta^{13}C$ by continuous-flow isotope ratio mass spectrometry (Thermo Finnigan Delta Plus XP mass spectrometer, Waltham, Massachusetts). Separate runs were conducted for $\delta^{15}N$ and $\delta^{13}C$. Isotope enrichment between successive trophic levels occurs as the heavier isotope accumulates in the consumer with each trophic transfer: an average of 2.3‰ for ^{15}N and 0.5‰ for ^{13}C (McCutchan et al. 2003). Higher delta values indicate higher proportions of the heavy isotope (^{15}N vs. ^{14}N, ^{13}C vs. ^{12}C) in a sample. Mass–balance equations were used to provide estimates of the percent SD nutrient assimilated by organisms (Johnston et al. 1997):

$$\text{(1)}\qquad \text{SD-nutrient enrichment (\%)} = (\delta X_{se} - \delta X_c)/((\delta X_s + (\text{TL}\cdot\delta X_e)) - \delta X_c) \times 100$$

where X refers to the element of interest (C or N), δX_{se} is the isotope ratio of the organism in areas enriched with salmon carcasses, δX_c is the isotope ratio of the organism in areas without carcasses, δX_s is the isotopic ratio of salmon tissue, and δX_e is the isotope enrichment factor per trophic level. TL is the trophic level correction factor: 1 for primary consumers (grazing and shredding insects), 2 for secondary consumers (predatory insects), and 3 for fish. These calculations would underestimate an organism's use of SD nutrients if they actually fed at a lower trophic level.

Statistical analyses

We limited statistical analyses of multiple responses measured over time to five response indicators to reduce exaggeration of the type-I error rate from multiple comparisons (Zar 1984). Tested responses were chosen a priori to determine basic trophic level effects: ammonium concentrations, biofilm AFDM, biofilm chlorophyll *a*, total insect density, and total insect biomass. To control for natural changes in response levels over time and meet model assumptions of normality, response values were calculated as the log$_e$ ratio of the response at a downstream site (10, 50, 150, or 250 m) to the upstream site (−50 m):

$$\text{(2)}\qquad Y_{ijk} = \log_e(\text{Downstream}_{ijk}/\text{Upstream}_{ik}) = \log_e(\text{Downstream}_{ijk}) - \log_e(\text{Upstream}_{ik})$$

where i represents stream, j represents distance downstream from the carcasses, and k is month sampled.

We expected responses to change over time naturally and assumed that this seasonal change was the same among the five sites within each stream. We measured responses in July, before carcass placement, and assumed those values to be background, or inherent, differences between upstream and downstream sites (~0). Responses measured after carcass addition were then compared to July's precarcass levels.

Randomized block, repeated measures analysis of variance (ANOVA) (SAS 1999) were used on the $\log_e$ ratio of responses. Because analyses were limited by small sample sizes, we could not model both spatial autocorrelation of sites within a stream and temporal autocorrelation of samples collected over time. Therefore, our model considered the streams as blocks and assumed equal correlation among sites within blocks. Distance from carcasses was modeled as a continuous variable, with response variables at each site repeatedly measured four times (July, August, September, and October 2003). July values were used as the reference level. To determine the covariance structure over time, we ran 10 common covariance models and chose the one with the best fit using Akaike's information criterion corrected for small sample sizes for each response (ammonium and insect density used UN(4) models and AFDM, chlorophyll *a*, and insect biomass used Toep(1) models) (Wolfinger 1993). In effect, we ended up with a comparison of regression line models. We expected that precarcass differences among sites would be spatially constant and approximately zero, i.e., regressions of July's responses would have an intercept and slope equal to zero (H_0: July = 0). After carcass addition, we hypothesized the greatest response to occur at the shortest distance from the carcasses, with the response decreasing downstream, i.e., post-July regressions would have intercepts and slopes differing from July.

Leaf-decomposition response values for each stream were calculated as the $\log_{10}$ ratio of the rates at a downstream site (10, 50, or 150 m) to the upstream site (–50 m). We used a one-tailed *t* test to make statistical comparisons (Zar 1984). No statistical analyses were conducted on $\delta^{15}N$ and $\delta^{13}C$ isotope values because of small sample sizes.

Results

Salmon carcasses

The carcasses, purposely kept under water to restrict birds and mammals from disturbing them, decomposed slowly. Caddisfly larvae, *Ecclisomyia*, were observed on carcasses within each stream, but only during early decomposition stages (2–3 weeks after carcass addition). They were distributed around the body and inside the gill cavities and mouth (~30–60 individuals per carcass). A thick mat of fungus covered most carcasses after 1 month of decomposition. No macroinvertebrates were seen on carcasses once the fungus developed.

After 2 months (late September), inner body tissues had decomposed with some skin and bones still intact. One week after the September sampling period, a black bear removed all the carcasses in Ninemile Creek. However, a large portion of the organic material probably had already leached from the carcasses, as the response pattern from Ninemile Creek in October was similar to those observed at the other study streams in October (see below). Therefore, it appears that early removal of the carcasses did not affect the stable isotope, water chemistry, biofilm, or invertebrate responses measured in October.

Stable isotopes

Before the addition of carcasses in July, mean $\delta^{15}N$ and $\delta^{13}C$ were similar for each taxonomic group among study sites (Table 2). Background $\delta^{15}N$ and $\delta^{13}C$, from sites upstream of carcasses, varied little from July through September 2003 (Table 2).

Carcass tissue was highly enriched in ^{15}N and ^{13}C (15.9‰ and –17.1‰, respectively), whereas leaf litter was relatively depleted (–3.1‰ and –29.2‰, respectively) (Table 2). Because pretreatment data indicated no spatial patterns in isotope ratios among sites within streams, an increase of $\delta^{15}N$ and $\delta^{13}C$ in August or September at the downstream sites compared with the upstream sites was attributed to the carcasses. In August, epilithon $\delta^{15}N$ and $\delta^{13}C$ increased relatively little at downstream sites compared with upstream sites (Fig. 2) (downstream sites were 5%–10% enriched with SD nitrogen (SDN) and 3%–5% enriched with SD carbon (SDC) compared with respective upstream site). In September, epilithon $\delta^{15}N$ showed more substantial ^{15}N enrichment (11%–16% SDN) and ^{13}C was inconsistently enriched or depleted (0%–9% SDC) (Table 2; Fig. 2).

Among insect feeding guilds, omnivorous *Ecclisomyia* caddisflies displayed the temporally most immediate and spatially greatest range in SDN uptake (Table 2; Fig. 2). In August, $\delta^{15}N$ and $\delta^{13}C$ of these limnephilids increased considerably at sites 10 m downstream of carcasses compared with upstream sites (36% SDN and 39% SDC). By September, limnephilid $\delta^{15}N$ increased at all downstream sites (12%–14% SDN), although $\delta^{13}C$ increased only slightly (2%–10% SDC). Neither shredding pteronarcid stoneflies nor predatory perlid stoneflies exhibited changes in $\delta^{15}N$ or $\delta^{13}C$ at downstream sites in August (Fig. 2). Predatory perlid stoneflies exhibited a delayed response of increased $\delta^{15}N$ at downstream sites in September (8%–13% SDN) (Fig. 2).

Only age-1 steelhead assimilated SD nutrients (Table 2; Fig. 2); their $\delta^{15}N$ increased at downstream sites compared with upstream sites in August and September (12% and 14% SDN, respectively), as did $\delta^{13}C$ (15% and 14% SDC, respectively). Neither sculpins nor age-0 steelhead were enriched in August or September.

Water chemistry

Only ammonium concentrations increased in response to carcass addition. Significant concentration changes in ammonium may have been more easily detected than other nitrogen forms because ammonium had the lowest background concentration. Ammonium concentrations were similar between upstream and downstream sites before carcass addition in July (Fig. 3; Table 3). In August and September, ammonium concentrations were significantly higher at downstream sites most near the carcasses compared with upstream sites ($p = 0.002$ and $p < 0.001$, respectively) (Fig. 3; Table 3). Compared with July, ammonium concentrations in September significantly decreased with distance from the carcasses ($p = 0.001$). By October, am-

Table 2. $\delta^{15}N$ and $\delta^{13}C$ (‰) isotope values for taxa collected from upstream (–50 m) and downstream (10, 50, 150 m) sites on 24 July, 12 August, and 21 September 2003.

	$\delta^{15}N$ (‰)				$\delta^{13}C$ (‰)			
	Upstream	Downstream sites			Upstream	Downstream sites		
	–50 m	10 m	50 m	150 m	–50 m	10 m	50 m	150 m
July — 1 week before carcass addition								
Epilithic biofilm	–1.2 (0.3)	–1.3 (0.2)	–1.3 (0.5)	–1.2 (0.3)	–32.5 (2.0)	–33.8 (1.4)	–33.1 (1.1)	–32.1 (2.3)
Limnephilidae	–0.5 (0.3)	0.1 (0.2)	–0.1 (0.3)	–0.1 (0.4)	–27.8 (0.6)	–26.8 (1.0)	–28.8 (1.1)	–28.4 (0.4)
Pteronarcyidae	–0.4 (0.1)	–0.3 (0.1)	–0.2 (0.1)	–0.3 (0.1)	–27.9 (0.2)	–27.9 (0.2)	–28.3 (0.1)	–27.9 (0.3)
Perlidae	1.9 (0.1)	1.8 (0.2)	1.9 (0.3)	2.0 (0.2)	–31.1 (1.4)	–30.9 (1.0)	–31.2 (1.5)	–31.1 (1.1)
August — 2 weeks after carcass addition								
Leaf litterfall[a]	–3.1 (0.4)				–29.2 (0.2)			
Epilithic biofilm	–1.1 (0.3)	**0.6 (0.8)**	–0.2 (0.4)	–0.1 (0.2)	–32.0 (2.9)	–31.6 (3.5)	–31.6 (2.5)	–31.2 (3.8)
Limnephilidae	0.0 (0.4)	**6.7 (1.4)**	0.5 (0.2)	0.5 (0.3)	–27.7 (1.3)	**–23.4 (0.6)**	–28.2 (1.7)	–25.8 (3.1)
Pteronarcyidae	–0.3 (0.1)	0.2 (0.3)	0.0 (0.2)	–0.2 (0.1)	–27.9 (0.2)	–27.8 (0.5)	–28.0 (0.4)	–28.2 (0.3)
Perlidae	2.1 (0.1)	2.2 (0.2)	2.2 (0.3)	2.1 (0.2)	–30.9 (1.5)	–31.1 (1.6)	–30.5 (1.3)	–30.8 (1.2)
Sculpin	4.1 (0.4)	3.5 (0.2)		–29.0 (1.4)	–27.9 (1.2)			
Steelhead age-0	5.0 (0.4)	5.7 (0.5)		–26.7 (1.0)	–26.2 (0.9)			
Steelhead age-1	5.5 (0.3)	**7.6 (2.0)**		–27.1 (0.2)	**–25.4 (2.1)**			
Carcass tissue		15.9 (0.1)				–17.1 (0.3)		
September — 8 weeks after carcass addition								
Leaf litterfall[a]	–3.1 (0.6)				–29.0 (0.3)			
Epilithic biofilm	–1.1 (0.3)	**1.5 (0.5)**	**1.1 (0.7)**	**0.7 (0.3)**	–30.0 (2.4)	–31.1 (2.5)	–28.9 (3.9)	–32.2 (3.2)
Limnephilidae	–0.4 (0.3)	**2.2 (1.4)**	**1.9 (0.8)**	**2.2 (1.3)**	–26.9 (3.0)	–26.6 (2.6)	**–25.8 (2.5)**	–26.1 (2.1)
Pteronarcyidae	–0.2 (0.2)	0.8 (0.1)	0.7 (0.1)	0.2 (0.1)	–27.4 (0.6)	–27.4 (0.4)	–27.9 (0.2)	–27.9 (0.1)
Perlidae	2.0 (0.3)	**4.3 (0.8)**	3.4 (0.3)	3.4 (0.2)	–29.1 (2.0)	–28.9 (0.9)	–30.2 (2.0)	–28.8 (1.3)
Sculpin	4.3 (0.5)	4.5 (0.5)		–27.9 (1.4)	–28.1 (1.6)			
Steelhead age-0	5.2 (0.3)	6.3 (0.6)		–26.2 (1.5)	–26.2 (1.0)			
Steelhead age-1	5.6 (0.4)	**8.0 (1.4)**		–27.0 (0.7)	**–25.3 (1.3)**			

Note: Values are the mean (±1 standard error in parentheses) of three streams. Isotope values in bold demonstrate taxa that assimilated at least 10% SD nutrients.

[a] Leaf litterfall samples represent an entire stream, formed from a composite of five samples per stream.

Fig. 2. Isotope signatures of representative trophic level taxa (mean $\delta^{15}N$ and $\delta^{13}C$) collected from upstream (–50 m) and downstream (10, 50, 150 m) sites among the three study streams: (*a*) 12 August and (*b*) 21 September 2003. Taxa collected: upstream sites, open symbols; 10 m sites, solid symbols; 50 m sites, lightly shaded symbols; and 150 m sites, medium shaded symbols. Symbols: leaf litter and biofilm, squares; insects, circles, fish and carcass tissues, diamonds.

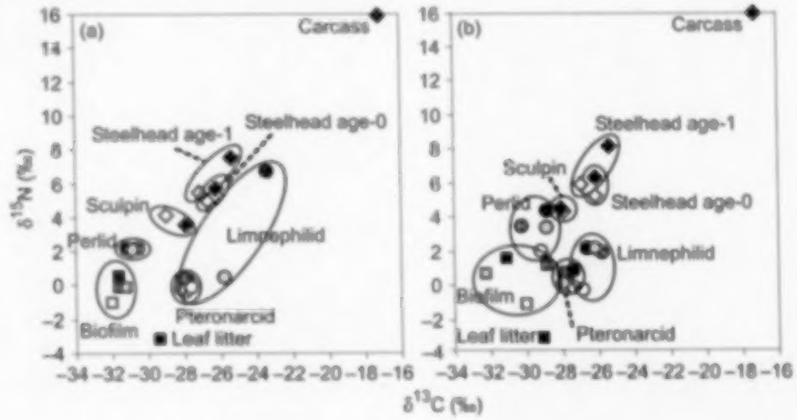

Fig. 3. Ammonium (NH_4-N) concentrations (μg·L^{-1}) from upstream (–50 m) and downstream (1, 10, 50, 150, 250 m) sites: (*a*) 28 July, (*b*) 6 August, (*c*) 2 September, and (*d*) 15 October 2003. Bars show the mean + 1 standard error of three streams. Open bars represent concentrations before or upstream of carcass addition; solid bars represent concentrations after or downstream of carcass addition.

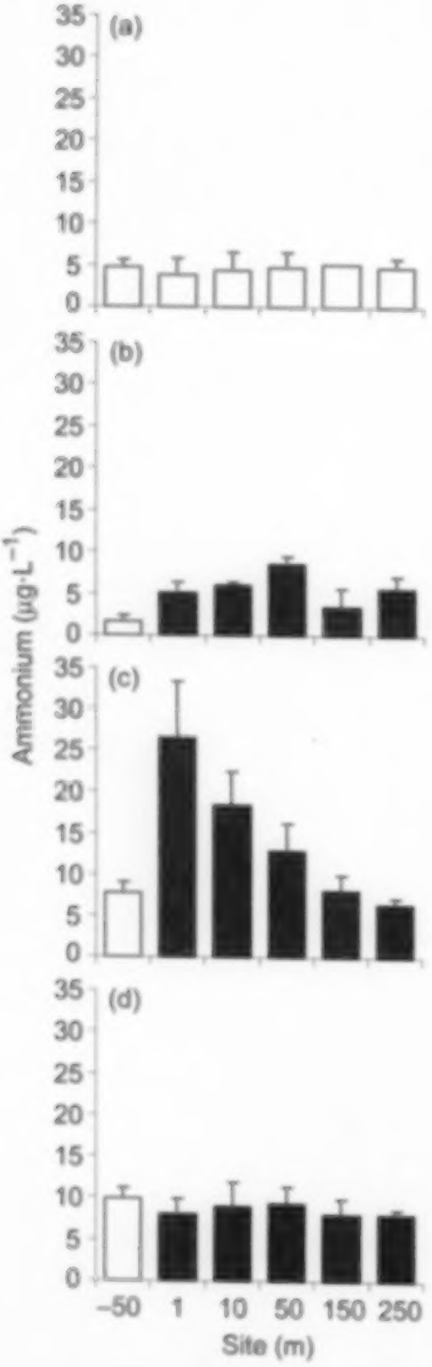

Fig. 4. Chlorophyll *a* levels (μg·cm^{-2}) from upstream (–50 m) and downstream (10, 50, 150, 250 m) sites: (*a*) 22 July, (*b*) 20 August, (*c*) 17 September, and (*d*) 14 October 2003. Bars show the mean + 1 standard error of three streams. Open bars represent levels before or upstream of carcass addition; solid bars represent levels after or downstream of carcass addition.

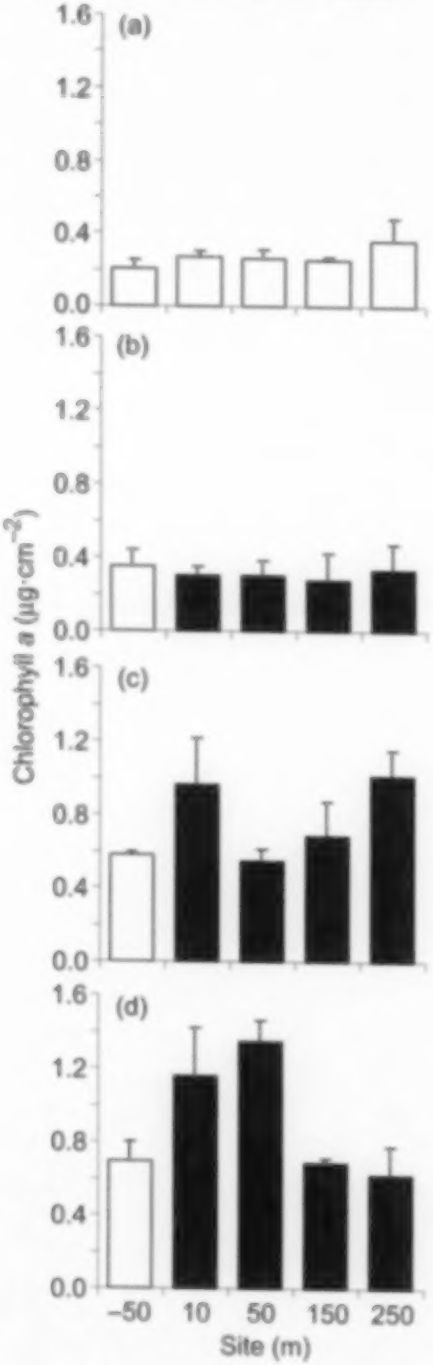

Table 3. Linear-fit regressions from repeated measures analysis of variance of response change as functions of distance downstream from carcasses for each month.

Month	Ammonium intercept, slope	AFDM intercept, slope	Chlorophyll *a* intercept, slope	Insect density intercept, slope	Insect biomass intercept, slope
July	–0.318, 0.002	–0.017, <0.001	–0.170, <0.001	–0.336, 0.001	–0.578, <0.001
p value	NS, NS	NS, NS	NS, NS	NS, NS	NS, NS
August	**1.062**, –0.001	0.110, <–0.001	–0.137, <–0.001	–0.052, <–0.001	0.396, <–0.001
p value	**0.002**, NS	NS, NS	NS, NS	NS, NS	NS, NS
September	**0.824, –0.004**	0.167, <0.001	0.131, 0.001	**0.693**, –0.002	0.131, –0.003
p value	**<0.001, 0.001**	NS, NS	NS, NS	**0.002**, NS	NS, NS
October	–0.144, <–0.001	–0.091, <0.001	0.570, **–0.003**	0.319, –0.002	–0.644, –0.002
p value	NS, NS	NS, NS	0.076, **0.022**	NS, NS	NS, NS

Note: Intercept and slope estimates are $\log_e$(downstream/upstream) ratios. Responses measured in July (before carcass addition) show background differences between upstream and downstream sites. Responses measures in August, September, and October show differences attributed to the carcass addition. Intercept or slope estimates in bold are significantly different from the null hypothesis ($p < 0.05$). NS indicates nonsignificant, $p > 0.10$. AFDM, ash-free dry mass.

monium concentrations returned to before carcass addition and upstream levels. Our data suggest that the peak ammonium release occurred in September, approximately 8 weeks after carcass addition.

Epilithon and leaf decomposition

In July, before carcasses were added to the study streams, epilithon AFDM and chlorophyll *a* levels were similar between sampling locations. After carcass addition, chlorophyll responses were highly variable and not significantly different between sites, yet there was a potentially biologically meaningful increase at sites downstream of carcasses compared with upstream in October, particularly at Ninemile and Paradise creeks ($p = 0.076$) (Fig. 4; Table 3). Chlorophyll responses significantly decreased with distance from carcasses ($p = 0.022$). AFDM did not respond to carcass addition. Given the large AFDM and chlorophyll standard errors and a significance level of <0.05, mean levels at downstream sites had to be 2 times and 1.4 times greater than upstream sites, respectively, to be significantly different from levels before carcass addition. Mean leaf-pack decomposition was faster at sites downstream than upstream of carcasses (Fig. 5), but responses were significant only at the 50 m site ($p = 0.010$).

Fig. 5. Leaf decomposition response: difference in $\log_{10}$-transformed decomposition rates (mg·day^{-1}) between respective downstream (10, 50, 150 m) and upstream (–50 m) sites. The decomposition study ran between 28 August and 25 September 2003. The star indicates a significant difference from zero. Bars show the mean + 1 standard error of three streams.

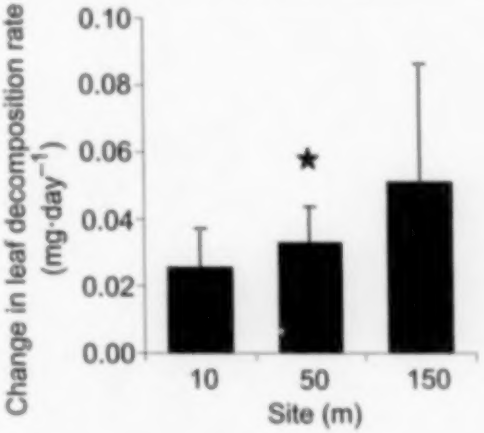

Benthic macroinvertebrates

Insect densities were similar between upstream and downstream sites in July, before carcass additions. Throughout the study, Diptera (primarily Chironomidae) and Ephemeroptera (primarily Baetidae and Heptageniidae) were the most abundant orders. Insect biomass was greater at sites upstream than downstream of carcasses in July. Plecoptera (primarily large-bodied Pteronarcyidae and Perlidae species) and several genera of Trichoptera constituted the greatest insect biomass. Non-insects (primarily water mites, worms, and snails) represented a small portion of the benthic macroinvertebrates collected per stream (9%–13%).

Macroinvertebrate responses to carcass addition were mixed, but certain taxa were more abundant near carcasses. In September, total insect abundance was significantly greater at sites downstream than upstream of carcasses ($p = 0.002$) (Fig. 6; Table 3). Heptageniidae (*Cinygmula*, *Rhithrogena*, *Epeorus*, and *Ironodes*) and Chironomidae (*Tanytarsini* and Orthocladiinae) larvae contributed most to increased densities in September; heptageniid density increased by an average of 298% (mean of 4693 individuals·m^{-2} at the 10 m sites compared with 1574 individuals·m^{-2} at the upstream sites), and chironomid density increased by an average of 249% (mean of 7769 individuals·m^{-2} at the 10 m sites compared with 3124 individuals·m^{-2} at the upstream sites). The density of elmid beetles (*Heterlimnius*), ubiquitous but less numerous at each site, increased by an average of 186% (mean of 321 individuals·m^{-2} at the 10 m sites compared with 172 individuals·m^{-2} at the upstream sites) in September. Unlike other insect groups, chironomid density continued to increase at sites downstream of carcasses in October, compared with sites upstream, with an average increase of 268% (mean of 8985 individuals·m^{-2} at the 10 m sites compared with 3358 individuals·m^{-2} at the upstream sites). Heptageniidae, Elmidae, and Chironomidae larval densities declined with distance downstream, and their densities 250 m downstream from carcasses were not different from upstream sites. Densities of other common insect taxa, in-

Fig. 6. Benthic insect density (insects·m^{-2}) from upstream (–50 m) and downstream (10, 50, 150, 250 m) sites: (*a*) 22 July, (*b*) 20 August, (*c*) 17 September, and (*d*) 14 October 2003. Bars show the mean + 1 standard error of three streams. Open bars represent insects collected before or upstream of carcass addition; solid bars represent insects collected after or downstream of carcass addition.

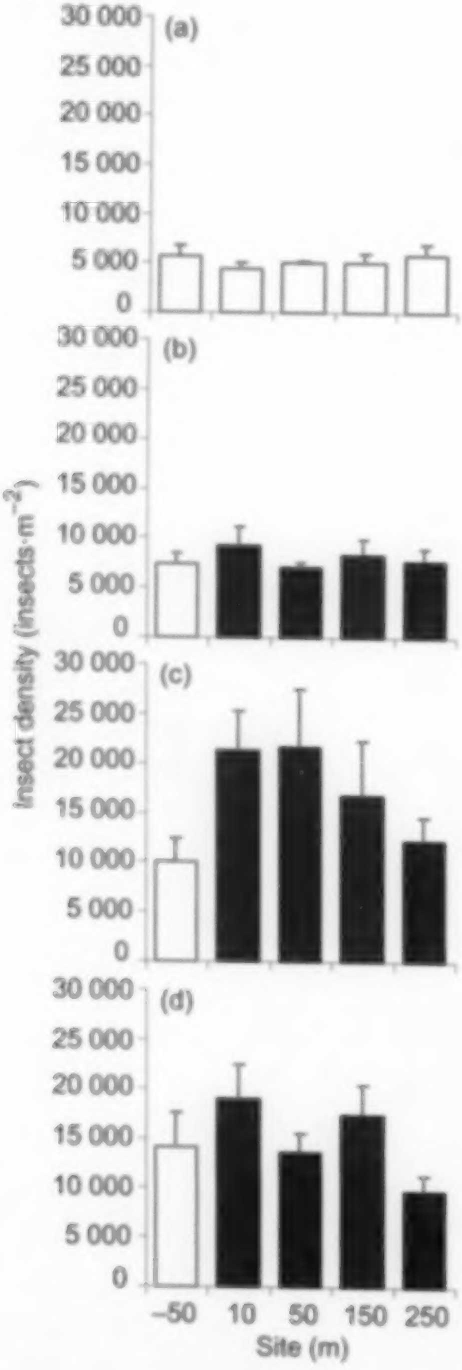

cluding the mayflies Baetidae, stoneflies Pteronarcyidae, Perlidae, Perlodidae, and Nemouridae, and caddisflies Limnephilidae, Lepidostomatidae and Hydropsychidae, did not display different abundance patterns along spatial or temporal distributions.

Insect biomass was highly variable among sampling locations and over time. No significant changes in total biomass, biomass of insect groups (order, family, or genera level), or abundance of different size classes were detected from carcass addition. Downstream total biomass needed to be five times greater than upstream biomass to be significantly different from levels before carcass addition, based on observed standard errors and a significance level of <0.05. In contrast to responses in insect abundance, carcass addition did not significantly affect insect biomass.

Discussion

This study tested the direct and indirect effects of decomposing salmon carcasses on primary producers and secondary consumers longitudinally downstream of introduced carcasses. SD nutrients were incorporated into the stream food web at all trophic levels. As in other studies, we observed higher ammonium and variable chlorophyll *a* levels in response to carcass addition (Chaloner et al. 2004; Mitchell and Lamberti 2005). Greater macroinvertebrate abundance, a response also reported in southeastern Alaska (Wipfli et al. 1998, 1999), was driven primarily by Chironomidae and Heptageniidae in these western Washington streams. Our examination of longitudinal effects downstream of carcass introductions suggested that changes to stream chemistry and biota tended to be transient and most apparent within 50 m of carcasses.

The addition of carcasses to increase nutrients has the potential to conflict between water quality and salmon restoration objectives. However, if carcass addition does not overstimulate algal growth, but increases stream secondary production, then salmon restoration objectives would be satisfied without compromising the intent of water quality goals. Carcass addition in Wind River streams did not strongly alter water chemistry or cause substantial algal blooms. We conducted this study during summer low-streamflow conditions, which should maximize any affects on water chemistry. Only ammonium levels responded to carcass addition. Following elevated levels in August, peak ammonium release occurred in September. In these montane, low-order streams, effects from carcass addition on stream chemistry appear minimal. Although highly variable, algal biomass, measured as chlorophyll *a*, tended to increase downstream of carcasses in October. This temporal lag in nutrient release and uptake was detected particularly in herbivores. Biofilm volumes were not apparently influenced by carcass addition, but biofilm production may have been masked by increased grazing. Measures of AFDM and chlorophyll *a* estimate standing stock and do not account for grazing by macroinvertebrates.

As chlorophyll *a* levels increased at some sites, densities of scraping (Heptageniidae) and collecting (Chironomidae and Elmidae) insects increased 2 months after carcass addition. Scrapers may have benefited from an increase in the quality or quantity of biofilms. Collectors may have benefited from increased organic particles from the breakdown of carcass tissues or from carcass fragments dislodged by foraging insects and water current. Predatory insects did not increase in density or biomass as expected, although perlid stoneflies had enhanced levels of $\delta^{15}N$, suggesting potential indirect effects in higher trophic levels. Increased macroinvertebrate densities within the treatment reaches may have resulted from a net increase per stream or, more likely, from invertebrates drifting into the carcass-treated reaches.

We hypothesized that decomposing salmon carcasses would stimulate microbial and invertebrate activity on leaf litter, leading to faster leaf decomposition. Leaf packs composed of alder and vine maple leaves decomposed significantly faster at the site 50 m downstream from carcasses compared with upstream sites. Average decomposition rates were also faster at 10 and 150 m sites, but these were more variable and not significantly different from the control site. Shredding insects did not increase in density or biomass in response to carcass addition. The shredder *Pteronarcys* did not assimilate SD nutrients, suggesting that the increase in decomposition rates resulted from an increase in microbial activity rather than by macroinvertebrates. In an artificial pond study, the addition of alewife carcasses caused microbial production and respiration on leaf litter to increase, indicating faster leaf processing by microbes (Durbin et al. 1979). Contrary results were observed when SD nutrients enhanced biofilm on wood debris but did not influence wood decomposition (Fisher-Wold and Hershey 1999). In our study, the addition of carcasses enhanced leaf litter breakdown, but we were not able to verify the biological agent causing the increase.

SD nutrients were incorporated into the stream food web through both direct (i.e., consumption of carcass tissues or eggs) and indirect (i.e., nutrients leached from the carcasses) pathways. The timing of changes in isotope ratios reflected the mechanistic differences between these pathways. Limnephilidae caddis larvae were observed feeding directly on salmon carcasses in early August, likely explaining their high $\delta^{15}N$ and $\delta^{13}C$. Age-1 steelhead were also observed to feed directly on carcasses, and salmon eggs were found in their stomachs during collection for isotope samples in August and September. Both organisms showed large increases in $\delta^{13}C$, indicating direct consumption of an enriched food source. Age-0 steelhead had no increased isotope activity and appeared to consume unenriched food resources. Sculpin also may have consumed unenriched prey. Unlike juvenile steelhead, the slow growth of sculpins may cause slow tissue turnover rates, resulting in a longer interval for tissues to change isotopic composition in response to changes in food (Hesslein et al. 1993).

As carcasses decomposed, observable direct consumption diminished and indirect nutrient pathways developed. SD nutrients were detected in September, 2 months after carcass addition, in epilithic biofilm, Perlidae stoneflies, and Limnephilidae caddisflies. Caddis larvae may have been exploiting ^{15}N derived from epilithon, as no insects were seen on carcasses in September, or possibly consuming dislodged carcass fragments within the stream substrate. Carcass biofilm may inhibit invertebrates from colonizing salmon carcasses and is not unique to the Wind River basin (Minshall et al. 1991; Johnston et al. 2004). Predatory stoneflies probably consumed enriched prey. SD-nutrient transfer via direct carcass consumption began quickly, whereas evidence of SD nutrients transferred indirectly required at least 2 months.

Measurable responses of secondary consumers, and to some extent primary producers, were seen at sites close to carcasses (1–50 m) and declined with increasing distance from the carcasses. Most effects were undetectable 250 m downstream of carcasses. However, SD nutrients were incorporated by some organisms (biofilm, Limnephilidae, and Perlidae) collected 150 m downstream from carcasses. SD nutrients may spiral downstream at levels detectable by isotope analysis, but measurable changes in the benthic community, which are more difficult to detect, may only occur in carcass-rich areas.

Adding frozen carcasses to streams and caging carcasses in wire mesh may have slowed fish decomposition by preventing some movement, resulting in fragmentation and possibly increasing the lag time observed in some responses. Nevertheless, dissolved ammonium concentrations increased significantly just 1 week after carcass addition, indicating that decomposition was well underway. Confining carcasses to one place and adding them at one time is somewhat different from the typically haphazard method of adding carcass to streams. It should be noted that streams receiving a single influx of salmon carcasses from manual addition may exhibit different responses than a stream that receives spawners annually and repeatedly over a spawning cycle. Local populations not adapted to or not present when carcasses are added may be limited by life history or morphology to take advantage of the new food source. Unlike natural spawning, supplementing carcasses omits substrate disturbance caused by redd excavation (Peterson and Foote 2000) and the slow release of nutrients through waste excretion (Braband et al. 1990).

Stream communities studied in the Wind River basin, although upstream of salmon spawning areas, exhibited many of the same biological responses observed from carcass addition elsewhere (Wipfli et al. 1999; Mitchell and Lamberti 2005). Our results differed in that we detected increased scraping mayflies (unlike Wipfli et al. 1998) but not significant increases in epilithic biofilm. Likewise, primary production was not measurably enhanced by rainbow trout addition in an Idaho stream (Minshall et al. 1991) or by salmon carcass addition in northern California streams (Ambrose et al. 2004). Thus, carcass supplementation in headwater streams may have a transient effect on lower trophic levels that could be readily consumed by secondary consumers. Detectable responses may be limited to select taxa or be limited by physical controls (e.g., sunlight, high gradient).

Carcass supplementation has become a popular, although unproven, method of adding marine-derived nutrients to headwater streams (Cederholm et al. 2001). Our study emphasizes the need for more research in natural streams. We found that relatively few significant changes in selected response variables could be differentiated from background variation and that these changes were observed only in close proximity to the carcasses. Although we were able to detect significant differences in ammonium concentrations and total insect densities, smaller and undetected effects may have had biologically meaningful consequences. Stable isotope analyses are useful for detecting more subtle responses in the food web, but as shown here, a strong stable isotope signal may not correspond with biological change. A variety of stream settings should be studied to understand the potential range of trophic responses to salmon carcasses at different densities so that scientists and managers can anticipate with greater certainty where carcass supplementation will have a demonstrated beneficial effect.

Acknowledgements

This study was supported by the Pacific Northwest Research Station, US Department of Agriculture Forest Service. The authors thank the Wind River Ranger Station and Gifford Pinchot National Forest for site access and logistical support, Spring Creek and Carson National Fish Hatcheries for providing salmon carcasses, and Susan Gutenberger for carcass disease testing. The authors greatly appreciate the efforts of Greg Stewart, Elizabeth Jones, Randall Colvin, Bill Gerth, Lance Wyss, and Justin Miles for their help in the field and lab. They also thank Patrick Connolly and Ian Jezorek at the US Geological Survey Columbia River Research Laboratory for fish collection, Bill Griffis at the US Environmental Protection Agency Integrated Stable Isotope Research Facility for isotope analysis, and the Willamette Research Station for water chemistry analysis. The authors are indebted to Manuela Huso for statistical advice. The authors thank Rick Edwards, Jon Honea, Hal Michael, and two anonymous reviewers for their insightful comments on this manuscript. The use of trade or firm names in this publication is for reader information and does not imply endorsement by the US Department of Agriculture of any product or service.

References

Ambrose, H.E., Wilzbach, M.A., and Cummins, K.W. 2004. Periphyton response to increased light and salmon carcass introduction in northern California streams. J. North Am. Benthol. Soc. **23**(4): 701–712.

Benfield, E.F. 1996. Leaf breakdown in stream ecosystems. *In* Methods in stream ecology. *Edited by* F.R. Hauer and G.A. Lamberti. Academic Press, New York. pp. 579–589.

Benke, A.C., Huryn, A.D., Smock, L.A., and Wallace, J.B. 1999. Length–mass relationships for freshwater macroinvertebrates in North America with particular reference to the southeastern United States. J. North Am. Benthol. Soc. **18**(3): 308–343.

Bilby, R.E., Fransen, B.R., Bisson, P.A., and Walter, J.K. 1998. Response of juvenile coho salmon (*Oncorhynchus kisutch*) and steelhead (*Oncorhynchus mykiss*) to the addition of salmon carcasses to two streams in southwestern Washington, U.S.A. Can. J. Fish. Aquat. Sci. **55**: 1909–1918.

Brabrand, A., Faafeng, B.A., and Nilssen, J.P.M. 1990. Relative importance of phosphorus supply to phytoplankton production: fish excretion versus internal loading. Can. J. Fish. Aquat. Sci. **47**: 364–372.

Cabrera, M.L., and Beare, M.H. 1993. Alkaline persulfate oxidation for determining total nitrogen in microbial biomass extracts. Soil Sci. Soc. Am. J. **57**: 1007–1012.

Cederholm, C.J., Johnson, D.H., Bilby, R.E., Dominguez, L.G., Garrett, A.M., Graeber, W.H., Greda, E.L., Kunze, M.D., Marcot, B.G., Palmisano, J.F., Plotnikoff, R.W., Pearcy, W.G., Simenstad, C.A., and Trotter, P.C. 2001. Pacific salmon and wildlife — ecological contexts, relationships, and implications for management. *In* Wildlife–habitat relationships in Oregon and Washington. *Edited by* D.H. Johnson and T.A. O'Neil. Oregon State University Press, Corvallis, Oregon. pp. 628–684.

Chaloner, D.T., Wipfli, M.S., and Caouette, J.P. 2002. Mass loss and macroinvertebrate colonization of Pacific salmon carcasses in south-eastern Alaska streams. Freshw. Biol. **47**: 263–273.

Chaloner, D.T., Lamberti, G.A., Merritt, R.W., Mitchell, N.L., Ostrom, P.H., and Wipfli, M.S. 2004. Variation in responses to spawning Pacific salmon among three south-eastern Alaska streams. Freshw. Biol. **49**: 587–599.

Durbin, A.G., Nixon, S.W., and Oviatt, C.A. 1979. Effects of the spawning migration of the alewife (*Alosa pseudoharengus*) on freshwater ecosystems. Ecology, **60**(1): 8–17.

Erway, M.M., Motter, K., and Baxter, K. 2001. Quality assurance plan. Willamette Research Station Analytical Laboratory, Corvallis, Oregon.

Fisher-Wold, A.K., and Hershey, A.E. 1999. Effects of salmon carcass decomposition on biofilm growth and wood decomposition. Can. J. Fish. Aquat. Sci. **56**: 767–773.

Gregory, S.C., Lamberti, G., Erman, D., Koski, K., Murphy, M., and Sedell, J.R. 1987. Influence of forest practices on aquatic production. *In* Streamside management: forestry and fishery interactions. *Edited by* E. Salo and T. Cundy. University of Washington Institute of Forest Resources, Seattle, Washington. No. 57. pp. 233–256.

Groot, C., and Margolis, L. 1991. Pacific salmon life histories. University of British Columbia Press, Vancouver, British Columbia.

Hesslein, R.H., Hallard, K.A., and Ramlal, P. 1993. Replacement of sulfur, carbon, and nitrogen in tissue of growing broad whitefish (*Coregonus nasus*) in response to a change in diet traced by δ^{34}S, δ^{13}C, and δ^{15}N. Can. J. Fish. Aquat. Sci. **50**: 2071–2076.

Johnston, N., Macdonald, J., Hall, K., and Tschaplinski, P. 1997. A preliminary study of the role of sockeye salmon (*Oncorhynchus nerka*) carcasses as carbon and nitrogen sources for benthic insects and fishes in the "Early Stuart" stock spawning streams, 1050 km from the ocean. Fisheries Project Report No. RD55, British Columbia Ministry of Environment, Lands and Parks, Victoria, British Columbia.

Johnston, N., MacIsaac, E., Tschaplinski, P., and Hall, K. 2004. Effects of the abundance of spawning sockeye salmon (*Oncorhynchus nerka*) on nutrients and algal biomass in forested streams. Can. J. Fish. Aquat. Sci. **61**: 384–403.

Kline, T.C., Goering, J.J., Mathisen, O.A., Poe, P.H., and Parker, P.L. 1990. Recycling of elements transported by runs of Pacific salmon: I. ^{15}N and ^{13}C evidence in Sashin Creek, southeastern Alaska. Can. J. Fish. Aquat. Sci. **47**: 136–144.

Mathisen, O.A. 1972. Biogenic enrichment of sockeye salmon lakes and stock productivity. Verh. Int. Ver. Limnol. **18**:1089–1095.

McCutchan, J.H.J., Lewis, W.M.J., Kendall, C., and McGrath, C.C. 2003. Variation in trophic shift for stable isotope ratios of carbon, nitrogen, and sulfur. Oikos, **102**(2): 378–390.

Merritt, R.W., and Cummins, K.W. 1996. An introduction to the aquatic insects of North America. 3rd ed. Kendall/Hunt Publishing Company, Dubuque, Iowa.

Meyer, J.L., and Johnson, C. 1983. The influence of elevated nitrate concentration on rate of leaf decomposition in a stream. Freshw. Biol. **13**: 177–183.

Minakawa, N., Gara, R.I., and Honea, J.M. 2002. Increased individual growth rate and community biomass of stream insects associated with salmon carcasses. J. North Am. Benthol. Soc. **21**(4): 651–659.

Minshall, G.W., Hitchcock, E., and Barnes, J.R. 1991. Decomposition of rainbow trout (*Oncorhynchus mykiss*) carcasses in a forest stream ecosystem inhabited only by nonanadromous fish populations. Can. J. Fish. Aquat. Sci. **48**: 191–195.

Mitchell, N.L., and Lamberti, G.A. 2005. Responses in dissolved nutrients and epilithon abundance to spawning salmon in Southeast Alaska streams. Limnol. Oceanogr. **50**(1): 217–227.

Peterson, D.P., and Foote, C.J. 2000. Disturbance of small-stream habitat by spawning sockeye salmon in Alaska. Trans. Am. Fish. Soc. **129**: 924–934.

Richey, J.E., Perkins, M.A., and Goldman, C.R. 1975. Effects of kokanee salmon (*Oncorhynchus nerka*) decompostion on the ecology of a subalpine stream. J. Fish. Res. Board Can. **32**: 817–820.

Robinson, C.T., and Gessner, M.O. 2000. Nutrient addition accelerates leaf breakdown in an alpine springbrook. Oecologia, **122**: 258–263.

SAS Institute Inc. 1999. SAS OnlineDoc®. Version 8. SAS Institute Inc., Cary, North Carolina.

Smock, L.A. 1980. Relationships between body size and biomass of aquatic insects. Freshw. Biol. **10**: 375–383.

Steinman, A.D., and Lamberti, G.A. 1996. Biomass and pigments of benthic algae. *In* Methods in stream ecology. *Edited by* F.R. Hauer and G.A. Lamberti. Academic Press, New York. pp. 295–313.

Wipfli, M.S., Hudson, J., and Caouette, J. 1998. Influence of salmon carcasses on stream productivity: response of biofilm and benthic macroinvertebrates in southeastern Alaska, U.S.A. Can. J. Fish. Aquat. Sci. **55**: 1053–1511.

Wipfli, M.S., Hudson, J.P., Chaloner, D.T., and Caouette, J.P. 1999. Influence of salmon spawner densities on stream productivity in southeast Alaska. Can. J. Fish. Aquat. Sci. **56**: 1600–1611.

Wolfinger, R. 1993. Covariance structure selection in general mixed models. Commun. Statist. Simulation Computation, **22**(4): 1079–1106.

Zar, J.H. 1984. Biostatistical analysis. 2nd ed. Prentice Hall, Englewood Cliffs, New Jersey.

Incorporating parameter uncertainty into evaluation of spawning habitat limitations on Chinook salmon (*Oncorhynchus tshawytscha*) populations

Timothy J. Beechie, Correigh M. Greene, Lisa Holsinger, and Eric M. Beamer

Abstract: Incorporating parameter uncertainty into a Monte Carlo procedure for estimating spawning habitat capacity helped determine that spawning habitat availability is unlikely to limit recovery of six populations of Chinook salmon (*Oncorhynchus tshawytscha*) in Puget Sound. Spawner capacity estimates spanned up to four orders of magnitude, yet there was virtually no overlap of distributions of capacity estimates with distributions of current spawner abundance (<0.2% overlap), except for the Suiattle River population (51% overlap). Empirical distributions of input parameters contained several important sources of uncertainty, insuring reasonably wide distributions of capacity estimates. The most defensible ranges of input parameters tended to produce conservative capacity estimates, indicating that increased model accuracy would only strengthen our conclusion that spawning habitat is not a constraint on these populations. There are insufficient data with which to develop parameter distributions that better represent historical capacity, which would certainly be higher than our estimates. Our results suggest that factors other than spawning capacity limit population size and that recovery efforts for Skagit River Chinook salmon need not focus on spawning habitat restoration.

Résumé : L'incorporation de l'incertitude des paramètres dans une procédure de Monte Carlo pour estimer la capacité de l'habitat de fraye a contribué à déterminer que la disponibilité de l'habitat ne limite vraisemblablement pas le rétablissement de six populations de saumons quinnat (*Oncorhynchus tshawytscha*) dans le détroit de Puget. Les estimations de capacité des reproducteurs s'étendent sur jusqu'à quatre ordres de grandeur, sans qu'il y ait virtuellement de chevauchement entre les estimations de capacité et les répartitions des abondances actuelles de reproducteurs (<0,2 % de chevauchement), sauf dans la population de la Suiattle (51 % de chevauchement). Les distributions empiriques des variables d'entrée contiennent plusieurs sources importantes d'incertitude, ce qui produit des distributions raisonnablement étendues des estimations de capacité. Les étendues les plus défendables des variables d'entrée ont tendance à générer des estimations de capacité conservatrices; cela indique qu'une précision accrue du modèle ne ferait que renforcer notre conclusion que l'habitat de fraye ne constitue pas une contrainte pour ces populations. Il n'existe pas assez de données pour produire une distribution de variables qui permettrait de mieux représenter la capacité de l'habitat dans le passé, qui serait certainement plus élevée que dans nos estimations. Nos résultats laissent croire que ce sont des facteurs autres que la capacité de fraye qui limitent la taille des populations et que les efforts de rétablissement des saumons quinnat de la Skagit ne doivent pas se concentrer seulement sur la restauration de l'habitat de fraye.

[Traduit par la Rédaction]

Introduction

A critical aspect of managing both freshwater and marine fish populations is understanding the role of habitat capacities in regulating population size (Ebersole and Liss 1997; Moussalli and Hilborn 1986; Myers et al. 2001). This issue is particularly vexing in the case of anadromous fish populations, which are influenced by both freshwater and marine habitats (Reeves et al. 1989; Cooney and Brodeur 1998; Hare et al. 1999), and multiple sources of uncertainty confound the identification of habitat constraints on populations (Steel et al. 2003). Habitat limitations on anadromous fish populations can be identified through two main avenues. First, comprehensive life stage analyses can identify habitat areas that might constrain populations (e.g., Moussalli and Hilborn 1986; Reeves et al. 1991). These analyses can be in the form of limiting-factor assessments that examine relative capacities of freshwater habitats (Reeves et al. 1989) or in the form of a complete life cycle model that compares both freshwater and marine life stages (Nickelson and Lawson 1998; Wilson 2003; Greene and Beechie 2004). Second, independent assessments of potentially limiting habitats can identify or rule out likely limiting factors, even when other factors are not known (e.g., Beechie et al. 1994). Single-factor

Received 15 March 2005. Accepted 13 October 2005. Published on the NRC Research Press Web site at http://cjfas.nrc.ca on 26 April 2006.
J18602

T.J. Beechie,[1] C.M. Greene, and L. Holsinger.[2] Watershed Program, Northwest Fisheries Science Center, NOAA Fisheries, 2725 Montlake Boulevard East, Seattle, WA 98112, USA.
E.M. Beamer. Skagit River System Cooperative, P.O. Box 368, La Conner, WA 98257, USA.

[1] Corresponding author (e-mail: tim.beechie@noaa.gov).

[2] Present address: US Forest Service, P.O. Box 8089, Missoula, MO 59807, USA.

Can. J. Fish. Aquat. Sci. **63**: 1242–1250 (2006) doi:10.1139/F06-015

assessments are also useful in estimating how many fish a currently inaccessible habitat might support should fish migration to that habitat be restored (Hanrahan et al. 2004).

In either approach there are considerable scientific uncertainties (Wilson 2003; Steel et al. 2003), and scientists and managers have long recognized the importance of explaining these uncertainties to better inform management decisions (e.g., Hall et al. 1988; Francis 1992; McAllister et al. 1994). However, uncertainty has rarely been explicitly incorporated into analyses of habitat restoration planning (Steel et al. 2003). Sources of uncertainty in model predictions include accuracy of model form (model uncertainty), accuracy and variability of parameter estimates (parameter uncertainty), extrapolation of data from other locations (prediction uncertainty), observer variation and measurement errors (measurement uncertainty), and stochastic variation (natural variability) (Rosenberg and Restrepo 1994; Francis and Shotton 1997; Steel et al. 2003). These are obviously intertwined to some degree in most models, and quantifying each explicitly is often difficult. However, these uncertainties can be expressed in a way that is useful to managers by incorporating multiple sources of uncertainty into a predictive model and then displaying the distribution of possible answers so that managers can appreciate the combined effect of those uncertainties (e.g., Hall et al. 1988; Francis 1992).

In this paper we incorporate parameter uncertainty into an assessment of habitat limitations on salmon populations, focusing on spawning habitat capacity. Spawning habitat capacity is one of many potential factors that might limit population size of anadromous salmonids (Reeves et al. 1989), particularly those species with short freshwater rearing phases and little opportunity for other freshwater factors to constrain population size (McNeil 1964; Fukushima et al. 1998). Spawning capacity is also well suited to examination of uncertainty issues because habitat capacity can be estimated simply, and there are empirical data with which to estimate uncertainties in model parameters. Our primary question in the paper is whether the size of six populations of Skagit River wild Chinook salmon (*Oncorhynchus tshawytscha*) might be constrained by spawning habitat limitations. We first develop simple models to estimate spawning habitat capacity based on previous studies of Chinook spawning habitats. We then use a Monte Carlo procedure to incorporate parameter uncertainty around the input variables into the predictions and generate probability distributions of the number of Chinook spawners that today's habitats can support. Finally, we compare these results with distributions of recent spawner population sizes and discuss the likelihood that spawning habitat availability currently limits population size.

Materials and methods

Our methodology for evaluating spawning habitat limitations in Chinook salmon consists of three main steps. We first use digital elevation models (DEMs), digital hydrography, and aerial photography to delineate and characterize spawning reaches for the six populations of Chinook salmon. We then synthesize multiple data sources to develop a simple model of spawner capacity and generate a distribution of capacity estimates for each population using Monte Carlo simulations. Finally, we test whether spawning capacity is likely limiting Skagit River salmon stocks by comparing the modeled distributions of spawner capacity with empirical distributions of spawner abundance based on up to 50 years of spawner data.

Study area

The Skagit River basin drains an area of 8544 km^2 in the North Cascades of Washington State, USA (Fig. 1). Precipitation ranges from 90 to 460 $cm \cdot year^{-1}$. Historically, dense coniferous forests covered hill slopes and terraces, and mixed deciduous and conifer forests covered the valley bottoms (Ayers 1899; Gannett 1899). Floodplain and riparian forests have been extensively modified to accommodate agricultural and residential uses (Lunetta et al. 1997), and the lower river reaches have been diked to protect agricultural lands from flooding (Beechie et al. 2001). These modifications have reduced available habitat area throughout the river basin, but most significantly in the lower reaches (Beechie et al. 1994, 2001).

Chinook salmon in the Skagit basin exhibit primarily the ocean-type life history (juveniles migrate to sea soon after emergence), although some populations have a significant proportion of stream-type fish (juveniles rear in freshwater for 1 year) (Ruckelshaus et al. 2006). Six distinct populations have been identified, all of which are untainted by hatchery stocks (Ruckelshaus et al. 2006). The current spawning distribution is concentrated mainly in the basins of the Skagit, Sauk, Suiattle, and Cascade rivers. Chinook salmon avoid spawning in the fine-grained bed of the lower mainstem Skagit River (33 km), so we excluded that reach from our capacity estimates. We also assumed no mainstem spawning in the Suiattle River, which has extremely high turbidity levels from glacial melt during the spawning period. Inundation of the Baker River by Shannon and Baker reservoirs eliminated 46.8 km of spawning habitat in the early 1900s (Beechie et al. 1994). Chinook adults are trapped and hauled past these reservoirs to spawn in upstream tributaries. Construction of Gorge Dam on the Upper Skagit River eliminated an additional 10 km of spawning habitat to just above the present Diablo Dam site, where Chinook salmon historically spawned (Ruckelshaus et al. 2006).

Mapping and classification of Chinook spawning streams

We mapped the range of potential Chinook salmon spawning areas based on the location of natural migration barriers and channel slope ($<0.04\ m \cdot m^{-1}$) (Vronskiy 1972; Lunetta et al. 1997). We then classified potential spawning reaches (including side channels) into small and large channels to facilitate the use of two separate equations for estimating spawner capacity. In small channels (5–25 m bankfull width), we based estimates of spawning capacity on number of redds per unit channel length (Montgomery et al. 1999). Because there are few data with which to develop a similar equation for large channels (>25 m width), we used an area-based method for estimating spawning habitat availability in the remaining reaches. Streams less than 5 m bankfull width were considered too small for consistent Chinook spawning based on data from the Stillaguamish, Snohomish, Skagit,

Fig. 1. Location of the independent spawning populations of Chinook salmon (*Oncorhynchus tshawytscha*) in the Skagit River basin (based on Ruckelshaus et al. 2006). Darker shading indicates Skagit River drainage basin. Inset maps show location of Skagit River basin (darkly shaded area) in Washington State and location of Washington State in North America.

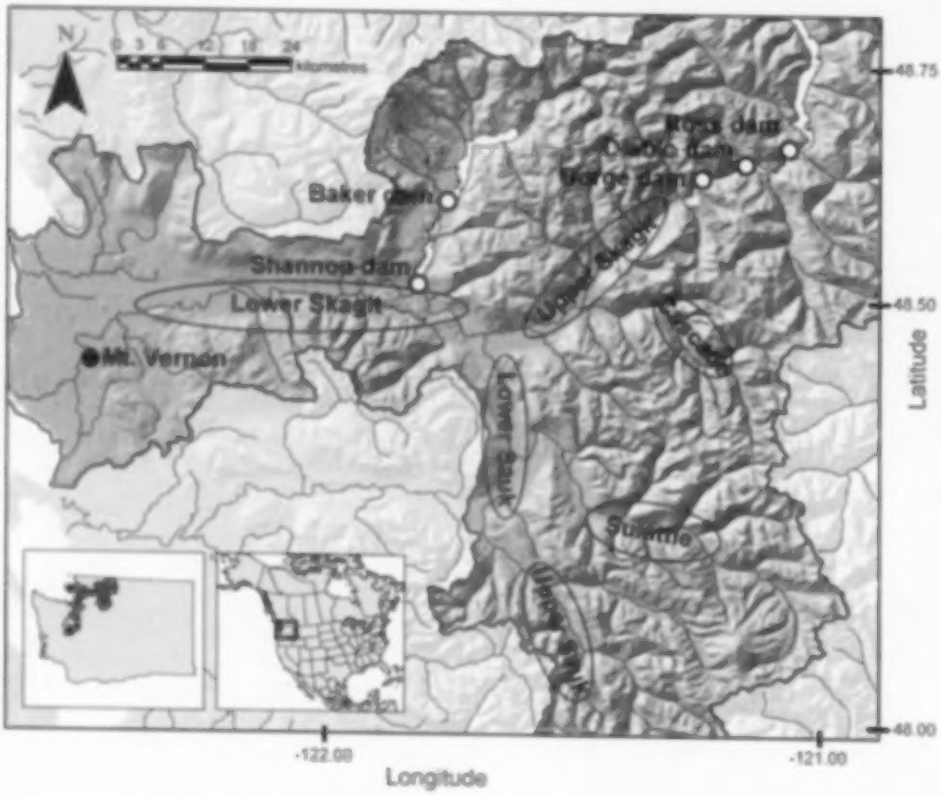

Suiattle, and White rivers (Holsinger and Pess 2003) and were not included in the analysis.

We mapped bankfull width throughout the channel network using an empirical relationship of bankfull channel width (w_{bf}) to drainage area (A) (Leopold et al. 1964):

$$(1) \qquad w_{bf} = aA^{b}$$

where a and b are empirical values. Basin drainage area was calculated from a 10 m DEM, and bankfull width was measured from 1998 1:12 000 scale digital orthophotography (obtained from Washington Department of Natural Resources (DNR)).

The resulting regression was

$$(2) \qquad w_{bf} = 7.6A^{0.37} \text{ (adjusted } r^2 = 0.73)$$

On average, aerial photograph measurements (w_a) ranged from 5 to 10 m smaller than field measurements (w_f) mainly because of overhanging tree cover in the aerial photographs (linear regression: $w_a = 1.0w_f + 5.9$, $r^2 = 0.98$) (Beechie et al. 2005). Therefore, we corrected channel width measured from aerial photography by +5.9 m, yielding a final bankfull width prediction equation of

$$(3) \qquad w_{bf} = 7.6A^{0.37} + 5.9$$

Using this equation, we mapped estimated channel width based on DEM-derived drainage areas and classified all streams in the DNR digital hydrography theme (derived from 1:12 000 scale orthophotography) as <5 m bankfull channel width (no spawning), 5–25 m width, and >25 m width.

Because width of side channels cannot be estimated based on drainage area, we manually measured width and length of side channels from digital orthophotographs. We included all side channels mapped in the digital hydrography data. Side channels were then classified into the width classes described above.

Estimating spawner capacity with the Monte Carlo procedure

We estimated Chinook spawner capacity (N) in small streams as a function of stream length in pool–riffle and forced pool–riffle channels (L), redd frequency (f_r, in redds·km^{-1}), and number of adults per redd (a_r):

$$(4) \; N = Lf_r a_r$$

Pool–riffle and forced pool–riffle channels (channels with relatively low slopes and short distances between pools; Montgomery and Buffington 1997) have similar densities of redds, and plane-bed and step–pool channels (channels with long distances between pools or slopes above ~3%) have virtually no Chinook spawning. Therefore we mapped pool–riffle and forced pool–riffle channels as potential spawning habitat and total their lengths for each population (L) and excluded plane-bed and step–pool channels. Channel types were mapped based on slope and adjacent forest cover (Lunetta et al. 1997). Frequency distributions of redds·km^{-1} (f_r) were derived from Montgomery et al. (1999), using values from the nearby Stillaguamish River, which represent long-term average numbers of Chinook spawners in a wide range of reach types (Table 1). To estimate number of adults per redd (a_r), we compiled male–female ratios from 40 unpublished carcass recovery and broodstock studies in north Puget Sound (survey periods range from 1 to 16 years) and then calculated number of adults per redd as the ratio of males to females plus one (i.e., we assumed one female per redd) (Table 1).

In large channels where areas of consistent Chinook spawning were mapped, we calculated number of spawners (N) based on total wetted area (A_w), the proportion of that area that is suitable for Chinook spawning (P_{sp}), redd area (A_r), and number of adults per redd (a_r):

$$N = a_r\left(\frac{A_w P_{sp}}{A_r}\right) \tag{5}$$

Wetted area (A_w) was calculated by multiplying reach length by wetted width (w_w), which was estimated with a regression model relating measured wetted width (from 1:12 000 scale digital orthophotographs, July 1998) to cumulative stream length (L_c, total stream length above each wetted width measurement) and stream order at the measurement point (o). We developed separate regressions for the Sauk and Skagit rivers because the Skagit River is regulated by five hydropower dams, whereas the Sauk River is unregulated.

Skagit River:

$$w_w = 0.024o^{1.34}L_c^{0.54} \text{ (adjusted } r^2 = 0.76) \tag{6}$$

Sauk River:

$$w_w = 0.008o^{-0.03}L_c^{1.04} \text{ (adjusted } r^2 = 0.74) \tag{7}$$

We estimated the percentage of wetted area that is suitable for spawning (P_{sp}) based on mapped areas where Chinook salmon spawn in most years, dividing the mapped spawning area by total wetted area of each sample reach. Percent spawnable area was calculated separately for each population. Chinook spawning was mapped in a significant proportion of each population's range (Table 2) to assure that the percent spawnable area applied to the full range of each population was representative of that population's habitat. Mean percent spawnable area for each of the five populations ranged from 4.2% to 9.7% (Table 2). Values of percent spawnable area are likely to be conservative because they reflect habitat selection by present-day spawning populations, which are considerably smaller than they were historically (Ruckelshaus et al. 2006). Nevertheless, we have no empirical or theoretical basis upon which to base larger numbers and therefore are limited to this approach for large channels.

Table 1. Median and 10th and 90th percentile values of distributions of input parameters for Chinook salmon (*Oncorhynchus tshawytscha*) spawner capacity estimates.

Parameter	10th percentile	Median	90th percentile
Redds·km^{-1}	0.0	6.1	54.3
Redd size (m^2)	4.9	14.1	27.9
Adults·redd^{-1}	1.35	1.9	3.5

Note: Regional redd size data and number of adults per redd from the Snohomish and Stillaguamish rivers (D. Hendricks, Washington Department of Fish and Wildlife, 600 Capitol Way North, Olympia, WA 98501, USA, unpublished data); number of redds per kilometre in pool–riffle and forced pool–riffle channels from the Stillaguamish River (Montgomery et al. 1999).

The most comparable data set for estimating redd areas (A_r) was from the nearby Stillaguamish River, where median redd size was 14 m^2 (Table 1). This value compared well with redd areas reported in two other studies, but four studies reported smaller redds (Table 3). Estimated inter-redd distances also compare well with those reported by Geist et al. (2000). Assuming redds are uniformly distributed and positioned immediately adjacent to one another (i.e., without a larger territorial boundary), we estimate that inter-redd distances in the Stillaguamish River average 2.1 m. This value falls within the range observed by Geist et al. (2000), who found that redds were uniformly distributed and inter-redd distances ranged from 2 to 5 m when spawners were near capacity. Number of spawners per redd (a_r) was estimated as described above for small streams.

Before running the Monte Carlo simulations, distributions of spawners per redd, redds per kilometre, and redd area were transformed to approximate normal distributions. Each variable required a unique transformation suited to the original data distribution. Redds per kilometre were highly skewed with a mode of zero, so we reflected the data around zero via an absolute value transformation. Redd areas were also highly skewed but slightly offset from zero, so we selected an absolute value transformation around a constant. Adults per redd were approximately log-normally distributed, so we selected a natural-log transformation. All three transformed distributions approximated normal distributions (Kolmogorov–Smirnov tests, $Z < 1.2$, $p > 0.1$) (Fig. 2). When back-transformed, simulated distributions of each variable (based on 2000 randomly sampled points) matched the empirical distributions (Kolmogorov–Smirnov test, $Z < 1.2$, $p > 0.05$), with the exception of redds per kilometre (Kolmogorov–Smirnov test, $Z = 2.79$, $p < 0.01$), which was oversampled at low to medium values (Fig. 2). This oversampling of low values tends to produce underestimates of spawning capacity. Once we obtained the transformed distributions of spawners per redd, redds per kilometre, and redd area, we used eqs. 4 and 5 in the Monte Carlo procedure to estimate spawner capacity 2000 times for each population, each time drawing randomly from the distributions. We discarded any capacity estimate if one of the three input measures exceeded the maximum empirical values, a procedure that eliminated 106 simulated capacities out of 2000.

Comparing simulated capacity to recent spawner abundances

To evaluate whether spawning habitat availability limits recovery of Skagit River Chinook salmon, we compared our distributions of spawning capacity estimates with em-

Table 2. Proportion of large-channel habitat areas sampled for estimation of percent spawnable area.

Population	Sampled area (million m^2)	Total area (million m^2)	Percent sampled	Mean percent spawnable area
Lower Skagit	10.71	12.38	87	5.8
Upper Skagit	3.31	6.59	50	9.7
Upper Cascade	NA	NA	NA	6.2[a]
Lower Sauk	2.54	3.44	74	5.3
Upper Sauk	0.63	2.05	31	4.2
Suiattle	NA	NA	NA	NA[b]

Note: Sampled area is the total wetted area of reaches in which spawning areas were mapped. Total area is the total wetted area of all reaches occupied by a population. Mean percent spawnable area is the average of all reaches in which percent spawnable area was estimated. NA, not available.

[a] No spawning areas were mapped in this population. Percent spawnable area for the Cascade River population was based on reaches with similar slope and discharge within the Upper Sauk population.

[b] The model assumes no mainstem spawning in the turbid Suiattle River.

Table 3. Summary of published redd sizes (adapted from Healey 1991).

Source	Type	Redd area (m^2)	
		Range	Mean
Chapman (1943)	—	2.4–4.0	
Burner (1951)	O	4.8–6.5	
Burner (1951)	S	2.4–4.1	
Vronskiy (1972)	S	4.0–15.0	
Neilson and Banford (1983)	S	0.5–27.5	9.5
Chapman et al. (1986)	O	2.1–44.8	17.0

Note: S, stream-type (spring-run) Chinook salmon (*Oncorhynchus tshawytscha*); O, ocean-type (fall and summer) Chinook salmon.

pirical distributions of population size for the six different Skagit River spawning populations. We assessed differences between the empirical and modeled distributions by examining the percentage overlap between them and by Kolmogorov–Smirnov tests for distribution differences. Spawning capacity estimates were based on annual redd counts conducted by the Washington Department of Fish and Wildlife between 1952 and 2001 (Washington Department of Fisheries and Wildlife and Western Washington Treaty Indian Tribes 1992; Hahn et al. 2001). Although not all spawning populations were continuously monitored during this time period, all spawning populations had at least 45 years of redd count estimates, with the exception of the Cascade River population, which had 17 years. These counts incorporate a combination of aerial and ground surveys to represent the entire spawning area of each population. Data from these surveys are then used to calculate total escapement using correction factors that include the amount of time that a redd is visible, the mean number of false redds, and the mean sex ratio (Hahn et al. 2001). In 1977, the Washington Department of Fisheries and Wildlife made a concerted effort to improve these estimates by standardizing much of the methodology. To examine whether this change in methodology resulted in differences in the distribution of escapements, we performed Kolmogorov–Smirnov tests on the five spawning populations with early (1952–1976) and later (1977–2001) escapement estimates. Distributions of escapement estimates based on the early and later methodologies were not significantly different for any of the five populations (Kolmogorov–Smirnov $Z < 1.56$, $p < 0.05$, for all populations after Bonferroni correction), so we used the complete time series of escapement estimates to generate the distribution of observed spawner abundance for each population.

Results

Available spawning area in large main channels and side channels (>25 m wide) ranged from 45 600 m^2 to over 718 100 m^2 (Table 4) (excluding the Suiattle River where we assume no mainstem spawning). Capacity estimates for most populations were dominated by the large area of mainstem channels, with large main channels accounting for more than 89% of the total spawning capacity in five of the six populations. Only when the mainstem was presumed unusable (the Suiattle River population) was the capacity estimate dominated by small channels. As much as 8% of the available spawning area in large channels was in side channels, with the highest percentages in the island-braided reaches occupied by the lower Sauk and lower Skagit populations. Within small channels, up to 35% of the available stream length was found in side channels.

Median estimated population sizes at capacity ranged from 1742 for the Suiattle population to 145 442 for the lower Skagit population (Table 5). Capacity estimates for individual populations spanned up to four orders of magnitude. None of the distributions approximated either a normal or lognormal distribution. Comparison of the distributions of capacity estimates to distributions of recent spawner population sizes revealed that all populations except the Suiattle population were well below estimated spawner capacities. In all cases except the Suiattle population, the distribution of spawners overlapped the distribution of capacity estimates by less then 0.2% (Table 5), and all populations showed significant frequency differences between escapement and capacity estimates based on Kolmogorov–Smirnov tests for distribution differences (Table 5).

Sensitivity analysis of the model for large channels indicated that spawner capacity estimates are most sensitive to underestimation of redd area (Fig. 3). Spawner capacity responds nonlinearly to redd area because total spawnable area is divided by redd area in the equation, and each doubling of redd area results in a halving of spawner capacity. Thus, relatively small decreases in the estimate of redd area lead to the largest incremental changes in the population

Fig. 2. Frequency distributions of (*a*) redds·km^{-1}, (*b*) redd area, and (*c*) adults per redd. First column in each panel shows the distribution of the original data, second column shows the transformed distribution (normal approximation shown by line), and third column shows the distribution created by the Monte Carlo procedure and back-transformed.

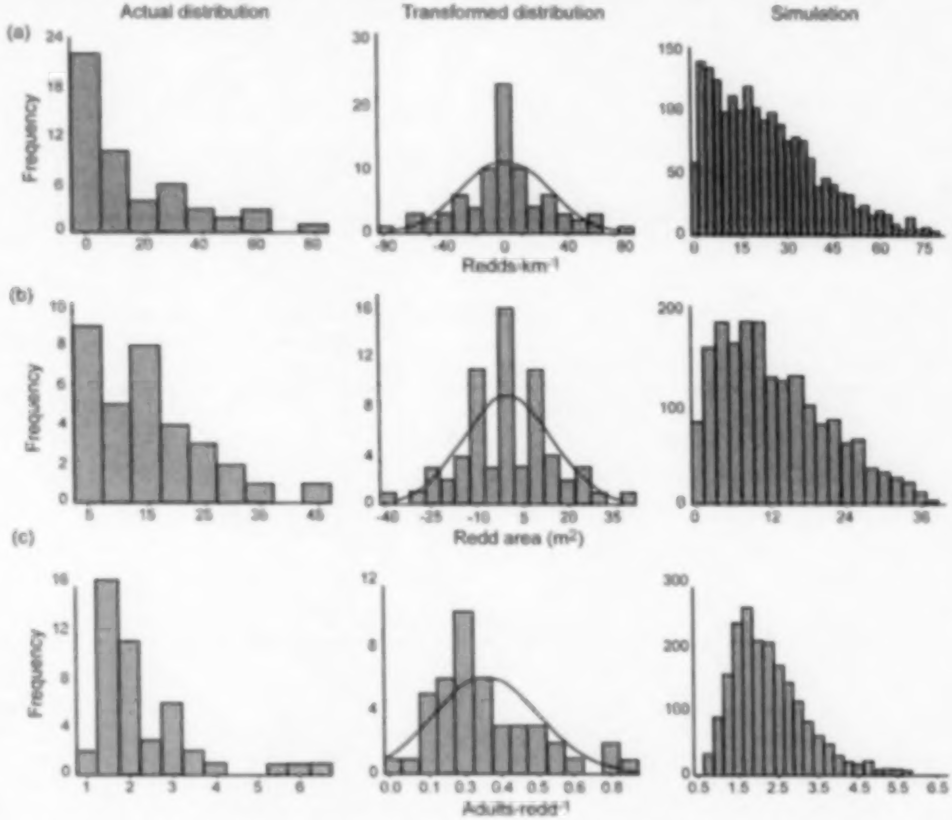

estimate. Nevertheless, percent spawnable area and number of spawners per redd also have substantial influence on the model results. Changes to other parameters cause capacity to increase linearly, an expected result shown by inspection of eq. 5. Inspection of eq. 4 for small channels indicates that estimates respond linearly to both number of redds per kilometre and number of spawners per redd and therefore are equally sensitive to changes in either parameter. However, the overall contribution of small streams to the estimated population size is small for all populations except for the Suiattle River population.

Discussion

Explicit recognition of uncertainties contained in model predictions is an important element of decision-making in fisheries management (Francis and Shotton 1997), although it is not commonly accounted for in planning freshwater habitat restoration efforts (Steel et al. 2003). In our example, accounting for several sources of uncertainty helped us determine that all six populations in the Skagit River basin are currently significantly below spawning capacity. Median spawner capacity estimates were more than one order of magnitude larger than recent population estimates for five of six populations and a factor of three larger for the remaining population. Accounting for uncertainty in the spawner capacity estimates provides a measure of confidence in the results over and above the statistical testing for differences in medians, allowing managers to more quantitatively judge the likelihood that spawning habitat limits population size. For the five populations with virtually no overlap between the distribution of estimated capacities and the distribution of current spawner estimates (<0.2% in all cases), the near complete separation of the two distributions indicates that there is almost no chance of spawning habitat limitation on population size. By contrast, there is a 51% overlap between the estimated and measured distributions for the Suiattle River population, indicating a greater chance of spawning habitat limitation for that population, especially in years when spawner abundance is relatively high and falls within the range of capacity estimates. However, we made the conservative assumption that there is no spawning at all in the turbid mainstem Suiattle River, even though it seems unlikely that capacity of the mainstem is actually zero. Thus, our estimates of spawner capacity are probably biased downwards in the one population in which there was overlap between capacity estimates and recent population sizes.

Quantifying each source of uncertainty in the data sets used to parameterize our model would be difficult and time consuming, so we chose to incorporate parameter uncer-

Table 4. Estimates of available spawning area (m^2) for large main channels and side channels (>25 m width) and length (km) of small main channels and side channels (5–25 m wide) for each population in the Skagit River basin.

Population	Large channels (m^2)	Large side channels (m^2)	Small channels (km)	Small side channels (km)
Lower Skagit	668 500	49 600	126.7	14.4
Upper Skagit	631 600	7 000	35.9	12.4
Cascade	44 100	1 500	3.1	1.7
Lower Sauk	168 400	14 000	51.0	20.6
Upper Sauk	84 600	1 600	19.7	6.1
Suiattle	NA	NA	38.7	0

Note: NA, no spawning because of high turbidity during the spawning period.

Table 5. Adult spawner population estimates (median based on the entire data set and the average for the four most recent years), median capacity estimates obtained from the Monte Carlo analysis, percent overlap of the population and capacity distributions, and statistical tests of these distributions for the six Chinook (*Oncorhynchus tshawytscha*) populations in the Skagit River basin.

				Kolmogorov–Smirnov	
Population	1952–2001 population median	Monte Carlo median	Percent overlap	*Z* test	*p* value
Lower Skagit	2606	145 442	<0.1	6.630	<0.001
Upper Skagit	6845	122 498	0.2	6.630	<0.001
Cascade	208	8 836	<0.1	4.105	<0.001
Lower Sauk	658	36 000	0.1	6.630	<0.001
Upper Sauk	492	18 226	0.1	6.980	<0.001
Suiattle	559	1 742	51.4	4.081	<0.001

Fig. 3. Sensitivity of capacity estimates for large streams (eq. 4) to changes in input parameters. Large streams have bankfull width >25 m. Heavy solid line indicates sensitivity to changes in the estimate of redd size, solid circles and thin solid line indicate sensitivity to changes in the estimate of adults per redd, and × and broken line indicate sensitivity to changes in the estimate of percent spawnable area. Range of each input variable is based on empirical data.

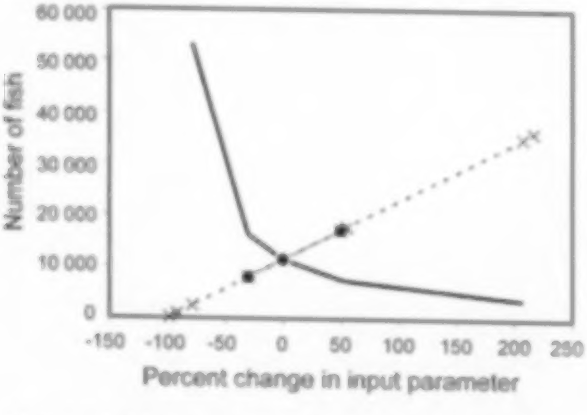

tainty a priori into a model of spawner capacity to illustrate the range of possible answers a simple model might yield. This approach recognizes that observer variation and natural variation are nested within parameter uncertainty. Thus, we cannot quantify each source of error separately, but all three are embedded in the parameter distributions that drive variation in model outputs. This approach yielded a range of up to four orders of magnitude in capacity estimates, yet there was still virtually no overlap of capacity estimates and current population sizes. Were we able to add additional parameter uncertainties into our model, the range of estimates would surely increase, but there is no indication that increased variation in the estimates would fundamentally alter our results.

An unaddressed uncertainty in our model is the possibility that some input parameters (particularly redd area) contain large errors because they are derived from studies in other rivers. This use of data from other sites results in prediction uncertainty, which is the uncertainty of model predictions for the Skagit basin resulting from input values being estimated from other populations. However, all of our input values are empirically derived, fall within the range of values found in several sites, and incorporate both natural variation and observer variation. Therefore, it is unlikely that such errors would be of sufficient magnitude to substantially shift the distributions of estimated capacities and therefore are unlikely to generate capacity estimates that are orders of magnitude higher than they should be. Moreover, where variation among studies allowed some choice of parameter ranges, the selected ranges produced conservative (low) estimates of spawner capacity and therefore increased confidence that our conclusions are not affected by overestimation of spawning capacity.

Were we to estimate spawning capacities using other than conservative values, the most significant change would be that estimated spawning capacity in tributaries would approximately double because number of redds per kilometre in preferred Chinook spawning reaches is roughly double the spatially averaged values we used (Montgomery et al. 1999). Nevertheless, this would have relatively little effect on most of our capacity estimates because tributary capacity accounts for <11% of total estimated spawning capacity in five of six populations. For the remaining population (Suiattle River), our capacity estimate would approximately double because we assumed no mainstem spawning for that population. The overlap of estimated spawning capacities and current spawner abundances would remain less than 2% for the five mainstem-spawning populations and would decrease to substantially less than the 51% overlap we found in our original estimate for the Suiattle River population. We might also increase our capacity estimates if we assumed a larger percentage of the mainstem was suitable for spawning or that redd areas would be smaller at higher spawning densities. Both changes would result in larger capacity estimates and therefore would increase certainty that spawning capacity is not limiting population size. Although our estimated spawner capacities may be low compared with true historical capacities, we had no local data upon which to base alternative parameter distributions that might better represent historical capacity.

Given the low likelihood that spawning habitat capacity limits recovery of Chinook salmon populations in the Skagit River basin, restoration efforts might be better focused on other factors that may limit salmon recovery. However, there remains considerable debate about what those actions should be. One possibility is that changes in spawning habitat quality keeps populations from recovering to levels at which they are constrained by available habitat area. For example, fine sediment in spawning gravels affects survival of eggs (Reiser and White 1988), as does the size of floods that occur during incubation (Seiler et al. 2003). However, typical values of survival from egg to outmigration for juvenile Chinook salmon in the Skagit River basin range from 10% to 16% in years with normal flood sizes (10 of 13 years; Seiler et al. 2003), suggesting that neither increased fines nor increased floods have been altered to the point that they explain current population sizes. Thus, our analysis shows that spawning habitat quantity is unlikely to constrain population sizes of Skagit River Chinook, but it leaves open the possibility that spawning habitat quality has been reduced and constrains population size.

A second possible constraint on recovery is that habitat change or loss has reduced capacity for some life stage other than adult spawners. For example, interannual variation in Puget Sound Chinook salmon population sizes is partly correlated with marine conditions, but the data do not suggest a strong constraint on population size in the marine environment (Coronado and Hilborn 1998). Freshwater rearing and nearshore or tidal delta habitats might also limit population size. However, there is currently little direct evidence that recovery of Skagit River Chinook salmon is constrained by changes in either freshwater rearing or nearshore habitat quality (Greene and Beechie 2004). Habitat limitations in the tidal delta are a more likely constraint because (*i*) there have been substantial habitat losses in the delta (Beechie et al. 2001; Collins et al. 2003), (*ii*) size of the Skagit metapopulation (all six populations combined) is sensitive to changes in delta area (Greene and Beechie 2004), and (*iii*) there is evidence of density dependence in the remaining delta habitat (E. Beamer, unpublished data).

Our approach to incorporating parameter uncertainty into evaluations of spawning habitat constraints on Chinook salmon populations is easily transferable to other populations or species. The model structure can remain essentially the same, but local data must be available to parameterize the capacity equations and to estimate distributions of recent spawner population sizes. When transferring this methodology to Chinook populations in other regions, care should be taken to use local data to create parameter distributions because river and habitat characteristics vary among ecoregions and populations. For example, percent spawnable area in the Skagit basin ranged from 4% to 10%, whereas percent spawnable areas in the Columbia River are >20% of the wetted area (Geist et al. 2000). Failure to account for such environmental and population-specific differences can lead to large errors in capacity estimates. When transferring this approach to other species (even nonsalmonids), the basic model structure can also remain the same, but capacity equations and parameter distributions must be adapted to accurately reflect species-specific habitat preferences and regional geomorphology and hydrology.

Acknowledgements

Numerous discussions with Mary Ruckelshaus and George Pess helped refine the goals and methods for this paper. We thank Beth Sanderson, Martin Liermann, and two anonymous reviewers for helpful comments on the manuscript.

References

Ayers, H.B. 1899. Washington Forest Reserve. *In* Nineteenth annual report of the United States Geological Survey, 1897–1898. Part V. Forest reserves. *Edited by* H. Gannett. Government Printing Office, Washington, D.C. pp. 283–313.

Beechie, T., Beamer, E., and Wasserman, L. 1994. Estimating coho salmon rearing habitat and smolt production losses in a large river basin, and implications for habitat restoration. N. Am. J. Fish. Manag. **14**: 797–811.

Beechie, T.J., Collins, B.D., and Pess, G.R. 2001. Holocene and recent geomorphic processes, land use and salmonid habitat in two north Puget Sound river basins. *In* Geomorphic processes and riverine habitat. Water science and application. Vol. 4. *Edited by* J.B. Dorava, D.R. Montgomery, F. Fitzpatrick, and B. Palcsak. American Geophysical Union, Washington, D.C. pp. 37–54.

Beechie, T.J., Veldhuisen, C.N., Schuett-Hames, D.E., DeVries, P., Conrad, R.H., and Beamer, E.M. 2005. Monitoring treatments to reduce sediment and hydrologic effects from roads. *In* Methods for monitoring stream and watershed restoration. *Edited by* P. Roni. American Fisheries Society, Bethesda, Maryland. pp. 194–225.

Burner, C.J. 1951. Characteristics of spawning nests of Columbia River salmon. Fish. Bull. Fish Wildl. Serv. **61**: 97–110.

Chapman, W.M. 1943. The spawning of Chinook salmon in the main Columbia River. Copeia, 1943: 168–170.

Chapman, D.W., Weitcamp, D.E., Welsh, T.L., Dell, M.B., and Schadt, T.H. 1986. Effects of river flow on the distribution of Chinook salmon redds. Trans. Am. Fish. Soc. **115**: 537–547.

Collins, B.D., Montgomery, D.R., and Sheikh, A.J. 2003. Reconstructing the historic river landscape of the Puget Lowland. *In*

Restoration of Puget Sound Rivers. *Edited by* D.R. Montgomery, S. Bolton, D.B. Booth, and L. Wall. University of Washington Press, Seattle, Wash. pp. 79–128.

Cooney, R.T., and Brodeur, R.D. 1998. Carrying capacity and North Pacific salmon production: stock-enhancement implications. Bull. Mar. Sci. **62**: 443–464.

Coronado, C., and Hilborn, R. 1998. Spatial and temporal factors affecting survival in coho and fall Chinook salmon in the Pacific Northwest. Bull. Mar. Sci. **62**: 409–425.

Ebersole, J.L., and Liss, W.J. 1997. Restoration of stream habitats in the western United States: restoration as reexpression of habitat capacity. Environ. Manag. **21**: 1–14.

Francis, R.I.C.C. 1992. Use of risk analysis to assess fishery management strategies: a case study using orange roughy (*Hoplostethus atlanticus*) on the Chatham Rise, New Zealand. Can. J. Fish. Aquat. Sci. **49**: 922–930.

Francis, R.I.C.C., and Shotton, R. 1997. "Risk" in fisheries management: a review. Can. J. Fish. Aquat. Sci. **54**: 1699–1715.

Fukushima, M., Quinn, T.J., and Smoker, W.W. 1998. Estimation of eggs lost from superimposed pink salmon (*Oncorhynchus gorbuscha*) redds. Can. J. Fish. Aquat. Sci. **55**: 618–625.

Gannett, H. 1899. Nineteenth annual report of the United States Geological Survey, 1897–1898. Part V. Forest Reserves. Government Printing Office, Washington, D.C.

Geist, D.R., Jones, J., Murray, C.J., and Dauble, D.D. 2000. Suitability criteria analyzed at the spatial scale of redd clusters improved estimates of fall chinook salmon (*Oncorhynchus tshawytscha*) spawning habitat use in the Hanford Reach, Columbia River. Can. J. Fish. Aquat. Sci. **57**: 1636–1646.

Greene, C.M., and Beechie, T.J. 2004. Habitat-specific population dynamics of ocean-type chinook salmon (*Onchorynchus tshawytscha*) in Puget Sound. Can. J. Fish. Aquat. Sci. **61**: 590–602.

Hahn, P., Kraemer, C., Hendrick, D., Castle, P., and Wood, L. 2001. Washington state Chinook salmon spawning escapement assessment in the Stillaguamish and Skagit Rivers, 1998. Washington Department of Fish and Wildlife, Olympia, Wash.

Hall, D.L., Hilborn, R., Stocker, M., and Walters, C.J. 1988. Alternative harvest strategies for Pacific herring (*Clupea harengus pallasi*). Can. J. Fish. Aquat. Sci. **45**: 888–897.

Hanrahan, T.P., Dauble, D.D., and Geist, D.R. 2004. An estimate of chinook salmon (*Oncorhynchus tshawytscha*) spawning habitat and redd capacity upstream of a migration barrier in the upper Columbia River. Can. J. Fish. Aquat. Sci. **61**: 23–33.

Hare, S.R., Mantua, N.J., and Francis, R.C. 1999. Inverse production regimes: Alaskan and West Coast Pacific salmon. Fisheries, **24**(1): 6–14.

Healey, M. 1991. Life history of Chinook salmon (*Oncorhynchus tshawytscha*). *In* Pacific salmon life histories. *Edited by* C. Groot and L. Margolis. University of British Columbia Press, Vancouver, B.C. pp. 176–185.

Holsinger, L., and Pess, G.R. 2003. Estimating Chinook spawner capacity of Stillaguamish River. *In* Ecosystem recovery planning for listed salmon: an integrated assessment approach for salmon habitat. *Edited by* T.J. Beechie, E.A. Steel, P.R. Roni, and E. Quimby. US Department of Commerce, NOAA Tech. Memo. NMFS-NWFSC-58. pp. 137–156.

Leopold, L.B., Wolman, M.G., and Miller, J.P. 1964. Fluvial processes in geomorphology. W.H. Freeman and Co., San Francisco, Calif.

Lunetta, R.S., Cosentino, B.L., Montgomery, D.R., Beamer, E.M., and Beechie, T.J. 1997. GIS-based evaluation of salmon habitat in the Pacific Northwest. Photogramm. Eng. Remote Sens. **63**: 1219–1229.

McAllister, M.K., Pikitch, E.K., Punt, A.E., and Hilborn, R. 1994. Bayesian approach to stock assessment and harvest decisions using the sampling/importance resampling algorithm. Can. J. Fish. Aquat. Sci. **51**: 2673–2687.

McNeil, W.J. 1964. Redd superimposition and egg capacity of pink salmon spawning beds. J. Fish. Res. Board Can. **21**: 1385–1396.

Montgomery, D.R., and Buffington, J.M. 1997. Channel-reach morphology in mountain drainage basins. Geol. Soc. Am. Bull. **109**: 596–611.

Montgomery, D.R., Beamer, E.M., Pess, G.R., and Quinn, T.P. 1999. Channel type and salmonid spawning distribution and abundance. Can. J. Fish. Aquat. Sci. **56**: 377–387.

Moussalli, E., and Hilborn, R. 1986. Optimal stock size and harvest rate in multistage life history models. Can. J. Fish. Aquat. Sci. **43**: 135–141.

Myers, R.A., MacKenzie, B.R., Bowen, K.G., and Barrowman, N.J. 2001. What is the carrying capacity for fish in the ocean? A meta-analysis of population dynamics of North Atlantic Cod. Can. J. Fish. Aquat. Sci. **58**: 1464–1476.

Neilson, J.D., and Banford, C.E. 1983. Chinook salmon (*Oncorhynchus tshawytscha*) spawner characteristics in relation to redd physical features. Can. J. Zool. **61**: 1524–1531.

Nickelson, T.E., and Lawson, P.W. 1998. Population viability of coho salmon, *Oncorhynchus kisutch*, in Oregon coastal basins: application of a habitat-based life cycle model. Can. J. Fish. Aquat. Sci. **55**: 2383–2392.

Reeves, G.H., Everest, F., and Nickelson, T. 1989. Identification of physical habitats limiting the production of coho salmon in western Oregon and Washington. US Department of Agriculture Forest Service Gen. Tech. Rep. PNW-GTR-245.

Reeves, G.H., Hall, J.D., Roelofs, T.D., Hickman, T.L., and Baker, C.O. 1991. Rehabilitating and modifying stream habitats. Am. Fish. Soc. Spec. Publ. **19**: 519–558.

Reiser, D.W., and White, RG. 1988. Effects of two sediment size-classes on survival of steelhead and Chinook salmon eggs. N. Am. J. Fish. Manag. **8**: 432–437.

Rosenberg, A.A., and Restrepo, V.R. 1994. Uncertainty and risk evaluation in stock assessment advice for U.S. marine fisheries. Can. J. Fish. Aquat. Sci. **51**: 2715–2720

Ruckelshaus, M., Currens, K., Graeber, B., Fuerstenberg, B., Rawson, K., Sands, N., and Scott, J. 2006. Independent populations of Chinook salmon in Puget Sound. US Department of Commerce, NOAA Tech. Memo. In press.

Seiler, D., Neuhauser, S., and Kiskimoto, L. 2003. 2002 Skagit River wild 0+ Chinook production evaluation annual report. Washington Department of Fish and Wildlife, Rep. FPA 03-11.

Steel, E.A., Liermann, M.C., McElhaney, P., Scholtz, N.L., and Cullen, A.C. 2003. Managing uncertainty in habitat recovery planning. *In* Ecosystem recovery planning for listed salmon: an integrated assessment approach for salmon habitat. *Edited by* T.J. Beechie, E.A. Steel, P.R. Roni, and E. Quimby. US Department of Commerce, NOAA Tech. Memo. NMFS-NWFSC-58. pp. 137–156.

Vronskiy, B.B. 1972. Reproductive biology of the Kamchatka River Chinook salmon (*Oncorhynchus tshawytscha* (Walbaum)). J. Ichthyol. **12**: 259–273.

Washington Department of Fish and Wildlife and Western Washington Treaty Indian Tribes. 1992. Washington State Salmon and Steelhead Stock Inventory (SASSI). Washington Department of Fish and Wildlife, Olympia, Wash.

Wilson, P.H. 2003. Using population projection matrices to evaluate recovery strategies for Snake River spring and summer Chinook salmon. Conserv. Biol. **17**: 782–794.

Using impact assessment methods to determine the effects of a marine reserve on abundances and sizes of valuable tropical invertebrates

M.P. Lincoln-Smith, K.A. Pitt, J.D. Bell, and B.D. Mapstone

Abstract: Procedures for impact assessment, including "beyond-BACI" (before–after control–impact) and proportional differences (ratios between impact and control treatments) were used to test population replenishment of marine invertebrates at a marine conservation area (MCA) and three fished (control) areas in the Solomon Islands of the southwestern tropical Pacific. Within shallow reef terrace habitat, the MCA caused abundance and size of the topshell *Trochus niloticus* to increase but did not affect holothurians (sea cucumbers) or the giant clam *Tridacna maxima*. Abundance of the nonexploited topshell *Tectus pyramis* was unchanged at the MCA but increased at the controls, possibly because of changes in abundance of *T. niloticus*. Within deep slope habitat, the MCA caused increased abundance of the sea cucumber *Holothuria fuscogilva* and prevented possible declines in abundances of *Thelanota anax* and all holothurians combined but had no effect on abundances of *Holothuria atra* or *Holothuria fuscopunctata*. Power analysis comparing the MCA with controls indicated that further, relatively modest increases in abundance or size of some species would have a good chance of being detected statistically. The beyond-BACI procedure holds promise for enabling rigorous evaluation of marine reserves as management tools at different spatial scales; the use of proportional differences is simpler but has limited management value.

Résumé : Des procédures d'évaluation des impacts, dont l'au-delà du BACI (« beyond-BACI »; avant–après témoin–impact) et des différences proportionnelles (rapports entre les conditions d'impact et les conditions témoins) nous ont servi à vérifier le renflouage des populations d'invertébrés marins dans une zone de conservation marine (MCA) et trois régions soumises à la pêche (témoins) dans les îles Salomon, sud-ouest du Pacifique tropical. Dans les habitats de récifs en terrasse de faible profondeur, la MCA cause un accroissement de l'abondance et de la taille du trocha, *Trochus niloticus*, mais n'affecte pas les holothuries (concombres de mer) ou la moule géante, *Tridacna maxima*. L'abondance du troca blanc, *Tectus pyramis*, non exploité reste inchangée dans les MCA, mais augmente dans les zones témoins, peut-être à cause des changements d'abondance de *T. niloticus*. Dans les habitats de pente profonds, la MCA a accru l'abondance du concombre de mer *Holothuria fuscogilva*, a empêché les déclins potentiels d'abondance de *Thelanota anax* et de toutes les holothuries combinées, mais est restée sans effet sur les abondances d'*Holothuria atra* ou d'*Holothuria fuscopunctata*. Une analyse de puissance qui compare la MCA aux zones témoins indique que des accroissements futurs relativement modestes d'abondance ou de taille de certaines espèces auraient de bonnes chances d'être détectées statistiquement. La méthode d'au-delà du BACI est prometteuse comme outil de gestion pour l'évaluation rigoureuse des réserves marines à différentes échelles spatiales; l'utilisation des différences proportionnelles est plus simple, mais elle possède une valeur limitée pour la gestion.

[Traduit par la Rédaction]

Introduction

Marine reserves have been advocated as a tool for managing fisheries resources (Roberts and Polunin 1993; Tegner 1993; Bohnsack 1998), particularly in tropical regions where conventional fisheries management theory and practice have been generally unsuccessful in sustaining complex, multispecies reef fisheries (Roberts and Polunin 1993). The potential benefits claimed for reserves include increases in abundance and size of individuals, increased diversity of

Received 15 April 2005. Accepted 24 January 2006. Published on the NRC Research Press Web site at http://cjfas.nrc.ca on 26 April 2006.
J18654

M.P. Lincoln-Smith.[1] The Ecology Lab Pty Ltd., 4 Green Street, Brookvale, New South Wales 2100, Australia.
K.A. Pitt. Centre for Aquatic Processes and Pollution and School of Environmental and Applied Science, Griffith University, PMB 50, Gold Coast Mail Centre, Queensland 9726, Australia, and The Ecology Lab Pty Ltd., 4 Green Street, Brookvale, New South Wales 2100, Australia.
J.D. Bell. The WorldFish Center, P.O. Box 500, GPO, 10670 Penang, Malaysia.
B.D. Mapstone. Antarctic Climate and Ecosystems Cooperative Research Centre, Private Bag 80, University of Tasmania, Hobart, Tasmania, 7001, Australia.

[1] Corresponding author (e-mail: mls@theecologylab.com.au).

Can. J. Fish. Aquat. Sci. **63**: 1251–1266 (2006) doi:10.1139/F06-033

species, and emigration of juveniles and adults or export of propagules to areas outside the reserve (Roberts and Polunin 1991; Dugan and Davis 1993; Bohnsack 1998). Although there are strong theoretical arguments in support of these benefits, data from field experiments have often been equivocal (Russ 2002; Willis et al. 2003; Sale et al. 2005; but see McClanahan and Arthur 2001). There is a pressing need to test the effectiveness of marine reserves for managing fisheries because the economic, social, and cultural costs associated with establishing and managing reserves can be considerable (Bergin 1993; Parrish 1999; Hilborn et al. 2004). Sound assessments will empower managers to decide whether marine reserves are the best way to use the often limited resources available to them for regulating fishing. A caveat here is that even where marine reserves are deemed to be an appropriate tool, they will be effective only if there is minimal illegal harvesting within the reserve. This requires the co-operation of local communities, especially in situations where organized enforcement of reserves is scarce or lacking.

An evaluation of a marine reserve requires separation of the effects of the reserve from natural spatial and temporal heterogeneity (Garcia-Charton and Perez-Ruzafa 1999). Specifically, increases in abundance or size of target species of interest within the reserve from before to after establishment of the reserve must exceed natural temporal fluctuations outside the reserve where harvest is occurring. Also, differences between the reserve and control (fished) areas must exceed natural variation among control areas. This requires sampling within the reserve, and at multiple control areas, several times before and after establishment of the reserve. This approach is known as a "beyond-BACI" (before–after control–impact) sampling design and was developed to assess environmental impacts when the affected location was unreplicated (Underwood 1993). With few exceptions (e.g., Edgar and Barrett 1997; Schroeter et al. 2001), sampling protocols for impact assessment have rarely been applied to assessments of marine reserves, although their use has been advocated (Carr and Reed 1993; Lincoln-Smith et al. 1997; Russ 2002).

The development of methods for measuring environmental impacts has been active since the 1970s. Eberhardt (1976) noted that essential inferences in modern experimental design rely on random assignment of experimental "treatments" and "controls", but many environmental impacts occur at a specific single location, and therefore, the impact treatment cannot be selected at random from an assortment of possible locations. Most studies of environmental impact are limited to one impacted area. Moreover, although one or more control areas may be available, randomization generally applies only to subsampling (Eberhardt 1976; Stewart-Oaten and Bence 2001). Beyond-BACI assumes that the location of a putative impact is selected randomly in terms of environmental indicators. That is not to say that social, economic, or logistical reasons for selecting that location are also random. In fact, they generally are not. This distinction has lead, in part, to debate regarding the suitability of beyond-BACI (Stewart-Oaten and Bence 2001; but see Keough and Mapstone 1997). Despite this debate, beyond-BACI has been applied in impact studies (e.g., Roberts et al. 1998). One alternative approach advocated has been to compare the difference ("delta" values) between impact and control locations as time series before and after the onset of the impact using a t test, which also facilitates simple calculation of statistical power (Schroeter et al. 1993; Osenberg et al. 1994).

The 83 km^2 Arnavon Islands Marine Conservation Area (MCA) was established in the Solomon Islands in 1995. Apart from Conservation Officers, no one lives on the Arnavon Islands. The islands were accessed before closure by boats from neighbouring villages. Three aspects of the Arnavon Islands MCA enabled testing of some of the anticipated benefits of marine reserves. First, surveys could be done at several spatial scales in the MCA and at several control locations before and after declaration of the MCA. Second, several species of invertebrates were harvested heavily throughout the Solomon Islands (Richards et al. 1994). Third, the MCA was established with the support of local communities.

The MCA was also suitable for applying the beyond-BACI design. Habitats and initial observations of species were similar to those in many other places within the general area. Thus, although selection of the MCA was not random for social reasons, it was reasonable to assume randomness for the performance indicators selected (i.e., abundance and size of commercially exploited invertebrates). Moreover, the ubiquitous nature of the habitat within the vicinity of the MCA provided ample opportunity to select control areas. Finally, there was time available (albeit limited) to do baseline surveys before the declaration of the reserve.

The major objective of this study was to test the hypothesis that the number and size of commercially exploited invertebrates would increase at the Arnavon Islands relative to fished areas nearby after establishment of the MCA. The hypothesis regarding increases in sizes was based on the assumption that fishers had previously targeted, or collected with greater efficiency, large individuals, although lower and upper size limits of 7 and 11 cm applied to one species, *Trochus niloticus*.

Materials and methods

Estimating changes in abundance

Invertebrates were sampled at four island groups (Arnavon, Waghena, Ysabel, and Suavanao; Fig. 1). The MCA was established at the Arnavon Islands in August 1995 and the remaining groups were controls. The number of control groups and sampling procedures were determined by pilot studies (Lincoln-Smith et al. 1997). Two islands were sampled in each group, and at each island, four sites were sampled within each of two habitats: shallow reef terrace habitat (depth range 0.5–3.5 m) and deeper sand and rubble slope habitat (15–22 m). Sites encompassed 5–10 ha and the same sites were sampled each time. Sites were selected in consultation with the local community and included only if the community had previously harvested target species there. Two habitats were sampled because trochus and giant clams were generally restricted to shallow reef terrace habitat, but several species of holothurians were more abundant in either of the two habitats. Invertebrates were counted by divers within six 50 m transects randomized within each site during

Fig. 1. Location of (*a*) the Arnavon Islands Marine Conservation Area in the Solomon Islands and (*b*) the three control locations, Waghena, Ysabel and Suavanao.

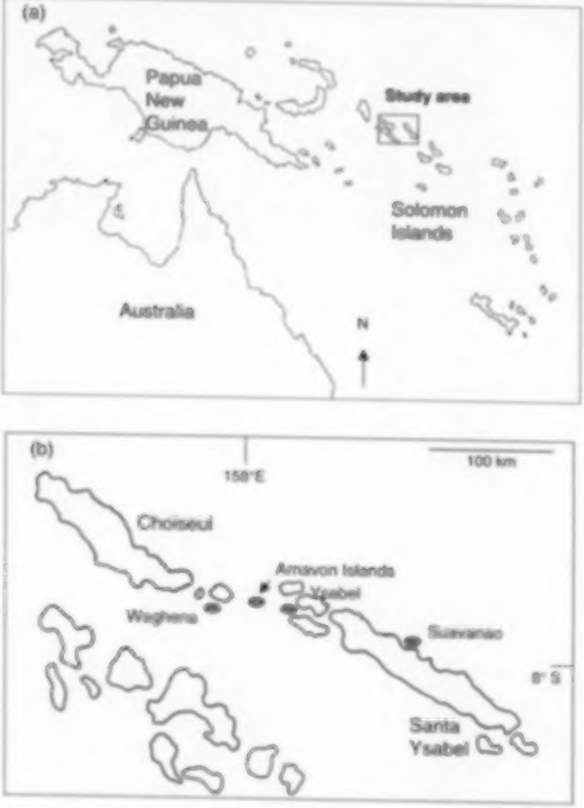

each survey. Transects were 2 m and 5 m wide in the terrace and slope habitats, respectively.

The MCA was declared in August 1995. Time was made available by local communities for us to do three surveys before and three surveys after closure: January–February, April–May, and July–August 1995 (before); and September 1998, January–February 1999, and April 1999 (after).

Analysis of abundance data using beyond-BACI

Variation in abundance was examined using five-factor beyond-BACI analyses of variance (ANOVA) (Underwood 1992, 1993). The model statement for the design is

$$\begin{aligned} X_{ijklmn} = {} & \mu + \mathrm{B}_i + \mathrm{T(B)}_{j(i)} + \mathrm{G}_k + \mathrm{I(G)}_{l(k)} \\ & + \mathrm{S(I(G))}_{m(l(k))} + \mathrm{BG}_{ik} + \mathrm{BI(G)}_{il(k)} \\ & + \mathrm{BS(I(G))}_{im(l(k))} + \mathrm{T(B)G}_{j(i)k} \\ & + \mathrm{T(B)I(G)}_{j(i)l(k)} + \mathrm{T(B)S(I(G))}_{j(i)m(l(k))} \\ & + \varepsilon_{n(ijklm)} \end{aligned}$$

where X_{ijklmn} is the value of any one datum made up of the overall mean (μ), residual (unexplained) variance ($\varepsilon_{n(ijklm)}$), and contributions of the five factors and their statistical interactions: (*i*) before vs. after (B); (*ii*) times (T(B)), which were nested within before vs. after and included the three "before" and three "after" surveys; (*iii*) groups (G), which included an asymmetrical comparison of the Arnavon group with the three control groups; (*iv*) islands (I(G)), which were nested within groups; and (*v*) sites (S(I(G))), which were nested within islands and groups. Other terms in the model were interactions. Before vs. after was a fixed factor. Times, groups, islands, and sites were random factors. Groups were treated as random because it was assumed that the habitats in which the species were sampled were representative subsamples of the region with no particular biases attributable to particular groups. Thus, even though the selection of the Arnavon Islands as a reserve was based largely on social considerations, habitats in that group were no different a priori than the same habitats in the other groups. Data from the two habitats were analysed separately because of the different methods used to sample each habitat.

The spatial factors in the model were orthogonal with respect to the temporal factors because the same groups, islands, and sites were sampled at each time, but different transects were sampled at each site at each time. The alternative of selecting new sites at random for each survey was not available because not enough sites were present at the MCA. In such cases, an alternative model would be to use repeated measures analyses (e.g., Green 1993; Keough and Mapstone 1997) with sites as the basic sampling unit, but given the small size of transects compared with the area of each site, the beyond-BACI approach was considered suitable.

Underwood (1992, 1993) described the mechanics of conducting asymmetrical ANOVAs. The sequence of tests required to detect a change varies depending on the results of initial tests. Two-tailed *F* tests were sometimes required, subsequent to initial tests, because temporal variation occurred at both the MCA and control areas after the establishment of the MCA. An impact could be identified by using a two-tailed test to compare the magnitude of variation within the MCA and control areas before and after establishment of the MCA (Underwood 1993). Similarly, if changes were identified from before to after establishment at the MCA and the controls, two-tailed tests were required to compare the magnitude of changes between the MCA and control areas. No tests were available for some factors, but tests were sometimes created by eliminating interaction terms that were nonsignificant at $P \geq 0.25$ (Underwood 1997). Cochran's *C* tests were used to test the assumption of homogeneity of variances, and data were transformed to $\ln(x + 1)$ where necessary to satisfy the assumption of homoscedasticity. However, if transformation failed to stabilize variances, raw data were analysed because ANOVA is robust to the assumption of homogeneous variances, particularly when the sampling design is balanced and has large numbers of replicates and treatments (Underwood 1997), as was the case here. Sometimes α is reduced to 0.01 when analyzing heteroscedastic data to control the probability of making a type I error because of heterogeneous variances. Reducing α, however, increases the potential for type II errors (Mapstone 1995; Underwood 1997). We retained α at 0.05, therefore, despite the potential for elevated risk of committing a type I error (i.e., concluding that the MCA had an effect when, in fact, it did not) in preference to increasing the likelihood of erroneously concluding that the MCA had no effect, when it actu-

Table 1. Asymmetrical analysis of variance comparing abundance of *Trochus niloticus* between the Arnavon Islands and reference locations, before and after declaration of the marine conservation area at the Arnavon Islands (MCA).

Sources of variation	df	MS	*F*	*p*	*F* vs.	Interpretation and implication for MCA
B	1	1.8368			Red.	
T(B)	4	0.2144			Red.	
G	3	6.7523			Red.	
I(G)	4	1.2448			Red.	
S(I(G))	24	1.1638			Red.	
B × G	3	4.5984				
B × M vs. C	1	11.8067	19.1574	0.0119	B × I(G)	Variation at the MCA group, relative to controls, from before to after declaration; MCA has caused a change in numbers at the scale of groups
B × G(C)	2	0.9942	1.6132	0.3062	B × I(G)	No variation among control groups from before to after declaration
B × I(G)	4	0.6163			No test	
B × I(M)	1	0.6806			No test	
B × I(G(C))	3	0.5949			No test	
B × S(I(G))	24	1.1117	2.9348	<0.0001	Residual	
B × S(I(M))	6	2.6528	7.0032	<0.0001	Residual	Variation at MCA sites from before to after declaration; MCA has caused a change in numbers at the scale of sites
B × S(I(G(C)))	18	0.5980	1.5787	0.0585	Residual	No variation among control sites from before to after declaration
T(B) × G	12	0.1866	0.3244	0.9728	T(B) × I(G)	Eliminate term
T(B) × M vs. C	4					
T(before) × M vs. C	2	0.3722				
T(after) × M vs. C	2	0.0300	0.0426	0.9584	T(B) × I(G)	No short-term temporal variation at MCA after declaration; no short-term effect detected at group scale
T(B) × G(C)	8					
T(before) × G(C)	4	0.1620				
T(after) × G(C)	4	0.1968	0.2795	0.8869	T(B) × I(G)	No short-term temporal variation among control groups after declaration
T(B) × I(G)	16	0.7040	1.8585	0.0208	Residual	
T(B) × I(M)	4					
T(before) × I(M)	2	0.1945				
T(after) × I(M)	2	3.5834	9.4599	<0.0001	Residual	Short-term temporal variation among MCA islands after declaration
T(after) × I(M)	2		18.4237	>0.10	T(before) × I(M), two-tailed	Short-term temporal variation between MCA islands, after declaration is similar to short-term variation between MCA islands before declaration; no short-term effect detected at island scale
T(B) × I(G(C))	12					
T(before) × I(G(C))	6	0.4421				
T(after) × I(G(C))	6	0.1759	0.4644	0.8349	Residual	No short-term temporal variation among control islands after declaration
T(B) × S(I(G))	96	0.2775	0.7326	0.973	Residual	Eliminate term
T(B) × S(I(M))	24					
T(before) × S(I(M))	12	0.2639				
T(after) × S(I(M))	12	0.7222	1.9065	0.0301	Residual	No short-term temporal variation among MCA sites after declaration; no short-term effect detected at site scale

---

Table 1 (*concluded*).

Sources of variation	df	MS	F	p	F vs.	Interpretation and implication for MCA
T(after) × S(I(M))	12		2.7366	>0.05	T(before) × S(I(M)), two-tailed	Short-term temporal variation among MCA sites after declaration is not different from short-term variation among MCA sites before declaration
T(B) × S(I(G(C)))	72					
T(before) × S(I(G(C)))	36	0.2438				
T(after) × S(I(G(C)))	36	0.1674	0.4419	0.9983	Residual	No short-term temporal variation among control sites after declaration
Residual	960	0.3788				
Total	1156					

Note: B, before vs. after; T, times; G, group; I, island; S, site; M, MCA; C, control; df, degrees of freedom; MS, mean square; Red., redundant term because of significant higher-order interaction; no test, no denominator mean square for creating F test; Cochran's $C = 0.1357$, $p < 0.01$.

ally did (i.e., a type II error) (Mapstone 1995). Post hoc Student–Newman–Keuls (SNK) tests were used to differentiate means where significant factors had >2 means.

Estimating changes in size using beyond-BACI

Target species observed within transects were measured with a flexible tape. Individuals observed just outside transects were also measured to increase sample sizes at each site. Trochus were measured across the widest point of the base of the shell. Holothurians were measured in situ, without disturbance, along the top of the body, from mouth to anus, using a tape measure. Clams were measured across the top of the shell as it was not possible to measure shell width because many individuals were embedded in coral.

Too few measurements were made for all taxa to enable a sensible comparison across all temporal and spatial scales, and hence data were pooled across spatial and (or) temporal scales to increase replication. Balanced replication (Underwood 1997) was achieved by randomly discarding data where necessary. Two analyses were used, depending on the number of animals available after pooling. For analysis 1, data were pooled at the group level in the MCA and across all groups within the controls. Data were also pooled across all three times sampled before and three times sampled after declaration of the MCA. A two-factor ANOVA compared (*i*) the MCA with controls and (*ii*) before and after declaration of the MCA. Both factors were fixed and orthogonal. Analysis 2 was an asymmetrical ANOVA used to compare sizes of *Tridacna maxima*. Data were pooled across sites and islands within each of the MCA and control groups. The factors analysed were before vs. after (fixed), times (nested in before vs. after and random), and groups (random), including an asymmetrical comparison of the MCA with the control groups.

Analysis of delta values for abundance and size

Delta values were calculated for each time before and after declaration of the MCA for data on abundance and size (cf. Osenberg et al. 1994). Here, the deltas were calculated as proportional differences using log-transformed data as

$$\Delta_B = \mathrm{MCA_B}/\mathrm{CA_B}$$

and

$$\Delta_A = \mathrm{MCA_A}/\mathrm{CA_A}$$

where Δ_B and Δ_A are the deltas for each time before and after declaration, respectively; $\mathrm{MCA_B}$ and $\mathrm{MCA_A}$ are the average total counts of an invertebrate per site within the MCA at each time before and after declaration; and $\mathrm{CA_B}$ and $\mathrm{CA_A}$ are the average total counts of an invertebrate per site within all control areas at each time before and after declaration. Delta values for size were based on average size across all sites within the MCA or control areas. Δ_B and Δ_A were compared using a one-tailed t test (H_0: $\Delta_B \geq \Delta_A$; H_a: $\Delta_B < \Delta_A$) for all invertebrates except *Tectus pyramis*, where a two-tailed test was used because we could not predict a direction of change for this species. Post hoc analysis of power $(1 - \beta)$ was used to determine (*i*) the number of samples (i.e., times each before and after declaration) required to achieve $1 - \beta \geq 0.80$, (*ii*) the power of t tests required to detect a significant reserve effect for a 25% and 50% change in the proportional difference between the MCA and the control areas before and after declaration of the MCA, using the observed mean abundance in $\mathrm{CA_B}$, and (*iii*) the size of the proportional difference required to achieve $1 - \beta \geq 0.80$, with $n = 3$. The use of 25% and 50% changes is consistent with published abundances of several species of invertebrates elsewhere in the tropical Pacific (e.g., Long and Skewes 1997; Preston and Lokani 1990); these changes were also used for evaluating sizes in the absence of available data from elsewhere.

Results

Twenty-seven species of commercially exploited invertebrates were recorded: seven species of giant clams, two species of pearl oysters, *T. niloticus*, and 17 species of holothurians. The nonharvested topshell *T. pyramis*, which was common in the shallow habitat, was also counted. Eight species were abundant enough to warrant statistical analysis. Total abundance of holothurians was also analysed for each habitat. Results of beyond-BACI analyses for *T. niloticus* are detailed to show the partitioning of variation and sequence of tests used, with details for other abundance variables analysed in the same way presented as summaries.

Abundance of invertebrates in the shallow terrace habitat

Trochus niloticus and Tectus pyramis

Establishment of the MCA facilitated an increase in the abundance of *T. niloticus* (Table 1; Fig. 2*a*). Abundance of *T. niloticus* increased threefold at the Arnavon Islands from before to after establishment, but numbers remained similar at the control groups over the same period (Fig. 2*a*). No test was available to compare islands (Table 1), but Fig. 2*b* suggests there was an increase in abundance at both islands within the MCA, whereas abundances remained similar or decreased at all but one of the control islands. Increases in abundance were inconsistent among sites within islands (Table 1) but tended to increase at all sites in the MCA (significantly so at two sites) while generally remaining similar or tending to decrease at most control sites from before to after declaration (Fig. 3).

The abundance of *T. pyramis*, which occurred in the same habitat as *T. niloticus*, was unchanged within the MCA from before to after its establishment (Table 2). Abundance varied among the 24 control sites, however, where numbers increased significantly at 11 sites, decreased at 2, and remained unchanged at 11.

Tridacna maxima

The MCA had no overall effect on the abundance of *T. maxima* (Table 2). Abundance, however, increased at seven of the eight sites in the MCA and at 20 control sites (Fig. 4). Because similar variation occurred at the MCA sites and control sites, the increase in abundance cannot be attributed to the MCA, suggesting broad-scale increases in the region.

Holothurians

The MCA had no detectable effect on the total abundance of holothurians or of *Stichopus chloronotus* in the shallow habitat (Table 2). This was despite abundances increasing twofold at the Arnavon Islands from before to after establishment of the MCA and numbers remaining similar at the control groups (Fig. 5*a*). The sensitivity of the test to identify changes at the MCA relative to control groups (B × MCA vs. controls interaction) was probably too low (df = 1,2) to detect the trend suggested graphically. Temporal variation occurred in the abundance of holothurians among sites at the Arnavons after establishment of the MCA, but this variation did not differ statistically from temporal variation before establishment and, hence, could not be attributed to an effect of the MCA.

Abundance of invertebrates in the deep slope habitat

Total holothurians

Establishment of the MCA did not cause a significant increase in the number of holothurians in the deeper slope habitat, but it may have prevented declines in abundance that were evident elsewhere in the region. Abundance varied at the MCA relative to the control groups from before to after declaration (Table 2*b*). SNK analyses indicated that abundance remained similar at the Arnavon group from before to after declaration but declined on average by one-third at the control groups (Fig. 5*b*). There was no variation in total abundance at the scale of sites at the Arnavon Islands from before to after establishment, but at the controls, abundance decreased at 11 sites, increased at 1, and was unchanged at 12 sites. This suggests that the MCA maintained populations but was ineffective at enhancing them.

Fig. 2. *Trochus niloticus*. Mean abundance (± standard error) among (*a*) groups ($n = 144$) and (*b*) islands ($n = 72$) before (shaded bars) and after (open bars) establishment of the Arnavon Marine Conservation Area. An asterisk (*) indicates significant difference (Student–Newman–Keuls test, $P \leq 0.05$).

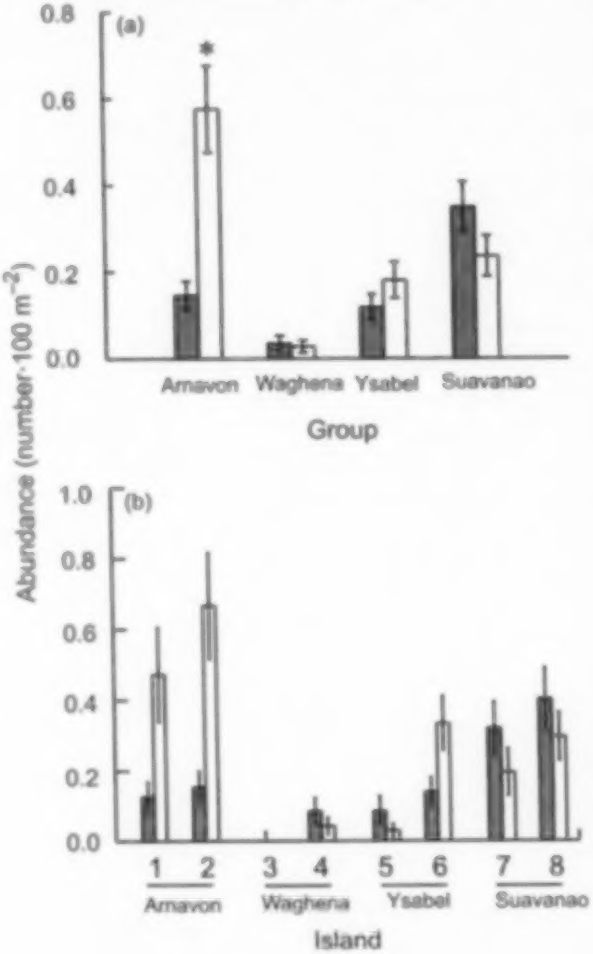

Holothuria fuscogilva

Establishment of the MCA had a limited effect on numbers of *H. fuscogilva* (Table 2; Fig. 5*c*). This species differed in abundance between the MCA and control groups from before to after declaration, but SNK tests failed to identify where the differences lay, probably because of the small number of degrees of freedom associated with the tests. Although not detected statistically, abundance almost doubled at the Arnavon group and decreased at the control groups following declaration (Fig. 5*c*). At the scale of sites, abundance increased greatly at two sites at the Arnavons and decreased at four sites at the control groups but did not change elsewhere (Fig. 6). Although there were few sites where differences occurred and overall numbers were small, the direction of change suggested that the MCA increased abundance at some sites and prevented declines at others compared with control areas.

Fig. 3. *Trochus niloticus*. Mean abundance (± standard error) among sites (n = 18) before (shaded bars) and after (open bars) establishment of the marine conservation area: (*a*) Arnavon Marine Conservation Area; (*b*) Waghena; (*c*) Ysabel; and (*d*) Suavanao. An asterisk (*) indicates significant difference (Student–Newman–Keuls test, $P \le 0.05$).

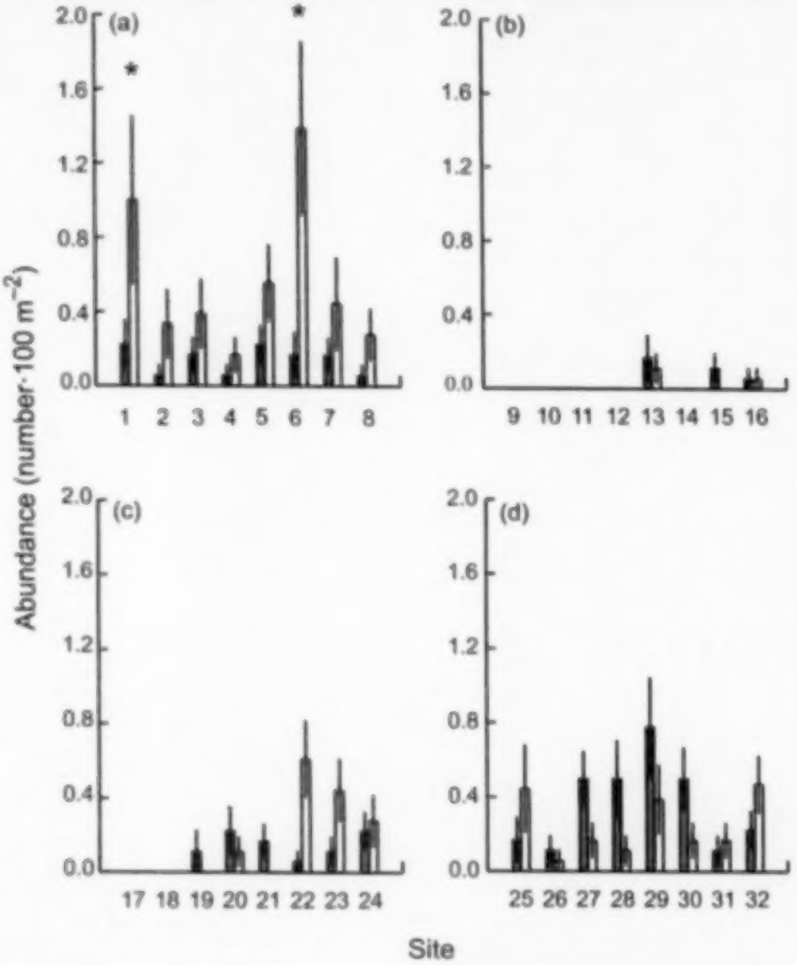

Holothuria atra

Establishment of the MCA had no measurable effect on the abundance of *H. atra* (Table 2). There were relatively large numbers of *H. atra* at the MCA, but patterns of abundance among groups did not change from before to after declaration. Short-term temporal variation was detected at the MCA after declaration but similar variation also occurred beforehand, indicating that it was not caused by the MCA (Table 2). Similarly, short-term temporal variation occurred among sites within the MCA after declaration. This variation was inconsistent from before to after declaration, but similar differences in temporal variation occurred at controls, thus temporal variation appeared unrelated to the MCA.

Thelanota anax and Holothuria fuscopunctata

Beyond-BACI indicated that the MCA did not affect abundances of *T. anax* or *H. fuscopunctata* (Table 2). *Thelanota anax* did not increase at any site in the MCA, but SNK tests indicated that abundance decreased at 4 of the control sites, remained unchanged at 19 sites, and increased at 1 site. Abundance of *H. fuscopunctata* increased at one site in the MCA after its establishment, but similar variation was recorded among control sites.

Effect of the MCA on sizes of invertebrates

Using analysis 1, the mean size of *T. niloticus* varied inconsistently through time (before vs. after × groups interaction, $F = 19.25$, $p < 0.0001$, df = 1,128, $n = 33$). Size increased within, and decreased outside, the MCA (Fig. 7*a*). Moreover, before declaration, *T. niloticus* tended to be smaller at the Arnavon Islands, but 3 years after declaration, they were significantly larger inside than outside the MCA. We did not observe recruitment of small juveniles during the study, which would tend to reduce mean size. *Holothuria fuscogilva* also showed a significant interaction between before vs. after and groups ($F = 4.919$, $p = 0.028$, df = 1,136, $n = 35$), i.e., animals tended to be smaller on average after

Table 2. Summary of asymmetrical analysis of variance examining temporal and spatial variation in the abundance of selected taxa and derived variables: (*a*) shallow terrace habitat and (*b*) deep slope habitat.

(*a*) Shallow terrace habitat.

Source of variation	*Tectus pyramis* (L)	*Tridacna maxima* (L)	Total holothurians (L)	*Stichopus chloronotus* (U)
Cochran's C	C = 0.0169, NS	C = 0.0167, NS	C = 0.0211, NS	C = 0.2353**
B × G	NS	NS	NS	NS
B × M vs. C	NS	NS	NS	NS
B × G(C)	NS	NS	NS	NS
B × I(G)	No test	No test	NS	NS
B × I(M)	No test	No test	NS	NS
B × I(G(C))	No test	No test	NS	NS
B × S(I(G))	**	**	NS	NS
B × S(I(M))	NS	*†	NS	NS
B × S(I(G(C)))	**	*	NS	NS
T(B) × G	NS	NS	NS	NS
T(B) × M vs. C				
T(before) × M vs. C				
T(after) × M vs. C	NS	NS	NS	NS
T(B) × G(C)				
T(before) × G(C)				
T(after) × G(C)	NS	NS	NS	NS
T(B) × I(G)	NS	NS	NS	NS
T(B) × I(M)				
T(before) × I(M)				
T(after) × I(M)	NS	NS	NS	NS
T(B) × I(G(C))				
T(before) × I(G(C))				
T(after) × I(G(C))	NS	NS	NS	NS
T(B) × S(I(G))	NS	NS	*	NS
T(B) × S(I(M))				
T(before) × S(I(M))				
T(after) × S(I(M))	NS	NS	***†	NS
T(B) × S(I(G(C)))				
T(before) × S(I(G(C)))				
T(after) × S(I(G(C)))	**	NS	NS	NS
†Two-tailed tests:				
B × S(I(M)) / B × S(I(G(C)))		NS		
T(after) × M / T(before) × M				
T(after) × S(I(M)) / T(before) × S(I(M))			NS	
T(after) × S(I(C)) / T(before) × S(I(C))				

(*b*) Deep slope habitat.

Source of variation	Total holothurians (L)	*Holothuria fuscogilva* (U)	*Holothuria atra* (U)	*Thelanota anax* (U)	*Holothuria fuscopunctata* (U)
Cochran's C	C = 0.0178, NS	C = 0.2308**	C = 0.1536*	C = 0.0937**	C = 0.0975**
B × G	*	NS	NS	NS	NS
B × M vs. C	**	*	NS	NS	NS
B × G(C)	NS	NS	NS	NS	NS
B × I(G)	NS	NS	NS	NS	NS
B × I(M)	NS	NS	NS	NS	NS
B × I(G(C))	NS	NS	NS	*	NS
B × S(I(G))	*	***	NS	***	**
B × S(I(M))	NS	**†	NS	NS	*†
B × S(I(G(C)))	**	***	NS	***	*
T(B) × G	NS	NS	NS	NS	NS
T(B) × M vs. C					
T(before) × M vs. C					
T(after) × M vs. C	NS	NS	**†	NS	NS

Table 2 (*concluded*).

Source of variation	Total holothurians (L)	*Holothuria fuscogilva* (U)	*Holothuria atra* (U)	*Thelanota anax* (U)	*Holothuria fuscopunctata* (U)
T(B) × G(C)					
T(before) × G(C)					
T(after) × G(C)	NS	NS	NS	NS	NS
T(B) × I(G)	NS	NS	NS	NS	NS
T(B) × I(M)					
T(before) × I(M)					
T(after) × I(M)	NS	NS	NS	NS	NS
T(B) × I(G(C))					
T(before) × I(G(C))					
T(after) × I(G(C))	NS	NS	NS	NS	NS
T(B) × S(I(G))	NS	NS	NS	NS	NS
T(B) × S(I(M))					
T(before) × S(I(M))					
T(after) × S(I(M))	NS	*†	***†	NS	NS
T(B) × S(I(G(C))					
T(before) × S(I(G(C)))					
T(after) × S(I(G(C)))	NS	NS	NS	NS	NS
†Two-tailed tests:					
B × S(I(M)) / B × S(I(G(C)))		NS			NS
T(after) × M / T(before) × M			NS		
T(after) × S(I(M)) / T(before) × S(I(M))			**		
T(after) × S(I(C)) / T(before) × S(I(C))		NS	**		

Note: Only terms relevant to determining whether the Arnavon Islands Marine Conservation Area (MCA) has been effective have been presented. See Table 1 for full design. B, before vs. after; T, times; G, group; I, island; S, site; NS, nonsignificant; *, $p < 0.05$; **, $p < 0.01$; ***, $p < 0.001$; U, untransformed data used; L, data $\ln(x + 1)$ transformed. † indicates that a subsequent two-tailed test was required.

declaration of the MCA at the Arnavons, but larger at the controls (Fig. 7*b*). In the period after declaration, mean size inside the MCA was significantly less than mean size outside. We did observe some smaller *H. fuscogilva* in the MCA after declaration. These individuals were ~30 cm and are unlikely to represent a recent settlement of small juveniles. Two other species examined using analysis 1 showed no variation consistent with a reserve effect. *Holothuria atra* ($n = 69$) and *H. fuscopunctata* ($n = 40$) both showed differences in size between the MCA and controls that did not differ through time. *Holothuria atra* were significantly smaller in the MCA (mean = 44.35 cm ± 0.52 cm standard error) than outside (46.34 cm ± 0.49 cm), whereas the reverse occurred for *H. fuscopunctata* (MCA, 48.30 cm ± 0.62 cm; controls, 46.53 cm ± 0.53 cm).

Using analysis 2, the mean size of *T. maxima* showed no effect consistent with declaration of the MCA (Table 3*a*). This was indicated by nonsignificant tests for the asymmetrical components of the analysis. Rather, there was variation among times before declaration that was consistent among groups and significant variation among groups that was consistent through time (Table 3*b*).

Analysis of delta values and calculation of power

The analysis of delta values was generally consistent with the beyond-BACI analyses at the largest spatial scale of the MCA vs. control areas (Table 4). An exception was the abundance of *T. anax*, which indicated more individuals within the MCA relative to the control areas from before to after declaration. The ratios of observed proportional differences between MCA and control areas from before to after declaration were generally quite small, suggesting a relatively small effect after 3 years of closure in the MCA. Post hoc power analysis for nonsignificant variables indicated that a large number of sampling times would have been required to have a good chance of detecting the observed ratios, and that estimates of power were variable among species (e.g., ranging from 0.262 for a 50% change in *Stichopus chloronotus* to 1 for a 25% change in *T. maxima*). Notwithstanding this, the study would have had a reasonable power to detect an even smaller effect for *T. niloticus* (abundance and size) and, in the deep habitat, for abundances of total holothurians, *H. fuscogilva*, and *T. anax*. Although power analyses were used to examine an increase in abundance and (or) size in most species, power was determined for a potential decrease in abundance of *T. pyramis* in the MCA relative to the controls based on the results of the beyond-BACI analysis. Here there would have been a large power to detect a 50% decrease in abundance of *T. pyramis* within the MCA compared with the controls.

Discussion

Effect of MCA on abundance

Commercially harvested marine invertebrates showed a range of responses to establishment of the MCA at the Arnavon Islands, which were evident using beyond-BACI and the comparison of delta values. Overall, the delta values simplified the interpretation of patterns in favour of either no effect or an increase in relative abundance in the MCA. The most notable response was that abundances of some of the most valuable and heavily exploited species (*T. niloticus* and

Fig. 4. *Tridacna maxima.* Mean abundances (± standard error) among sites before (shaded bars) and after (open bars) establishment of the marine conservation area ($n = 18$): (*a*) Arnavon Marine Conservation Area; (*b*) Waghena; (*c*) Ysabel; and (*d*) Suavanao. An asterisk (*) indicates significant difference (Student–Newman–Keuls test, $P \leq 0.05$).

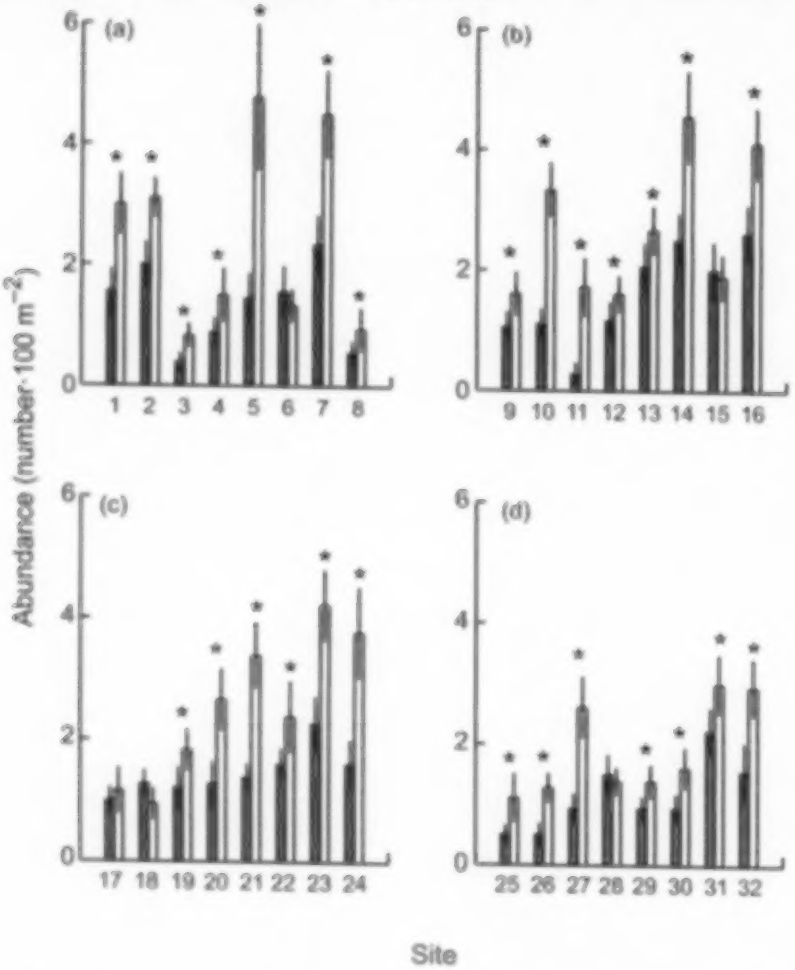

H. fuscogilva) increased in the MCA relative to fished (control) areas. The increase in abundance of *T. niloticus* was most evident at two of the eight sites at the Arnavon Islands. This small-scale variation may be due to (unknown) attributes of the habitat at different sites, variation in recruitment to an observable size, or stochastic processes. Alternatively, there were some reported instances of poaching within the MCA, which may have occurred more frequently at some sites than others, negating the potential benefits of protection. Thus, if social or logistical factors make it difficult to establish large areas for protection of trochus, effective replenishment of stocks may be possible within multiple smaller areas.

The MCA had one of three effects for other species. First, while numbers did not increase in the MCA, the reserve appeared to prevent declines in abundance apparent elsewhere in the region: total holothurians and *T. anax* in the deep habitat were in this category. Analysis of delta values did not identify this effect because the ratio estimator could have changed because of either an increase in the MCA or a decrease elsewhere. We cannot exclude the possibility that the MCA caused a redistribution of harvesting effort to areas outside the MCA, including controls (Halpern et al. 2004). Such an effect may accelerate declines, overemphasizing the benefits of the reserve. We do not consider this to be the case here, however, because the controls were distributed over a large area and the habitats studied were common throughout the general area, but the possibility does stress the need to understand how fishing effort may change after declaration of marine reserves.

Second, the MCA had no effect on abundance for five variables: *Stichopus chloronotus*, abundance of holothurians in the shallow habitat, *T. maxima*, *H. atra*, and *H. fuscopunctata*.

Third, *T. pyramis*, the only nonharvested species studied, appeared to increase at almost half the control sites, but at

Fig. 5. Mean abundances (± standard error) of (*a*) total holothurians in shallow habitat, (*b*) total holothurians in deep habitat, and (*c*) *Holothuria fuscogilva* in the deep habitat among groups before (shaded bars) and after (open bars) establishment of the Arnavon Marine Conservation Area (*n* = 144).

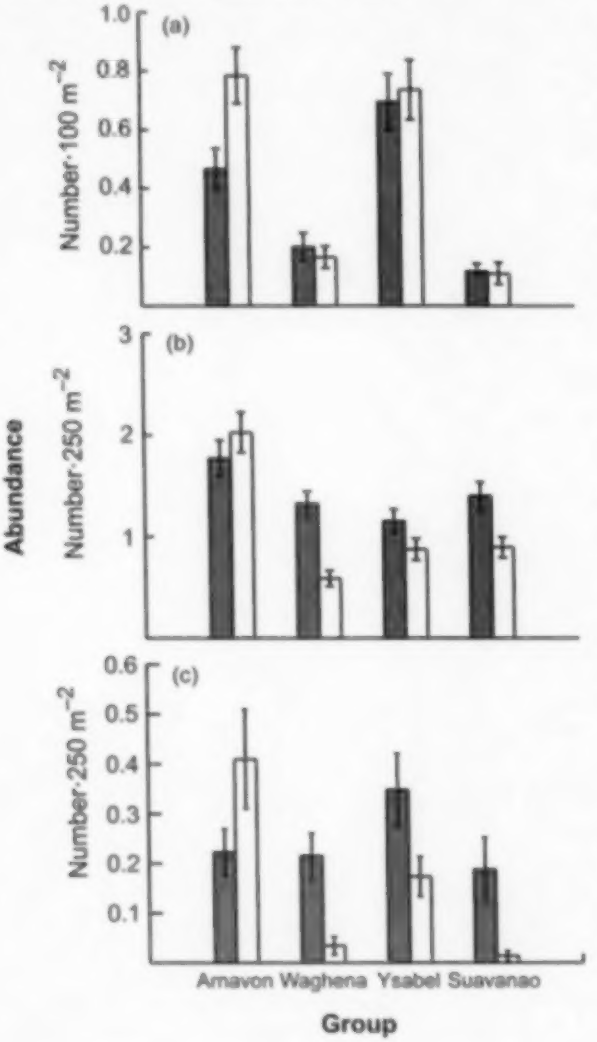

none of the Arnavon sites, suggesting that the MCA may have inhibited an increase in abundance there. One explanation for this pattern may be that *T. niloticus*, which increased in the MCA, limited abundance of *T. pyramis* through competition while depletion of *T. niloticus* at the control areas alleviated competition and allowed abundances of *T. pyramis* to increase. Both species graze on algae, grow to similar sizes, and occupy similar habitats on the reef terrace. Competition between these species remains to be demonstrated, but our results indicate that establishment of reserves to manage exploited species may have indirect effects on nontarget species. Effects on nontarget species occurring in marine reserves have not been examined widely but may occur because of changes in relative abundance of harvested and nonharvested species (e.g., Andrew and MacDiarmid 1991; McClanahan and Arthur 2001).

The lack of increases in abundance within the MCA for several species may mean that marine reserves are inappropriate for managing those species or that longer periods of time are needed for recovery, particularly for holothurians (Uthicke et al. 2004). Meagre spawning success, patchy distributions of larvae, and the size and location of the MCA may interact to reduce the probability of substantial settlement of species with pelagic larval phases. The cryptic nature of juvenile holothurians, which often have diel burrowing cycles and occur in different habitats to the adults (Reichenbach 1999; Mercier et al. 2000), would also reduce the likelihood of detecting a relatively rapid increase in abundance following protection from fishing if juvenile holothurians remained cryptic for several years.

The corollary to limited settlement is that *T. niloticus* and *H. fuscogilva*, which increased in the MCA, were present as cryptic juveniles before declaration or settled during the closure and then grew to a size where they could be seen during the "after" surveys. The smallest holothurians sampled were 100 mm long. Although growth varies among species of holothurians, some species have estimated growth rates of 0.5–1.7 cm·month^{-1} (Shelley 1985; Conand 1986) or 35–533 g·year^{-1} (Uthicke et al. 2004). This suggests that 3 years was sufficient time for newly recruited holothurians to grow to a size where they would be recorded by divers. Similarly, *T. niloticus* can grow to ~8 cm within 3 years (Nash 1993). The smallest *T. niloticus* we sampled were ~6 cm, again suggesting that 3 years was sufficient for recruits that settled at the time of establishment of the MCA to be sighted, though those that settled subsequently may not have been counted.

The time needed for a species to recover from harvesting will depend on factors such as generation time, severity and extent of previous fishing, local oceanographic features, location and size of the reserve, infringement of the reserve, and availability of nursery and adult habitat. Our study suggests that it may take many years to restore each of the target species to preharvest levels, assuming the reserve is an effective mechanism for mediating fishing. In the absence of data on the size of any local remnant unfished populations, comparison of data from the MCA with areas elsewhere in the western Pacific indicates that abundance of *T. niloticus* and *H. fuscogilva* in the MCA were still at the lower end of densities in the region. Three years after closure, densities of *H. fuscogilva* were estimated at 16 individuals·ha^{-1}, which was comparable with density estimates for unfished reefs in the eastern Torres Strait (7–30 individuals·ha^{-1}; Long and Skewes 1997) but well below maximum estimates of 82 individuals·ha^{-1} in Tonga (Preston and Lokani 1990). Uthicke et al. (2004) also suggested that recovery by *Holothuria nobilis* from harvesting could require decades. Although abundance of *T. niloticus* increased to 57 individuals·ha^{-1} in the MCA, this was also below estimates of densities from other areas (62–2016 individuals·ha^{-1}; Long et al. 1993; Nash et al. 1995). Further monitoring is needed to determine if longer closures can lead to densities similar to those found elsewhere in the region. Importantly, the power analyses suggest that the study would have had a good chance of de-

Fig. 6. *Holothuria fuscogilva*. Mean abundance (± standard error) among sites (n = 18) before (shaded bars) and after (open bars) establishment of the marine conservation area: (*a*) the Arnavon Marine Conservation Area; (*b*) Waghena; (*c*) Ysabel; and (*d*) Suavanao. An asterisk (*) indicates significant difference (Student–Newman–Keuls test, $P \leq 0.05$).

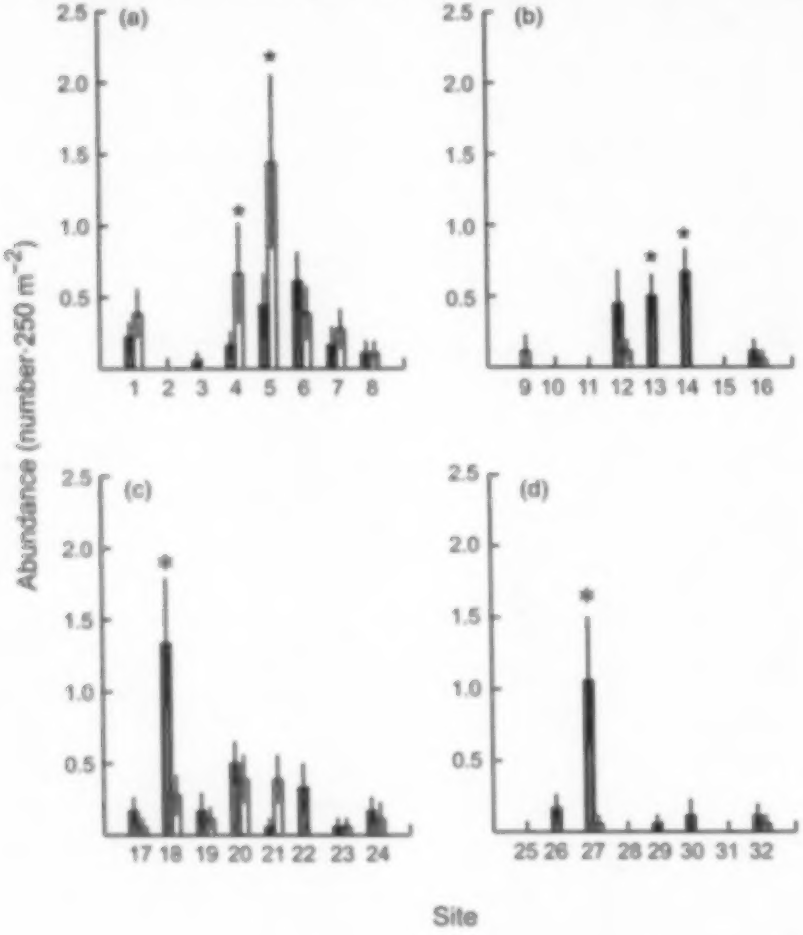

tecting effect sizes comparable with the densities of invertebrates recorded by others.

Effect of MCA on body size of species

The full beyond-BACI design could not be utilized for data on sizes because of limited numbers of individuals available for measurement. Using the reduced designs and the delta values, two of five species showed a change in size consistent with establishment of the reserve. The increase in size of *T. niloticus* meant that, on average, this species exceeded its upper legal size limit (11 cm) and hence had even greater protection because of difficulties in selling large individuals. Conversely, individuals outside the MCA were still within the legal size range but were significantly smaller after 3 years than previously. Thus, overharvesting could ultimately lead to *T. niloticus* outside the MCA being too small to harvest legally, and those within the MCA becoming too large.

The mean size of *H. fuscogilva* increased at the controls after establishment of the MCA, probably because of growth of smaller animals and an apparent lack of recruitment into smaller size classes. Some recruitment of smaller size classes was observed at the Arnavons, suggesting a small (but nonsignificant) decrease in the mean size of animals. Thus, the size distributions of animals may later change in various ways following protection from harvesting. This effect was not detected by analysis of delta values because our original hypothesis was that there would be an increase in size within the MCA. Our data suggest that responses in the size of harvested invertebrates to establishment of the MCA can be expected to be complex, especially where the fisheries are regulated by minimum and maximum size limits.

Advantages and disadvantages of the experimental design

This study has shown that it is possible to design sampling programmes to detect a reserve effect but that the interpretation of results is more complex than assessment of what happens within a reserve — changes must be considered in a regional context. Although the simpler approach to analyzing delta values has appeal at the broader scale of

Fig. 7. Mean size (± standard error) of (*a*) *Trochus niloticus* (n = 33) and (*b*) *Holothuria fuscogilva* (n = 35) at the Arnavon group and control groups (pooled) before (shaded bars) and after (open bars) establishment of the Arnavon Marine Conservation Area. Significant differences between means (Student–Newman–Keuls tests): *, $P \leq 0.05$; **, $P \leq 0.01$.

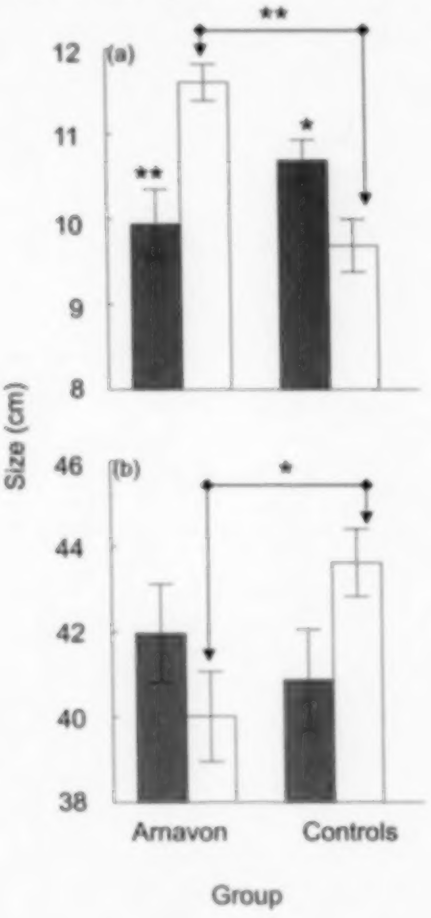

comparing a marine reserve with controls, it has limited value for interpretation and management, although it can provide a good indication of statistical power and effect sizes at the larger scale. Other critical factors affecting the sampling design and interpretation of data include the reason for the declaration of the reserve, duration of the sampling programme, and number of reserves and sites within reserves available for sampling. Our study illustrates this in three ways. First, the experimental design we used was based on the proposition that the term "groups" is a random factor (Eberhardt 1976; Stewart-Oaten and Bence 2001) with respect to the performance indicators selected. This implies that the beyond-BACI design is valid for marine reserves selected according to factors independent of the indicators. In some cases, however, reserves are selected for specific biological attributes, such as the presence of a spawning ground, particularly high biodiversity, etc. Therefore, there will be cases in which selection of a reserve would not be random with respect to performance indicators and an alternative approach is required (see also Willis et al. 2003).

Second, the temporal component of the design entailed three sampling times (spanning <1 year), each before and after declaration of the MCA, with 3 years between. It is unlikely that this relatively short time would be sufficient to establish a time series of change in abundance or size, but the study timing was constrained by external factors, including enlisting local co-operation and acceptance of the closure at the Arnavon Islands and, ultimately, poaching within the MCA resulting from civil strife within Solomon Islands between 1999 and 2002. The former types of constraints are likely to be a feature of the management of many marine reserves. This design, however, provides three replicated estimates of abundance and animal size, which enhances our confidence in the relationship between the Arnavon Islands and the control groups before and after declaration of the MCA. This can be critical where variable environmental conditions (water clarity, sea conditions, etc.) can bias counts among times and where population changes may occur over a short time scale (e.g., recruitment events). Therefore, although it may be desirable to establish a longer time series before declaration (cf. Stewart-Oaten and Bence 2001), there is merit in obtaining samples over shorter time periods, if time is limited.

Finally, the use of asymmetrical ANOVA provided a comprehensive method for testing the effectiveness of the MCA. Even so, the tests sometimes failed to verify strong apparent trends, particularly when the sensitivity of a test within the analytical model was likely to be low. Determining power for terms of interest in complicated asymmetrical designs is difficult, although this issue has been considered for impact studies by modelling with simulated data (Underwood and Chapman 2003). In our study, the calculation of power on the simplified design using delta values gave important insight into effect sizes at the MCA–control scale and may be a useful initial step for management. More broadly, lack of power can be addressed in several ways: (*i*) by increasing spatial replication, (*ii*) by incorporating multiple marine reserves (e.g., Russ 2002), and (*iii*) by including additional periods of sampling. Firstly, in our study, replication could have been increased within sites (i.e., the number of transects) or by increasing the number of sites and (or) control groups. Secondly, if practical, it would be preferable to sample two or more separate marine reserves within one design. This enhances the generality of results and enables the use of different types of design, with replication of both control and reserve treatments. This type of approach may not be possible in many areas for social and logistical reasons but would be useful in large managed areas, such as the Great Barrier Reef, Australia (Campbell et al. 2001). Thirdly, the same design could be used to compare data from the "before" period with three times the sampling taken, say, 6 years "after" declaration. Presumably, if the MCA is successfully enhancing the abundances and sizes of invertebrates, then the effect size will increase (to a limit) over time.

Wherever marine reserves are declared to help sustain fisheries, the key issue for assessing the effectiveness of the reserve for target species is to ensure that the data are ob-

Table 3. Analyses examining the effect of the establishment of the Arnavon Islands Marine Conservation Area on the size of *Tridacna maxima* ($n = 47$): (*a*) asymmetrical analysis of variance and (*b*) Student–Newman–Keuls results for significant terms.

(*a*) Asymmetrical analysis of variance.

Sources of variation	df	MS	*F*	*P*	F vs.
B	1	343.4235	0.8327	0.4131	T(B)
T(B)	4	412.3974	9.0108	<0.0001	T(B) × G
G	3	1039.2307	22.7069	<0.0001	T(B) × G
BG	3	11.0435	0.2413	0.8675	Residual
B × M vs. C	1	0.9941	0.0217	0.8829	Residual
B × C	2	16.0682	0.3511	0.7040	Residual
T(B) × G	12	73.6785	1.6099	0.0830	Residual
T(B) × M vs. C	4	94.4862			
T(before) × M vs. C	2	187.5333			
T(after) × M vs. C	2	1.4390	0.0314	0.9690	Residual
T(B) × among C	8	63.2746			
T(before) × among C	4	112.6054			
T(after) × among C	4	13.9439	0.3047	0.8749	Residual
Residual	1104	45.7672			

(*b*) Student–Newman–Keuls results for significant terms.

Sources of variation	Treatment means			
T(B): before	T1 (22.89±0.54) > T2 (20.58±0.47) = T3 (19.31±0.54)			
T(B): after	T4 (18.63±0.50) = T5 (20.34±0.52) = T6 (20.51±0.48)			
Groups	Waghena	= Suavanao	= Ysabel	<Arnavons
	18.30±0.40	20.07±0.42	20.19±0.40	22.95±0.42

Note: B, before vs. after; T, times; G, groups; C, controls; Cochran's C = 0.0568, $P < 0.05$. In (*b*), the numbers in parentheses represent the mean ± standard error.

Table 4. *t* tests and power analyses comparing the abundance or size (where indicated) of invertebrates in the Arnavon Islands Marine Conservation Area (MCA) with those in the control areas (CA) before and after declaration of the MCA.

Variable	Probability (*t* test)	Observed ratio[a]	*n* for $1 - \beta \geq 0.80$	$1 - \beta$ (25% change)	$1 - \beta$ (50% change)	Ratio for $1 - \beta \geq 0.80$[b]
Shallow habitat						
Trochus niloticus	0.009	2.67	—	—	—	2.10
T. niloticus size	0.018	1.25	—	—	—	1.20
Tectus pyramis[c]	0.254	0.85	10	0.643	0.989	0.65
Tridacna maxima	0.129	1.03	12	1	1	1.08
T. maxima size	0.562	0.98	—[d]	0.673	0.992	1.30
Total holothurians	0.165	1.34	16	0.170	0.390	2.00
Stichopus chloronotus	0.354	1.17	108	0.128	0.262	2.25
Deep habitat						
Total holothurians	0.002	1.30	—	—	—	1.15
Holothuria fuscogilva	0.029	4.49	—	—	—	4.25
H. fuscogilva size	0.923	0.88	—[d]	0.947	1	1.19
Holothuria atra	0.288	1.14	49	0.236	0.572	1.70
H. atra size	0.762	0.97	—[d]	0.999	1	1.11
Thelanota anax	0.012	2.40	—	—	—	1.80
Holothuria fuscopunctata	0.209	1.31	10	0.265	0.641	1.63
H. fuscopunctata size	0.664	0.99	—[d]	1	1	1.08

[a] Observed ratio = ((MCA/CA) after declaration) / ((MCA/CA) before declaration), $n = 3$ times before and after declaration.

[b] Ratio for $1 - \beta \geq 0.80$ = (MCA/CA before declaration) × iteration to achieve required power.

[c] Power calculation based on potential decrease in the MCA relative to the control areas.

[d] Not determined because observed ratio < 1.

tained within a rigorous experimental framework. Recent reviews (Russ 2002; Willis et al. 2003; Sale et al. 2005) suggest that there has not been enough emphasis on this. The use of impact assessment methods provides one such approach by helping managers and communities to understand the complexities of managing marine resources.

Acknowledgments

This project was commissioned through the Great Barrier Reef Marine Park Authority and funded by the Australian Centre for International Agricultural Research. The Nature Conservancy facilitated establishment of the MCA and trained and supported Conservation Officers with assistance from the South Pacific Regional Environmental Program. The Ministry of Forests, Environment and Conservation and the Department of Fisheries and Marine Resources, The Nature Conservancy, and The WorldFish Center, particularly Peter Ramohia, Moses Biliki, Nelson Kile, Ed Mayer, George Meyer, and Rayner Pitt, provided support. A.J. Underwood and T.M. Glasby gave statistical advice. This is WorldFish Center Contribution No. 1575.

References

Andrew, N.L., and MacDiarmid, A. 1991. Interactions between sea urchins and spiny lobsters in northeastern New Zealand. Mar. Ecol. Prog. Ser. **70**: 211–222.

Bergin, T. 1993. Marine and estuarine protected areas (MEPAs) — where did Australia get it wrong? *In* Protection of Marine and Estuarine Areas — a Challenge for Australians: Proceedings of the 4th Fenner Conference on the Environment, 9–11 October 1991, Canberra, Australia. *Edited by* A.M. Ivanovici, D. Tarte, and M. Olson. Australian Committee for IUCN, Canberra. pp. 148–155.

Bohnsack, J.A. 1998. Application of marine reserves to reef fisheries management. Aust. J. Ecol. **23**: 298–304.

Campbell, R.A., Mapstone, B.D., and Smith, A.D.M. 2001. Evaluating large scale experimental designs for management of coral trout on the Great Barrier Reef, Australia. Ecol. Appl. **11**: 1763–1777.

Carr, M.H., and Reed, D.C. 1993. Conceptual issues relevant to marine harvest refuges: examples from temperate reef fishes. Can. J. Fish. Aquat. Sci. **50**: 2019–2028.

Conand, C. 1986. Les resources halieutiques des pays insulaires du Pacifique. Deuxieme partie: Les holothuries. FAO Fisheries Technical Paper No. 272.2. Food and Agricultural Organisation, Rome, Italy.

Dugan, J.E., and Davis, G.E. 1993. Applications of marine refugia to coastal fisheries management. Can. J. Fish. Aquat. Sci. **50**: 2029–2042.

Eberhardt, L.L. 1976. Quantitative ecology and impact assessment. J. Environ. Manag. **4**: 27–70.

Edgar, G.J., and Barrett, N.S. 1997. Short term monitoring of biotic change in Tasmanian marine reserves. J. Exp. Mar. Biol. Ecol. **213**: 261–279.

Garcia-Charton, J.A., and Perez-Ruzafa, A. 1999. Ecological heterogeneity and the evaluation of the effects of marine reserves. Fish. Res. **42**: 1–20.

Green, R.H. 1993. Application of repeated measures designs in environmental impact and monitoring studies. Aust. J. Ecol. **18**: 81–98.

Halpern, B.S., Gaines, S.D., and Warner, R.R. 2004. Confounding effects of the export of production and the displacement of fishing effort from marine reserves. Ecol. Appl. **14**: 1248–1256.

Hilborn, R., Stokes, K., Maguire, J.J., Smith, T., Botsford, L.W., Mangel, M., Orensanz, J., Parma, A., Rice, J., Bell, J., Cochrane, K.L., Garcia, S., Hall, S.J., Kirkwood, G.P., Sainsbury, K., Stefansson, G., and Walters, C. 2004. When can marine reserve areas improve fisheries management? Ocean Coast. Manag. **47**: 197–205.

Keough, M.J., and Mapstone, B.D. 1997. Designing environmental monitoring for pulp mills in Australia. Water Sci. Technol. **35**: 397–404.

Lincoln-Smith, M.P., Bell, J.D., and Mapstone, B.D. 1997. Testing the use of a marine protected area to restore and manage invertebrate fisheries at the Arnavon Islands, Solomon Islands: choice of methods and preliminary results. Proc. 8th Int. Coral. Reef. Symp. (Panama), **2**: 1937–1942.

Long, B., and Skewes, T. 1997. Distribution and abundance of beche-de-mer on Torres Strait reefs. South Pac. Comm. (SPC) Beche-de-mer Information Bull. **9**: 17–22.

Long, B.G., Poiner, I.R., and Harris, A.N.M. 1993. Method of estimating the standing stock of *Trochus niloticus* incorporating Landsat satellite data, with application to the trochus resources of the Bourke Isles, Torres Strait, Australia. Mar. Biol. **115**: 587–593.

Mapstone, B.D. 1995. Scalable decision rules in environmental impact assessment: effect size, Type I, and Type II errors. Ecol. Appl. **5**(2): 401–410.

McClanahan, T.R., and Arthur, R. 2001. The effect of marine reserves and habitat on populations of east African coral reef fishes. Ecol. Appl. **11**: 559–569.

Mercier, A., Battaglene, S.C., and Hamel, J.F. 2000. Settlement preferences and early migration of the tropical sea cucumber *Holothuria scabra*. J. Exp. Mar. Biol. Ecol. **249**: 89–110.

Nash, W. 1993. Trochus. *In* Nearshore marine resources of the South Pacific. *Edited by* A. Wright and L. Hill. Forum Fisheries Agency and Institute of Pacific Studies, Honiara, Solomon Islands and Suva, Fiji. pp. 451–496.

Nash, W.J., Tuara, P., Terekia, O., Munro, D., Amos, M., Legata, J., Mataiti, N., Teopa, M., Whitford, J., and Adams, T. 1995. The Aitutaki trochus fishery: a case study. South Pacific Commission Inshore Fisheries Research Project Technical Document No. 9. South Pacific Commission, Noumea, New Caledonia.

Osenberg, C.W., Schmitt, R.J., Holbrook, S.J., Abu-Saba, K.E., and Flegal, A.R. 1994. Detection of environmental impacts: natural variability, effect size and power analysis. Ecol. Appl. **4**: 16–30.

Parrish, R. 1999. Marine reserves for fisheries management: why not. Calif. Coop. Ocean Fish. Invest. Rep. **40**: 77–86.

Preston, G., and Lokani, P. 1990. Report of a survey of the sea cucumber resources of Ha'apai, Tonga, June 1990. South Pacific Commission, Noumea, New Caledonia.

Reichenbach, N. 1999. Ecology and fishery biology of *Holothuria fuscogilva* (Echinodermata: Holothuroidea) in the Maldives, Indian Ocean. Bull. Mar. Sci. **64**: 103–113.

Richards, A.H., Bell, L.J., and Bell, J.D. 1994. Inshore fisheries resources of Solomon Islands. Mar. Poll. Bull. **29**: 90–98.

Roberts, C.M., and Polunin, V.C. 1991. Are marine reserves effective in management of reef fisheries? Rev. Fish Biol. Fish. **1**: 65–91.

Roberts, C.M., and Polunin, V.C. 1993. Marine reserves: simple solutions to managing complex fisheries? Ambio, **22**: 363–368.

Roberts, D.E., Smith, A.K., Ajani, P., and Davis, A.R. 1998. Rapid changes in encrusting marine assemblages exposed to anthropogenic point-source pollution: a 'Beyond BACI' approach. Mar. Ecol. Prog. Ser. **163**: 213–224.

Russ, G.R. 2002. Yet another review of marine reserves as reef fishery management tools. *In* Coral reef fishes, dynamics and diversity in a complex ecosystem. *Edited by* P.F. Sale. Academic Press (Elsevier Science), San Diego, Calif. pp. 421–443.

Sale, P.F., Cowen, R.K., Danilowicz, B.S., Jones, G.P., Kritzer, J.P., Lindeman, K.C., Planes, S., Polunin, N.V.C., Russ, G.R., Sadovy, Y.J., and Steneck, R.S. 2005. Critical science gaps impede use of no-take fishery reserves. Trends Ecol. Evol. **20**: 74–80.

Schroeter, S.C., Dixon, J.D., Kastendiek, J., and Smith, R.O. 1993. Detecting the ecological effects of environmental impacts: a case study of kelp forest invertebrates. Ecol. Appl. **3**: 331–350.

Schroeter, S.C., Reed, D.C., Kushner, D.J., Estes, J.A., and Ono, D.S. 2001. The use of marine reserves in evaluating the dive fishery for the warty sea cucumber (*Parastichopus parvimensis*) in California, U.S.A. Can. J. Fish. Aquat. Sci. **58**: 1773–1781.

Shelley, C. 1985. Growth of *Actinopyga echinites* and *Holothuria scabra* (Holothuroidea: Echinodermata) and their fisheries potential (as beche-de-mer) in Papua New Guinea. Proc. 5th Int. Coral Reef Congr. Tahiti, **5**: 297–302.

Stewart-Oaten, A., and Bence, J. R. 2001. Temporal and spatial variation in environmental impact assessment. Ecol. Monogr. **71**: 305–339.

Tegner, M.J. 1993. Southern California abalones: can stocks be rebuilt using marine harvest refugia? Can. J. Fish. Aquat. Sci. **50**: 2010–2018.

Underwood, A.J. 1992. Beyond-BACI: the detection of environmental impacts on populations in the real, but variable world. J. Exp. Mar. Biol. Ecol. **161**: 145–178.

Underwood, A.J. 1993. The mechanics of spatially replicated sampling programmes to detect environmental impacts in a variable world. Aust. J. Ecol. **18**: 99–116.

Underwood, A.J. 1997. Experiments in ecology: their logical design and interpretation using analysis of variance. Cambridge University Press, Cambridge, UK.

Underwood, A.J., and Chapman, M.G. 2003. Power, precaution, Type II error and sampling design in assessment of environmental impacts. J. Exp. Mar. Biol. Ecol. **296**: 49–70.

Uthicke, S., Welch, D., and Benzie, J.A.H. 2004. Slow growth and lack of recovery in overfished holothurians on the Great Barrier Reef: evidence from DNA fingerprints and repeated large-scale surveys. Conserv. Biol. **18**: 1395–1404.

Willis, T.J., Millar, R.B., Babcock, R.C., and Tolimieri, N. 2003. Burdens of evidence and the benefits of marine reserves: putting Descartes before des horse? Environ. Conserv. **30**: 97–103.

Threat and decline in fishes: an indicator of marine biodiversity

Nicholas K. Dulvy, Simon Jennings, Stuart I. Rogers, and David L. Maxwell

Abstract: Recent policy commitments aim to reduce biodiversity loss and integrate environmental concerns into fisheries management. However, there are few operational indicators for reporting biodiversity trends and judging progress in relation to management objectives. Here we develop a threat indicator based on the population status of a suite of 23 North Sea fishes from 1982 to 2001 estimated using World Conservation Union (IUCN) Red List decline criteria. The composite indicator was calculated from the weighted average of the threat scores of individual species in each year and varies from 0 to 3, where a score of 3 is equivalent to each species qualifying as "critically endangered". The proportion of threatened fishes, their degree of threat, and the composite indicator value increased steadily over time. The composite indicator value has been >1 since the late 1990s, equivalent to all species meeting the "vulnerable" criterion. A suitable reference trajectory, consistent with the World Summit on Sustainable Development commitment to "achieve by 2010 a significant reduction of the current rate of biodiversity loss" would be a significant reduction in the rate of increase in this indicator before 2010, a limit reference point could be 1 (all species vulnerable) and a target reference point could be 0 (no threatened species).

Résumé : Les engagements récents de la politique de gestion des pêches visent à réduire la perte de biodiversité et à intégrer les préoccupations environnementales dans la gestion. Il existe cependant peu d'indicateurs opérationnels pour décrire les tendances de la biodiversité et pour juger des progrès en fonction des objectifs de gestion. Nous développons ici un indicateur de menace basé sur le statut démographique d'une série de 23 poissons de la mer du Nord de 1982–2001 et estimé à partir des critères de déclin de la liste rouge de l'Union internationale de la conservation de la nature (IUCN). L'indicateur composé se calcule à partir des moyennes pondérées des valeurs de la menace pour chaque espèce individuelle pour chaque année et varie de 0–3; une valeur de 3 équivaut à chacune des espèces atteignant les critères de classification d'espèce gravement menacée. La proportion d'espèces en danger, le degré de menace contre elles et les valeurs de l'indicateur composé augmentent régulièrement au cours des années. L'indicateur composé a atteint une valeur >1 depuis la fin des années 1990, ce qui équivaut à toutes les espèces ayant atteint les critères de classification d'espèce vulnérable. Une trajectoire de référence appropriée, en accord avec les engagements du Sommet mondial sur le développement durable d'« atteindre avant 2010 une réduction significative du taux actuel de perte de biodiversité », serait une réduction significative du taux de croissance de cet indicateur avant 2010; un point de référence limite pourrait être une valeur de 1 (toutes les espèces vulnérables) et un point de référence cible pourrait être 0 (aucune espèce menacée).

[Traduit par la Rédaction]

Introduction

There are a number of national, regional, and international policy commitments to halt or reduce the rate of marine biodiversity loss by 2010 (Sainsbury and Sumaila 2003; Rogers and Greenaway 2005). The main threat to marine biodiversity is exploitation, which has resulted in population declines and extinctions, habitat degradation, and ecosystem changes (Jackson et al. 2001; Hutchings and Baum 2005; Myers and Worm 2005). Because fishing is a recognised cause of biodiversity loss, indicators of marine biodiversity are needed to support conservation and fisheries management (Rice 2003; Cury and Christensen 2005; Hutchings and Baum 2005). One option for developing an indicator of the biodiversity status of marine fishes is to tally up the number of species or populations that are listed as threatened, by all threat-listing schemes or one specific scheme, in any given region and year. This is the basis of the latest terrestrial threat indicators. The state and rate of change in terrestrial biodiversity is provided by World Conservation Union (IUCN) Red List indicators for birds, mammals, and amphibians (Baillie et al. 2004; Butchart et al. 2004). The development of a similar Red List indicator for marine species is not well advanced because the threat status of all marine species has not been comprehensively surveyed. Although this is due mainly to the magnitude of the task, fishes alone comprising

Received 9 May 2005. Accepted 22 December 2005. Published on the NRC Research Press Web site at http://cjfas.nrc.ca on 26 April 2006.
J18691

N.K. Dulvy,[1] S. Jennings, S.I. Rogers, and D.L. Maxwell. Centre for Environment, Fisheries and Aquaculture Science, Lowestoft Laboratory, Lowestoft, NR33 0HT, UK.

[1] Corresponding author (e-mail: nick.dulvy@cefas.co.uk).

doi:10.1139/F06-035

Table 1. Age of maturity of the species included in the analysis.

Common name	Species	Age at maturity	Reference
Starry ray	*Amblyraja radiata*	5†	Walker 1998
Wolf fish	*Anarhichas lupus*	6*	Maxwell and Jennings 2005
Grey gurnard	*Eutrigla gurnardus*	3*	Maxwell and Jennings 2005
Cod	*Gadus morhua*	3.8*	Maxwell and Jennings 2005
Tope	*Galeorhinus galeus*	9*	Maxwell and Jennings 2005
Witch	*Glyptocephalus cynoglossus*	5.5†	Muus and Neilsen 1999
Long rough dab	*Hippoglossoides platessoides*	2.6*	Maxwell and Jennings 2005
Cuckoo ray	*Leucoraja naevus*	8*	Maxwell and Jennings 2005
Dab	*Limanda limanda*	2.3*	Maxwell and Jennings 2005
Angler fish	*Lophius piscatorius*	4.5*	Maxwell and Jennings 2005
Haddock	*Melanogrammus aeglefinus*	2.5*	Maxwell and Jennings 2005
Whiting	*Merlangius merlangus*	1.5*	Maxwell and Jennings 2005
Hake	*Merluccius merluccius*	3.8*	Maxwell and Jennings 2005
Lemon sole	*Microstomus kitt*	4.5†	Muus and Neilsen 1999
Common ling	*Molva molva*	5.5†	Cohen et al. 1990; Deniel 1990
Plaice	*Pleuronectes platessa*	2.5*	Maxwell and Jennings 2005
Saithe	*Pollachius virens*	4.7*	Maxwell and Jennings 2005
Thornback ray	*Raja clavata*	10*	Maxwell and Jennings 2005
Spotted ray	*Raja montagui*	8*	Maxwell and Jennings 2005
Turbot	*Scophthalmus maximus*	6*	Maxwell and Jennings 2005
Brill	*Scophthalmus rhombus*	5†	Froese and Pauly 2005
Sole	*Solea solea*	2.5*	Denney et al. 2002
Spurdog	*Squalus acanthias*	6.5*	Maxwell and Jennings 2005

*Female age at 50% maturity.

†Sex and details of maturity stage were unknown.

half of all vertebrate species, the process may also have been delayed by ongoing debates about the validity of applying threat criteria to marine species (Hutchings 2001; Dulvy et al. 2003; Baillie et al. 2004).

Threat listings of terrestrial species, particularly birds and mammals, have been in place for some time, providing a time series that can be used to assess rate of change in aspects of terrestrial biodiversity (Butchart et al. 2004). Even if a comparable marine threat listing process were put in place now, it would take time to apply it comprehensively, and it would only provide the first data point in the time series necessary to assess the change in marine biodiversity. In the absence of capacity to assess the status of all marine species, or a suitable random sample, one option is to focus solely on fish. There are good reasons for focussing on fish: they comprise a large proportion of the biomass in marine ecosystems, their patterns of diversity are representative of other taxa, they provide ecosystem services to humans, and they show clear responses to fishing (Callaway et al. 2002; Rice 2003).

One possible approach to developing a biodiversity indicator is to assess threat for an assemblage of marine species for which time-series abundance data already exist. Fish species-abundance data are routinely collected to support existing fisheries management activities and can be used to provide descriptions of threat for marine fishes (Dulvy et al. 2005; Maxwell and Jennings 2005). Although a threat index derived from species-abundance data collected on trawl surveys will not provide a representative measure of marine biodiversity in the survey area, it does capture aspects of biodiversity about which society is concerned (Jennings 2004, 2005). This is broadly the sense in which the Red List indices for birds, mammals, and amphibians are already used to report on the state of the world's biodiversity, and they provide a pragmatic way of informing society about changing patterns of biodiversity (Butchart et al. 2004, 2005).

Declines of many vulnerable species occurred before the start of fisheries survey time series, and the application of decline criteria to survey data may underestimate the level of threat (Hutchings and Baum 2005). Moreover, if decline criteria are applied at any point in time and the last 10 years or three generations worth of data are used to assess decline, then threat will be underestimated for species that underwent major declines before this period and (or) that have become so scarce that the statistical power of surveys to detect contemporary trends is poor (Maxwell and Jennings 2005). These are examples of the shifting baseline effect, where the baseline represents an increasingly exploited state over time and may mask the true magnitude of fishing effects on biodiversity (Pauly 1995; Baum and Myers 2004; Sáenz-Arroyo et al. 2005).

Here we develop a biodiversity indicator for assessing and reporting the threat status of a suite of marine fishes. We assess threat for each species over time by applying the IUCN A1 decline criteria to fisheries-independent survey abundance data and derive a composite threat indicator based on the weighted average of species threat scores. To assess the effects of shifting baselines on the indicator, we determine how changes in the time window (survey years) used to calculate the indicator affect trends in the biodiversity indicator and the assumed status of the suite of fishes.

Materials and methods

We used the North Sea English groundfish survey data to assess changes in abundance and threat status of adult fishes. Currently, a survey grid of 75 stations is fished annually. Stations were fished with a Granton demersal trawl until 1991, but from 1992, a Grand Ouverture Verticale (GOV) demersal trawl was used. Tow duration for up to 1991 was 60 min, but for 1992 onwards, the tow duration was 30 min (B. Harley, Centre for Environment, Fisheries and Aquaculture Science (CEFAS), Lowestoft, Suffolk NR33 0HT, UK, personal communication). The Granton trawl gear was fitted with a cod-end liner of 14 mm stretched mesh and the GOV trawl was fitted with a cod-end liner of 20 mm stretched mesh. Both gears were towed at a speed of approximately 4 knots. All fishes caught were identified and measured. Catch rates were raised to number of individuals caught per 60 min tow. Not all stations in the survey grid are fished every year because of poor weather, equipment damage, or ship failure, and in the earlier surveys, more stations were sometimes surveyed (for more details see Maxwell and Jennings 2005).

Species were excluded if they were known to be poorly sampled by the gear, rare, or found in peripheral North Sea habitats and had a maximum length of <40 cm (Sparholt 1990; Knijn et al. 1993; Maxwell and Jennings 2005). Specifically, species were excluded if <150 individuals had been caught in the history of the survey, or if morphology, behaviour, and habitat preference were expected to lead to very low and variable catchability. Individuals <40 cm have increased in abundance in recent years, possibly as a result of the depletion of their larger predators, so we restricted this analysis to species with a maximum size greater than 40 cm total length (Daan et al. 2005). The 23 species retained for analysis were representative of the breadth of morphology, life histories, ecology, and taxonomic diversity of the larger bottom-dwelling fishes sampled on the English groundfish survey in the North Sea. The average age of maturity of all species in this suite of fishes was 4.9 years (Table 1.)

Threat was assessed using IUCN A1 decline criteria, which are based on the reduction in population size over the greater of 10 years or three generations in which causes are reversible, understood, and have ceased (IUCN 2004). The qualifying decline thresholds are "critically endangered" (≥90% decline), "endangered" (≥70% decline), and "vulnerable" (≥50% decline). Adult abundance estimates were $\log(x + a)$ transformed, where a was defined as one-half the minimum nonzero abundance value in the time series (Venables and Ripley 2002).

We measured threat retrospectively over the time series using two methods of measuring the change in adult numbers between two points in time: rate of decline and extent of decline. The rate of decline was estimated using subsets of the annual abundance data, as determined by a "moving window". A least squares linear model was fitted to a moving window spanning x years (we chose windows of 10 and 15 years) to represent the qualifying time spans used for measuring decline in the IUCN Red List A1 decline criteria. Fifteen years is approximately equivalent to three generations for the fishes considered here (Table 1). Specifically, the linear model was fit to the first x years of data, $t_1 - t_{1+x}$, and to each successive year, i.e., $t_2 - t_{2+x}$, $t_3 - t_{3+x}, \ldots, t_{\text{maximum}-x} - t_{\text{maximum}}$. Thus model fits and the estimates of percent change in abundance are determined by the span of the moving window and its placement in the time series. The extent of decline was calculated by comparing subsequent changes in adult abundance with a fixed start date of 1982. A linear model was fit to the first 10 years of data, $t_1 - t_{10}$, and to each successive year, i.e., $t_1 - t_{11}$, $t_1 - t_{12}, \ldots, t_1 - t_{\text{maximum}}$. The percent change in adult abundance was calculated from the start (t_1) and end (t_{10} to t_{maximum}) abundances as predicted from the least squares linear model fit (IUCN 2004).

Species that had met one of the decline criteria in any year of the time series and were thus identified as threatened were not delisted (categorized as not threatened) unless their numerical abundance had increased beyond a preset threshold. As an example, we chose a preset threshold of the mean catch rate averaged over the first 3 years of the time series. We chose the average of the first 3 years to minimize the

Fig. 1. Change in combined abundance of 23 large North Sea fishes over time: (*a*) average abundance ($\log_{10}$ numbers·h^{-1}); (*b*) differences in abundance between one year and the next ($\log_{10}$ numbers·h^{-1}); and (*c*) differences in abundance rescaled as a proportion of average abundance of the corresponding years ($\log_{10}$ numbers·h^{-1}). The vertical line indicates the year that the survey gear and tow length changed.

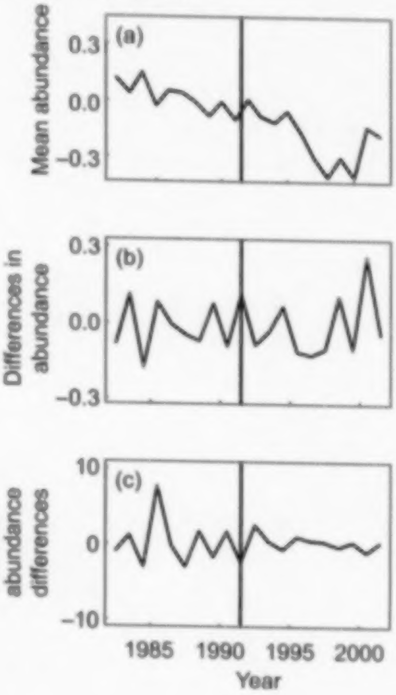

Fig. 2. Box-and-whisker plots of the distribution of the number of years of monitoring required to detect varying declines rates for two levels of power ($1 - \beta = 0.6$ and 0.8) and significance ($\alpha = 0.05$ and 0.3) across species. The dotted horizontal line denotes the qualifying time frames of (*a*, *b*, *c*) 10 years and (*c*, *d*, *e*) 15 years: (*a*) 10-year decline with $1 - \beta = 0.8$ and $\alpha = 0.05$; (*b*) 10-year decline with $1 - \beta = 0.8$ and $\alpha = 0.3$; (*c*) 10-year decline with $1 - \beta = 0.6$ and $\alpha = 0.05$; (*d*) 15-year decline with $1 - \beta = 0.8$ and $\alpha = 0.05$; (*e*) 15-year decline with $1 - \beta = 0.8$ and $\alpha = 0.3$; and (*e*) 15-year decline with $1 - \beta = 0.6$ and $\alpha = 0.05$.

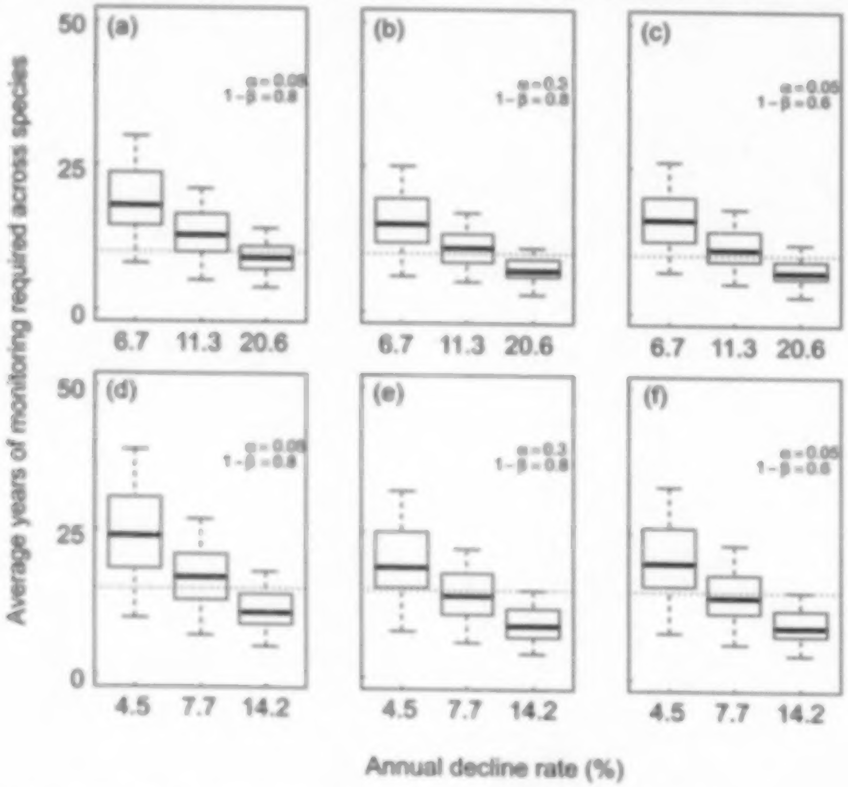

influence of exceptionally high or low abundance estimates in any given year.

The composite threat indicator was calculated for each year as the weighted average of species threat scores. Individual species threat categorisations were weighted as vulnerable = 1, endangered = 2, and critically endangered = 3, following Butchart et al. (2004), and allocated to the final year of the period over which the decline was measured. Species declining at increasing rates will increase in contribution to the threat index as their status worsens from vulnerable to critically endangered. A composite threat indicator was calculated as the weighted average threat score of all species for each year. This indicator is readily interpreted because the scores can vary from 0 to 3, such that a score of 0 is equivalent to no species meeting any of the threat criteria and a score of 3 is equivalent to each species being critically endangered.

We explored the power to detect trends in adult numbers underlying the individual threat assessments. The power analysis assumes an overall nonspecified smooth trend for 1982–2002 followed by declining trend, *q*, beginning in 2003 and lasting for *T* years (Nicholson and Fryer 1992; Maxwell and Jennings 2005). The number of years (*T*) required to detect a specified declining trend (*q*) were calculated based on the observed variance (ψ^2), specified significance (α), and power ($1 - \beta$). The IUCN A1 criteria qualifying decline rates of 50%, 70%, and 90% over 10 or 15 years were converted to annual decline rates (*q*) using $q = 1 - (1 - d)^{(1/n)}$, where *d* is the proportional decrease over *n* years (Maxwell and Jennings 2005). Variance (ψ^2) was calculated for adult abundance using a difference-based method (Gasser et al. 1986; Nicholson and Jennings 2004). When assessing threat, it can be reasonably argued that the cost of not correctly identifying a threatened species (which is actually at high risk of extinction) may be higher than the cost of raising a false alarm (resulting in unnecessary management action), so we considered a range of type I error rates up to 0.30 (Peterman and M'Gonigle 1992; Maxwell and Jennings 2005).

Results

The average adult abundance of this suite of 23 large North Sea demersal fishes declined by 34% over the 21 years since 1983 (Fig. 1*a*). There was no evidence for a large effect of the change in survey gear or tow time on composite abundance (Figs. 1*b*, 1*c*). The greatest year-to-year differences in abundance were at the start of the time series and decreased over time. The year-to-year differences (Fig. 1*b*) and differences expressed as a proportion of average abundance

Fig. 3. Species threat scores in each year measured as (*a*) rate of decline with a 10-year window, (*b*) rate of decline with a 15-year window, and (*c*) extent of decline. Species are plotted in descending rank order of body size, with smallest species at the top. Point size is proportional to threat scores, with the largest, intermediate, and smallest symbols representing declines over the qualifying time of ≥90%, ≥70%, and ≥50%, respectively.

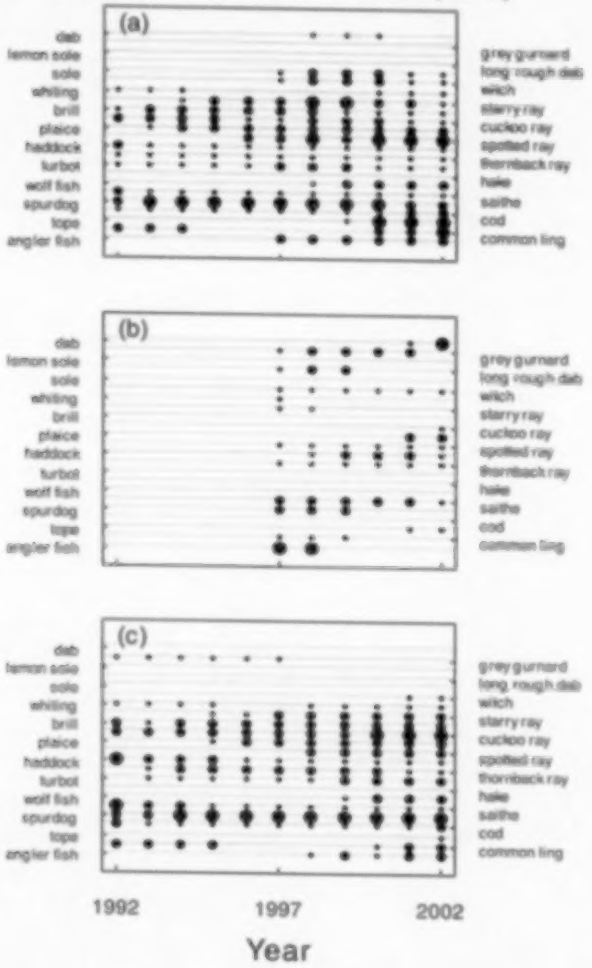

(Fig. 1*c*) spanning the survey changes in 1991–1992 are comparable to those in other years.

When averaged across species, the number of years of monitoring required to detect significant declines was usually longer than the qualifying time frame (Fig. 2). The qualifying time frame used was the longer of 10 years or 15 years, approximately three generations. Only the steepest annual declines >14.2% were detected within the qualifying time frames with high power ($1 - \beta = 0.8$) and significance ($\alpha = 0.05$) (Figs. 2*a*, 2*d*). Lower declines rates can be detected by accepting lower significance ($\alpha \leq 0.3$; Figs. 2*b*, 2*e*) or lower power ($1 - \beta \leq 0.6$; Figs. 2*c*, 2*f*).

Large-bodied species, including wolfish, cod, rays, and spurdog, consistently met one of the threat criteria (Fig. 3). The rate of decline criteria resulted in previously threatened species becoming less threatened toward the end of the time series (Figs. 3*a*, 3*b*). However, when using the extent of decline criteria, the number of threatened species and the degree of threat increased over time (Fig. 3*c*). The proportion of species declining by ≥70% and ≥50% and qualifying as endangered and vulnerable increased over time (Fig. 4). The proportion of endangered species increased to a peak and subsequently declined, and the proportion of vulnerable species increased before reaching a plateau for the rate of decline criteria (Figs. 4*a*, 4*b*). There is a continuing increase in the proportion of vulnerable and endangered species for the extent of decline criteria (Fig. 4*c*). There is a slight but highly variable increase in the number of species declining by ≥90% meeting the critically endangered criterion, with few (~5%) species qualifying (Figs. 4*a*–4*c*).

Fig. 4. Proportion of North Sea fishes meeting each of the three IUCN threatened categories (critically endangered, dotted line; endangered, broken line; and vulnerable, solid line), measured as (*a*) rate of decline with a 10-year window, (*b*) rate of decline with a 15-year window, and (*c*) extent of decline.

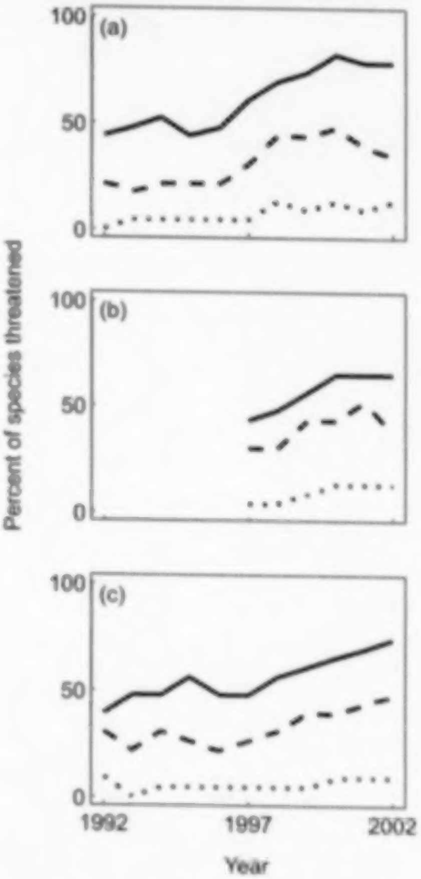

The composite threat score increased from ~0.7 in the early 1990s to a peak of >1 in the late 1990s (Fig. 5). The rate of decline criteria exhibited a peak and subsequent decline in threat score (Figs. 5*a*, 5*b*). The extent of decline criteria showed consistent year-on-year increases in threat score

Fig. 5. An indicator of threat over time for a suite of North Sea demersal fishes measured as (*a*) rate of decline with a 10-year window, (*b*) rate of decline with a 15-year window, and (*c*) extent of decline. The score can range from 0 to 3, and a score of 1 is equivalent to each species meeting the vulnerable criterion and is indicated with a dotted line.

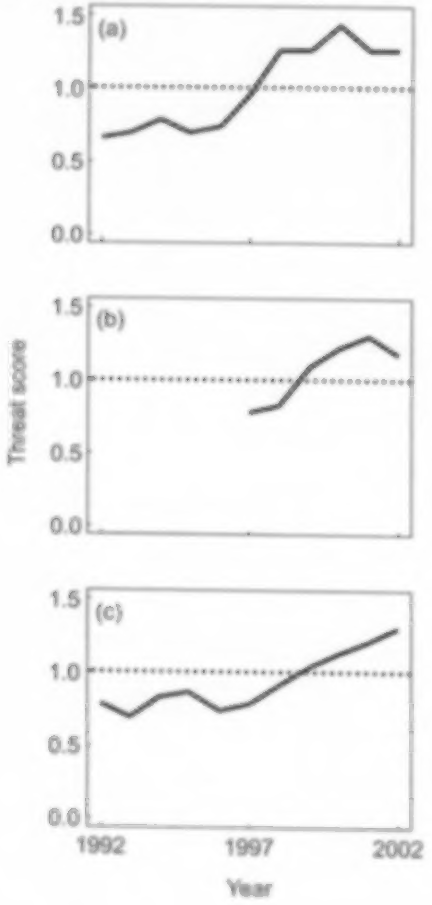

until the end of the time series (Fig. 5*c*). Rate of decline criteria differed in the timing of peak threat, and this peak was lower and increasingly delayed as a result of longer time windows (Figs. 4*a*, 4*b*), and this lag is reflected in the composite threat score (Figs. 5*a*, 5*b*).

Discussion

We have described a composite threat indicator based on year-on-year changes in the weighted average of individual species threat status. The proposed composite marine biodiversity indicator responds to changes in the proportion of threatened species in a specified fish assemblage. The indicator provides information on trends in aspects of biodiversity regarded as important by society and has potential to inform on progress toward management objectives. Because it is calculated from species size abundance survey data, it could be adopted immediately in many regions. This is fortuitous when political commitments to the introduction of an ecosystem approach have been rapid, but the development of a supporting science base has been relatively slow (Fulton et al. 2005; Rice 2005).

Values for the composite indicator were determined from trends in trawl survey catch per unit effort (CPUE) data but could equally be calculated using abundance estimates from stock assessments, underwater visual census, and other types of surveys. All the abundance estimates will be subject to some bias. In the case of trawl survey CPUE, distribution–abundance relationships (MacCall 1990) and changes in distribution due to climate change (Beare et al. 2004; Perry et al. 2005) are two processes that reduce the correlation between CPUE and true abundance. However, CPUE data are the only available measures of abundance for most fish species and bias can be reduced by basing the composite index on CPUE trends in a suite of species with distribution centres in the survey area.

In the North Sea, the overall abundance of the suite of species declined by ~34%. This relatively modest decline belies a high degree of threat for individual species. The composite threat indicator suggests that, on average, all species were threatened from the late 1990s onwards. This reiterates previous work that suggested that combining abundance trends of a number of species masks potentially important biodiversity issues (Dulvy et al. 2000). To support effective reporting and management decision making, the composite threat indicator should respond to signal rather than noise (Rice 2003; Rice and Rochet 2005). However, when assessing threat, the cost of not correctly identifying a threatened species (high risk of extinction) may be higher that the cost of raising a false alarm (unnecessary management action). Only the steepest declines were detected within the qualifying time frames when a type I error rate of 0.05 was accepted, but when this rate was increased to 0.30, then most declines were detected. Following Peterman and M'Gonigle (1992), we argue that a higher type I error rate, in this case 0.30 (falsely reporting a decline when one has not occurred on 30% of occasions) can be accepted when detecting declines and is consistent with the precautionary approach. If high type I error rates were unacceptable to users, then the indicator could be derived from the proportion of species undergoing the steepest declines (≥90%) in the qualifying time period. However, trends in the proportion of these (critically endangered) species are weak and highly variable, and an indicator based solely on the highest decline threshold may be unreliable or uninformative. Instead we suggest that the trends in each of the three threat categories be used to interpret the composite indicator, rather than be used as indicators. These component threat trends may be more informative if applied to surveys that yield less variable abundance estimates. Ultimately, the degree of acceptance of higher type I error rates and therefore the risk of unnecessary action (Di Stephano 2003) will be based on societal perceptions of risk, and one of the few aspects of marine biodiversity that policy makers have consistently emphasised is the risk of biodiversity loss (World Summit on Sustainable Development (WSSD) 2002). Moreover, nonsignificant trends in abundance can be informative (Jennings et al. 1998), and fish species have been shown to be threatened in the absence of suitable data for statistical treatment (Musick et al. 2000; Dulvy et al. 2003; Sadovy and Cheung 2003).

We suggest that the extent of decline method be used to assess the change in threat status and the composite indicator over time for two reasons. The extent of decline has the advantage of using all available data from the start of the time series to the year in which the indicator is calculated (IUCN 2004). Any threat indicator based on this method not only would minimise the influence of natural variability, but also would be consistent with the IUCN Red List guidelines. Thus species meeting one of the criteria as applied here could be considered for listing. Indeed, some of the species receiving high threat scores are already listed as threatened by the IUCN Red List, e.g., tope, spurdog, and cod (Baillie et al. 2004). The other key benefit of using the extent of decline method is that the decline is measured relative to abundance in the early years of the survey. This avoids the bias introduced by shifting baselines during the survey period, as occurs with the rate of decline method.

A possible disadvantage of using extent of decline is that the composite indicator may be biased against detecting genuine population recovery; however, our use of a delisting criterion safeguards against this problem. We delisted species once they recovered to the abundance (average catch rate) observed at the beginning of the time series. For assessed populations, standard assessment models could be used to calculate a more realistic baseline, based on the theoretical abundance in the absence of fishing mortality (Quinn and Deriso 1999).

Neither the decline methods used nor the data presented describe the dramatic reductions in abundance or regional extinctions of some North Sea species before 1982. Species thus affected include common sturgeon (*Acipenser sturio*), common skate (*Dipturus batis*), white skate (*Rostroraja alba*), long-nose skate (*Dipturus oxyrhinchus*), angel shark (*Squatina squatina*), northern bluefin tuna (*Thunnus thunnus*), and Atlantic halibut (*Hippoglossus hippoglossus*) (Brander 1981; Walker and Hislop 1998; Baillie et al. 2004). The disappearance of most of these species was identified using informal methods, such as historic and present-day comparisons of species lists or catch rates, and traditional knowledge (Quero 1998; Rogers and Ellis 2000; Wolff 2000). Although it would be possible to include some of these demersal species in the composite threat indicator, both to highlight their status and to allow for the effects of future recovery, such recovery is unlikely in the medium term. So, unless these species do start to reappear in research surveys, we suggest that lists of threatened species could be reported alongside the composite indicator, thereby avoiding reports of biodiversity change that are biased by the shifting baseline syndrome (Pauly 1995).

The composite threat indicator is a higher-level indicator and cannot directly guide management action. Moreover, although fishing has had a pervasive long-term impact on the overall abundance of large fishes in the North Sea (Jennings and Blanchard 2004), the abundance of individual species also responds to climate change, ecological interactions, and changes in primary production (Beaugrand et al. 2002; Brander 2005). Management to meet biodiversity targets would require that the species responsible for trends in the composite indicator be identified, as these species may need to be managed individually, in small groups, and (or) by region given the large spatial extent of the North Sea and the diverse fisheries that operate there.

Reference points, trajectories, or directions are used to relate the values of indicators to management objectives (Caddy and Mahon 1995; Jennings and Dulvy 2005; Link 2005). We suggest that a suitable reference trajectory would be a significant reduction in the rate of increase of the composite indicator before 2010. This is consistent with policy commitments to achieve a significant reduction in the rate of loss of biodiversity by 2010 (WSSD 2002). Limit and target reference points are more difficult to define from a policy perspective, but we suggest that a biologically defensible limit reference point for the composite threat indicator is a score of 1. This is based on previous findings that fish species qualifying as threatened under IUCN A1 decline criteria are also outside the safe biological abundance limits defined by stock assessment scientists (Dulvy et al. 2005). This suggested limit reference point has been exceeded by the threat index since the late 1990s, and the interpretation would be that on average all 23 species are overexploited. The most stringent target reference point would be a value of zero, if threat and extinction risk were regarded as unacceptable. However, even in the absence of fisheries exploitation, it may not be ecologically feasible to have no declining species in a community that is also affected by ecological interactions and environmental variation and change, and this target might be aspirational rather than realistic. Pragmatically, a less stringent but arbitrary target reference point of 0.25 or 0.5 could be set. These values would correspond to one-quarter (8 species) or one-half (15 species) of the suite of fishes qualifying as vulnerable (i.e., population decline rate between ≥50% and <70% over 10 years). Ultimately, the selection of the target would best be based on an assessment of the number of species that might be expected to be undergoing decline at any point in time as the result of factors other than fishing (Myers and Worm 2005).

Acknowledgements

The UK Department of Environment, Food and Rural Affairs funded this research (MF0729, AE 1148). We thank two anonymous referees for their constructive comments.

References

Baillie, J.E.M., Hilton-Taylor, C., and Stuart, S. 2004. 2004 IUCN Red List of Threatened Species: a global species assessment. World Conservation Union (IUCN), Gland, Switzerland, and Cambridge, UK.

Baum, J.K., and Myers, R.A. 2004. Shifting baselines and the decline of pelagic sharks in the Gulf of Mexico. Ecol. Lett. **7**: 135–145.

Beare, D.J., Burns, F., Greig, A., Jones, E.G., Peach, K., Kienzle, M., McKenzie, E., and Reid, D.G. 2004. Long-term increases in prevalence of North Sea fishes having southern biogeographic affinities. Mar. Ecol. Prog. Ser. **284**: 269–278.

Beaugrand, G., Reid, P.C., Ibanez, F., Lindley, J.A., and Edwards, M. 2002. Reorganization of North Atlantic marine copepod biodiversity and climate. Science (Washington, D.C.), **296**: 1692–1694.

Brander, K. 1981. Disappearance of common skate *Raia batis* from Irish Sea. Nature (London), **290**: 48–49.

Brander, K.M. 2005. Cod recruitment is strongly affected by climate when stock biomass is low. ICES J. Mar. Sci. **62**: 339–343.

Butchart, S.H.M., Stattersfield, A.J., Bennun, L.A., Shutes, S.M., Akçakaya, H.R., Baillie, J.E.M., Stuart, S.N., Hilton-Taylor, C., and Mace, G.M. 2004. Measuring global trends in the status of biodiversity: red list indices for birds. PLoS Biology, **2**: e383.

Butchart, S.H.M., Stattersfield, A.J., Baillie, J., Bennun, L.A., Stuart, S.N., Akçakaya, H.R., Hilton-Taylor, C., and Mace, G.M. 2005. Using red list indices to measure progress towards the 2010 target and beyond. Phil. Trans. R. Soc. Lond. B, **360**: 255–268.

Caddy, J.F., and Mahon, R. 1995. Reference points for fisheries management. Food and Agriculture Organisation, FAO Fisheries Technical Paper No. 347, Rome, Italy.

Callaway, R., Alsvåg, J., de Boois, I., Cotter, J., Ford, A., Hinz, H., Jennings, S., Krönke, I., Lancaster, J.E., Piet, G.J., Prince, P., and Ehrich, S. 2002. Diversity and community structure of epibenthic invertebrates and fish in the North Sea. ICES J. Mar. Sci. **59**: 1199–1214.

Cohen, D.M., Inada, T., Iwamoto, T., and Scialabba, N. 1990. Gadiform fishes of the world (Order Gadiformes). An annotated and illustrated catalogue of cods, hakes, grenadiers and other gadiform fishes known to date. Food and Agriculture Organisation, FAO Fisheries Synopsis 10 (125), Rome, Italy.

Cury, P., and Christensen, V. 2005. Quantitative ecosystem indicators: introduction. ICES J. Mar. Sci. **62**: 307–310.

Daan, N., Gislason, H., Pope, J.G., and Rice, J. 2005. Changes in the North Sea fish community: evidence of indirect effects of fishing? ICES J. Mar. Sci. **62**: 177–188.

Deniel, C. 1990. Comparative study of growth of flatfishes on the west coast of Brittany. J. Fish Biol. **37**: 149–166.

Denney, N.H., Jennings, S., and Reynolds, J.D. 2002. Life history correlates of maximum population growth rates in marine fishes. Proc. R. Soc. Lond. B, **269**: 2229–2237.

Di Stephano, J. 2003. How much power is enough? Against the development of an arbitrary convention for statistical power calculations. Funct. Ecol. **17**: 707–709.

Dulvy, N.K., Metcalfe, J.D., Glanville, J., Pawson, M.G., and Reynolds, J.D. 2000. Fishery stability, local extinctions and shifts in community structure in skates. Conserv. Biol. **14**: 283–293.

Dulvy, N.K., Sadovy, Y., and Reynolds, J.D. 2003. Extinction vulnerability in marine populations. Fish Fish. **4**: 25–64.

Dulvy, N.K., Jennings, S.J., Goodwin, N.B., Grant, A., and Reynolds, J.D. 2005. Comparison of threat and exploitation status in Northeast Atlantic marine populations. J. Appl. Ecol. **42**: 883–891.

Froese, R., and Pauly, D. 2005. FishBase. Available at www.fishbase.org.

Fulton, E.A., Smith, A.D.M., and Punt, A.E. 2005. Which ecological indicators can robustly detect effects of fishing? ICES J. Mar. Sci. **62**: 540–551.

Gasser, T., Sroka, L., and Jennen-Steinmetz, C. 1986. Residual variance and residual pattern in nonlinear regression. Biometrika, **73**: 625–633.

Hutchings, J.A. 2001. Conservation biology of marine fishes: perceptions and caveats regarding assignment of extinction risk. Can. J. Fish. Aquat. Sci. **58**: 108–121.

Hutchings, J.A., and Baum, J.K. 2005. Measuring fish biodiversity: temporal changes in abundance, life history and demography. Philos. Trans. R. Soc. Lond. B, **360**: 315–338.

IUCN. 2004. Guidelines for using the IUCN Red List categories and criteria. World Conservation Union, Gland, Switzerland.

Jackson, J.B.C., Kirby, M.X., Berger, W.H., Bjorndal, K.A., Botsford, L.W., Bourque, B.J., Bradbury, R.H., Cooke, R., Erlandson, J., Estes, J.A., Hughes, T.P., Kidwell, S., Lange, C.B., Lenihan, H.S., Pandolfi, J.M., Peterson, C.H., Steneck, R.S., Tegner, M.J., and Warner, R.R. 2001. Historical overfishing and the recent collapse of coastal ecosystems. Science (Washington, D.C.), **293**: 629–637.

Jennings, S. 2004. The ecosystem approach to fishery management: a significant step towards sustainable use of the marine environment? Mar. Ecol. Prog. Ser. (MEPS), **274**: 279–282.

Jennings, S. 2005. Indicators to support an ecosystem approach to fisheries. Fish Fish. **6**: 212–232.

Jennings, S., and Blanchard, J.L. 2004. Fish abundance with no fishing: predictions based on macroecological theory. J. Anim. Ecol. **73**: 632–642.

Jennings, S., and Dulvy, N.K. 2005. Reference points and reference directions for size-based indicators of community structure. ICES J. Mar. Sci. **62**: 397–404.

Jennings, S., Reynolds, J.D., and Mills, S.C. 1998. Life history correlates of responses to fisheries exploitation. Proc. R. Soc. Lond. B, **265**: 333–339.

Knijn, R.J., Boon, T.W., Heessen, H.J.L., and Hislop, J.R.G. 1993. Atlas of North Sea fishes. ICES Co-op Res. Rep. **194**: 1–268.

Link, J.S. 2005. Translating ecosystem indicators into decision criteria. ICES J. Mar. Sci. **62**: 569–576.

MacCall, A.D. 1990. Dynamic geography of marine fish populations. University of Washington, Seattle, Washington.

Maxwell, D.L., and Jennings, S. 2005. Power of monitoring programmes to detect decline and recovery of rare and vulnerable fish. J. Appl. Ecol. **42**: 25–37.

Musick, J.A., Harbin, M.M., Berkeley, S.A., Burgess, G.H., Eklund, A.M., Findley, L., Gilmore, R.G., Golden, J.T., Ha, D.S., Huntsman, G.R., McGovern, J.C., Parker, S.J., Poss, S.G., Sala, E., Schmidt, T.W., Sedberry, G.R., Weeks, H., and Wright, S.G. 2000. Marine, estuarine, and diadromous fish stocks at risk of extinction in North America (exclusive of Pacific salmonids). Fisheries, **25**: 6–30.

Muus, B.J., and Neilsen, J.G. 1999. Sea fish. Scandinavian fishing year book. Hedehusene, Copenhagen, Denmark.

Myers, R.A., and Worm, B. 2005. Extinction, survival and recovery of large predatory fishes. Phil. Trans. Roy. Soc. Lond. B, **360**: 13–20.

Nicholson, M.D., and Fryer, R.J. 1992. The statistical power of monitoring programmes. Mar. Poll. Bull. **24**: 146–149.

Nicholson, M.D., and Jennings, S. 2004. Testing candidate indicators to support ecosystem-based management: the power of monitoring surveys to detect temporal trends in fish community metrics. ICES J. Mar. Sci. **61**: 35–42.

Pauly, D. 1995. Anecdotes and the shifting baseline syndrome of fisheries. Trends Ecol. Evol. **10**: 430.

Perry, A.L., Low, P.J., Ellis, J.R., and Reynolds, J.D. 2005. Climate change and distribution shifts in marine fishes. Science (Washington, D.C.), **308**: 1912–1915.

Peterman, R.M., and M'Gonigle, M. 1992. Statistical power analysis and the precautionary principle. Mar. Poll. Bull. **24**: 231–234.

Quero, J.C. 1998. Changes in the Euro-Atlantic fish species composition resulting from fishing and ocean warming. PBZI J. Zool. **65**: 493–499.

Quinn, T.J., and Deriso, R.B. 1999. Quantitative fish dynamics. Oxford University Press, Oxford, UK.

Rice, J. 2003. Environmental health indicators. Ocean. Coast. Manag. **46**: 235–259.

Rice, J. 2005. Implementation of the ecosystem approach to fisheries management — asynchronous co-evolution at the interface between science and policy. Mar. Ecol. Prog. Ser. **300**: 265–270.

Rice, J., and Rochet, M.-J. 2005. A framework for selecting a suite of indicators for fisheries management. ICES J. Mar. Sci. **62**: 516–527.

Rogers, S.I., and Ellis, J.R. 2000. Changes in the demersal fish assemblages of British coastal waters during the 20th century. ICES J. Mar. Sci. **57**: 866–881.

Rogers, S.I., and Greenaway, B. 2005. A UK perspective on the development of marine ecosystem indicators. Mar. Poll. Bull. **50**: 9–19.

Sadovy, Y., and Cheung, W.L. 2003. Near extinction of a highly fecund fish: the one that nearly got away. Fish Fish. **4**: 86–99.

Sáenz-Arroyo, A., Roberts, C.M., Torre, J., Cariño-Olvera, M., and Enríquez-Andrade, R.R. 2005. Rapidly shifting environmental baselines among fishers of the Gulf of California. Proc. R. Soc. Lond. B, **272**: 1957–1962.

Sainsbury, K., and Sumaila, U.R. 2003. Incorporating ecosystem objectives into management of sustainable marine fisheries, including 'best practice' reference points and use of marine protected areas. *In* Responsible fisheries in the marine ecosystem. *Edited by* M. Sinclair and G. Valdimarsson. CAB International, Wallingford, UK. pp. 343–361.

Sparholt, H. 1990. An estimate of the total biomass of fish in the North Sea. J. Cons. Int. Explor. Mer, **46**: 200–210.

Venables, W.N., and Ripley, B.D. 2002. Modern and applied statistics. Springer-Verlag, New York.

Walker, P.A. 1998. Fleeting images: dynamics of North Sea ray populations. Ph.D. thesis, University of Amsterdam, Amsterdam, the Netherlands.

Walker, P.A., and Hislop, J.R.G. 1998. Sensitive skates or resilient rays? Spatial and temporal shifts in ray species composition in the central and north-western North Sea between 1930 and the present day. ICES J. Mar. Sci. **55**: 392–402.

Wolff, W.J. 2000. The south-eastern North Sea: losses of vertebrate fauna during the past 2000 years. Biol. Conserv. **95**: 209–217.

World Summit on Sustainable Development. 2002. Plan of implementation of the World Summit on Sustainable Development. UN Department of Economic and Social Affairs, Division of Sustainable Development, New York.

Whole-lake effects of invasive crayfish (*Orconectes* spp.) and the potential for restoration

Sadie K. Rosenthal, Samantha S. Stevens, and David M. Lodge

Abstract: Effects of invasive species are often extrapolated to whole systems based on small-scale, short-term, and (or) single-system studies. For example, previous laboratory studies and in-lake cage experiments suggest that invasive crayfish *Orconectes rusticus* and *O. propinquus* reduce macrophyte and snail abundance in north temperate lakes, and snapshot lake surveys provide supporting evidence. Still, these impacts have not been demonstrated in multiple whole lakes over time. Thus, in summer of 2003, we resurveyed benthic invertebrates and macrophytes in lakes originally surveyed by the Michigan Department of Natural Resources in the late 1930s. Our multilake survey supports the macrophyte results from small-scale and comparative studies: macrophyte species richness and abundance declined significantly in invaded lakes relative to uninvaded lakes. We next conducted a laboratory seed-bank study to examine the potential for macrophyte restoration in a lake occupied by rusty crayfish for at least 15 years. Only two macrophyte species (*Najas flexilis* and *Chara* spp.) germinated from sediments from the invaded lake compared with eight species from reference sediments. This suggests that invaded lakes may have depauperate seed banks and that restoration of invaded macrophyte communities may require manual planting, even if crayfish could be removed.

Résumé : Les effets des espèces envahissantes sont souvent extrapolés à systèmes entiers à partir d'études à petite échelle, à court terme ou sur un seul système. Par exemple, des études antérieures en laboratoire et des expériences en lac dans des cages laissent croire que les écrevisses envahissantes *Orconectes rusticus* et *O. propinquus* réduisent l'abondance des macrophytes et des gastéropodes dans les lacs tempérés nordiques; des inventaires instantanés de lacs fournissent des données qui appuient ces résultats. Néanmoins, ces impacts n'ont pas été démontrés dans un grand nombre de lacs entiers sur une longue période. C'est pourquoi, à l'été 2003, nous avons inventorié de nouveau les invertébrés benthiques et les macrophytes dans des lacs inventoriés à l'origine par le ministère des ressources naturelles du Michigan à la fin des années 1930. Notre inventaire de nombreux lacs confirme les résultats obtenus sur les macrophytes dans les études à petite échelle et les études comparatives : la richesse spécifique et l'abondance des macrophytes ont diminué de façon significative dans les lacs envahis par les écrevisses par comparaison aux lacs non envahis. Nous avons ensuite mené une étude en laboratoire de banques de graines pour déterminer le potentiel de restauration des macrophytes dans un lac occupé par l'écrevisse rousse depuis au moins 15 ans. Seules deux espèces de macrophytes, *Najas flexilis* et *Chara* spp., ont germé dans les sédiments recueillis dans le lac envahi, alors que huit espèces ont germé dans les sédiments témoins. Cela indique que les lacs envahis peuvent avoir des banques de graines appauvries et que, même si les écrevisses pouvaient être retirées, la restauration des communautés de macrophytes envahies par les écrevisses pourrait exiger des plantations manuelles.

[Traduit par la Rédaction]

Introduction

Invasive species have tremendous economic and ecological impacts. They are estimated to cost the US at least $137 billion annually (Pimentel et al. 2000), are a threat to imperiled species (Wilcove et al. 1998), and are the leading cause of biodiversity loss in lakes (Sala et al. 2000). Nevertheless, the impact of invasive species is often anecdotal and poorly quantified because pre-invasion data are lacking.

Given the potential for irreversible harm, it is unethical to experimentally introduce potentially invasive species into natural systems. Therefore, species are studied most often with laboratory experiments or with small-scale field experiments within an already invaded system. Unfortunately, such experiments often lack realism (Diamond 1986), and small-scale phenomena may not scale easily to a whole system (Lodge et al. 1998). One-time, multilake correlative studies incorporate more realism than do small-scale studies, but because correlation does not imply causation, we cannot confidently attribute observed ecological changes to invasive species. Short of a planned experiment, the most realistic type of study is a natural trajectory experiment in which multiple systems are studied before and after a disturbance (Diamond 1986). Often lacking, however, are both pre-

Received 3 June 2005. Accepted 22 December 2005. Published on the NRC Research Press Web site at http://cjfas.nrc.ca on 2 May 2006.
J18724

S.K. Rosenthal,[1] S.S. Stevens, and D.M. Lodge. Department of Biological Sciences, University of Notre Dame, Notre Dame, IN 46556, USA.

[1] Corresponding author (e-mail: srosenth@alumni.nd.edu).

Can. J. Fish. Aquat. Sci. 63: 1276–1285 (2006)   doi:10.1139/F06-037

invasion baseline data against which to measure change, and reference lakes to account for other potential drivers. In this study we have such data and are afforded a rare opportunity to test the effects of invasive crayfish in whole lakes over time.

The spread and impacts of crayfish have been studied in lakes of the US Upper Midwest since the 1970s (Capelli and Magnuson 1983). In the Northern Highland Lake District of Wisconsin and the upper peninsula of Michigan specifically, the focus has been on one native and two nonindigenous species. Virile crayfish (*Orconectes virilis*) are native throughout the region, northern crayfish (*O. propinquus*) are nonindigenous to some areas, and rusty crayfish (*O. rusticus*) are nonindigenous throughout (Creaser 1931, 1932). All three crayfish species are omnivores, feeding as shredders, collectors, scrapers, and predators (Lorman and Magnuson 1978), and studies suggest that invasive crayfish have strong trophic interactions in the littoral zones of lakes and reduce the abundance of macroinvertebrates, macrophytes, and periphyton (Lodge et al. 1994; Hill and Lodge 1995).

Rusty crayfish generally extirpate both congeners (Olsen et al. 1991), whereas northern crayfish either replace or coexist with virile crayfish (Lodge et al. 1986; Olsen et al. 1991). Of the other littoral invertebrates, snails are the best studied. Rusty crayfish reduced snail populations in a field experiment (Lodge et al. 1994) and were negatively associated with snail densities in a multilake correlative study (Lodge et al. 1998). Introduced crayfish affect macrophyte communities through consumption and nonconsumptive damage, reducing macrophyte biomass, shoot density, and species richness in field experiments (Lodge and Lorman 1987; Lodge et al. 1994). The reduction of macrophyte surface area may yield a net periphyton loss, even as periphyton-grazing snails decline (Lodge et al. 1994). Finally, the loss of macrophyte habitat, combined with egg predation by crayfish (Dorn and Mittelbach 2004), may lead to negative effects on fish populations.

Given the expected large negative effects stemming from crayfish invasions, the prospect of reversing these effects should be addressed to prioritize management efforts (Parker et al. 1999). Because macrophytes have major impacts on physical, chemical, and biological properties in lakes (Carpenter and Lodge 1986), they are a natural focus in testing the potential for recovery should rusty crayfish numbers decrease. Studies in other contexts suggest that a viable seed bank may provide the necessary rescue to reestablish a degraded plant community (McFarland and Rogers 1998; de Winton et al. 2000). However, if sustained herbivory results in seed-bank depletion, macrophyte communities may not recover even when herbivore populations are reduced or eliminated. This has never been tested with respect to crayfish invasions.

The thought that invasive crayfish cause dramatic shifts in macrophyte and macroinvertebrate communities in whole lakes has previously been inferred from correlative studies (Lodge et al. 1998; Wilson 2002), small-scale laboratory experiments (Olsen et al. 1991), short-term, in situ caging experiments (Lodge and Lorman 1987; Lodge et al. 1994), and single-lake studies (Wilson et al. 2004). Here we use a natural trajectory experiment to examine whether impacts of invasive crayfish predicted from small-scale experiments manifest at the whole-lake scale. For lakes in the upper peninsula of Michigan, we compare changes in the macrophyte and invertebrate communities between the 1930s and 2003 in invaded lakes and in uninvaded reference lakes. We then use a laboratory seed-bank study to test the potential for macrophyte recovery following crayfish removal. The results of this seed-bank experiment have implications for any restoration efforts.

Materials and methods

Multilake surveys

General

In the 1930s, biologists with the Michigan Department of Natural Resources (MI DNR) Institute for Fisheries Research (IFR) conducted comprehensive lake surveys in the upper peninsula of Michigan with the objective of better managing fish populations (McMurry et al. 1933; Eschmeyer 1936). Recognizing the importance of habitat and prey items to fish, they sampled macrophytes and benthic macroinvertebrates in a number of lakes, and we use these data as a baseline against which to compare ecological change between lakes invaded by crayfish and uninvaded reference lakes.

In 2003, we resampled macrophytes (in seven lakes) and macroinvertebrates (in nine lakes) (Table 1 and supplementary data[2]), using methods identical with those used in the 1930s, as best as we could determine from the available historical documentation (Eschmeyer and Hazzard 1936[3]; Miller 1936; Hazzard and Brown 1938[3]). Because we were interested in the effects of invasive cryfish on lake biota, we selected only lakes for which we found no obvious evidence (from the IFR records or from current long-term homeowners) of other contributing factors. For example, we excluded lakes that had been dammed at the outflow post-1930s because the resulting change in the water level may have had an effect on littoral communities. In 2003, we conducted surveys from late June through late August to approximate the dates surveyed in the 1930s and sampled at the same locations within lakes, as determined from IFR site descriptions and detailed maps of the sampling stations.

Crayfish

Crayfish were not specifically targeted in the 1930s sampling by the IFR or subsequently by the MI DNR. However, their occurrence was noted in the context of potential prey items for fish. In the records of the IFR and MI DNR, cray-

---

[2] Supplementary data for this article are available on the journal Web site (http://cjfas.nrc.ca) or may be purchased from the Depository of Unpublished Data, Document Delivery, CISTI, National Research Council Canada, Building M-55, 1200 Montreal Road, Ottawa, ON K1A 0R6, Canada. DUD 5027. For more information on obtaining material refer to http://cisti-icist.nrc-cnrc.gc.ca/irm/unpub_e.shtml.

[3] Dates of undated historical documents were approximated from dated documents referring back to these methods and from the authors' tenures at the IFR (Tina Tincher, Librarian, MI DNR, Fisheries Division, Institute for Fisheries Research, 212 Museums Annex Building, 1109 North University Avenue, Ann Arbor, MI 48109, USA, personal communication).

Table 1. Crayfish data.

Lake	Past crayfish (species)	No. crayfish·trap^{-1} (species) in 2003	Lakes sampled for		
			Benthos	Snails	Macrophytes
Beatons	1991 (Y)	0.3 (P)	×		×
Crooked	1938 (Y)	0.1 (R, P)	×	×	×
Gogebic	1940s (Y)	2.1 (P, V)	×	×	
Smoky	1989 (R)	0.0[a] (R)	×		
Sucker	1938 (Y)	1.0 (V)	×	×	×
Winslow	1938 (Y)	0.9 (P, I[b])	×		×
Hagerman	**1938 (Y)**	**25.1 (P, V[b])**	×		×
Ottawa	**1938 (Y); 1987 (R)**	**30.7 (R)**	×	×	×
Thousand Island	**1938 (Y); 1995 (R)**	**8.5 (R)**	×	×	×

Note: Lakes with high abundances of crayfish (in 2003) are in bold type. All lakes were originally sampled for other benthos in 1937 (Beatons) or 1938 (all other lakes), but for some lakes, information on crayfish is available only for later years. Crayfish species abbreviations: R, rusty (*Orconectes rusticus*); P, northern (*O. propinquus*); V, virile (*O. virilis*); I, immune (*O. immunis*); Y, crayfish unidentified.

[a] Rusty crayfish found by hand.

[b] In Winslow, only one of 17 crayfish trapped were immune crayfish; in Hagerman, only two of the 499 crayfish were virile crayfish.

fish were not identified to species, with the exception of rusty crayfish, which have been distinguished from other species since about 1987 (Bill Ziegler, Fisheries Management Biologist, MI DNR, Northern Lake Michigan Management Unit, 1420 US 2 West, Crystal Falls, MI 49920, USA, personal communication). However, in other pre-1931 surveys specifically targeting crayfishes, the only species of *Orconectes* found in the counties (Gogebic and Iron) of our study was the virile crayfish (*O. virilis*) (Creaser 1931), which we thus refer to as the native crayfish. The northern crayfish (*O. propinquus*) was found in Michigan's Upper Peninsula, but only in counties bordering the Great Lakes (Creaser 1931). Northern crayfish were thus either absent or rare in our counties until post-1931. The exact timing of their invasion is unknown, but by the 1970s, they occurred in many lakes of northern Wisconsin outside their original Great Lakes watershed distribution (Capelli and Magnuson 1983). Rusty crayfish, which are native to Indiana, Kentucky, and Ohio, were first noted in northern Wisconsin in the 1970s (Capelli and Magnuson 1983), where they have been used by anglers as bait.

In 2003, we determined crayfish composition of each lake by trapping with standard methods (Capelli and Magnuson 1983; Lodge et al. 1986) in August, an intermolt period during which adult males are active. Approximately 20 Gee minnow traps (Memphis Net and Twine, Memphis, Tennessee) with enlarged openings (~5 cm diameter) were baited with 120 ± 10 g beef liver and distributed roughly evenly around the perimeter of each lake. Traps were set in the afternoon at a depth of 1.5 ± 0.5 m and collected the following day. We recorded species, sex, and form for all crayfish caught.

Benthos sampling

We used maps made during the 1930s to relocate the 4–11 clearly marked benthos sampling stations for each of the nine lakes in which we resurveyed benthic communities. As in the 1930s, we took two standard 15.2 cm Ekman grabs at each station, for a combined sampling area of 464.5 cm^2. The sediments collected were sieved (850 μm mesh, previously No. 20) (Miller 1936) in the field, and organisms were immediately identified to the same taxonomic levels used in the 1930s (usually class or order).

Benthos analysis

To provide an index of lake-wide changes in total abundance of benthic invertebrates, we first calculated a metric of change at each station:

$$\text{Station metric} = \log\left(\frac{2003\ \text{abundance} + 1}{1930\text{s abundance} + 1}\right)$$

We then averaged this metric across all stations to calculate our lake-wide metric. We compared changes in macroinvertebrate abundance from the 1930s to 2003 between invaded and uninvaded lakes with t tests (SYSTAT 10.2; Systat Software Inc. 2002). Because we expected that crayfish would have strongest negative effects on littoral benthos, we did separate analyses for littoral (1–10 stations sampled in each lake) and profundal (1–5 stations per lake) benthos. Littoral stations were defined as either being shallower than maximum rooting depth for submergent macrophytes based on each lake's Secchi depth (Skogerboe et al. 2003) or containing snails. We expected no change in abundance for profundal macroinvertebrates but performed the analysis as a reference for littoral changes. We performed a separate analysis for snail abundance (one-tailed t test), because evidence from smaller-scale experiments suggests that snails are strongly reduced by crayfish (Lodge et al. 1994). We limited the snail analysis to littoral stations where snails were present in either sampling year. We did not analyze invertebrate species richness because of the course taxonomic classifications used in the 1930s.

Macrophyte sampling

The 1930s records indicate that submergent macrophytes were sampled visually at two scales. First, detailed observations for species presence and abundance were taken at 2–7 sampling stations in each lake, which were clearly indicated on lake maps. For the sampling stations, notes on species' aerial cover and depth indicated that vegetation was sampled from a broad area that differed among stations. We examined historical notes before sampling to best determine that area for each station. Second, the general presence of macrophytes was noted at the lake-wide scale.

For the detailed station surveys, we visually inspected sampling stations in seven lakes from a flat-bottomed boat, drifting slowly across the sampling area along 1–2 m depth contours. Most lakes were clear and we could easily identify species from above the water. Where we could not, we pulled plants to the surface with a modified rake (a 1.4 m tall rake with a 42 cm × 42 cm square of 12.7 mm mesh hardware cloth secured to the handle at the base). A photograph taken of early surveys (Hubbs and Eschmeyer 1938, their fig. 8) shows such a device, and Cooper (1974, p. 142) stated that scientists "dredge[d] for bottom food and weeds" in earlier surveys.

We identified submergent macrophytes to the taxonomic level assigned in the 1930s, which was generally species (Crow and Hellquist 2000). We assessed each species' abundance according to the 1938 classifications of sparse (S), medium (M), and dense (D). In 1937, five categories were used: I (rare), II (sparse), III (common), IV (abundant), and V (dense). To include in our analysis lakes that were sampled in different years, we converted the five 1937 categories (Beatons Lake) to the three 1938 categories (all other lakes) as follows: we designated I (1937) and II (1937) as sparse (1938), III (1937) as medium (1938), and IV (1937) and V (1937) as dense (1938). Sparse, medium, and dense were undefined in the section on lake sampling in the methods reported by Hazzard and Brown (1938)[3]. However, in the section on stream methods, a species was classified as sparse if seldom observed, medium if covering about half of the rocks or in patches and here and there, and dense if noticeable on practically every rock or if margining the stream. We followed these generalizations in our lakes: sparse if seldom observed, moderate if here and there, and dense if it was noticeable over most of the sampling station.

For the lake-wide surveys, markings on the lake maps indicated where submergent vegetation was historically present, in addition to the detailed sampling stations. We traveled the shoreline in these areas and classified the bottom as either firm (sand or gravel) or soft (muck), as we also did for each macrophyte sampling station. We then computed the proportion of the historically vegetated area with firm or soft bottom substrate. We did this because recent work has shown that crayfish are more abundant on firm than soft substrates (Kershner and Lodge 1995), and we therefore expected that the crayfish impact would be greater on firm than soft substrates.

Macrophyte analysis

To provide an index of change in species richness of submergent macrophytes for each station, we summed the number of taxa at each station and calculated a metric of change between years, as we did with invertebrate abundance above:

$$\text{Station metric of change} = \log\left(\frac{\text{2003 species richness} + 1}{\text{1930s species richness} + 1}\right)$$

We calculated the mean metric of change for firm and soft substrates separately and multiplied these by the proportion of shoreline historically occupied by submergent macrophytes in that substrate. We then summed across substrates to provide a lake-wide index of change for the area of the lake that was historically occupied by submergent macrophytes:

$$\begin{aligned}\text{lake metric} = {} & [(\text{proportion of lake in firm}) \\ & \times (\text{mean change on firm substrate})] \\ & + [(\text{proportion of lake in soft}) \\ & \times (\text{mean change on soft substrate})]\end{aligned}$$

Predicting that invaded lakes would have a more negative change than uninvaded lakes, we then compared this metric between invaded and uninvaded lakes with a one-tailed t test.

To provide an index of macrophyte abundance (regardless of species richness), we assigned each species at a station an index of abundance: 1 to sparse, 2 to medium, and 3 to dense. We summed the index of abundance across all submergent macrophyte species in a station for 1930s and 2003 data separately. We then did the same type of analysis as with species richness to calculate a metric of change (described above) for each lake. Recognizing that the assignment of 1, 2, and 3 is arbitrary, we examined the sensitivity of results to our classifications by repeating the analysis with postsampling estimations of average aerial cover for each category. On average, we estimated that macrophytes categorized as sparse covered 7% of the sampling station's surface area, medium 30%, and dense 53%.

Seed-bank experiment

Study sites

We began monitoring Lake Ottawa (223 ha, 27 m maximum depth), one of the study lakes above, in summer 2001. We caught an average of 36 male rusty crayfish·trap^{-1} in late July 2001 and observed that little of the vegetation noted on the 1930s map was still present. To test the potential for natural vegetation restoration if management efforts could reduce crayfish abundance, we tested the seed banks of two 1938 macrophyte sampling stations. Bay 1, the northernmost bay of Lake Ottawa, was dominated by light-colored muck over sand. Bay 2, the lake's southwestern bay, consisted of dark muck. We used Tenderfoot Lake (179 ha, 10 m maximum depth), at the mouth of Tenderfoot Creek, as a reference site. This site had abundant vegetation on muck substrate, with species overlapping those historically present in Lake Ottawa (Table 2).

Sample collection

On 16 August 2001, we took five sets of sediment cores at each of the two bays in Lake Ottawa and in Tenderfoot Lake to test for germination. A cylindrical metal-edged corer with an area of 0.018 m^2 was pushed into the sediments to a depth of 10 cm. A metal plate was slid underneath to collect the sediments (Lodge et al. 1998). Each set consisted of four cores taken at least 10 m apart at a given site at a water depth of 1 m.

Experiment and analysis

Sediment samples were placed in dark, cold storage (4 °C) at the University of Notre Dame (Notre Dame, Indiana) for 20 weeks to simulate winter conditions needed by some species to break seed dormancy (Baskin and Baskin 1998). Sediments from each sample (a layer approximately 4 cm deep) were then laid over a 5 cm layer of sand

Table 2. Macrophyte species present in the lakes and those that germinated in the seed-bank experiment.

Macrophytes	Lake Ottawa 1938	Lake Ottawa 2001–2003	Lake Ottawa Seed bank	Tenderfoot 2001	Tenderfoot Seed bank
Submergent species					
Ceratophyllum demersum	×			×	
***Chara* sp.**	×		×	×	×
Elodea canadensis		1 stem		×	
Megalodonta beckii				×	
Myriophyllum sp.	×			×	
Najas flexilis	×		×	×	×
Potamogeton amplifolius	×	×		×	
P. epihydrus		×			
P. gramineus				×	
P. illinoensis	×				×
P. natans	×				
P. pusillus	×			×	
P. richardsonii	×	2 plants		×	
P. robbinsii				×	×
P. spirillus				×	×
P. zosteriformis	×			×	×
Stuckenia pectinata	×				
Vallisneria americana				×	
Zosterella dubia	×			×	×
Floating species					
Nuphar variegata	×	×		×	×
Nymphaea odorata	×			×	
Polygonum amphibium	×	×			

Note: Species both historically present in Lake Ottawa and that germinated from either lake in the experiment are in bold type. 1938 data are from Institute for Fisheries Research (IFR) lake files. For current species presence, we snorkeled extensively in Lake Ottawa during the summers of 2001–2003 and surveyed Tenderfoot in the summer of 2001 from a boat.

(QUIKRETE© Play Sand, Atlanta, Georgia) in individual greenhouse tanks (0.457 m × 0.406 m) and covered with 12 cm of water. We put a single aquarium bubbler in each tank for aeration. The greenhouse was kept at about 20 °C (Haag (1983) germinated some of the same species at 19 °C), and 1000 watt, coated, metal halide lamps (400–700 nm spectrum bulbs) provided 14 h of daylight (0600–2000), supplementing natural light. A randomized block design was used to account for slight variability of light intensity resulting from light placement. In addition to the five replicates from each site, we set up one tank with 5 cm of sand to confirm the absence of macrophyte seeds in the sand. Thus a total of 16 tanks constituted the experiment, which ran from 28 January to 15 April 2002.

At the conclusion of the experiment, all germinated macrophytes were identified and counted. We used a randomized blocks analysis of variance with Tukey's multiple contrasts to test whether species richness, total number of macrophyte shoots, and total number of macrophyte shoots (excluding *Chara* spp.) differed between treatments.

Results

Lake surveys

Crayfish

Between the 1930s and 2003, three lakes were invaded such that the invader had attained high abundance by 2003: Lake Ottawa and Thousand Island Lake by rusty crayfish and Hagerman Lake by northern crayfish (Table 1). Rusty crayfish were first noted in Lake Ottawa in 1987 at which point they made up about 20% of the crayfish community (records in IFR lake files). By 1997, they were clearly the dominant species, comprising an estimated 75% of the crayfish community (records in IFR lake files). Since 2001, they have made up 100% of the crayfish trapped. In Thousand Island Lake, rusty crayfish were detected in 1995 (Perry and Lodge, unpublished data), but not quantified. Five additional lakes (Beatons, Crooked, Gogebic, Smoky, Winslow) have been invaded by rusty or northern crayfish, but the abundance of the invader is still very low (0–2 crayfish·trap^{-1}) (Table 1); thus for analysis these five lakes were included with the uninvaded lakes. Sucker Lake has only native virile crayfish.

Macroinvertebrates and macrophytes

In comparing invaded (n = 3) and uninvaded (n = 6) lakes, no significant difference existed in the changes of either littoral (p = 0.388; Fig. 1*a*) or profundal (p = 0.108; Fig. 1*c*) invertebrate abundance. The difference in the change of snail abundance was apparently large but not significant (p = 0.075, invaded n = 2, uninvaded n = 3; Fig. 1*b*). Low sample numbers limited the power of these analyses. Species richness of macrophytes in historically vegetated areas declined in invaded lakes (n = 3) as compared with uninvaded lakes (n = 4) (p = 0.007; Fig. 2*a*). Likewise, macrophyte abundance declined in invaded lakes as compared with uninvaded lakes, regardless of which categorical scale we used (with density categories of 1, 2, and 3, $p = 0.006$ (Fig. 2*b*), and with density categories of 7, 30, and 53, $p = 0.017$ (not shown)).

Seed-bank experiment

The number of macrophyte species that germinated was greater in sediments from the reference lake than in those from either site in Lake Ottawa ($p < 0.001$; Fig. 3*a*). Only *Najas flexilis* (hereafter referred to as *Najas*) and the macroalga *Chara* spp. (hereafter referred to as *Chara*) germinated from the Lake Ottawa sediments, whereas eight macrophyte species, including *Najas* and *Chara*, grew from the Tenderfoot Lake reference sediments (Table 2). More shoots germinated from the organic-rich sediments of Bay 2 than from the sandier sediments of Bay 1 or the reference sediments ($p = 0.002$; Fig. 3*b*). This trend was driven by high numbers of 5 cm tall sprouts of *Chara* in the sediments from Lake Ottawa's Bay 2. When *Chara* was excluded from the analysis, Tenderfoot Lake had a greater number of shoots than either site in Lake Ottawa ($p < 0.001$; Fig. 3*c*). No effects of treatment block were detected.

Discussion

Detailed historical sampling records in multiple lakes allowed us to examine long-term, whole-lake effects of invasive crayfish. As predicted from small-scale experiments, macrophyte species richness and abundance declined in invaded lakes relative to uninvaded lakes. For at least Lake Ottawa (the lake in which the timetable of invasion is clearest), these changes were quick (<15 years) relative to the 65-year duration of this study. The removal of macrophytes is expected to have many indirect effects not examined in this study. We expect lower periphyton biomass as a result of reduced colonizable surface area (Lodge et al. 1994) and fewer juvenile fish because of loss of habitat.

Effects on littoral benthos, though not statistically significant, were in the direction predicted from smaller-scale studies. We expected littoral invertebrate populations, especially snails, in invaded lakes to be low in abundance and diversity (Lodge et al. 1994, 1998). Our nonsignificant results (in the expected direction) may relate to both sampling bias and low power. When we sampled among macrophytes, the Ekman grab rarely retained vegetation, which is a primary habitat for snails (Brown and Lodge 1993); therefore the grabs likely underestimated snail abundance in vegetated habitats. Because vegetation occurred primarily in uninvaded lakes, the grabs likely underestimated snail abundance in uninvaded lakes relative to invaded lakes. Combined with the low power of our comparisons (limited by the small number of study lakes), these considerations suggest that our test of the impact of invasion on snails was conservative. Attributing biological significance to the apparent decline in snails after invasion is supported by the apparent opposite trend in profundal benthos, which occur at depths where crayfish predation is not important.

Fig. 1. Mean index of change (±1 standard error (SE)) in (*a*) littoral benthos, (*b*) snails, and (*c*) profundal benthos per station (profundal and littoral benthos: uninvaded, $n = 6$; invaded, $n = 3$; snails: uninvaded, $n = 3$; invaded, $n = 2$).

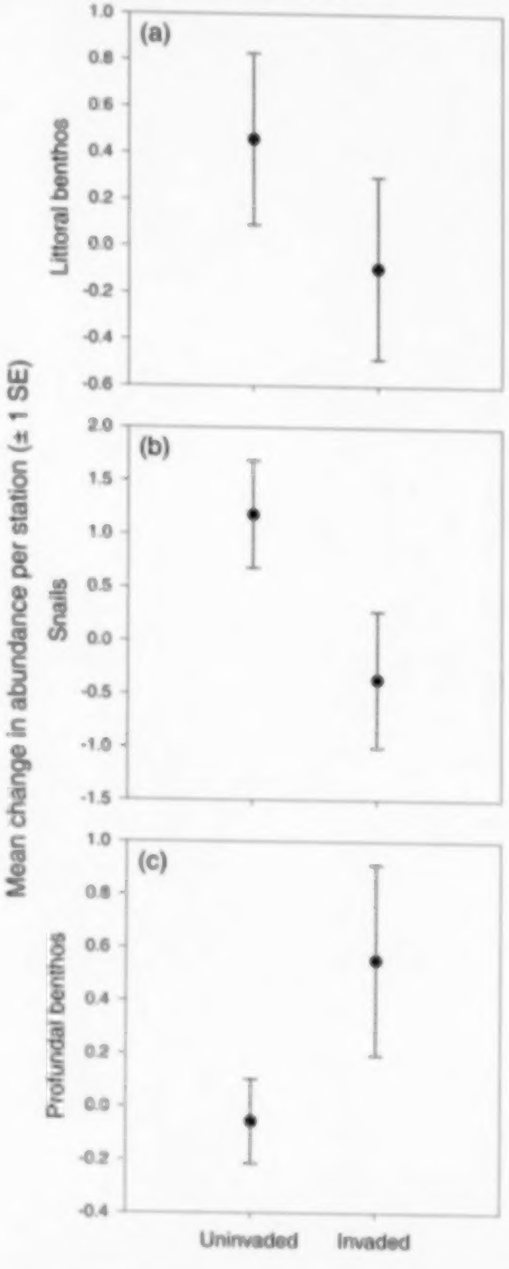

If uninvaded lakes were absolutely stable over time and our sampling methods in 2003 were exactly identical with those of the 1930s, the mean index of change for both macrophytes and invertebrates would have been zero. That our indices differed from zero may result from natural changes in the lake biota, although previous long-term studies of macrophytes in this northern highland lakes region suggest that without obvious drivers, changes in macrophyte composition are minor (Carpenter and Titus 1984; Lodge et al. 1989; Nichols 2001). Equally likely is that they are an in-

Fig. 2. Mean index of change (±1 standard error (SE)) in macrophyte species (*a*) richness and (*b*) abundance of the lake shoreline historically occupied by submergent macrophytes (uninvaded, $n = 4$; invaded, $n = 3$).

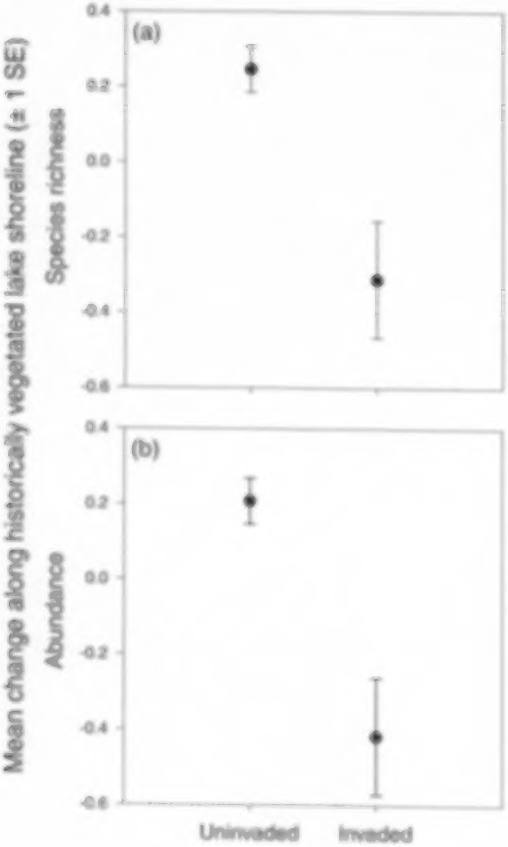

Fig. 3. Seed-bank experiment: mean (±1 standard error (SE)) species richness, shoots, and shoots excluding *Chara* per replicate ($n = 5$). Bay 1 and Bay 2 sediments are from invaded Lake Ottawa. Reference sediments are from uninvaded Tenderfoot Lake.

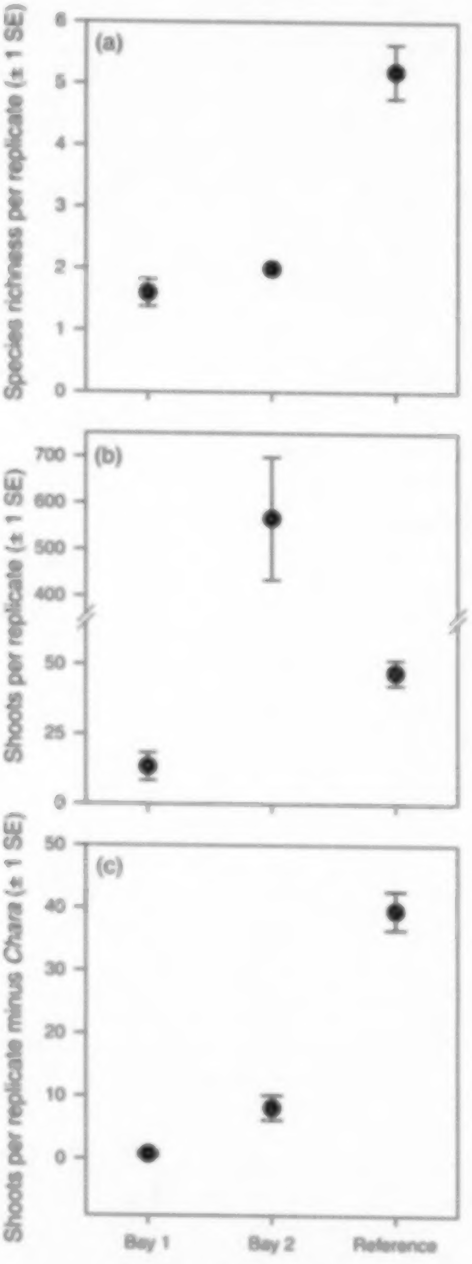

dication of different sampling efforts as opposed to large, lake-wide changes. This is especially true for macrophytes for which the details of the original sampling methods were less clear than for invertebrates. We consistently encountered more macrophyte species than were found by the 1930s biologists. The records indicate that the 1930s field crew spent about 3 days at each lake, and we suspect that they did not give sampling stations the same attention we did, because they had many additional duties including mapping the lake, testing water chemistry, and sampling fish.

This is the first study to suggest that northern crayfish, in addition to rusty crayfish, can cause community changes at the whole-lake scale. This is not particularly surprising, given the high abundance that northern crayfish achieve. However, other lakes in which this might have been observed have subsequently been invaded by rusty crayfish (Olsen et al. 1991), possibly masking the effects of northern crayfish.

Several lakes contained nonindigenous crayfish but are not "invaded" in the sense of high abundances of the introduced species. This may be a function of time, and repeated sampling of these lakes in the future might reveal an ongoing invasion. This seems most likely, given that it has happened in every other lake that we have observed to have a low abundance of the rusty crayfish (Olsen et al. 1991). On the other hand, it is possible that some lakes may simply not provide conditions or resources suitable for high population levels of crayfish and that such lakes would not experience community changes. Although we can relate certain lake attributes to whether crayfish will become established in a lake (Capelli and Magnuson 1983; Lodge and Hill 1994), we cannot yet predict in which lakes crayfish will become invasive, as defined by reaching population densities that cause large ecological effects.

Crayfish density may be related to amounts of preferred, shelter-providing substrate or to predation by fish, neither of which was examined in this study. Predators not only impact crayfish directly by consuming them, but also indirectly by causing them to be less active (Collins et al. 1983; Hill and Lodge 1995). Determining the degree to which shelter, predators, and other factors influence whether a community is likely to be invaded will help managers predict, and potentially prevent, future negative community shifts. This information could also help facilitate shifts to a lake's original status. In this respect, further understanding of the separate steps of invasion (Kolar and Lodge 2001) will be important for management. The ability to separately predict the lakes in which crayfish are likely to be introduced, establish, and achieve high densities would allow managers to focus their prevention and control efforts to specific waters.

Macrophyte restoration

Results from the seed-bank study indicate that if crayfish densities are reduced, depauperate seed banks may prevent lakes from returning to their previous, vegetated status. Laboratory seed-bank studies may not always be indicative of what emerges in the field (Brown 1998; Lundholm and Simser 1999). However, eight different macrophyte species germinated from the reference sediments, indicating that our experiment provided adequate germination and growing conditions for a number of species. Because they grew in the reference sediments and were previously found in Lake Ottawa, at least three submergent species (*Potamogeton illinoensis*, *P. zosteriformis*, and *Zosterella dubia*) in addition to *Najas* and *Chara* should have germinated from the Ottawa sediments if they were present. We cannot discount the possibility that propagules of these and other species are rare and that a larger volume of sediments may have yielded additional species. However, in contrast to detection from above the water by the 1930s biologists, we found no aboveground evidence of these species in 3 years of intensive snorkeling, suggesting that propagule abundance is lower than in the past.

Only *Najas* and *Chara* germinated from Lake Ottawa's sediments. These species have likely persisted because *Najas* germinates from seed annually (Voss 1972) and the macroalgae *Chara* reproduces from spores. Many other submergent macrophytes, on the other hand, rely on clonal reproduction, overwinter as turions, tubers, rhizomes, or standing plants, and rarely set seed (Sculthorpe 1967). The absence of aboveground *Chara* and *Najas* in Lake Ottawa is probably due to continuous herbivory by crayfish. In a lake enclosure–exclosure experiment, *Najas* occurred in exclosures but did not grow in the crayfish enclosures (Lodge et al. 1994), and in a stream experiment, Perry et al. (2000) found that macroalgae (*Chara* and *Nitella*) were completely removed from crayfish enclosures but remained in exclosures.

Potamogeton amplifolius was present in Lake Ottawa but did not germinate in the experiment. We think it is unlikely that this is an effect of laboratory conditions because we germinated species within the same genus and of the same general growth form (e.g., *P. illinoensis*). More likely is that *P. amplifolius* propagules are rare. Since 2001, we have not seen *P. amplifolius* flower or set seed in Lake Ottawa, and if it set seed in the past, the general sparseness of the species makes sampling seeds difficult.

The apparently limited reversibility of the impacts of invasion is not unexpected, because long lag times and (or) strong hysteresis occur in other systems in which community-wide changes are the result of a stressor. For example, reducing eutrophication in lakes does not always lead to macrophyte recovery, because turbidity and low light penetration maintain unfavorable conditions for macrophyte germination (Scheffer et al. 1993). Because of sustained crayfish herbivory for about 15 years, any restoration of many of the macrophyte species that inhabited Lake Ottawa in the 1930s would likely require manual planting, even if crayfish abundance could be reduced dramatically. Despite the small volume of sediments in our germination experiment, it seems unlikely that propagules of all 12 submergent species are sufficiently abundant in the lake for unaided restoration to occur in Lake Ottawa. Conclusions for other lakes would depend on lake-specific factors, including differences in invasion histories and macrophyte communities. Even in Lake Ottawa, an alternative strategy would be to remove crayfish and then observe which species of macrophytes reappear before any replanting effort.

Acknowledgments

Comments by Reuben Keller, Gary Lamberti, Gary Belovsky, and two anonymous reviewers have greatly improved this manuscript. We thank Tim Kreps, Brett Peters, Jody Murray, Jay Frentress, Justin Allen, Angela Bobeldyk, and Tim Davidson for field and laboratory assistance. We also thank the Michigan Department of Natural Resources (MI DNR) Institute for Fisheries Research (IFR) staff, especially Jim Breck, Ellen Grove, and Tina Tincher, for assistance with the lake archives, Bill Ziegler for DNR sampling information, and the US Forest Service Ottawa National Forest (ONF) personnel, including Jerry Edde, John Pagel, Bob Evans, and Michelle Holland. This project was supported by a challenge cost-share agreement between the University of Notre Dame and the ONF and by the National Science Foundation. A sabbatical fellowship (to DML) provided time for manuscript preparation.

References

Baskin, C.C., and Baskin, J.M. 1998. Seeds: ecology, biogeography, and evolution of dormancy and germination. Academic Press, San Diego, California.

Brown, S.C. 1998. Remnant seed banks and vegetation as predictors of restored marsh vegetation. Can. J. Bot. **76**: 620–629.

Brown, K.M., and Lodge, D.M. 1993. Gastropod abundance in vegetated habitats — the importance of specifying null models. Limnol. Oceanogr. **38**: 217–225.

Capelli, G.M., and Magnuson, J.J. 1983. Morphoedaphic and biogeographic analysis of crayfish distribution in northern Wisconsin. J. Crustac. Biol. **3**: 548–564.

Carpenter, S.R., and Lodge, D.M. 1986. Effects of submersed macrophytes on ecosystem processes. Aquat. Bot. **26**: 341–370.

Carpenter, S.R., and Titus, J.E. 1984. Composition and spatial heterogeneity of submersed vegetation in a softwater lake in Wisconsin. Vegetation, **57**: 153–165.

Collins, N.C., Harvey, H.H., Tierney, A.J., and Dunham, D.W. 1983. Influence of predatory fish density on trapability of crayfish in Ontario lakes. Can. J. Fish. Aquat. Sci. **40**: 1820–1828.

Cooper, G.P. 1974. Michigan fisheries centennial report (1873–1973). Michigan Department of Natural Resources Fisheries Division, Lansing, Michigan. Fisheries Management Rep. No. 6.

Creaser, E.P. 1931. The Michigan decapod crustaceans. Pap. Mich. Acad. Sci. Arts Lett. **13**: 257–276.

Creaser, E.P. 1932. The decapod crustaceans of Wisconsin. Trans. Wis. Acad. Sci. Arts Lett. **27**: 321–338.

Crow, G.E., and Hellquist, C.B. 2000. Aquatic and wetland plants of northeastern North America: a revised and enlarged edition of Norman C. Fassett's a manual of aquatic plants. University of Wisconsin Press, Madison, Wisconsin.

de Winton, M.D., Clayton, J.S., and Champion, P.D. 2000. Seedling emergence from seed banks of 15 New Zealand lakes with contrasting vegetation histories. Aquat. Bot. **66**: 181–194.

Diamond, J. 1986. Overview: laboratory experiments, field experiments, and natural experiments. *In* Community ecology. *Edited by* J. Diamond and T.J. Case. Harper and Row, New York. pp. 3–22.

Dorn, N.J., and Mittelbach, G.G. 2004. Effects of a native crayfish (*Orconectes virilis*) on the reproductive success and nesting behavior of sunfish (*Lepomis* spp.). Can. J. Fish. Aquat. Sci. **61**: 2135–2143.

Eschmeyer, R.W. 1936. Essential considerations for fish management in lakes. *In* Proceedings of the North American Wildlife Conference, Washington, D.C., 3–7 February 1936. US Government Printing Office, Washington, D.C. pp. 332–339.

Eschmeyer, R.W., and Hazzard, A.S. 1936. [Date approximate.] Notes on survey. Archives of the MI DNR Institute for Fisheries Research, 212 Museums Annex Bldg., 1109 North University Avenue, Ann Arbor, MI 48109, USA.

Haag, R.W. 1983. Emergence of seedlings of aquatic macrophytes from lake sediments. Can. J. Bot. **61**: 148–156.

Hazzard, A.S., and Brown, C.J.D. 1938. [Date approximate.] Institute for fisheries research inventory methods. Archives of the MI DNR Institute for Fisheries Research, 212 Museums Annex Bldg., 1109 North University Avenue, Ann Arbor, MI 48109, USA.

Hill, A.M., and Lodge, D.M. 1995. Multi-trophic-level impact of sublethal interactions between bass and omnivorous crayfish. J. North Am. Benthol. Soc. **14**: 306–314.

Hubbs, C.L., and Eschmeyer, R.W. 1938. The improvement of lakes for fishing: a method of fish management. Franklin DeKleine Company, Lansing, Michigan.

Kershner, M.W., and Lodge, D.M. 1995. Effects of littoral habitat and fish predation on the distribution of an exotic crayfish, *Orconectes rusticus*. J. North Am. Benthol. Soc. **14**: 414–422.

Kolar, C.S., and Lodge, D.M. 2001. Progress in invasion biology: predicting invaders. Trends Ecol. Evol. **16**: 199–204.

Lodge, D.M., and Hill, A.M. 1994. Factors governing species composition, population size, and productivity of cool-water crayfishes. Nord. J. Freshw. Res. **69**: 111–136.

Lodge, D.M., and Lorman, J.G. 1987. Reductions in submersed macrophyte biomass and species richness by the crayfish *Orconectes rusticus*. Can. J. Fish. Aquat. Sci. **44**: 591–597.

Lodge, D.M., Kratz, T.K., and Capelli, G.M. 1986. Long-term dynamics of 3 crayfish species in Trout Lake, Wisconsin. Can. J. Fish. Aquat. Sci. **43**: 993–998.

Lodge, D.M., Krabbenhoft, D.P., and Striegl, R.G. 1989. A positive relationship between groundwater velocity and submersed macrophyte biomass in Sparkling Lake, Wisconsin. Limnol. Oceanogr. **34**: 235–239.

Lodge, D.M., Kershner, M.W., Aloi, J.E., and Covich, A.P. 1994. Effects of an omnivorous crayfish (*Orconectes rusticus*) on a fresh-water littoral food-web. Ecology, **75**: 1265–1281.

Lodge, D.M., Stein, R.A., Brown, K.M., Covich, A.P., Bronmark, C., Garvey, J.E., and Klosiewski, S.P. 1998. Predicting impact of freshwater exotic species on native biodiversity: challenges in spatial scaling. Aust. J. Ecol. **23**: 53–67.

Lorman, J.G., and Magnuson, J.J. 1978. Role of crayfishes in aquatic ecosystems. Fisheries, **3**: 8–10.

Lundholm, J.T., and Simser, W.L. 1999. Regeneration of submerged macrophyte populations in a disturbed Lake Ontario coastal marsh. J. Gt. Lakes Res. **25**: 395–400.

McFarland, D.G., and Rogers, S.J. 1998. The aquatic macrophyte seed bank in Lake Onalaska, Wisconsin. J. Aquat. Plant Manag. **36**: 33–39.

McMurry, K.C., Eschmeyer, R.W., and Davis, C.M. 1933. Objectives and methods in the lake inventory in Michigan. Pap. Mich. Acad. Sci. Arts Lett. **18**: 259–276.

Miller, D.E. 1936. Michigan lake survey — a cooperative enterprise. Trans. Am. Fish. Soc. **66**: 128–130.

Nichols, S.A. 2001. Long-term change in Wisconsin lake plant communities. J. Freshw. Ecol. **16**: 1–13.

Olsen, T.M., Lodge, D.M., Capelli, G.M., and Houlihan, R.J. 1991. Mechanisms of impact of an introduced crayfish (*Orconectes rusticus*) on littoral congeners, snails, and macrophytes. Can. J. Fish. Aquat. Sci. **48**: 1853–1861.

Parker, I.M., Simberloff, D., Lonsdale, W.M., Goodell, K., Wonham, M., Kareiva, P.M., Williamson, M.H., von Holle, B., Moyle, P.B., Byers, J.E., and Goldwasser, L. 1999. Impact: toward a framework for understanding the ecological effects of invaders. Biol. Invasions, **1**: 3–19.

Perry, W.L., Lodge, D.M., and Lamberti, G.A. 2000. Crayfish (*Orconectes rusticus*) impacts on zebra mussel (*Dreissena polymorpha*) recruitment, other macroinvertebrates and algal biomass in a lake-outlet stream. Am. Midl. Nat. **144**: 308–316.

Pimentel, D., Lach, L., Zuniga, R., and Morrison, D. 2000. Environmental and economic costs of nonindigenous species in the United States. Bioscience, **50**: 53–65.

Sala, O.E., Chapin, F.S., Armesto, J.J., Berlow, E., Bloomfield, J., Dirzo, R., Huber-Sanwald, E., Huenneke, L.F., Jackson, R.B., Kinzig, A., Leemans, R., Lodge, D.M., Mooney, H.A., Oesterheld, M., Poff, N.L., Sykes, M.T., Walker, B.H., Walker, M., and Wall, D.H. 2000. Biodiversity — global biodiversity scenarios for the year 2100. Science (Washington, D.C.), **287**: 1770–1774.

Scheffer, M., Hosper, S.H., Meijer, M.L., Moss, B., and Jeppesen, E. 1993. Alternative equilibria in shallow lakes. Trends Ecol. Evol. **8**: 275–279.

Sculthorpe, C.D. 1967. The biology of aquatic vascular plants. St. Martin's Press, New York.

Skogerboe, J.G., Poovey, A.G., Getsinger, K.D., and Kudray, G. 2003. Invasion of Eurasian watermilfoil in lakes of the western upper peninsula, Michigan. U.S. Army Corps of Engineers, Washington, DC. Report No. ERDC/EL TR-03-10.

Systat Software Inc. 2002. SYSTAT 10.2 [computer program]. Systat Software Inc., Richmond, California.

Voss, E.G. 1972. Michigan flora: a guide to the identification and occurrence of the native and naturalized seed-plants of the state. Cranbrook Institute of Science, Bloomfield Hills, Michigan.

Wilcove, D.S., Rothstein, D., Dubow, J., Phillips, A., and Losos, E. 1998. Quantifying threats to imperiled species in the United States. Bioscience, **48**: 607–615.

Wilson, K.A. 2002. Impacts of the invasive rusty crayfish (*Orconectes rusticus*) in northern Wisconsin lakes. Ph.D. thesis, University of Wisconsin, Madison, Wisconsin, U.S.A.

Wilson, K.A., Magnuson, J.J., Lodge, D.M., Hill, A.M., Kratz, T.K., Perry, W.L., and Willis, T.V. 2004. A long-term rusty crayfish (*Orconectes rusticus*) invasion: dispersal patterns and community change in a north temperate lake. Can. J. Fish. Aquat. Sci. **61**: 2255–2266.

Factors influencing the distribution of chironomids in lakes distributed along a latitudinal gradient in northwestern Quebec, Canada

Isabelle Larocque, Reinhard Pienitz, and Nicolas Rolland

Abstract: The effect of 33 environmental variables on the distribution of chironomids was studied in 60 lakes of northwestern Quebec (Canada). A detrended canonical correspondence analysis detected linearity in the chironomid assemblages, thus redundancy analysis was used to identify the variables affecting the chironomid communities. Lake depth, dissolved organic carbon (DOC), mean August air temperature, and surface water temperature were the four variables that best explained the distribution of chironomids. Partial least squares analysis was used to develop new inference models. Among models, the one for mean August air temperature had the highest coefficient of determination (r^2_{jack} = 0.67) and the lowest root mean square error of prediction (= 1.17 °C). The results indicated that for downcore temperature reconstructions, it might be hard to dissociate the combined effects of temperature, DOC, and depth. Changes in taxa such as *Heterotrissocladius brundini*-type, *Heterotrissocladius subpilosus*-type, *Heterotrissocladius grimshawi*-type, *Micropsectra radialis*-type, *Tanytarsus lugens*-type, and *Microtendipes* can be attributed to changes in lake depth and (or) temperature. Changes in *Heterotanytarsus*, *Dicrotendipes*, *Cryptotendipes*, and *Cryptochironomus* might be attributed to shifts in temperature and DOC. Relationships among temperature, DOC, and lake depth should be studied in a "neo-ecology" design to better understand their impact on chironomid assemblage composition.

Résumé : L'effet de 33 variables environnementales sur la distribution des chironomides dans 60 lacs du nord-ouest du Quebec (Canada) a été étudié. Une relation linéaire dans les assemblages de chironomides a été démontrée par une analyse canonique des correspondances redressée. Une analyse de redondance a donc été utilisée pour identifier les variables influençant les communautés de chironomides. La profondeur du lac, le carbone organique dissous (DOC), la température moyenne de l'air en août et la température de l'eau en surface sont les quatre variables qui expliquent le mieux la distribution. Une analyse partielle des moindres carrés a été utilisée pour développer des modèles d'inférence. Le modèle qui prédit la température moyenne de l'air en août a le plus haut coefficient de détermination (r^2_{jack} = 0,67) et l'erreur quadratique moyenne de prédiction (= 1,17 °C) la plus faible. Les variations de certains taxons (type *Heterotrissocladius brundini*, type *Heterotrissocladius subpilosus*, type *Heterotrissocladius grimshawi*, type *Micropsectra radialis*, type *Tanytarsus lugens* et *Microtendipes*) peuvent être attribuées aux variations de la profondeur du lac et (ou) de la température. Les changements de *Heterotanytarsus*, *Dicrotendipes*, *Cryptotendipes* et *Cryptochironomus* peuvent être associés aux variations de température et de DOC. Les effets combinés de la température, du DOC et de la profondeur du lac sur les assemblages de chironomides devraient être étudiés selon un schéma de « néo-écologie » pour dissocier leurs influences respectives.

Introduction

Numerous chironomid transfer functions have been created since the early 1990s to quantitatively reconstruct air and water temperatures (e.g., Walker et al. 1997; Larocque et al. 2001; Porinchu et al. 2002), oxygen availability (Quinlan et al. 1998), water depth (Korhola et al. 2000), and chlorophyll *a* (Brodersen and Lindegaard 1999) from lake sediment sequences. These training sets are still limited geographically (Scandinavia, Switzerland, western Canada, eastern Canada, and the USA (Colorado and Maine)), and uncertainties remain regarding the applicability of a training set from one region to reconstruct temperature from lakes located outside of the geographical range of the training set (I. Larocque, unpublished data). Thus, it is still useful to develop new transfer functions that encompass the geographical range of the lakes to be used for paleoclimate (or any other variable) reconstructions. Training sets are useful to

Received 1 September 2005. Accepted 1 December 2005. Published on the NRC Research Press Web site at http://cjfas.nrc.ca on 29 April 2006.
J18872

I. Larocque[1] and N. Rolland. Institut National de Recherche Scientifique (INRS) : Eau, Terre et Environnement (ETE), 490 De La Couronne, QC G1K 9A9, Canada.
R. Pienitz. Paleolimnology–Paleoecology Laboratory, Centre d'Études Nordiques, Pavillon Abitibi-Price, Université Laval, QC G1K 7P4, Canada.

[1] Corresponding author (e-mail: isabelle_larocque@inrs-ete.uquebec.ca).

Can. J. Fish. Aquat. Sci. 63: 1286–1297 (2006) doi:10.1139/F06-020

identify the environmental factors influencing the distribution of chironomids in lakes over a large geographical transect (more than 1000 km), thereby contributing to a better understanding of their ecology and biogeographical distribution.

Northwestern Quebec (from Abitibi–Temiscamingue to northern Nunavik) covers a vast territory where rivers have been damned and where hydroelectricity plays a key role for the energy supply of industrial centers and communities in southern Quebec. It would be important to determine the effect of climate on future lake water levels and river discharge for the management and regulation of these aquatic ecosystems for the production of hydroelectricity. Although global climate models have shown that a substantial warming will occur in northern environments, regional to local predictions are needed to better manage the northern Quebec facilities. Climate data are thus necessary at regional to local scales. Meteorological data are available only at six locations in northwestern Quebec and data have been recorded only since 1993 (i.e., by Environment Canada). Only paleoarchives can provide longer temporal series of temperature inferences in areas where meteorological data are scarce. Here, we lay the foundations for future climate reconstructions along a south–north transect in northern Quebec by (*i*) determining those factors that statistically exert the strongest influence on the distribution of chironomids in the surface sediments of 60 lakes in northwestern Quebec and (*ii*) developing an inference model for the quantitative reconstruction of temperature based on fossil chironomid assemblages.

Materials and methods

Study area

Sixty lakes were sampled in August 1995, which resulted in the development of a dissolved organic carbon (DOC) – diatom transfer function (Fallu and Pienitz 1999). These lakes were located at the northern and southern part of the tree limit in northern Quebec (Fig. 1). The transect covers 1100 km, between 49°48′N to 59°32′N and 75°43′W to 78°78′W. Three eco-climatic zones are covered by this transect: the high boreal, the subarctic, and the low arctic (Environment Canada 1989). The mean annual temperature and precipitation vary from −0.1 °C and 920 mm in Matagami (49°45′N, 77°38′W) to −6.8 °C and 418 mm in Inukjuak (58°27′N, 78°07′W) (Environnement Canada 1993). These three eco-climatic zones are characterized by different vegetation types. The high boreal is composed mainly of spruce trees (*Picea mariana* and *Picea glauca*), with lichen cover (Payette 1983). In this paper, this zone will be referred to as the Boreal Forest. The subarctic has sporadic forest cover (spruce krummholz) and will be referred to as Forest–Tundra. This zone ends with the northern limit of trees. The last ecozone is described as Tundra with no krummholz and low ground vegetation. The southern zone is composed of granites and gneisses while the northern zone (starting at about 55° N) is composed of metamorphic rocks (Landry and Mercier 1992).

Study sites

Most of the 60 lakes had no affluent. The sampling procedures are described in Fallu and Pienitz (1999). Sediment cores were extracted with a modified Kajak–Brinkhurst or Glew gravity corer (Glew 1991) at the deepest part of the lake. The surface sediment (top 1 cm) was extracted and kept in a refrigerator at 4 °C. This centimetre likely represents the last 3–5 years of sedimentation (Richard et al. 1982; Larocque and Hall 2003).

Some physical and limnological parameters were measured on site, while water samples were taken at 40 cm depth and brought back for chemical analysis at the National Water Research Institute in Burlington, Ontario. Salinity, conductivity, and water temperature (WT) were measured in situ with a Yellow Spring Instrument 33 meter at a depth of 50 cm; transparency was measured with a Secchi disk; and pH was measured in the sampled water bottle at the Centre d'Études Nordiques research station in Kuujjuaraapik–Whapmagoostui. Altitude, area, and distance from the forest were measured on topographic maps (Fallu and Pienitz 1999). All parameters are summarized in Table 1.

Meteorological data were available from Environment Canada at six sites: Matagami (49°45′N, 77°38′W), Radisson (LG2; 53°63′N, 77°07′W), Kuujjuaraapik (55°28′N, 77°75′W), Umiujak (56°53′N, 76°52′W), and Inukjuak (58°27′N, 78°07′W). Air temperature data at each site were plotted against latitude, and a model was developed to extrapolate temperature at each studied lake. In other training set studies, July air temperature was one of the major factors controlling the distribution of chironomids (e.g., Lotter et al. 1997; Larocque et al. 2001), and in the present study we wanted to test if (*i*) air temperature was also important in explaining the distribution of chironomids in our training set and (*ii*) July air temperature (compared with June or August) was the important climate variable explaining the distribution of chironomids.

Chironomid analysis

All the sediment remaining after diatom analysis (Fallu and Pienitz 1999) in the top centimetre was used to extract chironomid head capsules. KOH (10%) was added overnight and the samples were sieved through a 100 µm mesh. The remaining solution was placed in a Bogorov counting tray and examined under a stereomicroscope at × 35 magnification. Head capsules were picked, one by one, and fixed in Hydromatrix mounting medium on a microscope slide. Head capsules were identified using a Van Guard light microscope at × 400 or × 1000. The taxonomy mainly followed Wiederholm (1983) and Oliver and Roussel (1983). Specific keys were used to separate the Tanytarsini subtribe (Brooks et al. 1997; S. Brooks, National History Museum, Cromwell Road, London SW7 5BD, UK, unpublished data). The Tanytarsini who could not be placed into taxonomic groups were separated following the presence (Tanytarsini with) or absence (Tanytarsini without) of a spur on the antenna pedicel. Tanypodinae groups were separated using the position of the setae following Rieradevall and Brooks (2001).

Statistical analysis

We used samples with at least 50 head capsules following the methods outlined in Quinlan and Smol (2000), Heiri and

Fig. 1. Location of the 60 sampled lakes in northern Quebec, Canada. Modified from Fallu and Pienitz (1999).

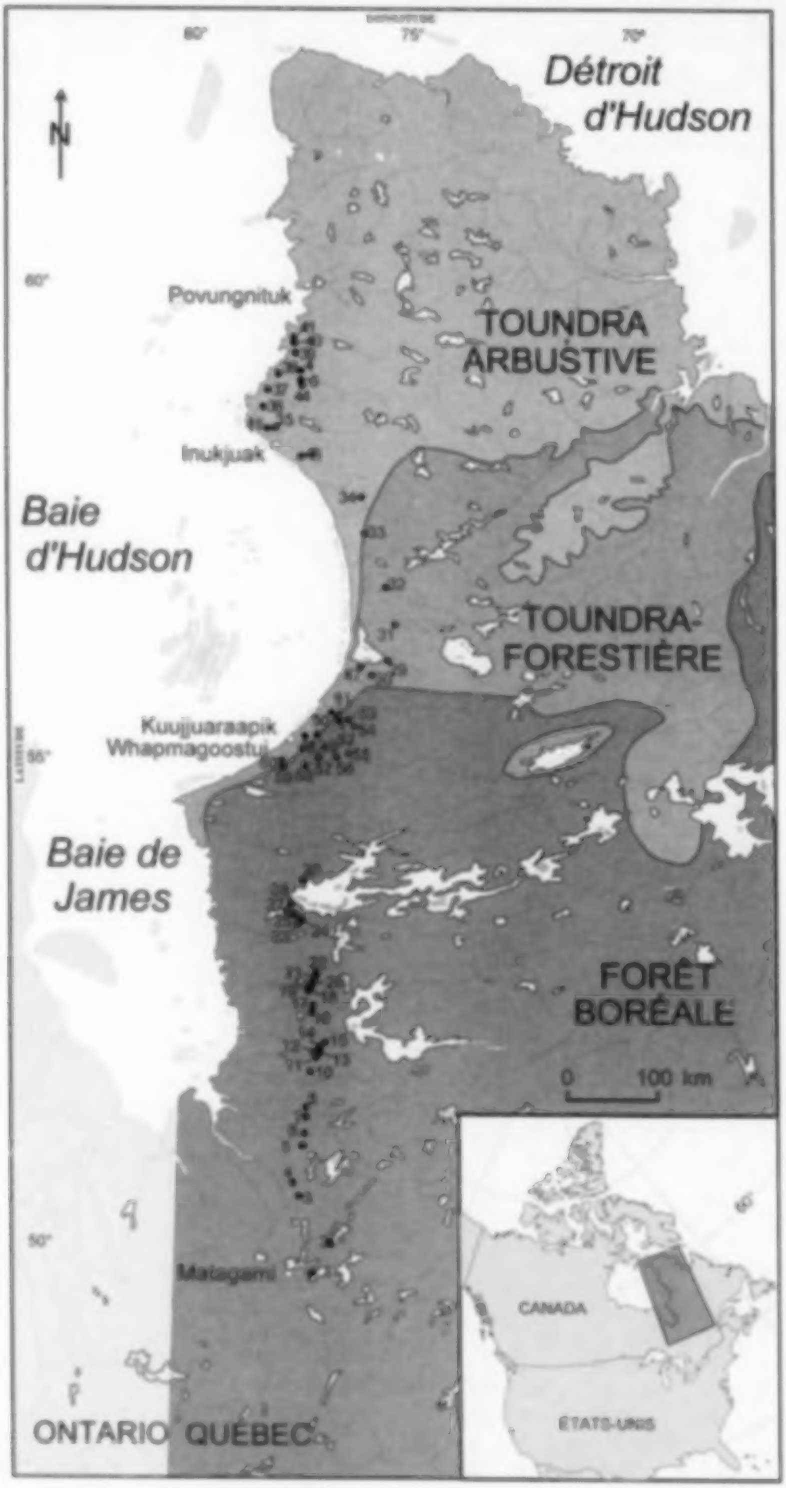
80°
75°
70°
Détroit d'Hudson
N
60°
Povungnituk
TOUNDRA ARBUSTIVE
Inukjuak
Baie d'Hudson
TOUNDRA-FORESTIÈRE
Kuujjuaraapik
Whapmagoostui
55°
Baie de James
FORÊT BORÉALE
0
100 km
50°
Matagami
ONTARIO
QUÉBEC
CANADA
ÉTATS-UNIS
60°

Table 1. Minimum, maximum, mean, and standard deviation (SD) of the environmental characteristics of the 52 studied lakes.

Lake characteristic	Min.	Max.	Mean	SD
TNP ($\mu g \cdot L^{-1}$)	1.0	48.9	11.6	7.8
TFP ($\mu g \cdot L^{-1}$)	0.6	10.6	3.9	2.3
PRS ($\mu g \cdot L^{-1}$)	0.4	7.7	1.9	1.5
TNK ($\mu g \cdot L^{-1}$)	32.0	396.0	233.5	83.9
NO_2 ($\mu g \cdot L^{-1}$)	0.0	8.0	2.5	1.8
DIC ($mg \cdot L^{-1}$)	0.2	4.8	1.3	1.1
DOC ($mg \cdot L^{-1}$)	2.3	19.4	8.1	4.3
Mg ($mg \cdot L^{-1}$)	0.2	4.3	0.7	0.6
Ca ($mg \cdot L^{-1}$)	0.3	6.2	1.9	1.3
Na ($mg \cdot L^{-1}$)	0.6	28.3	3.0	3.9
K ($mg \cdot L^{-1}$)	0.0	1.4	0.3	0.2
Cl ($mg \cdot L^{-1}$)	1.0	54.6	5.1	7.4
SO_4 ($mg \cdot L^{-1}$)	1.4	8.9	3.5	1.6
SiO_2 ($mg \cdot L^{-1}$)	0.1	5.5	1.5	1.5
CHLaN ($\mu g \cdot L^{-1}$)	0.4	17.7	3.7	2.7
CHLaC ($\mu g \cdot L^{-1}$)	0.0	13.1	2.6	2.1
POC ($mg \cdot L^{-1}$)	0.0	12.7	1.0	1.7
PON ($mg \cdot L^{-1}$)	0.0	1.4	0.1	0.2
Al ($\mu g \cdot L^{-1}$)	0.0	1000.0	142.8	191.6
Ba ($\mu g \cdot L^{-1}$)	0.8	11.1	3.2	2.3
Fe ($\mu g \cdot L^{-1}$)	5.0	1100.0	280.3	267.8
Mn ($\mu g \cdot L^{-1}$)	1.6	33.0	8.3	6.9
Sr ($\mu g \cdot L^{-1}$)	2.9	48.6	12.4	8.5
Altitude (m)	13.0	292.6	167.0	75.9
Area (ha)	4.5	292.6	80.2	162.7
Depth (m)	1.0	18.5	3.9	3.6
Transparency (Secchi)	0.5	6.6	2.2	1.6
Water temperature (°C)	13.0	23.6	18.4	3.2
Conductivity ($\mu S \cdot cm^{-1}$)	10.0	170.0	28.7	22.6

Note: TNP, total nonfilterd phoshorus; TFP, total filtered phosphorous; PRS, soluble phosphorous; NKT, total Kjedahl nitrogen; DIC, dissolved inorganic carbon; DOC, dissolved organic carbon; CHLaN, noncorrected chlorophyll *a*; CHLaC, chlorophyll *a* corrected for pheophytins; POC, particulated organic carbon; PON, particulated organic nitrogen.

Lotter (2001), and Larocque (2001). Taxa with an abundance of at least 2% in two lakes were kept for statistical analyses.

A detrended correspondence analysis (DCA) and a detrended canonical correspondence analysis (DCCA) were used to determine the unimodality or linearity in the chironomid data. A redundancy analysis (RDA) was used to determine those environmental variables that explained most of the variance in the distribution and composition of chironomid assemblages (ter Braak and Šmilauer 2002; Lepš and Šmilauer 2003). The CANOCO program (ter Braak and Šmilauer 2002) was used for all ordinations. The chironomid inference models were developed using partial least squares (PLS) methods using the program C2 (Juggins 2003).

Results

Chironomid distribution

Of the 60 lake sediment samples analysed, 52 contained enough chironomid head capsules (>50) to be used for statistical analyses. A total of 97 different chironomid taxa were identified in the surface sediments from the 52 lakes. Of those taxa, 64 had abundances of 2% and more in two lakes (Table 2) and were therefore used in statistical analyses. *Tanytarsus* without, *Tanytarsus* sp. B., *Procladius*, and the *Psectrocladius sordidellus* group were found in more than 40 of the 52 lakes. The *Heterotrissocladius grimshawi* group had the highest percentage (46%) in one lake (lake 29) followed by *Tanytarsus* without (42%), the *Psectrocladius sordidellus* group (30%), *Zalutschia lingulata pauca* (28%), *Sergentia* (27%), and *Procladius* (26%). Fourty-eight of the other taxa had maximum percentages of less than 10%.

The taxa presented in Fig. 2 are those showing the most variations with latitude and vegetation zones. *Cryptochironomus*, *Polypedilum* IIIC (fig. IIIC in Wiederholm 1983), and *Zalutschia zalutschicola* were found only in lakes located in the Boreal Forest zone. *Glyptotendipes*, *Chironomus plumosus*-type, *Paracladopelma*, *Heterotanytarsus*, *Pagastiella*, and *Cryptotendipes* were mainly restricted to the boreal zone, with some sporadic (<2) occurrences in lakes located in the two other zones. *Dicrotendipes* had higher percentages in low latitude lakes located in the boreal zone and was absent in the higher latitude lakes. *Tanytarsus lugens*-type and

Cladopelma were absent in lakes located in the Forest–Tundra zone, but were sporadically present in the Boreal Forest and the Tundra zones. *Microtendipes* had higher percentages in the higher latitude lakes in the Boreal Forest zone, but decreased with latitude in the Forest–Tundra zone and disappeared in lakes of the Tundra zone. *Heterotrissocladius grimshawi*-type and *Heterotrissocladius marcidus*-type had higher abundances in the lakes of the Forest–Tundra zone. *Heterotrissocladius subpilosus*-type was found mainly in lakes of the Forest–Tundra and Tundra zones. The *Psectrocladius sordidellus* group percentages were higher in Tundra lakes, although the taxon was present in most lakes. *Corynocera ambigua* was present only in some Tundra lakes, usually at low percentages (<7%).

Relationship with environmental factors

We provide all the meteorological data that were tested in an RDA to determine the ones explaining the best the distribution of chironomids (Table 3). Mean August air temperature in 1993 and 1994 was the air temperature variable that best explained the distribution of chironomids and was added to the 32 other environmental variables for statistical analysis.

Latitude, vegetation zones, and distance from the forest were highly correlated with temperature, so they were removed from statistical analyses. Two types of analyses can determine the unimodality of taxa: a DCA (ter Braak and Šmilauer 2002) or a DCCA (Lepš and Šmilauer 2003). In both cases, the gradient length expressed as standard deviation (SD) units is the measure of unimodality. The gradient length should be higher than 3 to indicate unimodality (Lepš and Šmilauer 2003). In the DCA, the gradient lengths for the first four axes were 2.01, 1.98, 1.44, and 1.99, indicating that chironomids had a linear distribution. The gradient lengths of the DCCA with all variables were 1.97, 1.95, 1.57, and 1.21. In a DCCA with WT as the sole variable, the gradient lengths were 1.139, 2.056, 1.718, and 1.486. Gradient lengths were longer in a DCCA with August temperature (1.537, 2.296, 2.229, and 1.692). Since all gradient lengths were <3, most chironomid taxa showed a linear relationship with surface water and mean August air temperature.

An RDA with 999 Monte Carlo permutations and forward selection of variables was used to determine the relationship between chironomid distributions in the 52 lakes and the 33 environmental data. All variables combined explained 84% of the variance in the chironomid assemblages. The first and second RDA axes explained 38% and 22%, respectively, of the variance. In general, the separation between the chironomid assemblages in Tundra lakes compared with those of the Boreal Forest lakes was clear (Fig. 3*a*), although 5 of the 37 Forest lakes had chironomid assemblages that resembled those found in Forest–Tundra or Tundra lakes. Seven variables (DOC, depth, area, WT, soluble phosphorus (PRS), dissolved inorganic carbon (DIC), and mean August air temperature) explained 33% of the variance in the distribution of chironomids in the 52 lakes. The variance explained by each environmental variable was estimated in partial RDAs. The variance explained, from highest to lowest, was DOC (9.2%) > depth (9.0%) > mean August air temperature (8.7%) > WT (8.5%) > PRS (6.9%) > DIC (4.4%) > area (3.7%). High λ1/λ2 ratios were obtained for depth (0.78),

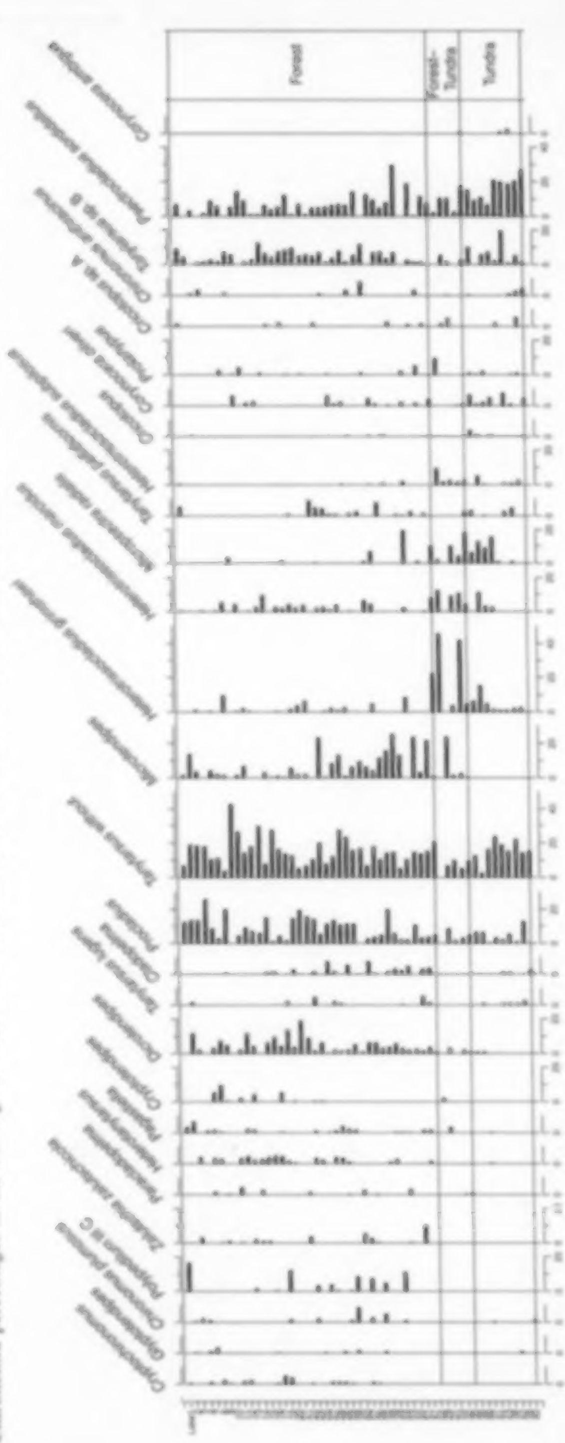

Fig. 2. Chironomid percentages in the training set lakes. Lakes are listed in order of decreasing latitude (°N). The zones indicate the limit of the three major vegetation types.

Table 2. Chironomid taxa with percentage of 2% in at least two lakes.

No.	Taxa	No. of lakes	Max. %
1	*Chironomus anthracinus*-type	14	8.4
2	*Chironomus plumosus*-type	12	8.7
3	*Cladopelma*	20	8.1
4	*Constempellina brevicosta*	21	6.9
5	*Cryptochironomus*	17	5.4
6	*Cryptotendipes*	12	10.2
7	*Dicrotendipes*	39	19.7
8	*Einfeldia*	8	7.2
9	*Endochironomus impar*-type	5	9.5
10	*Glyptotendipes*	10	3.7
11	*Microtendipes*	38	25.9
12	*Omisus*	7	4.1
13	*Pagastiella*	23	7.0
14	*Parachironomus*	5	2.2
15	*Paracladopelma*	12	4.6
16	*Polypedilum*	7	5.7
17	*Polypedilum* III C	12	16.8
18	*Sergentia*	19	27.3
19	*Stempellinella*	24	17.5
20	*Micropsectra bidentata*-type	12	6.9
21	*Micropsectra insignilobus*-type	13	13.1
22	*Micropsectra radialis*-type	19	20.0
23	*Cladotanytarsus*	18	7.0
24	*Paratanytarsus*	26	15.3
25	*Tanytarsus* without	51	43.0
26	*Tanytarsus* with	13	3.2
27	*Tanytarsus chinyensis*-type	9	6.9
28	*Tanytarsus* sp. B	44	19.8
29	*Tanytarsus* sp. C	6	4.3
30	*Tanytarsus lugens*-type	14	5.7
31	*Tanytarsus pallidicornis*-type	19	9.3
32	*Allopsectrocladius*	15	5.7
33	*Corynocera ambigua*	3	3.4
34	*Corynocera oliveri*	24	7.6
35	*Corynoneura*	5	3.0
36	*Cricotopus*	8	4.4
37	*Cricotopus* sp. A	16	6.0
38	*Cricotopus* sp. B	8	5.6
39	*Cricotopus sylvestris*	7	3.2
40	*Cricotopus cylindricus*	6	4.3
41	*Georthocladius*	2	2.5
42	*Heterotrissocladius grimshawi*-type	30	46.2
43	*Heterotrissocladius marcidus*-type	33	12.8
44	*Heterotrissocladius brundini*-type	7	7.1
45	*Heterotrissocladius subpilosus*	19	10.3
46	*Heterotanytarsus*	22	5.1
47	*Limnophyes*	6	3.0
48	*Mesocricotopus*	6	9.6
49	*Nanocladius*	8	3.4
50	*Orthocladius* sp. A	16	4.3
51	*Orthocladius* sp. D	7	2.8
52	*Paracricotopus*	8	3.2
53	*Parakiefferiella*	9	8.7
54	*Paraphaenocladius*	4	5.2
55	*Protanypus*	17	10.3
56	*Psectrocladius septentrionalis*-group	29	16.8
57	*Psectrocladius sordidellus*-group	49	30.0
58	*Smittia*	3	4.3
59	*Zalutschia lingulata pauca*	35	28.6
60	*Zalutschia zalutschicola*	15	10.4
61	*Ablabesmyia*	15	3.7
62	*Telopelopia*	22	5.6
63	*Pentaneurini*	34	7.4
64	*Procladius*	48	26.3

Note: The number of lakes indicates where the taxa was found; Max. % shows the percentage of the lakes where 2% of the taxa are found.

DOC (0.72), WT (0.71), and mean August air temperature (0.63), indicating that inference models could be created for these variables (Fallu and Pienitz 1999; ter Braak and Smilauer 2002).

Heterotrissocladius marcidus-type, *H. grimshawi*-type, *H. subpilosus*-type, *Micropsectra radialis*-type, *Protanypus*, and *Heterotrissocladius brundini*-type are taxa that were most influenced by depth (Fig. 3*b*). *Heterotanytarsus*, *Dicrotendipes*, *Cryptotendipes*, and *Cryptochironomus* seemed to be mostly influenced by WT, mean August air temperature, and DOC.

Transfer functions

Models for WT and mean August air temperature were developed using PLS. The coefficient of determination between mean August air temperature and chironomid percentages was higher ($r^2 = 0.67$) and the root mean square error of prediction (RMSEP) much lower (1.17 °C) than those for WT ($r^2 = 0.59$, RMSEP = 2.24 °C). When inferring WT, lakes with temperature lower than 16 °C were located further away from the 1:1 line of prediction (Fig. 4*a*), indicating that colder lakes were not so well predicted. In mean August predictions, the temperature in warmer lakes was generally underestimated, and the residuals for these lakes were more important (Fig. 4*b*).

Although our goal was to create chironomid transfer functions for temperature, models for DOC and depth were also attempted using PLS. While the transfer function for DOC had relatively good statistics ($r^2 = 0.62$, RMSEP = 2.78 $\text{mg}\cdot\text{L}^{-1}$), the model for depth had a low coefficient of correlation ($r^2 = 0.40$, RMSEP = 2.84 m).

Discussion

The chironomid distribution in our 52 lakes from northwestern Quebec was mainly influenced by four parameters: depth, DOC, WT, and mean August air temperature. The goal of this paper was to create a transfer function for temperature, and the model performance data showed that it was coherent to do so. Although the r^2 (0.67) was lower than that of the Eastern Canadian training set for WT (0.88; Walker et al. 1997), the RMSEP (1.17 °C) was lower (RMSEP Eastern Canadian = 2.26 °C). The better correlation in the Eastern Canadian training set might be explained by the fact that its

Table 3. Meteorological data analysed in a redundancy analysis.

Variable	Variance explained (%)
All variables	27
June 1993	—
July 1993	4
August 1993	—
Mean summer 1993	—
June 1994	4
July 1994	—
August 1994	—
Mean summer 1994	—
June 1995	—
July 1995	—
August 1995	—
Mean summer 1995	—
June 1993–1994	—
July 1993–1994	—
August 1993–1994	9
Mean summer 1993–1994	—
June 1993–1995	—
July 1993–1995	—
August 1993–1995	—
Mean summer 1993–1995	—

39 lakes were distributed over 3000 km and over a larger temperature gradient (20 °C). Our 52 lakes, however, were located within 1100 km in a temperature gradient of 10 °C. Similar results were obtained in Norway, where the first developed training set comprised only 44 lakes in a temperature gradient of 8.3 °C with $r^2 = 0.69$ (Brooks and Birks 2000), and the second training set comprised 153 lakes in Norway and Svalbard in a temperature gradient of 12.5 °C and an r^2 of 0.90 (S. Brooks, National History Museum, Cromwell Road, London SW7 5BD, UK; and H.J.B. Birks, Botanical Institute, University of Bergen, N-5007 Bergen, Norway, unpublished data). In general, training sets with longer temperature gradients have better r^2 (table 6 in Larocque et al. 2001). These results suggest that to obtain a better r^2, our training set should be extended, although training sets with lower r^2 also perform in general quite well. For example, inferences based on a Swedish training set with an r^2 of 0.65 were quite similar to meteorological data (Larocque and Hall 2003). It seems evident that the r^2 is not the only statistical parameter that is important for the relevance of the temperature inferences.

The lower RMSEP of our training set might result from higher taxonomic resolution. Here, we separated many of the taxa that were combined in the Eastern Canadian training set (especially the Tanytarsina), and we think we obtained better temperature optima for each taxon, thereby decreasing the error of temperature estimates. Similar results were obtained in Norway; increasing the taxonomic level probably decreased the error of temperature estimates in the 153-lake training set (S. Brooks, Natural History Museum, Cromwell Road, London SW7 5BD, UK, personal communication).

Fig. 3. (*a*) Redundancy analysis (RDA) of lake data. Solid circles are lakes located in the Boreal Forest zone, shaded circles represent lakes located in the Forest–Tundra ecotone, and open circles represent lakes within the Tundra zone. (*b*) RDA analysis of taxa. The numbers are associated to taxon names in Table 2. The arrows represent the vectors of the seven environmental data explaining the distribution of chironomids in the 52 lakes. DIC, dissolved inorganic carbon; Area, area of lakes; WT, water temperature; DOC, dissolved organic carbon; PRS, soluble reactive phosphorus; AUGUST AIR, mean August air temperature in 1993 and 1994; Depth, maximum lake depth.

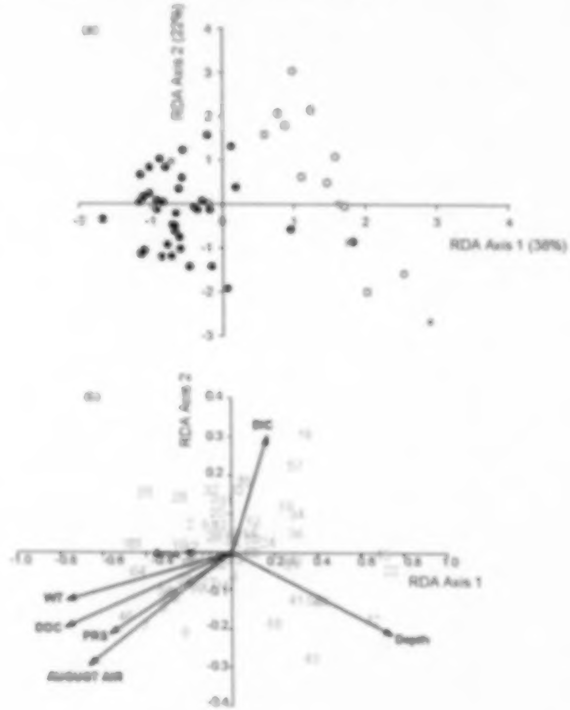

The PLS coefficients for each taxa (Table 4) identified the *Psectrocladius sordidellus* group, *Sergentia*, *Micropsectra radialis*-type, *Corynocera oliveri*, and *Heterotrissocladius subpilosus*-type as the coldest indicators. A review of temperature optima from four training sets is presented in Bennike et al. (2004) and is used for comparison with our results. The *Psectrocladius sordidellus* group was not considered as a cold indicator in northern Sweden (optimum = 11.6 °C), but *Psectrocladius* were the most abundant taxon in the cold early Holocene in a shrub–tundra lake in northern Quebec (Fallu et al. 2005). The species name *Psectrocladius sordidellus* is given to a group with similar characteristics of the head capsule but might comprise species with potentially different temperature optima. Here, the *Psectrocladius sordidellus* group is also located along the DIC vector in the RDA analysis and could be influenced by this factor more than by temperature. While *Sergentia* has a cold optimum in eastern Canada (6 °C) and is a cold indicator in our training

Fig. 4. (*a*) Relationship between observed and inferred water temperature. The solid line represents the 1:1 relationship. (*b*) Observed water temperature versus residuals. (*c*) Relationship between observed and inferred mean August air temperature. The solid line represents the 1:1 relationship. (*d*) Observed water temperature versus residuals.

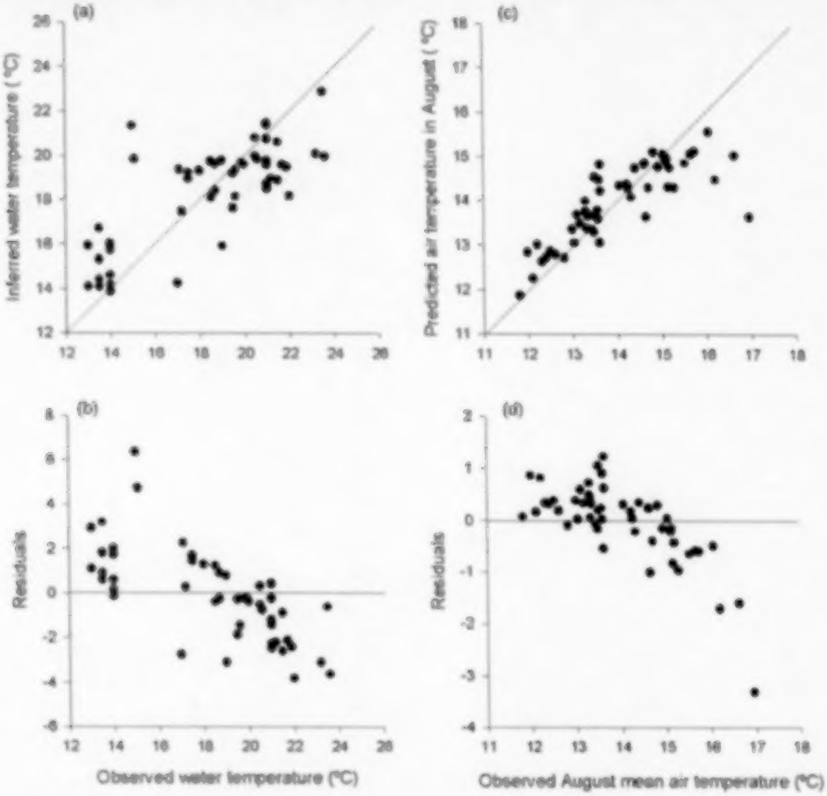

set, it had higher temperature optima (15 °C) in northern Finland and northern Sweden (Bennike et al. 2004). These contradictory results indicate that the taxa called "*Sergentia*" might not comprise the same species in Canada and in northern Europe. A special taxonomic effort could be given to this taxon to try to separate it into taxonomic groups. *Micropsectra radialis*-type, *Corynocera oliveri*, and *Heterotrissocladius* are cold indicators (optimum <7 °C) in the Canadian and in the North European training sets. *Dicrotendipes*, *Cryptochironomus*, and *Zalutschia* were identified as warm indicators in this training set and in the Eastern Canada and Northern Europe training sets (Bennike et al. 2004). Other taxa have contradictory results. *Cladotanytarsus* and *Cladopelma* were considered here as colder indicators, while they were warm indicators in other training sets; *Heterotanytarsus* is an intermediate taxon in other training sets, while it is a warmer indicator here. These differences might be attributed to the fact that we had linear relationships between the chironomid taxa and the temperature. By increasing the training set north and south, we might get a better distribution of all taxa and be able to calculate optima with unimodal techniques.

Although temperature was an important factor explaining the distribution of chironomids, other parameters obviously also had an influence on larval distribution. Depth and DOC effects on the chironomid distribution are further discussed below.

Depth

Depth has been identified as an important factor explaining the distribution of chironomids in many other training sets (e.g., Olander et al. 1997; Quinlan et al. 1998; Porinchu et al. 2002). Taxa such as *Micropsectra*, *Heterotrissocladius subpilosus*, and *H. brundini* are restricted to deep lakes or to the profundal zones (Walker 1990; Walker and MacDonald 1995; Simola et al. 1996). These taxa were also found in deeper lakes in our training set. Most *Tanytarsus*, *Tanytarsus lugens*, and *Microtendipes* prefer the littoral zone (Schmäh 1993; Walker and MacDonald 1995; Heiri et al. 2003). In the RDA ordination, these taxa were located at the opposite end of the depth vector, indicating that they prefer shallow lakes. Although an inference model has been built for the reconstruction of depth (Korhola et al. 2000), the low coefficient of determination we obtained here does not indicate that the model would be significant. The importance of depth in explaining the distribution of chironomids should be taken into account when interpreting temperature reconstructions, especially if the community changes involve

Table 4. Partial least square (PLS) coefficients of each taxon.

Taxa	PLS
Psectrocladius sordidellus-group	–0.331
Sergentia	–0.301
Micropsectra radialis-type	–0.177
Corynocera oliveri	–0.163
Heterotrissocladius subpilosus-type	–0.142
Cladopelma	–0.116
Heterotrissocladius grimshawi-type	–0.085
Tanytarsus pallidicornis-type	–0.083
Cladotanytarsus	–0.083
Tanytarsus lugens-type	–0.080
Tanytarsus sp. B	–0.075
Microtendipes	–0.072
Cricotopus sp. A	–0.067
Cricotopus	–0.061
Omisus	–0.058
Paracricotopus	–0.052
Orthocladius sp. A	–0.044
Chironomus anthracinus-type	–0.044
Corynocera ambigua	–0.044
Telopelopia	–0.032
Orthocladius sp. D	–0.029
Parachironomus	–0.026
Cricotopus cylindricus	–0.024
Chironomus plumosus-type	–0.023
Heterotrissocladius brundini-type	–0.020
Ablabesmyia	–0.014
Limnophyes	–0.008
Protanypus	–0.004
Parakiefferiella	–0.004
Paratanytarsus	–0.003
Micropsectra bidentata-type	–0.002
Micropsectra insignilobus-type	0.002
Nanocladius	0.002
Tanytarsus with	0.006
Georthocladius	0.008
Polypedilum	0.011
Einfeldia	0.018
Corynoneura scutellata	0.024
Psectrocladius septentrionalis-group	0.026
Allopsectrocladius	0.027
Glyptotendipes	0.029
Constempellina	0.035
Smittia	0.039
Heterotrissocladius marcidus-type	0.042
Tanytarsus without	0.044
Cricotopus sp. B	0.046
Paracladopelma	0.048
Tanytarsus sp. C	0.051
Paraphaenocladius	0.053
Cricotopus laricomalis	0.060
Polypedilum III C	0.069
Mesocricotopus	0.070
Pagastiella	0.074
Zalutschia lingulata pauca	0.086
Zalutschia zalutschicola	0.095
Tanytarsus chinyensis-type	0.112
Dicrotendipes	0.119
Endochironomus impar-type	0.131
Cryptochironomus	0.132
Cryptotendipes	0.136
Procladius	0.143
Heterotanytarsus	0.150
Stempellinella	0.151
Pentaneurini	0.192

changes in taxa such as *Micropsectra*, *H. subpilosus*-type and *H. brundini*-type, *Tanytarsus*, *Tanytarsus lugens*-type, and *Microtendipes*.

DOC

DOC was not an important parameter explaining the distribution of chironomids in most other training sets either because it was not measured as such (e.g., Walker et al. 1991; Olander et al. 1997 (total organic carbon, (TOC)); Porinchu et al. 2002 (particulate organic carbon) or the DOC gradient along the transect was weak (e.g., Larocque et al. 2001). Lotter et al. (1997) found a relationship between DOC and the chironomid distribution in Swiss lakes, but DOC did not solely explain a high proportion of the variance in the species data. In Finland, TOC was an important factor explaining the distribution of chironomids; high TOC lakes were surrounded by peatlands (Nyman et al. 2005).

In our study sites, DOC derives mainly from allochthonous sources (Fallu and Pienitz 1999). This has been shown also in other high latitude areas (e.g., Labrador, Engstrom 1987; Alaska, Kling et al. 1991; Yukon, Pienitz et al. 1997*a*; Northwest Territories, Pienitz et al. 1997*b*; Mackenzie Delta, Ramlal et al. 1994). The relationship between latitude and DOC is relatively important (Fig. 5): DOC is generally higher in lakes located in the Boreal Forest (average 9.8 mg·L^{-1}) and lower in Tundra lakes (average 4.8 mg·L^{-1}) (Fallu and Pienitz 1999). Similar results were obtained in northern Canada (Pienitz et al. 1997*a*, 1997*b*), in Siberia (Laing et al. 1999), and in Europe (Kingston and Birks 1990; Stevenson et al. 1991). The feeding habits of chironomid larvae vary, but many are detritivores and (or) filter-feeders, while others graze on bacteria (Walker 2001). These are feeding habits that involve DOC absorption. Binkley et al. (2005) showed that although DOC was thought to come primarily from bacteria degradation, *Chironomus* utilized DOC derived from terrestrial sources. Labile carbon was added to a stream in North Carolina, USA, and lead to a threefold increase in growth rate of chironomid larvae (Wilcox et al. 2005).

DOC can influence aquatic communities by attenuating light penetration (Vincent and Roy 1993) and by changing the thermal stratification of lakes (Scully 1998). In the RDA, DOC and temperature were represented by vectors that pointed in the same direction, indicating that separation of DOC and temperature effects on chironomid distribution

Fig. 5. Relationships between latitude and (*a*) dissolved organic carbon (DOC) and (*b*) water temperature. The solid line is the regression line.

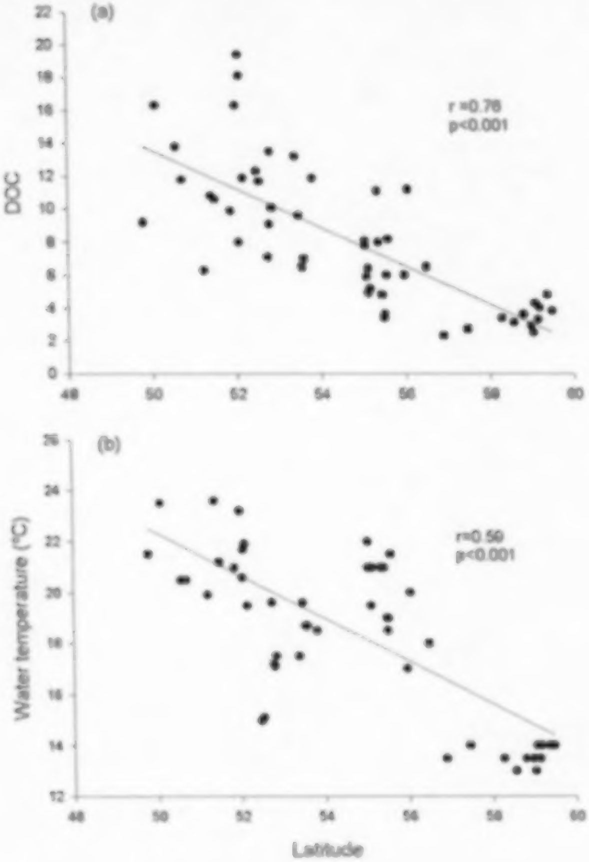

might be difficult, although the relationship between WT and DOC was weak (Fig. 5).

The DOC–diatom transfer function elaborated from the same set of lakes seems to be more relevant ($r^2 = 0.90$, RMSEP = 1.23 mg·L^{-1}) (Fallu and Pienitz 1999), and we therefore do not suggest to use the DOC–chironomid transfer function developed here.

Water, air, and August temperature

Based on other published transfer functions (e.g., Lotter et al. 1997; Brooks and Birks 2000; Larocque et al. 2001), it is not surprising that air temperature is better predicted with chironomids than with WT. This relationship is not entirely due to chironomid ecology and life cycle, although hatching of adults and reproduction might be related to air temperature (Armitage et al. 1995). It is mainly due to the fact that meteorological data have been sampled more frequently than WT. The air temperature data set is thus more representative than the punctual WT measurements.

Mean August air temperature 2 years prior to the sampling year is a better predictor of chironomid distribution than July air temperature of the sampling year, generally considered in other transfer functions (e.g., Brooks and Birks 2000; Larocque et al. 2001). Chironomid assemblages in surface sediment integrate several years (likely 2–5 years), and larvae might take more than 1 year to become fourth instar, especially in colder lakes (Armitage et al. 1995). August is the month when emergence was highest in temperate zone streams (Pinder 1974), and voltinism (number of annual generations per species in a habitat) decreases with latitude (Armitage et al. 1995). At high latitude sites, one generation per species is generally recorded every 2–3 years, and the adults of certain species (*H. grimshawi*, *Psectrocladius limbatellus*, *Rheocricotopus effusus*, and *Paracladopelma nigritula*) mainly emerge between mid-July and September (Welch 1976). These studies highlight the need for a better understanding of chironomid larval ecology when trying to explain the stronger impact of August (in this case) rather than July, mean June, or mean summer temperatures on the distribution of chironomids.

In conclusion, our results indicate that the northern Quebec lake training set should be extended to (*i*) get a unimodal response of taxa to better calculate optima of temperature and (*ii*) to better predict temperature in colder and warmer lakes. By extending the training set, we hope to achieve a better correlation (r^2) between temperature and chironomids. However, statistical analysis should not be the only approach for climate reconstruction. Understanding the relationship between temperature and chironomid larval life strategies (e.g., timing and duration of larval development, emergence) is still a research challenge for paleoecological studies using fossil chironomids. We plan to study more lakes along our transect with weekly sampling intervals to determine which taxa might be better indicators of temperature and to further refine the relationship between chironomids and lake DOC.

Acknowledgements

The environmental data were obtained through research funding obtained by R. Pienitz from the Natural Sciences and Engineering Research Council of Canada (NSERC) and Fonds de recherche sur la nature et les technologies (FQRNT). Thanks go to N. Allaire, M.-A. Fallu, and P. Tremblay who helped with field work.

References

Armitage, P., Cranston, P.S., and Pinder, L.C.V. (*Editors*). 1995. The Chironomidae: the biology and ecology of non-biting midges. Chapman and Hall, London, UK.

Bennike, O., Brodersen, K.P., Jeppesen, E., and Walker, I.C. 2004. Aquatic invertebrates and high latitude paleolimnology. *In* Long-term environmental change in arctic and Antarctic lakes. Developments in paleoenvironmental research. Vol. 8. *Edited by* R. Pienitz, S.V. Douglas, and J.P. Smol. Springer, Dordrecht, the Netherlands. pp. 159–185.

Binkley, E., Fontino, K., and Hershey, A.E. 2005. Importance of DOC from terrestrial sources in supporting benthic production in Arctic lakes. Chironomidae: linking biodiversity and bioassessment. *In* The Abiotic Template in Flowing Waters. The 2005 Joint Assembly of the American Geophysical Union

(AGU) and the North American Benthological Society (NABS), 22–27 May 2005, New Orleans, Louisiana. NABS, New Orleans, La.

Brodersen, K.P., and Lindegaard, C. 1999. Classification, assessment and trophic reconstruction of Danish lakes using chironomids. Freshw. Biol. **42**: 143–157.

Brooks, S.J., and Birks, H.J.B. 2000. Chironomid-inferred late-glacial and early-Holocene mean July air temperatures from Kråkenes Lake, Western Norway. J. Paleolimnol. **23**: 77–89.

Brooks, S.J., Lowe, J.J., and Mayle, F.E. 1997. The Late Devensian Lateglacial palaeoenvironmental record from Whitrig Bog, SE Scotland. 2. Chironomidae (Insecta: Diptera). Boreas, **26**: 297–308.

Engstrom, D.R. 1987. Influence of vegetation and hydrology on the humus budgets of Labrador lakes. Can. J. Fish. Aquat. Sci. **44**: 1306–1314.

Environment Canada. 1989. Ecoclimatic regions of Canada, first approximation. Ecoregions Working Group, Ottawa, Ont. Ecological Land Classification Series No. 23.

Environnement Canada. 1993. Normales climatiques au Canada, Québec, 1961–1990. Service de l'environnement atmosphérique, Ottawa, Ont.

Fallu, M.-A., and Pienitz, R. 1999. Diatomées lacustres de Jamésie-Hudsonie (Québec) et modèle de reconstitution des concentrations de carbone organique dissous. Ecoscience, **6**: 603–620.

Fallu, M.-A., Pienitz, R., Walker, I.R., and Lavoie, M. 2005. Paleolimnology of a shrub–tundra lake and response of aquatic and terrestrial indicators to climatic change in arctic Québec, Canada. Palaeogeogr. Palaeoclimatol. Palaeoecol. **215**: 183–203.

Glew, J. 1991. Miniature gravity corer for recovering short sediment cores. J. Paleolimnol. **5**: 285–287.

Heiri, O., and Lotter, A.F. 2001. Effect of low count sums on quantitative environmental reconstructions: an example using subfossil chironomids. J. Paleolimnol. **26**: 343–350.

Heiri, O., Lotter, A.F., Hausmann, S., and Kienast, F. 2003. A chironomid-based Holocene summer air temperature reconstruction from the Swiss Alps. Holocene, **13**: 477–484.

Juggins, S. 2003. Program C2 data analysis. Ver. 1.4.2. University of Newcastle, UK.

Kingston, J.C., and Birks, H.J.B. 1990. Dissolved organic carbon reconstruction from diatom assemblages in PIRLA project lakes, North America. Philos. Trans. R. Soc. Lond. B Biol Sci. **327**: 279–288.

Kling, G.W., Kipphut, G.W., and Miller, M.C. 1991. Arctic lakes and streams as gas conduits to the atmosphere: implications for tundra carbon budgets. Science (Washington, D.C.), **251**: 298–301.

Korhola, A., Olander, H., and Blom, T. 2000. Cladoceran and chironomid assemblages as quantitative indicators of water depth in subarctic Fennoscandian lakes. J. Paleolimnol. **24**: 43–54.

Laing, T.E., Pienitz, R., and Smol, J.P. 1999. Freshwater diatom assemblages from 23 lakes located near Norilsk, Siberia: a comparison with assemblages from other circumpolar treeline regions. Diatom Res. **14**: 285–305.

Landry, B., and Mercier, M. (*Editors*). 1992. Notions de géologie. 3rd ed. Modulo éditeur, Mont-Royal, Québec, Canada.

Larocque, I. 2001. How many chironomid head capsule is enough? A statistical approach to determine sample size for paleoclimatic reconstruction. Palaeogeogr. Palaeoclimatol. Palaeoecol. **172**: 133–142.

Larocque, I., and Hall, R.I. 2003. Chironomids as quantitative indicators of mean July air temperature: validation by comparison with century-long meteorological records from northern Sweden. J. Paleolimnol. **29**: 475–493.

Larocque, I., Hall, R.I., and Grahn, E. 2001. Chironomids as indicators of climate change: a 100-lake training set from a subarctic region of northern Sweden (Lapland). J. Paleolimnol. **26**: 307–322.

Lepš, J., and Šmilauer, P. 2003. Multivariate analysis of ecological data using CANOCO. Cambridge University Press, London, UK.

Lotter, A.F., Birks, H.J.B., Hofmann, W., and Marchetto, A. 1997. Modern diatom, cladocera, chironomid, and chrysophyte cyst assemblages as quantitative indicators for the reconstruction of past environmental conditions in the Alps. 1. Climate. J. Paleolimnol. **18**: 395–420.

Nyman, M., Korhola, A., and Brooks, S.J. 2005. The distribution and diversity of Chironomidae (Insecta: Diptera) in western Finnish Lapland, with special emphasis on shallow lakes. Global Ecol. Biogeogr. **14**: 137–153.

Olander, H., Korhola, A., and Blom, T. 1997. Surface sediment Chironomidae (Diptera) distribution along an ecotonal transect in subarctic Fennoscandia: developing a tool for palaeotemperature reconstructions. J. Paleolimnol. **18**: 45–59.

Oliver, D.R., and Roussel, M.E. 1983. The insects and arachnids of Canada, part II. The genera of larval midges of Canada. Agriculture Canada, Ottawa, Ont. Publ. 1746.

Payette, S. 1983. The forest tundra and present tree-lines of the northern Québec–Labrador peninsula. *In* Tree-line ecology. *Edited by* P. Morisset and S. Payette. Nordicana, **47**: 3–23.

Pienitz, R., Smol, J.P., and Lean, D.R.S. 1997*a*. Physical and chemical limnology of 50 lakes located between the southern Yukon and the Tuktoyatuk Peninsula, Northwest Territories (Canada). Can. J. Fish. Aquat. Sci. **54**: 330–346.

Pienitz, R., Smol, J.P., and Lean, D.R.S. 1997*b*. Physical and chemical limnology of 24 lakes located between Yellowknife and Contwoyoto Lake, Northwest Territories, Canada. Can. J. Fish. Aquat. Sci. **54**: 347–364.

Pinder, L.C.V. 1974. The Chironomidae of a small chalk-stream in southern England. Entomol. Tidsk. **95**(Suppl.): 195–202.

Porinchu, D.F., MacDonald, G.M., Bloom, A.M., and Moser, K.A. 2002. The modern distribution of chironomid sub-fossils (Insecta: Diptera) in the Sierra Nevada, California: potential for paleoclimatic reconstructions. J. Paleolimnol. **28**: 355–375.

Quinlan, R., and Smol, J.P. 2000. Setting minimum head capsule abundance and taxa deletion criteria in chironomid-based inference models. J. Paleolimnol. **26**: 327–342.

Quinlan, R., Smol, J.P., and Hall, R.I. 1998. Quantitative inferences of past hypolimnetic anoxia in south-central Ontario lakes using fossil midges (Diptera: Chironomidae). Can. J. Fish. Aquat. Sci. **55**: 587–596.

Ramlal, P.S., Hesslein, R.H., Hecky, R.E., Fee, E.J., Rudd, J.W.M., and Guildford, S.J. 1994. The organic carbon budget of a shallow arctic tundra lake on the Tuktoyaktuk Peninsula, NWT, Canada: arctic lake carbon budget. Biogeochemistry, **24**: 145–172.

Richard, P.J.H., Larouche, A., and Bouchard, M.A. 1982. Âge de la déglaciation finale et histoire postglaciaire de la vegetation dans la partie centrale du Nouveau-Québec. Geogr. Phys. Quat. **36**: 63–90.

Rieradevall, M., and Brooks, S.J. 2001. An identification guide to subfossil Tanypodinae larvae based on cephalic setation. J. Paleolimnol. **25**: 81–99.

Schmäh, A. 1993. Variation among fossil chironomid assemblages in surficial sediments of Bodensee–Untersee (SW-Germany): implications for paleolimnological interpretation. J. Paleolimnol. **9**: 99–108.

Scully, N.M. 1998. Les effets de la radiation ultraviolette et des facteurs hydrodynamiques sur les processus photobiochimiques des écosytèmes aquatiques. Thèse Ph.D., Université Laval, Québec.

Simola, H., Merilainen, J.J., Sandman, O., Marttila, V., Karjalainen, H., Kukkonen, M., Julken-Tiitto, R., and Hakulinen, J. 1996. Palaeolimnological analyses as information source for large lake biomonitoring. Hydrobiologia, **322**: 283–292.

Stevenson, A.C., Juggins, S., Birks, H.J.B., Anderson, D.S., Anderson, N.J., Battarbee, R.W., Berger, F., Davis, R.B., Flower, R.J., Hayworth, E.Y., Jones, V.J., Kingston, J.C., Kreiser, A.M., Line, J.J., Munro, M.A.R., and Renberg, I. 1991. The surface water acidification project paleolimnology programme: modern diatom/lake-water chemistry data. ENSIS Publishing, London, UK.

ter Braak, C.J.F., and Šmilauer, P. 2002. CANOCO reference manual. Version 4.5. Microcomputer Power, Ithaca, N.Y.

Vincent, W.F., and Roy, S. 1993. Solar ultraviolet-B radiation and aquatic primary production: damage, protection and recovery. Environ. Rev. **1**: 1–12.

Walker, I.R. 1990. Modern assemblages of arctic and alpine Chironomidae as analogues for late-glacial communities. Hydrobiologia, **214**: 223–227.

Walker, I.R. 2001. Midges: Chironomidae and related Diptera. *In* Tracking environmental change using lake sediments, volume 4. Zoological indicators. *Edited by* J.P. Smol, H.J.B. Birks, and W.M. Last. Kluwer Academic Publishers, Dordrecht, the Netherlands. pp. 43–66.

Walker, I.R., and MacDonald, G.M. 1995. Distributions of Chironomdiae (Insecta: Diptera) and other freshwater midges with respect to treeline, Northwest Territories, Canada. Arct. Alp. Res. **27**: 258–263.

Walker, I.R., Smol, J.P., Engstrom, D.R., and Burks, H.J.B. 1991. An assessment of Chironomidae as quantitative indicators of past climatic change. Can. J. Fish. Aquat. Sci. **48**: 975–987.

Walker, I.R., Levesque, A.J., Cwynar, L.C., and Lotter, A.F. 1997. An expanded surface-water palaeotemperature inference model for use with fossil midges from eastern Canada. J. Paleolimnol. **18**: 165–178.

Welch, H.E. 1976. Ecology of Chironomidae (Diptera) in a polar lake. J. Fish. Res. Board Can. **33**: 227–247.

Wiederholm, T. 1983. Chironomidae of the Holarctic region. Part 1. Larvae. Entomol. Scand. Suppl. 19.

Wilcox, H.S., Wallace, J.B., Meyer, J.L., and Benstead, J.P. 2005. Effects of labile carbon addition on a headwater stream food web. Limnol. Oceanogr. **50**: 1300–1312.

Temperature-dependent growth of the blue crab (*Callinectes sapidus*): a molt process approach

Bryce J. Brylawski and Thomas J. Miller

Abstract: Crustaceans display discrete and biphasic growth as a result of the molting process, so the traditionally used von Bertalanffy growth model does not capture well the phenomena associated with molting-based growth. A molt-process model can predict crustacean growth, including the temperature dependence of intermolt period that can produce the extended overwintering phenomena during which growth ceases. This study parameterized a molt-process model for the blue crab (*Callinectes sapidus*; Portunidae). Crab growth histories were observed for individual crabs held in field enclosures and temperature-controlled, recirculating tanks. A growth-based temperature of torpor (T_{min}) of 10.8 °C was determined. A mean growth per molt of 119.5% increase in carapace width was observed. The average intermolt period observed was 536 ± 231 degree-days. The predictive ability of these growth parameter estimates was evaluated against growth observed in the field based on data on interannual changes in size frequencies of crabs from a winter dredge survey. The evaluated model was used to explore recruitment timing in warm (1996) and cold (1998) years. A 10% shift in the timing of juvenile crabs becoming available for legal exploitation was predicted from the simulations.

Résumé : À cause du processus de la mue, les crustacés ont une croissance discontinue et biphasique; le modèle classique de croissance de von Bertalanffy ne décrit donc pas bien les phénomènes associés à cette croissance basée sur la mue. Un modèle de processus de la mue peut prédire la croissance des crustacés, y compris la dépendance de la température de la période inter-mue qui peut produire des phénomènes de longs hivernages pendant lesquels toute croissance cesse. Notre étude estime les paramètres d'un modèle de processus de la mue pour le crabe bleu (*Callinectes sapidus*; Portunidae). Le déroulement de la croissance a pu être observé chez des crabes individuels gardés dans des enclos de terrain et dans des aquariums à recirculation de température contrôlée. La température de torpeur (T_{min}) basée sur la croissance est estimée à 10,8 °C. La croissance moyenne observée par mue comprend une augmentation de 119,5 % de la largeur de la carapace. La durée observée moyenne des inter-mues est de 536 ± 231 degrés-jours. Nous avons évalué le pouvoir de prédiction de ces paramètres de croissance estimés par une comparaison avec la croissance en nature d'après les changements inter-annuels des fréquences des tailles de crabes dans un inventaire d'hiver à la benne. Nous avons utilisé le modèle à évaluer pour examiner la chronologie du recrutement dans une année chaude (1996) et une froide (1998). Les simulations prédisent un décalage de 10 % dans le moment où les jeunes crabes deviennent disponibles pour la récolte légale.

[Traduit par la Rédaction]

Introduction

The patterns and consequences of plant and animal growth have fascinated ecologists for more than a century (Thompson 1968). Researchers have sought to understand the consequences of differences in allocation of energy to growth among species and individuals. Such questions are at the heart of life history theory (Roff 1992). Development of much of this theory requires an accurate and quantitative description of growth. One of the most flexible and commonly used descriptions of growth is that of von Bertalanffy (1938).

A principal assumption of the von Bertalanffy model is that growth is continuous. However, crustaceans do not exhibit continuous growth; rather, in these animals, growth is discrete and biphasic. Their rigid exoskeleton limits external growth to the brief molting events (Hartnoll 1982). The saltatory nature of crustacean growth implies that the von Bertalanffy model is likely inadequate for defining crustacean growth dynamics. However, the biphasic nature of crustacean growth can be used as a foundation to develop a more appropriate model of crustacean growth. A saltatory growth pattern can be modeled by combining predictions of the amount of growth per molt (GPM) with estimates of the frequency of molting (the inverse of the intermolt period (IMP)) (Hiatt 1948). Such approaches are termed molt-process models (Smith 1997).

Molt-process models have been created for several crustaceans, including Alaskan king crab (*Paralithodes camtschatica*), American lobster (*Homarus americanus*), and Dungeness crab (*Cancer magister*) (McCaughran and Powel 1977; Fogarty and Idoine 1988; Wainwright and Armstrong 1993).

Received 15 March 2005. Accepted 23 November 2005. Published on the NRC Research Press Web site at http://cjfas.nrc.ca on 6 May 2006.
J18603

B.J. Brylawski[1,2] and T.J. Miller. University of Maryland Center for Environmental Science, Chesapeake Biological Laboratory, P.O. Box 38, Solomons, MD 20688, USA.

[1] Corresponding author (e-mail: brylawsk@vims.edu).
[2] Present address: Virginia Institute of Marine Science, College of William and Mary, P.O. Box 1346 Gloucester Point, VA 23062-1346, USA.

Can. J. Fish. Aquat. Sci. 63: 1298–1308 (2006)

doi:10.1139/F06-011

The previous models estimated IMP in days, based on molting-frequency estimates. For these instances, molting is infrequent (per year or longer). However, modeling IMP as a function of time alone ignores potential environmental influences on IMP. Temperature is one example of a factor that has a well-documented effect on IMP in crustaceans (Leffler 1972; Wainwright and Armstrong 1993). For example, in some temperate-climate crustaceans, growth ceases during the cold weather months because of the inhibitory effects of cold water (*Callinectes sapidus*; Leffler 1972; Ju et al. 2001). Thus, any growth-modeling framework for crustaceans must be sufficiently flexible to include temperature-dependent variation in intermolt period if it is to accommodate the diversity of growth patterns exhibited.

Smith (1997) developed a crustacean molt-process model that is flexible enough to include both overwintering and other temperature-dependent growth phenomena. In Smith's model, GPM is assumed to be a relatively constant proportion of the premolt size. However, Smith expressed IMP in physiological time, via a degree-day function, instead of in chronological time, as used in previous models.

The use of the degree-day approach permits the effects of time and temperature to be expressed simultaneously. Degree-days are calculated by multiplying the difference between the ambient temperature and a physiological minimum for growth (T_{min}) by the duration over which the temperature was experienced (days). Importantly, when the temperatures are below T_{min}, no degree-days are accumulated and the IMP becomes infinitely long, thereby inherently incorporating the phenomena of diapause. Smith's model accounts for variability in intermolt period by recognizing that accumulation of sufficient degree-day exposure is a necessary, but not sufficient, condition for molting. The probability of molting is determined by an exponential error function, shifted to account for the molting threshold. To parameterize the molt-process model, three parameters must be estimated: GPM, the minimum IMP (the minimum degree-days required for molting), and T_{min} (temperature of torpor, i.e., the lower temperature constraint below which all growth ceases). To gather the estimates of GPM and IMP, successive molts of individual animals must be observed, in either field or laboratory studies, under known physiological conditions.

Here we develop a molt-process model of the blue crab (*Callinectes sapidus*). Blue crab is distributed widely from Brazil to New England (Norse 1977). In the tropical and subtropical areas of this range, blue crab completes its life cycle within 1 year. However, from midlatitudes (~30°N), winter temperatures become sufficiently low that blue crab overwinter and thus require a minimum of 18 months to complete their life cycle (Hill et al. 1989). Throughout most of its range, blue crab supports important commercial fisheries. With recent concerns over declines in landings, there has been an increased interest in developing accurate growth models for blue crab as an aid to stock assessments (Miller and Smith 2003). There have been previously published studies on the growth of the blue crab (Tagatz 1968; Leffler 1972; Guerin and Stickle 1997). Yet, despite this earlier work, we lack data to develop the generic model of the type proposed by Smith to predict growth in blue crab.

Here, we report the results of controlled laboratory experiments conducted to provide preliminary estimates of T_{min}, GPM, and IMP for the blue crab. The growth of individual crabs of a range of sizes was monitored at four temperatures. Subsequently, field-enclosure experiments were conducted to test predictions of a molt-process growth model developed from the laboratory estimates. Additionally, the model was evaluated by comparing growth predicted by the model with growth observed in the field based on data on interannual changes in size frequencies of crabs from 1990 to 1997 from a winter dredge survey (Sharov et al. 2003). As an example of the model's utility, it is used to quantify the effect of interannual temperature variation on the dynamics of crab cohort recruitment to the commercial fishery.

Materials and methods

Growth studies

Laboratory study

We conducted a three-way factorial experiment, with three size classes of crabs of both sexes and four levels of temperature, to provide data to estimate model parameters. All experimental work was conducted at the Chesapeake Biological Laboratory (CBL, Solomons, Maryland) in 1999 and 2000. Crabs used in experiments were captured by dip-netting tidally migrating animals from the CBL pier located near the mouth of the Patuxent River, Maryland. Subsequently, crabs were held in an 2-m-diameter, outdoor, flow-through tank while they were trained onto artificial food (¼-inch trout chow pellets; Zeigler Brothers, Gardners, Pennsylvania) before use in the experiment.

Crabs with no missing limbs were separated by sex and carapace width (CW) into three size classes (small, <3.8 cm; medium, 3.8–5.1 cm; large, >5.1 cm). CW was measured at the base of the lateral spines. To begin the experiment, 40 individual crabs per tank were randomly assigned to one of 32 cylindrical chambers (17.8-cm-diameter cylinders) or one of eight rectangular enclosures (30.5 cm × 61 cm) within one of three 1.2 m × 2.4 m × 0.4 m temperature-controlled tanks. Each chamber and enclosure received an individual flow of temperature-controlled water and will be considered an independent experimental unit. Only large crabs were placed in the rectangular enclosures. Because of space constraints, only three of the four necessary temperatures could be run concurrently. Thus, two experimental trials were necessary to gather sufficient data. In 1999, a trial using 16, 20, and 24 °C temperature treatments was conducted. In 2000, a second trial, using 16, 20, and 28 °C temperature treatments, was performed. The two lower temperature trials were run in both trials to increase the amount of molt data collected from the slower molting crabs held at the colder temperature treatments.

During the course of the experiment, crabs were fed ad libitum every other day with the artificial pelletized food. There was always uneaten food present in the enclosure. Tanks were regularly siphoned to remove uneaten food and fecal matter. Every other day, 50% water changes were performed in the recirculating systems to prevent buildup of nitrogenous wastes and other exogenous compounds that may affect the molting patterns of the crabs. Replacement water was heated or chilled to the desired water temperature before addition. The amount of water added and the temperature of the source water were controlled so that the tank total temperature did not change by more than 2 °C.

Each crab was checked twice daily on weekdays and once per day on weekends for signs of molting or death. The presence of shell remains or a crab with an incompletely hardened new shell was used to determine a molt. After the new shell of a molted crab had hardened significantly (~48 h after observation of molt), the new CW was measured. Dead crabs were removed and replaced with animals of the same size class from the outdoor holding tank when possible. Crab mortality was highest within the first week of placement in the experimental setup. This was most likely caused by a portion of the animals refusing to eat the pelletized food. Later in the experimental trials, because of the advanced season, we were unable to procure the smaller size classes of crabs for replacement. When the abundance of crabs in the tanks was reduced to approximately 10% of capacity with no available replacement crabs, the trial was ended. This experimental plan yielded a 1999 trial of 182 days and a 2000 trial of 154 days.

Records of CW changes were processed to isolate individuals exhibiting single and multiple molts to determine the growth per molt (GMP; as a percentage of premolt CW). GPM was estimated by dividing the postmolt CW by the premolt carapace size and multiplying by 100 to get the percentage increase in crab size. Intermolt period (IMP) estimates were derived from information on both temperature exposure and number of days between observed molting events, based only on those crabs that had molted at least twice in an experiment.

$T_{\min}$ was estimated using the Curry and Feldman (1987) back-calculation method based on chronological IMP and temperature data. The inverses of the chronological IMP estimates for each temperature were plotted against the temperature treatment. A simple linear regression was performed to estimate the intersection of the function with the x axis to estimate the $T_{\min}$ value.

The individual chronological IMP estimates were expressed as physiological time using the estimated $T_{\min}$. Because the temperature was held constant, IMPs were estimated as

$$\text{(1)} \qquad \text{IMP}_{\text{degree-day}} = (\text{temperature} - T_{\min})\text{IMP}_{\text{days}}$$

All statistical analyses were conducted using SAS (version 8.12; SAS Institute Inc. 2001). Although the experiment was designed as a three-way factorial, inspection of the data collected in the experiment revealed overlaps in the sizes of animals in the different groups, particularly for animals tracked for multiple molts. Accordingly, the experiment was analyzed as a two-way factorial experiment using analysis of covariance (ANCOVA) to test for significant effects of temperature and sex, with initial size as a covariate.

Field-enclosure study

The results of the laboratory experiments described above were compared with data from an independent field-enclosure experiment conducted during the summer of 1997. Crabs were captured and held before the experiment in a flow-through indoor tank and fed frozen menhaden (*Brevoortia tyrannus*) and eel (*Anguilla rostrata*). After sufficient animals were collected for the trial, the crabs were separated into three size and two sex classes. The animals were then randomly assigned to one of three chambers within a 168 cm × 38 cm × 38 cm mesh enclosure. For the animals in the enclosures, the mesh was assumed to be sufficiently large to permit prey to enter, providing food. Ten enclosures, which could house a total of 30 crabs at any time, were deployed. The enclosures were tethered to the CBL pier in 3–5 m of water. The animals were checked weekly and measured to determine if they had molted in the previous week. Any animals that died during the trial were replaced with the same size class from the holding tank. Water temperature was recorded daily to convert chronological to physiological time.

IMP and GPM were estimated and tested as in the laboratory trials, without the tests associated with the differences among the experimental temperatures. As a result of the fluctuating temperature in the field, IMP was calculated as

$$\text{(2)} \qquad \text{IMP}_{\text{degree-day}} = \sum_{\text{IMP}} \text{daily temperature} - T_{\min}$$

where $T_{\min}$ is that estimated from the laboratory data. The IMP and GPM estimates from the field were compared with the laboratory estimates using analysis of variance (ANOVA).

Molt-process framework

Using the temperature-dependent growth parameters derived from our field and laboratory studies, we developed an individual-based molt-process model of crab growth that followed the growth of a cohort of up to 1000 individual crabs. The model predicts the growth of individual crabs using a daily time step. The individual predictions are then combined to predict the growth of the cohort. The model predicts an individual's growth using two submodels, intermolt period (IMP) and growth per molt (GPM), that in combination simulate the biphasic molting cycle of the blue crab. The IMP submodel predicts the time between molt events probabilistically, depending on the amount of physiological time elapsed since the last molt, which is tracked via a degree-day (DD) pool. The DD pool increases dependent on the daily water temperature and an estimate of the temperature of torpor ($T_{\min}$). The DD pool is used with a cumulative molting probability density function (CMPDF) to determine the percent chance of a crab molting on that day. The CMPDF was estimated by a maximum likelihood technique from the observed proportion molting. Multiple CMPDF forms were fitted using the available data, and a logarithmic form was determined to be the most appropriate (eq. 3). The CMPDF is given by

$$\text{(3)} \quad \text{Probability of molting} = A\log_e(\text{DD}_{\text{accumulated}}) - B$$

where A and B are the coefficients of the logarithmic model (values are given in Results). This molting probability is compared with a random number to determine if the crab should experience molt on the simulated day. This technique creates a soft-molt threshold that is reflective of the variation in intermolt periods observed in the growth studies.

When the IMP submodel determines that a molt event should occur, the GPM submodel is activated. The GPM submodel increases the crab's CW by a fixed amount, based on our laboratory and field data, and also resets the accumulated DD pool to zero. Zeroing the DD pool prevents additional molting activity until the pool has accumulated enough

Table 1. Number of observations, growth per molt (GPM) mean, chronological intermolt period (IMP), and range for each experimental temperature and sex class from a laboratory study of the growth of *Callinectes sapidus*.

Class	GPM observations	IMP observations	Mean GPM	Minimum GPM	Maximum GPM
Temperature (°C)					
16	27	1	118.1±8.7	104.44	139.8
20	50	6	121.4±6.9	105.06	141.8
24	40	17	116.1±6.3	106.43	137.8
28	30	12	121.8±6.9	1011.1	141.0
Sex					
Female	79	21	120.0±8.1	105.06	141.8
Male	68	15	118.7±6.6	104.44	135.5
Overall	147	36	119.5±7.4	104.44	141.8

physiological time to increase the molting probability sufficiently.

Simulations

We used the model in a series of three different simulations.

Performance simulations

We performed simple simulations designed to explore the model's ability to predict the patterns of growth observed in the field. To explore the model's reaction to temperature extremes and to determine if overwintering was being predicted, 100-day simulations were run with constant high (25 °C) and low (9 °C) temperature histories. To examine the reaction of the model to varying temperature conditions, a hypothetical 365-day cycle of temperatures between 6 °C and 25 °C was simulated. In all simulations, a cohort of 10 crabs was used.

Simulations of Chesapeake Bay crab growth (1990–1997)

We conducted simulations to predict the growth of cohorts of blue crabs in Chesapeake Bay. We used the size distribution of crabs <65 mm CW observed during winter as an initial description of the size distribution in a cohort comprised of 1000 crabs. The initial size distribution was derived from the data for a particular year from a winter dredge survey that has been conducted in the Chesapeake Bay since the winter of 1989–1990 (Sharov et al. 2003). The model was used to simulate the growth of the cohort, assuming no mortality, over the next 365 days using Chesapeake Bay water temperatures recorded for the modeled year at the Virginia Institute of Marine Science (VIMS) Ferry Pier (Gloucester Point, Virginia). The predicted size distributions were compared with the observed size distributions of crabs >65 mm observed in the winter dredge survey in the following year. Simulations of growth during 1991–1997 were conducted to compare the performance of the molt-process model against population-level data.

Fishery recruitment simulations

We conducted simulations to explore the impact of variations in seasonal temperature patterns on recruitment of crabs to the hard pot fishery. Simulations were run using starting distributions of 100 crabs with a mean CW of 30 mm. The temperature history came from the 1996 (cold) and 1998 (warm) VIMS Ferry Pier data. The output growth predictions were examined on a monthly basis to determine the partial recruitment vector. The partial recruitment vector was estimated by determining the proportion of the cohort that had attained legal size (127 mm CW) for the hard pot fishery.

Fig. 1. Sample growth trajectories for two individual crabs from (*a*) field- and (*b*) laboratory-raised *Callinectes sapidus*.

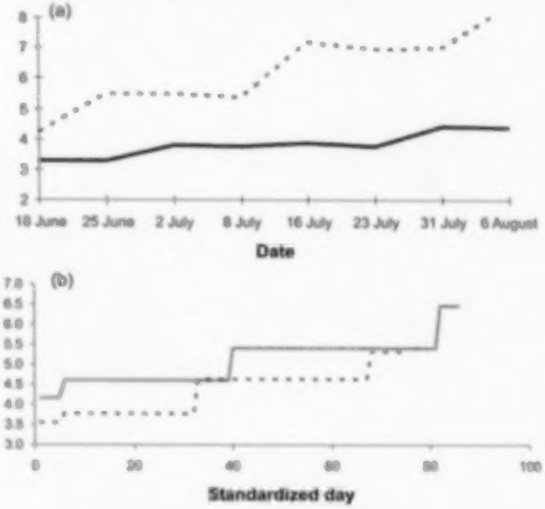

Results

Laboratory experiment and field-enclosure study

Our laboratory experiment yielded 147 estimates of GPM and 36 estimates of IMP (Table 1). The GPM observations outnumber the IMP observations, as IMP estimates require sequential molts that not every experimental crab provided. Sample growth trajectories of individual crabs are shown (Fig. 1*b*). All observations of IMP and GPM, including repeated molts of the same animal, were used in the model parameterization and treated as independent observations in order to maximize the quantity and scope of the data. We believe that the inclusion of all data collected increases the universality of the parameter estimates as the additional

Table 2. Analysis of covariance (ANCOVA; SAS PROC Mixed; SAS Institute Inc. 2001) results for laboratory growth per molt (GPM) observations for *Callinectes sapidus*.

Effect	NDF	DDF	*F*	Probability
Sex	1	141	2.13	0.1467
Temperature	3	141	5.26	0.0018
Size (covariate)	1	141	4.19	0.0426

Note: NDF, numerator degrees of freedom; DDF, denominator degrees of freedom.

Table 3. Regression output (SAS PROC REG; SAS Institute Inc. 2001) for laboratory growth per molt (GPM) estimates as a function of temperature and *Callinectes sapidus* premolt carapace width (CW). The reported probability is for a test that the parameter = 0.

Parameter	Estimate	*T*	Probability
Intercept	0.142	3.74	0.0003
Temperature	−0.000113	−0.07	0.9430
Premolt CW	0.0287	2.11	0.0370

Fig. 2. *Callinectes sapidus* laboratory growth per molt (GPM) as a function of temperature treatment.

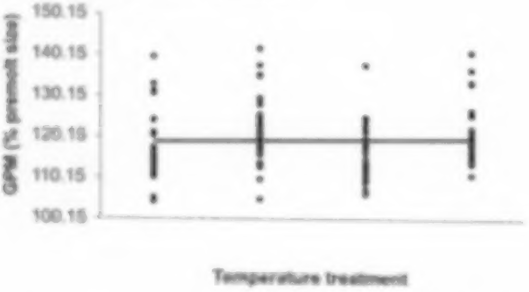

Fig. 3. *Callinectes sapidus* laboratory growth per molt (GPM) as a function of premolt carapace width.

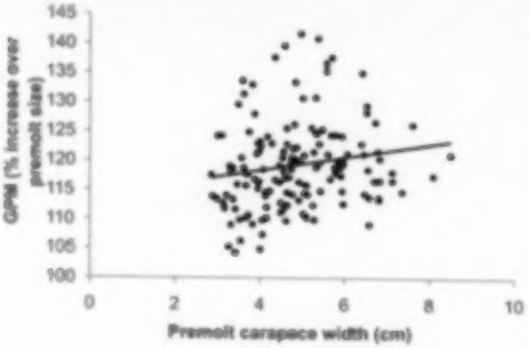

Fig. 4. *Callinectes sapidus* (*a*) intermolt period (IMP) and (*b*) inverse intermolt period (1/IMP) as a function of temperature. Regression relationship for the inverse intermolt period (*b*) is $IMP^{-1} = 0.00194 \times temperature - 0.02097$. The intercept of the regression line of the inverse intermolt period is the T_{min}. Mean values are represented by + signs.

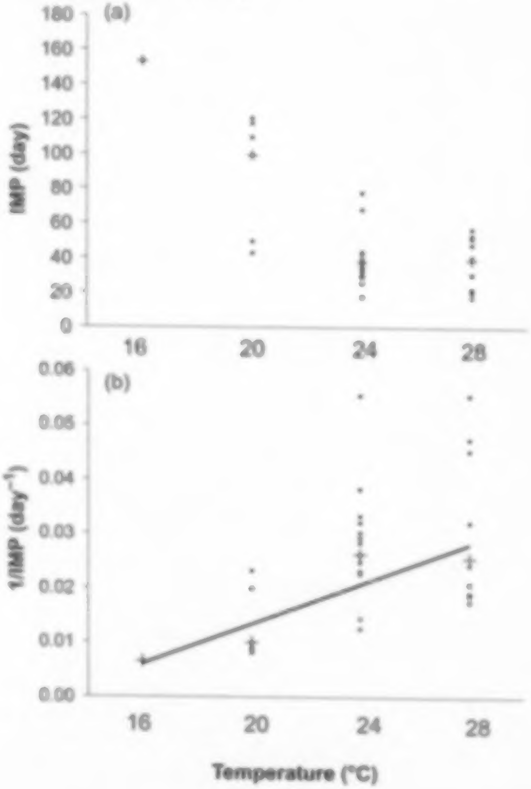

observations incorporate more sources of variability beyond the control of the experiment.

We observed molting in crabs from 2.9 to 8.5 cm CW. GPM data was highly variable. The lowest observed GPM was a 104.4% increase in CW for a 3.3 cm male crab held at 24 °C. The largest GPM was 141.8% for a 4.98 cm female crab held at 20 °C. The average GPM for the laboratory-reared crabs was 119.4% ± 7.5% (±1 standard deviation, SD) of the premolt CW. GPM estimates were normally distributed (Kolmogorov–Smirnov test, $F_{[147]} = 0.87$, $p = 0.09$). Average growth per molt varied among temperatures from 118.0% to 121.7% and among sexes by 118.7% to 120% (Table 1). ANCOVA analysis with sex and temperature as factors and initial size as a covariate indicated no significant difference with sex, but significant differences with initial size and temperature (Table 2). A multiple regression was performed to determine the extent of the effect of size and temperature on GPM. The slope of GPM with respect to temperature was nonsignificant (Table 3; Fig. 2). However, the GPM slope as a function of premolt CW was significantly different from zero (Table 3; Fig. 3). This result violates the molt-process model's assumption that GPM is completely invariant. Because the slope of the temperature – GPM relationship is minimal and not significant in the field results detailed below, we decided to accept Smith's (1997) assumption of invariability for this model application.

Fig. 5. *Callinectes sapidus* intermolt period as a function of premolt carapace width for field-raised (solid circles) and laboratory-raised (open circles) animals. The regression lines (field, solid line; laboratory, broken line) show the expected relationship indicating longer intermolt period (IMP) durations at larger sizes; however, they are nonsignificant.

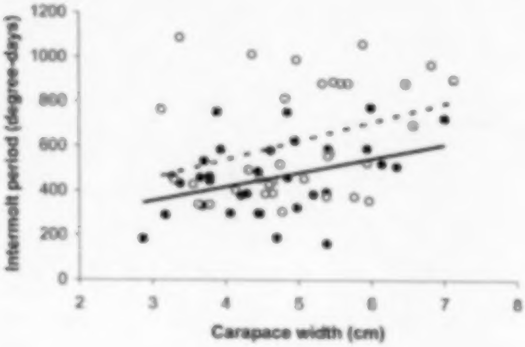

Intermolt period was significantly related to temperature (Fig. 4*a*): IMP decreased as temperature increased. The inverse of IMP was positively related to temperature (Fig. 4*b*). Extrapolation to the temperature intercept of the least squares regression fit to these data provides an estimate of $T_{\min}$ of 10.8 ± 0.015 °C (mean ± standard error, SE). This value was used to convert the chronological intermolt period observations into estimates of the physiological IMP. Because of a lack of data in the lower temperature trials, this $T_{\min}$ estimate may be biased, imparting error to the physiological IMP conversion. However, it is very close to Smith's (1997) original literature-based estimate and was assumed to be adequate for this initial parameterization of the molt-process model.

We observed chronological intermolt periods ranging between 18 days in the 28 °C crabs and 153 days in the 16 °C crabs. The mean physiological IMP in the laboratory experiments was 610 ± 259 degree-days. The lab-reared animals showed a significant difference in estimated physiological IMPs among temperature treatments. ANCOVA analysis indicated that sex and initial size did not significantly affect IMP (Table 5). Although the effect of size on physiological IMP was not significant, the IMP estimates appear to increase with increasing premolt size (Table 5; Fig. 5).

The average GPM of field-raised crabs was 122.4% ± 7.6%, similar to estimates of laboratory animals. GPM did not vary significantly with sex or with initial size in the field trials (Table 4). The average IMP for field animals was 428 ± 121 degree-days. The field and lab IMP estimates are not significantly different from each other (Table 5). The field-raised animals showed no significant IMP differences among the different sizes or sexes of animals (Table 5). IMP does appear to increase at increasing premolt size (Fig. 5). GPM estimates over both lab and field varied from 104.4% to 159.7%.

The final model parameters were derived from the combined field and laboratory growth data. A combined estimate of GPM = 119.5% and $T_{\min}$ = 10.8 °C was used in all simulation trials. The IMP estimates were used to derive the accumulated degree-days since the last molt event for the individual crabs. These individual estimates were used to calculate the CMPDF from the proportion of the population molting as a function of accumulated degree-days (Fig. 6).

Table 4. Analysis of covariance (ANCOVA) results on growth per molt (GPM) estimates of the field-enclosure-held *Callinectes sapidus*.

Effect	NDF	DDF	F	Probability
Sex	1	63	0.05	0.8167
Initial size	1	63	0.08	0.7775

Note: NDF, numerator degrees of freedom; DDF, denominator degrees of freedom.

Performance simulations

The constant high and low simulations produced the expected growth parameters. The constant 9 °C temperature input resulted in no molting activity, as if the crab was overwintering. The constant 24 °C temperature simulation produced multiple molting events with slightly different intermolt period lengths between each molt. The simulation of the hypothetical temperature cycle resulted in the expected model predictions. The intermolt periods shortened at higher temperatures and were longer at the lower simulated temperatures. Molting activity also ceased completely at the lower simulated "winter" temperatures and resumed once the water had warmed in the simulated "spring". The molt-process model appears to be able to predict the crab-specific growth phenomena.

Simulations of Chesapeake Bay crab growth (1990–1997)

The Chesapeake Bay crab growth simulations produced output distributions, the means of which were compared with the winter dredge survey (WDS) data for crabs >65 mm CW in the following year (Fig. 7). Both observed and predicted size distributions were approximately normal in all years simulated. In five out of seven cases, the model underestimated the mean CW of crabs after 1 year of growth (Table 6). The extent of the underestimation ranged from 15 mm to 41.3 mm CW (~15%–45% of the observed final size). In two cases, the model overestimated the observed size (Table 6). In these cases, the overestimation was relatively small (2.6 mm and 6.5 mm CW). For all 7 years simulated, the model, on average, underestimated the mean observed CW by 19.3 mm. In contrast, the standard deviations of all the predicted final size distributions were larger than the standard deviations observed in the WDS (Table 6).

Fishery recruitment simulations

The molt-process model was used to simulate the effects of warm and cold years to explore the effects of temperature on crabs recruiting to the fishery. The two years chosen differed by 2.1 °C in mean yearly temperature. The monthly predicted percentage of crabs entering the fishery was affected by the temperature history (Fig. 8). There was no apparent difference in the timing of initial recruitment to the fishery. For both warm and cool years, crabs recruited to the fishery in August. However, in subsequent months, the partial

Table 5. Analysis of variance (ANOVA) and analysis of covariance (ANCOVA) results for tests on the observed chronological intermolt period (IMP) estimates of *Callinectes sapidus* observed in the laboratory and field.

Experiment	Effect	NDF	DDF	*F*	Probability
Laboratory	Sex	1	30	1.14	0.295
	Temperature	3	30	35.79	0.001
	Initial size	1	30	3.05	0.091
Field	Sex	1	31	0	0.975
	Initial size	1	31	2.92	0.974
Both	Between trials	1	67	2.83	0.097

Note: NDF, numerator degrees of freedom; DDF, denominator degrees of freedom.

Fig. 6. Proportion of the experimental *Callinectes sapidus* molting (broken line) and the estimated logarithmic cumulative molting probability density function (CMPDF; probability of molting = $0.669\log_e(DD_{accumulated}) - 3.71$; solid line), as a function of degree-days (DD) accumulated since the previous molt event.

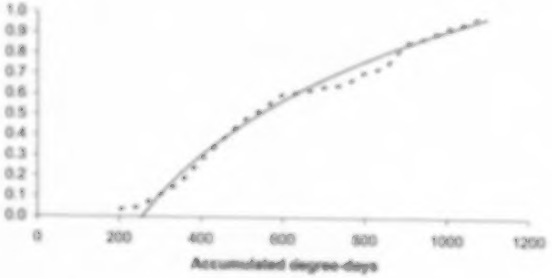

Fig. 7. 1990–1997 output distributions from Chesapeake Bay *Callinectes sapidus* growth simulation trials: model predictions (solid line) and observed distributions from the censored Virginia Institute of Marine Science winter dredge survey data (broken line).

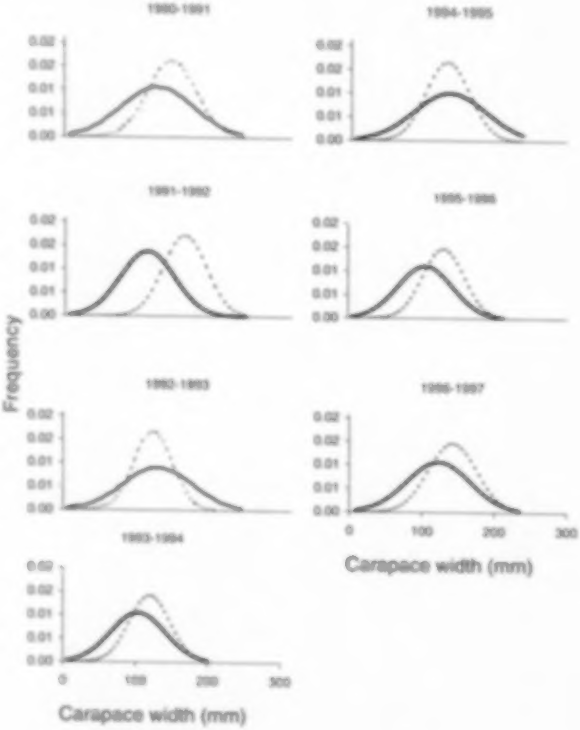

recruitment vector was on average 10% higher in any given month in the warm year than in the cool year.

Discussion

In this work, we attempted to parameterize and employ a molt-process model based on blue crab growth studies. Based on 213 molts observed under both laboratory and field conditions, the average growth per molt was estimated to increase by 119.5% ± 7.5% of premolt size. T_{min} was determined to be 10.8 °C, using the back-calculation technique described by Curry and Feldman (1987). An average intermolt period of 536 ± 231 degree-days was estimated from 69 observations of multiple molts under laboratory and field conditions.

The previous parameterization of the Smith (1997) molt-process model used meta-analysis to estimate the model parameters. There are several published experimental studies of growth in blue crab, but information on all parameters required for the molt-process model is limited. Some studies, such as Gray and Newcombe (1938), provided incomplete data required to parameterize the molt-process model. Gray and Newcombe (1938) estimated GPM to be 125%–133%; however, they did not quantify IMP or T_{min}. Other estimates of GPM include 122% and 120.9% (Leffler (1972) and Fitz and Wiegert (1991), respectively). Our estimate of 119.5% ± 7.5% is comparable to previous estimates. Additionally, the variation observed in our GPM estimates is similar to that seen in previous studies. Both Leffler (1972) and Tagatz (1968) reported highly variable GPM values, ranging between 113%–139% (aggregated by temperature rearing conditions) and 107.5%–150%, respectively. However, Tagatz (1968) reported sex-specific differences in GPM for blue crab and a size-dependent effect for GPM in male blue crab, neither of which was observed in our study.

In decapods, as with all animals that molt, GPM is limited primarily by the ability of the new cuticle, formed under the old shell, to expand during ecdysis (Cheng and Chang 1994). Salinity, nutrition, limb or eyestalk ablation, and container effects have been found to alter GPM (Hartnoll 1982; Smith 1990; Cheng and Chang 1993). These factors create physiological stress that can limit the ability of the crab to inflate the new cuticle. For example, if a crab is being fed an insuf-

Table 6. Simulations of Chesapeake Bay *Callinectes sapidus* growth (1990–1997).

	Initial observed		Final observed		Predicted		
	Mean	SD	Mean	SD	Mean	SD	Difference
1990–1991	26.2	11.3	118.0	26.0	102.3	39.8	15.7
1991–1992	28.7	10.2	132.0	24.0	90.7	27.9	41.3
1992–1993	34.3	12.8	118.0	24.9	124.5	45.6	–6.5
1993–1994	29.3	12.0	120.1	28.1	104.0	37.9	16.1
1994–1995	29.8	12.7	112.0	25.5	114.6	42.2	–2.6
1995–1996	29.34	11.2	122.8	26.57	99.3	35.4	23.5
1996–1997	27.7	11.2	119.4	24.8	89.8	34.0	29.6
Sum							117.1

Note: Initial observed data are the mean and standard deviation (SD) of the initial size distribution developed from the Virginia Institute of Marine Science winter dredge survey (WDS) data for the first year of the simulation. Final observed data are the mean and standard deviation of the initial size distribution developed from the WDS data for the second year of the simulation. Statistics provided are the difference between the final observed and predicted mean carapace widths.

Fig. 8. Predicted monthly percentages of a *Callinectes sapidus* population available for legal harvest (carapace width (CW) > 127 mm) outputted from warm (solid bars) and cold (open bars) year simulations.

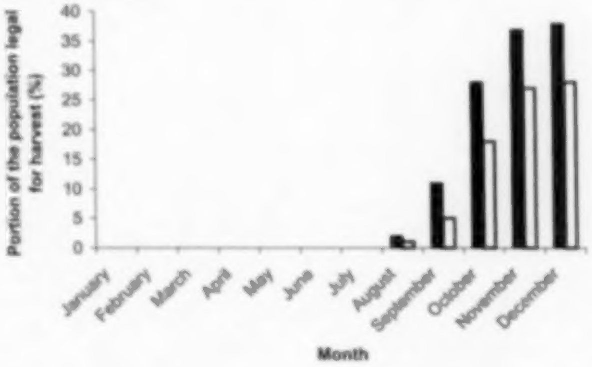

ficient diet or has multiple limbs to regenerate, it will not be able to devote as much energy to postmolt cuticle inflation as an unstressed crab. Thus, the similarities between the estimates of GPM likely reflect geometric constraints imposed by molting. The subtle difference between our GPM estimate results and those of the previously published studies is most likely a factor of the differing rearing conditions among the studies, combined with the natural variation in GPM between individuals.

A few estimates of T_{min} or IMP are reported in the literature. Van Engel (1958) estimated that growth ceased at 15 °C and true physiological torpor (subhibernation) occurred at 5 °C. However, these T_{min} estimates were based on physiological experiments and thus may not have a direct bearing on a minimum temperature for growth. Smith used previous estimates of IMP in a meta-analysis to generate estimates of T_{min} and IMP (Tagatz 1968; Leffler 1972; Cadman and Weinstein 1988). Smith (1997) estimated T_{min} to be 9.8 °C. The subsequent physiological IMP was 346.7–516.7 degree-days.

Variability in IMP can be due to forcing factors, other than temperature, imparted by the rearing conditions. Factors such as salinity, diet, and limb loss can significantly affect the molting process in crabs (Skinner and Graham 1972; Winget et al. 1976; Guerin and Stickle 1997). Variations between rearing conditions combined with behavioral effects may explain the differences in IMP estimates between the field and laboratory portions of our study and the previously published data. In addition to direct physiological effects, such as would be created by food limitation, indirect behavioral effects such as molt cycle variations resulting from the concentrated odor of other potentially cannibalistic crabs in the recirculating system may impart bias to the IMP estimates (Moksnes et al. 1997). Because we attempted to mediate these potentially confounding variables, we assume that they are not fatally biasing the parameter estimates for this application of the molt-process model.

The variation between the meta-analysis-derived parameters and ours can also be due to the inherent error imparted by combining multiple studies. The method of measurement of blue crab growth varies greatly among the published studies. For example, the measurement of crab size is reported as either a distance between the lateral spines or as measured at the base of the lateral spines. Equally, the different studies did not raise the animals in similar conditions; thus, container or feeding effects may skew the estimated growth parameters. Moreover, experimental animals were acclimated to different experimental environments that could have affected the growth of the animal. Additionally, the crabs used in the many growth studies were from multiple sources. Accordingly, population-specific differences cannot be ruled out. Previous studies used animals captured in Florida, Louisiana, and southern Virginia and yielded progressively larger T_{min} estimates with increasing latitude. Though the parameter estimates determined in this study may not fully reflect the growth dynamics of crabs in the field, they are rigorous enough to parameterize a preliminary molt-process model.

Our model was used to predict the growth of individual crabs and cohorts. The model is able to account for the crab-specific phenomena of discrete temperature-dependent growth and overwintering lacking in the currently used von Bertalanffy growth models. In the evaluation trials, observed and model-predicted increases in mean CW over one year differed by an average of 19.3 mm CW. This represents a sizeable error (~20%), suggesting that factors important to determining the observed distribution of crabs in the wild may have been left out. The deviations between the predicted and observed distributions in the Chesapeake Bay crab growth simulations most likely have three causes: inappropriateness of the temperature history inputs, error in censoring the WDS data, and error in parameterization of the model.

The temperature field used in the model may be an important source of the discrepancies between observed and predicted annual growth. As the temperature history drives the model through additions to the DD pool, it can drastically affect the output of the simulation. Crabs sampled in WDS have been living in a variety of temperature habitats, so there is no single best temperature for modeling. However, for practical reasons, we employed a temperature history in the model from a single geographic location, the VIMS Ferry Pier. This data set was chosen because it was complete for all simulation years and had daily temperature observations with very few missing data points. Though the data set was appropriate for evaluating in the molt-process model, it may lead to some of the deviation. Differences among the temperatures observed at one limited geographic location and the range of temperatures observed throughout the Chesapeake Bay will introduce error in the estimated output. We suggest that interannual differences in the degree of the mismatch in temperatures between the data used in the model and the temperature history of the bulk of the sampled crabs could be responsible for the variations observed in the degree of fit of observed and predicted size distributions.

A second possible source of error in the model simulations comes from the censoring technique used in the trials. We assumed that crabs under 65 mm CW were juveniles of the previous year and used their WDS distribution to provide the starting cohort for the simulation. We used the following year's size distribution of crabs over 65 mm CW as our basis for comparison. Our logic was that juvenile (<65 mm CW) crabs collected in the winter of one year would grow over the following year to be collected as immature and adult (>65 mm CW) crabs using the temperature history for the year of collection. The 65 mm CW cutoff was chosen because it fell at the minima between the two peaks of the bimodally distributed frequency data (Sharov et al. 2003). If this separation of the size distribution does not accurately reflect cohort dynamics, then the observed size distribution against which we compared our predictions may be biased.

A final source of error could be due to the incorrect parameterization of the model. An error in the estimation of any of the parameters could cause the deviation observed in the simulation runs. Though the experiments in this study were specifically designed to develop generalized and accurate parameter estimates, the data are limited in scope and robustness. By limiting the rearing conditions in order to isolate the effects of temperature, the dynamics of other important factors were not examined. This forced us to make assumptions, such as the invariability of GPM, that may bias the model's results. By excluding these more complex dynamics, we were forced to sacrifice some realism to create a simple model that could be widely applied. Future studies could be developed to provide the additional information necessary to include these dynamics.

A parameterization error may also be created by our inclusion of all the data collected in the experiments in the analysis and model parameterization. To maximize the scope and quantity of the data available, all observations were included in the parameter calculations, though they are not all fully independent or attributable to the experimental treatments. For example, in the laboratory experiment, we included the first molt observation where the animals were not held in the experimental conditions for the entire molt cycle, significantly increasing the data supporting the GPM calculation. This inclusion of the first GPM estimate per crab should not impart treatment-specific bias as all crabs were held in identical conditions before the experiment, although it incorporates more sources in intrinsic variation, increasing the robustness of the estimate. Similarly, we treated IMP estimates from crabs that exhibited multiple molts as independent observations in the analysis. This practice may have imparted bias if the rearing conditions were suboptimal; however, it incorporated the dynamics of sequential molts in the T_{min}, IMP, and CMPDF calculations. Additionally, we retained the 16 °C laboratory experiment in the determination of T_{min}, though only one estimate of IMP was collected from it because of the exceedingly long molt intervals. This paucity of low temperature data increased the relative weighting importance of the low temperature data. We believe that the error imparted by excluding the 16 °C data would be greater than the error created by the unequal weighting of it, so it was retained in the analysis. These limitations of the model framework and parameterization do instill error, as exemplified by the discrepancy between the variances of the observed and predicted CW distributions in the Chesapeake Bay blue crab growth simulations. The predicted standard deviation is always greater than the observed standard deviation. This is most likely due to the lack of mortality and emigration estimates in the model. The effects of size-dependent mortality can have a great effect on the variation in a population's size distribution (Rice et al. 1993). In the field, size-dependent mortality tends to truncate the variation in the frequency distribution of sizes. Mortality resulting from predation of crabs tends be the highest for the smallest members of the population (Hines and Ruiz 1995). Additionally, the mortality associated with molting caused by physical damage, physiological stress, and increased predation risk will reduce the numbers of larger crabs in the cohort as they experience more molt events (Leffler 1972). Additionally, the effects of the fishery and prespawning migration of females can significantly alter the population structure, as they remove larger animals selectively and can be significant but are not included in the current model form (Turner et al. 2003).

Future refinements of the model may include these additional complexities; however, despite these concerns, we believe that the model will predict crab growth accurately enough to examine some fisheries-important questions. The warm- and cold-year simulations showed the effect that temperature could have on the proportion of the population entering the fishery in a given year. The 1996 and 1998 sample history years varied by an average of 2.1 °C (709 degree-days), which resulted in a 10% shift in the timing of juvenile crabs becoming available for legal exploitation. A 10% shift in entrance to the fishery could cause potential yield to be overestimated and the fishery to be overharvested. This information can be used, in addition to traditional assessment techniques, to provide information to managers about some of the natural variation in crab growth and subsequent recruitment to the fishery.

This application of the molt-process model can also lay the foundations for a yield-per-recruit (YPR) model (Bunnell and Miller 2005). YPR attempts to maximize the total harvest by controlling the fishing mortality and age of entry into the fishery. In teleost fisheries, mortality is controlled by limiting effort, and age at first capture is set by net mesh sizes and exclusion devices. In the blue crab fishery, the age at which the bulk of the population enters the fishery has been unknown because of the lack of usable age markers and size structure overlap. By using the molt-process model to forecast the percent of a cohort entering the fishery at multiple ages, a YPR model can be constructed. This would allow the exploration of the effects of juvenile exclusion devices (cull rings) on the pot-based hard crab fishery that has not been possible without age markers.

In future, the molt-process model may be usable directly in the stock assessment framework in place of the von Bertalanffy growth model. However, at this time, the model is faced with some limitations preventing its easy inclusion. In an assessment, the molt-process model will be used to create an aggregate population using average inputs. It will be impossible to predict the temperature history that a crab will experience in the upcoming years, so a temperature average will be used instead. This will most likely take the form of average temperatures every day of the year for the past few years. Continuously updating this average history will account for trends; however, there will still be a mismatch between the average and actual temperatures that crabs experience. In a worst-case scenario, the average temperature history can lead to errors in years with abnormal temperature patterns and inappropriate suggestions being made to managers.

The molt-process model can be a tool for predicting the effects of temperature on crab growth and can be used in place of the more complex bioenergetic model to explore ecological questions. By using a molt-process model, one can predict the answer to questions of management concern, e.g., the number of seasons it takes for a crab to reach maturity or recruit to the fishery. Though the model may not be currently suitable as a direct replacement for the growth models used in stock assessments, it is a viable companion model to aid in the management of blue crabs. Once the limitations of inappropriate temperature history inputs and zoogeographical differences have been thoroughly explored, the model may be able to form the basis of a more accurate stock assessment; however, for now, it is still a tool for exploring other fisheries-important questions.

Acknowledgments

We thank the anonymous reviewers for comments on earlier drafts of this manuscript. This work was supported by a research grant from the Hudson River Foundation to TJM (HRF 008/98A). This is contribution number 3918 of the University of Maryland Center for Environmental Science, Chesapeake Biological Laboratory, Solomons, Maryland.

References

Bunnell, D.B., and Miller, T.J. 2005. An individual-based modeling approach to per-recruit models: blue crabs (*Callinecties sapidus*) in the Chesapeake Bay. Can. J. Fish. Aquat. Sci. **62**(11): 2560–2572.

Cadman, L.R., and Weinstein, M.P. 1988. Effects of temperature and salinity on the growth of the laboratory-reared juvenile blue crabs *Callinectes sapidus* Rathburn. J. Exp. Mar. Biol. Ecol. **121**: 193–207.

Cheng, J.H., and Chang, E.S. 1993. Determinants of postmolt size in the American lobster (*Homarus americanus*). I. $D_1{}^3$ is the critical stage. Can. J. Fish. Aquat. Sci. **50**: 2106–2111.

Cheng, J.H., and Chang, E.S. 1994. Determinants of postmolt size in the American lobster (*Homarus americanus*). II. Folding of premolt cuticle. Can. J. Fish. Aquat. Sci. **51**: 1774–1779.

Curry, G.L., and Feldman, R.M. 1987. Mathematical foundations of population dynamics. Texas A&M University Press, College Station, Texas.

Fitz, H.C., and Wiegert, R.G. 1991. Tagging juvenile blue crabs, *Callinectes sapidus*, with microwire tags: retention, survival, and growth through multiple molts. J. Crustac. Biol. **11**(2): 229–235.

Fogarty, M.J., and Idoine, J.S. 1988. Application of a yield and egg production model on size to an offshore American lobster population. Trans. Am. Fish. Soc. **117**: 350–362.

Gray, E.H., and Newcombe, C.L. 1938. Studies in moulting in *Callinectes sapidus* Rathbun. Growth, **2**: 285–196.

Guerin, J.L., and Stickle, W.B. 1997. A comparative study of two sympatric species within the genus *Callinectes*: osmoregulation, long-term acclimation to salinity and the effects of salinity on growth and molting. J. Exp. Mar. Biol. Ecol. **218**: 165–186.

Hartnoll, R.G. 1982. Growth. *In* The biology of the crustacea. Vol. 2. *Edited by* L.G. Abele. Academic Press, New York. pp. 111–196.

Hiatt, R.W. 1948. The biology of the lined shore crab *Pachygrahus crassipes*, Randal. Pac. Sci. **2**: 135–213.

Hill, J., Fowler, D.L., and Van Den Avyle, M.J. 1989. Species profiles: life histories and environmental requirements of coastal fishes and invertebrates (Mid-Atlantic) blue crab. Biol. Rep. US Fish. Wildl. Serv. **82**(11.100). US Corps of Engineers, TR EL-82-4.

Hines, A.H., and Ruiz, G.M. 1995. Temporal variation in juvenile blue crab mortality: nearshore shallows and cannibalism in Chesapeake Bay. Bull. Mar. Sci. **57**(3): 884–901.

Ju, S., Secor, D.H., and Harvey, R.H. 2001. Growth rates and lipofuscin accumulation rates in the blue crab *Callinecties sapidus*. Mar. Ecol. Prog. Ser. **224**: 197–205.

Leffler, C.W. 1972. Some effects of temperature on the growth and metabolic rate of juvenile blue crabs, *Callinectes sapidus*, in the laboratory. Mar. Biol. **14**: 104–110.

McCaughran, D.A., and Powel, G.C. 1977. Growth model for Alaskan king crab (*Paralithodes camtschatica*). J. Fish. Res. Board Can. **34**: 989–995.

Miller, T.J., and Smith, S.G. 2003. Modeling crab growth and population dynamics: insights from the blue crab conference. Bull. Mar. Sci. **72**: 537–541.

Moksnes, P-O., Lipcius, R.N., Phil, L., and van Monfrans, J. 1997. Cannibal–prey dynamics in young juveniles and postlarvae of the blue crab. J. Exp. Mar. Biol. Ecol. **215**(2): 157–187.

Norse, E.A. 1977. Aspects of the zoogeographical distribution of *Callinectes sapidus* (Brachyura: Portunidae). Bull. Mar. Sci. **27**(3): 440–447.

Rice, J.A., Crowder, L.B., and Rose, K.A. 1993. Interactions between size-structured predator and prey populations: experimental test and model comparison. Trans. Am. Fish. Soc. **122**: 481–491.

Roff, D.A. 1992. The evolution of life histories: theory and analysis. Chapman and Hall, New York.

SAS Institute Inc. 2001. SAS version 8.12 [computer program]. SAS Institute Inc., Cary, North Carolina.

Sharov, A.F., Vølstad, J.H., Davis, G.R., Davis, B.K., Lipcius, R.N., and Montane, M.M. 2003. Abundance and exploitation rate of the blue crab (*Callenecties sapidus*) in the Chesapeake Bay. Bull. Mar. Sci. **72**(2): 543–565.

Skinner, D.M., and Graham, D.E. 1972. Loss of limbs as a stimulus to ecdysis in Brachyura (true crabs). Biol. Bull. **143**: 222–233.

Smith, L.D. 1990. Patterns of limb loss in the blue crab, *Callinectes sapidus* Rathburn, and the effects of autonomy on growth. Bull. Mar. Sci. **46**(1): 23–36.

Smith, S.G. 1997. Models of crustacean growth dynamics. Ph.D. dissertation, University of Maryland College Park, College Park, Md.

Tagatz, M.E. 1968. Growth of Juvenile blue crabs, *Callinectes sapidus* Rathbun, in the St. Johns River, Florida. Fish. Bull. **67**: 281–288.

Thompson, D.W. 1968. On growth and form. Cambridge University Press, Cambridge, UK.

Turner, H.V., Wolcott, D.L., Wolcott, T.G., and Hines, A.H. 2003. Post-mating behavior, intramolt growth, and onset of migration to Chesapeake Bay spawning grounds by adult female blue crabs, *Callinecties sapidus* Rathbun. J. Exp. Mar. Biol. Ecol. **295**: 107–130.

Van Engel, W.A. 1958. The blue crab and its fishery in Chesapeake Bay. Part 1. Reproduction, early development, growth, and migration. Commer. Fish. Rev. **20**(6): 6–17.

von Bertalanffy, L. 1938. A quantitative theory of organic growth. Inquiries on growth laws. II. Human Biol. **10**: 181–213.

Wainwright, T.C., and Armstrong, D.A. 1993. Growth patterns in the Dungeness crab (*Cancer magister* Dana): synthesis of data and comparison of models. J. Crustac. Biol. **13**(1): 36–50.

Winget, R.R., Epifanio, C.E., Runnels, T., and Austin, P. 1976. Effects of diet and temperature on the growth and mortality of the blue crab, *Callinectes sapidus*, maintained in a recirculating culture system. Proc. Nat. Shellfish Assoc. **66**: 29–33.

Genetic structure in relation to movements in wild European grayling (*Thymallus thymallus*) in three Norwegian rivers

Jan Heggenes, Tore Qvenild, Michael D. Stamford, and Eric B. Taylor

Abstract: The relationship among genetic structure, movements, and barriers was studied in European grayling (*Thymallus thymallus*). Gene flow is closely related to movement patterns, and genetic differentiation may be negatively correlated with movement. Grayling movements in the Glomma River (8149 tagged) and the neighboring Trysilelva River (4070 tagged) were different among sampling sites. Most individuals were stationary (±0.5 km), but some individuals moved long distances (≤153 km). The movement data indicated potential for gene flow between the two upstream sampling sites in the Glomma River and between the two midstream sites in the Trysilelva River. Allele frequencies at seven microsatellite loci indicated pairwise differentiation across sampling sites. Genetic structuring was generally consistent with the observed movement pattern. Isolation-by-linear-distance or number of potential barriers (dams, lakes) was not significant among sites within streams or among sites within the two southern streams. They were significant, however, if two outlying northern populations in the Pasvik River were included. Our results suggest that although grayling may move long distances, they also exhibit genetic structuring within large continuous river systems. Fish movement, often the result of flexible and adaptive behavioral strategies, is the ecological mechanism for gene flow. Movements may be the adaptive link explaining how environmental conditions affect genetic structuring.

Résumé : Nous avons étudié la relation entre la structure génétique, les déplacements et les barrières chez l'ombre européen (*Thymallus thymallus*). Le flux génétique est étroitement relié aux patrons de déplacement et la différentiation génétique peut être en corrélation négative avec le déplacement. Les déplacements des ombres dans la Glomma (8149 ombres marqués) et la Trysilelva voisine (4070 ombres marqués) diffèrent d'un site d'échantillonnage à un autre. La plupart des individus sont sédentaires (± 0,5 km), mais certains se déplacent sur de grandes distances (≤153 km). Les données sur les déplacements indiquent une possibilité de flux génétique entre les deux sites d'échantillonnage d'amont de la Glomma et les deux sites du cours moyen de la Trysilelva. Les fréquences des allèles à sept locus microsatellites indiquent l'existence de différentiations par paires parmi les sites d'échantillonnage. La structure génétique est généralement en accord avec le patron des déplacements observé. Il n'y a pas d'isolement significatif dû à la distance linéaire, ni de nombre significatif de barrières (barrages, lacs) parmi les sites dans un même cours d'eau, ni parmi les sites dans les deux cours d'eau du sud. Il y en a cependant de significatifs lorsque qu'on inclut deux populations nordiques situées à l'écart dans la Pasvik. Nos résultats indiquent que, bien que les ombres puissent se déplacer sur de grandes distances, ils possèdent une structure génétique au sein de grands systèmes hydrographiques continus. Le déplacement des poissons, souvent le résultat de stratégies comportementales flexibles et adaptatives, est le mécanisme écologique du flux génétique. Les déplacements peuvent être les liens adaptatifs qui expliquent comment les conditions environnementales affectent la structuration génétique.

[Traduit par la Rédaction]

Introduction

Rapid microevolution, as found in many species (e.g., Hendry and Kinnison 1999), is often assumed to be the result of local adaptation through natural selection, corroborating the standard Darwinian view of evolution (e.g., Fisher 1930). It may also be caused, however, by nondirectional chance events through genetic drift (e.g., Wright 1931). Some of the best study organisms of rapid, genetically based evolution are freshwater fish. Salmonids in particular show life history variation and have been shown to form local phenotypic and genetic differentiation on small geographic scales across a diversity of environments (e.g., Taylor 1991; Kinnison et al. 1998; Palm and Ryman 1999). The spatial

Received 27 June 2005. Accepted 4 January 2006. Published on the NRC Research Press Web site at http://cjfas.nrc.ca on 2 May 2006.
J18761

J. Heggenes,[1] T. Qvenild,[2] M.D. Stamford,[3] and E.B. Taylor.[3] Telemark University College, N-3800 Bø i Telemark, Norway.

[1] Corresponding author (e-mail: jan.heggenes@hit.no).
[2] Present address: The Environment Agency Hedmark region, Statens hus, Parkgata 36, N-2306 Hamar, Norway.
[3] Present address: Department of Zoology, 6270 University Boulevard, The University of British Columbia, Vancouver, BC V6T 1Z4, Canada.

Can. J. Fish. Aquat. Sci. **63**: 1309–1319 (2006) doi:10.1139/F06-028

and temporal scale of genetic differentiation is important, being indicative of the scale of potential local adaptation, with its profound implications for conservation biology and management strategies. On the other hand, genetic drift plays an increasingly important role on smaller spatial and temporal scales because of the effects of environmental and demographic variation (e.g., Jorde and Ryman 1996; Hansen et al. 2002; Meldgaard et al. 2003).

European grayling (*Thymallus thymallus*) exhibit large-scale, among-population differences in life history traits (Northcote 1995; Haugen 2000) and genetic structuring (Snoj et al. 1999; Koskinen et al. 2000; Weiss et al. 2002). Other salmonids, e.g., brown trout (*Salmo trutta*), show considerable small-scale genetic variation (e.g., Ryman 1983; Ferguson 1989; Skaala 1992) and tend to be subdivided into local populations (e.g., Ruzzante et al. 2001; Ball-Ilosera et al. 2002). This may also be the case for grayling (Koskinen et al. 2001, 2002*a*, 2002*b*), but less is known about local genetic structuring in wild fish in continuous river systems with potential for gene flow (Meldgaard et al. 2003). Such microgeographic structuring probably reflects limited gene flow, which may promote genetic divergence via local adaptation and genetic drift. Conventionally, major genetic structure is considered to signal the potential existence of adaptive traits that enhance survival and reproduction in the local environment (e.g., Carvalho 1993). Reports of genetic results are, however, rarely accompanied with life history studies, which may corroborate the hypothesis of local adaptation (Koskinen et al. 2002*a*). There is a need, therefore, to document at which spatial and temporal scales genetic structuring is found, the extent of this structuring, and the possible ecological reasons for this.

Gene flow is closely related to movement patterns in individual fish. For brown trout (*S. trutta*), it has been argued that in resident populations, fry and adult movements are usually limited to a few hundred metres or less, although more extensive movements are related to spawning (e.g., Northcote 1992; Estoup et al. 1998). Populations may ultimately be structured genetically at the level of individual streams (e.g., Wenburg et al. 1998; Taylor et al. 2003) or sites within streams (Carlsson et al. 1999; Carlsson and Nilsson 2000), and both natural and man-made barriers to movement often play an important role (Carlsson and Nilsson 2001; Costello et al. 2003; Taylor et al. 2003). Anthropogenic modifications of rivers, e.g., dams or even relatively modest weirs, may disrupt movements and fragment populations (e.g., Meldgaard et al. 2003). Several recent studies, however, also indicate that extensive movements in salmonids may be more common than previously reported (e.g., Elliott 1994; Ovidio et al. 1998; Ovidio 1999), and salmonids are certainly capable of moving considerable distances. Furthermore, a fraction of the individuals may be particularly mobile (e.g., Armstrong et al. 1994), while the rest may be more stationary (e.g., Armstrong et al. 1998; Huntingford et al. 1998). Even a few dispersing individuals may have considerable genetic impact and impede development of local genetic structures (Frankham et al. 2002). Pilot studies suggest such a movement pattern in grayling (Andersen 1968; Kristiansen and Døving 1996).

The objective of this project was, therefore, to study potential genetic differentiation in European grayling at different spatial scales in relation to movement patterns. Data were collected from three large river systems in Norway. The Pasvik River is located at the northernmost distribution of European grayling, while the Trysilelva and Glomma rivers drain neighbouring watersheds in southeast Norway, where we also have collected extensive data on grayling movements. The Glomma and Pasvik rivers are affected by hydroelectric dams, while the Trysilelva River is free-flowing, except for a hydropower dam in the lowermost part. Our first hypothesis was that we would find local genetic structuring within rivers, but that levels of genetic differentiation assayed by neutral genetic markers would be negatively correlated with the extent of movement (and inferred gene flow) among sites within rivers that we assessed by physical tagging. A secondary hypothesis was that barriers to movement within streams (e.g., dams) would increase genetic differentiation among sites within individual rivers. Hence we predicted that intrariver genetic differentiation would be greatest among the completely isolated sites in the Pasvik River (dams with no fish ladders), followed by the Glomma River system (dams present that are accompanied by fish ladders), and finally the Trysilelva River would show the least among-site differentiation because it is free-flowing.

Materials and methods

Field sampling

All rivers have populations of wild European grayling, but there have been a few plantings of larvae of a local strain upstream in the Trysilelva River. The Glomma River in southeast Norway (Fig. 1) is a large, interconnected river–lake ecosystem inhabited by wild grayling. Historically, grayling movements were apparently extensive in the river (Qvenild and Linløkken 1989). All sampling sites are denoted using the first letter to indicate the river and a number indicating the relative order in stream, with site 1 being furthest upstream. Upstream of site G3 (mean flow 250 $m^3 \cdot s^{-1}$; total catchment area 15 440 km^2), the system has been regulated by four hydropower-related dams (1943–1979), all fitted with fish ladders, that are potentially semibarriers to movements (Fig. 1). Consequently, the grayling populations may have been artificially fragmented. Therefore, an extensive tagging program was initiated in 1985 (Floy FD-68BC Anchor tags during May–September; Qvenild 2001). We sampled grayling (May–June 1999) from two of the tagging sites (G3 and G2 153 km upstream) and in one additional location 212 km upstream (G1; Fig. 1). Grayling for genetic analysis were captured by sport fishing (G1) and in fish ladders (G2, G3). The Glomma River has a diverse fish fauna consisting of 29 species, with brown trout and grayling as the most widespread (Svarte 1983; Qvenild 2001).

The neighbouring free-flowing river system to the east is the Trysilelva River (Fig. 1; mean flow 77 $m^3 \cdot s^{-1}$; catchment area 5427 km^2), which has been separate from the Glomma River since postglacial times (about 8000 years). Trysilelva River grayling were tagged and movements recorded during a pilot project in the mid-1960s (Andersen 1968), and a new 5-year project was initiated in 1999. There are no barriers to fish movements among the three upstream sites. Between these three sites and the fourth lowermost site is a dam fitted with a fish ladder (5 km upstream of site four). We sampled

Fig. 1. Map of the study areas. Sampling sites are marked with letters and numbered dots. Glomma River (61°26′N, 11°04′E): G1 = Kvennan, G2 = Høyegga, G3 = Strandfossen; Trysilelva River (61°47′N, 11°46′E), upper part: T1 = Langsjøen, T2 = Galthue, T3 = Elvdalen, and lower part: T4 = Plassen; Pasvikelva River (69°24′N, 11°48′E): P1 = Grensefoss, P2 = Skogfoss. Bars indicate hydropower dams. Inset shows location in Norway.

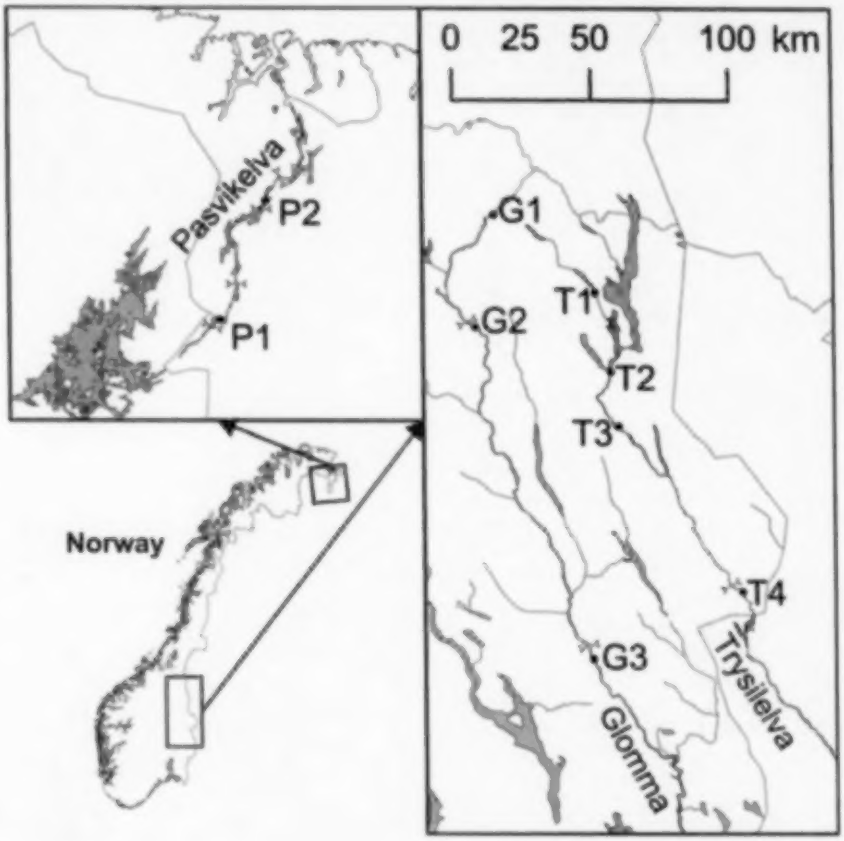

grayling (May–July 1999) for fin clips to use in genetic analyses at sites where fish were tagged (Fig. 1), but because sampling was done by sport fishing, it was somewhat more spatially spread out than in the Glomma River. At the upstream site T1, grayling were sampled for genetic analysis only. Site T2 is 34.5 km downstream of T1 at the outlet of Galten Lake, T3 is 31.5 km further downstream, and the lowermost site T4 was 78 km further downstream (Fig. 1). The fish fauna is dominated by brown trout and European grayling, but an additional 13 fish species inhabit the river (Qvenild and Nashoug 1998).

Finally, to compare diversity at an even larger geographic scale, we sampled grayling (July 1999) from the northernmost extreme of the distribution range of European grayling, the Pasvik River (Fig. 1; mean flow 185.9 $m^3 \cdot s^{-1}$; catchment area 18 510 km^2). The Norwegian part of the Pasvik River (lower 130 km) is regulated with four dams (with no fish passages), upstream at P1 (constructed in 1956, 129 km from the sea), 17 km downstream (constructed 1970), 68 km downstream at P2 (constructed 1964), and 10 km downstream (1978). Owing to its northern location, the Pasvikelva River has only eight fish species, with brown trout and grayling as widespread and common. Samples were collected below the two dams at P2 and P1, such that the sites are almost completely isolated from each other.

Adipose fins were clipped and stored individually in 96% ethyl alcohol. Data collected from each fish included total length, weight, sex (and gonad developmental stage, scales), and if previously tagged, tag number.

Microsatellite DNA

Genetic variation, within and among grayling sampling sites, was assayed at microsatellite DNA loci. Allelic variation at these loci was assayed using ^{32}P end-labelled, locus-specific primer pairs, then running the polymerase chain reaction (PCR) products on 6% polyacrylamide gels (see Costello et al. 2003). At least 20 loci have been isolated from European and Arctic grayling (*Thymallus arcticus*), and we selected the seven most variable loci known at the time of the study (Snoj et al. 1999; Susnik et al. 1999*a*, 1999*b*, 2000; Stamford and Taylor 2004). Genomic DNA was extracted from grayling fin clips using standard procedures (for details see Redenbach and Taylor 1999; Stamford and Taylor 2004).

Microsatellite data analysis

Microsatellite allele frequencies at individual loci were examined for departures from Hardy–Weinberg equilibrium within sites (exact test) and for departures from linkage-disequilibrium between loci using GENEPOP ver. 3.3 (Raymond and Rousset 1995). All probability tests were based on the Markov chain method with default values (Raymond and Rousset 1995). All tests involving multiple pairwise statistical tests incorporated the sequential Bonferroni correction (Rice 1989) to guard against inflated type I error rates. Microsatellite variation as expressed by F_{ST} was partitioned in a hierarchical fashion (using analysis of molecular variance, AMOVA; among rivers, sites within rivers, and within sites) as implemented in ARLEQUIN Ver. 2.000 (Schneider et al. 2000). Significance of F statistics was calculated and tested using FSTAT (Goudet 1995). The program GENECLASS (Cornuet et al. 1999) was used to assign individual grayling to the most likely site of origin (assignment tests).

The computer program TFPGA Ver. 1.3 (Miller 1997) was used to obtain descriptive statistics (number of samples, number of alleles, observed and expected heterozygosity, number of polymorphic loci) and to calculate co-ancestry identity–distance (Reynolds et al. 1983) between sites. This program was also used to test for differentiation between pairwise comparisons of sites using a contingency table and Markov chain approach with 10 batches of 1000 dememorizations and 2000 permutations per batch. Clustering among sites was examined using neighbour-joining trees from Cavalli-Sforza chord distance using PHYLIP ver. 5.5 (Felsenstein 1993). Mantel tests performed using FSTAT were used for matrices grouped by rivers to test for geographical correlates of genetic differentiation among sites (F_{ST}), i.e., the role of geographical distance, percent overlapping movements, or migration complexity (number of natural and human (dams) impediments to migration, presence of lakes between stream sections) in organizing genetic differentiation.

Assignment tests were performed by the program GENECLASS 1.0.02 (Cornuet et al. 1999) to determine how accurately individuals could be correctly assigned to their site of origin, based on their multilocus genotype, by a Bayesian statistical method, always using the "leave one out" option of GENECLASS. These direct assignment methods were also contrasted with the "rejection method", whereby individuals were rejected from populations based on their estimated assignment criterion values compared with the criterion distribution of each reference site. GENECLASS uses a "simulation" option to randomly generate a number of multilocus genotypes and criterion distributions for each site (marginal probability values, here 10 000) based on the estimates of allelic frequencies of the specific site (Cornuet et al. 1999).

We also utilized the microsatellite allele frequencies to test for evidence of recent bottlenecks in grayling using the mode-shift test and two-phased mutation model with default values (intermediate between infinite allele model and stepwise mutation model), as recommended and implemented in BOTTLENECK (Cornuet and Luikart 1996; Luikart et al. 1998). Bottlenecked populations may not have had time to adapt to potential problems imposed by small population sizes and may signify populations at risk of losing heterozygosity or variation at quantitative loci affecting fitness over the longer term (Luikart et al. 1998).

Fig. 2. Number of European grayling (*Thymallus thymallus*) tagged at site G2 in the Glomma River during the period 1985–2000.

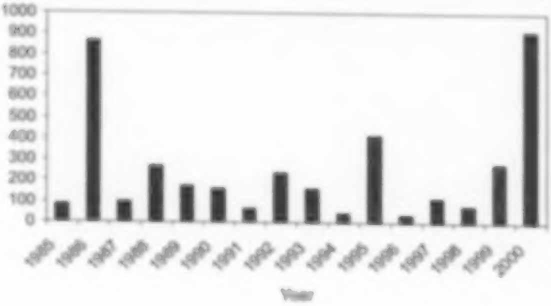

Results

Grayling movements

In the Glomma River at G2, 3919 grayling (46.5% 30–34 cm total length, range 20–58 cm, $n = 3178$) were captured for tagging during the period 1985–2000. Most fish moved through the fish ladder during June–July (43.8% and 44.6%, respectively). There was considerable variation in the number of grayling moving up the fish ladder among years (Fig. 2), with a mean of 251 (± standard deviation (SD) 269; range 38–915) grayling tagged per year. In all, 210 grayling (5.4%) were recaptured in the fish ladder: 17.6% (37 fish) the same year, 66.2% (139) the year after, and 16.2% (44) after 2 years or more. One fish (#20805) tagged in 1989 was recaptured five times, most recently in 1998, 9 years after tagging. Only four individuals, however, have been recaptured in three different years after tagging. Of 261 grayling recaptured by sport fishing, 36.8% (96 fish) were recaptured within ±0.5 km of the tagging site, 44.4% (116) were caught upstream (max. 70 km distance to recapture site) and 18.8% downstream (max. 46 km) (Table 1). Contingency tests of independence between recapture locations within rivers indicated that recaptures were nonrandomly distributed (χ^2 test, $P < 0.0001$).

Mean ± SD absolute movement distance for all recaptured grayling in the Glomma River ($n = 630$) was 12.0 ± 18.2 km (median 2.0), indicating limited but individually variable movements. A few individuals moved considerable distances. One grayling was captured and tagged at our downstream study site G3 on 31 May 1991 and was recaptured 153 km upstream at G2 on 29 June 1996, i.e., 5 years and 1 month later. This is the longest grayling movement recorded in our study. Some grayling also exhibited considerable movement speed. Twelve fish were recorded to move more than 1 km·day^{-1}, and one fish moved 54 km upstream within 8 days, i.e., 6.8 km·day^{-1}.

At the downstream site G3 in the Glomma River, 4230 grayling were tagged during the same period (1985–2000). The recaptures (369 fish) suggested more restricted move-

Table 1. Recaptures and gross movements of tagged grayling (*Thymallus thymallus*) in the Glomma and Trysilelva rivers in Norway.

	Glomma River		Trysilelva River	
	G2 (n = 261)	G3 (n = 369)	Upper part (T2 and T3; n = 88)	Lower part (T4; n = 379)
At site (%)	36.8	51.2	45.5	62.5
Upstream (%)	44.4	41.5	43.2	19.5
Downstream (%)	18.8	7.3	11.4	17.9
Mean (±SD) movement distance (km)	14.4 (19.6)	10.3 (17.0)	6.9 (10.6)	2.3 (8.0)

ments (mean ± SD = 10.3 ± 17.0 km, median 0.5) compared with G2 (14.4 ± 19.6 km, median 4.0; Table 1; Mann–Whitney *U* test, P = 0.0008). Movement patterns also tended to be different (Table 1) with fewer grayling moving downstream (7.3%) compared with G2 (18.8%; χ^2 test, $P < 0.0001$).

In the Trysileleva River, 4070 grayling (33.5% 30–34 cm total length, range 15–51 cm) were captured for tagging during the period 1999–2003, mostly by sport fishing. Of 467 grayling recaptured to date, 59% (277 fish) were at the tagging site (±0.5 km), while 24% (112) had moved upstream (max. 104.5 km) and 17% downstream (max. 30 km). Mean absolute movement distance was 3.2 ± 8.7 km (median 0 km), less than observed in the Glomma River (Mann–Whitney *U* test, $P < 0.0001$). The data indicated that the movement pattern changed considerably upstream of the Trysilelva River (Table 1; χ^2 test, $P < 0.0001$). In the upper part of the Trysilelva River (81.5 km) where the two upstream stations T2 and T3 are located (974 grayling tagged), 44%–46% of the fish were recaptured at the tagging site (±0.5 km). This increased to 62.5% in the lower part at the downstream (43.5 km) station T4 (3096 grayling tagged). Movement distances were higher in the upper part (6.9 ± 10.6 km, median 1 km) compared with the lower part (2.3 ± 8.0 km, median 0 km) (Table 1; Mann–Whitney *U* test, $P <$ 0.0001) and were higher with more upstream-directed movements (43.2% and 19.5%, respectively). This greater movement was reflected by the cumulative individual movement distances (Fig. 3). The longest movements, however, were recorded in the Glomma River system. For all sites within the Glomma River, few grayling individuals moved more than ±40 km (<2%), except at G2 (14%; Fig. 3). Twenty-two individuals (8.6%) tagged at G2 were recaptured at G1 (i.e., at 59 km further upstream), indicating considerable movement overlap between these two sites. However, overlapping movements between grayling moving downstream from G2 and upstream from G3 were limited; only three fish displayed such overlapping movements.

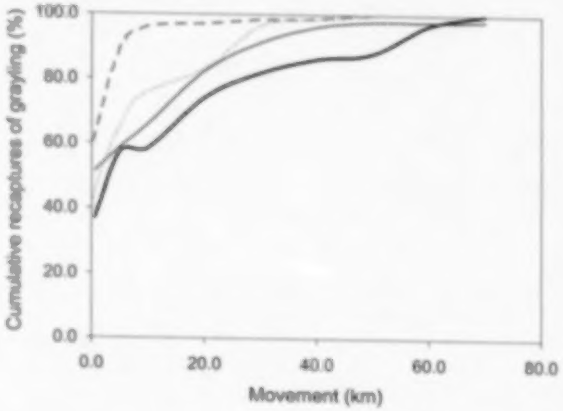

Fig. 3. Cumulative percentage of recaptures in relation to movement distance in the Glomma (site G3, solid thin line; site G2, solid thick line) and Trysilelva (upper part, broken line; lower part, dotted line) rivers.

In the Trysilelva River, overlapping movements between study sites were few. Of grayling tagged in the lower part around T4, the downstream site, 98% were recaptured within ±30 km (Fig. 3). One individual was recaptured 104 km upstream at T2. No downstream movements of fish tagged at the T3 site were recorded, indicating very little overlapping movements between the two downstream sites T3 and T4 (separated by 78 km). The more pronounced upstream movement pattern around the T3 site (above) resulted in more overlapping movements between T3 and T2 (six fish (15%) tagged at T3 were recaptured upstream at T2, i.e., 31.5 km). Only one tagged grayling moved from downstream to the upstream site T1 (>34.5 km), corroborating previous pilot studies (Andersen 1968) that indicated little movement between this and the other study sites.

In summary, the tagging studies indicated potential for gene flow between the two upstream study sites G2 and G1 in the Glomma River, while G3 appeared to be more isolated. In the Trysilelva River, tagging suggested potential gene flow between T3 and T2, but not between the other study sites.

Genetic population structure

The seven microsatellite markers (Table 2) were variable in revealing genetic diversity within and among the studied sites. All seven microsatellites were in linkage equilibrium for all locus pairs across all sites ($P > 0.05$), indicating that all loci segregate independently from one another. There were repeated PCR amplification failures for several individuals (total 27 fish) at *BFRO*018 that showed strong PCR product at all other loci. This suggested the presence of one or more null alleles at this locus in all but two populations (T3 and G2). Consequently, we estimated the pooled null allele frequency using maximum likelihood (Dempster et al. 1977) as implemented in GENEPOP.

The number of alleles (N_a in Table 2) per locus, as a measure of diversity, differed significantly among sites (G like tests, $P < 0.05$). *BFRO*004 and *BFRO*017 were represented with one or two alleles an all sites, while *BFRO*018 was most variable with up to 10 alleles at G1 (Glomma River)

Table 2. Various statistics for seven microsatellite loci found within and among populations of European grayling (*Thymallus thymallus*)

	BFRO004				*BFRO005*				*BFRO009*				*BFRO010*
Sampling site	N	N_a	H_e	A_r	N	N_a	H_e	A_r	N	N_a	H_e	A_r	N
Glomma River	121	1	na		119	4	59.7		120	3	39.4		122
G1	40	1	na	1.00	40	4	19.4	2.70	40	2	6.5	1.96	40
G2	32	1	na	1.00	30	4	12.9	2.93	32	3	10.1	2.44	33
G3	49	1	na	1.00	49	4	27.0	3.16	48	2	20.8	2.00	49
Trysilelva River	118	1	na		117	4	50.4		116	2	4.9		119
T1	30	1	na	1.00	30	2	8.5	2.00	31	2	2.9	1.84	31
T2	26	1	na	1.00	26	4	14.1	3.53	26	1	na	1.00	26
T3	24	1	na	1.00	24	4	13.0	3.56	24	2	1.0	1.58	24
T4	37	1	na	1.00	37	4	13.7	3.32	35	2	1.0	1.40	38
Pasvikelva River	53	2	1.0		53	3	5.8		53	3	33.5		55
P1	14	2	1.0	2.00	16	3	2.9	2.86	16	3	10.7	3.00	15
P2	37	1	na	1.00	37	2	2.9	1.77	37	3	23.0	3.00	40

Note: N, sample size; N_a, number of alleles; H_e, expected heterozygosity; A_r, allelic richness; na, not applicable. Significant departures from Hardy–

and eight or five alleles at the other sites: in all, 17 different alleles across sites (Table 2). Considerable differences among sites were also found for average observed (H_o) and expected (H_e) heterozygosity (Table 2), but the diversity measures N_a and H_o were not significantly correlated (simple linear model 2 regression, r^2 = 0.109, P = 0.38). Loci and sites were generally in Hardy–Weinberg equilibrium (Table 2). Out of 63 probability tests (nine sites and seven loci), four significant departures from HWE were found, about as expected under a 5% type I error.

G based exact tests indicated highly significant differentiation among sites, both overall among sites for each of the seven loci independently and combined and overall across all loci for all pairs of sites, except between the two sites T4 and T2 in Trysilelva (P = 0.12). In Pasvikelva River, the two sites P2 and P1 were also less differentiated (P = 0.016). Variation among rivers contributed 19.4%, and among sites within rivers 4.2%, whereas variation within individual sites contributed 76.3% to the total allele frequency variation (AMOVA, $P < 0.001$, $P < 0.004$, $P < 0.001$, respectively).

Pairwise estimates of F_{ST} and coancestry identity–distance among sites indicated differentiation among individual sites (Table 3). In particular, high F_{ST} values (>0.32) separated the two sites in the Pasvikelva River from the others, while divergence between sites within this river was small (F_{ST} = 0.0011, not significant; Table 3). Divergence was also found among sampling sites within the Trysilelva River (global F_{ST} = 0.093), except between T2 and T4 (Table 3). The genetic distance between T2 and T3 was also small (Table 3). The Glomma River sites generally showed lower pairwise F_{ST} values (Table 3; global F_{ST} = 0.027). Site G3 in the Glomma River and T1 in the Trysilelva River showed high pairwise F_{ST} values relative to the other sites (Table 3).

The neighbour-joining dendrogram (Cavalli-Sforzas chord distance; Fig. 4) illustrates much the same patterns with the within-river samples clustering together and with the Pasvik River as quite separate. The P2 and P1 sites clustered together with 100% bootstrap support (Fig. 4). Three Trysilelva River sites (T2, T3, T4) clustered together with 63% bootstrap support. The T1 population in the Trysilelva River was again distinct, while within the Glomma River, G3 was closer to G1 than to G2. Interestingly, the Pasvik River and Trysilelva River sites clustered (84% bootstrap support) separately from Glomma River sites. The cluster analysis also suggests, however, that the G1 site (Glomma River) is more closely related to sites in Trysilelva River and Pasvik River than to downstream Glomma River grayling (81% bootstrap support; Fig. 4).

Fig. 4. Neighbour-joining (NJ) tree generated from Cavalli-Sforzas chord distance among *Thymallus thymallus* populations sampled for this study. Genetic distances were calculated from allele frequency differences among populations using seven microsatellite loci. Consensus NJ cladogram was derived after 1000 bootstrap replicates; numbers at the branch forks indicate the proportion of times the populations to the right of the fork occurred among the trees.

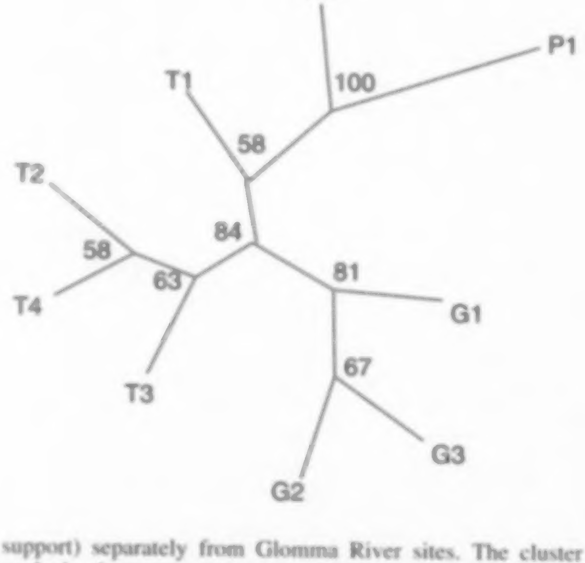

Mantel tests indicated that genetic differentiation (F_{ST}) and percent exchange between sites (as measured by movement indices) were negatively related (r = –0.23), but the relationship was not significant (P > 0.05). By contrast, a test of F_{ST} versus geographic distance was significant (r = 0.96, P < 0.005), mainly because of the two outlying populations in the Pasvikelva River. When these populations were excluded from the analysis, there was still a positive relation-in three rivers in Norway.

			BFRO015				*BFRO017*				*BFRO018*			
N_a	H_e	A_r	N	N_a	H_e	A_r	N	N_a	H_e	A_r	N	N_a	H_e	A_r
7	73.0		123	5	46.0		124	1	na		123	15	89.5	
4	20.8*	2.703	40	2	17.8	2.00	40	1	na	1.00	40	11	30.5	7.42
5	19.9	3.99	34	5	12.6	3.48	34	1	na	1.00	34	9	22.6	6.26
6	31.4	4.37	49	4	14.2	3.21	49	1	na	1.00	49	9	35.7	6.22
7	86.0		117	7	52.6		116	2	4.9		119	12	77.7	
5	22.0	4.37	31	2	4.7	1.96	31	1	na	1.00	31	5	24.3	5.42
6	17.9	5.28	25	6	14.6	5.18	26	1	na	1.00	26	6	12.9	5.01
4	15.2	3.58	24	5	13.9	4.55	24	2	2.9	1.83	24	6	8.1	4.91
4	22.0	3.66	37	4	16.8**	3.57	38	2	2.0	1.60	38	9	25.3*	5.98
3	24.1		55	4	28.7		57	2	9.2		57	10	40.4	
3	8.1	4.37	16	3	8.1	2.88	16	2	12.8	2.00	16	6	10.9	5.72
3	15.9	2.35	39	4	20.8	3.53	41	2	6.5	1.95	41	9	29.1*	6.82

Weinberg equilibrium (HWE) are marked with asterisks (*, significant departure from HWE; **, significant heterozygote deficit); Bonferroni-adjusted $P < 0.05$.

Table 3. Genetic differentiation between populations across all seven loci for European grayling (*Thymallus thymallus*) in three Norwegian rivers.

Population	G1	G2	G3	T1	T2	T3	T4	P1	P2
G1	—	0.0130	0.2037	0.1438	0.0565	0.1063	0.0695	0.4764	0.4505
G2	0.0188	—	0.1642	0.1140	0.0489	0.0763	0.0503	0.4384	0.4260
G3	0.0451	0.0120*	—	0.1916	0.2357	0.2478	0.2632	0.4821	0.5022
T1	0.1164	0.1059	0.1182	—	0.1759	0.1759	0.1456	0.4519	0.4310
T2	0.0526	0.0443	0.0841	0.1194	—	0.0490	0.0086	0.4983	0.4633
T3	0.1097	0.0759	0.1047	0.1646	0.0491	—	0.0888	0.5213	0.4904
T4	0.0578	0.0559	0.0978	0.0922	0.0202*	0.1120	—	0.5505	0.4998
P1	0.3395	0.3370	0.3183	0.3506	0.3474	0.3422	0.3831	—	0.0243
P2	0.3439	0.3447	0.3329	0.3479	0.3474	0.3386	0.3812	0.0011*	—

Note: Populations are denoted using the first letter to indicate the river (G, Glomma; T, Trysilelva; P, Pasvikelva) and a number indicating the relative order in stream, with site 1 being furthest upstream. Pairwise values of F_{ST} are given below the diagonal and co-ancestry distances are above the diagonal. F_{ST} values that were not significantly different ($\alpha < 0.05$) are marked with asterisks.

ship (but not significant) between genetic differentiation and geographic distance among the sites within the Glomma and Trysilelva rivers ($r = 0.25$, $P = 0.26$). There was also a positive association between genetic distances and number of potential movement barriers (dams, lakes; $r = 0.97$, $P < 0.005$; outlying northern sites removed, $r = 0.32$, $P = 0.16$).

The assignment tests showed variable results for the three rivers and sampling sites (Table 4). For the Pasvikelva River samples, individuals were generally assigned to the sites that they were sampled from and excluded from the other sites (71% and 75% assigned correctly, respectively; Table 4). In the Trysilelva River, most individuals were correctly assigned for T1 (65%) and T3 (64%), whereas overlap was considerable between the T4 and T2 samples (35% and 46% assigned correctly, 25% and 27% assigned to the other population, respectively). Few individuals were misassigned to any of the other rivers. If they were, it was to the G3 population in the Glomma River (16% from T1 and 12% from T3). In the Glomma River, fish captured at G3 were generally correctly assigned (74%), whereas a lower proportion was assigned for the two other sites (43% and 32%, respectively; Table 4). Most individuals were here "misassigned" to the G3 population (10% and 35%). Misassigned fish could be migrant individuals.

Our analyses indicated that five of the nine studied sites had allele frequency distributions consistent with their having experienced recent genetic bottlenecks. In the Trysilelva River, three of four sites in all cases exhibited a heterozygote excess relative to the observed number of alleles, as expected after a bottleneck (Wilcoxon two-tailed tests, $P < 0.03$). In the Glomma River, both G2 and G3 appeared to have been recently bottlenecked ($P < 0.04$), but not G1. In contrast, grayling from the two sites in the northern Pasvikelva River showed no sign of recent bottlenecks ($P > 0.2$).

Discussion

Within stream movements by grayling

The present study revealed considerable movements in European grayling, and for some individuals over much longer distances (153 km) than previously known. There are few published studies of movements in European grayling, in particular in larger river systems (but see Armstrong 1986; West et al. 1992; Hughes 1999 for Arctic grayling *T. arcticus*). It is believed, however, that grayling show more limited within-stream movements than other species such as brown trout, which are often sympatric with grayling. For instance, Parkinson et al. (1999) reported that spawning migrations of grayling did not exceed 5 km in a Belgian river, in contrast with brown trout (up to 25 km). Similarly, fish bypasses that are used extensively by brown trout appear to

Table 4. Results of assignment tests to estimate the most probable population of origin for individuals.

Population	Assignment	G1	G2	G3	T1	T2	T3	T4	P1	P2	Rejected all
G1	Assigned	0.43	0.10	0.35	0.00	0.10	0.00	0.03	0.00	0.03	
	Rejected	0.00	0.05	0.03	0.48	0.25	0.15	0.38	1.00	0.97	0.00
G2	Assigned	0.06	0.32	0.41	0.00	0.03	0.06	0.00	0.00	0.00	
	Rejected	0.32	0.12	0.21	0.56	0.56	0.32	0.41	1.00	1.00	0.12
G3	Assigned	0.00	0.20	0.74	0.00	0.02	0.02	0.02	0.00	0.00	
	Rejected	0.36	0.04	0.02	0.62	0.62	0.34	0.42	1.00	1.00	0.02
T1	Assigned	0.03	0.03	0.16	0.65	0.00	0.00	0.13	0.00	0.00	
	Rejected	0.52	0.42	0.16	0.07	0.48	0.42	0.29	1.00	1.00	0.00
T2	Assigned	0.00	0.00	0.04	0.00	0.46	0.19	0.27	0.00	0.00	
	Rejected	0.42	0.39	0.39	0.58	0.08	0.23	0.15	1.00	1.00	0.04
T3	Assigned	0.04	0.00	0.12	0.04	0.04	0.64	0.04	0.00	0.00	
	Rejected	0.64	0.32	0.36	0.44	0.20	0.08	0.24	1.00	1.00	0.08
T4	Assigned	0.00	0.03	0.10	0.00	0.25	0.10	0.35	0.00	0.00	
	Rejected	0.43	0.33	0.35	0.50	0.20	0.28	0.13	1.00	1.00	0.13
P1	Assigned	0.00	0.00	0.00	0.00	0.00	0.00	0.00	0.75	0.25	
	Rejected	1.00	1.00	1.00	1.00	1.00	1.00	1.00	0.00	0.13	0.00
P2	Assigned	0.00	0.00	0.00	0.00	0.00	0.00	0.00	0.22	0.71	
	Rejected	1.00	1.00	1.00	1.00	1.00	1.00	1.00	0.27	0.07	0.07

Note: Proportion of individuals from each population assigned to (highest likelihood of belonging) or rejected from ($\alpha = 0.05$) given reference population, based on the Bayesian simulation method.

be at least partial migration barriers for grayling (Linløkken 1993; Jungwirth 1996; Meldgaard et al. 2003).

In contrast, mean recorded movement in our study was 10.3–14.4 km in the impounded Glomma River and 2.3–6.9 km in the free-flowing Trysilelva River. Grayling movements in the two rivers were of the same order of magnitude, in spite of the presumed negative effect of dams and fish bypasses on grayling movements in the Glomma River. Movements may even have been more extensive prior to construction of dams, but historical data are anecdotal. Salmonids adapt to local and regional conditions through their behaviour and life histories, and grayling tend to thrive more in larger streams compared with trout (Northcote 1995; Parkinson et al. 1999). Varying movements is a flexible strategy for fish to adapt to environmental conditions and changes in most temperate streams. It may be expected, therefore, that behavioral movements and area use by grayling exhibit considerable variation between streams and thus between reported studies. Local environmental conditions and life history strategies in the resident grayling populations in the Glomma and Trysilelva rivers probably explain the longer movements observed here than in any other studies, which were limited to smaller river systems. The pattern of large individual variation, with relatively few individuals making long movements and most fish being relatively stationary, is typical for foraging activity in salmonids (e.g., Heggenes 1988; Armstrong et al. 1994; Huntingford et al. 1998) and for dispersal in vertebrates in general (Koenig et al. 1996). Directional movements, for example related to spawning or movement between seasonal habitats, may be more consistent between individuals (e.g., Clapp et al. 1990; Brown and MacKay 1995; Hughes 2000).

Graylings movements and genetic differentiation

Our study indicates that within-stream grayling movements, which we observed directly, corresponded with genetic structuring in the rivers. This was true whether we used F_{ST}-based measures of genetic differentiation, which tend to reflect longer-term processes on isolation and drift, or assignment test-based measures of differentiation, which may be more appropriate for assessing more recent restrictions in gene flow. Consequently, at least for the systems we studied, genetic markers provided meaningful, indirect measures of interlocality demographic isolation. The movement studies indicated overlapping movements, i.e., potential for gene flow, between the two upstream study sites G2 and G1 in the Glomma River. G3 was also overlapping with G2 but more isolated by distance. In the Trysilelva River, tagging suggested overlapping movements between T3 and T2, but not between the other study sites. This general movement pattern was reflected in the population genetic structuring, e.g., as expressed by F_{ST} values. The greatest differentiation in Glomma River was between G3 and G1. Likewise, F_{ST} was lower between T3 and T2 than between these two sites and the uppermost site T1. Genetic differentiation between T2 and the lowermost site T4 was, however, less than expected based on observed movement pattern. Gene flow between the sites appeared to be sporadic, as only one grayling was found to move the 104 km between these two sites. Sampling in fish ladders in Glomma River may be biased in favour of mobile individuals because mobile individuals may have been more likely to enter the fishways and be tagged. If anything, however, this would tend to produce conservative estimates of genetic differentiation, because our genetic analysis would be biased towards individuals that may have been more likely to move among sites. In the Trysilelva and Pasvikelva rivers, sampling was by sport fishing and, therefore, presumably representative of local sites.

To our knowledge, similar studies relating genetic structure in a continuous habitat to the ecological mechanism for potential gene flow, i.e., movement pattern, are rare in fish. In a study with a somewhat different design and spatial scale, Wenburg and Bentzen (2001) investigated population structure among 10 collections of anadromous coastal cutthroat trout (*Oncorhynchus clarkii clarkii*) from spatially separate creeks (2–100 km) within Puget Sound, Washington. These authors examined 3 years of tagging and recapture data and found a migration pattern that was associated with differences among populations in allele frequencies among three of the four creeks; higher F_{ST} measures between creeks were associated with lower degrees of movement between those same creeks. In a study of brook trout (*Salvelinus fontinalis*) in a watershed, Adams and Hutchings (2003) found good agreement between tagging and genetic data, indicating reproductively isolated populations in each lake, despite the absence of physical barriers. In a similar study, but in a different river, Wilson et al. (2004) reported no evidence of genetic differentiation between two brook trout populations with little migration from one population area to the other. They concluded that using indirect methods to estimate dispersal may be difficult on an ecological time scale. A combination of direct and indirect methods may provide a more complete picture.

It appears, as for example for site G1 and G3 in the Glomma River, that little or no migration do not necessarily imply genetic divergence, which may respond on a much longer time scale than migration patterns, for example when dams are constructed.

While most previous work on grayling have focused on rather large-scale population genetic structuring in space and time (e.g., Gross et al. 2001; Koskinen et al. 2002*c*; Weiss et al. 2002) and have reported between-river differentiation like in the present study, some recent studies also indicate considerable genetic structuring within continuous water systems at a spatial scale similar to our study. Koskinen et al. (2001, 2002*b*) reported substantial divergence between samples from spawning sites in different tributaries separated by 55 km or more in Lake Saimaa, Finland.

In a Danish river system fragmented by construction of numerous weirs during the last 60 years, Meldgaard et al. (2003) found significant differentiation between localities that were 10–20 km apart from each other. The authors found no significant pattern of isolation-by-distance; rather, genetic differentiation among European grayling localities appeared to largely be driven by the number of artificial partial barriers to fish migration (human-made weirs with ineffective fish bypasses) separating localities. The results of Meldgaard et al. (2003) suggested that relatively recent changes to habitats (e.g., weir construction) can have profound effects on the natural patterns of genetic differentiation. Studies by Haugen and Vøllestad (2001) indicate grayling may adapt rapidly to human impacts to habitat. The positive correlations between number of potential movement barriers (dams, lakes) and isolation-by-distance, and genetic differentiation in our study were at a much larger geographic scale and lower intensity and duration of potential fragmentation relative to the study by Meldgaard et al. (2003). When the outlying northern sites were removed, correlations were not significant. The fish ladders in our study area were, at least to some extent, effective at providing passage of grayling upstream and downstream, while the fish passages in the Danish study area were, until recently, apparently much less effective (Meldgaard et al. 2003).

Whether wild grayling in continuous natural water systems may show microscale genetic divergence and diversity similar to that reported, for example, for the often sympatric species brown trout (e.g., Carlsson et al. 1999; Carlsson and Nilsson 2001; Carlsson and Carlsson 2002) is not known. Koskinen et al. (2001, 2002*b*) found population divergence on a relatively small geographic scale (up to 55 km) for populations sampled at separate spawning sites in separate tributaries to a large lake. European grayling appears capable of rapid adaptation to local environmental conditions in small lakes (Koskinen et al. 2002*a*), suggesting a potential for microscale genetic differentiation also in stream environments. In contrast, our results may suggest less local genetic differentiation in continuous river systems. Both genetic distances and assignment tests indicated considerable overlap for some sites, mainly within rivers. We also found considerably longer movements by grayling in the Trysilelva and Glomma rivers than reported in any other study that we know of (but see e.g., Hughes 1999, 2000, for Arctic grayling). We suspect fish movement patterns vary locally depending on local ecological conditions and fish life histories. Therefore, local genetic divergence and diversity is likely to vary accordingly and should, when possible, be accompanied by movement studies such that conservation and management strategies can be tailored to specific ecological contexts. Our results indicate that conservation strategies for European grayling populations in the larger river systems may proceed by defining genetic populations over relatively large geographic scales compared with other sympatric salmonids, e.g., brown trout. Within the large river systems and time frame studied, and provided there are effective fishways, hydroelectric dams did not appear to have important genetic effects. This may, however, take time and may also be different in smaller systems because of different ecological conditions affecting movement behaviour.

References

Adams, B.K., and Hutchings, J.A. 2003. Microgeographic population structure of brook charr: a comparison of microsatellite and mark–recapture data. J. Fish. Biol. **62**: 517–533.

Andersen, C. 1968. Vandring hos harr, *Thymallus thymallus* L., i Trysilvassdraget belyst ved merkingsforsøk. M.Sc. thesis, Faculty of Mathematics and Natural Sciences, University of Oslo, Norway.

Armstrong, J.D., Shackley, P.E., and Gardiner, R. 1994. Redistribution of juvenile salmonid fishes after localized catastrophic depletion. J. Fish Biol. **45**: 1027–1039.

Armstrong, J.D., Braithwaite, V.A., and Fox, M. 1998. The response of wild Atlantic salmon parr to acute reductions in water flow. J. Anim. Ecol. **67**: 292–297.

Armstrong, R.H. 1986. A review of Arctic grayling studies in Alaska 1952–82. Alaska Cooperative Fisheries Research Unit, University of Alaska, Fairbanks, Alaska.

Ball-llosera, N.S., Garcia-Marin, J.L., and Pla, C. 2002. Managing fish population under mosaic relationships. The case of brown trout (*Salmo trutta*) in peripheral Mediterranean populations. Conserv. Genet. **3**: 385–400.

Brown, R.S., and MacKay, W.C. 1995. Fall and winter movements of and habitat use by cutthroat trout in the Ram River, Alberta. Trans. Am. Fish. Soc. **124**: 873–885.

Carlsson, J., and Carlsson, J.E.L. 2002. Micro-scale distribution of brown trout: an opportunity for kin selection? Ecol. Freshw. Fish, **11**: 234–239.

Carlsson, J., and Nilsson, J. 2000. Population genetic structure of brown trout (*Salmo trutta* L.) within a northern boreal forest stream. Hereditas, **132**: 173–181.

Carlsson, J., and Nilsson, J. 2001. Effects of geomorphological structures on genetic differentiation among brown trout populations in a Northern Boreal river drainage. Trans. Am. Fish. Soc. **130**: 36–45.

Carlsson, J., Olsén, K.H., Nilsson, J., Øverli, Ø., and Stabell, O.B. 1999. Microsatellites reveal fine-scale genetic structure in stream-living brown trout. J. Fish Biol. **55**: 1290–1303.

Carvalho, G.R. 1993. Evolutionary aspects of fish distribution: genetic variability and adaptation. J. Fish Biol. **43**: 53–73.

Clapp, D.F., Clark, R.D., and Diana, J.S. 1990. Range, activity, and habitat of large, free-ranging brown trout in a Michigan stream. Trans. Am. Fish. Soc. **119**: 1022–1034.

Cornuet, J.-M., and Luikart, G. 1996. Description and power analysis of two tests for detecting recent population bottlenecks from allele frequency data. Genetics, **144**: 2001–2014.

Cornuet, J.-M., Piry, S., Luikhart, G., Estoup, A., and Silignac, M. 1999. New methods employing mulitlocus genotypes to select or exclude populations as origins of individuals. Genetics, **153**: 1989–2000.

Costello, A.B., Down, T.E., Pollard, S.M., Pacas, C.J., and Taylor, E.B. 2003. The influence of history and contemporary stream hydrology on the evolution of genetic diversity within species: an examination of microsatellite DNA variation in bull trout, *Salvelinus confluentus* (Pisces: Salmonidae). Evolution, **57**: 328–344.

Dempster, A.P., Laird, N.M., and Rubin, D.B. 1977. Maximum likelihood for incomplete data via the EM algorithm. J. R. Stat. Soc. Ser. B, **39**: 1–38.

Elliott, J.M. 1994. Quantitative ecology and the brown trout. Oxford University Press, Oxford, UK.

Estoup, P., Rousset, F., Michalakis, Y., Cornuet, J.-M., Adriamanga, M., and Guyomard, R. 1998. Comparative analysis of microsatellite and allozyme markers: a case study investigating microgeographic differentiation in brown trout (*Salmo trutta*). Mol. Ecol. **7**: 339–353.

Felsenstein, J. 1993. PHYLIP (Phylogeny Inference Package). Version 3.5c. [Distributed by the author.] Department of Genome Sciences, University of Washington, Seattle, Wash.

Ferguson, A. 1989. Genetic differences among brown trout, *Salmo trutta*, stocks and their importance for the conservation and management of the species. Freshw. Biol. **21**: 35–46.

Fisher, R.A. 1930. The genetical theory of natural selection. Oxford University Press, Oxford, UK.

Frankham, R., Ballou, J.D., and Briscoe, D.A. 2002. Introduction to conservation genetics. Cambridge University Press, Cambridge, UK.

Goudet, J. 1995. FSTAT. Version 1.2. A computer program to calculate F-statistics. J. Hered. **86**: 485–486.

Gross, R., Kühn, R., Baars, M., Schröder, W., Stein, H., and Rottman, O. 2001. Genetic differentiation of European grayling populations across the Main, Danube and Elbe drainages in Bavaria. J. Fish Biol. **58**: 264–280.

Hansen, M.M., Ruzzante, D.E., Nielsen, E.E., Bekkevold, D., and Mensberg, K.L.D. 2002. Long-term effective populations sizes, temporal stability of genetic composition and potential for local adaptation in anadromous brown trout (*Salmo trutta*) populations. Mol. Ecol. **11**: 2523–2535.

Haugen, T.O. 2000. Life-history evolution in grayling. Evidence for adaptive phenotypic divergence during 8–28 generations. Ph.D. thesis, Faculty of Mathematics and Natural Sciences, University of Oslo, Norway.

Haugen, T.O., and Vøllestad, L.A. 2001. A century of life history evolution in grayling. Genetica, **112–113**: 475–491.

Heggenes, J. 1988. Effect of experimentally increased intraspecific competition on sedentary adult brown trout (*Salmo trutta*) movement and stream habitat choice. Can. J. Fish. Aquat. Sci. **45**: 1163–1172.

Hendry, A.P., and Kinnison, M.T. 1999. The pace of modern life: measuring rates of contemporary microevolution. Evolution, **53**: 1637–1653.

Hughes, N.F. 1999. Population processes responsible for larger-fish-upstream distribution patterns of Arctic grayling (*Thymallus arcticus*) in interior Alaskan runoff rivers. Can. J. Fish. Aquat. Sci. **56**: 2292–2299.

Hughes, N.F. 2000. Testing the ability of habitat selection theory to predict interannual movement patterns of a drift-feeding salmonid. Ecol. Freshw. Fish, **9**: 4–8.

Huntingford, F.A., Braithwaite, V.A., Armstrong, J.D., Aird, D., Thorpe, J.E., and Joiner, P. 1998. Social status and growth rates as determinants of site attachment in juvenile Atlantic salmon. J. Fish Biol. **53**: 314–321.

Jorde, P.E., and Ryman, N. 1996. Demographic genetics of brown trout (*Salmo trutta*) and estimation of effective population size from temporal changes of allele frequencies. Genetics, **143**: 1369–1381.

Jungwirth, M. 1996. Bypass channels at weirs as appropriate aids for fish migration in Rhinthal rivers. Regul. Rivers Res. Manag. **12**: 483–492.

Kinnison, M.T., Unwin, M.J., Hershberger, W.K., and Quinn, T.P. 1998. Egg size, fecundity, and development rate of two introduced New Zealand chinook salmon (*Oncorhynchus tshawytscha*) populations. Can. J. Fish. Aquat. Sci. **55**: 1946–1953.

Koenig, W.D., Vuren, D.V., and Hooge, P.N. 1996. Detectability, philopatry, and the distribution of dispersal distances in vertebrates. Trends Ecol. Evol. **11**: 514–517.

Koskinen, M.T., Ranta, E., Piironen, J., Veselov, A., Titov, S., Haugen, T.O., Nilsson, J., Carlstein, M., and Primmer, C.R. 2000. Genetic lineages and postglacial colonization of grayling (*Thymallus thymallus*, Salmonidae) in Europe, as revealed by mitochondrial DNA analyses. Mol. Ecol. **9**: 1609–1624.

Koskinen, M.T., Piironen, J., and Primmer, C.R. 2001. Interpopulation genetic divergence in European grayling (*Thymallus thymallus*, Salmonidae) at a microgeographic scale: implications for conservation. Conserv. Genet. **3**: 133–143.

Koskinen, M.T., Haugen, T.O., and Primmer, C.R. 2002*a*. Contemporary fisherian life-history evolution in small salmonid populations. Nature (London), **419**: 826–830.

Koskinen, M.T., Knizhin, I., Primmer, C.R., Schlotterer, C., and Weiss, S. 2002*b*. Mitochondrial and nuclear DNA phylogeography of *Thymallus* spp. (grayling) provides evidence of ice-age mediated environmental perturbations in the world's oldest body of fresh water, Lake Baikal. Mol. Ecol. **11**: 2599–2611.

Koskinen, M.T., Sundell, P., Piironen, J., and Primmer, C. 2002*c*. Genetic assessment of spatiotemporal evolutionary relationships and stocking effects in grayling (*Thymallus thymallus*, Salmonidae). Ecol. Lett. **5**: 193–205.

Kristiansen, H., and Døving, K.B. 1996. The migration of spawning stocks of grayling *Thymallus thymallus*, in Lake Mjøsa, Norway. Environ. Biol. Fishes, **47**: 43–50.

Linløkken, A. 1993. Efficiency of fishways and impact of dams on the migration of grayling and brown trout in the Glomma River system, south-eastern Norway. Regul. Rivers Res. Manag. **8**: 145–153.

Luikart, G., Allendorf, F.W., Cornuet, J.-M., and Sherwin, W.B. 1998. Distortion of allele frequency distributions provides a test of recent population bottlenecks. J. Hered. **89**: 238–247.

Meldgaard, T., Nielsen, E.E., and Loeschcke, V. 2003. Fragmentation by weirs in a riverine system: a study of genetic variation in time and space among populations of European grayling (*Thymallus thymallus*) in a Danish river system. Conserv. Genet. **4**: 735–747.

Miller, M.P. 1997. Tools for population genetic analysis (TFPGA) ver. 1.3. Department of Biological Sciences, Northern Arizona University, Flagstaff, Ariz.

Northcote, T.G. 1992. Migration and residency in stream salmonids — some ecological considerations and evolutionary consequences. Nord. J. Freshw. Res. **67**: 5–17.

Northcote, T.G. 1995. Comparative biology and management of Arctic and European grayling (Salmonidae, *Thymallus*). Rev. Fish Biol. Fish. **5**: 141–194.

Ovidio, M. 1999. Annual activity cycle of adult brown trout (*Salmo trutta* L.): a radio-telemetry study in a small stream of the Belgian Ardenne. Bull. Fr. Peche Piscic. **352**: 1–18.

Ovidio, M., Baras, E., Goffeaux, D., Birtles, C., and Philippart, J.C. 1998. Environmental unpredictability rules the autumn migration of brown trout (*Salmo trutta* L.) in the Belgian Ardennes. Hydrobiology, **372**: 263–274.

Palm, S., and Ryman, N. 1999. Genetic basis of phenotypic differences between transplanted stocks of brown trout. Ecol. Freshw. Fish, **8**: 169–180.

Parkinson, D., Philippart, J.-C., and Bara, B. 1999. A preliminary investigation of grayling in a small stream as determined by radiotracking. J. Fish Biol. **55**: 155–182.

Qvenild, T. 2001. Merkingsforsøk i fisketrappa i Høyegga i Glommavassdraget 1985–2000. Rapport nr. 7/2001, Fylkesmannen i Hedmark, miljøvernavdelingen, Hamar, Norway.

Qvenild, T., and Linløkken, A. 1989. Glomma — fisk og reguleringer. Sluttrapport fra Glommaprosjektet, Fylkesmannen i Hedmark, miljøvernavdelingen, Hamar, Norway.

Qvenild, T., and Nashoug, O. 1998. Driftsplan for Femund-/Trysilvassdraget. Del I: Fiskeressursene — status. Rapport nr. 9/98, Fylkesmannen i Hedmark, miljøvernavdelingen, Hamar, Norway.

Raymond, M., and Rousset, F. 1995. GENEPOP (Version 1.2). Population genetics software for exact tests and ecumenism. J. Hered. **86**: 248–249.

Redenbach, Z., and Taylor, E.B. 1999. Zoogeographical implications of mitochondrial DNA variation in Arctic grayling, *Thymallus arcticus*. Mol. Ecol. **8**: 23–35.

Reynolds, J., Weir, B.S., and Cockerham, C.C. 1983. Estimation of the coancestry coefficient: basis for a short-term genetic distance. Genetics, **105**: 767–779.

Rice, W.R. 1989. Analyzing tables of statistical tests. Evolution, **43**: 223–225.

Ruzzante, D.E., Hansen, M., and Meldrup, D. 2001. Distribution of individual inbreeding coefficients, relatedness and influence of stocking on native anadromous brown trout (*Salmo trutta*) population structure. Mol. Ecol. **10**: 2107–2128.

Ryman, N. 1983. Patterns and distribution of biochemical genetic variation in salmonids: differences between species. Aquaculture, **33**: 1–21.

Schneider, S., Roessli, D., and Excoffier, L. 2000. ARLEQUIN. Ver. 2.000. A software for genetics data anlysis. Genetics and Biometry Laboratory, University of Geneva, Switzerland.

Skaala, Ø. 1992. Genetic population structure of Norwegian brown trout. J. Fish Biol. **41**: 631–646.

Snoj, A., Susnik, S., Pohar, J., and Dovc, P. 1999. The first microsatellite marker (*BFRO 004*) for grayling, informative for its Adriatic population. Anim. Genet. **30**: 74–75.

Stamford, M.D., and Taylor, E.B. 2004. Phylogeographical lineages of Arctic grayling (*Thymallus arcticus*) in North America: divergence, origins, and affinities with Eurasian *Thymallus*. Mol. Ecol. **13**: 1333–1349.

Susnik, S., Snoj, A., and Dovc, P. 1999*a*. Microsatellites in grayling (*Thymallus thymallus*): comparison of two geographically remote populations from the Danubian and Adriatic river basin in Slovenia. Mol. Ecol. **8**: 1756–1757.

Susnik, S., Snoj, A., and Dovc, P. 1999*b*. A new set of microsatellite markers for grayling: *bfro014*, *bfro015*, *bfro016*, *bfro017* and *bfro018*. Anim. Genet. **30**: 462–478.

Susnik, S., Snoj, A., Jesensek, D., and Dovc, P. 2000. Rapid communication: microsatellite DNA markers (BFRO010 and BFRO011) for grayling. J. Anim. Sci. **78**: 488–489.

Svarte, Y. 1983. Oversikt over fiskeribiologiske undersøkelser i Glommavassdraget ovenfor Øyeren fram til 1983. Direktoratet for naturforvaltning-rapport nr. 2-1983. Trondheim, Norway.

Taylor, E.B. 1991. A review of local adaptation in Salmonidae, with particular reference to Pacific and Atlantic salmon. Aquaculture, **98**: 185–207.

Taylor, E.B., Stamford, M.D., and Baxter, J.S. 2003. Population subdivision in westslope cutthroat trout (*Oncorhynchus clarki lewisi*) at the northern periphery of its range: evolutionary inferences and conservation implications. Mol. Ecol. **12**: 2609–2622.

Weiss, S., Persat, H., Eppe, R., Schlotterer, C., and Uiblein, F. 2002. Complex patterns of colonization and refugia revealed for European grayling *Thymallus thymallus*, based on complete sequencing of the mitochondrial DNA control region. Mol. Ecol. **11**: 1393–1407.

Wenburg, J.K., and Bentzen, P. 2001. Genetic and behavioural evidence for restricted gene flow among coastal cutthroat trout populations. Trans. Am. Fish. Soc. **130**: 1049–1069.

Wenburg, J.K., Bentzen, P., and Foote, C.J. 1998. Microsatellite analysis of genetic population structure in an endangered salmonid: three coastal cutthroat trout (*Oncorhynchus clarki clarki*). Mol. Ecol. **7**: 733–749.

West, R.L., Smith, M.W., Barber, W.E., Reynolds, J.B., and Hop, H. 1992. Autumn migration and overwintering of Arctic grayling in coastal streams of the Arctic national wildlife refuge, Alaska. Trans. Am. Fish. Soc. **121**: 709–715.

Wilson, A.J., Hutchings, J.A., and Ferguson, M.M. 2004. Dispersal in a stream dwelling salmonid: Inferences from tagging and microsatellite studies. Conserv. Genet. **5**: 25–37.

Wright, S. 1931. Evolution in Mendelian populations. Genetics, **16**: 97–139.

Contribution of commonly analyzed polycyclic aromatic hydrocarbons (PAHs) to potential toxicity in early life stages of rainbow trout (*Oncorhynchus mykiss*)

Henrik Sundberg, Rasha Ishaq, Ulla Tjärnlund, Gun Åkerman, Kerstin Grunder, Cecilia Bandh, Dag Broman, and Lennart Balk

Abstract: In a series of bio-effect-directed fractionation experiments, we investigated the potential toxicity of sediment extracts from a contaminated bay. A previous study investigated abnormalities and hepatic ethoxyresorufin *O*-deethylase (EROD) activities in rainbow trout (*Oncorhynchus mykiss*) larvae by exposing newly fertilized eggs to the total extract and to fractions separated by degree of aromaticity. A major part of the potential toxicity was isolated in a fraction containing polycyclic aromatic compounds (PACs). In this study, we prepared a synthetic PAC mixture with 17 commonly analyzed polycyclic aromatic hydrocarbons (PAHs) in amounts equimolar to those found in the sediment PAC fraction. The 17 PAHs, which included 11 of the 16 United States Environmental Protection Agency (US EPA) priority PAHs, were unable to account for the toxicopathic effects observed and could explain less than 4% of the total EROD induction. The lack of a clear relationship between toxicopathic effects and EROD induction underlines the need for a battery of biomarkers for estimating environmental risk. These results reveal the limits of our knowledge regarding compounds responsible for potential toxicity in field situations.

Résumé : Dans une série d'expériences de fractionnement dirigé vers les bio-effets, nous avons étudié la toxicité potentielle d'extraits de sédiments provenant d'une baie contaminée. Une étude antérieure avait examiné les anormalités et les activités de l'éthoxyrésorufine *O*-déethylase (activités EROD) hépatiques chez les larves de truites arc-en-ciel (*Oncorhynchus mykiss*) en exposant des oeufs fraichement fécondés à un extrait complet et à des fractions séparées d'après leur degré d'aromaticité. Une partie importante de la toxicité potentielle a pu être isolée dans une fraction contenant des composés aromatiques polycycliques (PAC). Nous avons préparé dans notre étude un mélange synthétique de PAC contenant 17 hydrocarbures aromatiques polycycliques (PAH), fréquemment trouvés dans les analyses, dans des quantités équimolaires à celles présentes dans la fraction PAC des sédiments. Les 17 PAH, qui incluent 11 des 16 PAH sur la liste de priorité de l'EPA, ne peuvent expliquer les effets toxicopathiques observés et n'arrivent à élucider que 4 % de l'induction totale d'activité EROD. L'absence de relation nette entre les effets toxicopathiques et l'induction d'EROD souligne la nécessité d'avoir une batterie de biomarqueurs pour estimer les risques environnementaux. Nos résultats montrent les limites de nos connaissances sur les composés responsables de la toxicité potentielle dans les conditions de terrain.

[Traduit par la Rédaction]

Introduction

The complex mixture of compounds found in contaminated areas makes the determination of the major contributors to toxicity a formidable task, essential for risk assessments and for reliable monitoring of environmental improvement during remedial actions. One approach for pinpointing the major toxicants was developed in the late 1960s — the physicochemical fractionation of environmental samples combined with chemical analysis and biotests (e.g., Das et al. 1969). Recent investigations applying this approach to samples from a number of locations demonstrated that polycyclic aromatic compounds (PACs) could explain a major part of the potential toxicity in organic extracts. Boxall and Maltby (1997) could attribute a significant part of the lethal potential to the amphipod *Gammarus pulex* from sediment receiving motorway runoff (UK) to pyrene, fluoranthene, and phenanthrene. Other effects may be observed in exposed vertebrates, involving different mechanisms of toxicity that enable broader toxicological investigations. Brunström et al. (1992) found

---

Received 29 April 2005. Accepted 28 January 2006. Published on the NRC Research Press Web site at http://cjfas.nrc.ca on 6 May 2006.
J18670

H. Sundberg,[1] R. Ishaq,[2] U. Tjärnlund, G. Åkerman, K. Grunder, C. Bandh, D. Broman, and L. Balk. Department of Applied Environmental Science (ITM), Stockholm University, SE-106 91 Stockholm, Sweden.

[1] Corresponding author (e-mail: henrik.sundberg@itm.su.se).

[2] Current address: County Administrative Board of Stockholm, Box 22067, SE-104 22 Stockholm, Sweden.

Can. J. Fish. Aquat. Sci. **63**: 1320–1333 (2006)

doi:10.1139/F06-034

that a fraction containing PACs from settling particulate matter collected in the archipelago of Stockholm, Sweden, caused the major part of lethality and cytochrome P4501A (CYP1A) induction, measured as ethoxyresorufin *O*-deethylase (EROD) activity in chick embryos. However, the 15 analyzed polycyclic aromatic hydrocarbons (PAHs) — a subclass of PACs — were estimated to give only a minor contribution to the observed toxicity. Balch et al. (1995) demonstrated that the major carcinogenic effects in rainbow trout (*Oncorhynchus mykiss*) liver were caused by a fraction from the sediment of Hamilton Harbour (Ontario, Canada) that included PAHs and nitrogen-containing PACs.

Although samples from PAC-polluted areas cause mortality and toxicopathic effects such as edemas and spinal abnormalities in early life stages of fish (Carls et al. 1999; Heintz et al. 1999), the mechanisms of toxicity have been established only for a few PACs. The aryl hydrocarbon receptor (AhR) is suggested to be involved in this mechanism, since hemorrhagic and edematic rainbow trout larvae exposed to retene (7-isopropyl-1-methylphenanthrene) have elevated AhR-mediated CYP1A expression, measured by immunohistochemistry (Brinkworth et al. 2003) or as EROD activity (Billiard et al. 1999). The toxic effects of PAC exposure in early life stages of fish may, however, also involve other mechanisms. For instance, Incardona et al. (2004) demonstrated that edemas and spinal abnormalities could also be caused by three-ringed PAHs via an unknown mechanism affecting the cardiac function.

In a previous investigation, we fractionated sediment extract from a bay contaminated with polychlorinated biphenyls (PCBs) and found the fraction containing PACs caused more toxicopathic effects in rainbow trout larvae than the fraction containing PCBs and presumably other potent compounds, such as polychlorinated naphthalenes, dioxins, and furans (Sundberg et al. 2005). Consequently, to take our bioeffect directed fractionation approach a step further, we directed the present study at investigating the contribution of PAHs to potential toxicity in early life stages of rainbow trout. We also investigated the connection between AhR and toxicopathic effects caused by environmental PAC mixtures. For these purposes, we prepared a synthetic PAC mixture of 17 PAHs, including 11 of the 16 United States Environmental Protection Agency (US EPA) priority PAHs (Yan et al. 2004), in amounts equimolar to those we analyzed in the sediment PAC fraction. Ten subfractions each were isolated from the sediment PAC fraction and from the synthetic PAC mixture and injected into newly fertilized rainbow trout eggs. Toxicopathic variables and hepatic EROD activities were recorded in larvae. To the best of our knowledge, this is the first study investigating the contribution to potential toxicity in an intact vertebrate of 17 commonly analyzed PAHs in amounts equimolar to an environmental sample.

Materials and methods

Chemicals

Toluene (pro analysi (p.a.) grade), *n*-hexane (LiChrosolv®), cyclohexane (p.a. grade), silica gel (60 puriss), anhydrous sodium sulphate (p.a. grade), and copper (p.a. grade, fine powder < 63 µm) were obtained from Merck (Darmstadt, Germany). Water (HiPerSolve) was purchased from BDH Laboratory Supplies (Poole, UK). NADPH (N-0505, 98%), bovine serum albumin (A-7030), triolein (T-7140, 99%), sucrose (p.a. grade), ethoxyresorufin (E-3763), resorufin (R-3257), and Tris–HCL (p.a. grade) were purchased from Sigma (St. Louis, Missouri, USA). Agarose gel was bought from Pharmacia (Uppsala, Sweden). Benz[*a*]anthracene and benzo[*ghi*]perylene were kind gifts from Dr. Tomas Alsberg (Stockholm University, Stockholm, Sweden); the other native and deuterium-labelled PAH standards used for chemical analysis and in the exposure experiments were obtained from Cambridge Isotope Laboratories, Inc. (Andover, Massachusetts, USA). Benzo[*a*]pyrene, used as positive control in the exposure experiments, was bought from Fluka Chemie GmbH (Buchs, Switzerland).

Sediment sampling

Ten samples of the top 10 cm of bottom sediment were collected using a gravity corer from the polluted bay Örserumsviken, located southeast of the city of Västervik as described in Sundberg et al. (2005). Samples were stored at −20 °C in precleaned polypropylene jars with lids for 2 weeks prior to extraction.

Preparation of exposure solutions

The extraction and fractionation of sediment samples have been described in detail (Sundberg et al. 2005). Briefly, aliquots of the 10 pooled sediment samples were extracted wet for 50 h in toluene using a Soxhlet apparatus coupled to a Dean–Stark trap for water removal (Lamparski and Nestrick 1980). After solvent change to *n*-hexane, the total extract was obtained after cleanup (elemental sulphur removal by the addition of a small amount of elemental copper and running the extract on a silica gel column topped with sodium sulphate with *n*-hexane as eluent). An aliquot of the total extract was fractionated at room temperature (21–22 °C) on an automated high performance liquid chromatography (HPLC) system (Zebühr et al. 1993) with UV-VIS detection at $\lambda = 254$ nm. A semipreparative aminopropylsililated silica column (NH_2, µBondapak™, Waters, Milford, Massachusetts, USA, 7.8 mm × 300 mm, 10 µm) was used with *n*-hexane as the mobile phase. The retention times for toluene, anthracene, and phenanthrene (flow rate: 3 $mL \cdot min^{-1}$) were used to define three fractions, designated by their main components and eluting in the following order: (*i*) aliphatic and monocyclic aromatic compound fraction, (*ii*) dicyclic aromatic compound fraction, and (*iii*) PAC fraction. The latter fraction was collected by back-flushing the column at a flow rate of 5 $mL \cdot min^{-1}$. Total duration of one cycle was 30 min.

To track potentially active PAHs, the toxic sediment PAC fraction was further fractionated into 10 subfractions. The composition of PAHs found in the analyzed sediment PAC fraction were reconstructed by preparing a synthetic PAC mixture containing 17 PAHs, including 11 of 16 US EPA priority PAHs (Yan et al. 2004) (Table 1). Furthermore, to investigate the toxic contribution of PAHs in the sediment PAC subfractions and for quality control of the fractionation steps, an aliquot of the synthetic PAC mixture was fractionated analogously to the previous study (Sundberg et al. 2005). Subfractionation of the sediment PAC fraction and the synthetic PAC mixture was carried out on the same HPLC system. The first nine fractions (I–IX) were collected at time

Table 1. Dose (μg·kg wet egg^{-1}) of polycyclic aromatic hydrocarbons (PAHs) in the highest doses of the sediment polycyclic aromatic compound (PAC) fraction and the synthetic PAC mixture.

Compound	Sediment PAC fraction	Synthetic PAC mixture
Phenanthrene[a]	46	46
2-Methylanthracene	0.99	—
1-Methylphenanthrene	27	29
2-Phenylnaphtalene	19	18
Fluoranthene[a]	120	120
Pyrene[a]	110	96
Benzo[*a*]fluorene	16	—
Benzo[*b*]fluorene	20	—
2-Methylpyrene	13	—
1-Methylpyrene	14	—
Benzo[*ghi*]fluoranthene	11	13
Benz[*a*]anthracene[a]	35	37
Chrysene[a]	46	43
Naphthacene	5.6	Inc.[b]
Benzo[*b*]fluoranthene[a]	35	35
Benzo[*k*]fluoranthene[a]	29	40
Benzo[*e*]pyrene	29	29
Benzo[*a*]pyrene[a]	30	28
Perylene	8.1	7.2
2,2′-Dinaphthyl	2.8	—
Indeno[1,2,3-*cd*]pyrene[a]	22	23
Benzo[*ghi*]perylene[a]	22	23
Pentacene + dibenzo[*a,h*]anthracene[a]	7.7	—
Picene	8.5	—
Coronene	5.3	4.9
Dibenzo[*a,l*]pyrene	2.6	2.5
Total	680	590

Note: The doses were calculated from PAH analyses of the sediment PAC fraction, the synthetic PAC mixture, and from the known amount of each injected exposure solution (see Nanoinjection of exposure solutions in rainbow trout eggs). The high dose of the sediment PAC fraction corresponds to 70 g dry sediment·kg wet egg^{-1}. Dashes indicate that a compound was not added to the synthetic PAC mixture.

[a] US EPA priority pollutant (Yan et al. 2004).

[b] Included in the synthetic PAC mixture at a concentration equal to that found in the sediment PAC fraction. Naphthacene was degraded in samples and standards, and later analyses found much lower concentrations in both the sediment PAC fraction and in the synthetic PAC mixture. It has been excluded from further discussions.

intervals of approximately 5 min at a flow rate of 2 mL·min^{-1}, using the observed retention times for chrysene and perylene as markers. The tenth fraction (X) was isolated by backflushing the column at a flow rate of 5 mL·min^{-1} and collecting the UV-detected peak. The total duration of one cycle was 110 min.

PAH analyses

Internal standards phenanthrene-d_{10}, fluoranthene-d_{10}, pyrene-d_{10}, benzo[*a*]pyrene-d_{12}, and benzo[*ghi*]perylene-d_{12} were added to aliquots of the sediment PAC fraction, its 10 subfractions, and their synthetic analogues. Analyses were performed on a Fisons GC 8000 (Thermo Electron Corp, Waltham, Massachusetts, USA) equipped with a PTE™-5 capillary column (30 m × 0.25 mm, 0.25 μm film thickness; Supelco, Bellefonte, Pennsylvania, USA) coupled to a mass detector (Fisons MD800) operating in single ion monitoring (SIM) mode. Retention times and response factors of each analyte's molecular ion from a standard mixture containing 27 PAHs, including the five internal standards, were used for peak identification and quantification (Table 1). The total quantities (weight basis) of compounds in the PAC fraction were estimated by running the PAC fraction in the gas chromatography – mass spectrometry (GC/MS) system described above in full-scan mode (m/z: 70–700). Integrating unknown peaks and assuming equal response factors gave an estimate of unidentified compounds' weight. Detection limit was set at three times noise.

Handling of fish eggs

Eggs and seminal fluid from 4-year-old rainbow trout were collected and shipped to our laboratory from Älvdalslax, National Board of Fisheries (Älvdalen, Sweden), from Källefalls fiskodling (Källefall, Sweden), and from Kälarne fiskeriförsöksstation (Kälarne, Sweden) on the day of fertilization. To increase the homogeneity of the genetic material, one family pair was used on each occasion. After artificial fertilization and water swelling, eggs were placed in cup-shaped depressions in 1% agarose gel cast in square Petri dishes (Falcon, Becton Dickinson Labware, Franklin Lake, New Jersey, USA) with 36 eggs per dish (Åkerman and Balk 1995).

PAH contribution and mortality confirmation

The toxic contribution of PAHs in the sediment PAC fraction (PAH contribution experiment) was investigated using the family pair from Älvdalen. The surprisingly high mortality at the beginning of the PAH contribution experiment (see Results) was investigated twice by using the family pairs from Kälarne and Källefall (mortality confirmation experiment). The family pair from Kälarne was included in a larger study (Sundberg et al. 2005); the results of the controls from this family pair are therefore already published.

Nanoinjection of exposure solutions in rainbow trout eggs

The sediment PAC fractions, synthetic PAC mixture and its subfractions, and benzo[*a*]pyrene (positive control) were dissolved in the carrier substance, triolein. Two additional controls were used: carrier controls (eggs exposed solely to triolein) and uninjected controls. Owing to handling error in the first mortality confirmation experiment, the highest dose of benzo[*a*]pyrene was not investigated. To investigate a possible plateau in dose response of EROD induction caused by benzo[*a*]pyrene, an additional dose (8000 μg·kg wet egg^{-1}) was included in the second mortality confirmation experiment. The day after fertilization, rainbow trout eggs were exposed by the nanoinjection technique (Åkerman and Balk 1995; Walker et al. 1996). Briefly, triolein-dissolved exposure solutions were transferred using a vacuum suction pump into aluminium silicate capillaries (Sutter Instrument Co., Novato, California, USA) with sharp elliptical tips. Exposures were performed under a stereomicroscope (Leica MZ8, Leica Microscopy and Scientific Instruments Group, Heerburg, Switzerland) with the aid of a one-dimensional hydraulic manipulator (Narishige, Tokyo, Japan) and a Pico injector (Medical Systems Corp., Greenvale, New York, USA). After penetration of the chorion and the vitelline membrane, the solutions were injected into the yolk of the egg. Before injection, each capillary was individually calibrated by adjusting the nitrogen gas pressure and the time of injection so that the diameter of the triolein droplet corresponded to the desired dose (less than 1‰ (*v/v*) of the egg volume). Eggs were exposed to three graded doses of the sediment PAC fraction, each separated by a factor five, with the high dose corresponding to 70 g dry sediment·kg wet egg^{-1} (Table 1). The synthetic PAC mixture was injected into eggs in three graded doses corresponding to the analyzed amount of PAHs in the sediment PAC fraction. The 10 sediment PAC subfractions and the 10 synthetic PAC subfractions were injected into eggs at doses corresponding to the highest dose of the sediment PAC fraction on a PAH basis (Tables 2 and 3).

Eggs and larvae maintenance

Petri dishes were kept dark in individual flow-through aquariums containing 2 L Stockholm municipal drinking water filtered in three consecutive steps (nominal pore size 50 μm; active carbon; nominal pore size 10 μm) and aerated. The water temperatures were 5.2–7.9 °C (PAH contribution experiment) and 8.5–9.1 °C and 7.2–8.1 °C (mortality confirmation experiments). Dead eggs and larvae were removed every second or third day. Abnormalities in newly hatched larvae, investigated under the stereomicroscope, included hemorrhages in the yolk sac, head, trunk, and tail region; edemas in the yolk sac, pericardium, and fins; and asymmetric yolk sacs — an abnormality first described in our previous investigation (Sundberg et al. 2005). For brevity and to give an impression of the severity of the abnormalities, we present data on asymmetric yolk sacs, hemorrhages, and multiple abnormalities.

Severing larval spinal columns when two-thirds of yolk consumption was reached terminated fish exposure experiments. At termination, 33–36 days (240–260 degree-days (°C)) had elapsed post-hatch in the PAH contribution experiment and 27–28 days (210–240 degree-days (°C)) in the two mortality confirmation experiments. While submerged in ice-cold 0.9% saline, individual lengths were recorded and livers were dissected. Pooled livers (three larval livers corresponded to $n = 1$ for the enzymatic analyses) were homogenized with 300 μL 0.25 mol·L^{-1} sucrose, immediately portioned into ice-kept cryo vials, and plunged into liquid nitrogen (Sundberg et al. 2005). The number of dissected livers in the different exposure groups and the control groups ranged from 12 to 45 (n = 4–15).

Measurement of EROD activity

CYP1A activity, measured as EROD activity, was analyzed according to a method based on Prough et al. (1978) using a Jasco FP-777 spectrofluorometer (Japan Spectroscopic Co., Ltd., Tokyo, Japan). Measurements of liver homogenates were performed at room temperature (21–22 °C) in glass cells with a final volume of 2 mL as previously described (Sundberg et al. 2005). Emission intensities were recorded at $\lambda = 583$ with excitation $\lambda = 530$.

Statistics

Statistical differences in mortalities and abnormalities between exposure and control groups were determined using Fisher's exact test with Bonferroni correction. Kruskal–Wallis and Dunn's multiple comparison tests were performed to investigate statistical differences in EROD activities and larval length. Statistical significance between groups was set at $p <$ 0.05.

Results

PAH analyses

The composition of PAHs in the synthetic PAC mixture was confirmed by chemical analysis (Table 1). The synthetic PAC mixture represents approximately 13% (weight basis) of the compounds present in the sediment PAC fraction, assuming similar response factors for unidentified compounds. Although PAH standards and samples were stored at –20 °C, naphthacene was degraded; analyses of both the sediment PAC fraction and the synthetic PAC mixture found much lower concentrations than were initially determined. Naphthacene was therefore excluded from our further discussions. Doses of individual PAHs in the sediment PAC subfractions and synthetic PAC subfractions are shown in Tables 2 and 3, respectively. The sum of PAH concentration in the synthetic PAC subfractions agreed within factors 1.0–2.3 with the sum in the sediment PAC subfractions and within

Table 2. Dose (μg·kg wet egg^{-1}) of polycyclic aromatic hydrocarbons (PAHs) in the 10 sediment polycyclic aromatic compound (PAC) subfractions.

Compound	Sediment PAC subfraction										Total
	I	II	III	IV	V	VI	VII	VIII	IX	X	
Phenanthrene	56										56
2-Methylanthracene	1.4										1.4
1-Methylphenanthrene	22										22
2-Phenylnaphtalene	13										13
Fluoranthene		120	0.60								120
Pyrene	81	48	0.36								130
Benzo[*a*]fluorene		17	9.3								27
Benzo[*b*]fluorene		1.5	24								25
2-Methylpyrene		12									12
1-Methylpyrene		6.8		0.63							7.4
Benzo[*ghi*]fluoranthene			13								13
Benz[*a*]anthracene				31	13						43
Chrysene				24	45						69
Benzo[*b*]fluoranthene							14	24			38
Benzo[*j*+*k*]fluoranthene							10	22	9.0		41
Benzo[*e*]pyrene							23	8.2			31
Benzo[*a*]pyrene						15	19				33
Perylene								9.6	1.6		11
2,2′-Dinaphtyl						2.3					2.3
Indeno[1,2,3-*cd*]pyrene										33	33
Benzo[*ghi*]perylene										33	33
Pentacene + dibenzo[*a,h*]anthracene										9.0	9.0
Picene										11	11
Coronene										6.5	6.5
Dibenzo[*a,i*]pyrene										4.4	4.4
Total	170	210	47	55	58	17	65	64	11	97	790

Note: Missing values indicate not detected (<three times noise). The doses were calculated from PAH analyses of the sediment PAC fraction and from the known amount of each injected exposure solution (see Nanoinjection of exposure solutions in rainbow trout eggs).

factors 1.0–2.2 with the synthetic PAC mixture. Note that benzo[*k*]fluoranthene was separated from benzo[*j*]fluoranthene in the analysis of the sediment PAC fraction and was thus included in the synthetic PAC mixture. In the analysis of the sediment PAC subfractions, however, we were not able to discriminate them, since benzo[*j*]fluoranthene was not included in the standard.

In general, the proportions of individual PAHs in the sediment PAC subfractions were similar to those of the synthetic PAC subfractions. However, benzo[*b*]fluoranthene, benzo[*k*]fluoranthene, benzo[*e*]pyrene, benzo[*a*]pyrene, and perylene, eluted in earlier sediment PAC subfractions, compared with their corresponding synthetic PAC subfractions.

Mortalities and abnormalities

Mortalities and abnormalities were not statistically different between carrier controls and uninjected controls; exposure groups were therefore compared with carrier controls for the statistical analyses. Abnormalities were recorded among newly hatched larvae within 2 days to investigate them at similar developmental stages and to minimize a possible bias due to regenerating tissues (e.g., edema). Owing to several exposure groups and thus several samples in the PAH contribution experiment, only larvae exposed to the highest doses of benzo[*a*]pyrene, the sediment PAC fraction, and the synthetic PAC mixture were examined. The only larvae found at dissection to be significantly shorter than carrier controls were larvae receiving 5000 μg benzo[*a*]pyrene·kg wet egg^{-1} in the PAH contribution experiment.

PAH contribution experiment

Total mortalities were significantly elevated compared with carrier controls at the highest doses of both the sediment PAC fraction and the synthetic PAC mixture (Fig. 1*a*). The highest dose of the sediment PAC fraction was the only exposure that caused a significant increase of larval mortality (Fig. 1*a*). No significant effects on mortalities were caused by sediment PAC and synthetic PAC subfractions (Figs. 1*b*, 1*c*). Surprisingly high mortalities were observed among embryos exposed to the highest dose of the synthetic PAC mixture — 6 of 34 embryos — within 18 days post-exposure, a time point where no other exposure group had such high mortality this early (not shown). We therefore repeated the exposure of the synthetic PAC mixture using the two additional family pairs to investigate if this early mortality was caused by the exposure or by other unknown factors (mortality confirmation experiment).

Cases of asymmetric yolk sac were significantly increased in larvae exposed to 5000 μg benzo[*a*]pyrene·kg wet egg^{-1} (Fig. 2*a*), the sediment PAC fraction (Fig. 2*a*), and sediment PAC subfraction II (Fig. 2*b*). This disorder was not observed in any other exposure groups, except for one larva exposed

Table 3. Dose (μg·kg wet egg^{-1}) of polycyclic aromatic hydrocarbons (PAHs) in the 10 synthetic polycyclic aromatic compound (PAC) subfractions.

	Synthetic PAC subfraction										
Compound	I	II	III	IV	V	VI	VII	VIII	IX	X	Total
Phenanthrene	29	0.17									30
1-Methylphenanthrene	14	0.037									14
2-Phenylnaphtalene	8.2	0.025									8.2
Fluoranthene		80	1.1								81
Pyrene	24	42	0.15								66
Benzo[*ghi*]fluoranthene			13	0.32							13
Benz[*a*]anthracene				10	21						31
Chrysene				6.5	31						38
Benzo[*b*]fluoranthene								19	1.5		20
Benzo[*k*]fluoranthene								31	1.2		32
Benzo[*e*]pyrene								20	0.40		20
Benzo[*a*]pyrene							24	1.6			26
Perylene									6.5		6.5
Indeno[1,2,3-*cd*]pyrene										18	18
Benzo[*ghi*]perylene										14	14
Coronene										3.1	3.1
Dibenzo[*a,i*]pyrene										2.1	2.1
Total	76	120	14	17	52	0.0	24	71	9.7	38	420

Note: Missing values indicate not detected (<three times noise). The doses were calculated from PAH analyses of the synthetic PAC mixture and from the known amount of each injected exposure solution (see Nanoinjection of exposure solutions in rainbow trout eggs).

to sediment PAC subfraction VI (Fig. 2*b*, nonsignificant). Hemorrhages were not significantly increased in any exposure group, but frequencies of hemorrhagic larvae among those exposed to the sediment PAC fraction (Fig. 2*a*) were approximately three times higher than carrier controls. Multiple abnormalities were significantly increased among larvae exposed to the sediment PAC fraction (Fig. 2*a*) and to sediment PAC subfraction II (Fig. 2*b*).

Mortality confirmation experiment

The synthetic PAC mixture caused no significant increase in mortalities compared with carrier controls in the two mortality confirmation experiments (Figs. 3*a*, 3*b*). The lowest dose of synthetic PAC mixture in the first mortality confirmation experiment (Fig. 3*a*) caused the highest embryonal mortality (nonsignificant) in these experiments. Tendencies (nonsignificant) of dose response of embryonal mortalities were observed in larvae exposed to benzo[*a*]pyrene in both mortality confirmation experiments (Figs. 3*a*, 3*b*).

The synthetic PAC mixture caused no significant effects on abnormalities in the two mortality confirmation experiments. Asymmetric yolk sacs were only found among larvae exposed to benzo[*a*]pyrene (Figs. 4*a*, 4*b*). In the first mortality confirmation experiment, hemorrhagic larvae were found among all exposures, including carrier controls (Fig. 4*a*), while in the repeated mortality confirmation experiment, this abnormality was only observed among those exposed to benzo[*a*]pyrene (Fig. 4*b*).

EROD induction in larval liver homogenates

No statistical differences were found between EROD activities in carrier controls and uninjected controls. EROD inductions in the exposure groups were therefore calculated as percentage of carrier control.

PAH contribution experiment

The specific activity in carrier controls was 16 ± 2 pmol resorufin·mg protein^{-1}·min^{-1} (95% confidence limit). Dose response effects were significant for benzo[*a*]pyrene and the sediment PAC fraction (Fig. 5*a*). The highest dose of the synthetic PAC mixture caused a nonsignificant twofold EROD induction (220%), whereas the lowest dose of the sediment PAC fraction caused a significant fivefold EROD induction (520%). The sediment PAC subfractions caused similar significant EROD inductions that ranged from 270% (subfraction VII) to 460% (subfraction II), except for subfraction X, which caused a significant ninefold EROD induction (880%; Fig. 5*b*). The only synthetic PAC subfraction to cause significant EROD induction was subfraction X (260%; Fig. 5*c*).

Mortality confirmation experiment

EROD activities in carrier controls in the repeated mortality confirmation experiment (24 ± 3 pmol resorufin·mg protein^{-1}·min^{-1}, 95% confidence limit) were significantly higher than those of the carrier controls in both the first mortality confirmation experiment (14 ± 5 pmol resorufin·mg protein^{-1}·min^{-1}, 95% confidence limit) and in the PAH contribution experiment. The dose response relationships and induction potentials for both benzo[*a*]pyrene and the synthetic PAC mixture, however, were similar in all three experiments (Figs. 5*a*, 6*a*, 6*b*).

Discussion

Contribution of PAHs to early life-stage toxicity in fish

The 17 PAHs used in the present investigation could explain only a small amount of the potential toxicity of the sediment PAC fraction. The synthetic PAC mixture caused

Fig. 1. Mortalities in early life stages of rainbow trout (*Oncorhynchus mykiss*) in the polycyclic aromatic hydrocarbon (PAH) contribution experiment. Embryonal mortalities (pre-hatch) are indicated as solid bars and larval mortalities (post-hatch) as open bars. Rainbow trout were exposed as newly fertilized eggs using the nanoinjection technique. The sediment polycyclic aromatic compound (PAC) fraction was isolated from sediment extract from the polluted bay. The synthetic PAC mixture was prepared from 17 PAHs in amounts equimolar to those found in the sediment PAC fraction. High doses are presented on a PAH basis in Tables 1, 2, and 3; the two other graded doses are separated by a factor of five; and *n* denotes number of injected eggs. Triolein-injected eggs were used as carrier controls, and graded doses of benzo[*a*]pyrene (μg·kg wet egg^{-1}) served as positive controls. An asterisk (*) indicates where data are significantly higher than carrier controls ($p < 0.0014$, 36 repeats, Fisher's exact test with Bonferroni correction). Brackets denote that the total mortality was significantly higher than carrier controls.

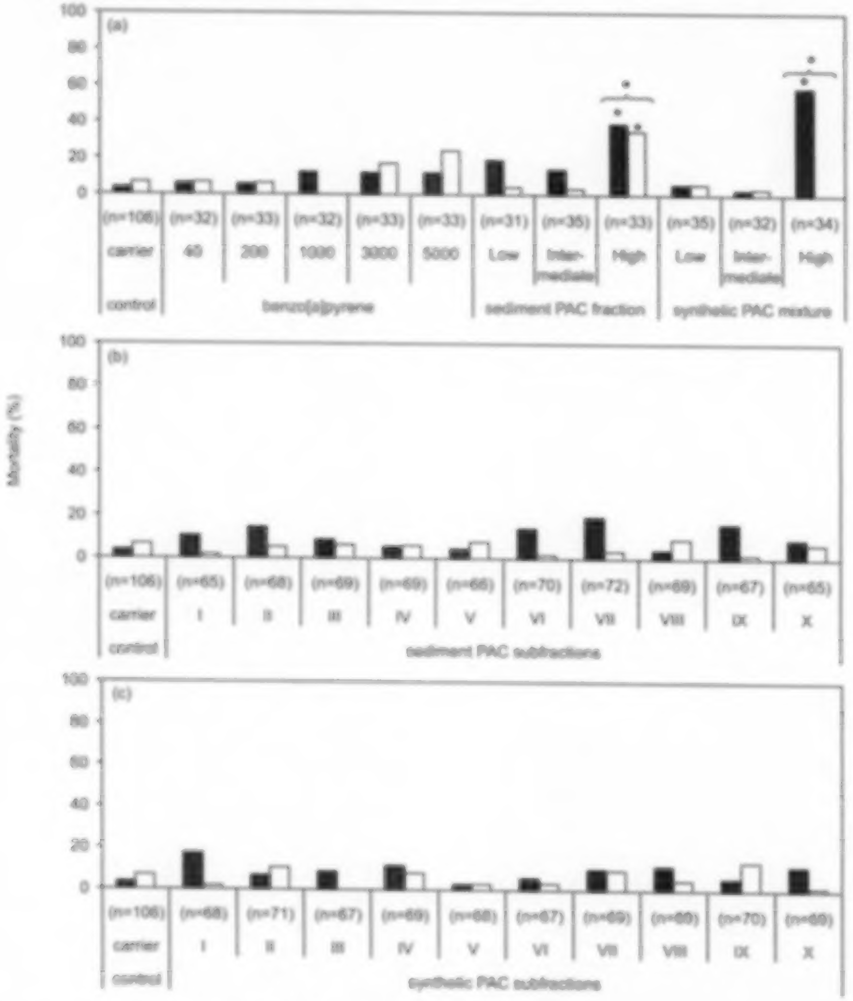

mortalities only during the embryonal stage and did not cause any significant increase in multiple abnormalities in larvae. The sediment PAC fraction, however, caused both embryonal and larval mortalities and a significant increase in larvae suffering from asymmetric yolk sac and multiple abnormalities. The numbers of mortalities caused by the subfractions, both sediment and synthetic, were not significantly higher than carrier controls, indicating that the mortalities are an effect of a combination of compounds in the sediment PAC fraction and in the synthetic PAC mixture.

In the PAH contribution experiment, the 17 PAHs appeared to explain embryonal mortality, while in the two mortality confirmation experiments, no significant increase of embryonal mortality was caused by the synthetic PAC mixture. This discrepancy suggests that the rainbow trout used in the PAH contribution experiment were more sensitive to mortality in the embryonic stage than the two other family pairs. Different degrees of background abnormalities and mortalities among the three experiments might also indicate differences in egg quality. Though one family pair is insufficient for comparing strains, variability in early life-stage mortality in different strains has been demonstrated in rainbow trout exposed to 2,3,7,8-tetrachlorodibenzo-*p*-dioxin (TCDD) (Walker and Peterson 1991).

Fig. 2. Percentage of newly hatched rainbow trout (*Oncorhynchus mykiss*) larvae in the polycyclic aromatic hydrocarbon (PAH) contribution experiment suffering from asymmetric yolk sac (hatched bars), hemorrhaging (open bars), or multiple abnormalities (solid bars). Rainbow trout were exposed as newly fertilized eggs using the nanoinjection technique. The sediment polycyclic aromatic compound (PAC) fraction was isolated from sediment extract from the polluted bay. The synthetic PAC mixture was prepared from 17 PAHs in amounts equimolar to those found in the sediment PAC fraction. High doses are presented on a PAH basis in Tables 1, 2, and 3; the two other graded doses are separated by a factor of five; and *n* denotes number of investigated larvae. Triolein-injected eggs were used as carrier controls, and graded doses of benzo[*a*]pyrene (μg·kg wet egg^{-1}) served as positive controls. An asterisk (*) indicates where data are significantly higher than carrier controls ($p < 0.0014$, 36 repeats, Fisher's exact test with Bonferroni correction).

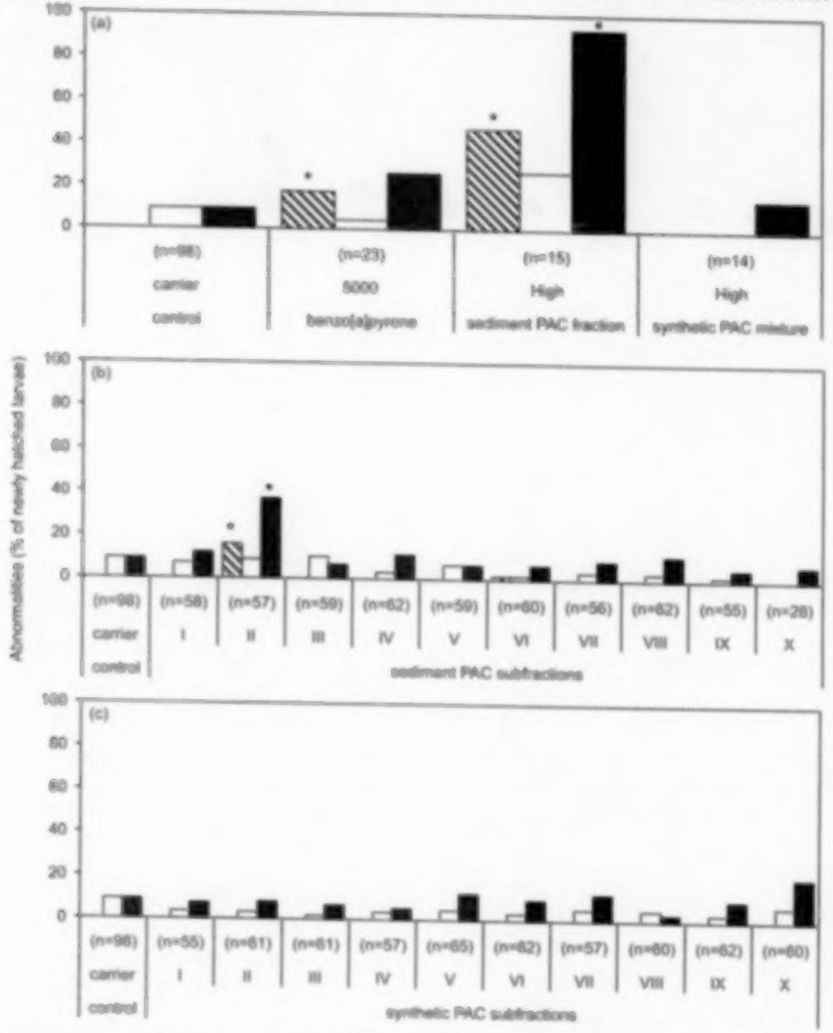

Nevertheless, the 17 PAHs were unable to explain the majority of the toxicopathic effects caused by the sediment PAC fraction, since the other effects were preserved when exposures were repeated. The sediment PAC fraction caused similar degrees of increased larval mortalities, abnormalities, and EROD induction as previously observed (Sundberg et al. 2005). The degrees of abnormalities and EROD induction among larvae exposed to the highest doses of benzo[*a*]pyrene were similar in all three experiments and our previous investigation (Sundberg et al. 2005). The synthetic PAC mixture caused no significant increase of larval mortalities or abnormalities, but it caused equal EROD induction in all three experiments. These results might also illustrate that the toxicopathic effects for the doses presented here hold thresholds effects. Hence, background abnormalities and mortalities differed among the experiments, but the most potent exposure solutions regarding abnormalities and EROD induction (the sediment PAC fraction and benzo[*a*]pyrene) preserved their toxicity when re-exposed, underlining the importance of including positive and negative controls in animal experiments.

Since no significant difference in terms of abnormalities was observed among larvae exposed to the synthetic PAC mixture and its 10 subfractions, we conclude that there is a

Fig. 3. Mortalities in early life stages of rainbow trout (*Oncorhynchus mykiss*) in the mortality confirmation experiment. The high early embryonal mortality in the polycyclic aromatic hydrocarbon (PAH) contribution experiment was investigated by repeating the exposure of the synthetic polycyclic aromatic compound (PAC) mixture twice (panels *a* and *b*). Embryonal mortalities (pre-hatch) are depicted as solid bars, and larval mortalities (post-hatch) as open bars. Rainbow trout were exposed as newly fertilized eggs using the nanoinjection technique. The synthetic PAC mixture was prepared from 17 PAHs in amounts equimolar to those found in the sediment PAC fraction from the polluted bay. High doses are presented on a PAH basis in Table 1; the two other graded doses are separated by a factor of five; and *n* denotes number of injected eggs. Triolein-injected eggs were used as carrier controls, and graded doses of benzo[*a*]pyrene (μg·kg wet egg^{-1}) served as positive controls.

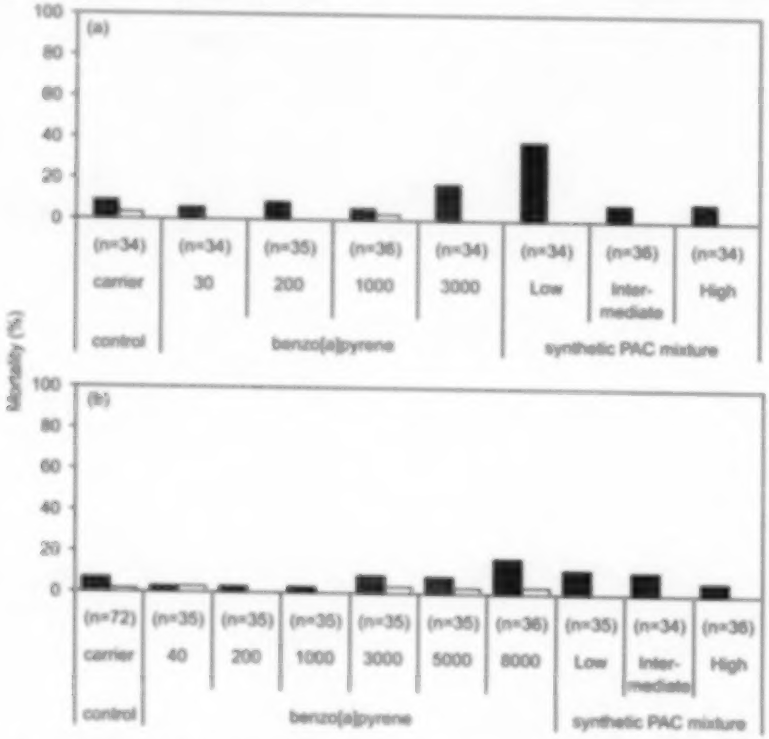

limited contribution of the 17 PAHs to the potential toxicopathic effects caused by compounds in the sediment. The only subfraction to cause a significant increase in larvae with multiple abnormalities was the sediment PAC subfraction II. This subfraction contained high concentrations of alkylated (C_1 to C_4) phenanthrene, fluoranthene, and three alkylation degrees (C_0 to C_2) of the thiaarene benzonaphtothiophene (Sundberg et al. 2005). Alkylated PAHs are found in higher concentrations than nonalkylated PAHs in polluted sediment (Barron and Holder 2003) and are demonstrated to be more toxic to early life stages of aquatic animals than their nonalkylated homologues (Rice et al. 1977; Hawkins et al. 2002; Barron et al. 2004), indicating a need for increased emphasis of these compounds.

Since the EROD induction caused by the highest dose of the synthetic PAC mixture was less than that caused by a 25 times lower dose (based on PAH concentration) of the sediment PAC fraction, the 17 PAHs used in this study can be said to explain less than 4% of the total EROD induction. The induction potential of the synthetic PAC mixture could be traced to subfraction X, providing evidence that indeno[1,2,3-*cd*]pyrene, benzo[*ghi*]perylene, coronene, and dibenzo[*a,l*]pyrene are the major causative compounds in the synthetic PAC mixture. The EROD induction in larvae exposed to the synthetic PAC subfraction X was slightly higher than in those exposed to the synthetic PAC mixture, suggesting nonadditive effects from the 13 other PAHs. Since sediment PAC subfractions were separated by their degree of aromaticity and all caused significant EROD induction, the compounds responsible for the portion of the sediment PAC fraction's EROD induction that cannot be explained by the 17 PAHs may have widely varying aromatic structures (three–five rings). The sum of EROD activity caused by the 10 sediment PAC subfractions, after background subtraction, was 530 pmol·mg protein^{-1}·min^{-1}, while the highest dose of the sediment PAC fraction caused an induction of 350 pmol·mg protein^{-1}·min^{-1}. The same comparison in our previous investigation (Sundberg et al. 2005) was more similar — 690 pmol·mg protein^{-1}·min^{-1} for the sum of the sediment PAC subfraction and 600 pmol·mg protein^{-1}·min^{-1} for the sediment PAC fraction. The larger difference we observed in the present investigation was most probably due to larger sample sizes in the present investigation (n = 10) than in the previous (n = 5), giving rise to smaller 95% confidence limits. Though larvae of one family pair had significantly higher background EROD activity than larvae of the other two family pairs, their EROD inductions were similar when exposed to the same substances. In addition, all

Fig. 4. Percentage of newly hatched rainbow trout (*Oncorhynchus mykiss*) larvae in the mortality confirmation experiment suffering from asymmetric yolk sac (hatched bars), hemorrhaging (open bars), or multiple abnormalities (solid bars). The high early embryonal mortality in the polycyclic aromatic hydrocarbon (PAH) contribution experiment was investigated by repeating the exposure of the synthetic polycyclic aromatic compound (PAC) mixture twice (panels *a* and *b*). Rainbow trout were exposed as newly fertilized eggs using the nanoinjection technique. The synthetic PAC mixture was prepared from 17 PAHs in amounts equimolar to those found in the sediment PAC fraction from the polluted bay. High doses are presented on a PAH basis in Table 1; the two other graded doses are separated by a factor of five; and *n* denotes number of investigated larvae. Triolein-injected eggs were used as carrier controls, and graded doses of benzo[*a*]pyrene (μg·kg wet egg^{-1}) served as positive controls. An asterisk (*) indicates where data are significantly higher than carrier controls (panel *a*: $p < 0.0063$, 8 repeats; panel *b*: $p < 0.005$, 10 repeats, Fisher's exact test with Bonferroni correction).

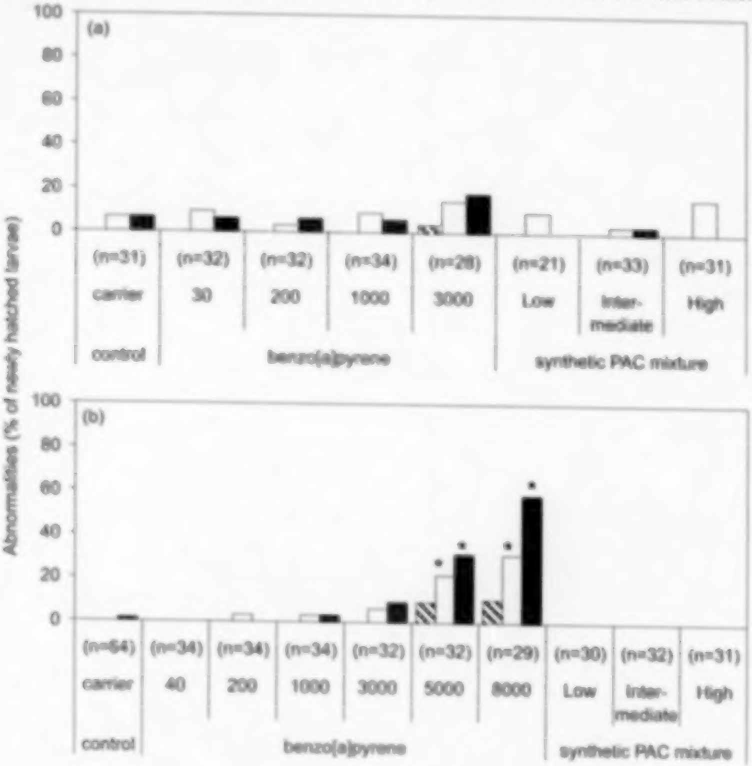

three family pairs, and one previously (fig. 3*b* in Sundberg et al. 2005), were equally prone to developing asymmetric yolk sacs, suggesting that if this abnormality develops via a specific mechanism, as does EROD induction, it might be less affected by variations in egg quality and genetic material of rainbow trout than endpoints that can be developed via several mechanisms.

The sums of analyzed PAHs in the synthetic PAC subfractions agreed well with the weighed amount (within factors 1.0–2.2) considering that analytical errors in PAH analyses have been demonstrated to be up to 8% relative standard deviation (Pettersen et al. 1999). The smaller PAHs found in synthetic PAC subfraction I differed the most from the weighed amounts, which may be explained by co-evaporation with the solvent, *n*-hexane, during fractionation. The sum of individual PAHs in the sediment PAC subfractions were greater than those in the sediment PAC fraction, which also contributed to differences between the sediment PAC subfractions and the synthetic PAC subfractions. This deviation may be explained by the fact that the sediment PAC subfractions contain fewer compounds than the sediment PAC fraction and thus less noise interfering with the chromatography and the MS detector. Some PAHs were distributed somewhat differently in the sediment PAC subfractions compared with their synthetic analogues, which could be explained by a matrix effect from unidentified compounds in the complex sediment PAC fraction interfering with the separation mechanism in the HPLC system. An alternative for investigating the contribution of the analyzed compounds to the toxicity would be to prepare synthetic subfractions directly. We chose, however, to fractionate the synthetic PAC mixture to investigate if this multistep bio-effect-directed fractionation approach could be reproduced. Consequently, when comparing environmental samples from different locations and fractionating the samples in several steps, chemical analyses are needed to confirm the separation.

Mechanisms of mortality and toxicopathic effects

Our results indicate that the mortalities caused by complex environmental PAC mixtures may involve mechanisms other than AhR mediation. The only synthetic subfraction to significantly induce EROD activity, X, caused no increased

Fig. 5. Hepatic ethoxyresorufin *O*-deethylase (EROD) induction (percentage of carrier control) in rainbow trout (*Oncorhynchus mykiss*) larvae exposed as newly fertilized eggs by nanoinjection in the polycyclic aromatic hydrocarbon (PAH) contribution experiment. The sediment polycyclic aromatic compound (PAC) fraction was isolated from sediment extract from the polluted bay. The synthetic PAC mixture was prepared from 17 PAHs in amounts equimolar to those found in the sediment PAC fraction. High doses are presented on a PAH basis in Tables 1, 2, and 3; the two other graded doses are separated by a factor of five. Triolein-injected eggs were used as carrier controls, and graded doses of benzo[*a*]pyrene (μg·kg wet egg^{-1}) served as positive controls. Mean values ± 95% confidence limits (error bars) are shown for each treatment; carrier control responses are defined by the upper and lower 95% confidence limits (broken lines). Sample size in each exposure group was $n = 5$, except for the following exposures: carrier control, $n = 15$; highest doses of the sediment PAC fraction and the synthetic PAC mixture, $n = 4$ (*a*); the sediment PAC subfractions (*b*) and the synthetic PAC subfractions (*c*), $n = 10$. An asterisk (*) indicates where data are significantly higher than carrier controls ($p < 0.05$, Kruskal–Wallis and Dunn's multiple comparison tests).

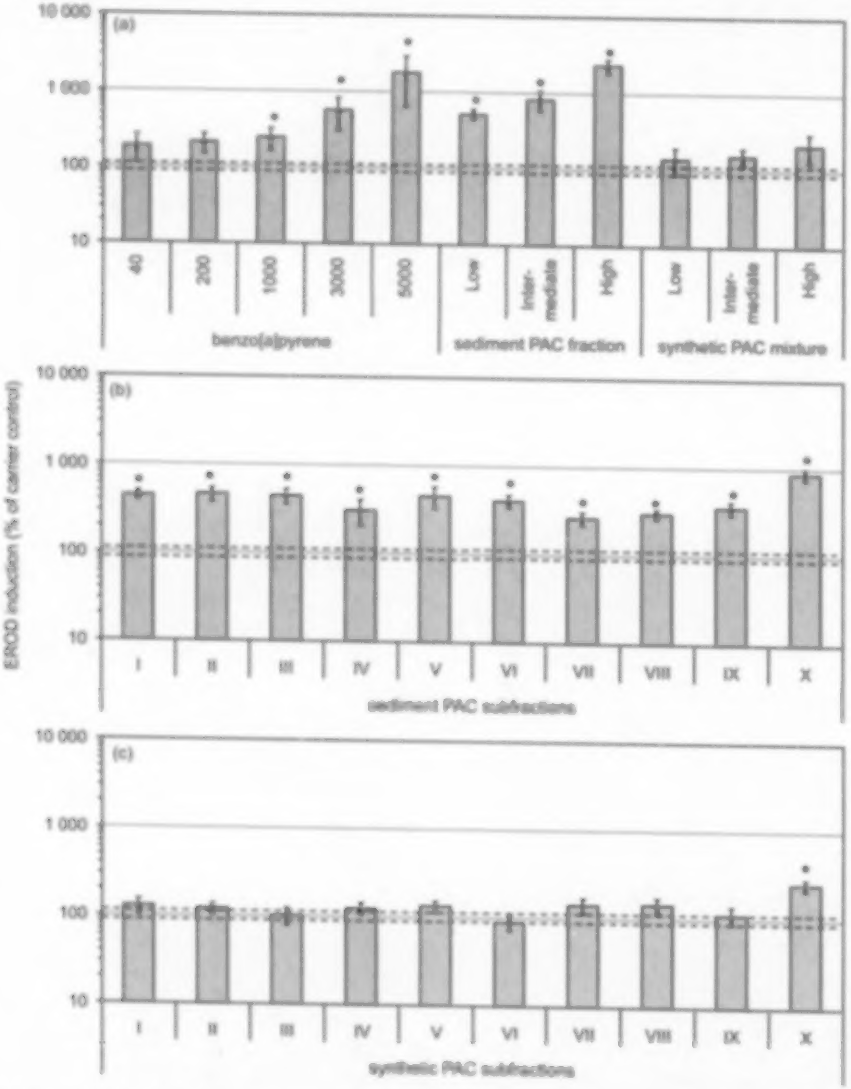

mortality. While the sediment PAC fraction caused high mortality coinciding with high EROD induction, its 10 subfractions, all of which caused significant EROD induction, caused no increase in mortality. AhR-meditated toxicity is often studied using TCDD, since this pollutant is one of the most potent AhR agonist in fish (Tanguay et al. 2003). One hypothesized AhR-mediated mechanism of mortality is the exhaustion of energy stores in terms of liver glycogen depletion (Viluksela et al. 1999). In embryonic salmonids, glycogen is the primary energy source by generating energy via glycolysis (Terner 1979). Though dose-dependent depletion of hepatocyte glycogen has been observed in moribund TCDD-exposed lake trout (*Salvelinus namaycush*) (Spitsbergen et al. 1991), Marty et al. (1997) did not find

Fig. 6. Hepatic ethoxyresorufin *O*-deethylase (EROD) induction (percetange of carrier control) in rainbow trout (*Oncorhynchus mykiss*) larvae exposed as newly fertilized eggs by nanoinjection in the mortality confirmation experiment. The high early embryonal mortality in the polycyclic aromatic hydrocarbon (PAH) contribution experiment was investigated by repeating the exposure of the synthetic polycyclic aromatic compound (PAC) mixture twice (panels *a* and *b*). Rainbow trout were exposed as newly fertilized eggs using the nanoinjection technique. The synthetic PAC mixture was prepared from 17 PAHs in amounts equimolar to those found in the sediment PAC fraction from the polluted bay. High doses are presented on a PAH basis in Table 1; the two other graded doses are separated by a factor of five. Triolein-injected eggs were used as carrier controls, and graded doses of benzo[*a*]pyrene (μg·kg wet egg^{-1}) served as positive controls. Mean values ± 95% confidence limits (error bars) are shown for each treatment; carrier control responses are defined by the upper and lower 95% confidence limits (broken lines). Sample sizes were $n = 5$ except for carrier control in *b* where $n = 10$. An asterisk (*) indicates where data are significantly higher than carrier controls ($p < 0.05$, Kruskal–Wallis and Dunn's multiple comparison tests).

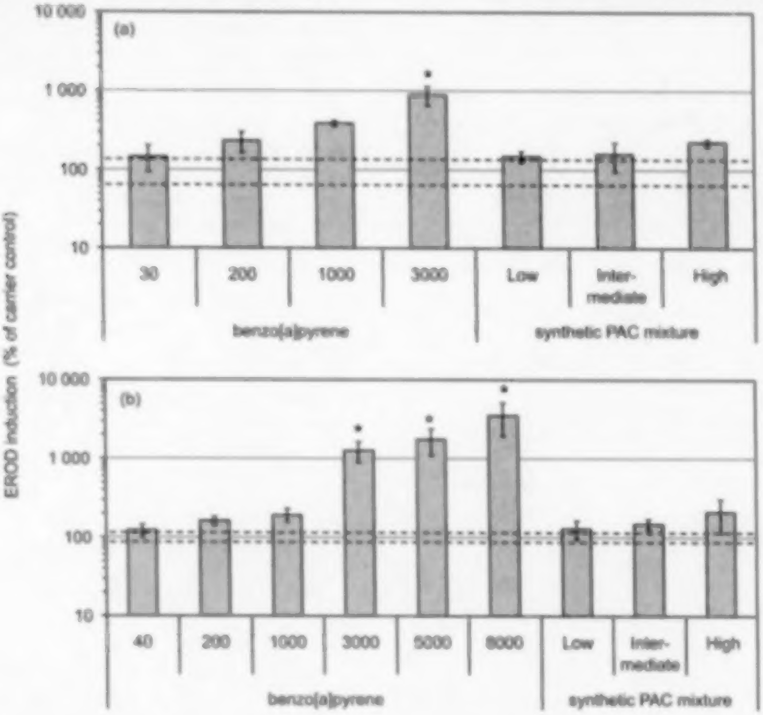

any decrease of glycogen in embryos and larvae of pink salmon (*Oncorhynchus gorbuscha*) exposed to PACs (weathered crude oil).

Abnormalities are also observed in TCDD-exposed teleost larvae for PAHs and other PACs; however, different mechanisms of early life-stage toxicity are evident. Edemas and hemorrhages are demonstrated to be caused by peripheral circulation failure and cell death in vascular endothelium (Guiney et al. 1997; Teraoka et al. 2003). Cell death is believed to be caused by AhR-mediated lipid peroxidation, since pharmaceutical treatment with a CYP1A antagonist (piperonyl butoxide) and an antioxidant (*N*-acetylcysteine) provided significant protection against early life-stage toxicity in TCDD-exposed medaka (Japanese rice fish, *Orizias latipes*) (Cantrell et al. 1996). Guiney et al. (1997) demonstrated an elevated CYP1A expression (immunohistochemical analysis) in vascular endothelium that correlated with hemorrhages and edemas in TCDD-exposed lake trout larvae. We found, however, that the most potent EROD inducer among the sediment PAC subfractions, X, caused no significant increase of abnormalities, while the EROD induction ability of subfraction II — the sediment PAC subfraction that caused most abnormalities — was similar to the other eight subfractions. Since EROD induction did not completely coincide with prevalence of the asymmetric yolk sac, this specific abnormality might be caused by the involvement of another unknown mechanism. This multimechanistic hypothesis is supported by findings from others. Incardona et al. (2004) demonstrated that zebrafish (zebra danio, *Danio rerio*) exposed to phenanthrene and dibenzothiophene experienced a direct effect on cardiac function by an unknown mechanism. Barron et al. (2004) could best predict early life-stage toxicity in fish exposed to PAC mixtures by considering several mechanisms.

In summary, only a small percentage of the potential toxicity from a polluted sediment sample to early life stages of fish can be attributed to 17 commonly analyzed and environmentally monitored PAHs. These 17 PAHs represent 13% of the compounds in the sediment PAC fraction, and our results suggest that our knowledge of which compounds actually are responsible for potential toxicity in field situations is alarmingly limited. Four PAHs (indeno[1,2,3-*cd*]pyrene, benzo[*ghi*]perylene, coronene, and dibenzo[*a,l*]pyrene) contributed less than 4% to the EROD induction potential, and the 17 PAHs could not explain larval mortalities or abnormalities. We have also demonstrated that AhR mediation is not solely responsible for toxicopathic effects in early life stages of rainbow trout.

Acknowledgements

The municipality of Västervik, Sweden, funded this study. The authors thank Marsha Hanson (Stockholm University, Stockholm, Sweden) for revising the language.

References

Åkerman, G., and Balk, L. 1995. A reliable and improved methodology to expose fish in the early embryonic stage. Mar. Environ. Res. **39**(1–4): 155–158.

Balch, G.C., Metcalfe, C.D., and Huestis, S.Y. 1995. Identification of potential fish carcinogens in sediment from Hamilton Harbor, Ontario, Canada. Environ. Toxicol. Chem. **14**(1): 79–91.

Barron, M.G., and Holder, E. 2003. Are exposure and ecological risks of PAHs underestimated at petroleum contaminated sites? Hum. Ecol. Risk. Assess. **9**(6): 1533–1545.

Barron, M.G., Carls, M.G., Heintz, R., and Rice, S.D. 2004. Evaluation of fish early life-stage toxicity models of chronic embryonic exposures to complex polycyclic aromatic hydrocarbon mixtures. Toxicol. Sci. **78**(1): 60–67.

Billiard, S.M., Querbach, K., and Hodson, P.V. 1999. Toxicity of retene to early life stages of two freshwater fish species. Environ. Toxicol. Chem. **18**(9): 2070–2077.

Boxall, A.B.A., and Maltby, L. 1997. The effects of motorway runoff on freshwater ecosystems: 3. Toxicant confirmation. Arch. Environ. Contam. Toxicol. **33**(1): 9–16.

Brinkworth, L., Hodson, P., Tabash, S., and Lee, P. 2003. CYP1A induction and blue sac disease in early developmental stages of rainbow trout (*Oncorhynchus mykiss*) exposed to retene. J. Toxicol. Environ. Health, **66A**(7): 627–646.

Brunström, B., Broman, D., Dencker, L., Näf, C., Vejlens, E., and Zebühr, Y. 1992. Extracts from settling particulate matter collected in the Stockholm Archipelago waters — embryolethality, immunotoxicity and EROD-inducing potency of fractions containing aliphatics/monoaromatics, diaromatics or polyaromatics. Environ. Toxicol. Chem. **11**(10): 1441–1449.

Cantrell, S.M., Lutz, L.H., Tillitt, D.E., and Hannink, M. 1996. Embryotoxicity of 2,3,7,8-tetrachlorodibenzo-*p*-dioxin (TCDD): the embryonic vasculature is a physiological target for TCDD-induced DNA damage and apoptotic cell death in medaka (*Orizias latipes*). Toxicol. Appl. Pharmacol. **141**(1): 23–34.

Carls, M.G., Rice, S.D., and Hose, J.E. 1999. Sensitivity of fish embryos to weathered crude oil: Part I. Low-level exposure during incubation causes malformations, genetic damage, and mortality in larval Pacific herring (*Clupea pallasi*). Environ. Toxicol. Chem. **18**(3): 481–493.

Das, B.S., Reid, S.G., Betts, J.L., and Patrick, K. 1969. Tetrachloro-*o*-benzoquinone as a component in bleached kraft chlorination effluent toxic to young salmon. J. Fish. Res. Board Can. **26**(11): 3055–3067.

Guiney, P.D., Smolowitz, R.M., Peterson, R.E., and Stegeman, J.J. 1997. Correlation of 2,3,7,8-tetrachlorodibenzo-*p*-dioxin induction of cytochrome P4501A in vascular endothelium with toxicity in early life stages of lake trout. Toxicol. Appl. Pharmacol. **143**(2): 256–273.

Hawkins, S.A., Billiard, S.M., Tabash, S.P., Brown, R.S., and Hodson, P.V. 2002. Altering cytochrome P4501A activity affects polycyclic aromatic hydrocarbon metabolism and toxicity in rainbow trout (*Oncorhynchus mykiss*). Environ. Toxicol. Chem. **21**(9): 1845–1853.

Heintz, R.A., Short, J.W., and Rice, S.D. 1999. Sensitivity of fish embryos to weathered crude oil: Part II. Increased mortality of pink salmon (*Oncorhynchus gorbuscha*) embryos incubating downstream from weathered Exxon Valdez crude oil. Environ. Toxicol. Chem. **18**(3): 494–503.

Incardona, J.P., Collier, T.C., and Scholz, N.L. 2004. Defects in cardiac function precede morphological abnormalities in fish embryos exposed to polycyclic aromatic hydrocarbons. Toxicol. Appl. Pharmacol. **196**(2): 191–205.

Lamparski, L.L., and Nestrick, T.J. 1980. Determination of tetra, hexa, hepta, and octachlorodibenzo-para-dioxin isomers in particulate samples at parts per trillion levels. Anal. Chem. **52**(13): 2045–2054.

Marty, G.D., Short, J.W., Dambach, D.M., Willits, N.H., Heintz, R.A., Rice, S.D., Stegeman, J.J., and Hinton, D.E. 1997. Ascites, premature emergence, increased gonadal cell apoptosis, and cytochrome P4501A induction in pink salmon larvae continuously exposed to oil-contaminated gravel during development. Can. J. Zool. **75**(6): 989–1007.

Pettersen, H., Axelman, J., and Broman, D. 1999. The relative contribution of spatial-, sampling- and analytical variation to the PAH and PCB concentrations in Baltic Sea sediments. Chemosphere, **38**(5): 1025–1034.

Prough, R.A., Burke, M.D., and Mayer, R.T. 1978. Direct fluorometric methods for measuring mixed-function oxidase activity. *In* Methods in enzymology. Vol. L II. Part C. *Edited by* S. Fleicher and L. Packer. Academic Press, New York, USA. pp. 372–377.

Rice, S.D., Short, J.W., and Karinen, J.F. 1977. Comparative oil toxicity and comparative animal sensitivity. *In* Fate and effects of petroleum hydrocarbons in marine organisms and ecosystems. *Edited by* D.A. Wolfe. Pergamon, Elmsford, New York, USA. pp. 78–94.

Spitsbergen, J.M., Walker, M.K., Olson, J.R., and Peterson, R.E. 1991. Pathologic alterations in early life stages of lake trout, *Salvelinus namaycush*, exposed to 2,3,7,8-tetrachlorodibenzo-*p*-dioxin as fertilized eggs. Aquat. Toxicol. **19**(1): 41–71.

Sundberg, H., Ishaq, R., Åkerman, G., Tjärnlund, U., Zebühr, Y., Linderoth, M., Broman, D., and Balk, L. 2005. A bio-effect directed fractionation study for toxicological and chemical characterization of organic compounds in bottom sediment. Toxicol. Sci. **84**(1): 63–72.

Tanguay, R.L., Andreasen, E.A., Walker, M.K., and Peterson, R.E. 2003. Dioxin toxicity and aryl hydrocarbon receptor signaling in fish. *In* Dioxins and health. 2nd ed. *Edited by* A. Schecter and T.A. Gasiewicz. John Wiley & Sons, Inc., Hoboken, New Jersey, USA. pp. 603–628.

Teraoka, H., Dong, W., Tsujimoto, Y., Iwasa, H., Endoh, D., Ueno, N., Stegeman, J.J., Peterson, R.E., and Hiraga, T. 2003. Induction of cytochrome P450 1A is required for circulation failure and edema by 2,3,7,8-tetrachlorodibenzo-*p*-dioxin in zebrafish. Biochem. Biophys. Res. Commun. **304**(2): 223–228.

Terner, C. 1979. Metabolism and energy conversion during early development. *In* Fish physiology, bioenergetics and growth. Vol. VIII. *Edited by* W.S. Hoar, D.J. Randall, and J.R. Brett. Academic Press, New York, USA. pp. 261–278.

Viluksela, M., Unkila, M., Pohjanvirta, R., Tuomisto, J.T., Stahl, B.U., Rozman, K.K., and Tuomisto, J. 1999. Effects of 2,3,7,8-tetrachlorodibenzo-*p*-dioxin (TCDD) on liver phosphoenolpyruvate carboxykinase (PEPCK) activity, glucose homeostasis and plasma amino acid concentrations in the most TCDD-susceptible and the most TCDD-resistant rat strains. Arch. Toxicol. **73**(6): 323–336.

Walker, M.K., and Peterson, R.E. 1991. Potencies of polychlorinated dibenzo-*p*-dioxin, dibenzofuran, and biphenyl congeners, relative to 2,3,7,8-tetrachlorodibenzo-*p*-dioxin, for producing early life stage mortality in rainbow trout (*Oncorhynchus mykiss*). Aquat. Toxicol. **21**(3–4): 219–238.

Walker, M.K., Zabel, E.W., Åkerman, G., Balk, L., Wright, P., and Tillitt, D.E. 1996. Fish egg injection as an alternative exposure route for early life stage toxicity studies. Description of two unique methods. *In* Techniques in aquatic toxicology. *Edited by* G.K. Ostrander. CRC Press, Boca Raton, Florida, USA. pp. 41–72.

Yan, J., Wang, L., Fu, P.P., and Yu, H. 2004. Photomutagenicity of 16 polycyclic aromatic hydrocarbons from the US EPA priority pollutant list. Mutat. Res. **557**(1): 99–108.

Zebühr, Y., Näf, C., Bandh, C., Broman, D., Ishaq, R., and Pettersen, H. 1993. An automated HPLC separation method with 2 coupled columns for the analysis of PCDD/Fs, PCBs and PACs. Chemosphere, **27**(7): 1211–1219.

Aggregated yield and fishing effort in multispecies fisheries: an empirical analysis

Kai Lorenzen, Oriana Almeida, Robert Arthur, Caroline Garaway, and Sophie Nguyen Khoa

Abstract: Many tropical fisheries are inherently of a multispecies nature, with any given type of fishing gear harvesting a wide range of species. Species-aggregated relationships between fishing effort and yield or catch per unit of effort (CPUE) provide important information for the management of such fisheries, as well as insights into ecosystem-level responses to fisheries exploitation. We used a model selection approach to study species-aggregated, yield–effort relationships in spatially replicated, multispecies inland fisheries. Of three alternative models considered, the data strongly supported a sigmoid functional form (Akaike weight 0.95) over the alternative, asymptotic exponential or quadratic (Schaefer) models (Akaike weights 0.03 and 0.02, respectively). The sigmoid form implies the occurrence of an inflexion point in the rising part of the yield–effort curve and no decline in aggregated yield even at the highest effort levels observed. Aggregated CPUE declines steeply near the origin of the effort scale before stabilizing or rising to a local maximum and then declining inversely with further increases in effort. This highly nonlinear response suggests that extreme caution is required when interpreting aggregated CPUE as an indicator of fishing impacts on exploited communities. Further research is required to identify the mechanisms generating the observed relationship.

Résumé : Plusieurs pêches tropicales sont multispécifiques de nature et tout type d'engin de pêche y récolte une gamme étendue d'espèces. Les relations pour l'ensemble des espèces entre l'effort de pêche et le rendement ou les captures par unité d'effort (CPUE) fournissent des informations importantes pour la gestion de telles pêches, ainsi que des perspectives sur les réactions écosystémiques à l'exploitation par la pêche. Nous utilisons une méthodologie de sélection de modèles afin d'étudier les relations rendement–effort pour l'ensemble des espèces dans des pêches intérieures multispécifiques qui se répètent à l'échelle spatiale. Des trois modèles considérés, les données appuient fortement le choix d'une forme fonctionnelle sigmoïde (pondération d'Akaike de 0,95) plutôt que des modèles de rechange asymptotique exponentiel ou quadratique de Schaefer (poids respectifs d'Akaike de 0,03 et de 0,02). La forme sigmoïde implique l'existence d'un point d'inflexion dans la partie croissante de la courbe rendement–effort et l'absence de déclin du rendement de l'ensemble des espèces même aux niveaux les plus élevés d'effort observés. La CPUE de l'ensemble des espèces décline abruptement près de l'origine de l'échelle des efforts avant de se stabiliser ou de remonter pour atteindre un maximum local, pour ensuite diminuer en fonction inverse des augmentations subséquentes de l'effort. Cette réaction qui est loin d'être linéaire indique qu'il faut être très prudent lorsqu'on interprète la CPUE de l'ensemble des espèces comme indicateur des impacts de la pêche sur les communautés exploitées. Des recherches supplémentaires pourraient identifier les mécanismes responsables de la relation observée.

[Traduit par la Rédaction]

Introduction

Many tropical fisheries are inherently of a multispecies nature, with any given gear type exploiting a wide range of species (Pauly 1979; Welcomme 1985). Species-aggregated yield and catch per unit of effort (CPUE) are important indicators of the exploitation status of such fisheries for two reasons. First, aggregated yield and CPUE relate directly to the production and socio-economic benefits derived from the fishery. Second, they reflect, at least in part, community-level responses to exploitation. Aggregated yield and CPUE therefore complement indicators of structural impacts of fishing on exploited communities and ecosystems, such as the mean trophic level of landings, mean size of fish in the catch, or the slope of biomass size spectra (Pauly et al. 1998; Welcomme 1999; Rochet and Trenkel 2003). Aggre-

Received 5 June 2005. Accepted 24 January 2006. Published on the NRC Research Press Web site at http://cjfas.nrc.ca on
6 May 2006.
J18727

K. Lorenzen,[1] O. Almeida,[2] R. Arthur,[3] C. Garaway,[4] and S. Nguyen Khoa.[5] Division of Biology, Imperial College London, Silwood Park, Ascot SL5 7PY, UK.

[1] Corresponding author (e-mail: k.lorenzen@imperial.ac.uk).

[2] Present address: Instituto de Pesquisa Ambiental da Amazônia (IPAM), Av. Nazare 669, Centro - 66.035–170 Belem, PA, Brasil.

[3] Present address: MRAG Ltd., 18 Queen Street, London W1J 5PN, UK.

[4] Present address: Department of Anthropology, University College, Gower Street, London WC1E 6BT, UK.

[5] Present address: International Water Management Institute (IWMI), P.O. Box 2075, Colombo, Sri Lanka.

doi:10.1139/F06-038

Fig. 1. Overview of the alternative relationships between fishing effort and (*a*) yield and (*b*) catch per unit of effort (CPUE): sigmoid (heavy solid line), asymptotic (thin solid line), and quadratic (dashed line) functional form. Yield and effort are in arbitrary units.

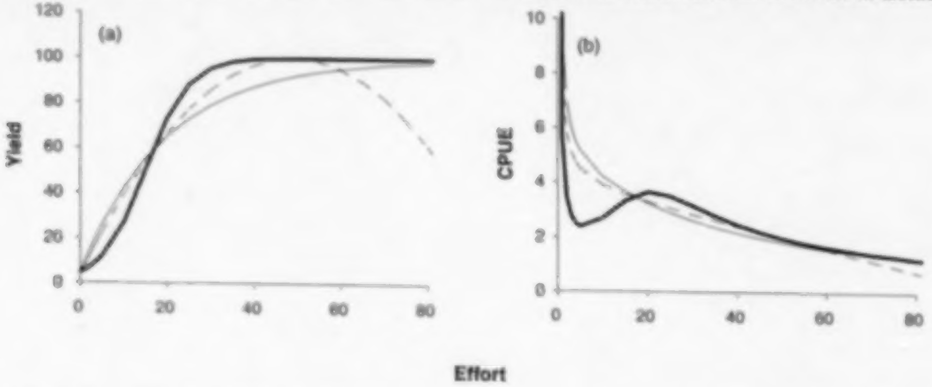

gated yield and CPUE have been used in several recent studies on impacts of fishing and environmental modifications on fish communities (e.g., Lorenzen et al. 1998; Myers and Worm 2003; Nguyen Khoa et al. 2005). However, the ecological interpretation of observed patterns in aggregated multispecies CPUE is far from straightforward, as illustrated by the controversy surrounding Myers and Worm's (2003) study on the rapid apparent depletion of predatory fish communities (Walters 2003; Hampton et al. 2005; Polacheck 2006).

Interpretation or prediction of aggregated yield and CPUE responses to variation in effort requires a quantitative understanding of the relationship between yield or CPUE and effort. This leads to the question of whether there is a general relationship between species-aggregated yield or CPUE and effort that applies to a wide range of fisheries. In single species fisheries, this role has long been effectively played by the Schaefer and related surplus production models, assuming a dome-shaped relationship between yield and effort, and continuously declining CPUE (Hilborn and Walters 1992). The Schaefer model has also been applied to aggregated yield in multispecies fisheries (e.g., Pauly 1979), but systematic discrepancies between the model and aggregated data have been widely noted. In particular, aggregated yield does not tend to decline even at very high levels of fishing effort (Pauly 1979; Marten and Polovina 1982), and CPUE may show a local maximum at intermediate levels of effort rather than a monotonous decline (Welcomme 1985, 1999). Disaggregation into ecologically defined species groups (Ralston and Polovina 1982) or transformation of variables (Bayley 1988) are usually required for species-aggregated data to conform to a Schaefer-type relationship. Theoretical studies suggest that aggregated yield–effort relationships are unlikely to follow the shape of Schaefer or similar surplus production models unless very restrictive conditions apply, but have not identified any general alternative models (Pope 1979; Kirkwood 1982).

Bayley (1988) provides the most extensive empirical analysis of aggregated yield–effort relationships, using comparative data for a range of tropical lakes, river floodplain systems, and lagoons. He assumes a quadratic (Schaefer) functional form a priori, but tests different transformations (none, log, and square-root) of both yield and effort data to obtain the best fit to the quadratic curve. While this approach has resulted in a good statistical description of the comparative data, it has three shortcomings. First, the a priori assumption of a quadratic functional form imposes a strong, theoretically based constraint and effectively makes the resulting model theoretical rather than empirical (Mangel et al. 2001). Second, the use of transformed variables confounds error structure and functional form and therefore obscures the underlying relationship. Third, fitting of the model to data from ecologically and technologically very heterogeneous systems poses problems in terms of effort standardization and potential confounding factors. For this reason, Bayley (1988) called for systematic comparative studies within more homogeneous systems.

Our study aims to further the empirical analysis of aggregated yield–effort relationships by confronting alternative functional relationships with data collected from ecologically and technologically homogeneous systems. We also reanalyze the data for more heterogeneous systems as used in Bayley (1988). Three candidate models are considered, which represent the major functional forms advanced in previous conceptual or empirical studies (Fig. 1). (*i*) A sigmoid model as developed conceptually by Welcomme (1985, 1999) and supported empirically by Laë (1997) for lagoon fisheries. The model is asymptotic at high effort levels and has an inflexion point in the rising section of the yield curve. Consequently the CPUE curve may show a more or less pronounced local maximum at intermediate effort levels and declines only gradually at higher levels. (*ii*) An asymptotic exponential model, which shows the same asymptotic behaviour at high effort levels, but does not have an inflexion point in the rising section. It thus implies a monotonous decline in CPUE with increasing effort. This form has been proposed as a conceptual model by Jul-Larsen and van Zwieten (2002). (*iii*) A quadratic (Schaefer) model, as often assumed for single species stocks and used in multispecies systems by Pauly (1979) and, with transformed variables, Bayley (1988). While our selection of candidate models is inspired by previous empirical and conceptual studies, none of the models have a direct phenomenological basis. The aim of our analysis is the identification of a robust empirical model, rather than the testing of alternative biological hypotheses. Using a model selection approach based on maximum likelihood estimation (Burnham and Anderson 2002; Johnson and Omland 2004), we account for log-normal error structure without distorting the functional form of the underlying yield–effort relationship.

Materials and methods

Data

Primary data were obtained from subsistence-oriented inland fisheries in the Brazilian Amazon and in Laos. In both study areas, the majority of the rural population engages in fishing as part of a diversified semisubsistence livelihood strategy (Garaway 1999; Almeida 2004; Smith et al. 2005). Primary data were collected from four independent study systems: Amazon lakes, Lao nonstocked lakes, Lao stocked lakes, and Lao floodplains (Table 1). Amazon lakes were located in the floodplain of the lower Amazon and ranged in size from 10 to 1200 ha. Their fisheries were exploited by local communities predominantly with gill nets, cast nets, and hook and line. The Lao lakes were much smaller than those studied in the Amazon, covering between 1 and 20 ha in area. Nonstocked lakes contained only native, wild stocks and were exploited by local households on an individual basis, using mostly gill nets and cast nets. Stocked lakes contained populations of exotic species maintained largely by continued stocking, in addition to native wild fish. Exotic species comprised Indian major carp (*Labeo rohita*, *Cirrhinus mrigala*) and Chinese carp (*Aristichthys nobilis*, *Hypophthalmichthys molitrix*), which do not reproduce naturally in small lakes, and Nile tilapia (*Oreochromis niloticus*), which established self-reproducing populations in the more eutrophic lakes (Arthur 2004). Only wild fish catches from the stocked lakes were used in the current analysis. Previous studies indicated that stocking of exotic species had no measurable impact on wild fish catches, abundance, or species composition (Lorenzen et al. 1998; Arthur 2004). Catches and abundance of exotic species, on the other hand, were strongly influenced by stocking and cannot therefore be included in the analysis of multispecies yield–effort responses. Stocked lakes were exploited on a communal basis by fishing teams using gill nets and cast nets, and overall effort levels were often low because of either intentional restriction or low incentives to participate in communal harvesting (Garaway 1999). Lao floodplain fisheries are based on a mixture of aquatic habitats that become interconnected during the wet season, including rivers, floodplain lakes, and rice paddies (Nguyen Khoa et al. 2005), and are exploited by a plethora of different gears. For the purpose of this study, wetland areas were delineated on a village basis, and catch and effort were expressed per unit of village wetland area.

Catch and effort data were collected by means of household surveys, with the exception of stocked Lao lakes, where catches were recorded directly by the village administration. Household surveys based on recall of catches by respondents are widely used to quantify catch and effort in subsistence-oriented and recreational fisheries, where diffuse landings make the use of conventional catch assessment surveys all but impossible (Bayley and Petrere 1989; Cahoon et al. 1993; SEAFDEC 2004). Recall of catches by fishers tends to be reasonably accurate as long as recall periods are short (i.e., days up to one week). A comparison of catch weights esti-

Table 1. Overview of the data sets used.

System	Description	Replicates	Area range (ha)	Data collection	Year of sampling	Source
Amazon lakes	Floodplain lakes in the lower Amazon	23 lakes fished by one village each	20–1 125	Household surveys	2000–2001	This study
Laos						
Lakes (nonstocked)	Floodplain lakes in Laos	11 lakes fished by three villages	1–10	Household surveys with aided recall	1995–1997	This study
Lakes (stocked)	Wild fish catches from floodplain lakes in Laos also stocked with exotic species	39 lakes fished by one village each	0.3–5.5	Direct recording of catches	1999–2002	This study
Floodplain	Floodplain area dominated by rain-fed rice fields	18 aquatic habitat areas attributed to one village each	3–1 400	Household surveys with aided recall	1998–1999	This study
African lakes	Large lakes	31 lakes	11 300 – 6 880 000	Catch and market flow surveys	1960–1975	Henderson and Welcomme 1974; Bayley 1988
River floodplains	Tropical rivers with floodplains	14 rivers with floodplains	4 000 – 3 325 000	Catch and market flow surveys	1977–1981	Welcomme 1979; Bayley 1988
Lagoons	Tropical coastal lagoons	13 lagoons	100 – 1 434 400	Catch and market flow surveys	1960–1980	Kapetsky 1984; Bayley 1988

mated by Amazonian fishers with subsequent direct measurement showed that fishers' estimates were within 10% of the true weight in 70% of cases and within 20% in 90% of cases (G. Moisés, Project Mamiraua, Cx. Postal 38, 69470-000 Tefe, AM, Brazil, personal communication). Our surveys were designed with a 1-week recall period, and in Laos visual aids such as sticks and bowls to aid recall were used (Garaway 1999). Surveys covered two 1-week periods in the dry and wet seasons, respectively, in the case of Amazon lake and Lao floodplain fisheries, twelve 1-week periods (one per month) in the case of Lao nonstocked lake fisheries, and continuous village records in Lao stocked lake fisheries. In the Amazon and Lao lake fisheries where fishers often had access to several local lakes, catch and effort data were disaggregated within households and combined by lake.

In the Lao floodplain fisheries, which were exploited by a plethora of gears, effort was measured as hours fished without reference to gear type. In the Amazon and Lao lake fisheries that were exploited by fewer gear types, effort expended by different gear types was standardized as follows (Gulland 1983). The fishing power P_g of gear g relative to standard gear s was calculated as the average of the CPUE ratio for the two gear types over all lakes i where both gears were used:

$$(1)\qquad P_g = \frac{1}{n}\sum_{i=1}^{n}\frac{\mathrm{CPUE}_{g,i}}{\mathrm{CPUE}_{s,i}}$$

The combined fishing effort E_i of all gears in lake i is then given by

$$(2)\qquad E_i = \sum_{g} E_{g,i}P_g$$

Annual yield and fishing effort for each replicate were calculated per unit lake area or per maximum flooded area in the case of the floodplain study. Gear composition was unrelated to total fishing effort per unit area within studies. However, the gears used differed between systems, with the Amazon lake fisheries targeting larger species, while the Lao lake or floodplain fisheries targeted virtually the full size range of fish present. Hence effort measures are comparable within, but not across systems.

We also reanalysed the secondary data used in Bayley's (1988) study. These data were derived predominantly from catch surveys and some market flow studies, mostly conducted as part of United Nations Food and Agricultural Organization (FAO) projects (Henderson and Welcomme 1974; Welcomme 1979; Kapetsky 1984). In all data used in Bayley's (1988) study, effort was expressed in terms of fishers per square kilometre.

Analysis

Three alternative models, as described above, were fitted to the aggregated yield–effort data. All models had three parameters, did not force the relationship through the origin, and were written with maximum or asymptotic yield $Y_{\max}$ as an explicit parameter. The sigmoid model with an inflexion point in the rising section is of the form

$$(3)\qquad Y(E) = \frac{Y_{\max}}{1+\exp[a(b-E)]} + \varepsilon$$

where $Y(E)$ is the aggregated yield at aggregated effort level E, $Y_{\max}$ is the maximum yield, a determines the steepness of the curve, b is the effort level at which yield equals 50% of the asymptotic yield, and ε is a log-normally distributed random error. This model is asymptotic with $Y(E) \rightarrow 0$ for $E \rightarrow -\infty$ and $Y(E) \rightarrow Y_{\max}$ for $E \rightarrow \infty$; hence $Y(0) > 0$. The asymptotic exponential model with monotonically declining slope is of the form

$$(4)\qquad Y(E) = Y_{\max}\{1-\exp[-a(E-b)]\} + \varepsilon$$

where a determines the steepness of the curve, and b is the effort at the origin of the yield curve. The quadratic (Schaefer) model is of the form

$$(5)\qquad Y(E) = Y_{\max}(1-\{1-[a(E-b)]\}^2) + \varepsilon$$

where a is the inverse of effort at maximum yield, and b is the effort at the origin of the yield curve.

The models were fitted using the method of maximum likelihood. Omitting constant terms, the minimum negative log likelihood L for each of the candidate models j is given by

$$(6)\qquad L_j = \frac{n}{2}\ln\left\{\frac{1}{n}\sum_{i=1}^{n}\ln(Y_i) - \ln[M_j(E_i, Y_{\max,j}, a_j, b_j)]^2\right\}$$

where n is the number of observations, Y_i is the observed yield for replicate i, and $M_j(E_i, Y_{\max,j}, a_j, b_j)$ is the yield predicted by model M_j for effort E_i given the maximum likelihood estimate of parameters $Y_{\max,j}$, a_j, b_j (Hilborn and Mangel 1997; Burnham and Anderson 2002). Because the same set of models is compared on several independent data sets, the negative log likelihood $L_{j,\mathrm{combined}}$ of the combined data for each candidate model j may be calculated as the sum of the negative log likelihoods $L_{j,t}$ associated with the same model in the independent systems t (Edwards 1992):

$$(7)\qquad L_{j,\mathrm{combined}} = \sum_{t} L_{j,t}$$

Note that this is the combined L for model j given separate parameter estimates for each of the independent systems. The combined L thus applies to the common functional form of the model; it does not imply that a joint set of parameters is estimated for all systems.

Because only the differences between L_j values of the data given alternative models are of interest, we report likelihoods as

$$(8)\qquad \Delta L_j = L_j - L_{\min}$$

where $L_{\min}$ is the minimum L_j among the candidate set of models. The relative weight of evidence for each model can be expressed by the normalized likelihood

$$(9)\qquad W_j = \frac{\exp(-\Delta L_j)}{\sum_{k=1}^{3}\exp(-\Delta L_k)}$$

which may be interpreted as the probability that model j is the best model for the given data given the candidate set of models. The expression given here is the Akaike weight (W)

Table 2. Parameter estimates of the yield–effort models of Amazon lakes and Lao lakes and floodplains.

System	Model	Y_{max} (kg·ha^{-1}·year^{-1})	a (h^{-1}·ha·year)	b (h·ha^{-1}·year^{-1})	n	ΔL	W
Amazon lakes	Sigmoid	92	0.11	30	23	0.00	0.63
	Asymptotic	2993	0.000 4	−1.4	23	1.25	0.18
	Quadratic	5220	0.000 1	−1.6	23	1.24	0.19
Laos							
Lakes (nonstocked)	Sigmoid	199	0.002	1967	11	0.05	0.32
	Asymptotic	1878	0.000 02	−15	11	0.00	0.34
	Quadratic	609	0.000 05	−13	11	0.01	0.34
Lakes (stocked)	Sigmoid	547	0.002 3	1630	39	0.00	0.55
	Asymptotic	1087	0.000 1	−73	39	0.90	0.22
	Quadratic	1012	0.000 05	−74	39	0.86	0.23
Floodplain	Sigmoid	129	0.018	184	18	0.08	0.33
	Asymptotic	321	0.001 1	−8.1	18	0.16	0.31
	Quadratic	157	0.001 1	−7.6	18	0.00	0.36

Note: Y_{max}, a, and b are the model parameters; n is the number of observations; L is the negative log likelihood; and W is the Akaike weight.

Table 3. Parameter estimates of the yield–effort models of African lakes, river floodplains, and lagoons.

System	Model	Y_{max} (kg·ha^{-1}·year^{-1})	a (fishers^{-1}·km^{2}·year)	b (fishers·km^{-2}·year^{-1})	n	ΔL	W
African lakes	Sigmoid	76	5.30	0.74	31	0.00	0.58
	Asymptotic	153	0.29	0.07	31	0.70	0.29
	Quadratic	155	0.11	0.07	31	1.52	0.13
River floodplains	Sigmoid	99	1.04	1.97	14	0.00	0.50
	Asymptotic	97	0.32	−0.22	14	0.76	0.23
	Quadratic	186	0.06	−0.22	14	0.60	0.27
Lagoons	Sigmoid	106	0.51	2.88	13	0.29	0.29
	Asymptotic	120	0.18	−0.52	13	0.00	0.39
	Quadratic	132	0.05	−1.32	13	0.19	0.32

Note: Y_{max}, a, and b are the model parameters; n is the number of observations; L is the negative log likelihood; and W is the Akaike weight.

(Burnham and Anderson 2002) when all alternative models have the same number of free parameters.

Results

Akaike weights (W) favour the sigmoid model in our primary data for Amazon lakes and stocked Lao lakes and in the secondary data for African lakes and river floodplains. In the remaining systems, Ws are equivocal in their support for the alternative models (Tables 2, 3). When likelihoods are combined among systems (Table 4), Ws strongly favour the sigmoid functional form in our primary data (W = 0.80), the secondary data (W = 0.69), and overall (W = 0.95). Comparison of fitted models with data and examination of standardized residuals for the sigmoid model show that the sigmoid functional form provides a good description of all systems (Figs. 2, 3). Note that because of use of a log-normal error model, deviations of data from the fitted models in the yield and CPUE plots are not the same as the actual residuals.

Empirical support for the sigmoid model points to three regularities in the relationship between effort and aggregated yield or CPUE. These are evident in the data and fitted models for individual systems (Figs. 2, 3), but are best demonstrated when the fitted sigmoid models are normalized and plotted on the same graph (Fig. 4). First, there is no evidence of aggregated yield declining with effort throughout the effort range observed in the systems under study. Second, observed and predicted CPUE are very high near the origin of the effort scale and decline steeply to much lower values at moderate effort levels. This steep decline in CPUE occurs while the overall level of exploitation is very low, with aggregated yield less than 10% of the system potential. Third, after the initial steep decline, aggregated CPUE tends to rise to a more or less pronounced local maximum before declining very gradually with increasing effort. It is also noticeable that the normalized models for all systems represented in our primary data and to one system (African lakes) represented in the secondary data show a very similar normalized slope (Fig. 4). Only the relationships estimated for the small and comparatively heterogeneous secondary data sets on river floodplains and lagoons show substantially different (lower) normalized slopes. Three distinct regions may be identified in the aggregated relationship with respect to yield and CPUE responses (Fig. 4). In the lightly exploited range (A in Fig. 4), yield is relatively constant, but CPUE declines steeply with increasing effort. This is followed by a moderately exploited range (B), where yield increases almost linearly with effort, while CPUE also increases slightly

Table 4. Combined likelihood (*L*) and Akaike weights (*W*) associated with the alternative models.

Model	Our studies		Bayley (1988)		All studies combined	
	ΔL	*W*	ΔL	*W*	ΔL	*W*
Sigmoid	0.00	0.82	0.00	0.69	0.00	0.95
Asymptotic	2.16	0.09	1.17	0.22	3.34	0.03
Quadratic	1.97	0.11	2.02	0.09	3.99	0.02

Fig. 2. Yield, catch per unit of effort (CPUE), and standardized residuals of yield in relation to fishing effort in the Amazon lake, Lao lake (nonstocked and stocked), and Lao floodplain fisheries. Lines indicate the fitted sigmoid (solid line), asymptotic (long dashed line), and quadratic (short dashed line) models. Standardized residuals are given for the sigmoid model, which shows the best fit overall.

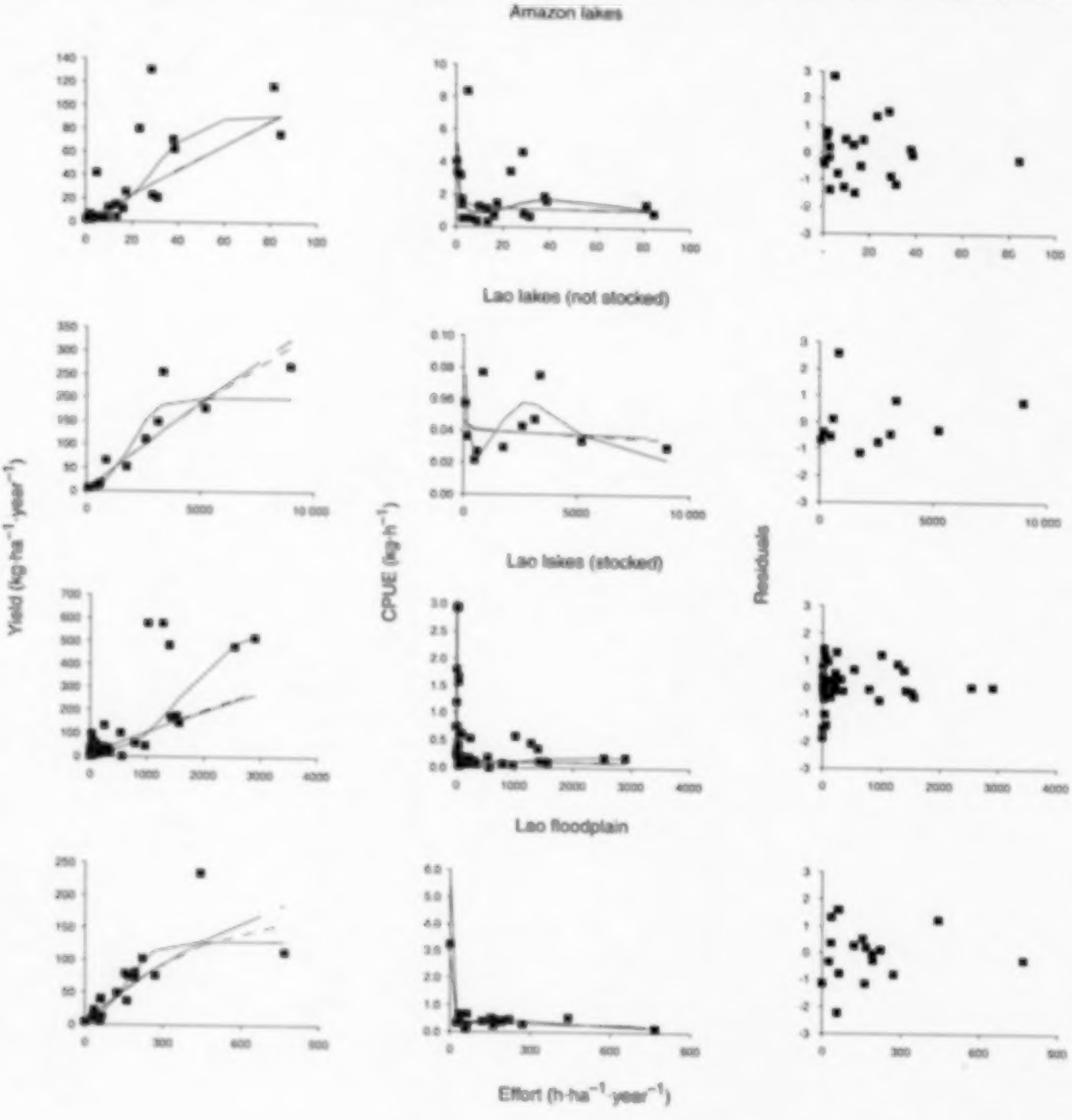

Fig. 3. Yield, catch per unit of effort (CPUE), and standardized residuals of yield in relation to fishing effort in the African lake, river, and lagoon fisheries data compiled by Bayley (1988). Lines indicate the fitted sigmoid (solid line), asymptotic (long dashed line), and quadratic (short dashed line) models. Standardized residuals are given for the sigmoid model, which shows the best fit overall.

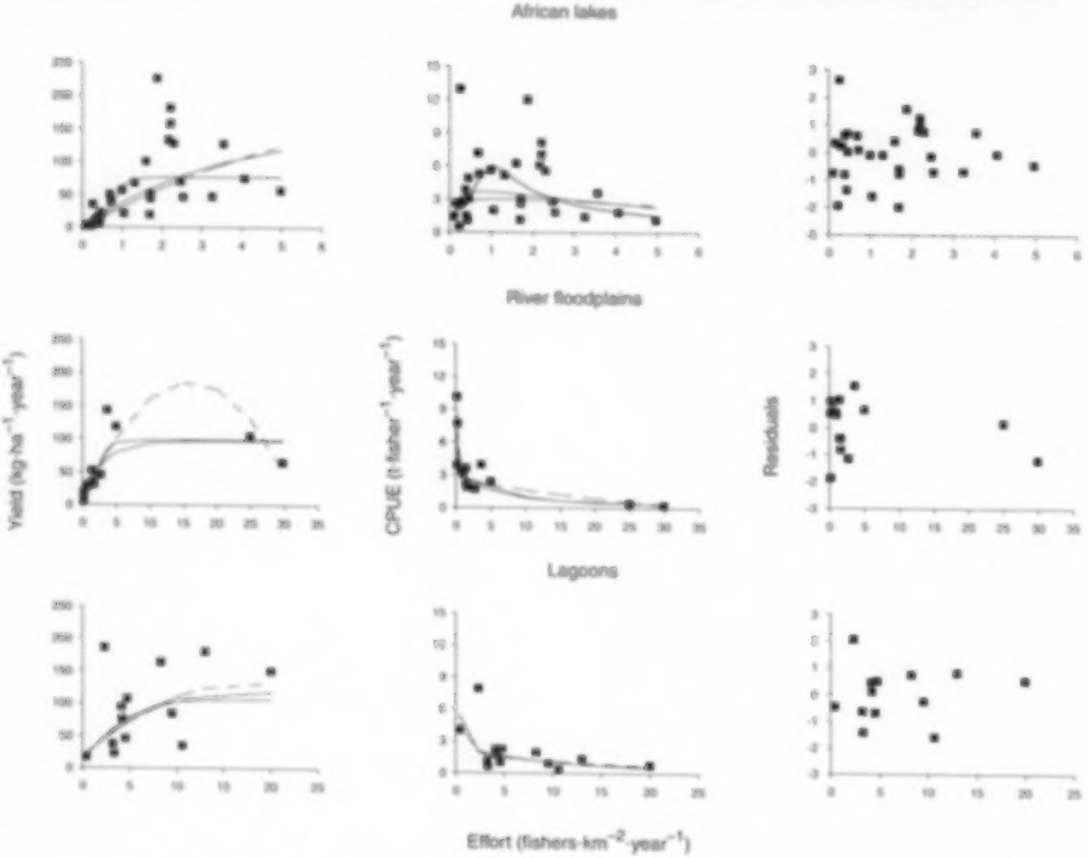

or remains constant. Finally, in the highly exploited range (C), yield is insensitive to effort while CPUE declines inversely.

Discussion

A sigmoid functional form provides a better empirical model for the multispecies fisheries analysed than either an asymptotic exponential or a quadratic (Schaefer) model. This holds for both our primary studies of relatively homogeneous systems and the data for more heterogeneous systems first analysed by Bayley (1988). The sigmoid model performs best overall, and in no system performs substantially worse than any of the alternative models. We have thus identified a functional form for aggregated yield–effort relationships that appears to hold some generality and is substantially different from the forms assumed or observed in single species fisheries. Key attributes of the relationship within the moderate-to-high effort range have been proposed conceptually or are implicit in earlier studies (Welcomme 1985; Bayley 1988; Laë 1997). Transformation of variables and a priori selection of models, however, may have obscured the true relationships and in particular prevented appreciation of its complex behaviour at low effort levels. Our use of a model selection approach, combined with new comparative data from relatively homogeneous systems, has thus allowed us to generalize previously suggested attributes and identify new attributes in aggregated yield–effort relationships.

Our analysis assumes that fishing effort is an independent control affecting the response variables yield and CPUE (i.e., effort is not in turn affected by the response variables). Dynamic effort responses to spatial variation in CPUE would require observations to be treated as joint outcomes of underlying variation in production factors that influence both yield and effort (Walters and Martell 2004). Effort levels are unlikely to be influenced strongly by yield or CPUE in our studies, where fishing involved the majority of the local populations and was carried out in a part-time, subsistence-oriented manner. Effort per unit water area was thus determined by two factors: human population density relative to water area and the level of effort expended by individuals. Population density relative to water area varied widely within study systems, as a result of settlement patterns influenced mainly by agricultural land availability (agriculture being the dominant livelihood activity in the study areas).

Fig. 4. Normalized (*a*) yield and (*b*) catch per unit of effort (CPUE) as a function of normalized effort in the fitted sigmoid models for our primary data (solid lines) and the secondary data (dashed lines). Effort has been normalized relative to the effort at which 50% of the asymptotic yield is obtained (model parameter *b*), while yield has been normalized relative to asymptotic yield. Also shown are the three effort regions: (A) lightly exploited — yield is relatively constant but CPUE declines steeply with increasing effort; (B) moderately exploited — yield increases almost linearly with effort while CPUE remains constant; (C) highly exploited — yield is insensitive to effort while CPUE declines inversely.

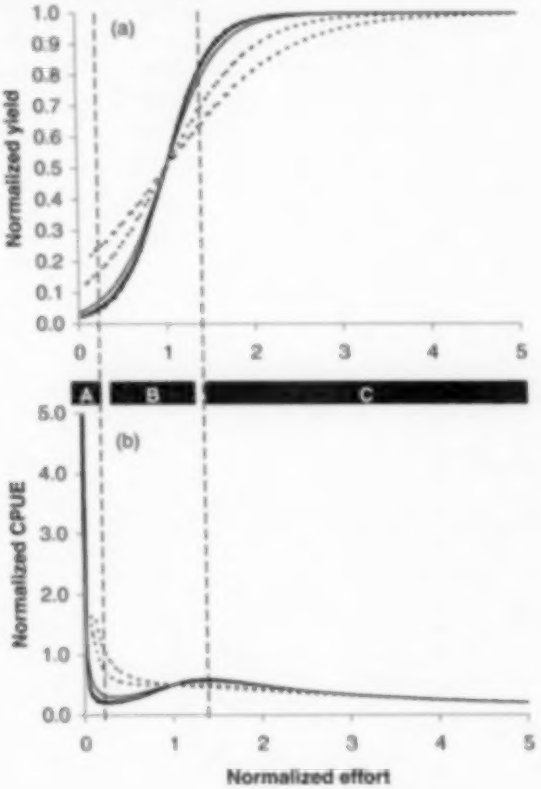

Our household surveys showed that the level of fishing effort expended, and where relevant, its allocation to different water bodies, were influenced primarily by labour availability, convenience of access, and local fishing restrictions rather than CPUE (Garaway 1999; Almeida 2004). No correlations were found between CPUE achieved and average household fishing effort expended in different replicates. While we could not directly examine determinants of effort in the data sets previously analysed by Bayley (1988), it is likely that once again local population density relative to water area is the dominant factor influencing effort variation within the study systems.

The identified relationships have direct implications for the management of multispecies fisheries, in particular those where aggregated yield and CPUE (as opposed to those of only a few species) are important to management stakeholders. This is likely to be the case in tropical inland and coastal fisheries, where high demand exists for a broad range of species. Where such fisheries are highly exploited (range C), aggregated yields will be sustained but CPUE and thus the economic returns to fishers will decline as effort increases. This implies that total yield levels may be maintained even in situations where low opportunity costs for fishers (lack of alternative employment or nutrition) result in very high levels of effort (Allison and Ellis 2001; Jul-Larsen and van Zwieten 2002; Smith et al. 2005). Maintenance of aggregated yield, of course, does not imply absence of changes in ecosystem structure or functioning that may be of conservation concern. Effort reduction within the high-effort range will improve CPUE (i.e., returns to effort), and this can provide incentives for regulation where alternative opportunities exist and institutional arrangements are conducive. In moderately exploited fisheries (range B), effort restriction will reduce aggregated yield proportionally, but not bring increased returns (CPUE) to fishers. Incentives to reduce effort are thus low for all stakeholders. Reducing effort (and yield) to very low levels within range A will always result in a very substantial increase in CPUE, regardless of the initial level of effort. This result is consistent with the observation that drastic fishing restrictions such as no-take reserves tend to increase CPUE or survey abundance substantially by a factor of three on average (Lorenzen et al. 1998; Mosquera et al. 2000). Our analysis also shows, however, that the impact of restrictions is highly nonlinear and that more moderate effort reductions will not bring proportional gains in CPUE. Finally, it is noteworthy that all systems studied included fisheries in all regions of effort (A, B, C), with about 30% being lightly, 40% moderately, and 30% highly exploited (excluding the stocked Lao lakes, where effort was very restricted and 68% were lightly exploited). Hence it should not automatically be assumed that tropical inland fisheries are highly exploited, not that effort reduction will necessarily increase yield or CPUE. Whereas aggregated yield and CPUE are unlikely to be the only considerations in the management of multispecies fisheries, both variables are of great interest to key stakeholders. As such, they will be important even where conservation objectives and criteria are the primary focus of management.

The highly nonlinear aggregated CPUE response to effort variation suggests that extreme caution is required when interpreting aggregated CPUE as an indicator of fishing impacts on the exploited community. Unfortunately we do not have sufficient data to provide more than a speculative interpretation of the mechanisms underlying the observed response. Variation in CPUE may arise from variation in stock biomass or in catchability (the effectiveness of fishing), and it is likely that both factors play a part in shaping the aggregated CPUE–effort relationship. While constant catchability and thus proportionality between CPUE and biomass is often assumed in stock assessments, this needs not hold true in all fisheries or over a wide range of effort levels (Hilborn and Walters 1992; Hampton et al. 2005; Polacheck 2006). The steep decline in CPUE at very low fishing effort and biomass removal is very unlikely to reflect a proportional decline in community biomass, particularly given that a further tenfold increase in effort and biomass removal fails to produce any further decline in CPUE. Rather, the initial steep decline in CPUE is likely to reflect "hyperdepletion": declining catchability owing to changes in species and size composition of the fish community and the spatial dynamics of fish and fishers (Hilborn and Walters 1992; Walters 2003; Hampton et al. 2005). By contrast, the relative stability of CPUE over a wide range of higher effort levels may result from maintenance of community biomass through successive replacement of large, slow-growing predators by smaller, faster growing forage fish as effort increases (May et al. 1979; Duplisea et al. 1997; Pauly et al. 1998). However, a degree of "hyperstability" (stability of CPUE despite declining biomass) may also be implicated (Hilborn and Walters 1992). The more or less notable increase in CPUE at intermediate effort levels could reflect an increase in community biomass because of release from predation pressure (a trophic cascade), but could also be generated through a transition in the CPUE–biomass relationship from hyperdepletion at low levels to proportionality or hyperstability at higher effort levels. Further research is required to elucidate the mechanisms underlying the identified, apparently general relationship between effort and aggregated yield or CPUE.

Even though our understanding of mechanisms remains limited and speculative, knowledge of the aggregated CPUE–effort relationship aids in the interpretation of observed temporal trends. Rapid declines in aggregated CPUE during the early development of multispecies fisheries, as observed by Myers and Worm (2003), are to be expected and do not imply that the fisheries are highly exploited. Given the overall CPUE–effort relationship, it also seems unlikely that such declines reflect proportional declines in biomass as implied by Myers and Worm (2003), but we cannot conclusively reject this interpretation. It is clear, however, that substantial changes affecting CPUE do occur at very low effort levels and may well be ecologically important (Walters 2003; Hampton et al. 2005). Stabilization of CPUE following initial decline, again observed by Myers and Worm (2003), is also consistent with relationship identified here and may occur despite large increases in effort and possible change in community structure and ecosystem functioning. Overall, this suggests that aggregated CPUE is not a very useful indicator of community or ecosystem impact. Nonetheless, the mechanisms underlying the consistently observed rapid decline in CPUE at low effort levels require further investigation to assess their ecological significance.

Acknowledgements

This study was supported by the Darwin Initiative, the Department for International Development of the United Kingdom, and the Gordon and Betty Moore Foundation. Guillermo Moisés provided data on the accuracy of Amazon fishers' catch estimates. Comments by Geoff Kirkwood, Carl Walters, Robin Welcomme, Paul van Zwieten, and an anonymous referee improved the manuscript.

References

Allison, E.H., and Ellis, F. 2001. The livelihoods approach and management of small-scale fisheries. Mar. Policy, **25**: 377–388.

Almeida, O.T. 2004. Fisheries management in the Brazilian Amazon. Ph.D. thesis, University of London, UK.

Arthur, R.I. 2004. Adaptive learning and the management of small waterbody fisheries: a case study in Lao PDR. Ph.D. thesis, University of London, UK.

Bayley, P.B. 1988. Accounting for effort when comparing tropical fisheries in lakes, river-floodplains and lagoons. Limnol. Oceanogr. **33**: 963–972.

Bayley, P.B., and Petrere, M. 1989. Amazon fisheries: assessment methods, current status and management options. Can. Spec. Publ. Fish. Aquat. Sci. **106**: 385–398.

Burnham, K.P., and Anderson, D.R. 2002. Model selection and multi-model inference: a practical information-theoretic approach. Springer, New York.

Cahoon, L.S., Riker, C.A., and Moore, T.F. 1993. Recall bias in the national survey of fishing, hunting, and wildlife associated recreation. *In* Proceedings of the Survey Research Methods Section, American Statistical Association. Available from http://www.amstat.org/sections/SRMS/Proceedings/papers/1993_083.pdf [accessed 18 May 2005]. pp. 508–513.

Duplisea, D.E., Kerr, S.R., and Dickie, L.M. 1997. Demersal fish biomass size spectra on the Scotian Shelf, Canada: species replacement at the shelfwide scale. Can. J. Fish. Aquat. Sci. **54**: 1725–1735.

Edwards, A.W.F. 1992. Likelihood. Johns Hopkins University Press, Baltimore, Md.

Garaway, C.J. 1999. Small waterbody fisheries and the potential for community-led enhancement: case studies in Lao PDR. Ph.D. thesis, University of London, UK.

Gulland, J.A. 1983. Fish stock assessment: a manual of basic methods. Wiley, Chichester, UK.

Hampton, J., Sibert, J.R., Kleiber, P., Mazunder, M.N., and Harley, S.J. 2005. Decline in Pacific tuna populations exaggerated? Nature (London), **434**: 38.

Henderson, H.F., and Welcomme, R.L. 1974. The relationship of yield to morpho-edaphic index and number of fishermen in African inland fisheries. CIFA Occas. Pap. 1.

Hilborn, R., and Mangel, M. 1997. The ecological detective: confronting models with data. Princeton University Press, Princeton, N.J.

Hilborn, R., and Walters, C.J. 1992. Quantitative fisheries stock assessment. Chapman and Hall, London, UK.

Johnson, J.B., and Omland, K.S. 2004. Model selection in ecology and evolution. Trends Ecol. Evol. **19**: 101–108.

Jul-Larsen, E., and van Zwieten, P. 2002. African freshwater fisheries: what needs to be managed? NAGA WorldFish Ctr. Quart. **25**(3–4): 35–40.

Kapetsky, J.M. 1984. Coastal lagoon fisheries around the world: some perspectives on fishery yields, and other comparative fishery characteristics. Stud. Rev. GFCM **61**(1): 97–139. FAO, Rome, Italy.

Kirkwood, G.P. 1982. Simple models for multispecies fisheries. *In* Theory and management of tropical fisheries. *Edited by* D. Pauly and G.I. Murphy. International Center for Living Aquatic Resources Management, Manila. pp. 83–97.

Laë, R. 1997. Does overfishing lead to a decrease in catches and yields? An example of two West African coastal lagoons. Fish. Manag. Ecol. **4**: 149–164.

Lorenzen, K., Garaway, C.J., Chamsingh, B., and Warren, T.J. 1998. Effects of access restrictions and stocking on small water body fisheries in Laos. J. Fish Biol. **53**(S1): 345–357.

Mangel, M., Fiksen, O., and Giske, J. 2001. Theoretical and statistical models in natural resource management and research. *In* Modeling in natural resource management: development, interpretation and application. *Edited by* T.M. Schrenk and A.B. Franklin. Island Press, Washington. pp. 57–72.

Marten, G.G., and Polovina, J.J. 1982. A comparative study of fish yields from various tropical ecosystems. *In* Theory and management of tropical fisheries. *Edited by* D. Pauly and G.I. Murphy. International Center for Living Aquatic Resources Management, Manila. pp. 255–283.

May, R.M., Beddington, J.R., Clark, C.W., Holt, S.J., and Laws, R.M. 1979. Management of multispecies fisheries. Science (Washington, D.C.), **205**: 267–277.

Myers, R.A., and Worm, B. 2003. Rapid worldwide depletion of predatory fish communities. Nature (London), **423**: 280–283.

Mosquera, I., Cote, I.M., Jennings, S., and Reynolds, J.D. 2000. Conservation benefits of marine reserves for fish populations. Anim. Conserv. **4**: 321–332.

Nguyen Khoa, S., Lorenzen, K., Garaway, C., Chamsinhg, B., Siebert, D.J., and Randone, M. 2005. Impacts of irrigation on fisheries in rain-fed rice-farming landscapes. J. Appl. Ecol. **42**: 892–900.

Pauly, D. 1979. Theory and management of tropical multispecies stocks: a review, with emphasis on the Southeast Asian demersal fisheries. ICLARM Stud. Rev. 1.

Pauly, D., Christensen, V., Dalsgaard, J., Froese, R., and Torres, F. 1998. Fishing down marine food webs. Science (Washington, D.C.), **279**: 860–863.

Polacheck, T. 2006. Tuna longline catch rates and in the Indian Ocean: Did industrial fishing result in a 90% rapid decline in the abundance of large predatory species? Mar. Pol. doi:10.1016/j.marpol.2005.06.016.

Pope, J.G. 1979. Stock assessment in multi-species fisheries. South China Seas Fisheries Development Coordination Programme. SCS/DEV/79/19. FAO, Rome, Italy.

Ralston, S., and Polovina, J.J. 1982. A multispecies analysis of the commercial deep-sea handline fishery of Hawaii. Fish. Bull. **80**: 435–448.

Rochet, M.J., and Trenkel, V.M. 2003. Which community indicators can measure the impact of fishing? A review and proposals. Can. J. Fish. Aquat. Sci. **60**: 86–99.

SEAFDEC. 2004. Handbook on collecting fishery statistics for inland and coastal fisheries. Southeast Asian Fisheries Development Center, Bangkok, Thailand.

Smith, L.E.D., Nguyen Khoa, S., and Lorenzen, K. 2005. Livelihood functions of inland fisheries: policy implications in developing countries. Water Policy, **7**: 359–383.

Walters, C. 2003. Folly and fantasy in the analysis of spatial catch rate data. Can. J. Fish. Aquat. Sci. **60**: 1433–1436.

Walters, C.J., and Martell, S.J.D. 2004. Fisheries ecology and management. Princeton University Press, Princeton, N.J.

Welcomme, R.L. 1979. Fisheries ecology of floodplain rivers. Longman, London, UK.

Welcomme, R.L. 1985. River fisheries. FAO Fish. Tech. Pap. 262. FAO, Rome, Italy.

Welcomme, R.L. 1999. Review of a model for qualitative evaluation of exploitation levels in multi-species fisheries. Fish. Manag. Ecol. **6**: 1–20.

A length-based multispecies model for evaluating community responses to fishing

Stephen J. Hall, Jeremy S. Collie, Daniel E. Duplisea, Simon Jennings, Mark Bravington, and Jason Link

Abstract: Quantitative ecosystem indicators are needed to fulfill the mandate for ecosystem-based fisheries management. A variety of community metrics could potentially be used, but before reference levels for such indices can be established the sensitivity of candidate indices to fishing and other disturbances must be determined. One approach for obtaining such information is to test candidate indicators with models that mimic real ecosystems and can be manipulated experimentally. Here we construct a size-based multispecies model of a community of fish species that interact by predation. The model was parameterized for 21 fish species to obtain a predation-regulated community. Following an analysis of the sensitivity of the model to parameter uncertainty, we tested the sensitivity of community-level indicators to increasing levels of fishing mortality (*F*). Abundance and biomass spectra were sensitive to fishing mortality, with the slope decreasing with increasing *F*. Species diversity size spectra were also very sensitive to *F*, with diversity in the largest size classes declining rapidly. In contrast, *k*-dominance curves were less sensitive to fishing pressure. Importantly, however, although most community-level metrics showed clear trends in response to fishing, single-species declines in spawning stock biomass were the most sensitive indicators of fishing effects.

Résumé : Des indicateurs écosystémiques quantitatifs sont nécessaires afin de remplir le mandat de la gestion des pêches basée sur les écosystèmes. On peut utiliser une variété de métriques de la communauté, mais avant que les niveaux de référence de ces indices puissent être établis, il faut déterminer la sensibilité des indices à la pêche et aux autres perturbations. Une façon d'obtenir cette information est de tester les indicateurs considérés avec des modèles qui reproduisent de vrais écosystèmes et qui peuvent être manipulés expérimentalement. Nous construisons ici un modèle multispécifique structuré d'après la taille d'une communauté de poissons qui interagissent par prédation. Nous avons déterminé les paramètres pour 21 espèces de poissons de manière à obtenir une communauté contrôlée par la prédation. Après une analyse de sensibilité du modèle à l'incertitudes des paramètres, nous avons évalué la sensibilité des indicateurs de type communautaire à des niveaux croissants de mortalité due à la pêche (*F*). Les spectres d'abondance et de biomasse sont sensibles à la mortalité due à la pêche et leur pente diminue en fonction inverse de *F*. Les spectres de diversité spécifique en fonction de la taille sont aussi très sensibles à *F* et la diversité dans les classes de tailles plus grandes décline rapidement. En revanche, les courbes de dominance *k* sont moins sensibles à la pression de pêche. De façon importante, cependant, alors que la plupart des métriques de type communautaire montrent des tendances claires en réaction à la pêche, les diminutions de la biomasse du stock des reproducteurs d'espèces individuelles sont les indicateurs les plus sensibles aux effets de la pêche.

[Traduit par la Rédaction]

Introduction

There is increasing recognition of the need for ecosystem considerations in fisheries management (Food and Agricultural Organisation of the United Nations 2001), but progress with defining and setting management objectives has been slow. Reference points provide measurable criteria for determining whether quantitative management objectives are met. For example, to ensure the long-term sustainability of a target stock, a short-term management goal may be to minimize the risk that it will fall below some specified biomass level (a limit reference point), while a simultaneous longer-

Received 4 January 2006. Accepted 24 January 2006. Published on the NRC Research Press Web site at http://cjfas.nrc.ca on 9 May 2006.
J19088

S.J. Hall.[1] WorldFish Center, P.O. Box 500 GPO, 10670 Penang, Malaysia.
J.S. Collie. University of Rhode Island, Graduate School of Oceanography, Narragansett, RI 02882, USA.
D.E. Duplisea. Division of Fish and Marine Mammals, Maurice Lamontagne Institute, Fisheries and Oceans Canada, 850 route de la Mer, Mont-Joli, QC G5H 3Z4, Canada.
S. Jennings and M. Bravington.[2] CEFAS, Lowestoft Laboratory, Lowestoft, NR33 0HT, United Kingdom.
J. Link. NMFS/NEFSC, Food Web Dynamics Program, 166 Water Street, Woods Hole, MA 02543, USA.

[1] Corresponding author (e-mail: s.hall@cgiar.org).

[2] Present address: CSIRO (CMIS), P.O. Box 1538, Castray Esplanade, Hobart, TAS 7001, Australia.

Can. J. Fish. Aquat. Sci. **63**: 1344–1359 (2006) doi:10.1139/F06-039

term goal might be the rebuilding of the stock to a target reference point (Sissenwine and Shepherd 1987). The benefits of using reference points for managing target stocks is now widely recognized and some efforts have been made to use the same approach for some nontarget species of conservation interest (Hall and Mainprize 2004).

A potentially useful extension of the above approach would be the development of quantitative management objectives using reference point metrics, which capture valued aspects of whole communities or ecosystems. To date, however, although there have been efforts to understand the sensitivity to trophic interactions of single-species metrics for which reference points might be set (Collie and Gislason 2001), multispecies or ecosystem level metrics are still being proposed and evaluated (Rochet and Trenkel 2003).

Although the ideal properties of metrics for which reference points might be selected are well known, the development of a sound body of theory that would allow us to understand the mechanisms controlling the sensitivity and behaviour of candidate community- or ecosystem-level reference points is required (Rochet and Trenkel 2003). Such understanding is the first step towards identifying appropriate metrics because underpinning theory would allow rigorous evaluation of the alternatives. As it did with the development of single-species reference points, we expect the construction of defensible mathematical models to provide a basis for development and testing of multispecies and ecosystem metrics. Using a modelling approach we are already beginning to appreciate, for example, how trophic interactions might determine community size distributions and how fishing might modify them (Rice and Gislason 1996; Duplisea and Bravington 1999; Bianchi et al. 2000). Recent analyses with size-structured models indicate, for example, that the slope of size spectra becomes steeper if the predator–prey size ratio is smaller (predators can eat larger prey) and (or) predator growth efficiency is lower (Benoit and Rochet 2004; Shin and Cury 2004). Increased fishing mortality also results in a steeper slope and downward curvature at the largest sizes.

With the exception of biomass size distributions, however, approaches remain to a large extent phenomenological — we describe changes (or lack of them) in community attributes such as species diversity, but the underlying causes and consequences of these changes are largely unknown. At this stage, therefore, most metrics of community structure do not have practical value for assessing the significance of fisheries effects and deciding on management actions.

As a general rule, species that have larger body size, mature later, and have lower rates of potential population increase experience larger population declines in response to fishing, even when differences in fishing mortality rate are accounted for (Jennings et al. 1999). Such differences imply that different life-history characteristics may explain underlying responses to fishing at both the individual species level and the community level (Jennings et al. 1999). If we are to fully develop an ecosystem level theory of fishing, the life-history attributes of component species seem most likely to be at its core. In an effort to help further develop the necessary theory we have developed a size-structured multispecies model of a fish community with a realistic distribution of life-history attributes. The purpose of this paper is to describe that model, examine its sensitivity to key model parameters, and present some preliminary results examining the utility of various community-level metrics of fishing effects.

Model assumptions and equations

Our approach differs from that reported from most other size-based models in that it maintains both the identity of the species in the system and the size structure of the individual populations. To maintain a level of realism and to help ensure internal consistency, we have chosen to develop a model that is loosely based on a single real fish community and have selected the Georges Bank fish community for this purpose because of the large body of information available on the fish species and their dynamics in this region. Despite this specificity, however, our model should be considered as strategic in focus and is directed explicitly at understanding the dynamics of the emergent properties of fish communities rather than providing quantitative predictions for species abundances in any particular system. This approach builds on the results obtained with entirely abstract size-structured models (Benoit and Rochet 2004; Shin and Cury 2004), while ensuring that the model can be parameterized for a real fish community. Although the model has been parameterized for Georges Bank in an effort to ground our parameterization in a defensible manner, we would not necessarily expect the results to mimic either the relative abundances of species or the temporal trends that have been observed there.

A food web matrix defines the feeding relationships between the 21 species represented in the model system (Table 1). Building on previous work by Murawski and Idoine (1992) and Duplisea and Bravington (1999), the model follows length cohorts of individuals from each species throughout their life. The baseline or standard model includes fifteen 10 cm length classes, though the model is programmed to allow for variable numbers and widths of size classes. All key parameters and state variables are listed in Table 2. For convenience, we have named the model LeMANS (length-based multispecies analysis by numerical simulation). In the following sections we begin by describing how each of the key biological processes has been modelled before going on to describe the sequence in which they were implemented.

Growth

We assume that fish grow continuously throughout their lives according to the von Bertalanffy growth equation:

$$(1) \qquad L_{t,i} = L_{\infty,i}(1 - e^{-k_i(t-t_0)})$$

where both $L_{\infty,i}$, the asymptotic length, and k_i, the instantaneous growth rate, are estimated empirically for each species i (Penttila et al. 1989).

For convenience, we represent growth in the model as a deterministic process, parameterised from field data, which is not affected by the abundance of prey resources. Thus, there is no feedback between variations in predation mortality (and hence predator food intake), resulting from time-varying prey abundances, and predator growth. In addition, the formulation does not account for the increased variance

Table 1. The food web matrix for the 21 species represented in the model.

		Predator species																				
Prey species	Scientific name	1	2	3	4	5	6	7	8	9	10	11	12	13	14	15	16	17	18	19	20	21
1. Sand lance	*Ammodytes americanus*	0	1	1	1	1	1	1	1	1	1	1	1	1	1	1	1	1	1	1	1	1
2. Longhorn sculpin	*Myoxocephalus octdecemspinosus*	0	1	0	0	0	0	0	0	0	1	0	0	0	0	1	0	1	1	0	0	0
3. Atlantic herring	*Clupea harengus*	0	1	0	0	0	0	0	0	0	1	1	1	1	1	1	1	1	1	1	0	1
4. Witch flounder	*Glyptocephalus cynoglossus*	0	0	0	0	0	1	0	0	0	0	0	0	0	0	1	0	0	1	0	0	0
5. Windowpane	*Scophthalmus aquosus*	0	0	0	0	1	0	0	0	0	0	0	0	0	0	1	0	0	1	0	0	0
6. Winter flounder	*Pseudopleurinectes americanus*	0	0	0	0	0	0	0	0	0	0	0	0	0	0	1	0	0	1	0	0	0
7.Atlantic mackerel	*Scomber scombrus*	0	0	0	0	0	0	0	0	0	1	1	1	0	0	1	1	1	1	1	0	1
8. Fourspot flounder	*Paralichthys oblongus*	0	0	0	0	0	0	0	0	0	0	0	0	0	0	1	0	0	1	0	0	0
9. Yellowtail flounder	*Limanda ferruginae*	0	0	0	0	0	0	0	0	0	0	0	0	0	0	1	0	0	1	0	0	0
10. Little skate	*Leucoraja erinacea*	0	0	0	0	0	0	0	0	0	0	0	0	0	0	1	0	0	1	0	0	0
11. Red hake	*Urophycis chuss*	0	0	0	0	1	0	0	0	0	1	1	0	1	1	1	0	1	1	0	1	1
12. Silver hake	*Merlucius bilinearis*	0	0	0	0	1	0	0	1	0	1	1	1	1	1	1	0	1	1	1	1	1
13. Sea raven	*Hemitripterus americanus*	0	0	0	0	0	0	0	0	0	1	0	0	0	0	0	0	1	1	0	0	0
14. Haddock	*Melanogrammus aeglefinus*	0	0	0	0	0	0	0	0	0	1	0	0	1	1	1	0	1	1	0	0	0
15. Spiny dogfish	*Squalus acanthias*	0	0	0	0	0	0	0	0	0	0	0	0	0	0	1	0	0	1	0	0	0
16. Pollock	*Pollachius virens*	0	0	0	0	0	0	0	0	0	1	0	0	0	1	1	1	1	1	0	0	1
17. Winter skate	*Raja ocellata*	0	0	0	0	0	0	0	0	0	0	0	0	0	0	1	0	0	0	0	0	0
18. Goosefish	*Lophius americanus*	0	0	0	0	0	0	0	0	0	0	0	0	0	0	0	0	0	1	0	0	0
19. White hake	*Urophycis tenuis*	0	0	0	0	1	0	0	0	0	1	1	0	1	1	1	0	1	1	1	1	1
20. Summer flounder	*Paralichthys dentatus*	0	0	0	0	0	1	0	0	0	0	0	0	0	0	1	0	0	1	0	0	0
21. Atlantic cod	*Gadus morhua*	0	0	0	0	0	0	0	0	0	1	0	0	1	1	1	0	1	1	0	0	1
No. of prey species		0	3	1	1	5	3	1	2	1	11	6	4	7	8	19	4	11	20	5	4	8
No. of predator species		20	5	12	3	3	2	9	2	2	2	10	13	3	6	2	7	1	1	11	3	7

Note: In the matrix, which predators eat which prey is denoted by the number 1. The matrix is derived from food habits data in Link (2002).

Table 2. State variables and key model parameters.

Symbol		Description	Units
State variables			
$N_{i,j}$		Number of individuals of species *i* in size class *j*	individuals
S_i		Spawning stock biomass of species *i*	tonnes
R_i		The number of recruits of species *i* in a given year	individuals
t		Time	t
Parameters			
a_i	*	The intercept parameter of the length–weight relationship for species *i*	—
b_i	*	The slope parameter of the length–weight relationship for species *i*	—
$L_{\infty,i}$	*	Asymptotic length parameter of the von Bertalanffy growth equation	cm
k_i	*	Growth parameter of the von Bertalanffy growth equation	t^{-1}
$\varphi_{i,j}$		The proportion of species *i* in size class *j* that move to the next size class in a single time step	—
α_i		Productivity parameter of the Ricker stock–recruitment equation for species *i*	—
β_i		Density dependence parameter of the Ricker stock-recruitment equation for species *i*	tonne^{-1}
$S_{\max,i}$	*	The maximum observed spawning stock biomass of species *i*	tonnes
κ_i	*	Curvature parameter for the maturity ogive of species *i*	—
L_{M50}	*	The length at which 50% of species *i* are mature	cm
$\bar{\omega}_{i,j}$		The proportion of species *i* in size class *j* that are mature	—
$F_{i,j}$		Instantaneous rate of fishing mortality on species *i* in size class *j*	t^{-1}
ϕ_i	*	A binary variable indicating whether species *i* is fished	
$F_{\max}$		The maximum annual fishing mortality rate for a fully recruited fish	t^{-1}
η		Steepness parameter for the fishing selectivity ogive	
$L_{\varphi 50}$		The length at which 50% selection by the fishery occurs	cm
$M1_{i,j}$		Natural (nonmodelled) mortality for species *i* in size class *j*	t^{-1}
Ψ, υ		Parameters of the beta distribution for $M1$	—
$M2_{i,j}$		Predation mortality for species *i* in size class *j*	t^{-1}
$\tau_{m,i}$	*	The preference for prey species *m* by predator species *i*	—
$\zeta_{n,j}$		Size preference for prey of size *n* by predator of size *j*	—
$\nu_{i,j,m,n}$		The relative preference (suitability) for predator *i* of size *j* of prey *m* of size *n*	—
$I_{i,j}$		The ration (ingestion rate) that must be consumed by species *i* in size class *j* to account for modeled growth in a given time step	tonnes · t^{-1}
Ge_j		The growth efficiency (proportion of food consumed that is converted to body mass) of fish in size class *j*	—

Note: Asterisks denote species-specific input parameters, estimated from empirical data and input directly to the model.

in body size of a cohort as it gets older. The assumption of growth rates independent of feeding levels is consistent with the multispecies virtual population analysis (MSVPA) equations (Magnusson 1995) and with a lack of evidence for food-dependent growth rates in temperate fish communities (Collie 2001). However, this assumption may not hold for boreal communities, where there is some evidence of food-limited growth (Livingston and Tjelmeland 2000).

Because the von Bertalanffy equation provides a continuous description of growth but our model deals with discrete size classes, it is necessary to discretize the growth function. This discretization was achieved in the following way. For each species – length class combination, the time taken for an individual to grow from the lower to the upper limit of length class *j* was calculated from the following equation (Hilborn and Walters 1992, p. 428):

$$t_{i,j} = \frac{1}{k_i}\left[\log\left(1 - \frac{L_{\mathrm{lower}}}{L_\infty}\right) - \log\left(1 - \frac{L_{\mathrm{upper}}}{L_\infty}\right)\right]$$

This equation can be simplified to

$$(2) \qquad t_{i,j} = \frac{1}{k_i}\log\left(\frac{L_\infty - L_{\mathrm{lower}}}{L_\infty - L_{\mathrm{upper}}}\right)$$

Assuming that individuals are evenly distributed across a size class, the proportion that leave the size class solely because of growth in any given time interval is then given by $\varphi_{i,j} = 1/t_{i,j}$. However, because time steps in the model are arbitrary and, for computational convenience, we wish to avoid the possibility that individuals could skip more than one size class in a given time step, we set the time step so that, in the absence of mortality, all individuals in the fastest-growing species – length class combination ($t_{\min}$) would always reach the next length class in a single time step by rescaling the times such that $\varphi_{i,j} = t_{\min}/t_{i,j}$.

Because growth in length is entirely deterministic with no feedback from the abundance of prey resources, this matrix of proportions had only to be calculated at the beginning of a model run. For the parameter values used here, this led to

Table 3. Species-specific parameters used in base model run, as defined in Table 2.

Species	Scientific name	a	b	k	L_∞	$L_{50\%}$	κ	$S_{\max}$	τ
Sand lance	*Ammodytes americanus*	0.003	3.211	0.500	24.0	12.0	0.587	13.1	0
Longhorn sculpin	*Myoxocephalus octdecemspinosus*	0.010	3.078	0.720	30.0	15.0	0.587	10.0	0
Atlantic herring	*Clupea harengus*	0.010	2.990	0.280	35.0	25.0	0.587	165.0	1
Witch flounder	*Glyptocephalus cynoglossus*	0.003	3.428	0.230	39.3	20.0	0.392	28.0	1
Windowpane	*Scophthalmus aquosus*	0.011	3.000	0.242	41.0	22.0	2.43	29.0	1
Winter flounder	*Pseudopleurinectes americanus*	0.011	3.138	0.283	45.5	25.0	0.587	21.0	1
Atlantic mackerel	*Scomber scombrus*	0.007	3.319	0.243	46.1	30.0	0.641	183.0	1
Fourspot flounder	*Paralichthys oblongus*	0.008	3.000	0.335	50.0	25.0	0.306	29.0	1
Yellowtail flounder	*Limanda ferruginae*	0.008	3.129	0.335	50.0	23.0	0.487	52.0	1
Little skate	*Raja erinacea*	0.005	3.141	0.352	53.0	50.0	0.587	15.0	1
Red hake	*Urophycis chuss*	0.005	3.222	0.190	60.2	25.0	0.507	16.0	1
Silver hake	*Merlucius bilinearis*	0.007	3.050	0.180	65.4	23.0	0.587	465.0	1
Sea raven	*Hemitripterus americanus*	0.019	3.100	0.720	68.0	25.0	0.587	10.0	0
Haddock	*Melanogrammus aeglefinus*	0.010	3.068	0.376	73.8	28.0	0.375	421.0	1
Spiny dogfish	*Squalus acanthias*	0.003	3.122	0.100	100.0	80.0	0.587	136.0	1
Pollock	*Pollachius virens*	0.010	3.028	0.100	111.0	40.0	0.154	200.0	1
Winter skate	*Raja ocellata*	0.004	3.317	0.144	114.1	85.0	0.587	30.0	1
Goosefish	*Lophius americanus*	0.020	2.897	0.108	126.0	49.0	0.587	10.0	1
White hake	*Urophycis tenuis*	0.006	3.220	0.106	136.0	34.0	0.137	16.0	1
Summer flounder	*Paralichthys dentatus*	0.007	3.278	0.173	137.0	26.0	0.306	29.0	1
Atlantic cod	*Gadus morhua*	0.009	3.052	0.120	148.0	40.0	0.149	72.1	1

Note: Species ordered by body size (L_∞). Data sources for direct input parameters: a and b, US National Marine Fisheries Service databases (J.S. Link, personal communication); k and L_∞, Penttila et al. (1989); $L_{50\%}$, O'Brien et al. (1993); $S_{\max}$, Myers et al. (1995); κ, O'Brien et al. (1993); τ, US National Marine Fisheries Service food-habits database (J.S. Link, personal communication).

a time step in the standard model that was equivalent to approximately 80 days.

All conversions between length (cm) and weight (g) that were required by the model were calculated with species-specific values for a and b, empirically estimated parameters of the standard length–weight relationship $W = aL^b$, obtained from the US National Marine Fisheries Service (Table 3).

Recruitment

Perhaps the most difficult aspect of any model of fish population dynamics is the choice and parameterization of the stock–recruitment relationship. This difficulty is particularly acute when a relationship is required for many species. For this model, recruitment was described by the Ricker stock–recruitment equation:

$$(3)\qquad R_i = \alpha_i S_i e^{-\beta_i S_i}$$

where R_i is recruitment, S_i is spawning stock biomass, and α_i and β_i are species-specific parameters. For some of the species in our model community, no direct study of stock and recruitment has been undertaken, whereas for others a variety of estimates are available. Our approach to this problem was to use estimates of the two parameters of the Ricker equation for 65 of the stocks collated by Myers et al. (1995) for which recruitment was estimated at age 1. Both parameters were scaled to common recruit and spawning stock size units (individuals × 10^6 and tonnes × 10^3, respectively) and the relationship between α and the parameters of the von Bertalanffy growth equation were examined to determine whether there was any empirical basis for a generalized relationship between life-history attributes describing individual growth and spawners per recruit at low population size (Myers et al. 1999). Our analysis showed that there was a significant negative linear relationship between log α and log L_∞ and a positive linear relationship with k. Of these two, the relationship with L_∞ fitted best ($\ln(\alpha) = 11 - 2.30\ln(L_\infty)$, $r^2 = 0.33$, $P < 0.001$; Fig. 1a). This regression equation was used to estimate α values from empirical estimates of L_∞ for all species in the model.

In contrast to Ricker's α, we found no clear relationship between Ricker's β and the von Bertalanffy growth parameters. This result is not surprising, however, because β, the term reflecting density dependence in recruitment, is highly sensitive to the existence of recruitment data for large stock sizes. Unfortunately, the presence of such data differs between stocks, depending on whether they were assessed early or late in the history of exploitation. The question arises, therefore, of how one can obtain estimates of β for modeling purposes?

The approach that we have adopted is to exploit the fact that $S_{r\_\max} = 1/\beta$. It follows from this equation that there should be a linear relationship between the stock size (S) at which recruitment is maximized ($S_{r\_\max}$) and β when plotted on logarithmic scales. Because β has units of $1/S$, this linearity with β should hold for other metrics related to stock size. To test this assumption we extracted maximum observed spawning stock size ($S_{\max}$) for each of the time series data in Myers et al. (1995), where recruitment was estimated at age 1, and plotted this against the estimate of β (Fig. 1b). As one would expect, the majority of data fit our expectation extremely well. By omitting four outliers, we obtain the relationship $\ln(\beta) = 0.1513 - 0.9484\ln(S_{\max})$, $r^2 = 0.8476$, $P < 0.001$.

It is perhaps important to stress at this point that our purpose here is to obtain a reasonable spread of β values that are broadly consistent with the life-history characteristics of

Fig. 1. (*a*) The relationship between Ricker stock–recruitment parameter α and the von Bertalanffy growth parameter L_∞. (*b*) The relationship between maximum observed stock size $S_{\max}$ and β. Data are for 65 stocks described in Myers et al. (1995).

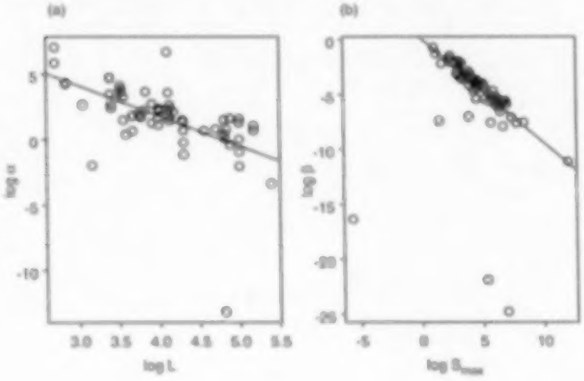

the modeled species. Therefore, using the above fit, maximum observed stock size for each fish species in the Georges Bank time series was used to obtain the relative size of β for the species in our model. These estimates were then scaled upward or downward by a constant amount (for all stocks) to tune the model to obtain reasonable equilibrium population sizes in the absence of fishing. New recruits were introduced into the model into the smallest modeled size class during a single time step each year, which corresponded to an approximately 80-day period.

One difficulty of calculating *S* when discrete size classes are used is that not all individuals in the class will be mature, unless size at first maturity corresponds with the lower bound of a size class. To overcome this difficulty, the proportion of mature individuals ($\bar{\omega}$) for each species – size class combination was calculated with maturity ogives. The ogive can be described by a logistic model such that

$$(4)\qquad \bar{\omega}_{i,j} = \frac{1}{1 + e^{-\kappa_i (L_{i,j} - L_{M50,i})}}$$

where L_{M50} is the length at which 50% of individuals are mature and κ is a steepness parameter. Estimates of κ and L_{M50} for Georges Bank species were obtained from O'Brien et al. (1993). For species for which estimates were unavailable, we used the mean κ for the species for which estimates were available (κ = 0.587) and the L_{M50} value of the most closely related species. For this analysis no distinction between males and females was made and only data on maturity schedules for females were used to parameterize the model.

Fishing mortality

The instantaneous rate of fishing mortality was modelled according to the following equation:

$$(5)\qquad F_{i,j} = \frac{\phi_i F_{\max}}{1 + e^{-\eta(L - L_{F50})}}$$

where $F_{i,j}$ represents the fishing mortality on species *i* of size class *j*, ϕ_i is a binary variable indicating whether species *i* is fished, $F_{\max}$ is the maximum annual fishing mortality rate for a fully recruited fish, η is a steepness parameter, and L_{F50} is the size at 50% selection by the fishery. For all model runs described here, η was set at 0.25 and L_{F50} was set at 25 cm.

Residual natural mortality (*M*1)

Natural mortality from causes other than predation by the modeled species is known as residual natural mortality (*M*1). The instantaneous rate, *M*1, was described by a U-shaped function with rapidly decreasing mortality during the early period of life, a fairly constant mortality for middle-sized fish, and increasing mortality in very large fish, because of increasing senescence, disease, etc. Although we have no data to support such a functional form, it seems intuitively obvious that it must occur at the limit in unexploited fish populations to prevent the buildup of very large fish (Quinn and Collie 2005). A suitably shaped curve was provided by the beta function

$$(6)\qquad M1_j = \frac{1}{B(\psi, \upsilon)} \left(\frac{L_j}{L_{\max}}\right)^{\psi - 1} \left(1 - \frac{L_j}{L_{\max}}\right)^{\upsilon - 1}$$

where $0 < \psi < 1$, $0 < \upsilon < 1$, L_j is the midlength of size class *j*, and $L_{\max}$ is the maximum size of fish observed in the model. The shape of this function is shown for $\psi = 0.8$, $\upsilon = 0.4$ (Fig. 2*a*), which provides a suitable description of our intuition about natural mortality. Initial runs of the model suggested that the parameterization adopted was reasonable.

Predation mortality (*M*2)

Using the von Bertalanffy growth equation we can calculate the growth increment for an average-sized individual (*L*) in each size class during a given time step from the following equation:

$$\Delta L = (L_\infty - L)(1 - e^{-K\Delta t})$$

Converting this increment to weight and dividing by a conversion efficiency will provide an estimate of the ration, $I_{i,j}$, that must be consumed by that predator – size class combination to account for the growth. Growth efficiency (Ge), the efficiency with which consumed food was converted to body mass, was estimated by

$$(7)\qquad \mathrm{Ge}_{i,j} = \left(1 - \left(\frac{W_{i,j}}{W_{i,\infty}}\right)^{0.11}\right) \times 0.5$$

where $\mathrm{Ge}_{i,j}$ is the growth efficiency of species *i* in size class *j*, $W_{i,j}$ is the weight at the midpoint of size class *j*, and W_∞ is the weight at L_∞. The above relationship exploits the observed allometric relationship between production, ingestion, and energy expenditure, where production = $\pi W^{0.75} - \pi' W^{0.86}$ (Jobling 1994), along with the fact that when maximum size is reached all energy is used for metabolism (i.e., there is no growth). This approach gave growth efficiencies by size ranging from 0.35 for very small individuals of a species and close to zero for the largest fish.

For prey species *m* in size class *n*, the predation mortality is then given by

Fig. 2. (*a*) Residual natural mortality (*M*1) as a function of body size (length). (*b*) Relative food preference, modeled as a function of prey–predator weight ratio, using a lognormal distribution function with μ = –3.5, σ = 1.

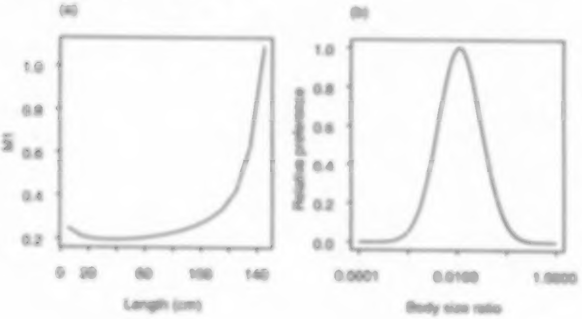

$$M2_{m,n} = \sum_{i}\sum_{j} I_{i,j}N_{i,j}\frac{\nu_{i,j,m,n}}{\sum_{k}\sum_{l}\nu_{i,j,k,l}W_{k,l}N_{k,l} + \text{other}} \tag{8}$$

where *W*, *N*, and *I* are weight, abundance, and ration, respectively, for a given species – size class combination, "other" is food available from prey (other food) that is not explicitly represented in the model, and $\nu_{i,j,m,n}$ is the relative preference (suitability) for predator *i* of size *j* of prey *m* of size *n*. Equation 8 corresponds to a Holling type-II functional response, as implemented in MSVPA (Magnusson 1995). Although total feeding rate is constant in the model, predator feeding rate on a particular prey saturates at high prey abundance such that *M*2 is a decreasing function of prey abundance. The suitability parameter, ν, allows the total predator ration to be apportioned among prey species. Suitability is defined as

$$\nu_{i,j,m,n} = \zeta_{n,j}\,\tau_{m,i}$$

where the parameter $\zeta_{n,j}$ is the preference for a prey of size *n* by predator of size *j*, and $\tau_{m,i}$ is the vulnerability of prey species *m* to predator species *i*.

The size-preference parameter, ζ, was calculated as a function of the ratio of prey-to-predator body weight at the midpoint in a length class (or at the midpoint between the lower bound of the largest length class for a species and L_∞). This preference function was modelled with a lognormal distribution using initial parameter values of μ = –3.5, σ = 1 (Fig. 2*b*). This parameterization gives a maximal preference for prey that is approximately 1/33rd of the weight of the predator (Hahm and Langton 1984) and is broadly consistent with recent observations (Scharf et al. 2000).

Values for τ were set at either 0 or 1, indicating whether a particular species was known to eat a given prey. By varying the matrix of τ values, the food web topology can be altered. The suitability values (ν) for all prey size-class combinations were normalized for each predator size-class combination such that they summed to 1 (Magnusson 1995).

Other food

With the above formulation, it is the contribution by other (nonmodelled) food that scales *M*2 values to sensible levels. In the future, it may be possible to back-calculate to determine what amount of other food would be required to satisfy the system, but for now, other food was used as a tuning parameter to produce a stable system with all species persisting and *M*2 levels broadly comparable with the annual average predation mortalities estimated by Tsou and Collie (2001) for selected Georges Bank species. Annual average *M*2 values ranged from a maximum of 1.63 for silver hake (*Merluccius bilinearis*) to a minimum of 0.03 for spiny dogfish (*Squalus acanthias*).

Implementation sequence

Using the formulations described above, the following implementation sequence was used within each time step. First, if it was the correct time step within the year, recruits were added to the smallest size class. Mortality was then imposed on all size classes, after which the growth function was applied to move the appropriate proportion of individuals to the next size class.

The general sequence and form for the model's governing equations to update abundance *N* for each species *i* in size class *j* at time *t* can be written as follows:

(*i*) introduce recruits: $N'_{i,1,t} = N_{i,1,t-1} + R_{i,t}$

(*ii*) impose mortality: $N''_{i,j,t} = N'_{i,j,t}e^{-(F_{i,j,t}+M1_{i,j,t}+M2_{i,j,t})}$

(*iii*) impose growth: $N_{i,j,t} = N''_{i,j,t}(1 - \phi_{i,j}) + N''_{i,j-1,t}(\phi_{i,j-1})$

Model runs

As noted above, the model was tuned by adjusting the "other food" parameter to obtain reasonable *M*2 values. We then ran the model until it reached equilibrium and used the equilibrium abundances as the initial values for all subsequent model runs. Runs of the standard model with 10 cm size class intervals were for 114 time steps, the equivalent of approximately 25 years. To test for discretization error, we also constructed a second version of the model with thirty 5 cm length intervals, which we ran for 228 time steps, again corresponding to an approximately 25-year period. As with the standard model, this second model was tuned by altering the other food parameter to obtain quantitatively similar equilibrium behaviour under a no-fishing scenario. The behaviour of this second model in response to changes in fishing mortality was then compared with that of the standard model.

As a further test of sensitivity, we also examined the effects of uncertainty in the standard model to five of the key input parameters: the stock–recruitment parameters α and β, the size-preference parameters μ and σ, and growth efficiency, Ge. Each of these five parameters was either increased or decreased by 10% of the base level for all species at the same time. With two levels of five parameters, the full factorial design had 32 sensitivity runs. Each sensitivity trial was run for 114 time steps to reach equilibrium. The response variables were the numbers and predation mortality for each species and a set of community indices proposed by Rochet and Trenkel (2003). We then fit linear models to estimate the first-order effect of each parameter on each response variable. The sensitivities were plotted, relative to the mean of the response variable, with the S-PLUS function plot.design (Insightful 2001).

To examine the response of alternative descriptors of community structure to fishing pressure, we undertook 10 runs

Table 4. Summary of the effects of size-class width on a range of univariate community metrics.

Community metric	$F = 0$	$F = 0.4$	$F = 0.8$
Total number of individuals	–1.2	3.2	6.6
Total community biomass	–5.1	–8.0	–14.3
Mean weight of an individual	–3.9	–10.9	–19.7
Mean length of an individual	–1.2	–0.1	–0.3
Mean L_∞ of an individual	2.7	2.3	1.9
Mean L_{M50} of an individual	0.3	1.7	0.5
Community diversity (Hill's N1)	0.5	–8.9	–2.8
Proportion of piscivores[a]	3.5	–0.6	0.3
Proportion of noncommercial species	12.1	40.6	51.1

Note: The table entries show the percentage change resulting from the use of 30 cm × 5 cm size classes rather than the 15 cm × 10 cm size classes used in the model key runs. Community metrics were chosen from the list proposed by Rochet and Trenkel (2003).

[a] Piscivores have been arbitrarily defined as species with more than six prey species.

of the standard model using the parameter set shown (Table 3). All direct input parameters were held constant with the exception of fishing mortality, which ranged from 0 to 1 at 0.1 intervals.

Results

Sensitivity analysis

Comparison of the output from our standard model (10 cm) with that from the 5 cm interval model revealed very similar behaviour. For example, the correlation coefficients for the logarithm of total abundances and annualized $M2$ values for each species at year 25 were both 0.99 in the absence of fishing. When a fishing mortality of 0.8 was imposed, similarly high correlations were also obtained (r^2 = 0.98 and 0.99 for log N and log $M2$, respectively). These data indicate that the numbers and mortality calculations in our model are quite insensitive to the choice of size interval. A comparison of the relative change in a variety of other univariate community metrics for the two different models also showed a relative insensitivity to size-class interval in the absence of fishing (Table 4). The only difference between the two models that was greater than 10% at $F = 0$ was the proportion of noncommercial species. However, because this proportion was low (~0.1) in the community, normalizing by this small fraction amplified the differences between models.

With increased fishing mortality, the community structure shifted to the smaller size classes where growth is more rapid through the size-class boundaries, which lead to some divergence between the outputs of the two models for mean weights and other weight-based indices (Table 4). Numbers at length were quite insensitive to the choice of size interval, but at low abundance, small differences were amplified by the power relationship between weight and length. Although the choice of size interval can impact the absolute values of weight-based community metrics, our primary concern here is the impact of these choices on our conclusions about the effects of fishing. In this respect, we are confident of our findings because the trends in community metrics with respect to fishing remained the same as those shown later, regardless of the choice of size interval.

To illustrate the results of the sensitivity analyses for the key model parameters, percentage deviations from the mean for a series of community response variables were plotted (Fig. 3). The largest deviations, of the order of ±5%–8%, were for total numbers and total biomass and were in response to variations in β, the density-dependence parameter of the stock–recruitment relationship. Variations of ±5% were also observed in these same two variables in response to changes in the stock–recruitment parameter α. As one would expect, a low level of β results in an increase in numbers and biomass, whereas a lower level of α results in a decrease. For the remaining variables, deviations from the mean response were less than 1% with a varying pattern of relative sensitivity to the different parameters. In general, sensitivity was greatest to μ, the logarithmic ratio of prey weight to predator weight, and Ge, the growth efficiency. Taken overall, the results indicate that our model was not unduly sensitive to uncertainty in model parameters.

Species population trajectories

As one might expect, the spawning stock biomass of all species subject to fishing mortality declined under fishing (Fig. 4). After 25 years of fishing at $F = 0.8$, seven of the modeled populations had become extinct, although six of these persisted and were approaching positive equilibrium abundances with $F = 0.4$ over the same time period. In contrast, sand lance (*Ammodytes americanus*), longhorn sculpin (*Myoxocephalus octdecemspinosus*), and sea raven (*Hemitripterus americanus*) increased in biomass, owing to the release from predation caused by the declines in predators resulting from fishing. Of these latter species, the largest response was shown by sand lance, a feature that is to be expected because this species serves as prey for 20 of the 21 modelled species compared with 5 and 3 for the other two species.

In contrast to the pattern for spawning stock biomass, trends in numerical abundance showed a more variable pattern with fishing, leading to an increase in numerical abundance for some of the exploited species (Figs. 5 and 6). At intermediate levels of fishing, small increases occurred for four relatively small-bodied species with only two or three predators (witch flounder, *Glyptocephalus cynoglossus*; windowpane, *Scophthalmus aquosus*; winter flounder, *Pseudopleurinectes americanus*; and yellowtail flounder, *Limanda ferruginae*) (Fig. 5). Increases were also observed in mackerel (*Scomber scombrus*, which had nine predators) and the

Fig. 3. Sensitivity of community indices to 10% increases and decreases in the value of key model parameters (stock–recruitment parameters, α and β; size-preference parameters, μ and σ; growth efficiency, Ge). In each subplot, the vertical lines indicate the sensitivity to each parameter, relative to the overall mean level, indicated by the horizontal line. H indicates a 10% increase and L indicates a 10% decrease in each parameter. Noncommercial species, noncomm. spp.

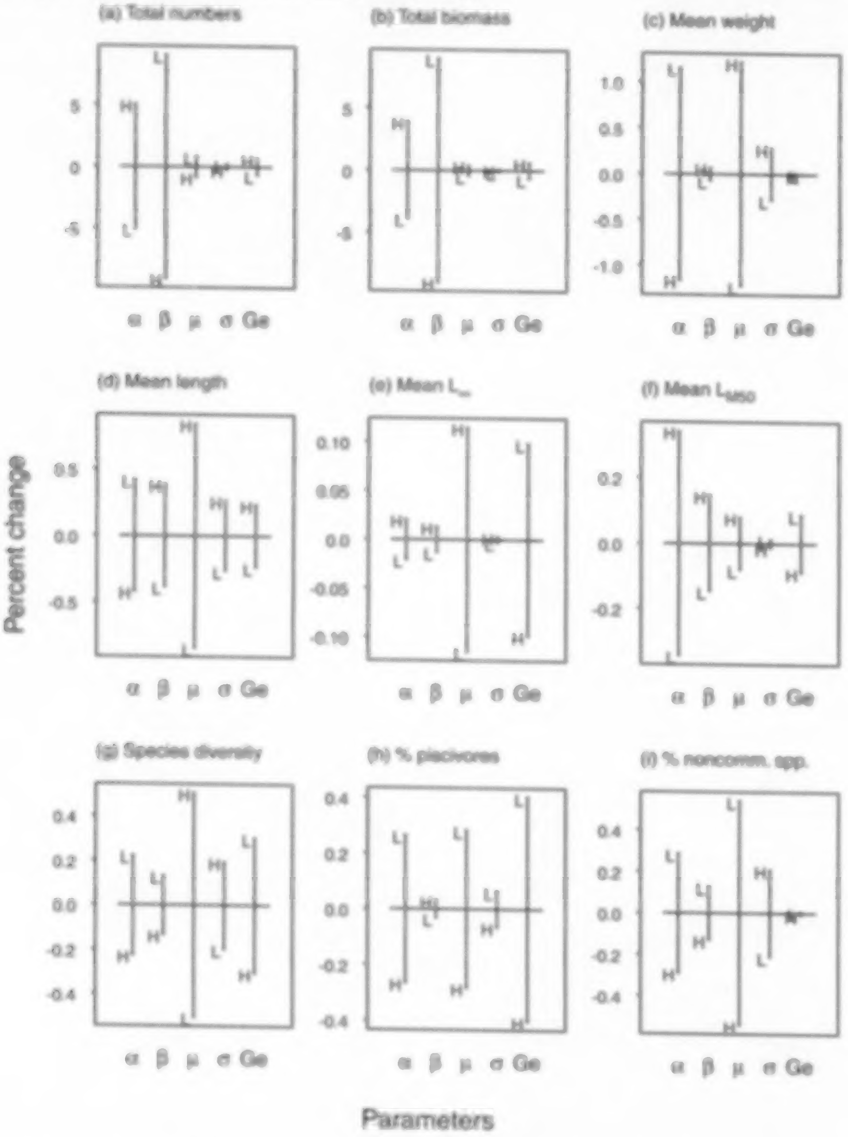

larger-bodied summer flounder (*Paralichthys dentatus*) and haddock (*Melanogrammus aeglefinus*). At high levels of fishing mortality, notable increases in abundance were only sustained for mackerel and winter flounder, as well as sand lance, which was unfished.

With no fishing mortality ($F = 0$), the community was numerically dominated by herring, mackerel, silver hake, and haddock (Fig. 6). These relative abundances are qualitatively similar to the abundance levels observed on George Bank, with the exception of Atlantic cod (*Gadhus morhua*), which has historically been more abundant (Fogarty and Murawski 1998). With increasing fishing mortality, numerical dominance shifted towards sand lance, mackerel, and haddock and away from silver hake, which was very sensitive to fishing. These levels of fishing mortality are comparable with those experienced during the period of overfishing on Georges Bank (Fogarty and Murawski 1998).

Logically these increases in abundance combined with a decrease in spawning stock biomass must have arisen because the affected populations comprised a larger proportion of smaller individuals when these species were fished. This counterintuitive result must be a consequence of indirect

Fig. 4. Time series of spawning stock biomass for each modeled species under different fishing mortalities. Species are ordered from top left to bottom right according to size (L_∞). $F = 0$, solid line; $F = 0.4$, broken line; $F = 0.8$, dashed–dotted line.

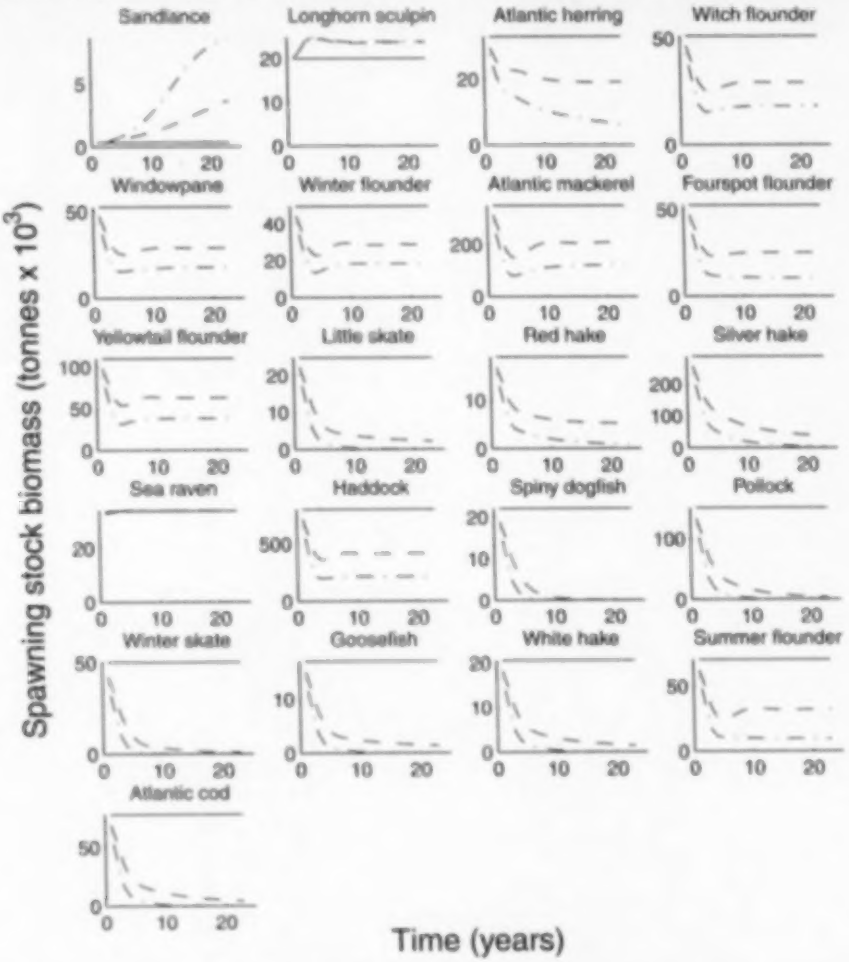

predation effects propagated through the food web, which allowed small individuals of some species to escape predation and persist in the system, despite being subject to fishing pressure.

Community structure

The effects of fishing at the community level can be represented in a variety of ways, each emphasizing a particular aspect of structure. Here we explore the behaviour of some of the size and rank abundance based approaches that have been suggested in the literature (Rice and Gislason 1996; Bianchi et al. 2000; Rochet and Trenkel 2003).

The biomass and abundance size spectra in our model are consistent in pattern with those found in natural communities and show a steady pattern of decrease after 25 years of fishing history (Figs. 7*a* and 7*b*). As one would expect, effects are most marked in the largest size classes, with both abundance and biomass falling to very low levels under high fishing pressure for the largest individuals. These results are consistent with both a priori expectations and previous empirical findings (Rice and Gislason 1996; Greenstreet and Hall 1996).

In contrast to the size spectra, rank abundance plots expressed using the *k*-dominance approach (Clarke 1990) show relatively little separation between fishing regimes (Figs. 7*c* and 7*d*). However, some patterns are discernable, most notably that there is an increase in the numerical dominance of the most abundant species with increasing fishing, whereas the pattern for biomass shows an increase at intermediate levels of fishing and a decline when fishing increases further. This result would appear to be related to the effects on the biomass and abundance trajectories of individual species described earlier.

When species diversity within size classes is plotted against body size, a clear bimodality is apparent with a trough at about 75 cm. This feature of diversity size spectra has not previously been identified in field data and is a result of the gap in the distribution of L_∞ values for species in our model between 74 cm and 100 cm. In a model system where a more even distribution of body sizes was represented, this

Fig. 5. Time series of abundances for each modeled species under different fishing mortalities. Data have been smoothed with a 1-year running mean to dampen within-year dynamics. Species are ordered from top left to bottom right according to size (L_∞). $F = 0$, solid line; $F = 0.4$, broken line; $F = 0.8$, dashed-dotted line.

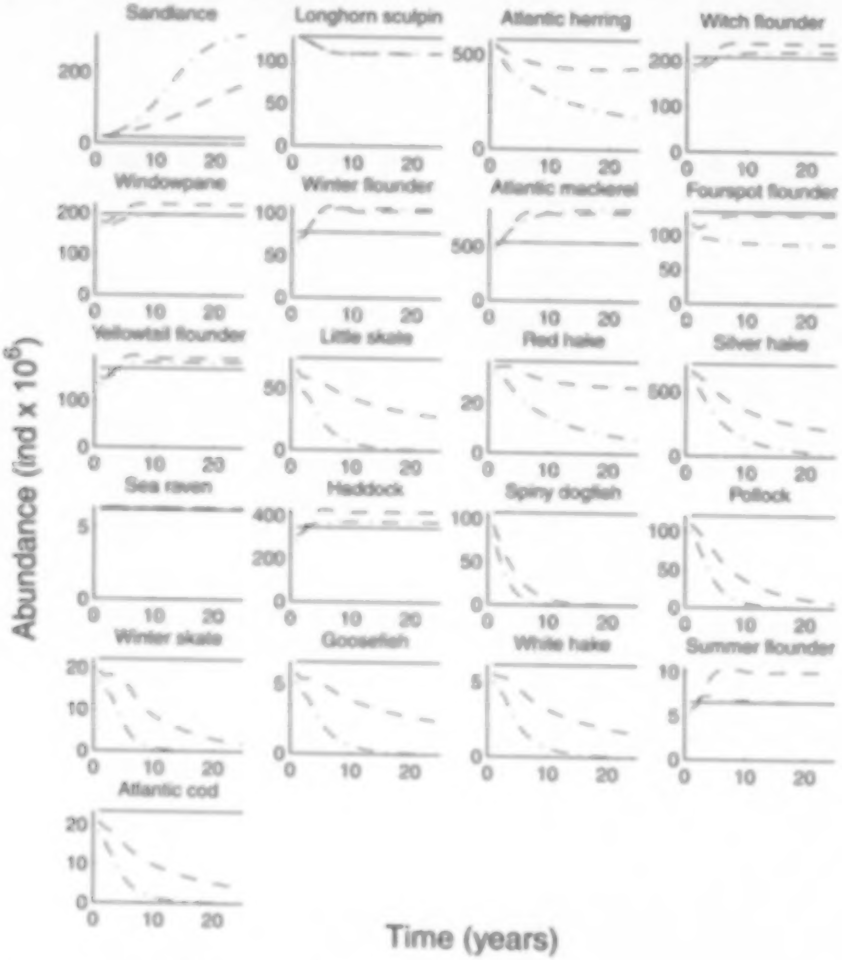

feature would not occur and, as far as we are aware, has not been examined for Georges Bank.

For sensitivity of the diversity size spectrum to fishing, it would appear that the diversity of individuals in larger size classes is much more affected by fishing. Indeed, the contrast between predictions for the biomass size spectrum (Fig. 7*b*) and the diversity size spectrum (Fig. 7*f*) suggests that the latter may show the effects of fishing more clearly.

In considering these results (Fig. 7), it should be borne in mind that these represent predicted changes resulting from 25 years of fishing. Clearly, for a metric to be useful for management purposes, it needs to respond over a much shorter time scale. An appreciation of temporal responsiveness can be obtained by examining the evolution of these patterns over time (Fig. 8). These data suggest that abundance and biomass size spectrum and *k*-dominance curves diverge rapidly from the zero fishing condition and that these features are broadly similar after 6 years. In contrast, a greater separation between time periods can be seen for the larger part of the diversity size spectrum, suggesting that changes in this attribute of community structure as the result of fishing should be observable over a longer time frame.

We also tested the sensitivity of a number of aggregate metrics to fishing mortality (Fig. 9). Total biomass declined more steeply with F than total numbers because fishing targeted the larger fish while allowing the numbers of some small fish species to increase (Fig. 9*a*). Total catch was maximized at $F = 0.6$, which can be interpreted as the community-level maximum sustainable yield (Fig. 9*b*). All the measures of mean length declined with F as expected (Figs. 9*b*, 9*c*). Of these, mean length was the most sensitive to F (~30% decline between $F = 0$ and 1), and mean length at maturity was the least sensitive (~15% decline). Mean length at maturity was not a sensitive metric because there is less variation among species in L_{M50} than L_∞ (Table 3). Mean weight decreased more steeply with F than mean length because of the power relationship between weight and length and because fishing increased the numbers of some small fish species. Even so,

Fig. 6. Bar plots indicating changes in abundance (number of individuals × 10^6) for each species after 25 years under different levels of fishing mortality: (*a*) $F = 0$; (*b*) $F = 0.4$; (*c*) $F = 0.8$; (*d*) percent change in species abundance between $F = 0$ and $F = 0.8$ simulations.

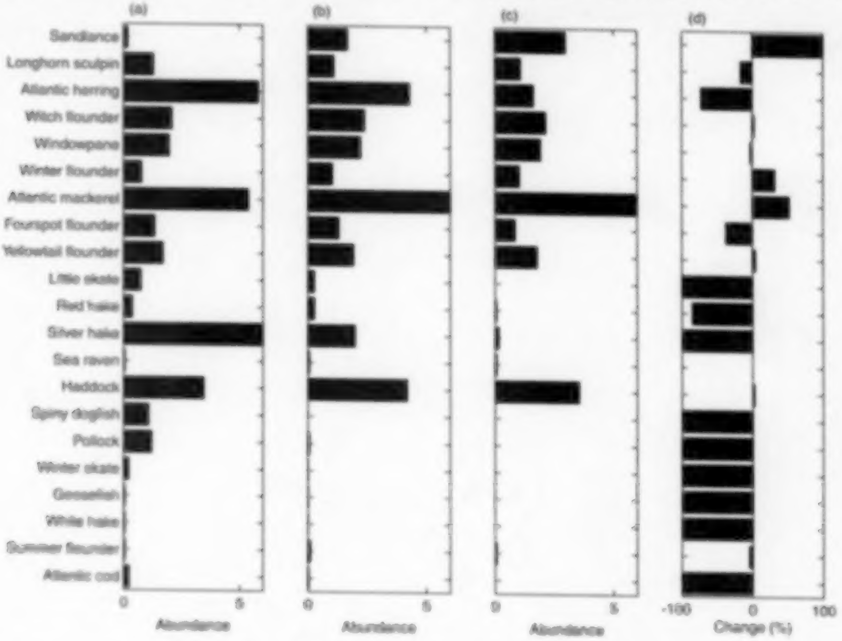

the decrease in mean weight of ~44% over the F range of 0 to 1 did not match the decrease in total biomass of ~80%.

Species diversity decreased most steeply between the range of $F = 0.2$ to 0.7 (Fig. 9*d*). In addition to declines in the evenness of abundances, this was also the range over which individual species were being lost from the community. The biomass of piscivorous species as a proportion of the total biomass declined only slightly with fishing mortality. This lack of sensitivity occurred because F was applied equally to all fished species and some of the species that we classified as nonpiscivorous are quite large (e.g., red hake (*Urophycis chuss*), white hake (*Urophycis tenuis*); Table 2). The biomass of noncommercial species (sand lance, longhorn sculpin, and sea raven) increased with F because of their release from predation (Fig. 9*d*). In summary, these aggregate metrics responded to fishing mortality in the expected directions (Rochet and Trenkel 2003). Metrics based on mass were more sensitive to F than those based on numbers or length. All metrics varied monotonically with F except total catch and species diversity, which had a threshold or inflection point at intermediate levels of fishing.

Discussion

The purpose of this paper was to describe a size-based model of a fish community, examine its sensitivity to key model parameters, and present some preliminary results examining the utility of various community-level metrics of fishing effects. As noted earlier, this model should be considered as strategic in focus and is directed explicitly at understanding the dynamics of the emergent properties of fish communities rather than providing quantitative predictions for species abundances in any particular system. Thus, although the model has been parameterized for Georges Bank in an effort to ground our parameterization in a defensible manner, we would not necessarily expect the results to mimic either the relative abundances of species or the temporal trends that have been observed.

Of the community-level indices we calculated, only total numbers and biomass in the community were somewhat sensitive to changes in the stock–recruitment parameters. This lack of sensitivity to possible parameter misspecification suggests that the responses of the community-level indices to fishing mortality are general to size-structured communities. The modeled community was more sensitive to the choice of size interval, especially at high levels of fishing mortality. With no fishing, numbers changed more gradually over the entire size range and were insensitive to the position of size-class boundaries relative to the size-specific demographic processes (growth, maturity, fishing, and predation). In contrast, with high fishing mortality, numbers were compressed in the lower size classes, where the positions of the size intervals affected the distribution of mean weights. Even so, the community-level indices had the same qualitative responses to fishing and most had the same quantitative patterns when comparing runs with different size-class intervals. The choice of size class is application dependent and depends partly on the size resolution of the data. For consistency, comparisons to assess the effects of fishing should be made within the same model parameterization.

The functional form of LeMANS is largely consistent with other recent size-based models (Benoit and Rochet 2004; Shin and Cury 2004); growth is described by the von Bertalanffy model, growth efficiency is on the order of 20% and nonpredation and fishing mortality both increase with size. However, unlike other models in which predation is de-

Fig. 7. The response of various community-level attributes to differing fishing mortalities imposed for 25 years: (*a*–*b*) abundance and biomass size spectra, total abundance of individuals (ind.) or total biomass in each size class; (*c*–*d*) *k*-dominance curves, log species rank versus cumulative proportional abundance or biomass; (*e*–*f*) diversity–size spectrum, species diversity, calculated as Hill's N1 (exp Shannon's H), of individuals in each size class. $F = 0$, solid line; $F = 0.4$, broken line; $F = 0.8$, dashed–dotted line.

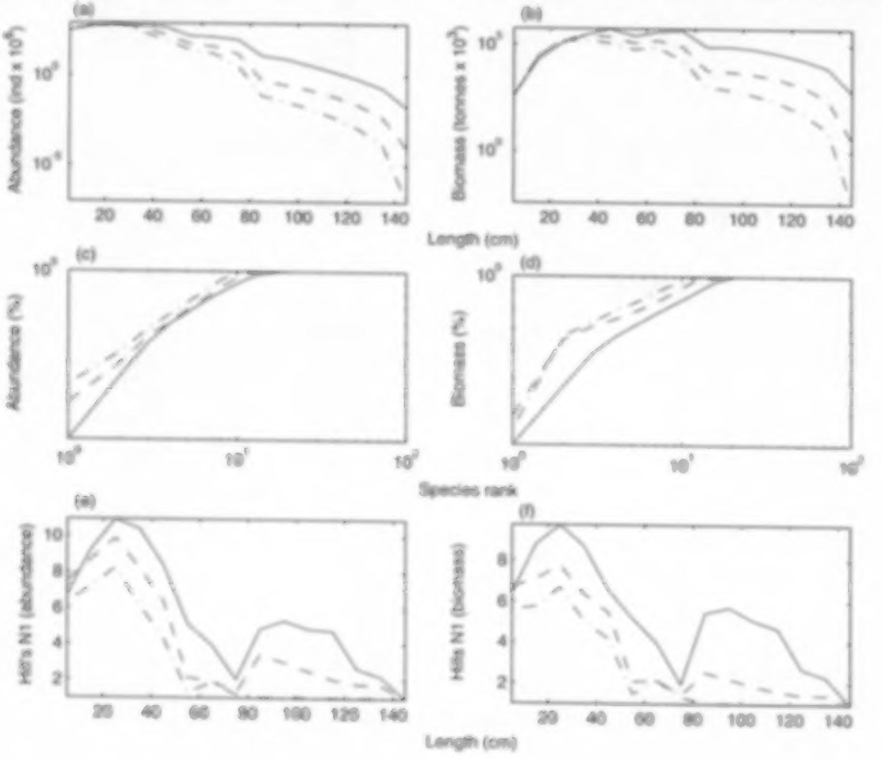

termined by encounter probabilities, LeMANS incorporates a type-II predator functional response. Density dependence is necessary at some point in the life cycle to stabilize the model dynamics. In LeMANS, density dependence occurs in the stock–recruitment functions, which is consistent with fisheries theory. The results obtained with LeMANS and the metrics calculated from them are also consistent with previous studies. Similarities with other work also extend to model sensitivity; as with MSVPA, our model was more sensitive to parameters related to recruitment (α and β) than to predation (μ, σ, and Ge) (Gislason 1991; Collie et al. 2003).

While individual population trajectories might not reflect those observed in the real world, we would expect our model to represent the emergent features of a natural community. In this respect, it is comforting that the patterns in community structure observed are largely consistent with those observed elsewhere (Rice and Gislason 1996; Duplisea and Bravington 1999; Bianchi et al. 2000). This degree of consistency increases our confidence that predictions made about fishing effects are robust. The trends in the various community attributes with increases in fishing pressure are also consistent with a priori expectations and previous work, which shows a loss of larger-bodied species, although until now we had relatively little feel for how quickly changes might be observed or of the scale of change to be expected (Gislason and Rice 1998; Duplisea and Bravington 1999).

Using a forward-projecting version of MSVPA, previous work by Rice and Gislason (1996) suggested that biomass size spectra may be a more useful approach than diversity size spectra for examining community-level effects. Their analysis, however, was based on a model with only 11 species and analysis of diversity effects with such a model may have been constrained. Although very preliminary, our results suggest that abundance or biomass size spectra may be very responsive to fishing effects as we observed changes after 6 years that did not change further for the next 18 years. In contrast, *k*-dominance representations show relatively little sensitivity to fishing effects and would appear to be of limited utility. This result contrasts markedly with findings for benthic communities, where *k*-dominance curves have become one of the "industry standards" for examining the effects of anthropogenic disturbance (Clarke and Warwick 1994). Contrary to Rice and Gislason (1996), we also found the diversity size spectra to show a marked effect from fishing that evolved steadily over the 25-year period.

It is encouraging that most of the community-level indices are sensitive to fishing mortality and respond in the directions predicted by theory (Rochet and Trenkel 2003). In data-limited situations, where not all metrics are calculable, simple metrics, such as mean length in the catch, can serve as proxies for the community-level effects. However, most of these metrics change monotonically with fishing and,

Fig. 8. Evolution of community-level attributes over time for $F = 0.4$: (*a*–*b*) abundance and biomass size spectra, total abundance of individuals (ind) or total biomass in each size class; (*c*–*d*) *k*-dominance curves, log species rank versus cumulative proportional abundance or biomass; (*e*–*f*) diversity–size spectrum, species diversity, calculated as Hill's N1 (exp Shannon's H), of individuals in each size class. $t = 0$ years, solid line; $t = 6$ years, broken line; $t = 12$ years, dotted line; $t = 25$ years, dashed–dotted line.

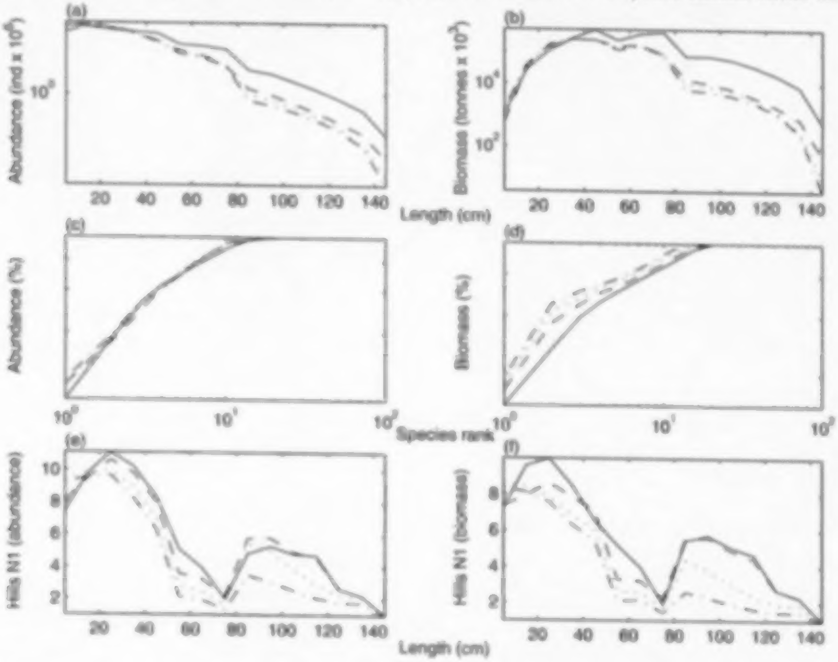

Fig. 9. Sensitivity of community-level metrics to fishing mortality: (*a*) total abundance, solid line; total biomass, dashed–dotted line; (*b*) total catch, solid line; mean length in catch, dashed–dotted line; (*c*) mean L_∞, solid line; mean length, dotted line; mean L_{M50}, dashed–dotted line; mean weight, broken line; (*d*) proportion of piscivores, solid line; proportion of noncommercial species, dashed–dotted line; species diversity (Hill's N1), broken line. Individuals, ind.

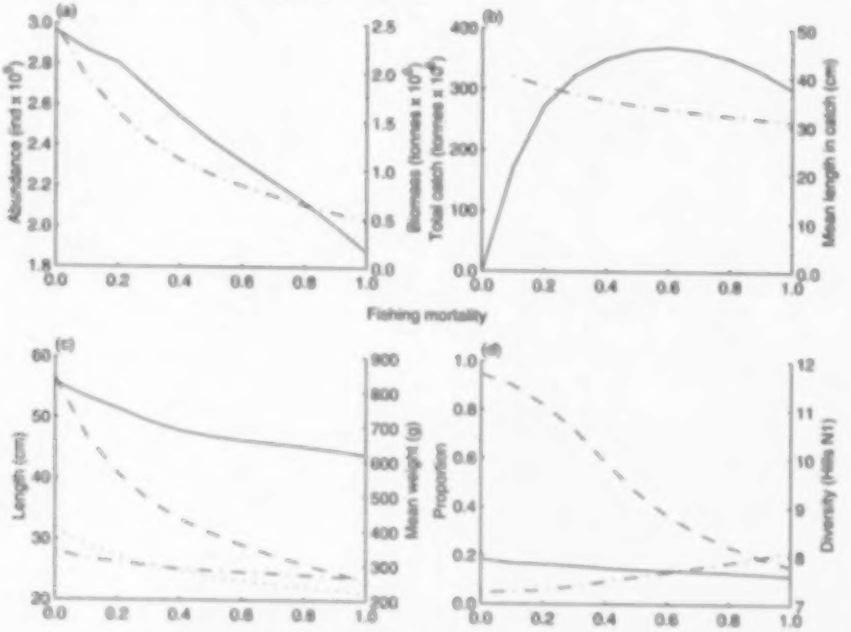

therefore, lack obvious points at which one might set reference levels. If the aggregate fish community is considered a "super species", then the aggregate fishing mortality for maximum sustainable yield (MSY) could be a reference level. However, community-level metrics do not guarantee the persistence of all species in the community; at the community-level MSY of $F = 0.6$ in our model, for example, six species had been eliminated. Thus, the adoption of community- or ecosystem-level reference points alone may be insufficient to protect all the species that are considered threatened. Instead, it may be necessary to adapt single-species reference points to nontarget species and to incorporate these additional reference levels into fishery management plans. In this regard it should be noted that, in our simulations, the single-species declines in spawning stock biomass were the most sensitive indicators of fishing effects. Although single-species fisheries management has been roundly criticized for ignoring ecosystem considerations (Pikitch et al. 2004), there may be no simple alternative to species-by-species monitoring and assessment (Quinn and Collie 2005).

The primary purpose of this paper was to describe a new length-based multispecies model and to provide an illustration of its potential utility for understanding how community-level attributes change under fishing. Further work will be required to fully explore the behaviour of the model and what it can tell us about the dynamics of exploited fish communities. In particular, we need to ask how the topology of the food web alters behaviour, what the effects of differential fishing pressure (selectivity by fishing fleets) might be, and how a wider range of community-level indices responds to fishing. We also need to more fully confront the model's predictions with data and explore its behaviour when parameterized with data from other communities.

Acknowledgements

This project was supported by the Pew Fellows Program in Marine Conservation, an initiative of The Pew Charitable Trusts in partnership with the New England Aquarium. J.S.C. acknowledges support from the Georges Bank GLOBEC Program.

References

Benoit, E., and Rochet, M.-J. 2004. A continuous model of biomass size spectra governed by predation and the effects of fishing on them. J. Theor. Biol. **226**: 9–21.

Bianchi, G., Gislason, H., Graham, K., Hill, L., Jin, X., Koranteng, K., Manickchand-Heileman, S., Paya, I., Sainsbury, K.J., Sanchez, F., and Zwanenburg, K. 2000. Impact of fishing on size composition and diversity of demersal fish communities. ICES J. Mar. Sci. **57**: 558–571.

Clarke, K.R. 1990. Comparisons of dominance curves. J. Exp. Mar. Biol. Ecol. **138**: 143–157.

Clarke, K.R., and Warwick, R.M. 1994. Change in marine communities: an approach to statistical analysis and interpretation. Natural Environmental Research Council, Plymouth, UK.

Collie, J.S. 2001. Multispecies dynamics. *In* Encyclopedia of ocean sciences. *Edited by* J.H. Steele, S. Thorpe, and K. Turekian. Academic Press, London. pp. 1002–1010.

Collie, J.S., and Gislason, H. 2001. Biological reference points for fish stocks in a multispecies context. Can. J. Fish. Aquat. Sci. **58**: 2167–2176.

Collie, J.S., Gislason, H., and Vinther, M. 2003. Using AMOEBAs to display multispecies, multifleet fisheries advice. ICES J. Mar. Sci. **60**: 709–720.

Duplisea, D.E., and Bravington, M.V. 1999. Harvesting a size-structured ecosystem. ICES CM 1999/Z:01.

Fogarty, M.J., and Murawski, S.A. 1998. Large-scale disturbance and the structure of marine ecosystems: fishery impacts on Georges Bank. Ecol. Appl. **8**: S6–S22.

Food and Agricultural Organisation of the United Nations. 2001. What is the code of conduct for responsible fisheries? Food and Agricultural Organisation of the United Nations, Rome, Italy.

Gislason, H. 1991. The influence of variations in recruitment on multispecies yield predictions in the North Sea. ICES Mar. Sci. Symp. **193**: 50–59.

Gislason, H., and Rice, J. 1998. Modeling the response of size and diversity spectra of fish assemblages to changes in exploitation. ICES J. Mar. Sci. **55**: 362–370.

Greenstreet, S.P.R., and Hall, S.J. 1996. Fishing and groundfish assemblage structure in the northwestern North Sea: an analysis of long-term and spatial trends. J. Anim. Ecol. **65**: 577–598.

Hahm, W., and Langton, R. 1984. Prey selection based on predator/prey weight ratios for some Northwest Atlantic fish. Mar. Ecol. Prog. Ser. **19**: 1–5.

Hall, S.J., and Mainprize, B. 2004. Towards ecosystem-based fisheries management. Fish Fish. **5**: 1–20.

Hilborn, R., and Walters, C.J. 1992. Quantitative fisheries stock assessment: choice, dynamics and uncertainty. Chapman & Hall, New York.

Insightful Corp. 2001. S-PLUS 6 for Windows [computer program]. Guide to statistics. Insightful Corporation, Seattle, Wash.

Jennings, S., Greenstreet, S.P.R., and Reynolds, J.D. 1999. Structural changes in an exploited fish community: a consequence of differential fishing effects on species with contrasting life histories. J. Anim. Ecol. **68**: 617–627.

Jobling, M. 1994. Fish bioenergetics. Kluwer Academic, Dordrecht, the Netherlands.

Link, J.S. 2002. Does food web theory work for marine ecosystems? Mar. Ecol. Prog. Ser. **230**: 1–9.

Livingston, P.A., and Tjelmeland, S. 2000. Fisheries in boreal ecosystems. ICES J. Mar. Sci. **57**: 619–627.

Magnusson, K.G. 1995. An overview of the multispecies vpa — theory and applications. Rev. Fish Biol. Fish. **5**: 195–212.

Murawski, S., and Idoine, J. 1992. Multispecies size composition: a conservative property of exploited fishery systems? J. Northwest Atl. Fish. Sci. **14**: 79–85.

Myers, R.A., Bridson, J., and Barrowman, N.J. 1995. Summary of worldwide stock and recruitment data. Can. Tech. Rep. Fish. Aquat. Sci. No. 2024.

Myers, R.A., Bowen, K.G., and Barrowman, N.J. 1999. Maximum reproductive rate of fish at low population sizes. Can. J. Fish. Aquat. Sci. **56**: 2404–2419.

O'Brien, L.O., Burnett, J., and Mayo, R.K. 1993. Maturation of nineteen species of finfish off the northeast coast of the United States, 1985–1990. NOAA Tech. Rep. NMFS 113.

Penttila, J.A., Nelson, G.A., and Burnett, J.M. 1989. Guidelines for estimating lengths at age for 18 Northwest Atlantic finfish and shellfish species. NOAA Tech. Memo. NMFS-F/NEC-66.

Pikitch, E.K., Santora, C., Babcock, E.A., Bakun, A., Bonfil, R., Conover, D.O., Dayton, P.K., Doukakis, P., Fluharty, D., Heneman, B., Houde, E.D., Link, J.S., Livingston, P.A., Mangel, M., McAllister, M.K., Pope, J., and Sainsbury, K.J. 2004.

Ecosystem-based fishery management. Science (Washington, D.C.), **305**: 346–347.

Quinn, T.J., and Collie, J.S. 2005. Sustainability in single-species population models. Philos. Trans. R. Soc. B, **360**: 147–162.

Rice, J., and Gislason, H. 1996. Patterns of change in the size spectra of numbers and diversity of the North Sea fish assemblage, as reflected in surveys and models. ICES J. Mar. Sci. **53**: 1214–1225.

Rochet, M.-J., and Trenkel, V.M. 2003. Which community indicators can measure the impact of fishing? A review and proposals. Can. J. Fish. Aquat. Sci. **60**: 86–99.

Scharf, F.S., Juanes, F., and Rountree, R.A. 2000. Predator size – prey size relationships of marine fish predators: interspecific variation and effects of ontogeny and body size on trophic-niche breadth. Mar. Ecol. Prog. Ser. **208**: 229–248.

Shin, Y.-J., and Cury, P. 2004. Using an individual-based model of fish assemblages to study the response of size spectra to changes in fishing. Can. J. Fish. Aquat. Sci. **61**: 414–431.

Sissenwine, M.P., and Shepherd, J.G. 1987. An alternative perspective on recruitment overfishing and biological reference points. Can. J. Fish. Aquat. Sci. **44**: 913–918.

Tsou, T., and Collie, J.S. 2001. Estimating predation mortality in the Georges Bank fish community. Can. J. Fish. Aquat. Sci. **58**: 908–922.

Effects of ontogeny, season, and temperature on the swimming performance of juvenile green sturgeon (*Acipenser medirostris*)

Peter J. Allen, Brian Hodge, Inge Werner, and Joseph J. Cech, Jr.

Abstract: Because some salmonids show decreased swimming performance (U_{crit}) during their parr–smolt transformation, we tested the hypothesis that juvenile anadromous green sturgeon (*Acipenser medirostris*) decrease U_{crit} during their analogous ontogenetic stage. Juvenile green sturgeon (mean age: 98 days) that had not reached seawater tolerance had a positive relationship of U_{crit} (cm·s^{-1}) with total length (TL), whereas seawater-tolerant sturgeon (mean age: 150 days) had a negative relationship of U_{crit} with TL. This U_{crit} decrease was presumably seasonal because a similar-sized group of fish tested later (mean age: 288 days) showed a linear increase in U_{crit} with TL. Smaller sturgeon displayed both morphological (larger relative pectoral fin surface areas) and behavioral (rostrum wedging and pectoral fin holding) attributes for station holding in a riverine environment. In a second experiment to test the effects of increased river temperature near the predicted time of downstream migration, U_{crit} and heat-shock protein concentrations increased at 24 °C compared with at 19 °C (mean age: 155 days). Thus, although there was evidence for cellular stress, the swimming ability of the fish was not compromised. Therefore, water velocity, temperature, and time of year should be considered in life-stage-specific efforts to manage or protect green sturgeon.

Résumé : Parce que certains salmonidés accusent une baisse de performance natatoire (U_{crit}) durant leur transformation de tacon en saumoneau, nous avons évalué l'hypothèse qui veut que les jeunes esturgeons verts (*Acipenser medirostris*) anadromes réduisent leur U_{crit} durant leur stade ontologique analogue. Les jeunes esturgeons verts (âge moyen de 98 jours) qui n'ont pas encore atteint leur tolérance à l'eau de mer montrent une relation positive entre U_{crit} (cm·s^{-1}) et la longueur totale (TL), alors que les esturgeons tolérants à l'eau de mer (âge moyen de 150 jours) ont une relation négative entre U_{crit} et TL. Cette réduction d'U_{crit} est sans doute saisonnière puisque qu'un groupe de taille semblable testé plus tard (âge moyen de 288 jours) montre une augmentation linéaire d'U_{crit} avec TL. Les esturgeons plus petits possèdent des caractéristiques morphologiques (surface relative plus grande des nageoires pectorales) et comportementales (insertion du rostre et position des nageoires pectorales) pour se maintenir sur place dans un environnement de rivière. Dans une seconde expérience d'évaluation des effets d'une augmentation de la température de la rivière près du moment prédit de l'émigration vers l'aval, U_{crit} et les concentrations de protéines du choc thermique sont plus élevées à 24 °C qu'à 19 °C (âge moyen de 155 jours). Ainsi, bien qu'il y ait des indices d'un stress cellulaire, la capacité de nage des poissons n'est pas compromise. Il faut donc prendre en considération la vitesse du courant, la température de l'eau et le moment de l'année dans les efforts reliés au stade de vie que l'on fait pour aménager ou protéger l'esturgeon vert.

[Traduit par la Rédaction]

Introduction

Maximum aerobic swimming performance of fish has been widely measured as critical swimming velocity (U_{crit}). Typically determined in a water flume or tunnel, U_{crit} can be described as sustainable swimming in stepped water velocity increases until fatigue (Brett 1964; Beamish 1978; Hammer 1995). Despite some inherent limitations in simulating natural environments, this laboratory-based measurement has correlates with ecological performance and relationships to swimming abilities in a fish's natural environment (reviewed by Plaut 2001; Wolter and Arlinghaus 2003). U_{crit} has been studied extensively in juvenile salmonids, and some of these studies have directly compared freshwater parr with seawater-tolerant smolts. Whereas most fishes increase U_{crit} as they grow and develop (Beamish 1978; Hammer 1995), several studies have reported decreased U_{crit}, increased tail beat frequency (TBF), and increased refusal to swim during the

Received 1 August 2005. Accepted 13 January 2006. Published on the NRC Research Press Web site at http://cjfas.nrc.ca on 11 May 2006.
J18819

P.J. Allen,[1] B. Hodge, and J.J. Cech, Jr. Department of Wildlife, Fish, and Conservation Biology and the Center for Aquatic Biology and Aquaculture, University of California at Davis, 1 Shields Avenue, Davis, CA 95616, USA.
I. Werner. Department of Anatomy, Physiology and Cell Biology, School of Veterinary Medicine, University of California, 1 Shields Avenue, Davis, CA 95616, USA.

[1] Corresponding author (e-mail: pjallen@ucdavis.edu).

doi:10.1139/F06-031

parr–smolt transformation (PST; Thorpe and Morgan 1978; Flagg and Smith 1982). A recent study shows evidence of locomotory muscle restructuring (including thyroid hormone induced restructuring) during the PST, affecting muscle contractility and fiber type, and decreasing U_{crit} (Katzman and Cech 2001). Thus, the downstream movements of these juveniles is facilitated by a decrease in aerobic, red muscle fibers and the associated ability to maintain position in stream currents (Katzman and Cech 2001). However, questions remain concerning the swimming performance and downstream migration in nonsalmonid anadromous fishes, including sturgeon.

There have been several studies on swimming performance in juvenile sturgeons (McKenzie et al. 2001; Peake 2004). Most of the sturgeon swimming studies used limited size and age ranges of fish (McKenzie et al. 2001; Adams et al. 2003) or did not study anadromous species (Peake et al. 1995; Adams et al. 1999). Therefore, the potential age- and size-related changes in swimming performance have not been elucidated for anadromous species of sturgeon. Green sturgeon (*Acipenser medirostris*) are anadromous and are known to spawn in three river systems: the Sacramento and Klamath in northern California and the Rogue in southern Oregon. Adults range from Ensenada, Mexico, to the Bering Sea (Moyle 2002), but there is little information on their early life stages, particularly on size and age of juvenile seawater entry. Populations appear to be declining (Moyle 1994, 2002), and their natal rivers are modified by anthropogenic changes such as dams and water diversions, which in turn have increased summer water temperatures over historic levels (Bartholow 2005).

The effects of these temperature increases on early life stages of green sturgeon, including the life stages during which seawater adaptation occurs, are not fully understood. In salmonids, temperature is known to influence endogenous changes that occur during the PST (McCormick et al. 2002; Handeland et al. 2004; Marine and Cech 2004), as well as affect swimming performance (Johnston and Ball 1997; Taylor et al. 1997). In green sturgeon, embryos and larger, older (yearling) juveniles have been found to be negatively impacted by warm temperatures (Mayfield and Cech 2004; Van Eenennaam et al. 2005), which has included depressed swimming abilities (Mayfield and Cech 2004), although smaller, younger (~1–2 months old) juveniles may not be adversely affected (Allen et al. 2006). Heat-shock protein (hsp) expression, a cellular measure of temperature-related stress, may show complementary changes with swimming performance. Although hsps have not been shown to be directly linked to many measures of physiological performance (a tertiary physiological stress response), this has been primarily due to a paucity of studies (Iwama et al. 2004). Therefore, measurements of swimming performance and hsp expression can provide an integrated whole-organism and cellular evaluation of the effects that temperature may have on juvenile green sturgeon during the critical period of seawater adaptation.

There were two main objectives of this study. The first was to measure changes in U_{crit} with ontogeny in juvenile green sturgeon. Because of their anadromy, we hypothesized that they would display a "smolt-like" temporary decrease in U_{crit} when they reached seawater tolerance. To aid in the comparisons of swimming performance with increasing sizes of fish, a concurrent study was carried out on the ontogeny of salinity tolerance in green sturgeon with size and age (Allen 2005). The second objective was to measure temperature-related effects on juvenile green sturgeon swimming performance and hsp expression. Larger (yearling) juvenile green sturgeon show decreased swimming performance at 24 °C (Mayfield and Cech 2004). Because of this we hypothesized that U_{crit} would decrease at 24 °C compared with at 19 °C and that hsp expression would increase.

Materials and methods

Fish rearing and holding

Green sturgeon were hatched according to the methods described by Van Eenennaam et al. (2001). Briefly, adult wild fish were obtained from the Klamath River and were artificially induced to spawn, and first generation fish (73–288 days posthatch (dph) or 2.5–9.5 months old) were used in experiments. Larval to juvenile fish were reared, under natural (springtime) photoperiods, in circular (1 m diameter) fiberglass tanks with continuous flows of nonchlorinated well water at 18.6 ± 0.3 °C (mean ± standard deviation, SD). Inflowing water was oriented with a spray bar to provide a very slight current in the tank. Ad libitum rations of commercial diet (Silver Cup Soft-Moist Trout Diet; Nelson & Sons, Inc., Murray, Utah) and small amounts of tubifex were added once the fish started exogenous feeding. Currents in holding tanks were gradually increased as the fish grew larger and were better able to hold position. Before experiments, fish were transferred into a 1 m diameter tank similar to the holding tanks except that water currents were increased throughout the tank. Increased flows from a small, submersible pump better simulated currents found in the fishes' natal river environment. Fish were always acclimated to the stronger currents (6–12 $cm \cdot s^{-1}$) for 3–14 days before experimentation. Fish were fed commercial diet according to the optimal growth feeding chart derived for white sturgeon (S.I. Doroshov, Department of Animal Science, University of California at Davis, Davis, CA 95616, unpublished data). Experimental tanks were measured daily for temperature (19.2 ± 0.02 °C), pH (7.78 ± 0.02), dissolved oxygen (always >7.75 $mg \cdot L^{-1}$ or 84.4% saturation; mean 8.33 ± 0.04 $mg \cdot L^{-1}$ or 90.4 ± 0.5%), and dissolved total ammonia (unionized ammonia always <11.0 $\mu g \cdot L^{-1}$; mean 5.5 ± 0.3 $\mu g \cdot L^{-1}$).

Experiment 1: changes in swimming performance (U_{crit}) with ontogeny

We measured ontogenetic changes in swimming performance (weekly U_{crit} tests) with increasing age (73–177 dph or 2.5–6 months old; July–October) and total length (TL) from fish of the same cohort. The experiment was conducted until fish had far surpassed a length and age threshold at which all fish were surviving in seawater, based on concurrent salinity-tolerance experiments with the same cohort. Fish in all U_{crit} experiments were used only once.

A Brett-type swim chamber (Brett 1964) that generated rectilinear flow was used to measure U_{crit}. Fish were individually netted, placed in a water-filled plastic container, and transferred (3.3 m distance) to the cylindrical swimming chamber (65 cm length, 15 cm diameter). Each fish was acclimated for 30–60 min at a low water velocity (5 cm·s^{-1}) to orient it to the current and chamber. Fish were shielded from observers by black plastic or opaque plastic sheets, and swimming was observed via a mirror oriented at an angle over the top of the swimming chamber. After acclimation, water velocity was increased in increments of 10 cm·s^{-1} at 20 min intervals. U_{crit}, as a measure of the maximum aerobic swimming ability (Beamish 1978), was calculated from Brett (1964):

$$(1) \qquad U_{\text{crit}} = V_f + V_i(T_f / T_i)$$

where V_f is the final velocity at which the fish swam for the entire 20 min period, V_i is the increment of water velocity increase (10 cm·s^{-1}), T_f is the time swum at the water velocity of fatigue, and T_i is the time increment for each water velocity (20 min). The swimming chamber was maintained at a constant temperature by a thermostat-controlled water bath, and its water was partially exchanged with fresh, air-equilibrated well water between experiments to ensure dissolved oxygen levels near air saturation. No solid blocking corrections were used, because the maximum cross-sectional area of the fish was always <10% of the cross-sectional area of the swimming chamber (Bell and Terhune 1970).

U_{crit} swimming tests were concluded when fish impinged three times at the same water velocity. Impingement was determined as either impingement (one-third or greater of body in contact with the rear screen) or fatigue (sustained contact with the rear screen for 60 s). After the initial impingement, the water velocity was decreased for <60 s until the fish came off the rear screen. If the fish did not come off the rear screen within 60 s, the experiment was ended. If the fish did come off the rear screen, the water velocity was increased until it was at the same velocity of impingement. Usually, the second and third impingements occurred in rapid succession at the water velocity of the first impingement. In contrast, 23% of fish were excluded from analyses because of either tail propping (caudal fin supporting fish on rear screen despite rapid increases and decreases in water velocity to coax the fish into swimming) or rostrum wedging (rostrum thrust into front screen holding nonswimming fish in the current). Fish would occasionally use their pectoral fins to help brace against the currents on the bottom of the swimming chamber. This bracing was usually very temporary, because fish were unable to hold their position without swimming for more than a few seconds because of the cylindrical shape of the swimming chamber. Fish were not touched, prodded, or shocked during the experiment.

During experiment 1, TBF and ventilation frequency (VF) were also measured. Both measurements were means from watching the fish for 30 s periods three times at every water velocity interval: 5, 10, and 15 min after water velocity increases. Data from water velocities >45 cm·s^{-1} were not used because of the difficulty in accurately observing TBF and VF.

The possible effects of flume size on swimming performance in larger juvenile green sturgeon (330–450 mm TL) were tested using a larger-sized flume (91 cm long × 25.4 cm diameter, cylindrical) and found not to be significantly different from the flume size used above (t test, $p < 0.05$, $n = 6$ per flume, 54.49 ± 1.19 cm·s^{-1} vs. 55.03 ± 2.14 cm·s^{-1}). These fish were from a different cohort, were swum in winter (February) instead of in late summer – early autumn (August–October), and were older (287–288 dph or 9.5 months old) than the other comparably sized experiment 1 fish (3.5–6 months old).

After experiment 1, fish were immediately euthanized in 500 mg·L^{-1} tricaine methanesulfonate (MS 222) and pectoral fin dimensions, TL, and wet mass were measured (for pectoral fin dimensions, $n = 47$, with 29 of the smallest fish, out of the total 76 fish, not measured). Each pectoral fin (right and left) was measured for length (anterior to posterior) and width (insertion to fin tip). Relative pectoral fin surface area was estimated by the following equation:

$$(2) \qquad \text{surface area} = (\text{length} \cdot \text{width})/\text{TL}^2$$

Experiment 2: elevated temperature effects

Twenty fish were placed in a tank with water flows and feeding regimes similar to those in the 19 °C pre-experimental tank. These fish were acclimated to 24 °C (1 °C·day^{-1}) and were held at 24 °C for 2.5–5 weeks before swimming performance experiments. The experimental tank was measured daily for temperature (24.3 ± 0.08 °C), pH (8.21 ± 0.03), dissolved oxygen (always >6.43 mg·L^{-1} or 77.3% saturation; mean 7.21 ± 0.09 mg·L^{-1} or 86.4 ± 1.0%), and dissolved total ammonia (unionized ammonia always <44.1 µg·L^{-1}; mean 22.2 ± 1.1 µg·L^{-1}). Experimental parameters were the same as those previously described, and fish were from the same cohort as those used in experiment 1. These experiments were conducted during the late summer to early autumn period (September–October) when sturgeon were 123–177 dph (4–6 months old). The 24 °C level was chosen because it is a high summer water temperature in their natal rivers (Erickson et al. 2002; US Geological Survey (USGS) 2004).

Following TL and wet mass measurements in experiment 2, dorsal muscle samples (1 cm^2 section from the right side adjacent to the third and fourth dorsal scutes) were removed by scalpel and forceps for hsp analyses. For pelvic fin samples, a 1 cm^2 section of the right pelvic fin was removed. All samples were placed into individual frozen-sample vials, frozen on dry ice, and stored at –80 °C until hsp analyses (<3 months). Fish acclimated to 24 °C for 2.5–5 weeks (n = 16) and fish of the same age and size (n = 15) held at 19 °C were sampled regardless of whether they cooperated during swimming trials or not. Hsp60, hsp70, and hsp90 were analyzed using Western blotting techniques as described by Werner et al. (2001) and Viant et al. (2003), with protein bands being quantified by densitometry (Bio-Rad GS710; Bio-Rad Laboratories, Hercules, California).

Statistical analyses

For the relationship of swimming performance with TL, two separate linear regressions were used (Sall et al. 2001): one for TLs of fish from 120 to 266 mm and another for TLs of fish from 267 to 475 mm because of the results of the concurrent salinity-tolerance experiment, which found that 100% salinity tolerance was achieved in an experimental group of fish with a mean ± standard error (SE) TL of 266 ± 24 mm (Allen 2005). After both relationships were found to be significant ($p < 0.05$), a piecewise regression (Neter et al.

Fig. 1. Experiment 1 relationship between U_{crit} and total length (TL) for juvenile green sturgeon (*Acipenser medirostris*) during summer and early autumn: ●, fish that were less than 100% seawater (SW) tolerant; ○, fish that were 100% SW tolerant based on a concurrent experiment. The regression line represents the linear relationship $y = 0.077x_1 + 31.348 - 0.160(x_1 - 266)x_2$, where x_1 = TL and $x_2 = 1$ if $x_1 > 266$, otherwise $x_2 = 0$ ($r^2 = 0.26$, $n = 76$).

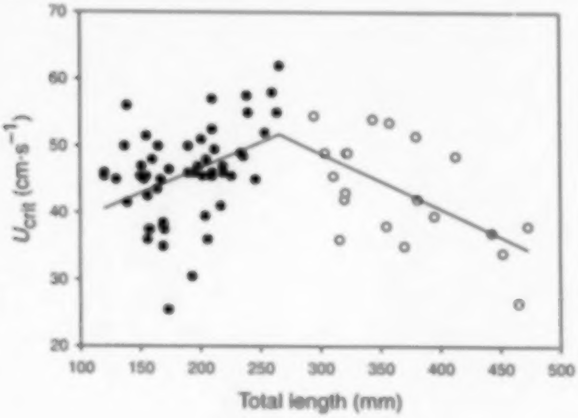

1996) was used to combine the two regressions at the TL that accounted for the maximum amount of variance, which happened to be 266 mm. Regressions also characterized the relationships between pectoral fin dimensions and TL. All regressions were found to be significant ($p < 0.05$). For TBF and VF, data were divided into four groups (10–20, 20–30, 30–40, and 40–50 cm) to analyze size effects at each water velocity using analyses of variance. No differences were found, so data from all sizes of fish were combined and analyzed for water velocity. Multiple comparison tests (Tukey's honestly significant difference test) were used only if the overall one-way analysis of variance (ANOVA) was found to be significant. Student's *t* tests were used to compare 24 °C and 19 °C groups for U_{crit} and hsp results. In all cases, differences were considered significant at $p < 0.05$. All statistical values for measurements are reported as means ± SE.

Results

Experiment 1: changes in swimming performance (U_{crit}) with ontogeny

U_{crit} increased in fish with TLs from 120 to 266 mm ($n = 56$) and decreased in fish with TLs from 267 to 475 mm ($n = 20$; $y = 0.077x_1 + 31.348 - 0.160(x_1 - 266)x_2$, where x_1 = TL and $x_2 = 1$ if $x_1 > 266$, otherwise $x_2 = 0$, $r^2 = 0.26$; Fig. 1). The change from increasing to decreasing U_{crit} with increasing fish size also corresponded with the mean TL (266 ± 24 mm) of fish achieving full-strength seawater tolerance in a concurrent experiment (Allen 2005), supporting our hypothesis.

There were no differences in TBF or VF among the four size groups; therefore, all the size groups were combined and TBF and VF were analyzed between water velocities. TBF and VF both increased with water velocity (Fig. 2).

Fig. 2. Mean (± standard error) juvenile green sturgeon (*Acipenser medirostris*) gill ventilation ($n = 50$–73, ▲) and tail beat frequencies ($n = 49$–76, ●) with swimming velocity, experiment 1, summer to early autumn fish. Different letters and numbers represent significant differences in gill ventilation and tail beat frequency, respectively (analysis of variance, $p < 0.05$).

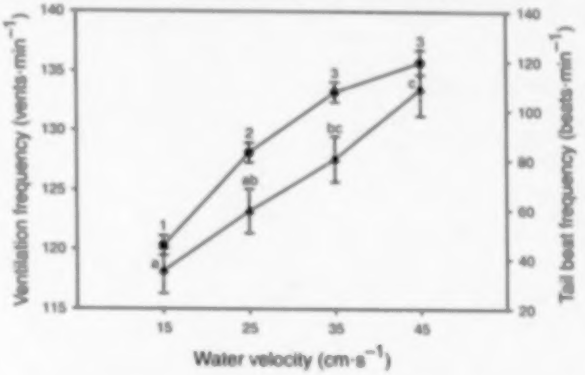

As fish TL increased, pectoral fin length ($y = 0.664x - 0.046$, $r^2 = 0.86$, $n = 47$; Fig. 3*a*), width ($y = 0.882x - 0.743$, $r^2 = 0.89$, $n = 47$; Fig. 3*b*), and surface area ($y = 1.546x - 0.789$, $r^2 = 0.896$, $n = 47$; Fig. 3*c*) all had negative allometric relationships (slope <1 for length and width, slope <2 for surface area).

Experiment 2: elevated temperature effects

U_{crit} was 14.9% greater in fish acclimated to 24 °C (U_{crit} = 51.77 ± 1.93 cm·s^{-1}, TL = 357 ± 12 mm, wet weight = 203.6 ± 19.0 g, $n = 11$) compared with fish at 19 °C (U_{crit} = 45.14 ± 2.03 cm·s^{-1}, TL = 355 ± 11 mm, wet weight = 197.2 ± 17.6 g, $n = 11$, $p = 0.028$), rejecting our hypothesis of decreased swimming ability at 24 °C.

Chronically elevated temperatures (24 °C) caused an increase in hsp expression, a measure of the temperature-induced cellular stress response, in both muscle and fin tissue (representative gels shown in Allen 2005). Soluble dorsal muscle tissue samples from fish acclimated to 24 °C had significantly elevated hsp72, hsp78, and hsp90 levels, but not hsp60 (Fig. 4*a*). The membrane-associated portions of the dorsal muscle tissue samples had significantly elevated hsp72 levels, but not hsp90. Soluble pelvic fin tissue samples from fish acclimated to 24 °C had significantly elevated hsp72 and hsp78 levels, but not hsp60 and hsp90 (Fig. 4*b*). The membrane-associated portions of the pelvic fin tissue samples had significantly elevated hsp72, hsp78, and hsp90 levels.

Discussion

Changes in swimming performance (U_{crit}) with ontogeny

Most studies of swimming performance in juvenile sturgeons did not investigate changes in swimming performance with body length (Adams et al. 1999, 2003; McKenzie et al. 2001), assess anadromous species (Peake et al. 1995), or incorporate fish sizes smaller than those typifying seawater tolerance (Mayfield and Cech 2004). Our study provides the

Fig. 3. Relationships between juvenile green sturgeon (*Acipenser medirostris*) pectoral fin dimensions and total length (TL; mm), experiment 1, summer to early autumn fish. (*a*) For pectoral fin length (mm) to TL, the regression line represents the linear relationship $y = 0.664x - 0.046$ ($r^2 = 0.86$, $n = 47$ fish). (*b*) For pectoral fin width (mm) to TL, the regression line represents the linear relationship $y = 0.882x - 0.743$ ($r^2 = 0.89$, $n = 47$ fish). (*c*) For pectoral fin surface area (length × width; mm^2) to TL, the regression line represents the linear relationship $y = 1.546x - 0.789$ ($r^2 = 0.896$, $n = 47$ fish).

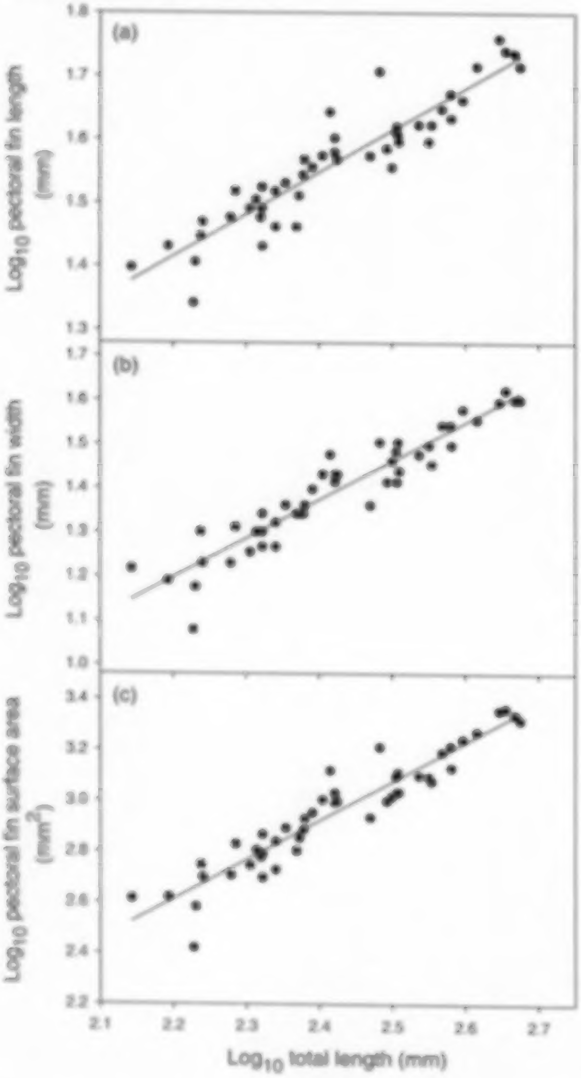

Fig. 4. Juvenile green sturgeon (*Acipenser medirostris*) soluble and membrane-bound (M) (*a*) muscle and (*b*) pelvic fin heat-shock proteins (hsps) with temperature, experiment 2. Data represent means + standard error (n = 15–16 for each hsp and temperature); asterisks represent significant differences (t test, $p < 0.05$) between temperatures, with each hsp analyzed separately.

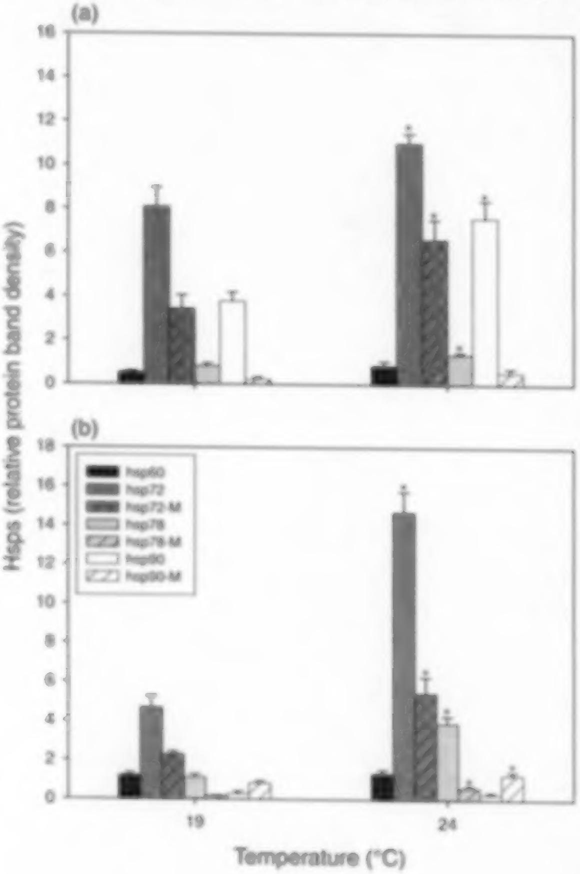

first information on the relationship between ontogeny interval and swimming ability in an anadromous sturgeon species. The relationship between U_{crit} and body size in juvenile green sturgeon is remarkable in how closely it parallels the onset of seawater tolerance (based on concurrent studies on the same cohort of fish). The positive relationship of U_{crit} with body size in smaller fish that could not tolerate seawater changed to a negative one at the same size at which fish were able to tolerate full-strength seawater (based on mean size of a group of fish with 100% survival in 34‰ seawater). Interestingly, Kynard et al. (2005) found that green sturgeon show a behavioral preference for downstream movement at 110–181 dph, which is similar to the ages (106–177 dph) of seawater-tolerant fish in our study.

In experiment 1, pooled mean U_{crit} (54.8 ± 1.9 cm·s^{-1}, n = 12) of winter fish was significantly greater than late summer – early autumn data for fish >266 mm TL (43.3 ± 1.5 cm·s^{-1}, n = 20). When plotted along with data from experiment 1 for fish ≤266 mm TL and with U_{crit} data for larger green sturgeon (Mayfield and Cech 2004), a steady increase in U_{crit} with TL ($y = 0.065x + 33.320$, $r^2 = 0.67$, $n = 79$) is apparent (Fig. 5). The comparatively greater swimming abilities of this winter group of fish fit much better with data from Mayfield and Cech (2004) on larger juvenile green sturgeon and with linear relationships seen in swimming abilities of other sturgeon (Peake et al. 1995) and salmonid species (Glova and McInerney 1977; Peake and McKinley 1998).

Fig. 5. Juvenile green sturgeon (*Acipenser medirostris*) relationship between U_{crit} and total length, excluding fish that are newly tolerant to seawater from the late summer to early autumn period: ●, summer fish with <100% seawater (SW) tolerance; ■, winter fish with 100% SW tolerance; ▲, fish from Mayfield and Cech (2004). The regression line represents the linear relationship $y = 0.065x + 33.320$ ($r^2 = 0.67$, $n = 79$).

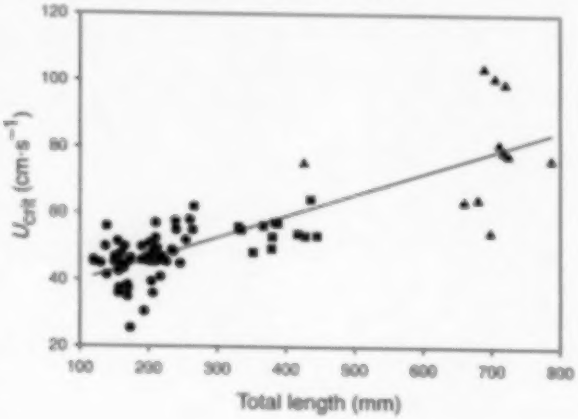

Katzman and Cech (2001) discussed a potential mechanism leading to changes in swimming performance related to endogenous changes during the PST. They found a thyroid hormone mediated developmental shift in mosaic locomotory muscle kinetics and a resulting depression in swimming performance in coho salmon (*Oncorhynchus kisutch*) smolts compared with parr. In fish of the same size, thyroid hormone (tri-iodothyronine, T_3) implanted smolts decreased U_{crit}, increased muscle twitch and tetanic contraction forces, and increased muscle contraction and relaxation rates compared with sham-implanted or control fish. They pointed out that the increased contraction and relaxation rates indicate an upregulation of fast-type fiber contractile proteins, which would probably promote burst swimming over sustained swimming and may be an adaptation for downstream migration in escaping cataracts or predators.

Although sustainable swimming ability is suggested to decrease during the PST based on these muscle tissue changes, evidence in wild or hatchery populations is lacking (Table 1). Smith (1982) proposed that a decrease in swimming performance aids in downstream migration by the inability to hold station in strong currents. However, the early studies used in support of this hypothesis by Thorpe and Morgan (1978) and Flagg and Smith (1982) were limited in that they did not demonstrate statistically significant decreases in swimming performance during the PST, based on studies on both parr and smolts. Furthermore, although several studies have suggested a plateau (Graham et al. 1996) or slight decrease in swimming or holding abilities associated with the time of smolting (Virtanen and Forsman 1987; Castleberry et al. 1991; Taylor and Foote 1991), none of these studies demonstrated statistically significant decreases in swimming ability. In contrast, there have been several studies that have shown a statistically significant increase in swimming ability during the time of the PST (Glova and McInerney 1977; Peake and McKinley 1998). These results support Hammer (1995), who in a review of swimming experiments found that the absolute (cm·s^{-1}) swimming ability of fish generally increases with length. Other studies on swimming during the PST have been designed for other purposes (Moore et al. 1990) and therefore did not compare parr–smolt swimming differences or had concurrent changes in temperature (Muir et al. 1994).

Likewise, studies contrasting the swimming ability of anadromous or downstream-migrating fishes with freshwater forms have generally found improved, not decreased, swimming performance. Taylor and Foote (1991) found that the anadromous form of sockeye salmon (*Oncorhynchus nerka*) had better swimming performance (U_{crit}) than the freshwater form (kokanee) at the same body sizes. Taylor and McPhail (1986) found that anadromous threespine sticklebacks (*Gasterosteus aculeatus*) had greater prolonged swimming abilities but slower maximum and mean burst swimming velocities than freshwater sticklebacks. Ellerby et al. (2001) found that catadromous, silver-phase (migrate to seawater) European eels (*Anguilla anguilla*) have a greater mass-specific power output of slow-twitch aerobic muscle fibers than similar-sized freshwater, yellow-phase eels, yielding more efficient swimming capabilities.

In our study, three factors were different between the late summer – early autumn fish and winter fish of experiment 1: cohort, age, and time of year. Any one of these differences could contribute to the observed U_{crit} differences, such as through endogenous thyroid hormone levels, as suggested by Katzman and Cech (2001). Age and time of year (seasonal cues) are known to influence thyroid hormone levels and migration propensity (reviews by Folmar and Dickhoff 1980; Hoar 1988; Hogasen 1998) in juvenile salmonids. Thyroid hormone levels were measured in the same cohort of fish concurrently with experiment 1 summer – early autumn fish, and a peak in plasma T_3 concentration was observed near the time of the depression in swimming performance (P.J. Allen and J.J. Cech, Jr., unpublished data). However, thyroid hormones were not measured during the winter runs. Late summer – early autumn experiment 1 fish may represent migrating fish and winter fish may represent nonmigratory fish based on the times of year when the two experiments were conducted and the juveniles' respective ages.

A second point of interest is the relationship of TBF with the PST. Webb et al. (1984) found that TBF increases linearly with water velocity and decreases with increasing TL at the same water velocity in rainbow trout (*Oncorhynchus mykiss*). However, Flagg and Smith (1982) found an increase in TBF (relative to body length) in coho salmon during the smolt stage, which decreased in postsmolts. Coughlin et al. (2001*a*) found decreased TBF (relative to body length) in older rainbow trout juveniles compared with parr that was related to a change in muscle fiber type and could be induced by the administration of thyroxine (T_4; Coughlin et al. 2001*b*). Ellerby et al. (2001) found that TBF increased in nonmigratory yellow-phase eels, compared with migratory silver-phase eels, to maintain the same swimming speeds by changes in muscle power output.

In our study, TBF increased with water velocity, which is similar to studies on juvenile Adriatic sturgeon (*A. naccarii*; McKenzie et al. 2001), juvenile lake sturgeon (*A. fulvescens*; Webb 1986), and shovelnose sturgeon (*Scaphirhynchus*

Table 1. Swimming ability during the parr–smolt transformation (PST).

Study	Species, source	Temperature (°C)	Swimming methods
Virtanen and Forsman 1987	Atlantic salmon (*Salmo salar*), W	10–12	50 cm·s^{-1}, 8 h
Moore et al. 1990	Atlantic salmon (*S. salar*), H	11–13.5	5 cm·s^{-1} every 10 min
Graham et al. 1996[a]	Atlantic salmon (*S. salar*), H	2–15	1 BL·s^{-1} every 60 min
Peake and McKinley 1998	Atlantic salmon (*S. salar*), W	12–20	Parr, 3 cm·s^{-1}; smolts, 6 cm·s^{-1} for 2, 5, or 10 min
Peake and McKinley 1998	Atlantic salmon (*S. salar*), W	12–20	Fixed velocity: 200 min
Glova and McInerney 1977	Coho salmon (*Oncorhynchus kisutch*), W	3–23	~6 cm·s^{-1} every 60 min
Katzman and Cech 2001[b]	Coho salmon (*O. kisutch*), H	19	10 cm·s^{-1} every 20 min
Castleberry et al. 1991[c]	Chinook salmon (*O. tshawytscha*), W	10–25	10 cm·s^{-1} every 5 min
Muir et al. 1994[d]	Chinook salmon (*O. tshawytscha*), H	4–12	15–26 cm·s^{-1} every 15 min
Taylor and Foote 1991	Sockeye salmon (*O. nerka*), 1G	10	~8–9 cm·s^{-1} every 60 min
This study (exp. 1, summer – early autumn)	Green sturgeon (*Acipenser medirostris*), 1G	19	10 cm·s^{-1} every 20 min
This study (exp. 1, summer and winter) and Mayfield and Cech 2004	Green sturgeon (*A. medirostris*), 1G	19	10 cm·s^{-1} every 20 min

Note: Data are either means ± standard error or a range based on information provided in the study. Abbreviations: W, wild; H, hatchery; 1G, first

[a] Graham et al. (1996) made holding not swimming measurements, data are for parr and smolts.

[b] Katzman and Cech (2001) "smolts" = parr + T_3 implant.

[c] Castleberry et al. (1991) data are for parr and smolts.

[d] Muir et al. (1994) results are not independent of temperature (parr, 4–5 °C; smolts, 10–12 °C).

platorynchus; Parsons et al. 2003). Our results did not support the findings of Flagg and Smith (1982) in relation to changes in TBF before and after seawater tolerance. Tail beat amplitude and body curvature has been noted to relate to swimming speed in sturgeon (Webb 1986; Long 1995); however, this was not investigated in our study.

McKenzie et al. (2001) found a decrease in Adriatic sturgeon VF at high water velocities, reflecting a partial shift to ram ventilation. We did not find this result in green sturgeon, possibly because we were only able to conduct measurements reliably up to a swimming velocity of 45 cm·s^{-1}.

Sturgeon actively use the posterior portions of their pectoral fins to control their body angle and initiate maneuvering movements in the water column (Wilga and Lauder 1999). Therefore, the larger pectoral fins, relative to TL, of the smaller juvenile green sturgeon should confer better station-holding ability in riverine life. Similarly, Pelis and McCormick (2003) found larger pectoral fins in parr compared with similar-sized smolts. In our experiments, the smaller fish used their pectoral fins to hold station (including propping) against water currents more often than did the larger fish. Several other sturgeon (Adams et al. 1997, 1999) and salmonid species (Arnold et al. 1991; Peake and McKinley 1998) have shown similar behavioral use of pectoral fins. As juvenile green sturgeon grow larger and move into seawater, large pectoral fins would presumably be less useful for station holding in currents. During steady horizontal swimming in sturgeon, pectoral fins are not used to generate lift (Wilga and Lauder 1999). Therefore, because green sturgeon from the San Francisco Estuary are known to migrate long distances (Miller 1972), large pectoral fins might be disadvantageous for extensive marine migratory movements because of increased drag. Webb (1986) noted that lake sturgeon have 3.5 times more drag per unit area than rainbow trout, and 18% less overall thrust. Thus, small decreases in drag from smaller (relative to fish TL) pectoral fins may improve swimming efficiencies, particularly when available thrust may be less than that of other migratory species. Our data supported this with negative allometric relationships with increasing TL for pectoral fin length, width, and surface area.

The most interesting behavior that was observed in small juvenile green sturgeon was rostral wedging. Fish would wedge their rostrum into the wire mesh in the front of the swim chamber to avoid swimming. Then they would tilt their bodies downward slightly using their pectoral fins to lever their rostrum into the mesh. Rostrally wedged fish (n = 11) were able to withstand water velocities far above their U_{crit}, as they were immediately impinged after losing their hold and, therefore, were not included in the data analyses. Perhaps the small green sturgeon have a behavioral propensity for wedging their rostrum into crevices or under rocks or debris in strong currents to avoid being swept downstream.

Elevated temperature effects

The effects of elevated temperatures during the time period when juvenile green sturgeon may be moving downriver are generally contrary to what was hypothesized. Green sturgeon exposed to a chronically elevated temperature (24 °C) actually increased in swimming performance compared with sturgeon acclimated to a lower temperature (19 °C). However, hsp expression did increase with temperature, showing a possible indirect relationship between these two measurements representing the whole-organism and cellular levels, respectively.

The increases in swimming speeds at 24 °C in juvenile green sturgeon are likely due to a complex interaction of fac-

Parr / pre-SW tolerant		Smolt / SW tolerant		
Length (cm)	Swimming ability (cm·s^{-1})	Length (cm)	Swimming ability (cm·s^{-1})	PST swimming relationship
13.3±1.5	All lasted 8 h	16.1±0.9	10 of 14 lasted 8h	Possibly decreasing
12.7–17.2	~69–108	12.2–18.9	~66–105	Not compared
5.7–12.5	~20–60			Possible plateau in smolts
4.8–13 FL	44–90	12.4–18 FL	76–164	Increasing
5–13.1 FL	53–86	13–17 FL	99–126	Increasing
Mean ~9.5 FL	~35–59	Mean ~11.5 FL	~40–63	Increasing
10.53±0.14 FL	Mean 77.7	10.23±1.6 FL	Mean 61.8	Decreasing
3–9 SL	~30–55			Plateau or decrease: 5–9 cm
10.2–17.6 FL	~24–80			Increasing
7.0–8.5 FL	60.1±0.52	8.6–10.0 FL	58.5±0.56	Plateau or slight decrease
12–26.6 TL	25.5–62	26.7–47.3 TL	54.5–26.5	Decreasing
12–26.6 TL	25.5–62	26.7–78.7 TL	48.3–103.9	Increasing

generation that is reared in captivity; SW, seawater; T_3, tri-iodothyronine; SL, standard length; FL, fork length; TL, total length; BL, body length.

tors (Taylor et al. 1997). Johnston and Ball (1997) noted that swimming speeds usually increase with temperature up to a species' thermal tolerance limit, at which performance declines. Therefore, juvenile green sturgeon of the ages and sizes studied clearly tolerate 24 °C. This conclusion is supported by increased growth rates at 24 °C compared with at 19 °C in post-yolk-sac juvenile green sturgeon that were fed ad libitum, showing that the fish were not overly stressed (Allen et al. 2006). In juvenile shovelnose and pallid (*Scaphirhynchus albus*) sturgeons, Adams et al. (2003) found increased U_{crit} at 20 °C compared with at 10 °C. Interestingly, Mayfield and Cech (2004) found that swimming performance in older (age-1) juvenile green sturgeon decreased at 24 °C and that fish were severely stressed at these temperatures. They also found that metabolic costs (Mo_2) increased between 19 and 24 °C but not between 11 and 19 °C. It is possible that juvenile green sturgeon of the ages and sizes studied in this experiment can perform at an increased level at warm summer river temperatures compared with larger fish, despite the increase in energy costs, if ample rations are available.

The increased metabolic costs that Mayfield and Cech (2004) found between 24 and 19 °C may be partly accounted for by increases in hsp production. In our experiment, the increased hsps in both muscle and pelvic fin tissues indicated that the chronically high temperature (24 °C) caused some temperature-related cellular stress (Iwama et al. 1998, 1999). It is interesting that hsp levels were elevated after the long-term (2.5–5 weeks) 24 °C temperature exposure, as compared with the more typical acute temperature exposures used in most hsp studies. Viant et al. (2003) observed a transient (3 day) increase of hsp72 in steelhead trout parr exposed for several weeks to 20 °C, a temperature that is not acutely stressful, and concluded that hsp72 remained elevated until other temperature adaptation mechanisms could be activated. Podrabsky and Somero (2004) found that hsp70 and hsp90 tended to be more responsive to longer-term temperature elevations, whereas smaller hsps tended to be more responsive to fluctuating temperatures. Perhaps the difference in hsp levels between the temperature treatments is more reflective of an hsp expression Q_{10} between temperatures. Because hsps remained elevated throughout the exposure period, this may indicate that juvenile green sturgeon are unable to adapt, needing increased hsp synthesis to counteract the damaging effects of high temperature. Finally, because the temperature-related differences in hsps were comparable between muscle tissue and pelvic fin clips, our results suggest that hsp studies could be incorporated into field sampling using the much less invasive pelvic fin clips, provided immediate and rapid freezing of samples is accomplished (i.e., dry ice or liquid N_2).

In conclusion, U_{crit} studies are most relevant in simulating conditions that riverine fishes might experience (Plaut 2001). As juvenile green sturgeon develop, U_{crit} increases until fish reach the size at which they can tolerate seawater. Once fish reach this size, U_{crit} either decreases or continues to increase, depending on time of year, age, and related thyroid hormone levels. Decreases in U_{crit} during this time may facilitate downstream movements, although juvenile green sturgeon movements have not been investigated in relation to seasonally peaking flow rates or freshets. Comparison with swimming abilities in developing anadromous salmonids during the PST reveals that some studies have only demonstrated trends for decreasing U_{crit}, whereas others have shown a steady increase in swimming abilities during this developmental period. The evidence from recent studies on thyroid hormone effects on muscle development and swimming abilities during these life stages indicates that further research on both salmonid and nonsalmonid anadromous species is needed.

Juvenile green sturgeon clearly have morphological and behavioral adaptations to riverine life, with relative pectoral fin surface areas decreasing as fish grow larger and the presence of behaviors such as rostral wedging. Juvenile green sturgeon responded to warmed (24 °C) conditions with increased U_{crit}, despite increased hsp production. Management or protection efforts for green sturgeon should thus consider effects of changing seasonal flow rates and water temperature.

Acknowledgements

We thank the Yurok Tribal Council and the Yurok Fisheries Program for broodstock fish; S. Doroshov, J. Van Eenennaam, and J. Linares-Casenave for providing larval fish from the broodstock; P. Lutes for facility assistance and recommendations; T. Allen, C. Woodley, and J. Zamora for technical assistance and insight; R. Mayfield for the use of his swimming performance data; S. Doroshov, P. Moyle, D. Kültz, and two anonymous reviewers for providing constructive comments in the review of this manuscript; and the California Bay-Delta Authority (grant no. ERP-02D-P57), the Anadromous Fish Restoration Program (US Fish and Wildlife Service, US Bureau of Reclamation; grant no. 11332-1-G005), the University of California Agricultural Experiment Station (grant no. 3455-H to JJC), Marin Rod and Gun Club, Granite Bay Flycasters, and the California Federation of FlyFishers for financial assistance.

References

Adams, S.R., Parsons, G.R., Hoover, J.J., and Killgore, K.J. 1997. Observations of swimming ability in shovelnose sturgeon (*Scaphirhynchus platorynchus*). J. Freshw. Ecol. **12**: 631–633.

Adams, S.R., Hoover, J.J., and Killgore, K.J. 1999. Swimming endurance of juvenile pallid sturgeon, *Scaphirhynchus albus*. Copeia, 1999(3): 802–807.

Adams, S.R., Adams, G.L., and Parsons, G.R. 2003. Critical swimming speed and behavior of juvenile shovelnose sturgeon and pallid sturgeon. Trans. Am. Fish. Soc. **132**: 392–397.

Allen, P.J. 2005. Seawater adaptation in juvenile green sturgeon, *Acipenser medirostris*. Ph.D. dissertation, University of California at Davis, Davis, California.

Allen, P.J., Nicholl, M., Cole, S., Vlazny, A., and Cech, J.J., Jr. 2006. Growth of larval to juvenile green sturgeon in elevated temperature regimes. Trans. Am. Fish. Soc. **135**: 89–96.

Arnold, G.P., Webb, P.W., and Holford, B.H. 1991. The role of the pectoral fins in station-holding of Atlantic salmon parr (*Salmo salar* L.). J. Exp. Biol. **156**: 625–629.

Bartholow, J.M. 2005. Recent water temperature trends in the lower Klamath River, California. N. Am. J. Fish. Manag. **25**: 152–162.

Beamish, F.W.H. 1978. Swimming capacity. *In* Fish physiology. Vol. VII. *Edited by* W.S. Hoar and D.J. Randall. Academic Press, Inc., New York. pp. 101–187.

Bell, W.H., and Terhune, L.D.B. 1970. Water tunnel design for fisheries research. Fish. Res. Board Can. Tech. Rep. No. 195. pp. 1–69.

Brett, J.R. 1964. The respiratory metabolism and swimming performance of young sockeye salmon. J. Fish. Res. Board Can. **21**: 1183–1226.

Castleberry, D.T., Cech, J.J., Jr., Saiki, M., and Martin, B.A. 1991. Growth, condition and physiological performance of juvenile salmonids from the lower American River: February through June 1991. University of California at Davis, US Fish and Wildlife Service, National Fisheries Research Contaminant Center, Dixon, California.

Coughlin, D.J., Burdick, J., Stauffer, K.A., and Weaver, F.E. 2001*a*. Rainbow trout display a developmental shift in red muscle kinetics, swimming kinematics and myosin heavy chain isoform. J. Fish Biol. **58**: 701–715.

Coughlin, D.J., Forry, J.A., McGlinchey, S.M., Mitchell, J., Saporetti, K.A., and Stauffer, K.A. 2001*b*. Thyroxine induces transitions in red muscle kinetics and steady swimming kinematics in rainbow trout (*Oncorhynchus mykiss*). J. Exp. Zool. **290**: 115–124.

Ellerby, D.J., Spierts, I.L., and Altringham, J.D. 2001. Slow muscle power output of yellow- and silver-phase European eels (*Anguilla anguilla* L.): changes in muscle performance prior to migration. J. Exp. Biol. **204**: 1369–1379.

Erickson, D.L., North, J.A., Hightower, J.E., Weber, J., and Lauck, L. 2002. Movement and habitat use of green sturgeon *Acipenser medirostris* in the Rogue River, Oregon, USA. J. Appl. Ichthyol. **18**: 565–569.

Flagg, T.A., and Smith, L.S. 1982. Changes in swimming behavior and stamina during smolting of coho salmon. *In* Proceedings of the Salmon and Trout Migratory Behavior Symposium, Seattle, Washington. 3–5 June 1981. *Edited by* E.L. Brannon and E.O. Salo. School of Fisheries, University of Washington, Seattle, Wash. pp. 191–195.

Folmar, L.C., and Dickhoff, W.W. 1980. The parr–smolt transformation (smoltification) and seawater adaptation in salmonids: a review of selected literature. Aquaculture, **21**: 1–38.

Glova, G.L., and McInerney, J.E. 1977. Critical swimming speeds of coho salmon (*Oncorhynchus kisutch*) fry to smolt stages in relation to salinity and temperature. J. Fish. Res. Board Can. **34**: 151–154.

Graham, W.D., Thorpe, J.E., and Metcalfe, N.B. 1996. Seasonal current holding performance of juvenile Atlantic salmon in relation to temperature and smolting. Can. J. Fish. Aquat. Sci. **53**: 80–86.

Hammer, C. 1995. Fatigue and exercise tests with fish. Comp. Biochem. Physiol. A, **112**: 1–20.

Handeland, S.O., Wilkinson, E., Sveinsbo, B., McCormick, S.D., and Stefansson, S.O. 2004. Temperature influence on the development and loss of seawater tolerance in two fast-growing strains of Atlantic salmon. Aquaculture, **233**: 513–529.

Hoar, W.S. 1988. The physiology of smolting salmonids. *In* Fish physiology. Vol. XI. *Edited by* W.S. Hoar and D.J. Randall. Academic Press, Inc., San Diego, California. pp. 275–343.

Hogasen, H.R. 1998. Physiological changes associated with the diadromous migration of salmonids. NRC Research Press, Ottawa, Ontario.

Iwama, G.K., Thomas, P.T., Forsyth, R.B., and Vijayan, M.M. 1998. Heat shock protein expression in fish. Rev. Fish Biol. Fish. **8**: 35–56.

Iwama, G.K., Vijayan, M.M., Forsyth, R.B., and Ackerman, P.A. 1999. Heat shock proteins and physiological stress in fish. Am. Zool. **39**: 901–909.

Iwama, G.K., Afonso, L.O.B., Todgham, A., Ackerman, P., and Nakano, K. 2004. Are hsps suitable for indicating stressed states in fish? J. Exp. Biol. **207**: 15–19.

Johnston, I.A., and Ball, D. 1997. Thermal stress and muscle function in fish. *In* Global warming: implications for freshwater and marine fish. *Edited by* C.M. Wood and D.G. McDonald. Cambridge University Press, New York. pp. 79–104.

Katzman, S., and Cech, J.J. 2001. Juvenile coho salmon locomotion and mosaic muscle are modified by *3′,3′,5′*-tri-iodo-L-thyronine (T_3). J. Exp. Biol. **204**: 1711–1717.

Kynard, B., Parker, E., and Parker, T. 2005. Behavior of early life intervals of Klamath River green sturgeon, *Acipenser medirostris*, with a note on body color. Environ. Biol. Fishes, **72**: 85–97.

Long, J.H. 1995. Morphology, mechanics, and locomotion: the relation between the notochord and swimming motions in sturgeon. Environ. Biol. Fishes, **44**: 199–211.

Marine, K.R., and Cech, J.J., Jr. 2004. Effects of high water temperature on growth, smoltification, and predator avoidance in juvenile Sacramento River Chinook salmon. N. Am. J. Fish. Manag. **24**: 198–210.

Mayfield, R.B., and Cech, J.J., Jr. 2004. Temperature effects on green sturgeon bioenergetics. Trans. Am. Fish. Soc. **133**: 961–970.

McCormick, S.D., Shrimpton, J.M., Moriyama, S., and Bjornsson, B.T. 2002. Effects of an advanced temperature cycle on smolt development and endocrinology indicate that temperature is not a zeitgeber for smolting in Atlantic salmon. J. Exp. Biol. **205**: 3553–3560.

McKenzie, D.J., Cataldi, E., Romano, P., Owen, S.F., Taylor, E.W., and Bronzi, P. 2001. Effects of acclimation to brackish water on the growth, respiratory metabolism, and swimming performance of young-of-the-year Adriatic sturgeon (*Acipenser naccarii*). Can. J. Fish. Aquat. Sci. **58**: 1104–1112.

Miller, L.W. 1972. Migrations of sturgeon tagged in the Sacramento – San Joaquin estuary. Calif. Fish Game, **58**: 102–106.

Moore, A., Russell, I.C., and Potter, E.C.E. 1990. The effects of intraperitoneally implanted dummy acoustic transmitters on the behaviour and physiology of juvenile Atlantic salmon, *Salmo salar* L. J. Fish Biol. **37**: 713–721.

Moyle, P.B. 1994. The decline of anadromous fishes in California. Conserv. Biol. **8**: 869–870.

Moyle, P.B. 2002. Inland fishes of California. University of California Press, Berkeley, California.

Muir, W.D., Giorgi, A.E., and Coley, T.C. 1994. Behavioral and physiological changes in yearling chinook salmon during hatchery residence and downstream migration. Aquaculture, **127**: 69–82.

Neter, J., Kutner, M.H., Nachtsheim, C.J., and Wasserman, W. 1996. Applied linear statistical models. 4th ed. WCB McGraw-Hill, Boston, Massachusetts.

Parsons, G.R., Hoover, J.J., and Killgore, K.J. 2003. Effect of pectoral fin ray removal on station-holding ability of shovelnose sturgeon. N. Am. J. Fish. Manag. **23**: 742–747.

Peake, S., and McKinley, R.S. 1998. A re-evaluation of swimming performance in juvenile salmonids relative to downstream migration. Can. J. Fish. Aquat. Sci. **55**: 682–687.

Peake, S., Beamish, F.W.H., McKinley, R.S., Katopodis, C., and Scruton, D.A. 1995. Swimming performance of Lake Sturgeon, *Acipenser fulvescens*. Can. Tech. Rep. Fish. Aquat. Sci. No. 2063.

Peake, S.J. 2004. Swimming and respiration. *In* Sturgeons and paddlefish of North America. *Edited by* G.T.O. LeBreton, F.W.H. Beamish, and R.S. McKinley. Kluwer Academic Publishers, Dordrecht, Netherlands. pp. 147–166.

Pelis, R.M., and McCormick, S.D. 2003. Fin development in stream- and hatchery-reared Atlantic salmon. Aquaculture, **220**: 1–4.

Plaut, I. 2001. Critical swimming speed: its ecological relevance. Comp. Biochem. Physiol. A, **131**: 41–50.

Podrabsky, J.E., and Somero, G.N. 2004. Changes in gene expression associated with acclimation to constant temperatures and fluctuating daily temperatures in an annual killifish *Austrofundulus limnaeus*. J. Exp. Biol. **207**: 2237–2254.

Sall, J., Lehman, A., and Creighton, L. 2001. JMP Start Statistics: a guide to statistics and data analysis using JMP and JMPIN software. 2nd ed. SAS Institute Inc., Cary, N.C.

Smith, L.S. 1982. Decreased swimming performance as a necessary component of the smolt migration in the Columbia River. Aquaculture, **28**: 153–161.

Taylor, E.B., and Foote, C.J. 1991. Critical swimming velocities of juvenile sockeye salmon and kokanee, the anadromous and non-anadromous forms of *Oncorhynchus nerka* (Walbaum). J. Fish Biol. **38**: 407–419.

Taylor, E.B., and McPhail, J.D. 1986. Prolonged and burst swimming performance in anadromous and freshwater threespine stickleback, *Gasterosteus aculeatus*. Can. J. Zool. **64**: 416–420.

Taylor, E.B., Egginton, S., Taylor, S.E., and Butler, P.J. 1997. Factors which may limit swimming performance at different temperatures. *In* Global warming: implications for freshwater and marine fish. *Edited by* C.M. Wood and D.G. McDonald. Cambridge University Press, New York. pp. 105–133.

Thorpe, J.E., and Morgan, R.I.G. 1978. Periodicity in Atlantic salmon *Salmo salar* L. smolt migration. J. Fish Biol. **12**: 541–548.

US Geological Survey. 2004. Klamath River temperature data. *In* National Weather Information Service surface web data for California. Available online at http://nwis.waterdata.usgs.gov/ca/nwis.

Van Eenennaam, J.P., Webb, M.A.H., Deng, X., Doroshov, S.I., Mayfield, R.B., Cech, J.J., Jr., Hillemeier, D.C., and Willson, T.E. 2001. Artificial spawning and larval rearing of Klamath River green sturgeon. Trans. Am. Fish. Soc. **130**: 159–165.

Van Eenennaam, J.P., Linares-Casenave, J., Deng, X., and Doroshov, S.I. 2005. Effect of incubation temperature on green sturgeon embryos, *Acipenser medirostris*. Environ. Biol. Fishes, **72**: 145–154.

Viant, M.R., Werner, I., Rosenblum, E.S., Gantner, A.S., Tjeerdema, R.S., and Johnson, M.L. 2003. Correlation between heat-shock protein induction and reduced metabolic condition in juvenile steelhead trout (*Oncorhynchus mykiss*) chronically exposed to elevated temperature. Fish Physiol. Biochem. **29**: 159–171.

Virtanen, E., and Forsman, L. 1987. Physiological responses to continuous swimming in wild salmon (*Salmo salar* L.) parr and smolt. Fish Physiol. Biochem. **4**: 157–163.

Webb, P.W. 1986. Kinematics of lake sturgeon, *Acipenser fulvescens*, at cruising speeds. Can. J. Zool. **64**: 2137–2141.

Webb, P.W., Kostecki, P.T., and Stevens, E.D. 1984. The effect of size and swimming speed on locomotor kinematics of rainbow trout. J. Exp. Biol. **109**: 77–95.

Werner, I., Koger, C.S., Hamm, J.T., and Hinton, D.E. 2001. Ontogeny of the heat shock protein, hsp70 and hsp60, response and developmental effects of heat-shock in the teleost, medaka (*Oryzias latipes*). Environ. Sci. **8**: 13–30.

Wilga, C.D., and Lauder, G.V. 1999. Locomotion in sturgeon: function of the pectoral fins. J. Exp. Biol. **202**: 2413–2432.

Wolter, C., and Arlinghaus, R. 2003. Navigation impacts on freshwater fish assemblages: the ecological relevance of swimming performance. Rev. Fish Biol. Fish. **13**: 68–89.

Population structure and divergence using microsatellite and gene locus markers in Chinook salmon (*Oncorhynchus tshawytscha*) populations

Daniel D. Heath, J. Mark Shrimpton, Russell I. Hepburn, Sara K. Jamieson, Sarah K. Brode, and Margaret F. Docker

Abstract: Using different classes of genetic markers can provide insight into the role of selection, as well as a broader context for identifying population differentiation. We used nine microsatellite loci and polymorphisms at eight gene loci (major histocompatibility complex (MHC) classes I and II, growth hormones 1 and 2, transferrin, and immunoglobin heavy-chain) to determine population structure in six coastal populations (Vancouver Island, VI) and five interior populations (Fraser River, FR) of Chinook salmon (*Oncorhynchus tshawytscha*) in British Columbia, Canada. F_{ST} and G'_{ST} values for specific VI gene loci were significantly higher than those for the FR and VI microsatellite loci or the FR gene loci. Pairwise microsatellite F_{ST} values were correlated with geographic distance across regions, but not using the gene locus marker data. Neighbor-joining cluster analyses showed one VI population as particularly divergent based on the gene locus data, while the VI and FR microsatellite locus and the FR gene locus analyses yielded no anomalous population divergence. The VI MHC class II marker F_{ST} values were exceptionally high, indicative of probable directional selection acting on MHC class II. Our results are consistent with local adaptation in Chinook salmon, but the nature of the local adaptation likely differs among regions.

Résumé : L'utilisation de différentes classes de morqueurs génétiques ouvre des perspectives sur le rôle de la sélection et fournit un contexte élargi pour l'identification de la différenciation des populations. Nous avons étudié neuf locus microsatellites ainsi que le polymorphisme à huit locus géniques (complexe majeur des histocompatibilité (MHC) classes I et II, hormones de croissance 1 et 2, transferrine et chaine lourde de l'immunoglobine) afin de déterminer la structure génétique de six populations côtières (île de Vancouver, VI) et de cinq populations de l'intérieur (fleuve Fraser, FR) de saumons quinnat (*Oncorhynchus tshawytscha*) en Colombie-Britannique, Canada. Les valeurs de F_{ST} et de G'_{ST} des locus géniques spécifiques VI sont significativement plus élevées que celles des microsatellites FR et VI et des locus géniques FR. Les valeurs paire par paire de F_{ST} des microsatellites sont en corrélation avec la distance géographique d'une région à une autre, mais ce n'est pas le cas des données des marqueurs des locus géniques. Des analyses de groupement avec fusion des groupes voisins montrent qu'une population VI est particulièrement divergente d'après ses données de locus géniques, alors que les analyses des microsatellites VI et FR et des locus géniques FR n'indiquent aucune divergence exceptionnelle de population. Les valeurs F_{ST} des marqueurs MHC de classe II de VI sont particulièrement élevées, ce qui indique qu'il y a probablement une sélection directionnelle qui agit sur les MHC de classe II. Nos résultats sont compatibles avec une adaptation locale chez le saumon quinnat, mais la nature de cette adaptation locale varie vraisemblablement d'une région à l'autre.

[Traduit par la Rédaction]

Introduction

Given barriers to gene flow, populations and species may genetically diverge through mutation, drift, or selection. Although the early controversy over drift versus selection as the driving force behind genetic divergence has not been completely resolved, current interests focus on partitioning the contribution of drift versus selection (Miller et al. 2001; Ford 2002). Although a vast number of studies of population genetic differentiation have been published, most used only neutral (or assumed neutral) markers. The employment of presumed neutral markers (such as microsatellite loci or synonymous substitutions; but see Li et al. 2004) is clearly indicated if the analysis assumes drift as the primary mechanism

Received 24 May 2005. Accepted 20 February 2006. Published on the NRC Research Press Web site at http://cjfas.nrc.ca on 13 May 2006.
J18704

D.D. Heath,[1] **R.I. Hepburn, S.K. Jamieson, S.K. Brode, and M.F. Docker.** Great Lakes Institute for Environmental Research, and the Department of Biological Sciences, University of Windsor, 401 Sunset Avenue, Windsor, ON N9B 3P4, Canada.
J.M. Shrimpton. Biology Program, University of Northern British Columbia, 3333 University Way, Prince George, BC V2N 4Z9, Canada.

[1] Corresponding author (e-mail: dheath@uwindsor.ca).

Can. J. Fish. Aquat. Sci. **63**: 1370–1383 (2006)   doi:10.1139/F06-044

for divergence (e.g., determining reproductive isolation, effective population size, or number of migrants; Beaumont and Nichols 1996). However, neutral markers by themselves are of limited value for determining potential functional divergence among populations (Miller et al. 2001). Thus a simultaneous evaluation of both neutral marker and functional gene-coding polymorphisms is the ideal solution for partitioning the effects of isolation (drift) and functional divergence (selection). Until quite recently, such an approach was constrained by our limited knowledge of possible candidate genes that were a priori expected to show selective effects in organisms of conservation and evolutionary interest (i.e., not genetic "model species"; see Vasemägi and Primmer 2005). Given recent advances in vertebrate genome research, those constraints are no longer a serious limitation for studies of functional genetic divergence and evolution (Vasemägi and Primmer 2005).

The role of drift versus selection has been investigated at a number of known-function loci, primarily through sequence analysis among species, and many of those loci show evidence of positive selection (see Ford 2002). Ford (2002) identified nine classes of functional loci that appear to have undergone positive selective effects, based on the ratio of synonymous to nonsynonymous substitutions. Although selecting candidate loci based on the expectation of adaptive significance is a reasonable approach for studies of gene-level selection, finding among-population coding polymorphisms at such loci can be logistically difficult. One alternative is to use noncoding polymorphisms (e.g., intron sequence variation or expressed sequence tag (EST)-linked microsatellite DNA) that are closely linked to gene-coding regions (Vasemägi et al. 2005). The available level of polymorphism for such markers is much higher than for true coding polymorphisms, but they can still reflect recent selection effects via their tight linkage with coding regions (Vasemägi and Primmer 2005; Vasemägi et al. 2005). We refer to our intron and coding region polymorphisms as gene locus markers, since they are polymorphisms at known-function gene loci.

We chose candidate gene loci for this study based on the expectation for potentially high levels of population-specific selective effects and hence genetic divergence and local adaptation. Polymorphisms in the peptide-binding regions of the major histocompatibility complex (MHC) genes have been shown to be under the effects of selection in a variety of organisms, including salmonids (Landry and Bernatchez 2001; Miller et al. 2001; Wegner et al. 2003). Since MHC diversity is directly related to the breadth of the specific immune response as the basis for antigen recognition, it is not surprising that MHC has been shown to be under strong selection for diversity (Landry and Bernatchez 2001; Miller et al. 2001; Wegner et al. 2003). Although less frequently reported than diversifying selection, MHC genes may also be under selection for specific alleles (Miller et al. 1997, 2001, 2004; Grimholt et al. 2003; Wegner et al. 2003). Similarly, other immune function-related genes would be expected to be highly sensitive to selective effects (Ford 2002). The other immune function-related marker loci we chose for this study have also been shown to play a role in pathogen challenge survival, although the supporting evidence is not as consistent as that for the MHC class II. Despite a demonstrated relationship between transferrin genotype and resistance to bacterial infection (e.g., Winter et al. 1980), presumably because of the nonspecific, antibacterial function of transferrin's iron-binding properties (Hirst and Ellis 1996), there have only been a few studies reporting genotype differences among populations of salmon (e.g., Van Doornik et al. 1996) and some evidence for selective effects on transferrin gene sequence (Ford 2000, 2001). Although there have been, to our knowledge, no reports of selective effects on the immunoglobin heavy-chain (IgH) genes in salmon, Moran et al. (1997) reported strong population divergence among 11 populations of Chinook salmon. Thus we included both IgH and transferrin gene locus markers in the present study.

Genes related to critical life history parameters (such as growth or reproduction) are also expected to experience selection; however, the intensity of selection would likely be less, since selection at such loci would act indirectly via selection on phenotypic life history variation in diverse environments. Differences among populations of salmon in both freshwater and saltwater growth rates are well known (Groot and Margolis 1991); however, such differences are probably strongly affected by environmental factors. Although we are aware of no studies on population-level selection or divergence at the growth hormone (GH) genes in salmon, differences in growth patterns among populations have been identified as adaptive, and thus selection is implied. Since Moran et al. (1997) reported a very high F_{ST} value (0.53) based on GH-2 intron D RFLP data from 11 populations of Chinook salmon, we included both GH-1 and GH-2 gene loci in the present study.

Despite a very large body of published studies of population genetic divergence among salmonid populations, only recently have researchers attempted to partition the observed divergence into drift versus selective effects, despite the strong expectation for local adaptation in philopatric salmon populations (Taylor 1991; Adkinson 1995; Waples et al. 2004). The expectation for functional genetic differences among populations of salmonids is further strengthened as a result of the diverse environments and life history patterns observed among populations within a species (Adkinson 1995; Waples et al. 2004). Coastal and interior life histories in Chinook salmon (*Oncorhynchus tshawytscha*) have been well documented (see Groot and Margolis 1991; Waples et al. 2004), and some of the differences have been shown to have an additive genetic component (see Waples et al. 2004). Populations of Chinook salmon inhabiting such diverse environments and displaying diverse life histories are likely to have experienced quite different selective pressures.

Here we report an analysis of genetic structure among 11 populations of Chinook salmon taken from two different regions of British Columbia, Canada. We determine population structure and differentiation using both microsatellite and gene locus markers at immune function (MHC, transferrin, and immunoglobin heavy-chain) and growth-related (GH-1 and GH-2) loci. The "neutral" markers used here are strictly speaking presumed neutral, since microsatellite loci can occur within (or, in linkage disequilibrium, with) coding regions (e.g., Vasemägi et al. 2005) and hence may respond to selection pressures (see Li et al. 2004). On the other hand,

Fig. 1. Map of southern British Columbia and Vancouver Island, with the location of the six Vancouver Island and five upper Fraser River populations marked. Vancouver Island populations: NR, Nimpkish River; SR, Salmon River; QR, Quinsam River; PF, Puntledge River (Fall run); PS, Puntledge River (Summer run); BQ, Big Qualicum River. Fraser River populations: NcR, Nechatko River; StR, Stuart River; WR, Willow River; DC, Dome Creek; BR, Bowron River.

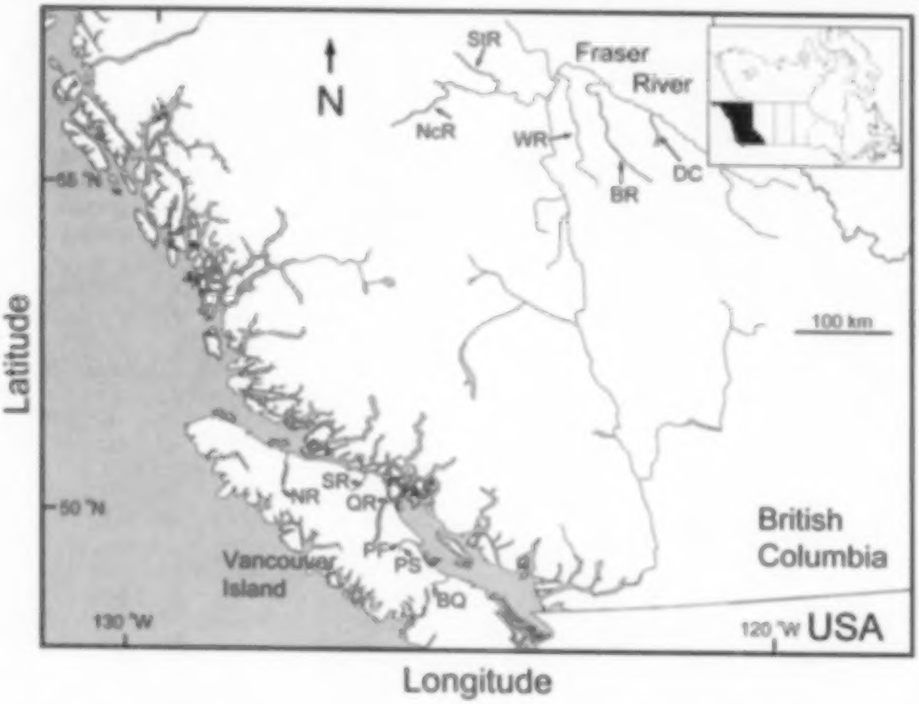

our gene locus markers include true coding polymorphisms (MHC) as well as intron-based polymorphisms that are closely linked to functional coding regions, but are not directly functional. The Chinook salmon populations in this study are from Vancouver Island (VI, six populations) and from tributaries of the upper Fraser River (FR, five populations); all were colonized approximately 10 000 – 14 000 years ago after the last glaciation (see Ford 1998). The VI populations are coastal and thus have a short freshwater–saltwater migration distance, coupled with an ocean-type juvenile life history (i.e., short freshwater residency; Groot and Margolis 1991; Waples et al. 2004). The FR tributary populations are interior and thus have a long migration distance, coupled with a stream-type juvenile life history (i.e., long freshwater residency; Groot and Margolis 1991; Waples et al. 2004). There are also profound environmental differences between the two regions. We chose our gene locus markers to maximize the likelihood of detecting evidence for selection, since growth and immune function genes are expected to be under strong selection in anadromous, semelparous salmon populations. Specifically, we expected that the MHC classes I and II (MHC-I and MHC-II, respectively) markers would show high levels of population structure and divergence (e.g., Landry and Bernatchez 2001; Miller et al. 1997, 2001) relative to the presumed neutral microsatellite markers, while the intron-based immune function and growth-related markers would show an intermediate level of genetic divergence. Furthermore, we predicted that the pattern would be independent of life history or environmental differences, since diversifying selection should act within populations across the species range; thus we expected to see similar patterns of divergence among populations in both of the sampled regions.

Materials and methods

Sampling

Six populations of VI Chinook salmon and five populations in tributaries of the upper FR, British Columbia, (Fig. 1) were sampled between 1988 and 1992. (VI populations were all sampled in 1989.) All fish were sampled as sexually mature adults during the peak of the return distribution; either blood (VI) or scale (FR) samples were collected. Fish from the Puntledge River system (VI) form two separate subpopulations (Summer and Fall runs), based on the timing of their return migration. These two groups are managed as separate populations and utilize different areas of the river for spawning; however, there is some question of the validity of the designation of these two runs as separate populations. The Puntledge River populations have received egg and fry transfers over multiple years, primarily from the Big Qualicum River, but also from the Quinsam River. The Salmon River received minimal egg transfer from the Quinsam River in 1981 and 1988. There are no recorded transfers to the Nimpkish River or any of the FR populations.

DNA extraction and marker application

DNA was extracted from blood and scale samples from 30–52 individuals per population using proteinase K digestion followed by phenol–chloraform–isoamyl alcohol extraction and salt precipitation. Two classes of markers were applied to the DNA samples. The neutral markers are published microsatellite DNA markers, optimized for use in Chinook salmon (Olsen et al. 1996; O'Reilly et al. 1996; Scribner et al. 1996; Nelson and Beacham 1999; Banks et al. 1999; Olsen and Bentzen 2000; Williamson et al. 2002). We used a total of 13 loci, five of which were used in both the VI and FR populations (Ots104 (VI & FR), Ots4 (VI & FR), Ots1 (FR), Ots3 (FR), Omy207 (FR), OtsG3 (VI), OtsG311 (VI), Omy325 (VI & FR), Sfo8 (VI), One114 (VI), Ssa85 (VI & FR), Oneu3 (FR), Ssa197 (VI & FR)). The optimized polymerase chain reaction (PCR) conditions determined for Chinook salmon were as follows: a 1 min denaturation step (94 °C), followed by 35 cycles of a 1 min denaturation step (94 °C), a 1 min annealing step (50 °C — Ots3, Sfo8; 52 °C — Ots4, Ots1, Omy207, Oneu3, Ssa197, One114; 54 °C — Ots104, OtsG3, OtsG311; 56 °C — Omy325, Ssa85), and a 1.5 min extension step (72 °C). Each 25 µL reaction contained 2.5 µL of 10× reaction buffer (100 $\text{mmol}\cdot\text{L}^{-1}$ Tris–HCl pH 8.4, 500 $\text{mmol}\cdot\text{L}^{-1}$ KCl, 15 $\text{mmol}\cdot\text{L}^{-1}$ $MgCl_2$), 2.5 $\text{mmol}\cdot\text{L}^{-1}$ $MgCl_2$, 0.1 $\text{mmol}\cdot\text{L}^{-1}$ each dNTP, 2.0 $\mu\text{mol}\cdot\text{L}^{-1}$ of each primer, 1.0 µL of the extracted DNA, 1.0 U (1 U = 16.67 nkat) *Taq* polymerase (GIBCO BRL, Gaithersburg, Maryland), and ddH_2O to make up the 25 µL reaction volume. The forward primer for all PCR was dye-labeled, and the resulting dye-labeled, amplified fragments were run on an automated sequencer (Beckman Coulter Inc., Fullerton, California, or Visible Genetics, Toronto, Ontario) with appropriate size standards.

The gene locus markers are based on both intron (IgH, GH-1 and GH-2, and transferrin) and coding region (MHC-I and MHC-II) polymorphisms, and all are restriction fragment length polymorphisms (RFLPs). For IgH, amplification and restriction digest protocols followed those described in Moran et al. (1997); GH-1, GH-2, transferrin, and MHC-II PCR–RFLP protocols are described in Docker and Heath (2002); and the MHC-I markers were developed for this project (see below). The MHC-II markers are situated within a common amplified fragment; one (*Rsa*I) represents a nonsynonymous substitution in the putative peptide-binding region, and the second RFLP (*Dde*I) detects polymorphisms at a synonymous site that was always linked to a nonsynonymous substitution in the next codon.

The two novel MHC-I markers are situated in the A1 domain of the MHC-I gene, which was initially amplified using primers described in Miller et al. (1997) following PCR conditions described in Docker and Heath (2002) for MHC-II (primer annealing temperatures of 58, 55, and 52 °C for 10, 10, and 20 cycles, respectively). PCR product from 21 Chinook salmon was cloned into pBluescript SK(+) vector, and we sequenced 1–20 (average 8.4) subclones per individual using the Beckman Coulter CEQ2000XL automated sequencer and supplied chemistry. A total of 57 alleles were detected among 177 sequences; alleles were either 222 or 228 bp in length and also differed from one another at 1–18 sites. The majority of allele sequence variants were observed in only one subclone sequence, and they were deemed artifacts. PCR–RFLP-based assays capable of detecting variation among common alleles were developed using the six most common alleles (found in 55% of the subclones) and were then verified with the rare alleles (presumed artifacts) to ensure that each assay produced only two possible fragment length patterns. RFLPs were detected with endonucleases *Alw*26I (267 bp (uncut) versus 87 bp and 180 bp) and *Rsa*I (93 bp and 174 bp versus 32 bp, 61 bp, and 174 bp). Restriction fragment sizes varied depending on the length variant present (we report the large size variant RFLPs above). Restriction digests were carried out according to the manufacturer's instructions (Promega Corporation, Madison, Wisconsin), and fragments were visualized on 1.8% agarose gels. Both MHC-I markers represent nonsynonymous substitutions in the peptide-binding region.

Analysis

Except where noted, all genetic analyses were performed using Tools for Populations Genetic Analyses (TFPGA) software (v. 1.3) (M. Miller, Department of Biology, Utah State University, Logan, UT 84322-5305, USA; http://www.marksgeneticsoftware.net/). An exact test for Hardy–Weinberg equilibrium was employed at each locus within each population to test for significant ($P < 0.05$) departures from equilibrium; the Monte Carlo method included a total of 20 000 permutations. The results were corrected for multiple simultaneous comparisons using the sequential Bonferroni procedure (Rice 1989). Genetic differentiation among populations was quantified by calculating F_{ST} following Weir and Cockerham (1984), and the 95% confidence intervals were estimated using bootstrap analysis over loci. Weir and Cockerham's (1984) unbiased F_{ST} estimator assumes no specific mutation model, since it is predicated upon divergence resulting from primarily genetic drift. We calculated F_{ST} for the neutral (microsatellite) and the gene locus markers separately. One microsatellite locus (OtsG13; Williamson et al. 2002) exhibited unacceptably high levels of departure from Hardy–Weinberg equilibrium in all populations assayed, and we excluded it from this study. Since F_{ST} is expected to vary with heterozygosity (Beaumont and Nichols 1996; Hedrick 1999, 2005), we also calculated G'_{ST}, a modification of F_{ST} that scales the estimate to reflect limitations imposed by high heterozygosity, a situation common to most microsatellite loci (Hedrick 2005). Finally, we plotted F_{ST} for each marker against mean expected heterozygosity and evaluated the likelihood of selective effects on the observed range of F_{ST} values using the simulation approach described in Beaumont and Nichols (1996). Simulations were performed using FDist2 (software available online from http://www.rubic.rdg.ac.uk/~mab/software.html); we used mean weighted F_{ST} estimates for each class of marker in both FR and VI regions (FR gene locus F_{ST} = 0.06; FR microsatellite F_{ST} = 0.05; VI gene locus F_{ST} = 0.24; VI microsatellite F_{ST} = 0.03) and performed 60 000 simulations with 50 demes using a stepwise mutation model for the microsatellite data and an infinite allele model for the gene locus data. We plotted the resulting 95% confidence intervals for each class of marker for each region.

We performed unrooted neighbor-joining (NJ) cluster analyses with Cavalli-Sforza and Edwards' (1967) chord distance (D_C) using Populations version 1.2.14 (O. Langella,

Table 1. Sample size (N), number of alleles (A), and observed (H_O) and expected (H_E) heterozygosity at nine microsatellite loci and eight gene loci markers for six populations of Chinook salmon (*Oncorhynchus tshawytscha*) on Vancouver Island.

Locus	Big Qualicum River	Nimpkish River	Puntledge River (Fall)	Puntledge River (Summer)	Quinsam River	Salmon River
Microsatellite						
Ots104						
N	36	29	32	41	24	39
A	23	26	25	18	28	23
H_O	0.94	0.86	0.84	0.83	0.92	0.77
H_E	0.92	0.94	0.94	0.89	0.94	0.90
Ots4						
N	40	37	38	43	35	41
A	12	11	11	10	10	9
H_O	0.85	0.87	0.74	0.88	0.77	0.78
H_E	0.86	0.84	0.82	0.84	0.77	0.76
OtsG3						
N	35	35	36	42	33	40
A	2	2	2	2	2	2
H_O	0.14	0.06	0.08	0.14	0.05	0.05
H_E	0.13	0.06	0.08	0.13	0.06	0.04
OtsG311						
N	18	25	20	20	18	20
A	22	30	20	14	18	16
H_O	0.87	1.00	0.90	0.75	0.69	0.82
H_E	0.92	0.96	0.93	0.86	0.84	0.88
Omy325						
N	40	37	38	43	35	41
A	9	8	8	9	8	10
H_O	0.87	0.71	0.76	0.72	0.63	0.73
H_E	0.78	0.69	0.68	0.73	0.63	0.78
Sfo8						
N	39	37	37	43	35	41
A	17	9	19	17	22	22
H_O	0.94	0.57*	0.66**	0.90	0.80	0.78*
H_E	0.89	0.79	0.91	0.89	0.93	0.93
One114						
N	36	25	32	29	18	33
A	22	16	21	13	10	17
H_O	0.97	0.96	0.93	0.95	0.89	0.81
H_E	0.93	0.91	0.88	0.87	0.87	0.89
Ssa85						
N	40	37	38	43	35	41
A	14	17	15	20	16	16
H_O	0.8	0.60**	0.86	0.85	0.94	0.78**
H_E	0.86	0.88	0.88	0.90	0.90	0.90
Ssa197						
N	39	36	38	43	34	41
A	27	29	23	29	25	36
H_O	0.94	0.97	0.86	0.81*	0.71**	0.95
H_E	0.94	0.93	0.91	0.92	0.94	0.95
Gene locus						
GH-1D						
N	52	47	50	44	47	47
A	2	2	2	2	2	2
H_O	0.48	0.38	0.34	0.14	0.15	0.21
H_E	0.42	0.38	0.37	0.20	0.14	0.22

Table 1 (*concluded*).

Locus	Big Qualicum River	Nimpkish River	Puntledge River (Fall)	Puntledge River (Summer)	Quinsam River	Salmon River
GH-2D						
N	52	47	50	44	47	47
A	2	2	2	2	2	2
H_O	0.06	0.13	0.08	0.05	0.11	0.11
H_E	0.06	0.16	0.08	0.04	0.10	0.10
IgH						
N	52	47	50	44	47	47
A	2	2	2	2	2	2
H_O	0.52	0.23	0.42	0.50	0.51	0.45
H_E	0.46	0.32	0.39	0.44	0.49	0.48
Transferrin						
N	52	47	50	44	47	47
A	2	2	2	2	2	2
H_O	0.35	0.00	0.30	0.41	0.08	0.11
H_E	0.44	0.00	0.31	0.43	0.08	0.10
MHC-I						
*Alw*26I						
N	49	44	48	43	44	45
A	2	2	2	2	2	2
H_O	0.31	0.27	0.42	0.37	0.45	0.44
H_E	0.49	0.39	0.47	0.36	0.48	0.49
*Rsa*I						
N	50	45	48	43	45	45
A	2	2	2	2	2	2
H_O	0.12**	0.00	0.02**	0.23	0.09	0.13
H_E	0.44	0.00	0.36	0.24	0.12	0.19
MHC-II						
*Dde*I						
N	52	47	50	44	47	47
A	2	2	2	2	2	2
H_O	0.06	0.02	0.04	0.07	0.00	0.23
H_E	0.06	0.02	0.04	0.07	0.00	0.34
*Rsa*I						
N	52	47	50	44	47	47
A	2	2	2	2	2	2
H_O	0.38	0.06	0.36	0.11	0.49	0.32
H_E	0.37	0.06	0.34	0.14	0.44	0.40

Note: Significant departures from Hardy–Weinberg equilibrium (after sequential Bonferroni correction) are indicated with asterisks (**, $P < 0.01$; *, $P < 0.05$).

Centre National de la Recherche Scientifique, Laboratoire Populations, Génétique et Evolution, Gif sur Yvettev, France; http://www.cnrs-gif.fr/pge/bioinfo/populations) and Treeview (Page 1996) software. We used D_C because of expectations for better tree topology estimation for closely related populations (Angers and Bernatchez 1998), although branch length estimation may be somewhat compromised (Angers and Bernatchez 1998). We performed the cluster analysis for the two categories of markers in the VI and FR populations separately. We bootstrapped, with replacement, among loci using 1500 permutations to get an estimate of tree topology consistency.

To test for agreement with an isolation-by-distance model of genetic divergence among the Chinook salmon populations within the two marker categories, we regressed pairwise F_{ST} on geographic distance using all pairwise comparisons of populations within the two regions only. We did not include comparisons between VI and FR populations, since the two regions are functionally isolated, and we used some microsatellite markers that were unique to each region. Geographic distance was measured along the shortest river and ocean pathway within each region (measured on 1:250 000 scale maps). Since we did not include all pairwise comparisons, we did not perform Mantel tests, but rather used linear regression and the Spearman's rank correlation to test for a relationship between F_{ST} and geographic distance. We used Mantel tests for correlation between geographic distance and F_{ST} within each region for each class of marker separately.

We tested for linkage disequilibrium among loci within the two marker types using a likelihood ratio test with the

Table 2. Sample size (N), number of alleles (A), and observed (H_O) and expected (H_E) heterozygosity at nine microsatellite loci and eight gene locus markers for five populations of Chinook salmon (*Oncorhynchus tshawytscha*) from tributaries of the upper Fraser River.

Locus	Nechako River	Stuart River	Willow River	Bowron River	Dome Creek
Microsatellite					
Ots1					
N	43	28	23	24	39
A	2	2	2	2	2
H_O	0.56	0.62	0.70	0.42	0.46
H_E	0.50	0.50	0.51	0.49	0.47
Ots3					
N	47	27	24	24	50
A	7	10	3	5	3
H_O	0.66	0.63*	0.65	0.50	0.71
H_E	0.73	0.71	0.56	0.49	0.51
Ots4					
N	42	21	24	25	48
A	9	9	7	8	7
H_O	0.74	0.64	0.76	0.80	0.81
H_E	0.81	0.75	0.69	0.77	0.79
Ots104					
N	46	22	22	25	49
A	20	22	18	21	19
H_O	0.91	0.94	0.88	0.92	0.96
H_E	0.94	0.90	0.92	0.93	0.93
Omy207					
N	41	28	24	25	51
A	3	3	3	2	2
H_O	0.30	0.04	0.04	0.20	0.04
H_E	0.37	0.04	0.04	0.18	0.04
Omy325					
N	43	27	24	25	51
A	12	11	7	10	13
H_O	0.79	0.89	0.87	0.76	0.90
H_E	0.85	0.83	0.74	0.76	0.87
Oneu3					
N	46	28	24	24	48
A	3	2	4	5	3
H_O	0.32	0.64	0.71	0.61	0.38
H_E	0.27	0.45	0.62	0.57	0.40
Ssa85					
N	44	25	24	22	51
A	19	16	10	11	14
H_O	0.89	0.72*	0.88	0.91	0.84
H_E	0.88	0.90	0.85	0.81	0.87
Ssa197					
N	45	28	24	24	51
A	31	19	20	13	22
H_O	0.84	0.85	0.86	0.75	0.77
H_E	0.94	0.91	0.93	0.84	0.92
Gene locus					
GH-1D					
N	39	35	20	32	51
A	2	2	2	2	2
H_O	0.33	0.71	0.25	0.38	0.02
H_E	0.28	0.49	0.29	0.31	0.02

Table 2 (*concluded*).

Locus	Nechako River	Stuart River	Willow River	Bowron River	Dome Creek
GH-2D					
N	39	35	20	32	51
A	2	2	2	2	2
H_O	0.08	0.42	0.40	0.19	0.17
H_E	0.07	0.45	0.32	0.17	0.16
Transferrin					
N	39	35	20	32	51
A	2	2	2	2	2
H_O	0.21	0.34	0.50	0.19	0.59
H_E	0.18	0.28	0.38	0.17	0.42
MHC-II					
*Rsa*I					
N	39	35	20	32	51
A	2	2	2	2	2
H_O	0.61	0.40	0.20	0.47	0.25
H_E	0.43	0.36	0.32	0.36	0.22
*Dde*I					
N	39	35	20	32	51
A	2	2	2	2	2
H_O	0.13	0.43	0.20	0.22	0.33
H_E	0.12	0.37	0.32	0.19	0.35
IgH					
N	39	35	20	32	51
A	2	2	2	2	2
H_O	0.46	0.43	0.20	0.38	0.18
H_E	0.36	0.34	0.26	0.34	0.16
MHC-I					
*Alw*26I					
N	39	35	20	32	51
A	2	2	2	2	2
H_O	0.74	0.46	0.65	0.53	0.49
H_E	0.50	0.48	0.50	0.44	0.47
*Rsa*I					
N	39	35	20	32	51
A	2	2	2	2	2
H_O	0.05**	0.31	0.00**	0.13**	0.02**
H_E	0.18	0.50	0.32	0.40	0.31

Note: Significant departures from Hardy–Weinberg equilibrium (after sequential Bonferroni correction) are indicated with asterisks (**, $P < 0.01$; *, $P < 0.05$).

distribution approximated by a permutation procedure (100 000 permutations) as implemented in ARLEQUIN 3.0 software (Excoffier et al. 2005; also available online from http://cmpg.unibe.ch/software/arlequin3/). This test assumes Hardy–Weinberg equilibrium; thus results for loci not in agreement with Hardy–Weinberg equilibrium should be interpreted with caution. The results of the test for linkage disequilibrium were corrected for multiple simultaneous comparisons using the sequential Bonferroni procedure (Rice 1989).

Results

The various marker loci showed a very large range of diversity among the populations (Tables 1, 2). Generally, the microsatellite markers had the highest heterozygosity (except for OtsG3), but both types of marker showed considerable variability. The microsatellite loci showed low to moderate departure from Hardy–Weinberg equilibrium (9 out of 99 comparisons); all departures were due to an excess of homozygotes (Tables 1, 2). There were six significant departures from Hardy–Weinberg equilibrium for the MHC-I (*Rsa*I) marker, all due to an excess of homozygotes; these departures included four VI populations and two FR populations (Tables 1, 2). None of the other gene locus markers significantly departed from equilibrium in any population.

Among the VI populations, the microsatellite-based F_{ST} estimate was significantly lower than the gene locus marker F_{ST} estimate, while there was no significant difference between mean F_{ST} estimates derived from the two marker categories in the FR populations (Table 3). Although the magnitude of the differences was reduced when the G'_{ST} sta-

Table 3. Microsatellite and gene locus-specific F_{ST} and G'_{ST} for Vancouver Island (VI) and upper Fraser River (FR) populations.

Microsatellite locus	F_{ST}	G'_{ST}	Gene locus	F_{ST}	G'_{ST}
VI					
Omy325	0.045	0.19	GH-1D	0.045	0.07
Ssa85	0.033	0.19	GH-2D	0.001	0.001
Sfo8	0.021	0.10	Transferrin	0.144	0.19
Ots4	0.034	0.21	MHC-II (*Rsa*I)	0.382	0.57
Ssa197	0.016	0.14	MHC-II (*Dde*I)	0.770	0.84
Ots104	0.019	0.15	IgH	0.133	0.25
OtsG3	0.000	0.00	MHC-I (*Alw*26I)	0.087	0.15
OtsG311	0.020	0.14	MHC-I (*Rsa*I)	0.102	0.12
One114	0.032	0.32			
All loci[a]	0.027 (0.02–0.04)	0.16 (0.10–0.23)		0.239 (0.11–0.41)	0.27 (0.07–0.47)
FR					
Ots1	0.01	0.013	GH-1D	0.174	0.29
Ots3	0.12	0.37	GH-2D	0.120	0.17
Ots4	0.021	0.099	Transferrin	0.048	0.083
Ots104	0.012	0.19	MHC-II (*Rsa*I)	0.020	0.036
Omy207	0.078	0.092	MHC-II (*Dde*I)	0.032	0.046
Omy325	0.070	0.52	IgH	0.019	0.031
Oneu3	0.132	0.31	MHC-I (*Alw*26I)	0.035	0.94
Ssa85	0.025	0.19	MHC-I (*Rsa*I)	0.097	0.11
Ssa197	0.021	0.13			
All loci[a]	0.048 (0.02–0.08)	0.21 (0.11–0.33)		0.066 (0.04–0.10)	0.11 (0.04–0.17)

[a] Means across all loci and 95% confidence limits (CI) are given.

tistic was used, a similar pattern emerged (Table 3). When individual marker locus F_{ST} was plotted against expected heterozygosity with the simulated 95% confidence limits calculated in FDist2, one of the MHC-II markers in the VI populations significantly deviated from neutral expectations, while the GH-1D marker in the FR populations was marginally significantly outside of the expected range for neutral loci (Fig. 2*a*). Those departures from neutral expectations are even more marked, and the second MHC-II marker significantly departed from neutrality when tested using the simulations based on the microsatellite data (Figs. 2*a*, 2*b*). When the clearly divergent MHC-II data were removed from the FDist2 simulation calculations (Beaumont and Nichols 1996), the second MHC-II marker was also significantly outside the expected neutral range (data not shown). One microsatellite locus in the FR populations (Ots104) was also marginally outside of the expected neutral range; however, this locus exhibited lower than expected F_{ST} (Fig. 2*b*). To test for the specific effect of the MHC-II marker data on our analysis within the VI populations, we removed the MHC-II data and recalculated mean F_{ST} and the 95% confidence limits for the remaining gene locus markers. The elimination of the MHC-II data reduced the mean F_{ST} (mean = 0.10, 95% confidence limits = 0.064–0.125), but it was still significantly different from the microsatellite F_{ST} (Table 3). Individual F_{ST} and G'_{ST} estimates based on the eight gene locus polymorphisms varied substantially among loci and between VI and FR populations (Table 3). The MHC-II markers showed the highest divergence among the VI populations, while the GH markers yielded the highest divergence estimates among the FR populations (Table 3).

The NJ cluster diagrams for the VI and FR populations using microsatellite markers showed a pattern similar to many reported for Pacific salmon populations over limited geographic ranges (Waples et al. 2004), that is, long branch lengths with little topology (Fig. 3). The VI microsatellite marker data weakly cluster the Big Qualicum and Puntledge (Fall) populations separately from the other populations (Fig. 3*a*), which is consistent with the known movement of zygotes and fry from the Big Qualicum to the Puntledge (Fall) populations. However, there is no consistent clustering of the Puntledge (Summer) with either the Big Qualicum or Quinsam river populations, nor do the Salmon River or Nimpkish River populations show any particular divergence (Fig. 3*a*). The FR microsatellite clustering pattern is consistent with geographic relationships (see Fig. 1), with the Stuart and Nechako clustering together, the Bowron and Dome clustering together, and the Willow being intermediate (Fig. 3*b*). The clustering pattern generated from the VI gene locus markers shows a dramatic difference in topology relative to that generated using microsatellite data; the Big Qualicum, Puntledge (Summer), and Puntledge (Fall) populations cluster together, with the Quinsam River and Salmon River populations diverging from that cluster and the Nimpkish River population showing extreme divergence (Fig. 3*c*). The clustering based on FR gene locus markers shows a divergence pattern closer to the microsatellite marker clustering patterns; however, the concordance with geographic distribution is lost, since the Nechako and Bowron cluster together, as do the Willow and Dome, with the Stuart showing an intermediate position (Fig. 3*d*). Generally, bootstrap values were high, although we do not show bootstrap values below 50%.

The isolation-by-distance regression analysis produced a significant relationship between F_{ST} and geographic distance for the pairwise microsatellite marker F_{ST} when data from

Fig. 2. Weir and Cockerham's (1984) unbiased F_{ST} plotted against expected population heterozygosity (H_E) for each marker locus used in this study; 95% confidence limits (CI) shown were calculated based on 60 000 simulations in FDist2. (*a*) Gene locus marker data: Vancouver Island values, solid circles (95% CI = solid lines); Fraser River values are open circles (95% CI = broken lines). (*b*) Microsatellite marker data: Vancouver Island values, solid circles (95% CI = solid lines), Fraser River values, open circles (95% CI = broken lines). Labeled data (MHC-II, GH-1D, and Ots104) are those identified as statistical outliers based on neutral marker simulations.

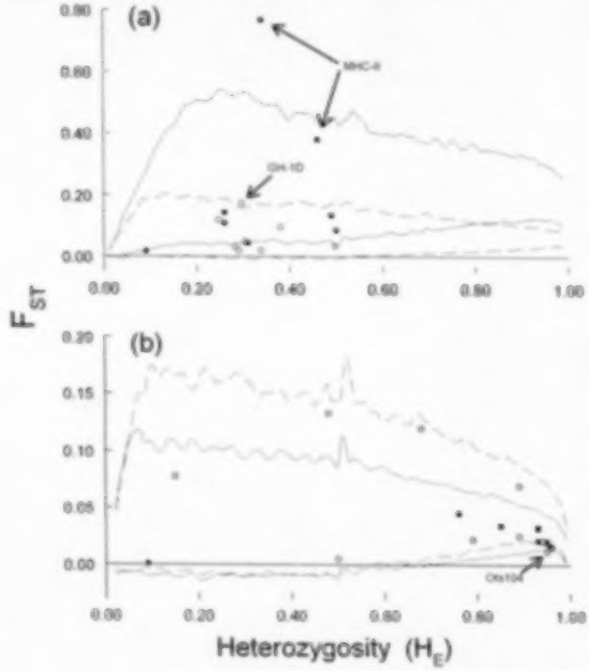

both regions were included (Fig. 4*a*; linear regression r^2 = 0.35; Spearman's rank correlation coefficient = 0.69, $P <$ 0.001). However, no relationship was observed using the gene locus marker-based F_{ST} estimates (Fig 4*b*; $P >$ 0.20), nor was there a significant relationship when we removed the MHC-II marker data from our analysis (Fig. 4*c*; $P >$ 0.10). When we tested for a relationship between microsatellite F_{ST} and geographic distance within the VI and FR populations separately, neither were significant based on a Mantel's test (Fig. 4*a*; $P >$ 0.05), although the VI microsatellite F_{ST}-based analysis approached significance (P = 0.06). Using the gene locus data, we found no significant Mantel tests (Figs. 4*b*, 4*c*) except for within the VI population using the gene locus polymorphism data with the MHC-II data removed (Fig. 4*c*; $P < 0.01$, $r^2 = 0.64$). Since the populations in the two regions have pronounced life history differences and are separated by a large geographic distance, we did not include any cross-region pairwise comparisons.

There was no significant linkage disequilibrium between any of the microsatellite loci in any population after Bonferroni correction ($P > 0.05$), nor were there any significant linkage disequilibria among the growth-related marker loci (GH-1 and GH-2). Among the immune function loci, MHC-II (*Rsa*I) and MHC-II (*Dde*I) were in weak linkage disequilibrium ($P < 0.05$) in 2 out of 11 populations (Salmon River and Dome Creek). MHC-I (*Alw*26I) was in weak linkage disequilibrium with MHC-I (*Rsa*I) in 6 of 11 populations. The RFLP polymorphisms in the MHC-I and MHC-II PBRs are apparently not tightly linked within our study populations, and although the inclusion of both RFLPs as independent markers in our analysis in not likely to have biased our results (because of the low level of linkage disequilibrium), we cannot rule out the possibility of a bias. There were no significant linkage disequilibria at the transferrin and IgH loci compared with any of the MHC loci.

Discussion

The comparison of divergence among natural populations using putative neutral genetic markers (including synonymous substitutions) and markers of unknown selective status is becoming recognized as a potentially powerful approach (e.g., Kim et al. 1999; Landry and Bernatchez 2001; Canino et al. 2005). Such an approach has two main benefits: first, it can detect selection acting in natural or seminatural situations, and second, it provides a basis for detailed evolutionary analyses of selection acting at specific genes, which in turn can be of considerable conservation value for the identification of the genetic basis of local adaptation. In our study, the divergence (F_{ST} and G'_{ST}) among populations varied with marker type and between coastal and interior populations. Gene locus polymorphisms identified higher levels of population structure among the VI populations than neutral marker loci, but no significant difference was observed in the interior populations (FR). Limitations to comparisons between such diverse marker loci due to differences in heterozygosity and allele numbers have been noted (Beaumont and Nichols 1996; Hedrick 1999, 2005); however, our results were consistent when we corrected for the possible effects of heterozygosity on F_{ST} estimation (G'_{ST}; Hedrick 2005) and using Beaumont and Nichols (1996) simulation approach. The nature of the genetic divergence between the VI and FR Chinook salmon populations was further clarified by our cluster analyses based on the two categories of markers. The microsatellite NJ cluster diagrams show a pattern typical of divergence under migration–drift equilibrium, while the gene locus marker NJ cluster diagrams differ in both branch length and topology from those of the microsatellite markers, especially for the VI populations. The most likely explanation of these results is selection acting on specific gene loci assayed in this study, although we cannot rule out possible effects of the quite different mutational mechanisms characteristic of the two marker types. Selective effects acting on our gene locus markers are further supported by their nonsignificant isolation-by-distance relationship compared with the significant microsatellite relationship. Although some of the gene loci included in this study appear to be under selection, the selection effects clearly differ between the coastal (VI) and the interior (FR) populations.

Our gene locus markers are predominantly intron-based polymorphisms, hence they reflect variation at the candidate loci only through linkage disequilibrium, and thus apparent locus-specific selection effects must be interpreted with cau-

Fig. 3. Unrooted neighbor-joining cluster analysis diagrams based on Cavalli-Sforza and Edwards' (1967) chord distance for the gene locus and microsatellite markers in the Vancouver Island (VI) and Fraser River (FR) populations: (*a*) VI microsatellite markers, (*b*) FR microsatellite markers, (*c*) VI gene locus markers, (*d*) FR gene locus markers. The data were bootstrapped over loci, with replacement, for 1500 replicates; the numbers represent the percent support of the branch (support less than 50% is not shown). Puntledge S, Puntledge River Summer run; Puntledge F, Puntledge River Fall run.

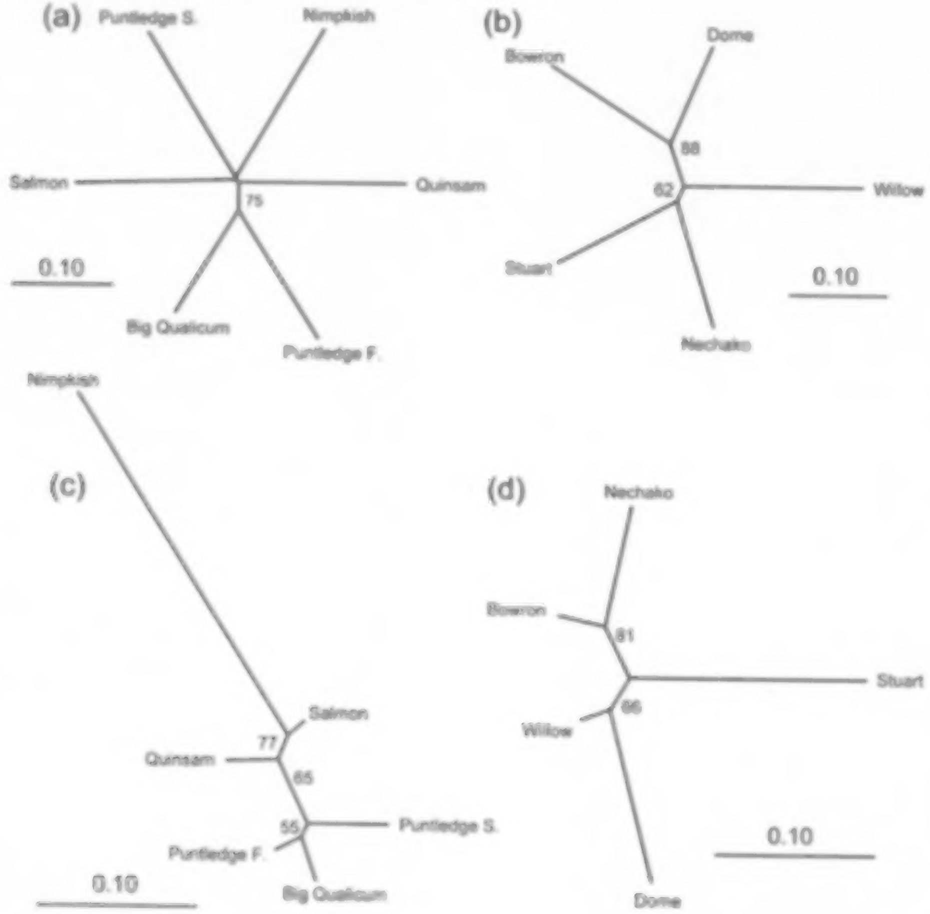

tion. Nevertheless, two of the markers (both are MHC-II markers and are thus coding region polymorphisms) stand out as being exceptionally divergent among the six VI populations. Such a pattern is indicative of directional selection at that locus in the VI study populations, especially since the removal of the MHC-II data yielded a significant isolation by distance relationship. In fact, all of the immune function markers generally showed elevated levels of population divergence within the VI populations. Interestingly, none of the immune function marker F_{ST} estimates (including MHC-II) were elevated among the FR populations. MHC-II allele diversity (as well as specific allele combinations) has been shown to have direct effects on survival and immune response in pathogen challenges (e.g., Grimholt et al. 2003; Miller et al. 2004). Such functional relationships between gene diversity and survival suggest obvious mechanisms for selection acting at the population level in salmonids, where each population typically experiences diverse pathogen exposure (e.g., Wood et al. 1989), although the pathogen exposure of the specific populations studied here are not known. Other studies that focused on MHC evolution within and among salmon populations have shown both higher than expected levels of heterogeneity (ascribed to balancing selection) and lower than expected levels of diversity (tentatively identified as evidence for directional selection) in specific populations (Langefors et al. 1998; Kim et al. 1999; Miller et al. 2001). In salmon, MHC PBR polymorphisms have generated high estimates of population divergence (e.g., MHC-II F_{ST} = 0.13, Langefors et al. 1998; MHC-II F_{ST} = 0.129, Kim et al. 1999; MHC-II F_{ST} = 0.19, Miller et al. 2001); however, none of those studies reported F_{ST} values as high as reported here for MHC-II marker data. Other studies that present population divergence data from both microsatellite and MHC markers in salmonids have shown that MHC markers often detect higher levels of divergence (e.g., Landry and Bernatchez 2001).

Although we are not aware of studies on population-level selection or divergence at GH genes, differences in growth

Fig. 4. Regression of Weir and Cockerham's (1984) unbiased F_{ST} on geographic distances measured as the shortest waterway distance using pairwise population comparisons within the Vancouver Island (solid circles) or Fraser River (open circles) populations for all microsatellite data (*a*), all gene locus marker data (*b*), and gene locus data with the MHC-II markers removed (*c*). No pairwise comparisons were made between Vancouver Island and Fraser River populations. Regression lines for the microsatellite marker data (*a*) were significant based on Spearman's rank correlation ($P < 0.001$; $r^2 = 0.35$), while the regressions using the gene locus marker data (*b*) and the modified gene locus data (*c*) were not significant ($P > 0.10$). Within regions, the Mantel tests were statistically significant only for the Vancouver Island modified gene locus data ($P < 0.01$; $r^2 = 0.64$), denoted as the broken line in panel *c*.

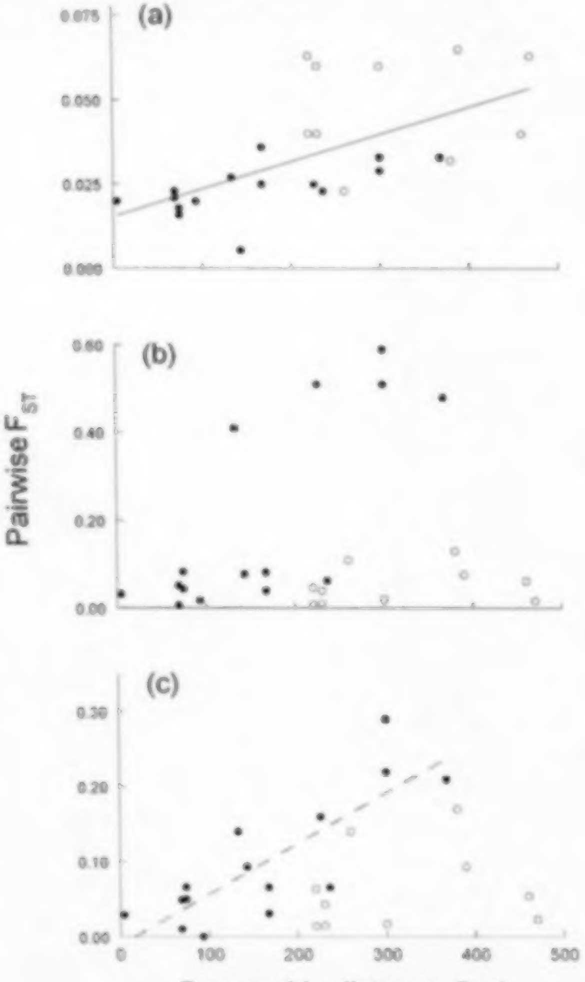

patterns among populations have been identified as adaptive, and thus selection is implied. Our data show a weak signal for possible selective effects at the growth-related markers (e.g., GH-1D) within the FR populations. Within the interior, stream-type populations assayed here, growth rate may be a more critical life history parameter than in the VI populations, where a shorter, freshwater residency time coupled with milder winter conditions may relax size threshold limitations. Overall, however, selection acting on freshwater or saltwater growth rates would be expected to be weaker than selection acting on immune function, since it would act indirectly via differences in life history performance in changing environments.

Curiously, with the exception of the clustering of the Big Qualicum and Puntledge (Fall) river populations, neither the microsatellite NJ cluster diagram nor the isolation-by-distance analyses reflect the known movement of eggs and fry among VI study populations for supplementation purposes. However, the pattern of population clustering in the gene locus marker NJ analysis is consistent with the known transfer of eggs and fry, raising the possibility of differential introgression into the native gene pool for the microsatellite versus gene locus markers in the supplemented populations. One possible explanation for the lack of a consistent genetic signal from the supplementation efforts may be that the supplemented fish are not readily integrated into the reproductive population (e.g., Ruzzante et al. 2004). Although the genetic status of the two Puntledge River populations has been questioned, particularly since both groups have received considerable transfer from the Big Qualicum River, the divergence between the fall and summer runs was strongly supported by the NJ cluster analysis, as well as by the exact tests for allele frequency differences and pairwise F_{ST} in all marker classes.

Our data provide evidence for selective effects on immune function loci in Chinook salmon on Vancouver Island, British Columbia, and weaker evidence for possible growth-related selection in the interior populations of the upper Fraser River drainage. It has been hypothesized that the role of bacterial and parasitic infection on salmon survival in the wild is important, and our MHC-II marker results show that it may contribute to the genetic architecture of coastal populations of Chinook salmon, but curiously, not in interior populations. Our results also have applications to salmon conservation and management, since the population structure revealed using functional gene-linked markers was fundamentally different from that expected based on drift (or migration) or even extrinsic environmental selection. Overall, our comparison of microsatellite and gene locus marker divergence among Chinook salmon populations provides evidence for locally relevant adaptive differences among populations and regions.

Acknowledgements

We thank N. Bernier, G. Iwama, the staff at the Salmon Enhancement Program hatcheries, and the Age Analysis Laboratory at the Pacific Biological Station for the collection and access to the tissue samples used for this study. C. Busch, S. Gibson, L. Rankin, J. Kelly, M. Simms, and E. Fillatre all contributed to the lab work. J. Ovenden provided valuable comments on the manuscript. The research was funded through a Natural Sciences and Engineering Research Council of Canada Discovery Grant and Canada Research Chair funding to DDH and an Applied Research and

Development Grant from Fisheries Renewal British Columbia to JMS and DDH.

References

Adkinson, M.D. 1995. Population differentiation in Pacific salmon: local adaptation, genetic drift, or the environment? Can. J. Fish. Aquat. Sci. **52**: 2762–2777.

Angers, B., and Bernatchez, L. 1998. Combined use of SMM and non-SMM methods to infer fine structure and evolutionary history of closely related brook charr (*Salvelinus fontinalis*, Salmonidae) populations from microsatellites. Mol. Biol. Evol. **15**: 143–159.

Banks, M.A., Blouin, M.S., Baldwin, B.A., Rashbrok, V.K., Fitz-Gerald, H.A., Blankenship, S.M., and Hedgecock, D. 1999. Isolation and inheritance of novel microsatellites in chinook salmon (*Oncorhynchus tschawytscha*). J. Hered. **90**: 281–288.

Beaumont, M.A., and Nichols, R.A. 1996. Evaluating loci for use in the genetic analysis of population structure. Proc. R. Soc. Lond. B Biol. Sci., **263**: 1619–1626.

Canino, M.F., O'Reilly, P.T., Hauser, L., and Bentzen, P. 2005. Genetic differentiation in walleye pollock (*Theragra chalcogramma*) in response to selection at the pantophysin (*PanI*) locus. Can. J. Fish. Aquat. Sci. **62**: 2519–2529.

Cavalli-Sforza, L.L., and Edwards, A.W.F. 1967. Phylogenetic analysis: models and estimation procedures. Evolution, **32**: 550–570.

Docker, M.F., and Heath, D.D. 2002. PCR-based markers detect genetic variation at growth and immune function-related loci in chinook salmon (*Oncorhynchus tshawytscha*). Mol. Ecol. Notes, **2**: 606–609.

Excoffier, L., Laval, G., and Schneider, S. 2005. Arlequin ver. 3.0: an integrated software package for population genetics data analysis. Evolutionary Bioinformatics Online, **1**: 47–50.

Ford, M.J. 1998. Testing models of migration and isolation among populations of chinook salmon (*Oncorhynchus tshawytscha*). Evolution, **52**: 539–557.

Ford, M.J. 2000. Effects of natural selection on patterns of DNA sequence variation at the transferrin, somatolactin, and p53 genes within and among chinook salmon (*Oncorhynchus tshawytscha*) populations. Mol. Ecol. **9**: 843–855.

Ford, M.J. 2001. Molecular evolution of transferrin: evidence for positive selection in Salmonids. Mol. Biol. Evol. **18**: 639–647.

Ford, M.J. 2002. Applications of selective neutrality tests to molecular ecology. Mol. Ecol. **11**: 1245–1262.

Grimholt, U., Larsen, S., Nordmo, R., Midtlyng, P., Kjoeglum, S., Syorset, A., Saebø, S., and Stet, R.J.M. 2003. MHC polymorphism and disease resistance in Atlantic salmon (*Salmo salar*); facing pathogens with single expressed major histocompatibility class I and class II loci. Immunogenetics, **55**: 210–219.

Groot, C., and Margolis, L. 1991. Pacific salmon life histories. University of British Columbia Press, Vancouver, B.C.

Hedrick, P.W. 1999. Perspective: highly variable loci and their interpretation in evolution and conservation. Evolution, **53**: 313–318.

Hedrick, P.W. 2005. A standardized genetic differentiation measure. Evolution, **59**: 1633–1638.

Hirst, I.D., and Ellis, A.E. 1996. Utilization of transferrin and salmon serum as sources of iron by typical and atypical strains of *Aeromonas salmonicida*. Microbiology, **142**: 1543–1550.

Kim, T.J., Parker, K.M., and Hedrick, P.W. 1999. Major histocompatibility complex differentiation in Sacramento River chinook salmon. Genetics, **151**: 1115–1122.

Landry, C., and Bernatchez, L. 2001. Comparative analysis of population structure across environments and geographical scales at major histocompatibility complex and microsatellite loci in Atlantic salmon (*Salmo Salar*). Mol. Ecol. **10**: 2525–2539.

Langefors, Å., Schantz, T.V., and Widegren, B. 1998. Allelic variation of Mhc class II in Atlantic salmon; a population genetic analysis. Heredity, **80**: 568–575.

Li, Y.-C., Korol, A.B., Fahima, T., and Nevo, E. 2004. Microsatellites within genes: structure, function, and evolution. Mol. Biol. Evol. **21**: 991–1007.

Miller, K.M., Withler, R.E., and Beacham, T.D. 1997. Molecular evolution at Mhc genes in two populations of chinook salmon *Oncorhynchus tshawytscha*. Mol. Ecol. **6**: 937–954.

Miller, K.M., Kaukinen, T.D., Beacham, T.D., and Withler, R.E. 2001. Geographic heterogeneity in natural selection on an MHC locus in sockeye salmon. Genetica, **111**: 237–257.

Miller, K.M., Winton, J.R., Schulze, A.D., Purcell, M.K., and Ming, T.J. 2004. Major histocompatibility complex loci are associated with susceptibility of Atlantic salmon to infectious hematopoietic necrosis virus. Environ. Biol. Fishes, **69**: 307–316

Moran, P., Dightman, D.A., Waples, R.S., and Park, L.K. 1997. PCR–RFLP analysis reveals substantial population-level variation in the introns of Pacific salmon (*Oncorhynchus* spp.). Mol. Mar. Biol. Biotechnol. **6**: 315–327.

Nelson, R.J., and Beacham, T.D. 1999. Isolation and cross species amplification of microsatellite loci useful for study of Pacific salmon. Anim. Genet. **30**: 228–229.

Olsen, J.B., and Bentzen, P. 2000. Microsatellites reveal population identity of individual pink salmon to allow supportive breeding of a population at risk of extinction. Trans. Am. Fish. Soc. **129**: 232–242.

Olsen, J.B., Wenburg, J.K., and Bentzen, P. 1996. Semiautomated multilocus genotyping of Pacific salmon (*Oncorhnychus* spp.) using microsatellites. Mol. Mar. Biol. Biotechnol. **5**: 259–272.

O'Reilly, P.T., Hamilton, L.C., McConnell, S.K., and Wright, J.M. 1996. Rapid analysis of genetic variation in Atlantic salmon (*Salmo salar*) by PCR multiplexing of dinucleotide and tetranucleotide microsatellites. Can. J. Fish. Aquat. Sci. **53**: 2292–2298.

Page, R.D.M. 1996. TREEVIEW: an application to display phylogenetic trees on personal computers. Comput. Appl. Biosci. **12**: 357–358.

Rice, W.R. 1989. Analyzing tables of statistical tests. Evolution, **43**: 223–225.

Ruzzante, D.E., Hansen, M.M., Meldrup, D., and Ebert, K.M. 2004. Stocking impact and migration pattern in an anadromous brown trout (*Salmo trutta*) complex: where have all the stocked spawning sea trout gone? Mol. Ecol. **13**: 1433–1445.

Scribner, K.T., Gust, J.R., and Fields, R.L. 1996. Isolation and characterization of novel salmon microsatellite loci: cross-species amplification and population genetic applications. Can. J. Fish. Aquat. Sci. **53**: 833–841.

Taylor, E.B. 1991. A review of local adaptation in Salmonidae, with particular reference to Pacific and Atlantic salmon. Aquaculture, **98**: 185–207.

Van Doornik, D.M., Milner, G.B., and Winans, G.A. 1996. Transferrin polymorphism in coho salmon, *Oncorhynchus kisutch*, and its application to genetic stock identification. Fish. Bull. **94**: 566–575.

Vasemägi, A., and Primmer, C.R. 2005. Challenges for identifying functionally important genetic variation: the promise of combining complementary research strategies. Mol. Ecol. **14**: 3623–3642.

Vasemägi, A., Nilsson, J., and Primmer, C.R. 2005. Expressed sequence tag-linked microsatellites as a source of gene-associated polymorphisms for detecting signatures of divergent selection in Atlantic salmon (*Salmo salar* L.). Mol. Biol. Evol. **22**: 1067–1076.

Waples, R.S., Teel, D.J., Myers, J.M., and Marshall, A.R. 2004. Life-history divergence in Chinook salmon: historic contingency and parallel evolution. Evolution, **58**: 386–403.

Wegner, K.M., Reusch, T.B.H., and Kalbe, M. 2003. Multiple parasites are driving major histocompatibility complex polymorphism in the wild. J. Evol. Biol. **16**: 224–232.

Weir, B.S., and Cockerham, C.C. 1984. Estimating *F*-statistics for the analysis of population structure. Evolution, **38**: 1358–1370.

Williamson, K.S., Cordes, J.F., and May, B. 2002. Characterization of microsatellite loci in chinook salmon (*Oncorhynchus tshawytscha*) and cross-species amplification in other salmonids. Mol. Ecol. Notes, **2**: 17–19.

Winter, G.W., Schreck, C.B., and McIntyre, J.D. 1980. Resistance of different stocks and transferrin genotypes of coho salmon, *Oncorhynchus kisutch*, and steelhead trout, *Salmo gairdneri*, to bacterial kidney disease and vibriosis. Fish. Bull. **77**: 795–802.

Wood, C.C., Rutherford, D.T., and McKinnell, S. 1989. Identification of sockeye salmon (*Oncorhynchus nerka*) stocks in mixed-stock fisheries in British Columbia and Southeast Alaska using biological markers. Can. J. Fish. Aquat. Sci. **46**: 2108–2120.

Assessing possible thermal rearing restrictions for juvenile coho salmon (*Oncorhynchus kisutch*) through thermal infrared imaging and in-stream monitoring, Redwood Creek, California

M.A. Madej, C. Currens, V. Ozaki, J. Yee, and D.G. Anderson

Abstract: We quantified patterns in stream temperature in a northern coastal California river using thermal infrared (TIR) imaging and in-stream monitoring and related temperature patterns to the historical and present distributions of juvenile coho salmon (*Oncorhynchus kisutch*). In Redwood Creek, California, water temperature increased from the headwaters to about 60 km downstream, then gradually decreased over the next 40 km as the river approaches the Pacific Ocean. Despite the lack of fish migration barriers, juvenile coho are currently only observed in the downstream-most 20 km, whereas historically they were found in 90 km of river channel. Maximum daily temperatures and duration of elevated stream temperatures were not significantly different in the headwater and downstream reaches but were significantly higher in the 50 km long intervening reach, where maximum weekly maximum temperatures ranged from 23 to 27 °C. An increase in stream temperatures in the middle basin during the last three decades as a result of channel aggradation, widening, and the removal of large riparian conifers may play an important role in restricting juvenile coho to one-fifth of their historical range.

Résumé : Nous avons mesuré quantitativement les patrons de température dans une rivière côtière du nord de la Californie à l'aide d'imagerie thermique infrarouge (TIR) et d'enregistrements de température dans les cours d'eau et nous avons relié ces patrons thermiques aux répartitions passées et actuelles des jeunes saumons coho (*Oncorhynchus kisutch*). Dans Redwood Creek, Californie, la température augmente depuis l'amont sur environ 60 km vers l'aval, puis elle baisse graduellement sur les prochains 40 km alors que la rivière s'approche du Pacifique. Malgré l'absence de barrière à la migration des poissons, les jeunes saumons coho s'observent actuellement seulement dans les 20 km les plus en aval, alors que dans le passé ils se retrouvaient sur 90 km du cours de la rivière. Les températures journalières maximales et la durée des températures élevées ne diffèrent pas significativement dans les sections d'amont et d'aval, mais elles sont significativement plus élevées dans la section intermédiaire de 50 km, où le maximum des températures maximales hebdomadaires varient de 23 à 27 °C. Un accroissement de la température dans le bassin moyen de la rivière au cours des trois dernières décennies à cause de l'aggradation du chenal, de l'élargissement du lit et de l'enlèvement des grands conifères de la rive peut jouer un rôle important dans la restriction des jeunes saumons coho à un cinquième de leur aire de répartition historique.

[Traduit par la Rédaction]

Introduction

Water temperature is an important physical factor that regulates the distribution of fish (Li et al. 1994; Welsh et al. 2001). High water temperatures have been shown to limit the distribution of salmonids within streams (Meisner 1990), reduce abundance (Ebersole et al. 2001), and fragment populations within a watershed (Matthews and Zimmerman 1990). Elevated water temperatures can also decrease growth and increase juvenile mortality (Brett 1979). High water temperatures can negatively influence salmonid egg development and juvenile appetite and growth (Dockray et al. 1996), as well as negatively alter behavior and interspecies interactions (De Staso and Rahel 1994; Beschta et al. 1987).

Coho (or silver) salmon (*Oncorhynchus kisutch*) juveniles, like most salmonids, prefer cool-water rearing and typically reside in the stream for a minimum of 1 year after hatching. However, in Prairie Creek, a tributary to Redwood Creek in

Received 22 July 2005. Accepted 22 December 2005. Published on the NRC Research Press Web site at http://cjfas.nrc.ca on 13 May 2006.
J18805

M.A. Madej[1] and C. Currens. US Geological Survey Western Ecological Research Center, 1655 Heindon Road, Arcata, CA 95521, USA.
V. Ozaki and D.G. Anderson. Redwood National and State Parks, 1655 Heindon Road, Arcata, CA 95521, USA.
J. Yee. US Geological Survey Western Ecological Research Center, 3020 State University Drive East, Room 3006, Sacramento, CA 95819, USA.

[1] Corresponding author (e-mail: mary_ann_madej@usgs.gov).

Can. J. Fish. Aquat. Sci. **63**: 1384–1396 (2006) doi:10.1139/F06-043

northern coastal California, about one-quarter of the smolts reside in-stream for 2 years before migrating to the Pacific Ocean (Bell 2001) so they are especially vulnerable to stressful summer temperatures. Redwood Creek is currently listed as temperature- and sediment-impaired under the Clean Water Act, section 303d, because of past timber harvest, removal of riparian vegetation, widespread streamside landsliding, and channel aggradation. The upstream reach of the river is beginning to recover from past damage in terms of pool frequency and depth (Madej 2001). A recent reconnaissance-level assessment of fish habitat in the upper reach of Redwood Creek indicates that the aquatic habitat (high pool frequency, extensive shading from alders, a moderate channel gradient (0.5%), and adequate spawning gravel size) should now support salmonids (California Resources Agency 2005); nevertheless, coho salmon are absent.

Juvenile coho salmon distribution in the Redwood Creek basin is presently limited to the downstream-most 20 km of mainstem and a few large low-gradient tributaries in the lower basin, but historically coho were found throughout most of the mainstem of Redwood Creek (Snyder 1931). This apparent lack of coho in upper Redwood Creek under present conditions is puzzling, and we hypothesize that the summer thermal environment on Redwood Creek restricts juvenile coho rearing for most of the mainstem length. To evaluate this concern, Redwood National and State Parks and the US Geological Survey (USGS) initiated a study in 1997 to document the basin-wide summer water temperature regime of Redwood Creek using continuous-recording temperature probes. This effort provided in-stream and air temperature data at several locations along Redwood Creek. To supplement this study, an airborne thermal infrared (TIR) survey was conducted in the summer of 2003 to provide a longitudinal profile of spatially continuous water temperature data for Redwood Creek. The objectives of this multiscale study were (*i*) to determine longitudinal trends in summer water temperature (maxima, minima, and durations of elevated temperatures), (*ii*) to compare temperature regimes in the stream reach bearing coho with those in the reach not bearing coho, and (*iii*) to identify warm reaches of Redwood Creek that may be limiting thermal environments for rearing coho.

Materials and methods

Study site description

Redwood Creek drains an area of 738 km^2 in northern coastal California and enters an estuary at Orick, California (Fig. 1). The basin receives an average of 200 cm of rainfall annually, most of which occurs between October and March. In the upstream-most 72 km, the river flows through privately owned lands primarily under timber management, and in the lower 36 km, it flows through Redwood National and State Parks (RNSP). Except for a steep, 10 km long reach in the headwaters of the basin, channel gradient in Redwood Creek is less than 2% and averages 0.3% (Madej 1995). There are no barriers to fish migration for 100 km of the mainstem. Median particle size (D_{50}) decreases from 40 mm near Minon Creek to 16 mm at Orick.

Aerial photographs from 1936 and 1947 show that before commercial timber harvesting, Redwood Creek was narrow and sinuous in most reaches and covered with a thick canopy of coniferous trees. Large-scale timber harvesting began in the basin in the 1950s. By 1966, 55% of the forest had been logged, and by 1992, ~80% of the basin had been logged (Best 1995). Large floods in 1953, 1955, 1964, 1972, 1975, and 1997 initiated widespread road and stream-crossing failures, gullying, and streamside landsliding in the basin. The floods before 1997 caused extensive channel aggradation and bank erosion throughout Redwood Creek, although channel changes were most extensive in the upper basin, where logging activity had been the most intense. Aerial photographs and field observations documented that the channel widened, pool size and frequency diminished, channel bed material became finer, and the channel bed aggraded up to 9 m at some sites (Madej 1995). Concomitantly, the dominant riparian vegetation changed dramatically. In 1948, 86% of the length of the riparian zone along Redwood Creek was dominated by conifers, which decreased to 15% by 1997, with canopy density decreasing as well (Urner and Madej 1998). Most of the intact old-growth conifer riparian zones are located on the downstream-most 20 km of Redwood Creek within RNSP.

This transition from a riparian zone dominated by old-growth redwood and Douglas fir to brush or smaller hardwoods (primarily red alder, *Alnus rubra*) presumably increased water temperatures in Redwood Creek, but few data are available to assess time trends. Interviews with long-time residents living in the middle basin of Redwood Creek provide anecdotal evidence of summer water temperature in the early to mid-20th century. All remember that the water in Redwood Creek used to be like "ice" when they were kids, but the river is warmer today (Van Kirk 1994). They also described Redwood Creek as having a thick canopy of trees. Between 1953 and 1959, average daily maximum of water temperature in July and August in this area was 22 °C, based on periodic measurements at the USGS O'Kane (or "near Blue Lake") stream gaging station (Blodgett 1970). In contrast, from 1975 to 1980, the station recorded daily water temperatures that exceeded 28 °C on average 7 consecutive days per year. Annual peak water temperatures were between 29 and 32 °C for that time period (USGS 1975–1980).

The fish fauna of Redwood Creek is typical of the coastal streams of northern California (Anderson 1988; Brown 1988). Both anadromous and resident fish species are present in the basin and include coho and Chinook (*Oncorhynchus tshawytscha*) salmon, steelhead (*Oncorhynchus mykiss*) and coastal cutthroat (*Oncorhynchus clarkii*) trout, lamprey (*Lampetra tridentata*), sculpins (*Cottus* spp.), and stickleback (*Gasterosteus aculeatus*). Anecdotal evidence, including interviews with local residents, photographs, and newspaper articles, provides some evidence of coho along the length of Redwood Creek (Anderson 1988; Van Kirk 1994; James O'Barr, RNSP, P.O. Box 7, Orick, CA 95555, USA, unpublished data). In addition, limited scientific observations (Briggs 1953; California Department of Fish and Game (CDFG) 1965, 2002) portray historical distribution of coho throughout most of the Redwood Creek basin. Snyder (1931) reports that the middle basin of Redwood Creek was

Fig. 1. Redwood Creek watershed in California, USA. Continuous in-stream data loggers were deployed in the main flow of Redwood Creek at each of the monitoring sites.

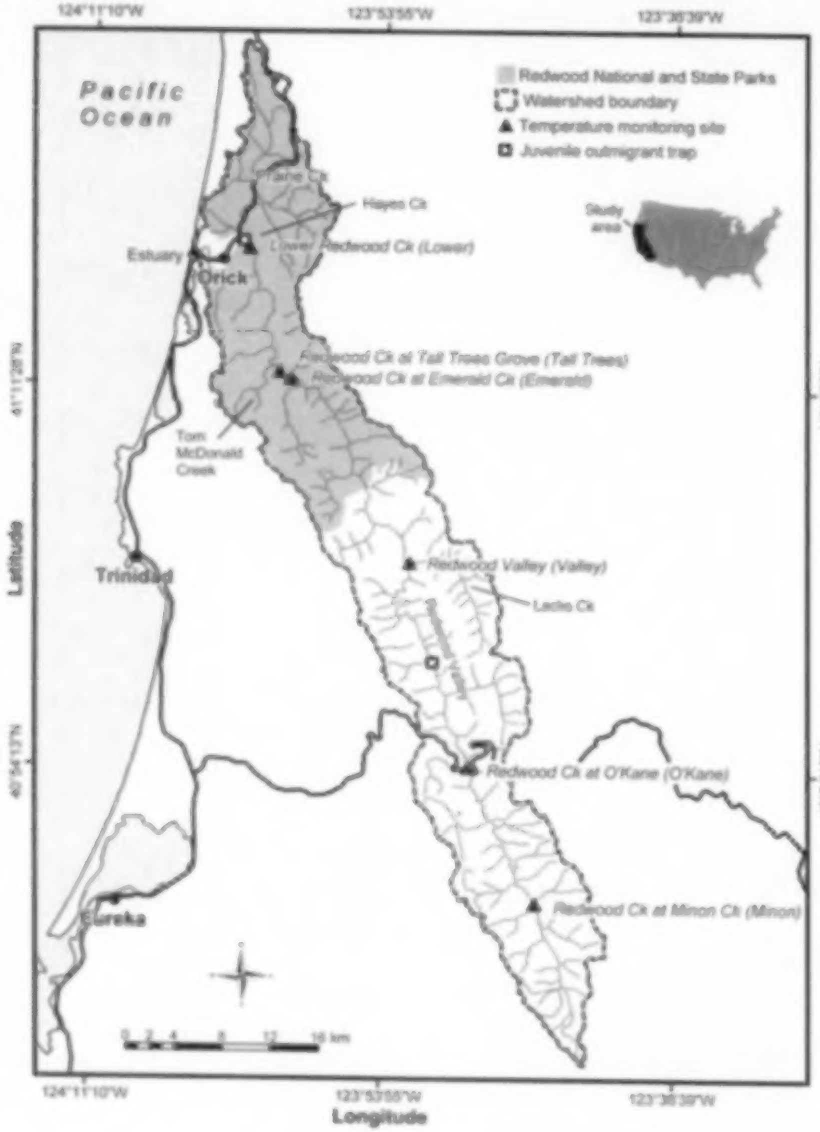
124°11'10"W
123°53'55"W
123°36'39"W
41°11'28"N
40°54'13"N
Latitude
Longitude
Pacific Ocean
Redwood National and State Parks
Watershed boundary
Temperature monitoring site
Juvenile outmigrant trap
Prairie Ck
Hayes Ck
Lower Redwood Ck (Lower)
Estuary
Orick
Study area
Redwood Ck at Tall Trees Grove (Tall Trees)
Redwood Ck at Emerald Ck (Emerald)
Tom McDonald Creek
Trinidad
Redwood Valley (Valley)
Lacks Ck
Redwood Valley
Redwood Ck at O'Kane (O'Kane)
Eureka
Redwood Ck at Minon Ck (Minon)
0 2 4 8 12 16 km

used as a silver salmon egg source for a Trinity River hatchery in the mid- to late 1890s. Hallock et al. (1952) described mainstem Redwood Creek as an "excellent silver salmon stream" with pools too deep to seine.

During the last 25 years, however, coho distribution has become much more limited. In 1997, coho salmon were federally listed as threatened in the Southern Oregon/Northern California Evolutionary Significant Unit, where Redwood Creek is located. A combination of direct observation (snorkel surveys), spawning surveys, and downstream migrant trapping has been used to document fish presence in various reaches of Redwood Creek. In 1980–1981, Brown (1988) and Anderson (1988) surveyed the entire Redwood Creek basin for fish presence. Adult spawning surveys were conducted on the mainstem in the middle basin of Redwood Creek during the winters of 1989 and 1990. During the summer of 2003, RNSP fishery biologists surveyed juvenile coho "presence–absence" using direct observation by snorkeling the downstream half of Redwood Creek (Lacks Creek downstream to Hayes Creek). The CDFG operates two downstream migrant traps, one in the middle basin at river kilometre 53 (rkm 53, Redwood Valley) and the other in lower Redwood Creek (rkm 6.5, "Lower"). Traps typically operate from March until late July, when juvenile Chinook outmigration slows significantly.

Juvenile coho salmon temperature requirements

Juvenile coho salmon require cool water to survive and grow and are susceptible to increased summer water temperatures because they rear in freshwater for at least a year. The estimated upper lethal temperature for juvenile coho varies depending on the techniques used. Brett (1952) reported that when five species of Pacific salmon, including coho, were exposed to various temperature gradients, all juvenile salmonid species preferred temperatures between 12 and 14 °C and juveniles generally avoided stream temperatures above 15 °C. He also reported 26.0 °C as the upper lethal temperature based on the incipient lethal temperature. In this test, fish were acclimated at 20 °C before being placed into higher temperature water. However, because of an accidental loss of coho during the experiment, he based his findings on the upper thermal limits of spring Chinook salmon. Becker and Genoway (1979), as referenced in Bjornn and Reiser (1991), reported 28.8 °C as the upper lethal temperature based on the critical thermal maximum technique in which the water and fish were slowly heated. Using the same technique, McGeer et al. (1991) determined that juvenile coho survived at temperatures up to 23 °C, but none survived at water temperatures higher than 25.5 °C.

In the absence of lethal effects, stream temperature can still influence the distribution and growth of juvenile salmonids. For a nearby northern California basin, Welsh et al. (2001) reported that juvenile coho were not present in streams where the maximum weekly maximum temperature (MWMT) exceeded 18.1 °C or where the maximum weekly average temperature (MWAT) exceeded 16.8 °C. Growth stops when water temperatures exceed 18–20.3 °C (Stein et al. 1972; Bell 1973; Armour 1991). Many factors, such as food availability, habitat quality, and competition, as well as water temperature, affect salmonids. Willey (2004) modeled bioenergetics of juvenile coho salmon in northern California streams and concluded that in streams with limited food resources, juvenile coho growth may decrease as daily average temperatures increase above 15.7 °C. Because no clear temperature thresholds have been established regarding coho health, in this study we compare ranges of temperatures, as well as maximum temperatures, in various stream reaches.

Stream temperature monitoring

Two types of temperature monitoring were used in this study to provide multiscale information: ground-based measurements and remote-sensing techniques. In-stream data loggers measured summer stream temperatures at point locations along Redwood Creek for 5–7 consecutive years. Remote-sensing techniques using TIR imagery provided a spatially continuous longitudinal profile of surface water temperature at a given point in time. Thus the two methods are complementary in assessing both spatial and temporal trends in the water temperature regime.

Data loggers (Onset Computer Corporation, Bourne, MA 02532, USA) collected continuous water temperature data at seven sites along Redwood Creek during the summers of 1997–2003 (Fig. 1). We selected sampling sites based on study objectives and available stream access. Data loggers were calibrated before use and were deployed from June through September with sampling intervals that ranged from 15 to 60 min. Stream data loggers were submerged in the water column in areas of shade and mixed water. At a subset of stream study sites, we placed air temperature data loggers in a shaded area of the riparian zone in close proximity to the stream data logger. Cool air temperature is a reliable indicator of fog presence during summer months (and consequently less solar radiation is reaching the stream on those days). The accuracy of the probes is ±0.2 °C, and the resolution is ±0.2 °C.

On 29 July 2003, a helicopter flight surveyed 95 km of Redwood Creek by collecting TIR and color video imagery of Redwood Creek and its riparian zone from a flight altitude of 425 m above ground level. Visible-band and TIR (8–12 μm) cameras attached to a gyro-stabilized mount on the underside of the helicopter collected 2500 images. The TIR data captured water temperatures at midafternoon when stream temperatures reached their daily maximum. The contractors recorded TIR images directly from the sensor to an on-board computer, and individual images were referenced with time and position data provided by a global-positioning system (Watershed Sciences Inc. (WSI) 2004). They converted measured radiance values contained in the raw TIR images to surface water temperatures based on the emissivity of water, atmospheric transmission effects, ambient background reflections, and the calibration characteristics of the sensor. They then compared the radiant temperatures with the temperatures measured by 11 in-stream data loggers. Calibration parameters were fine-tuned to provide the most accurate fit between the radiant and in-stream temperatures. The average absolute differences between the temperatures recorded by the in-stream data loggers and the radiant temperature derived from the TIR images were within the desired accuracy of 0.5 °C (WSI 2004).

Once the TIR images were calibrated, WSI interpreted stream temperatures for each of the 2500 images by determining the radiant temperature (pixel values) of 10 points along the center of the stream channel. The temperature value for each thermal image was estimated by using the median value of the 10-point sample. The temperatures of detectable surface inflows (e.g., surface springs, tributaries) were also sampled. In some cases, tributaries or other features detected in the imagery were not sampled because of their small size. In addition, data processing focused on interpreting spatial variations in surface temperatures observed in the images. The images were assigned a distance based on a 1:24 000 routed GIS (geographic information system) stream coverage obtained from the National Park Service, Arcata, California. The median temperatures for each sampled image were then plotted against the corresponding river kilometre to develop a longitudinal temperature profile (WSI 2004). The location and median temperature of all sampled surface water inflows were also mapped to illustrate how these inflows influence mainstem temperature patterns.

Variable water surface conditions (such as riffle versus pool), slight changes in viewing aspect, and variable background temperatures (e.g., sky versus trees) can result in differences in the calculated radiant temperatures within the same image or between consecutive images. The apparent temperature variability is generally less than 0.6 °C (Torgerson et al. 2001). In general, apparent stream temperature changes of <0.6 °C are not considered significant unless associated with a tributary or other source.

Data analysis

We used several metrics to define temperature regimes and compare stream temperatures at various locations along Redwood Creek: daily maxima and minima, weekly average maxima (MWAT and MWMT, defined below), duration of exceedance of a given temperature, and number of consecutive hours over specific high temperatures ("stress intervals"). MWAT was originally defined by Brungs and Jones (1977) as a limit to the maximum temperature, for a species and life stage that should not be exceeded in a regulatory sense, but more recently MWAT is the term used to describe the maximum value of a 7-day moving average of daily average temperatures (Welsh et al. 2001). This latter usage is the definition used in the present study. Similarly, MWMT is the maximum value of a 7-day moving average of daily maximum temperatures.

Cumulative frequency–distribution curves illustrate the percentage of time that a stream temperature was exceeded for each monitoring site for the critical period of 1 July to 31 August when stream temperatures are highest. These curves are useful indicators of the seasonal exposure to high temperatures, but they do not indicate if thermal recovery (periods of time <18 °C) occurred at night. Thermal recovery, if present, would help ameliorate temperature stress on fish. To examine the daily stress levels more closely, we defined "stress intervals" by the number of consecutive hours that a particular temperature was exceeded during July and August in 2000–2003. For example, if on 2 July, a probe recorded 10 consecutive hours of >18 °C, a 10-h stress interval of >18 °C would be counted for that date. Stress intervals were computed for consecutive hours >18 °C, >20 °C, >22 °C, and >24 °C for all sites. We compared the mean duration and frequency of stress intervals for these temperature values among sites.

Statistical analyses

Differences in daily maximum and minimum temperatures for July and August 1997 to 2003 among sites were analyzed using a repeated-measures analysis of variance model to account for temporally correlated daily measurements from the same site that might undermine the independence of the data (PROC MIXED, SAS Institute Inc. 1999). We modeled temporal correlations using various correlation types, including no correlations, and Akaike's information criterion (AIC) was used to select the correlation type corresponding to the best-fitting model (lowest AIC value) (Littell et al. 1996; Burnham and Anderson 1998). We assumed temperatures from different years to be temporally independent, and a year effect was included in the model to account for any variation associated with year differences. Temperatures from different sites on the same day were considered spatially correlated, therefore the data were converted into pairwise differences between sites to isolate site-related differences and eliminate any shared spatial effects between sites. We determined differences among sites by statistically testing the null hypothesis that all paired difference data had a mean of zero. The data were fitted to an ANOVA model containing site pair, year, and interaction effects, and the interaction was removed if not found to be significant. All tests were conducted at $\alpha = 0.05$ significance level.

We compared multiple pairs of sites by using an approach adapted from Fisher's protected least significant difference (LSD) tests. We first determined whether the F test for pairings indicated an overall significant difference among sites. If the F test was significant, then we used individual t tests to determine which mean paired differences between sites were statistically different from 0. If the F test was not significant, then no differences were concluded and no individual t tests were conducted.

Similar to the analysis of daily maxima data, the daily minima and the stress durations at each of the four temperature values were compared across sites using a repeated-measures ANOVA followed by pairwise comparisons based on Fisher's protected LSD tests. We log-transformed stress durations before analysis to remove skewness. Because a long stress interval at one site could occur in association with either a long interval or two short intervals at a nearby site, we did not model any spatial correlations in the durations of stress intervals between sites. We determined differences among sites by statistically testing the null hypothesis that all sites had equivalent mean durations of stress intervals.

Results

Fish observations

Recent surveys and trapping efforts document that juvenile coho salmon are currently limited to the downstream-most 20 km of Redwood Creek and tributaries entering that reach. In the 1980–1981 survey of the entire Redwood Creek basin, only three tributaries in the middle basin had single observations of juvenile coho (Brown 1988), and only a handful of tributaries in the lower basin contained rearing juvenile coho (Anderson 1988). Although spawning surveys are difficult to conduct because of low visibility and high stream flow during the winter, the 1989 surveys documented several adult coho salmon in the middle basin of Redwood Creek. Adult coho salmon spawners were observed in Redwood Valley during the winter 2000–2001 spawning season (Pacific Coast Fish, Wildlife and Wetlands Restoration Association 2002); however, a downstream migrant trap located in the middle basin of Redwood Creek (rkm 53) has never captured a juvenile coho in the past 5 consecutive years of trapping (Sparkman 2005). Juvenile coho were captured at the lower trap (rkm 6.5) in 2003 and 2004. In 2003, unusually high flow conditions early in the season made the lower trap inoperable for several weeks and low juvenile coho numbers precluded determining population estimates (Bill Pinnix, US Fish and Wildlife Service, 1655 Heindon Road, Arcata, CA 95521, USA, personal communication). Only 29 young-of-the-year (YOY) and 12 age-1+ coho were trapped in 2003. In 2004, 202 YOY juvenile coho and 69 age-1+ coho salmon were caught at the lower trap (Sparkman 2004). During the summer of 2003, RNSP biologists conducted an extensive juvenile coho "presence–

Fig. 2. Average daily maximum stream temperatures measured in Redwood Creek at O'Kane for two time periods: 1975–1980, solid line; 1998–2003, broken line.

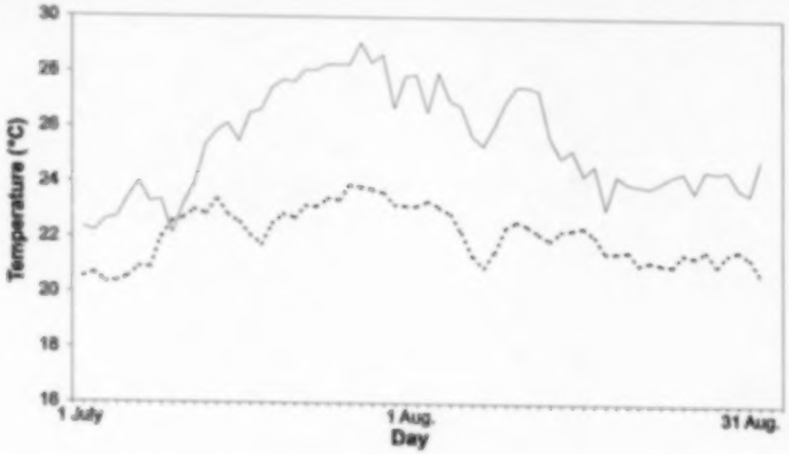

Table 1. Means and standard deviations (SD) of daily minimum and maximum temperatures for period of record (1 July to 31 August 1997 to 2003).

Redwood Creek site	Daily temperature (°C)	
	Mean minimum ± SD	Mean maximum ± SD
Estuary	17.0±1.2c	18.9±1.2a
Lower	16.1±0.6b	20.6±1.4b
Tall Trees	18.3±0.8d	21.9±1.1c
Emerald	18.3±0.8d	22.2±1.2c
Valley	18.3±1.1d	24.6±1.9d
O'Kane	17.3±1.4c	22.3±1.6c
Minon	14.5±1.5a	20.0±1.5b

Note: Sites not sharing a common letter were statistically different from one another ($p < 0.05$). Sites with increasing temperatures are classified by alphabetically increasing letters.

absence" snorkel survey on the lower half of Redwood Creek, including areas along the channel margins such as undercut banks and side pools. No coho were observed in the main channel above rkm 20 (Tom McDonald Creek), and juvenile coho were only observed in nine locations in the lower 20 km of channel (Ozaki and Anderson 2005). Of the few juvenile coho sighted in Redwood Creek, seven of the nine locations were side pools. Side pools were separated from the main channel by a gravel bar but were open to Redwood Creek on the downstream end. Many of the pools were influenced by cool seeps and springs, intragravel flow, groundwater, or small tributaries. These pools were generally cooler than the mainstem. The other two mainstem sightings were at the downstream end of the surveyed reach, near the coast.

Daily maximum temperatures

During a period of channel aggradation in upper Redwood Creek from 1975 to 1980, average daily stream temperatures at O'Kane were very high (Fig. 2). Maximum daily temperature data were not available from 1980 to 1998, but the period from 1998 to 2003 exhibited a considerable decrease in average daily maxima. Presently the peak temperatures of 22–24 °C are comparable with the 22 °C peak measured between 1953 and 1959.

Based on the recent data set, average daily maximum temperatures were similar in the uppermost and downstream reaches of Redwood Creek but were higher in the middle basin (Table 1). A model based on temporal correlations exponentially declining over days was found to have a superior fit compared with a model assuming no temporal correlations (AIC difference = 1318). There were no statistical differences between lower Redwood Creek (coho-bearing reach) and the Minon reach (no coho present) (20 °C and 20.6 °C, respectively). In contrast, sites in intervening reaches (Tall Trees, Emerald, Valley, and O'Kane) had significantly higher daily maximum temperatures, averaging over 21 °C, with Valley exhibiting the highest value (24.6 °C).

Daily minimal temperatures

In addition to maximum daily stream temperatures, we were interested in how the stream thermally recovers at night, and so we examined the minimum daily temperatures. Upper Redwood Creek (Minon) is the coolest site in terms of mean daily minimum temperatures, and the middle basin sites (Tall Trees, Emerald and Valley) are the warmest (Table 1). If we examine the daily pattern of minima more closely, some interesting differences in thermal patterns in Redwood Creek appear (Fig. 3). Using 2003 as an example, we show that at the Minon site, temperatures dropped below 18 °C on

Fig. 3. Daily minimum temperatures recorded in July and August 2003. These patterns were typical of all the years studied. Bold horizontal line represents the 18.1 °C threshold of concern for coho (Welsh et al. 2001).

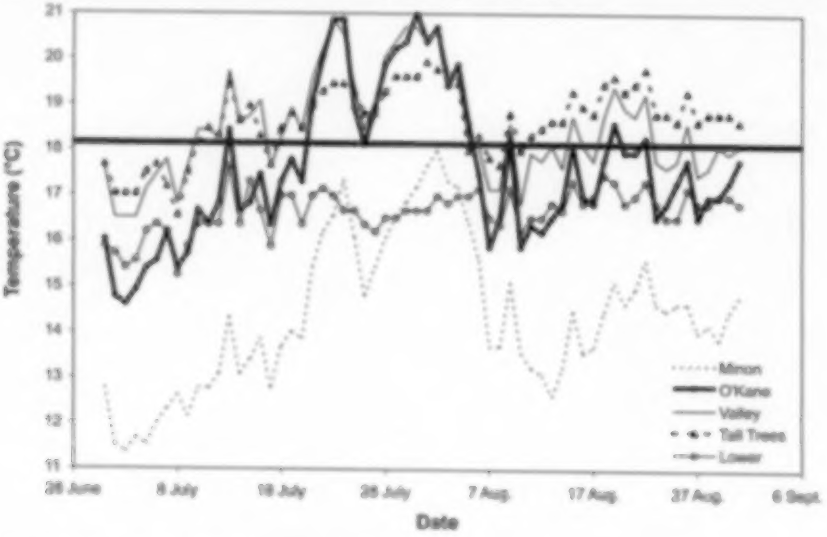

Table 2. Maximum weekly average temperatures (MWAT) at Redwood Creek monitoring stations.

Redwood Creek site	Drainage area (km^2)	Distance to mouth (km)	MWAT (°C) 1997	1998	1999	2000	2001	2002	2003
Estuary	730	0.3		19.1	17.4	18.4	18.9	18.7	20.2
Lower	611	7.7			17.6	18.5	18.2	18.1	18.7
Tall Trees	533	22.0		21.0	19.7	21.0	20.8	20.4	21.2
Emerald	520	23.3					20.9	20.5	21.3
Valley	314	46.7	22.0	22.3		22.1	21.9	21.8	22.5
O'Kane	175	72.9	21.4	21.7	20.1	21.4	21.0	21.4	22.2
Minon	86	91.0	18.4	18.5	17.6			18.3	19.0
Valley (air)*			28.7	27.9	25.7	25.6	27.7	29.8	29.3

Note: All MWAT records occurred in July or August of their respective year. Temperatures were not recorded at all stations for every year of the study. MWAT is the maximum of a 7-day moving average of daily average temperatures.

*Mean daily maximum air temperature for 1 July – 31 August.

each day for the entire summer season. Valley and O'Kane exhibited the highest values for minimum daily temperatures in late July and early August 2003. However, by 7 August, those reaches showed greater cooling at night than the downstream reach of Tall Trees. Even though the Tall Trees reach is within the old-growth redwood forest, daily minimum temperatures remained above 18 °C for most of the summer. Not until Lower were minimum daily temperatures consistently below 18 °C. These data indicate that at least half the length of Redwood Creek (Tall Trees to O'Kane, 50 km) had daily minimum temperatures above the desired range for coho. Lower also showed a more subdued pattern in terms of seasonal variation (Fig. 3). This reach has the highest discharge (so greater thermal mass) but also has more frequent coastal fog than upstream reaches.

A model based on temporal correlations exponentially declining over days was found to have a superior fit compared with a model assuming no temporal correlations (AIC difference = 1541). The daily minimum temperatures between the uppermost and downstream reaches of Redwood Creek were dissimilar, with the Minon site at the uppermost reach having lower minimum temperatures than lower Redwood Creek (Table 1). Stations in intervening reaches (Tall Trees, Emerald, and Valley) had significantly higher daily minimum temperatures, averaging >18 °C.

Maximum weekly average and maximum weekly maximum temperatures

Water temperatures reached their summer maxima in late July or early August for all years of record. MWAT and MWMT show similar patterns throughout Redwood Creek (Table 2; Fig. 4). Overall, the summer of 1999 exhibited the lowest MWAT values for all monitoring sites, as well as one of the coolest average air temperatures. Redwood Valley (Valley), located in the middle basin of Redwood Creek, had the highest values for MWAT

Fig. 4. Maximum weekly maximum temperatures, 1997 to 2003. Coho (*Oncorhynchus kisutch*) presence and absence thresholds are derived from studies in a nearby river basin, the Mattole (Welsh et al. 2001).

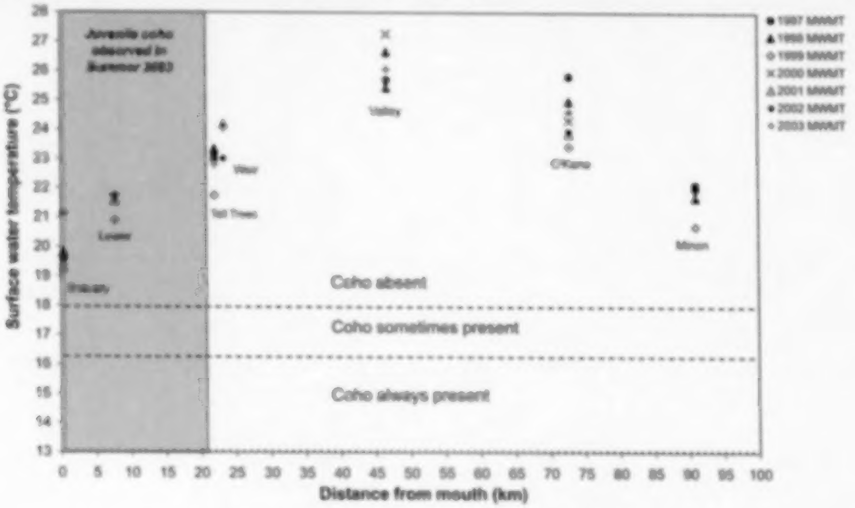

Fig. 5. Cumulative frequency distributions for July and August 2002 showing the total time that a given stream temperature was exceeded during these months. These distributions are typical for all the years studied.

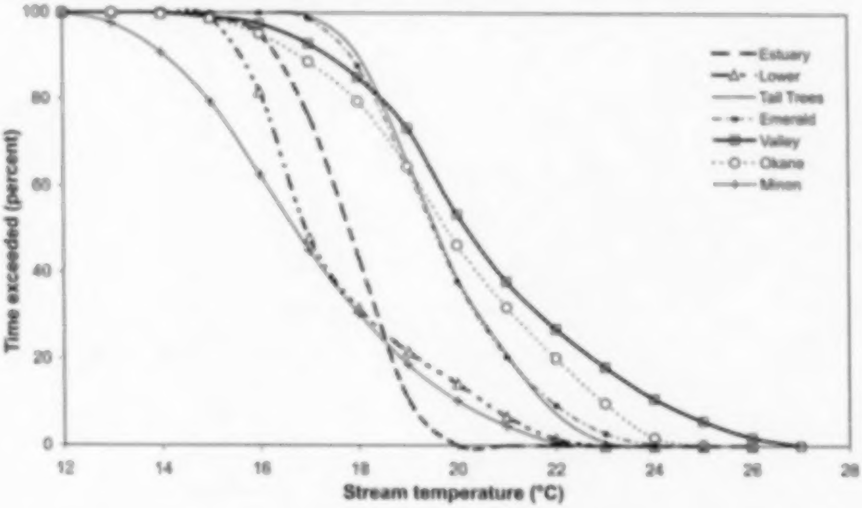

and MWMT. MWMT values increased sharply upstream of Redwood Creek at Tall Trees Grove (Tall Trees, rkm 22) (Fig. 4), which coincides with the upstream extent of coho documented during the 2003 presence–absence survey. MWAT also increased between the lower Redwood Creek (rkm 7.7) and the Tall Trees monitoring sites. Minon and Lower have the lowest temperature values, except for the Redwood Creek estuary (Estuary, rkm 0.3), which is moderated by inflow from the ocean.

Duration of exposure to high temperatures

Upper Redwood Creek (Minon) had the longest duration of cool temperatures (<18 °C) and Valley had the longest duration of high temperatures (>20 °C) (Fig. 5). These cumulative frequency distribution patterns are typical of the period of record (1997–2003). The temperature distributions for Tall Trees and Emerald were virtually the same, which is not surprising because they are located within 1.3 km of each other. Although these two sites exhibit less time at the highest temperatures than Valley and O'Kane, they also had less time at cool temperatures (<18 °C). Lower and Minon had similar exceedence curves for temperatures >18 °C, but Minon experienced a longer time span at cooler temperatures. Finally, Estuary had the most modulated temperature regime, with temperatures ranging from 16 °C to 20 °C most of the time.

The cumulative frequency–distribution curves represent the total number of hours that a given temperature was exceeded during the summer season. These curves can be examined in

Table 3. Geometric means of duration of stress intervals for temperatures exceeding 18, 20, 22, and 24 °C and frequency of stress intervals.

Site	Duration of stress intervals (h)				Frequency of stress intervals			
	>18 °C	>20 °C	>22 °C	>24 °C	>18 °C	>20 °C	>22 °C	>24 °C
Estuary	7.7ab	4.6a	1.0a	ND	148	20	1	ND
Lower	8.4b	4.4a	2.4ab	ND	223	178	11	ND
Tall Trees	26d	9.2b	3.6b	ND	98	237	107	ND
Emerald	26d	9.8b	4.3bc	2.2a	58	166	101	13
Valley	23c	11c	5.9d	2.8a	107	222	225	180
O'Kane	17c	9.0b	5.3cd	3.5b	163	219	133	27
Minon	5.7a	3.6a	1.8a	ND	174	68	12	ND

Note: Sites not sharing a common letter were statistically different from one another ($p < 0.05$). Sites with increasing stress interval durations are classified by alphabetically increasing letters. Sites indicated with ND had no stress intervals >24 °C. A stress interval is the number of consecutive hours over a specific high temperature.

Fig. 6. Median surface water temperature based on thermal infrared (TIR) imaging along Redwood Creek. Some surface flow temperatures in tributaries were recorded by the TIR imagery. Note that the locations of in-stream monitoring sites were distributed to detect the main temperature trends in the basin. (Modified from WSI (2004).)

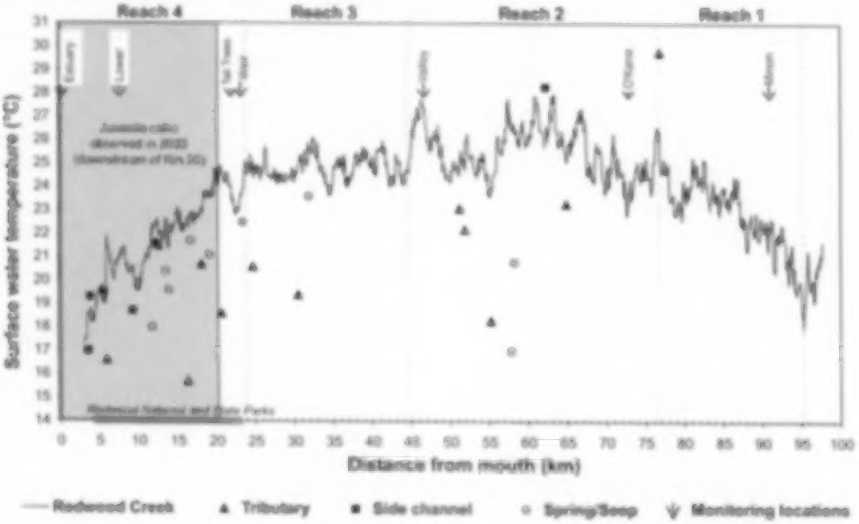

finer detail through the tabulation of stress intervals, which examines total consecutive hours exceeding a specific temperature. Statistical comparisons of stress intervals at the seven sites are summarized (Table 3). As with the daily minimum and maximum temperature models, a repeated-measures model based on temporal correlations exponentially over the sequence of stress intervals was superior to a model assuming no temporal correlations for >18, >20, >22, and >24 °C stress temperatures (AIC difference ≥100). The exposure to consecutive hours of high temperature was similar in the uppermost and downstream reaches of Redwood Creek. There were no statistical differences detected in the durations of >20 and >22 °C stress intervals between lower Redwood Creek (coho-bearing reach) and the Minon reach (no coho present). However, there was a difference between these two reaches for stress intervals >18 °C, where Minon had statistically shorter stress intervals. Neither station had any stress intervals of >24 °C. In contrast, stations in intervening reaches (Tall Trees, Emerald, Valley, and O'Kane) had significantly longer >18 and >20 °C stress intervals than the Lower or Minon stations. The Valley and O'Kane sites also had longer >22 °C stress intervals than the Lower and Minon stations. It is interesting to note that the Tall Trees and Emerald sites had significantly longer intervals of >18 °C than O'Kane (so less nighttime cooling), even though the MWATs and MWMTs are consistently higher at O'Kane.

TIR imaging

Surface water temperature data collected through TIR imaging in Redwood Creek is summarized (Fig. 6). The thermal profile of Redwood Creek generally increases from the headwaters to the middle part of the basin and then cools as it approaches the coast. This thermal signature has also been observed on the nearby Mattole River (Russ Faux, Watershed Sciences Inc., 230 SW 3rd Street, Corvallis, OR 97333, USA, personal communication). Water temperature varied on a shorter scale as well, e.g., changing more than 1 °C within a kilometre of the stream channel in several areas. Many such changes were associated with the inflow of tributaries or springs. Based on the TIR data for 29 July 2003, Redwood Creek can be divided into four main reaches that showed similar temperature characteristics (Fig. 6): reach 1, warming zone, water temperature in Redwood Creek increased from 17.9 °C in the headwaters to 26.5 °C downstream at rkm 76; reach 2, hot zone, the middle basin, where surface water temperatures ranged from 23 °C to 28 °C, exhibited the highest water temperatures of the survey; reach 3, warm zone, stream temperatures cooled slightly in the next 20 km, where the average surface water temperature was 24.8 °C; reach 4, cooling zone, in the downstream-most reach of Redwood Creek, closer to the ocean, stream temperatures cooled. The highest number of cool tributaries, springs, and seeps were also detected in this reach.

Discussion

TIR remote-sensing technology successfully provided spatially continuous stream temperature data for a 90 km reach of river in a large basin. This technology enabled stream temperature assessment across mixed ownership and inaccessible areas of the Redwood Creek basin. The longitudinal temperature profile from TIR imagery provides a clear snapshot of the current thermal regime in Redwood Creek and a baseline for monitoring future changes in stream temperature. Although TIR data for Redwood Creek provided a surface temperature profile at a limited temporal scale (one afternoon), the survey supplemented a 7-year temperature monitoring program conducted at a more limited spatial scale (seven sites). The TIR data identified four general stream reaches with differing thermal characteristics, which corroborated patterns detected by the continuous in-stream monitoring. Small cool-water seeps, springs, and side channels within the warmer river channel were also identified with TIR imagery.

TIR longitudinal profile data were also used to evaluate the adequacy of locations of long-term temperature monitoring sites. In-stream data loggers provide point data along the length of Redwood Creek, but TIR data integrate the spatial distribution and general thermal characteristics of the creek. We compared the location of stream temperature monitoring sites with the spatial distribution of water temperature throughout the basin from the TIR survey, which indicated that the current in-stream monitoring locations provide an adequate representation of stream temperature distribution in Redwood Creek. An additional data logger near rkm 60 would help better define the thermal regime in the hot zone, however.

The longitudinal temperature data revealed that Redwood Creek reaches its maximum temperature in the middle basin and becomes cooler farther downstream, unlike many rivers reported in the literature (Allan 1995). Lewis et al. (2000) demonstrated that the highest daily maximum temperatures in coastal streams in northern California were less than those in inland streams. In Redwood Creek, it is probable that coastal fog, old-growth redwood trees in the riparian zone, and an abundance of cool-water tributaries and seeps in the lower basin all contribute to the cooling trend there, but the relative importance of each of these factors is a subject for further research.

A comparison of thermal regimes at several sites in Redwood Creek shows some limited recovery of cool temperatures in upper Redwood Creek. From 1953 to 1959, before widespread basin disturbances, the maximum summer water temperature measured at Redwood Creek at O'Kane was 22 °C. Following severe floods, channel aggradation, and extensive timber harvest in the 1960s and 1970s, maximum water temperatures increased and peak summer water temperatures between 29 and 33.5 °C were measured in the period from 1975 to 1980. Since 1997, however, the peak temperatures in July and August have decreased to between 24.9 and 26.8 °C and the average daily maximum temperature decreased almost 3.5 °C to 22 °C. Some physical characteristics of the channel are recovering in this reach, based on the return to former streambed levels after aggradation (Madej and Ozaki 1996) and the re-establishment of riparian vegetation and canopy closure over Redwood Creek (Urner and Madej 1998), which may be contributing to the thermal recovery.

Our monitoring indicates that thermal recovery may be more complete in upper Redwood Creek (Minon) than at sites farther downstream. Thermal regimes differed markedly in the middle basin compared with the lower and upper basin. We used several metrics to compare the temperature regimes in upper Redwood Creek (Minon) and mid-upper Redwood Creek (O'Kane), where coho are absent, with lower Redwood Creek (Lower), where coho are still found. Daily maximum temperatures were not significantly different between Minon and Lower, and Minon had significantly lower minimum temperatures than Lower. Based on this analysis, we do not believe that summer water temperature is a limiting factor to juvenile coho rearing in the upper (Minon) reach.

In contrast, even though the temperature regime at O'Kane has improved since 1978, average maximum water temperature is significantly higher at O'Kane than at Lower, and MWMTs and MWATs are consistently higher at O'Kane. The duration of stress intervals was significantly longer at O'Kane than at Lower. The intervening reach between O'Kane and Tall Trees was significantly warmer than either Minon or Lower in terms of daily maxima and duration of stress intervals, and MWATs and MWMTs were also higher here. In addition, TIR data documented water temperatures of >22 °C for this 50 km reach. In the middle basin, MWATs and MWMTs for several years were >21.8 and >25 °C, respectively. Studies by Welsh et al. (2001) on tributaries of the Mattole River, California, suggest that streams with MWMT greater than 18.1 °C or MWAT greater than 16.8 °C may restrict the presence of juvenile coho salmon. (Coho salmon in Redwood Creek and the Mattole River are grouped within the same Evolutionary Significant Unit). Although the main channel of Redwood Creek is accessible to salmon and steelhead for most of its length and historically coho ranged throughout most of Redwood Creek, juvenile coho salmon are noticeably lacking in the middle and upper basins. High temperatures in the middle basin likely restrict juvenile rearing habitat there.

Many studies evaluate stream temperature regimes by only using daily and weekly means and maxima. Although these metrics give a useful snapshot of thermal conditions, an analysis of duration of high temperatures revealed additional thermal patterns of interest to us. For example, Redwood Creek at Tall Trees, despite having cooler maximum temperatures than the hot middle reach, exhibited longer durations of moderately high temperatures (>18 °C) than the middle reach (Valley) and so represents a different type of thermal stress for fish. Minon also had significantly shorter durations of stress intervals (consecutive hours above 18, 20, and 22 °C) than Lower. The difference in patterns between MWMT and stress interval data suggests that duration of elevated temperatures should be considered in addition to daily maximum and average temperatures to more fully represent water temperature regimes. The relative importance of short durations of high temperatures versus longer durations of moderately high temperatures on fish physiology in Redwood Creek is not known, and we encourage the use of additional metrics, such as cumulative distribution curves and stress intervals, to assess duration characteristics of thermal regimes.

The coho presence–absence surveys indicated that juvenile coho rearing is currently limited to the downstream-most section of Redwood Creek, and less than 20% of the main channel currently supports young coho during the summer. Stream temperature monitoring indicated that there is a sharp decrease in the MWAT, MWMT, and maximum daily water temperature on the lower river between rkm 22 and rkm 7.7 across all years. In addition, the TIR profile showed the greatest thermal complexity in the downstream-most reach of Redwood Creek, where many cools springs, seeps, side channels, and tributaries were measured.

During the last 5 years, no juvenile coho have been caught at the downstream migrant trap in Redwood Valley (rkm 53.0), indicating no use by juvenile coho upstream of the trap site (Sparkman 2004). TIR data indicate that Redwood Valley is the hottest reach in Redwood Creek. In-stream temperature monitoring supports this conclusion, and since monitoring began in 1997, Redwood Valley has had the highest maximum daily water temperatures, MWATs, and MWMTs of all the monitoring sites along the entire length of the creek. During 2004, Sparkman (2004) caught YOY coho salmon at the lower downstream migrant trap (rkm 6.4) on Redwood Creek every month from April to July. This indicates that lower Redwood Creek and the estuary may still provide important rearing habitat for juvenile coho salmon. Unfortunately, there is limited information on coho distribution in the Redwood Creek basin through time. Nevertheless, we have shown that a headwater reach (O'Kane) that was historically cool and then experienced increased temperatures for at least 5 years has begun to thermally recover, and upstream of that reach (at Minon), conditions are similar to those in a coho-bearing reach of stream. However, the intervening 50 km reach of stream has summer water temperature several degrees warmer than what is reported to be acceptable for coho in the nearby Mattole River basin (Welsh et al. 2001). The only reach that currently supports coho is the downstream-most 20 km of the 100 km long Redwood Creek. Based on this study and the Mattole River coho distribution data, we suggest that a thermal restriction may be reducing the historical range of rearing for juvenile coho for about three-quarters of the length of Redwood Creek.

There are several limitations to this study. Although TIR remote sensing can map surface water temperature, it cannot be used as a tool to identify thermally stratified pools, which may be several degrees cooler at depth. Past studies have shown that although few in number, cold pools exist in lower Redwood Creek (Moses 1984; Ozaki 1988; Keller et al. 1995) and provide important coldwater refugia for salmonids during periods of thermal stress (Nielsen et al. 1994). For the past couple of years, juvenile steelhead have been observed using cooler thermal areas in Redwood Valley (Valley) during periods of high water temperature (Michael Sparkman, 50 Ericson Court, Arcata, CA 95521, USA, personal communication). Some of the most interesting cool-water interactions occur along the channel banks. Unfortunately, with TIR data, the riparian vegetation commonly obscures the channel edges where cool groundwater seeps and springs may emerge. Small areas (<3 m^2) of groundwater seeps or cool upwelling are nondetectable at the scale of the TIR flight used in this study. Likewise, in-stream monitoring by probes emplaced in the main flow will not detect small cool-water sources. As a result, small cool-water refugia may exist in warm reaches of Redwood Creek, but these must be quantified by a different method

Based on the results of this study, stream temperature appears to be a dominant factor controlling distribution of juvenile coho salmon. Nevertheless, past land use and large floods caused extensive channel aggradation, which adversely affected aquatic and riparian habitat and destroyed juvenile rearing habitat in Redwood Creek. Timber harvest and stream bank erosion resulted in a loss of riparian trees and habitat. Surveys of longitudinal profiles of the lower river in 1977 indicated that the channel bed was filled in with sediment and lower Redwood Creek was flat and featureless after large storms in 1964 and the early 1970s. Pool depths and frequencies have subsequently increased (Madej 1999). Although aquatic and riparian habitat in Redwood Creek is recovering, there are still lingering effects such as the lack of large riparian trees to provide both stream shading and a source for in-stream wood and the lack of functional large woody debris in the channel to scour pools and provide cover and channel complexity (California Resources Agency 2005). The lack of high-quality rearing habitat, large wood, and channel complexity may also contribute to the limited upstream distribution of coho.

Other possible factors may affect the distribution of coho in the Redwood Creek basin. The influence of fish hatchery operations in Prairie Creek, a tributary entering Redwood Creek near its mouth, from 1894 to 1993 is not known. The Prairie Creek hatchery produced coho salmon from 1924 to 1993, with the exception of 1945–1960. Hatchery operations may have introduced higher numbers of coho to the basin and coho runs in Redwood Creek may have been artificially increased. Presently, no invasive or exotic fish species exist in Redwood Creek. Nevertheless, there may be shifts in the native fish communities in response to changing channel conditions and warmer stream temperature regimes.

In addition, lower Redwood Creek was severely altered following the construction of flood control levees in 1968. Historically, Redwood Creek near its mouth meandered across a wide floodplain. The levees channelized the downstream-most 5 km of channel into a narrow straight chute, isolating the river from its floodplain. Consequently, access to favorable backwater and alcove habitat by coho in this reach was eliminated. Because the riparian zone along two-thirds of Redwood Creek has been converted from a conifer-dominated system in 1947 to a deciduous system (Urner and Madej 1998), nutrient and invertebrate prey availability has probably changed, as suggested by Murphy and Meehan (1991). Turbidity levels in Redwood Creek frequently exceed 300 nephelometric turbidity units (NTU) during winter flows (R. Klein, RNSP, 1655 Heindon Road, Arcata, CA 95521, USA, unpublished data). Bisson and Bilby (1982) reported that juvenile coho salmon avoided water with turbidities that exceeded 70 NTU. High winter turbidity levels may affect the ability of juvenile coho to feed and thus affect their growth, but these factors have not been quantified. Future research will examine the influence of such factors on coho distribution. Nevertheless, our study highlights the importance of temperature monitoring over a long time period along the entire length of river, as well as the need for integrative studies incorporating bioenergetics and physiology with temperature monitoring and modeling.

Acknowledgements

Carrie Jones, Brian Barr, and Heather Ambrose processed the raw temperature files, and Jeremy Hunter and Van Hare helped process the TIR data. Greg Bundros and Tom Marquette deployed temperature probes at many of the Redwood Creek locations. Green Diamond Resource Company, Barnum Timber Company, and the Stover family granted access to Redwood Creek monitoring sites. Baker Holden, Terry Hines, Kyle Max, Jeanne Mayer, and Ben Littlefied assisted in the snorkel surveys. We are grateful to two anonymous reviewers for their thought-provoking comments.

References

Allan, J.D. 1995. Stream ecology: structure and function of running waters. Chapman & Hall, New York.

Anderson, D.G. 1988. Juvenile salmonid habitat of the Redwood Creek basin, Humboldt County, California. M.S. thesis, Humboldt State University, Arcata, Calif.

Armour, C.L. 1991. Guidance for evaluating and recommending temperature regimes to protect fish. US Fish Wildl. Serv. Biol. Rep. No. 90(22).

Becker, C.D., and Genoway, R.G. 1979. Evaluation of the critical thermal maximum for determining thermal tolerance of freshwater fish. Environ. Biol. Fishes, **4**: 245–256.

Bell, M.C. 1973. Fisheries handbook of engineering requirements and biological criteria. US Army Corps of Engineers, Fish Passage Development and Evaluation Program, North Pacific Division, Portland, Oregon, Contract No. DACW57-68-0086.

Bell, E. 2001. Survival, growth and movement of juvenile coho salmon (*Oncorhynchus kisutch*) over-wintering in alcoves, backwaters, and main channel pools in Prairie Creek, California. M.S. thesis, Humboldt State University, Arcata, Calif.

Beschta, R.L., Bilby, R.E., Brown, G.W., Holtby, L.B., and Hofstra, T.D. 1987. Stream temperature and aquatic habitat: fisheries and forestry interactions. *In* Forestry and fisheries interactions. *Edited by* E.O. Salo and T.W. Cundy. University of Washington Institute of Forest Resources, Seattle, Wash., Contribution No. 57. pp. 191–232.

Best, D.W. 1995. History of timber harvest in the Redwood creek basin, Northwestern California. Chapter C. *In* Geomorphic processes and aquatic habitat in the Redwood Creek Basin, Northwestern California. *Edited by* K.M. Nolan, H.M. Kelsey, and D.C. Marron. US Geological Survey Professional Paper 1454. pp. C1–C7.

Bisson, P.A., and Bilby, R.E. 1982. Avoidance of suspended sediment by juvenile coho salmon. N. Am. J. Fish. Manag. **2**: 371–374.

Bjornn, T.C., and Reiser, D.W. 1991. Habitat requirements of salmonids in streams. *In* Influences of forest and rangeland management on salmonid fishes and their habitats. *Edited by* W.R. Meehan. Am. Fish. Soc. Spec. Publ. No. 19. pp. 112–133.

Blodgett, J.C. 1970. Water temperatures of California streams: North Coastal Subregion. US Geological Survey Open-File Report, USGS, Menlo Park, Calif.

Brett, J.R. 1952. Temperature tolerance in young Pacific salmon, genus *Oncorhynchus* sp. J. Fish. Res. Board Can. **9**: 265–323.

Brett, J.R. 1979. Environmental factors and growth. *In* Fish physiology. Vol. 8. *Edited by* W.S. Hoar, D.J. Randall, and J.R. Brett. Academic Press, New York. pp 599–675.

Briggs, J.C. 1953. The behavior and reproduction of salmonid fishes in small coastal streams. Calif. Dep. Fish Game Bull. No. 94, Sacramento, Calif.

Brown, R.A. 1988. Physical rearing habitat for anadromous salmonids in the Redwood Creek Basin, Humboldt County, California. M.S. thesis, Humboldt State University, Arcata, Calif.

Brungs, W.A., and Jones, B.R. 1977. Temperature criteria for freshwater life: protocol and procedures. US Environmental Protection Agency EPA-600/3-77-061.

Burnham, K.P., and Anderson, D.R. 1998. Model selection and inference: a practical information-theoretic approach. Springer-Verlag Inc., New York.

California Department of Fish and Game. 1965. California Fish and Wildlife Plan. Vols. I, II, and IIIB. State of California Resources Agency, Department of Fish and Game, Sacramento, Calif.

California Department of Fish and Game. 2002. Status review of California coho salmon north of San Francisco. Report to the California Fish and Game Commission, April 2002. California Fish and Game Commission, Sacramento, Calif.

California Resources Agency. 2005. North Coast Watershed Assessment Program: Redwood Creek assessment implementation summary. California Resources Agency, Sacramento, Calif.

De Staso, J., III, and Rahel, F.J. 1994. Influence of water temperature on interactions between juvenile Colorado River cutthroat trout and brook trout in a laboratory stream. Trans. Am. Fish. Soc. **123**: 289–297.

Dockray, J.J., Reid, S.D., and Wood, C.M. 1996. Effects of elevated summer temperatures and reduced pH on metabolism and growth of juvenile rainbow trout (*Oncorhynchus mykiss*) on unlimited ration. Can. J. Fish. Aquat. Sci. **53**: 2752–2763.

Ebersole, J.L., Liss, W.J., and Frissell, C.A. 2001. Relationship between stream temperature, thermal refugia and rainbow trout *Oncorhynchus mykiss* abundance in arid-land streams in the northwestern United States. Ecol. Freshw. Fish, **10**: 1–10.

Hallock, R.J., Warner,G.H., and Fry, D.H., Jr. 1952. California's part in a three-state salmon fingerling marking program. Calif. Fish Game Rep. **38**: 301–332.

Keller, E.A., Hofstra, T.D., and Moses, C. 1995. Summer "cold pools" in Redwood Creek near Orick, California. Chapter U. *In* Geomorphic processes and aquatic habitat in the Redwood Creek Basin, Northwestern California. *Edited by* K.M. Nolan, H.M. Kelsey, and D.C. Marron. US Geological Survey Professional Paper Paper No. 1454. pp. U1–U9.

Lewis, T.E., Lamphear, D.W., McCanne, D.R., Webb, A.S., Krieter, J.P., and Conroy, W.D. 2000. Regional assessment of stream temperatures across northern California and their relationship to various landscape-level and site-specific attributes. Forest Science Project, Humboldt State University Foundation, Arcata, Calif.

Li, H.W., Lamberti, G.A., Pearsons, T.N., Tait, C.K., Li, J.L., and Buckhouse, J.C. 1994. Cumulative effects of riparian disturbances along high desert trout streams of the John Day Basin, Oregon. Trans. Am. Fish. Soc. **123**: 627–640.

Littell, R.C., Milliken, G.A., Stroup, W.W., and Wolfinger, R.D. 1996. SAS system for mixed models [computer program]. SAS Institute Inc., Cary, N.C.

Madej, M.A. 1995. Changes in channel-stored sediment, Redwood Creek, Northwestern California, 1947–1980. Chapter *O*. *In* Geomorphic processes and aquatic habitat in the Redwood Creek Basin, Northwestern California. *Edited by* K.M. Nolan, H.M. Kelsey, and D.C. Marron. US Geological Survey Professional Paper No. 1454. pp. O1–O27.

Madej, M.A. 1999. Temporal and spatial variability in thalweg profiles of a gravel-bed river. Earth Surf. Processes Landforms, **24**: 1153–1169.

Madej, M.A. 2001. Development of channel organization and roughness following sediment pulses in single-thread, gravel bed rivers. Water Resour. Res. **37**(8): 2259–2272.

Madej, M.A., and Ozaki, V. 1996. Channel response to sediment wave propagation and movement, Redwood Creek, California, USA. Earth Surf. Processes Landforms, **21**: 911–927.

Matthews, W.J., and Zimmerman, E.G. 1990. Potential effects of global warming on native fishes of the southern Great Plains and the Southwest. Fisheries, **15**: 26–32.

McGeer, J.C., Baranyi, L., and Iwama, G.K. 1991. Physiological responses to challenge tests in six stocks of coho salmon (*Oncorhynchus kisutch*). Can. J. Fish. Aquat. Sci. **48**: 1761–1771.

Meisner, J.D. 1990. Potential loss of thermal habitat for brook trout, due to climatic warming, in two southern Ontario streams. Trans. Am. Fish. Soc. **119**: 282–291.

Moses, C.G. 1984. Pool morphology of Redwood Creek, California. M.S. thesis, University of California at Santa Barbara, Santa Barbara, Calif.

Murphy, M.L., and Meehan, W.R. 1991. Stream ecosystems. *In* Influences of forest and rangeland management on salmonid fishes and their habitats. *Edited by* W.R. Meehan. Am. Fish. Soc. Spec. Publ. No. 19. pp. 17–46.

Nielsen, J.L., Lisle, T.E., and Ozaki, V. 1994. Thermally stratified pools and their use by steelhead in northern California streams. Trans. Am. Fish. Soc. **123**: 613–626.

Ozaki, V. 1988. Geomorphic and hydrologic conditions for cold pool formation on Redwood Creek, California. Redwood National Park Technical Report No. 24, Redwood National Park, Arcata, Calif.

Ozaki, V., and Anderson D. 2005. Evaluation of stream temperature regimes for juvenile coho salmon in Redwood Creek using thermal infrared. National Park Service, Water Resources Division, Ft. Collins, Co., Tech. Rep. NPS/NRWRD/NRTR-2005/331.

Pacific Coast Fish, Wildlife and Wetlands Restoration Association. 2002. Redwood Creek Salmon Spawner Survey 2000/01 Season. Pacific Coast Fish, Wildlife and Wetlands Restoration Association, Arcata, Calif.

Snyder, J.O. 1931. Salmon of the Klamath River, California. Division of Fish and Game of California, Sacramento, Calif., Fish Bull. No. 34.

Sparkman, M.D. 2004. Redwood Creek Juvenile Salmonid Downstream Migration Study, study year 2004. Annual Report Project 2i3. California Department of Fish and Game, Anadromous Fisheries Resource Assessment and Monitoring Program, Northern California, North Coast Region, Arcata, Calif.

Sparkman, M.D. 2005. Upper Redwood Creek Juvenile Salmonid Downstream Migration Study. A Five-Year Summary Report. Project 2i4 (Draft). California Department of Fish and Game, Anadromous Fisheries Resource Assessment and Monitoring Program, Northern California, North Coast Region, Arcata, Calif.

Stein, R.A., Reimers, P.E., and Hall, J.D. 1972. Social interaction between juvenile coho (*Oncorhynchus kisutch*) and fall Chinook salmon (*O. tshawytscha*) in Sixes River, Oregon. J. Fish. Res. Board Can. **29**(12): 1737–1748.

Torgerson, C.E., Faux, R.N., McIntosh, B.A., Poage, N.J., and Norton, D.J. 2001. Airborne thermal remote sensing for water temperature assessment in rivers and streams. Remote Sens. Environ. **76**: 386–398.

Urner, S., and Madej, M.A. 1998. Changes in riparian composition and density following timber harvest and floods along Redwood Creek, California. The Society for Ecological Restoration Northwest Chapter, Seattle, Wash. pp. 32–34. [Abstracts.]

US Geological Survey. 1975–1980. Water resources data for California water year 1975–1980. Vol. 2. Pacific slope basins. Annual Water Data Reports, US Geological Survey, Sacramento, Calif.

Van Kirk, S. 1994. Historical information on Redwood Creek. Report prepared for Redwood National Park, Arcata, Calif. (www.krisweb.com/biblio/redwood_nps_vankirk_1994.pdf).

Watershed Sciences Inc. 2004. Aerial survey of Redwood Creek. Thermal infrared and color videography. Final report to Redwood National and State Parks, Corvallis, Oregon.

Welsh, H.H., Jr., Hodgson, G.R., Harvey, B.C., and Roche, M.E. 2001. Distribution of juvenile coho salmon in relation to water temperatures in tributaries of the Mattole River, California. N. Am. J. Fish Manag. **21**: 464–470.

Willey, W.S. 2004. Energetic response of juvenile coho salmon (*Oncorhynchus kisutch*) to varying water temperature regimes in northern California streams. M.S. thesis, Humboldt State University, Arcata, Calif.

Pure spatial and spatially structured environmental variables explain *Skistodiaptomus* copepod range limits in the northeastern USA

Ryan A. Thum and Richard S. Stemberger

Abstract: We assessed the ability of present-day environmental factors to explain the nonoverlapping range boundaries of *Skistodiaptomus* copepods in the northeastern USA. Variance partitioning using partial canonical correspondence analysis (CCA) attributed 21% of the variance in species occurrences to spatial location, 20% to spatially structured environmental variation, and 12% to environmental factors that are not spatially structured. Discriminant function analysis (DFA) aided our interpretation of the variance in species' occurrences attributed to spatially structured environmental variation. *Skistodiaptomus pallidus* lakes were discriminated from *Skistodiaptomus oregonensis* and *Skistodiaptomus pygmaeus* lakes along a productivity gradient, with *S. pallidus* occurring in more productive lakes. In contrast, *S. oregonensis* and *S. pygmaeus* lakes were environmentally similar. Thus, a large portion of the spatially structured variation in the variance-partitioning analysis most likely reflected the shared correlations between the spatial locations and environmental conditions of *S. pallidus* lakes. Taken together, the results from CCA and DFA analyses suggested that *S. pallidus*' range boundary is controlled by environmental factors (lake productivity), while the range boundaries for *S. oregonensis* and *S. pygmaeus* were related more to their biogeographic histories than to present-day environments. We discuss alternative explanations for range limits that are independent of environmental conditions.

Résumé : Nous avons évalué dans quelle mesure les facteurs environnementaux d'aujourd'hui permettent d'expliquer les répartitions des aires géographiques discrètes des copépodes *Skistodiaptomus* dans le nord-est des É.-U. Une partition de la variance par analyse des correspondantes canoniques (CCA) partielles attribue 21 % de la variance dans la présence des espèces à la position géographique, 20 % à de la variation environnementale à structure spatiale et 12 % à des facteurs environnementaux qui ne sont pas structurés en fonction de l'espace. Une analyse des fonctions discriminantes (DFA) a contribué à l'interprétation de la variance dans la présence des espèces attribuée à la variation environnementale reliée à l'espace. Les lacs à *Skistodiaptomus pallidus* se distinguent des lacs à *Skistodiaptomus oregonensis* et à *Skistodiaptomus pygmaeus* d'après un gradient de productivité, *S. pallidus* se retrouvant dans les lacs plus productifs. En revanche, les lacs à *S. oregonensis* et à *S. pygmaeus* possèdent des environnements semblables. Ainsi, une portion importante de la variation à structure spatiale dans l'analyse de partition de la variance reflète très vraisemblablement les corrélations communes entre les positions géographiques et les conditions environnementales des lacs à *S. pallidus*. Pris dans leur ensemble, les résultats des analyses CCA et DFA indiquent que les limites de l'aire de répartition de *S. pallidus* sont contrôlées par des facteurs environnementaux (productivité des lacs), alors que les limites d'aire de *S. oregonensis* et de *S. pygmaeus* sont reliées plus à leur histoire biogéographique qu'à leur environnement d'aujourd'hui. Des explications de rechange des limites d'aire qui sont indépendantes des conditions environnementales font l'objet d'une discussion.

[Traduit par la Rédaction]

Introduction

Species' ranges may reflect both contemporary ecological interactions and historical contingencies (Endler 1982*a*, 1982*b*). When dispersal opportunities are not limiting, species' ranges should reflect present-day variation in environmental conditions that define geographic boundaries between local habitats that do or do not support positive population growth (e.g., Caughley et al. 1987; Root 1988). For example, range limits may be set by physiological constraints to abiotic conditions (e.g., Root 1988), habitat selection (e.g., States 1976; Howard and Harrison 1984; Alkon and Saltz 1988), or the presence of natural enemies that exclude them. However, geographic ranges may also be limited by factors that are not necessarily related to environmental conditions. For example, limitations to dispersal (e.g., dependence on continuous water routes) can influence species' range limits if dispersal opportunities are available in some but not all di-

Received 6 July 2005. Accepted 22 December 2005. Published on the NRC Research Press Web site at http://cjfas.nrc.ca on 13 May 2006.
J18776

R.A. Thum[1,2] and R.S. Stemberger. Department of Biological Sciences, Dartmouth College, Hanover, NH 03755, USA.

[1] Corresponding author (e-mail: rat38@cornell.edu).
[2] Present address: Department of Ecology and Evolutionary Biology, E303 Corson Hall, Cornell University, Ithaca, NY 14853, USA.

Can. J. Fish. Aquat. Sci. 63: 1397–1404 (2006) doi:10.1139/F06-046

rections (Gaylord and Gaines 2000). Similarly, populations may experience Allee effects that prevent range expansion beyond their current limits (Keitt et al. 2001). Finally, range limits may be defined by biological interactions (e.g., interference competition, reproductive interference, hybridization) with adjacently distributed (parapatric) species, and these interactions need not be mediated by the environment (Bull 1991; Case et al. 2005).

Biogeographic analyses of zooplankton distributions in areas of North America that were glaciated during the Pleistocene have revealed strong associations between the current distributions of many species and historical waterway connections (e.g., proglacial lakes) to presumed areas of glacial refugia (Dadswell 1974; Carter et al. 1980; Stemberger 1995). While these associations suggest that dispersal limitation across wide biogeographic spatial scales contributes substantially to species' geographic range limits, they do not preclude an important role of contemporary environmental conditions for maintaining range limits. For example, strong correlations may exist between the geological history of an area and present-day environmental conditions. Moreover, zooplankton are thought to disperse effectively because of the prevalent production of resting stages that can presumably disperse readily through animal vectors (Maguire 1963; Proctor 1964). In addition, recent experimental evidence suggests that local processes are more important than dispersal limitation in determining local zooplankton composition across small spatial scales (Shurin 2000). However, the influence of dispersal versus environmental limitations on zooplankton distributions may vary across taxa (Jenkins and Buikema 1998; Jenkins and Underwood 1998; Bohonak and Jenkins 2003). Thus, biogeographic studies should explicitly test for an influence of contemporary environmental conditions and factors that are independent of the environment in determining species' ranges.

Copepods in the genus *Skistodiaptomus* that occur in the northeastern United States and adjacent Canada provide a unique opportunity to study the relative importance of present-day environmental factors versus other factors for determining species' range limits. Associations between current distributions and historical waterways suggest historical dispersal limitation to the large proglacial lakes that formed along the retreating edge of the Wisconsinan glacier, and these lakes ultimately connected to the isolated glacial refugia from which they likely colonized (Stemberger 1995; Fig. 1). Moreover, these species do not appear to be as effective dispersers as other zooplankton groups (Stemberger 1995), and thus their distributions may be limited by factors that are not necessarily related to present-day environmental conditions. However, differences in contemporary environmental conditions among lakes occupied by these species have not been explicitly evaluated as a factor maintaining *Skistodiaptomus* distributions.

A variety of statistical techniques have been developed to relate variance in species' occurrences to variance in environmental conditions (e.g., Legendre and Legendre 1998; ter Braak and Šmilauer 2002). In addition, the inclusion of spatial locations (i.e., geographic location of lakes in the study area) as explanatory variables can be used to decompose the explained variance in species' occurrences into three fractions that correspond to (*a*) spatially independent environmental variance, (*b*) spatially structured environmental variance, and (*c*) pure spatial variance that is independent of environmental variance (Borcard et al. 1992). If species' distributions correspond to variation in environmental factors, then the explained variance in species' occurrences should be attributed to either pure or spatially structured environmental variation. On the other hand, when species' distributions are limited by factors other than environmental conditions, we expect spatial location independent of environmental variation to largely explain species' occurrences. Thus, the relative importance of spatial and environmental variables can be used to infer the relative influence of contemporary environment in determining species' range limits.

Here we take advantage of a large data set of environmental conditions for lakes across the range boundaries of northeastern USA *Skistodiaptomus* to evaluate the relative influences of contemporary environmental differences versus factors unrelated to the environment in maintaining their distribution boundaries. We use partial canonical correspondence analysis (CCA; ter Braak 1986; Borcard et al. 1992; ter Braak and Šmilauer 2002) to determine the relative influences of environmental variables and spatial locations to explain *Skistodiaptomus* occurrences. We then use discriminant function analysis (DFA) to determine whether lakes occupied by different species are discriminated by local environmental conditions. Although similar to the CCA in its methodology, DFA is used to explicitly test the hypothesis that *Skistodiaptomus* species occupy lakes that are significantly different in their environmental conditions. The DFA allows multiple comparisons between species, which in turn facilitates the interpretation of the spatially structured environmental component (*b*) in the CCA. For example, discriminant functions that significantly distinguish *Skistodiaptomus oregonensis* lakes from *Skistodiaptomus pygmaeus* lakes indicate longitudinal gradients in environmental variables contributing heavily to that function, since these species are spatially segregated across the landscape along a longitudinal axis (see Fig. 1).

Using CCA and DFA in conjunction, we show that spatially structured environmental variation largely explains *Skistodiaptomus pallidus* occurrences, while spatial location independent of environmental variation explains the majority of variation in *S. oregonensis* and *S. pygmaeus* occurrences.

Materials and methods

Skistodiaptomus and environmental data were obtained from the US Environmental Protection Agency Environmental Monitoring and Assessment Program – Surface Waters survey of northeastern USA lakes (available from http://www.epa.gov/emap/html/datal/surfwatr/data/nelakes/index.html). This data set consists of 614 sampling dates for 373 lakes in New England, New Jersey, and New York during the months of July–August 1991–1996. Of these lakes, 253 were sampled once and 120 were sampled more than once (up to seven times). Six lakes were excluded because they lacked zooplankton data.

We selected a single sampling date from each of the lakes that were sampled more than once over the period of 1991–1996 to satisfy assumptions of statistical independence. We randomly selected a sampling date from each lake where a

Fig. 1. Distributions of *Skistodiaptomus* species in the northeastern USA based on species occurrence from the Environmental Monitoring and Assessment Program data (available from http://www.epa.gov/emap/html/datal/surfwatr/data/nelakes/index.html). *Skistodiaptomus* species show little overlap in their distributions except in southern New England. Shaded circles, *Skistodiaptomus oregonensis*; solid triangles, *Skistodiaptomus pygmaeus*; open squares, *Skistodiaptomus pallidus*.

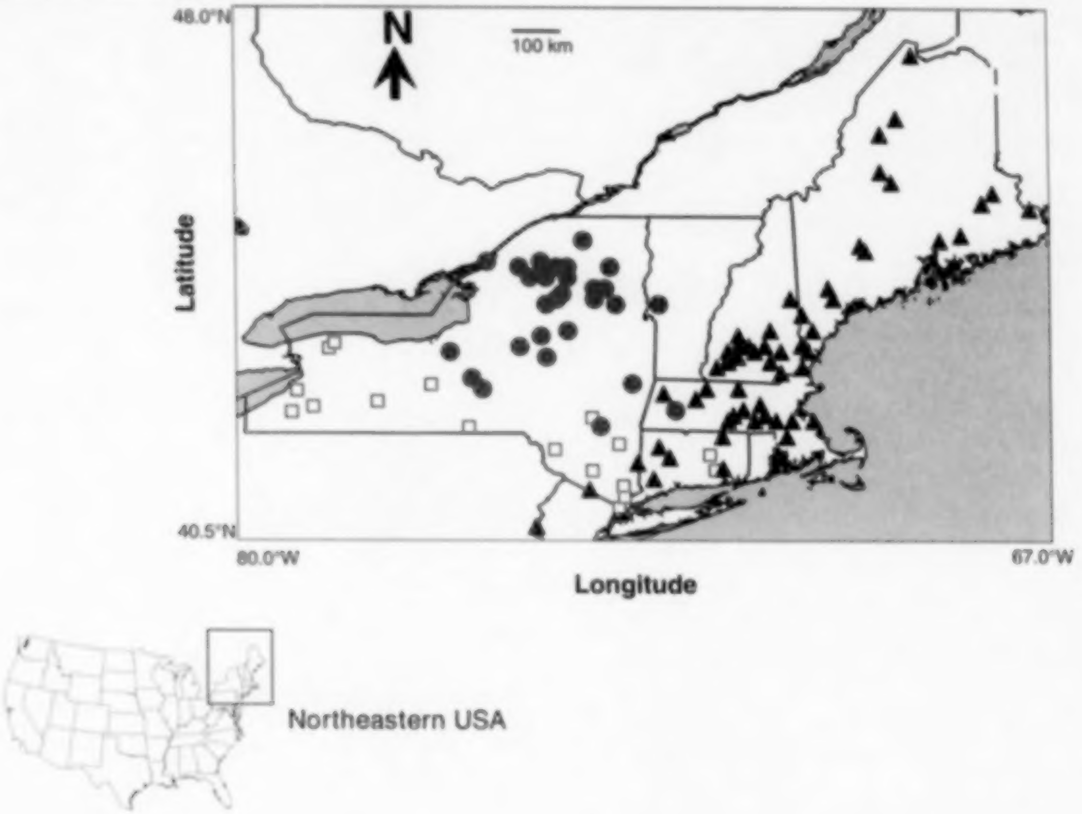

Skistodiaptomus was either present or absent on all visits (354 lakes). If a *Skistodiaptomus* was present in some but not all sampling visits, we randomly chose a sampling date from which the species was present (13 lakes) to maximize our power to discriminate among lakes inhabited by different species. *Skistodiaptomus* may have been present in some lakes without detection if the adult stages upon which species identifications are based were not observed. However, failure to detect *Skistodiaptomus* in some lakes did not bias our analyses because we only made statistical comparisons among lakes where *Skistodiaptomus* were present; we did not attempt to compare lakes with and without particular *Skistodiaptomus*. Sample sizes of lakes containing *S. pallidus*, *S. oregonensis*, and *S. pygmaeus* were 24, 34, and 72, respectively.

In all analyses, we related presence or absence data for *Skistodiaptomus* to a number of physicochemical, nutrient, hydrological, and biological variables (see Table 1). We used conductivity, pH, and acid-neutralizing capacity (ANC) as surrogates for all ion concentrations because they are highly correlated ($r > |0.8|$). We $\log_{10}$-transformed continuous variables such as chemical variables and species abundances to satisfy assumptions of normality and equal variance. Similarly, we square-root-transformed species richness variables. pH was not transformed, as it was already measured on a log scale. Because of negative values, ANC was transformed by taking the $\log_{10}$ of the absolute value of each measurement and then adjusting the sign depending on the sign of the original measurement.

Influence of environmental versus spatial factors on *Skistodiaptomus* occurrences

We performed partial CCA (ter Braak 1986) using CANOCO, version 4.5 (ter Braak and Šmilauer 2002) for variance partitioning described by Borcard et al. (1992). CCA is the preferred method for relating explanatory variables to presence or absence data (Legendre and Legendre 1998). Briefly, three separate CCAs were performed: one using environmental variables, one using spatial variables, and one using both environmental and spatial variables. Because of the potential for shared portions of variance due to correlations between environmental variables and spatial location, the environmental CCA explains a fraction of variance ($a + b$) that includes a spatially structured component (b). Similarly, the spatial CCA explains a fraction of variance ($b + c$) that includes this same spatially structured environmental

Table 1. Means and ranges of environmental variables used in canonical correspondence and discriminant function analyses for three *Skistodiaptomus* species.

Variable	*S. oregonensis*		*S. pygmaeus*		*S. pallidus*	
	Mean	Min.–Max.	Mean	Min.–Max.	Mean	Min.–Max.
Hydrological						
Lake area (ha)	201.9	1.6–1229.7	205.2	1.5–4284.5	49.5	1.8–730.9
Average depth (m)	4.7	0.6–19.4	4.1	0.6–21.9	2.9	0.6–18.5
Retention (years)	0.5	0–4.1	0.5	0–3.4	0.2	0–2.3
Elevation (m)	365.8	22.0–600.0	176.5	2–555.0	218.4	11.0–568.0
Physicochemical						
pH	7.3	4.5–8.7	7.2	4.2–8.5	8.2	7.5–8.6
ANC (µequiv.·L^{-1})	484.1	–2621.5	208.5	–1612.2	1099.1	188.0–2963.0
Conductivity (µS·cm^{-1})	92	10.4–692.2	86.2	17.6–688.0	223	76.6–660.0
Color (PCU)	28.6	3.0–193.0	27.8	2.0–299.0	24.3	3.0–126.0
Turbidity (NTU)	1	0.3–3.2	1.1	0.3–6.7	6.2	0.6–31.0
Total suspended solids (mg·L^{-1})	1.9	0.3–4.8	1.6	0–7.8	11.9	0.6–116.0
Nutrients						
Total P (µg·L^{-1})	15.3	3.6–62.0	12.7	0–55.0	441.3	6.0–8740.0
Total N (µg·L^{-1})	406.9	202.0–1018.0	382.6	148.0–2524.0	1088.9	300.0–4013.0
N/P	3.5	2.0–4.4	3.4	0–6.6	2.7	0–4.1
Biological						
Chlorophyll *a* (µg·L^{-1})	7.9	1.2–43.5	4.9	0–28.5	42	1.8–191.9
Species richness (no. of species)						
Small cladocerans	3.2	0–7.0	3.7	1.0–9.0	4.2	1.0–10.0
Large cladocerans	3.1	0–6.0	3.1	0.0–10.0	2	1.0–7.0
Small cyclopoids	0.4	0–1.0	0.6	0.0–1.0	0.6	0–1.0
Large cyclopoids	1.7	0–5.0	1.5	0–4.0	1.3	0–5.0
Calanoid copepods	1.8	0–3.0	1.9	1–5.0	1.3	0–5.0
Crustaceans	10.2	0–16.0	10.6	1.0–24.0	9.1	0–21.0
Rotifers	20.2	0–35.0	18.4	0–37.0	18.6	0–38.0
Species abundance (individuals·L^{-1})						
Small cladocerans	7.3	0–59.9	6.5	0–123.3	39.8	0.2–267.1
Large cladocerans	5.8	0–27.1	9.3	0–263.5	15.9	0–138.3
Large adult cyclopoids	3.4	0–22.8	4	0–28.3	14.3	0–154.2
Adult *Epischura*	0.1	0–1.3	0.1	0–1.0	0.1	0–7.8
Rotifers	292.6	0–2273.2	244.7	0.3–1701.4	1041.2	18.4–5466.7

Note: Not all variables entered into the analyses significantly ($\alpha = 0.05$; see text for details). ANC, acid-neutralizing capacity; PCU, platinum–cobalt units; NTU, nephelometric turbidity units.

component. The CCA incorporating both spatial and environmental variables explains the total variation in species occurrences ($a + b + c$). Thus, the spatially structured environmental component of variance (b) can be determined from the equation:

$$b = [(a + b) + (b + c)] - (a + b + c)$$

The pure environmental (a) and pure spatial (c) components can then be determined by subtraction:

$$a = (a + b) - b$$

and

$$c = (b + c) - b$$

We used the forward selection procedure in CANOCO and 1000 Monte Carlo permutation tests for selecting environmental (see Table 1) and spatial variables to include in the partial CCAs (ter Braak and Šmilauer 2002) with an $\alpha = 0.05$. Spatial variables consisted of decimal degrees longitude and latitude coordinates of lake locations. Variables were included if they explained a significant amount of additional variance at $\alpha = 0.05$. In addition, we inspected variance inflation factors (VIFs) and eliminated variables with VIFs > 20 (ter Braak and Šmilauer 2002).

Environmental differences among *Skistodiaptomus* lakes

We used DFA to determine if lakes occupied by different *Skistodiaptomus* species could be distinguished from one another based on their environmental conditions using STATISTICA, version 7.1 (StatSoft Software, Inc., Tulsa, Oklahoma).

As in the CCA, we chose the environmental variables to include in the DFA by using the forward selection procedure with $\alpha = 0.05$. In addition, we only allowed variables with tolerances >0.1 to enter. Tolerance ranged from 0 to 1 and is a measure of the unique contribution of an environmental

Table 2. Variance partitioning and associated *P* values for canonical correspondence analyses with spatial and environmental variables based on 1000 Monte Carlo permutations.

Partition	Variance explained (%)	*P*
a + *b* + *c*	53.0	0.001
a + *b*	32.2	0.001
a + *c*	40.6	0.001
a	12.4	
b	19.6	
c	21.0	
Unexplained	47.0	

Note: Values represent the percentage of variation in *Skistodiaptomus* occurrences explained by the first two canonical axes. Pure environmental (*a*), spatially structured (*b*), and pure spatial (*c*) variance components and their combinations are shown. Both canonical axes were significant at $\alpha = 0.001$.

variable to the overall analysis — higher numbers reflect greater unique contribution to the analysis. We applied Levene's tests on all environmental variables to check for heterogeneity of variances among groups.

Predation by fish is a major factor structuring body size and species composition of zooplankton assemblages (Currie et al. 1999). We did not include any fish variables in our multivariate analyses because of missing data for many lakes (only 11 and 18 lakes with *S. oregonensis* and *S. pallidus* present, respectively, had fish data). To maintain the higher sample sizes for multivariate analyses, we analyzed the total counts of fish (which included young-of-the-year fish, juveniles, and adults) for all *Skistodiaptomus* lakes for which these data were available using univariate analysis of variance (ANOVA). These data were $\log_{10}$-transformed before analysis to satisfy the assumption of homogeneity of variances among groups. Collection effort was dependent on lake size and is described in Baker et al. (1997).

Results

Influence of environmental versus spatial factors on *Skistodiaptomus* occurrences

Forward selection identified four environmental variables that entered significantly into the CCA: turbidity, total nitrogen, elevation, and pH. ANC was significant using forward selection but had a high VIF because of its high correlation with pH. Therefore, we included pH and eliminated ANC. All other environmental variables (see Table 1) failed to enter significantly into the analysis using forward selection criteria. Both longitude and latitude entered significantly into the model using a forward procedure with only spatial variables.

Spatial and environmental variables together explained 53% of the variation in *Skistodiaptomus* occurrences (Table 2). The majority (40%) of this variation was attributed to spatial location independent of the environment. In fact, forward selection revealed that longitude alone was the greatest single predictor of species occurrences (Table 3). However, a pure spatially structured environmental component also contributed heavily to the explained variance (37%). Pure environmental variation explained the least amount of variance in species occurrences (23%). Moreover, the relative importance of environmental variables in explaining species occurrences decreased when spatial variables were also included (Table 3). For example, elevation failed to explain any additional variance in species occurrences when spatial location was also considered (Table 3).

Table 3. Comparison of marginal and conditional λ values for canonical correspondence analyses.

Variable	Marginal λ	Conditional λ		
		a	*b*	*c*
Longitude	0.57	—	0.57	0.57
Latitude	0.23	—	0.12	0.24
Turbidity	0.41	0.41	0.30	—
Total N	0.36	0.09	0.03	—
Elevation	0.12	0.08	0	—
pH	0.18	0.06	0.04	—

Note: Marginal λ refers to the variance in species occurrences explained by the variable alone. Conditional λ refers to the additional variance in species occurrences explained after the inclusion of other variables in the forward selection procedure. Variance components: pure environmental (*a*), spatially structured (*b*), and pure spatial (*c*).

Table 4. Factor structures of the two discriminant functions (DF) for *Skistodiaptomus* lakes.

Variable	DF1	DF2	Tolerance*
pH	0.39	–0.09	0.82
Color	–0.04	0.06	0.56
Turbidity	0.70	–0.46	0.51
Total N	0.67	–0.06	0.37
Lake area	–0.29	–0.06	0.64
Average lake depth	–0.22	0.22	0.50
Elevation	0.00	0.81	0.89

*Tolerance is a measure of the redundancy of explanatory variables.

Environmental differences among *Skistodiaptomus* lakes

Seven environmental variables entered significantly into the DFA: pH, color, turbidity, total nitrogen, average lake depth, and elevation. Turbidity, total nitrogen, and pH contributed most heavily to discriminant function one (DF1), while elevation, turbidity, and average lake depth contributed most heavily to DF2 (Table 4).

The DFA produced two canonical axes (discriminant functions) that were significant at $\alpha = 0.01$. The overall DFA had a Wilks' λ (a measure of discriminatory power, where 0 is perfect discrimination and 1 is no discriminatory power) of 0.38. However, the second discriminant function had poor discriminatory power (Wilks' $\lambda = 0.84$). This poorer discriminatory power of the second discriminant function is because DFA partitions variance among groups such that the most variance is explained by the first axis, followed by the second axis, and so on.

Multiple comparisons of species indicated that the environments of lakes occupied by different *Skistodiaptomus* were significantly different at $\alpha = 0.001$. A scatterplot of DF1 scores versus DF2 scores demonstrates that DF1 discriminates *S. pallidus* from *S. oregonensis* and *S. pygmaeus*, while

Fig. 2. Scatterplot of scores from overall discriminant functions among lakes occupied by different *Skistodiaptomus* species. There is clear separation of *Skistodiaptomus pallidus* from *Skistodiaptomus oregonensis* and *Skistodiaptomus pygmaeus* along discriminant function 1, which is driven largely by variables related to productivity. Discriminant function 2 is largely driven by elevation, which separates *S. oregonensis* and *S. pygmaeus*. Shaded circles, *S. oregonensis*; solid triangles, *S. pygmaeus*; open squares, *S. pallidus*.

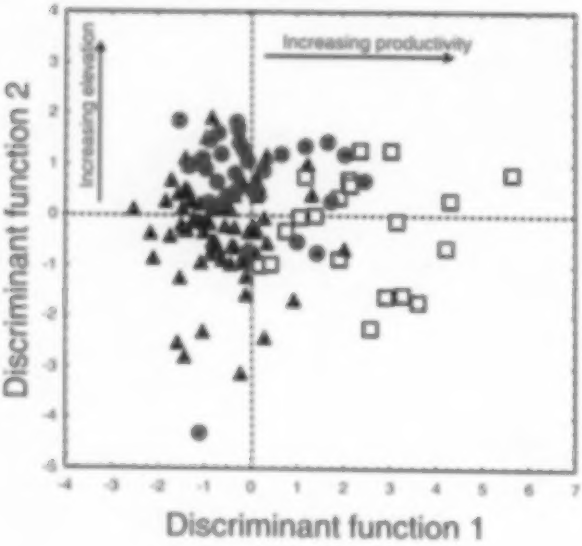

DF2 discriminates *S. oregonensis* from *S. pallidus* and *S. pygmaeus* (Fig. 2). Although significantly different, examination of the classification of cases based on the discriminant functions revealed that *S. oregonensis* lakes were commonly misclassified as *S. pygmaeus* lakes (47% of *S. oregonensis* lakes misclassified as *S. pygmaeus* lakes). *Skistodiaptomus pallidus* and *S. pygmaeus* lakes were correctly classified as such in 75% and 90% of the cases, respectively.

Finally, one-way ANOVAs performed on the total fish counts further supported strong environmental differentiation of lakes occupied by *S. pallidus*. Total fish counts significantly differed among lakes occupied by different *Skistodiaptomus* ($F_{[2,58]} = 5.2$, $p = 0.008$); Newman–Keuls multiple comparisons showed that *S. pallidus* lakes had significantly more fish (mean of $\log_{10}$-transformed data = 2.8, $n = 18$) than lakes having either *S. pygmaeus* (mean of $\log_{10}$-transformed data = 1.2, $n = 33$) or *S. oregonensis* (mean of $\log_{10}$-transformed data = 1.5, $n = 11$). However, total fish counts between *S. oregonensis* lakes and *S. pygmaeus* lakes did not significantly differ (Fig. 3).

Discussion

The variance-partitioning CCA demonstrates that spatial location explains the vast majority of the variation in *Skistodiaptomus* occurrences in the northeastern USA. Although the largest component of variance is attributed to pure spatial variance independent of environmental variation (fraction *a*), spatially structured environmental variation (fraction *b*) also explains a sizeable fraction of *Skistodiaptomus* occurrences. The pure spatial component of variance is consistent with Stemberger's (1995) suggestion that dispersal limitation to historical waterway connections to isolated glacial refugia explains the nonoverlapping ranges of *Skistodiaptomus* in the northeastern USA. However, the spatially structured environmental component of variance suggests that landscape-level environmental gradients may also maintain these nonoverlapping boundaries.

Fig. 3. Mean and standard errors for total fish counts for lakes occupied by different *Skistodiaptomus* species. Letters above bars indicate multiple comparisons, where identical letters indicate groups that are not significantly different (α = 0.05).

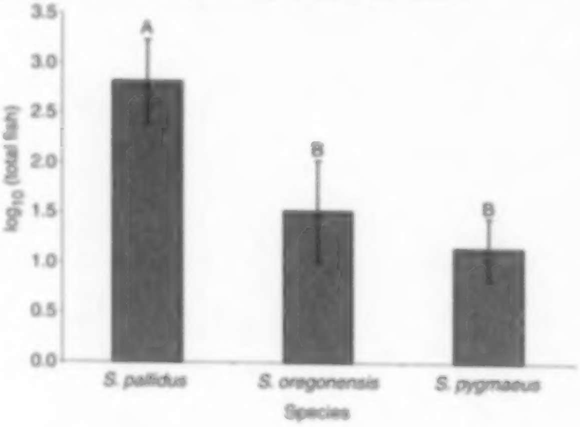

DFA further revealed the relative contributions of spatial versus environmental factors accounting for *Skistodiaptomus* occurrences in northeastern lakes. In particular, it suggests that the northern range limit of *S. pallidus* in the northeastern USA is determined by environmental factors, while the eastern and western range limits of *S. oregonensis* and *S. pygmaeus*, respectively, are determined by spatial location independent of environmental variables.

Lakes occupied by *S. pallidus* were clearly different in their environmental characteristics from those occupied by *S. oregonensis* or *S. pygmaeus*. In short, *S. pallidus* lakes were more productive than *S. oregonensis* or *S. pygmaeus* lakes: they were more turbid and had higher total nitrogen and pH. In addition, *S. pallidus* lakes also had higher numbers of fish and smaller-bodied zooplankton assemblages dominated by high abundances of small cladocerans, early instars of cyclopoid copepods, and rotifers although these variables were either not included (i.e., fish data) or did not enter significantly into the overall DFA or CCA. Dominance by small-bodied species most likely reflected the intensity of size-selective predation by fish (Stemberger and Miller 2003). However, lake productivity was also positively correlated with higher numerical abundances of small cladocerans, cyclopoid copepods, and rotifers (Stemberger and Lazorchak 1994). Thus, *S. pallidus* occupation of more productive lakes may reflect either its physiological tolerance to abiotic conditions, its ability to prey on small zooplankton-like rotifers (Williamson and Butler 1987), or its ability to reduce impacts on its population growth rate by effectively avoiding fish predators. Regardless of the biological mechanism, *S. pallidus*' northern boundary in the northeastern USA appears to be environmentally controlled by variables associated with higher productivity.

The environmental differences between *S. pallidus* lakes versus *S. oregonensis* and *S. pygmaeus* lakes are consistent with previous descriptions of *S. pallidus*. For example, cultural eutrophication of lakes has been recognized as a factor promoting *S. pallidus*' range expansion in the western USA (Byron and Saunders 1981) and Wisconsin (Torke 2001) from areas in which it historically occurred. Recent land use changes due to increased agricultural development in the southern region of our study area have occurred to a greater extent than in the northern region and may therefore explain why *S. pallidus* is the most dominant *Skistodiaptomus* in this region.

In contrast with *S. pallidus*, lakes occupied by *S. oregonensis* and *S. pygmaeus* were similar in the majority of environmental variables, with the exception of lake elevation: *S. oregonensis* tended to occur in higher-elevation lakes. However, lake elevation itself is spatially structured across the landscape: lakes in the western portions of our study area (where *S. oregonensis* occurs) are generally higher than in eastern portions (where *S. pygmaeus* occurs). In a separate DFA (not shown), we included longitude as an independent variable. The inclusion of longitude in the forward selection procedure resulted in the elimination of elevation as a significant variable in the model ($p = 0.55$). This indicates that the strong influence of lake elevation on the discrimination of *S. oregonensis* and *S. pygmaeus* lakes results from the correlation between lake location and elevation. Another DFA (not shown) where neither elevation of longitude was included resulted in insignificant differences between *S. oregonensis* and *S. pygmaeus* lakes ($p = 0.25$).

The slight difference in mean lake elevations between *S. oregonensis* and *S. pygmaeus* probably has little biological relevance and more likely reflects the influence of dispersal from geographically isolated glacial refugia, as suggested by Stemberger (1995). The higher elevations of lakes currently occupied by *S. oregonensis*, particularly in the Adirondack province, are at much higher elevation today than they were at the onset of glacial retreat because of extensive isostatic rebound of the underlying bedrock since deglaciation. Although lake elevation can influence environmental conditions such as water chemistry (e.g., Webster et al. 1996; Webster et al. 2000), elevation differences between *S. oregonensis* and *S. pygmaeus* lakes are not accompanied by environmental differences in other variables.

The environmental similarities among lakes occupied by *S. oregonensis* and *S. pygmaeus* suggest that factors other than contemporary environments may have played an important role in maintaining their historic range limits following their initial colonization of the northeastern USA at the end of the Pleistocene. As Stemberger (1995) suggested, dispersal limitation to water vector transport may have preserved the historical range limits of these two species following colonization of interior North America from isolated glacial refugia using the extensive proglacial lake and drainage connections. This interpretation implicitly invokes Allee effects that prevent range expansion beyond current limits (e.g., Keitt et al. 2001), and there is some evidence that Allee effects may play an important role in determining occurrences for copepods. For example, weak overland dispersal ability and Allee effects appear to limit the ability of the diaptomid copepod *Hesperodiaptomus shoshone* to reestablish populations in ponds where it occurred before the introduction of fish populations, even after fish removal (Sarnelle and Knapp 2004). However, zooplankton are generally thought to disperse effectively because of their production of resting stages that can be easily transported by animal vectors, such as birds (Maguire 1963; Proctor 1964; Figuerola et al. 2005). Thus, dispersal limitation is not expected to be a major factor involved in limiting species' distributions (e.g., Shurin 2000). An alternative explanation is that direct interactions between *S. oregonensis* and *S. pygmaeus* prevent their range overlap despite their dispersal abilities. Although models for competitive parapatry over homogeneous space are rare (Bull 1991), one mechanism is reproductive interference (decreases in the reproductive fitness of females due to physical blocking or damaging of genitalia by indiscriminant mating with heterospecific males; Bull 1991; Case et al. 2005). *Skistodiaptomus oregonensis* and *S. pygmaeus* males will mate readily with heterospecific females despite zero production of offspring (*S. oregonensis* males crossed with female *S. pygmaeus*) or the production of intrinsically incompatible offspring that die before their first molt (*S. pygmaeus* males crossed with *S. oregonensis* females; Thum 2004). Moreover, a recently completed experiment demonstrates that the presence of heterospecific males decreases the probability of successful fertilization of both *S. oregonensis* and *S. pygmaeus* females (R. Thum, unpublished data). Thus, there is a strong opportunity for reproductive interference, which has been demonstrated to maintain stable parapatry (Anderson 1977; Bull 1991; Case et al. 2005).

It is possible that our analysis failed to incorporate some spatially structured environmental variables that influence *Skistodiaptomus* occurrences (Legendre and Legendre 1998), and 37% of the variance in species occurrences remains unexplained. This explanation is unlikely because important environmental variables that we failed to incorporate would have to be uncorrelated with all of the variables that we included, and this list is comprehensive.

Separating the influence of history and contemporary environmental factors that explain occurrences of these species will likely require a variety of investigations that address alternative hypotheses, as suggested by Endler (1982*b*). Our analyses make important headway on untangling the relative influences of contemporary environmental factors and historical contingencies in determining species' ranges. Specifically, we extend our understanding of the drivers of range limits for zooplankton following colonization from Pleistocene refugia. Previous interpretations of zooplankton distributions in the northeastern USA and Canada were based almost solely on spatial occurrence data (e.g., Dadswell 1974; Carter et al. 1980; Stemberger 1995); we have explicitly incorporated environmental and spatial factors into a single analysis. Our results suggest that environmental factors related to lake productivity may limit the spread of some zooplankton species that expanded from their Pleistocene refugia following glacial retreat. However, environmental similarities among lakes occupied by different species of these copepods suggest that factors other than environmental differences have prevented the spread of some species from the areas they originally colonized via extensive waterway connections following ice sheet retreat. Further investigation of alternative hypotheses for range limits that do not depend on environmental conditions should broaden our understanding of the interactions between species' ecologies and their histories in determining geographic ranges.

Acknowledgements

We thank K.L. Cottingham, J.J. Gilbert, R.G. Harrison, M.A. McPeek, J. Jones, K. Peterson, B. Brown, N.G. Hairston, Jr., T. Yoshida, C. Kearns, and J. Fox for helpful comments.

References

Alkon, P.U., and Saltz, D. 1988. Foraging time and the northern range limits of the Indian crested porcupine (*Hystrix indica* Kerr). J. Biogeogr. **15**: 403–408.

Anderson, R.F.V. 1977. Ethological isolation and competition of allospecies in secondary contact. Am. Nat. **111**: 939–949.

Baker, J., Peck, D., and Sutton, D. 1997. Environmental monitoring and assessment program surface waters: field operations manual for lakes. US Environmental Protection Agency, Washington, D.C.

Bohonak, A.J., and Jenkins, D.G. 2003. Ecological and evolutionary significance of dispersal by freshwater invertebrates. Ecol. Lett. **6**: 783–796.

Borcard, D., Legendre, P., and Drapeau, P. 1992. Partialling out the spatial component of ecological variation. Ecology, **73**: 1045–1055.

Bull, C.M. 1991. Ecology of parapatric distributions. Annu. Rev. Ecol. Syst. **22**: 19–38.

Byron, E.R., and Saunders, J.F. 1981. Colonization of Lake Tahoe and other western habitats by the copepod, *Skistodiaptomus pallidus* (Herrick) (Calanoida). Southwest. Nat. **26**: 82–83.

Carter, J.C.H., Dadswell, M.J., Roff, J.C., and Sprules, W.G. 1980. Distribution and zoogeography of planktonic crustaceans and dipterans in glaciated eastern North America. Can. J. Zool. **58**: 1355–1387.

Case, T.J., Holt, R.D., McPeek, M.A., and Keitt, T.H. 2005. The community context of species' borders: ecological and evolutionary perspectives. Oikos, **108**: 28–46.

Caughley, G., Grice, D., Barker, R., and Brown, B. 1987. The edge of the range. J. Anim. Ecol. **57**: 771–785.

Currie, D.J., Dilworth-Christie, P., and Chapleau, F. 1999. Assessing the strength of top-down influences on plankton abundance in unmanipulated lakes. Can. J. Fish. Aquat. Sci. **56**: 427–436.

Dadswell, M.J. 1974. Distribution, ecology and postglacial dispersion of certain crustaceans and fishes in eastern North America. Natl. Mus. Can. Pub. Zool. 11.

Endler, J.A. 1982*a*. Aternative hypotheses in biogeography: introduction and synopsis of the symposium. Am. Zool. **22**: 349–354.

Endler, J.A. 1982*b*. Problems in distinguishing historical from ecological factors in biogeography. Am. Zool. **22**: 441–452.

Figuerola, J., Green, A.J., and Michot, T.C. 2005. Invertebrate eggs can fly: evidence of waterfowl-mediated gene flow in aquatic invertebrates. Am. Nat. **165**: 274–280.

Gaylord, B., and Gaines, S.D. 2000. Temperature or transport? Range limits in marine species mediated solely by flow. Am. Nat. **155**: 769–789.

Howard, D.J., and Harrison, R.G. 1984. Habitat segregation in ground crickets: the role of interspecific competition and habitat selection. Ecology, **65**: 69–76.

Jenkins, D.G., and Buikema, A.L., Jr. 1998. Do similar communities develop in similar sites? A test with zooplankton structure and function. Ecol. Monogr. **68**: 421–443.

Jenkins, D.G., and Underwood, M.O. 1998. Zooplankton may not disperse readily in wind, rain, or waterfowl. Hydrobiologia, **387/388**: 15–21.

Keitt, T.H., Lewis, M.A., and Holt, R.D. 2001. Allee effects, invasion pinning, and species' borders. Am. Nat. **157**: 203–216.

Legendre, P., and Legendre, L. 1998. Numerical ecology. 2nd ed. Elsevier, Amsterdam.

Maguire, B.J. 1963. The passive dispersal of small aquatic organisms and their colonization of isolated bodies of water. Ecol. Monogr. **33**: 161–185.

Proctor, V.W. 1964. Viability of crustacean eggs recovered from ducks. Ecology, **45**: 656–658.

Root, T. 1988. Energy constraints on avian distributions and abundances. Ecology, **69**: 330–339.

Sarnelle, O., and Knapp, R.A. 2004. Zooplankton recovery after fish removal: limitations of the egg bank. Limnol. Oceanogr. **49**: 1382–1392.

Shurin, J.B. 2000. Dispersal limitation, invasion resistance, and the structure of pond zooplankton communities. Ecology, **81**: 3074–3086.

States, J.B. 1976. Local adaptations in chipmunk *Eutamias amoenus* populations and evolutionary potential at species borders. Ecol. Monogr. **46**: 221–256.

Stemberger, R.S. 1995. Pleistocene refuge areas and postglacial dispersal of copepods of the northeastern United States. Can. J. Fish. Aquat. Sci. **52**: 2197–2210.

Stemberger, R.S., and Lazorchak, J.M. 1994. Zooplankton assemblage responses to disturbance gradients. Can. J. Fish. Aquat. Sci. **51**: 2435–2447.

Stemberger, R., and Miller, E. 2003. Cladoceran body length and Secchi disk transparency in northeastern U.S. lakes. Can. J. Fish. Aquat. Sci. **60**: 1477–1486.

ter Braak, C.J.F. 1986. Canonical correspondence analysis: a new eigenvector technique for multivariate direct gradient analysis. Ecology, **67**: 1167–1179.

ter Braak, C.J.F., and Šmilauer, P. 2002. CANOCO reference manual and CanoDraw for Windows user's guide: software for canonical community ordination (Version 4.5). Microcomputer Power, Ithaca, N.Y.

Thum, R.A. 2004. The influences of environmental differences and incomplete reproductive isolation on parapatry in *Skistodiaptomus* copepods. Ph.D. thesis, Dartmouth College, Hanover, N.H.

Torke, B. 2001. The distribution of calanoid copepods in the plankton of Wisconsin lakes. Hydrobiologia, **453**: 351–365.

Webster, K.E., Kratz, T.K., Bowser, C.J., Magnuson, J.J., and Rose, W.J. 1996. The influence of landscape position on lake chemical responses to drought in northern Wisconsin. Limnol. Oceanogr. **41**: 977–984.

Webster, K.E., Soranno, P.A., Baines, S.B., Kratz, T.K., Bowser, C.J., Dillon, P.J., Campbell, P., Fee, E.J., and Hecky, R.E. 2000. Structuring features of lake districts: landscape controls on lake chemical responses to drought. Freshw. Biol. **43**: 499–515.

Williamson, C.E., and Butler, N.M. 1987. Temperature, food and mate limitation of copepod reproductive rates: separating the effects of multiple hypotheses. J. Plankton Res. **9**: 821–836.

Energy expenditure during hatching in rainbow trout (*Oncorhynchus mykiss*) embryos

Marcie M. Ninness, E. Don Stevens, and Patricia A. Wright

Abstract: The objective of our study was to estimate the overall (aerobic and anaerobic) energy expenditure involved in hatching in rainbow trout (*Oncorhynchus mykiss*) embryos. During hatching, there were significant increases (50% and 19%, respectively) in movement and oxygen consumption. There were no differences in tissue indicators of anaerobic metabolism (adenosine triphosphate (ATP), adenosine monophosphate (AMP) deaminase, ammonia) between embryos that hatched naturally (chorionated) compared with embryos in which the chorion had been manually removed and therefore did not hatch (dechorionated). Furthermore, phosphocreatine (PCr), ATP, and lactate were unaltered immediately after hatching compared with embryos at rest before hatch. The anaerobic capacity of just hatched larvae was further evaluated by forced exercise and hypoxic exposure. PCr and ATP were unaltered following a 2 min manual chase, whereas lactate concentration was significantly increased (30%). Hypoxia (5 mg $O_2 \cdot L^{-1}$, 5 days) resulted in a 2.7-fold elevation of tissue lactate concentration. Our results reveal that the increase in activity during hatch may be involved in escaping the egg capsule, but the metabolic cost of this increased movement is relatively small. Moreover, the anaerobic capacity of newly hatched rainbow trout is low relative to juvenile or adult fish.

Résumé : L'objectif de notre étude est d'estimer la dépense globale (aérobie et anaérobie) d'énergie impliquée dans l'éclosion des embryons de la truite arc-en-ciel (*Oncorhynchus mykiss*). Durant l'éclosion, il y a des augmentations significatives de 50 % du mouvement et de 19 % de la consommation d'oxygène. Il n'y a pas de différence dans les indicateurs tissulaires de métabolisme anaérobie (triphosphate d'adénosine (ATP), monophosphate d'adénosine (AMP), déaminase, ammoniaque) entre les embryons (chorionés) qui éclosent naturellement et les embryons (déchorionés) dont le chorion a été retiré manuellement et qui n'éclosent donc pas. De plus, la phosphocréatine (PCr), l'ATP et le lactate demeurent inchangés immédiatement après l'éclosion par comparaison avec des embryons au repos avant l'éclosion. Nous avons aussi évalué la capacité anaérobie des larves fraîchement écloses à l'aide d'exercices imposés et d'une exposition à l'hypoxie. La PCr et l'ATP restent inchangées après une poursuite manuelle de 2 min, alors que la concentration de lactate s'accroît significativement de 30 %. Une hypoxie (5 mg $O_2 \cdot L^{-1}$, 5 jours) cause une augmentation de 2,7 fois de la concentration tissulaire de lactate. Nos résultats montrent que l'augmentation de l'activité durant l'éclosion permet peut-être la libération de la capsule de l'oeuf, mais que le coût métabolique de ces mouvements additionnels est relativement bas. De plus, la capacité anaérobie des truites arc-en-ciel à l'éclosion est basse par comparaison à celle des poissons juvéniles et adultes.

[Traduit par la Rédaction]

Introduction

The chorion is a tough, acellular shell that surrounds and protects salmonid embryos during their development. Following fertilization, the chorion undergoes a calcium-dependant hardening that increases the mechanical strength of the egg 10-fold (for review, see Kørsgaard et al. 1995). At the time of hatch, the embryo must penetrate the chorion. It is fairly well established that a proteolytic hatching enzyme released into the perivitelline fluid by the embryo plays a major role in the hatching process by digesting the inner layer of the chorion (Hayes 1942; Yamagami 1988). The mechanical component of hatching, or movement by the embryo, is generally thought to play only a minor role in hatching but has been considered by only a few studies. Peterson and Martin-Robichaud (1983) observed that in Atlantic salmon (*Salmo salar*), the head of the embryo broke through the chorion requiring very little mechanical effort on the part of the embryo; however, the number of movements during hatching was not quantified. Speer-Blank and Martin (2004) reported an increase in the number of movements once hatching was artificially triggered in California grunion (*Leuresthes tenuis*) embryos. Thus, the data is sparse on the mechanical component of hatching.

Wright et al. (1995) and Wright and Fyhn (2001) have suggested that any activity during hatching is exhaustive, relying partly on anaerobic energy expenditure. Their reasoning is based on their observation that tissue ammonia

Received 27 May 2005. Accepted 22 December 2005. Published on the NRC Research Press Web site at http://cjfas.nrc.ca on 18 May 2006.
J18713

M.M. Ninness, E.D. Stevens, and P.A. Wright.[1] Department of Integrative Biology, University of Guelph, 50 Stone Road East, Guelph, ON N1G 2W1, Canada.

[1] Corresponding author (e-mail: patwrigh@uoguelph.ca).

Can. J. Fish. Aquat. Sci. **63**: 1405–1413 (2006)   doi:10.1139/F06-036

concentrations are elevated at the time of hatching in rainbow trout (*Oncorhynchus mykiss*) embryos (Wright et al. 1995; Essex-Fraser et al. 2005). Ammonia formation is known to occur under anaerobic conditions in fish white muscle (for review, see Wood 2001). Under these conditions, adenosine triphosphate (ATP) stores are metabolized through adenosine diphosphate (ADP) and the adenylate kinase reaction to adenosine monophosphate (AMP), which in turn is deaminated via AMP deaminase, resulting in increases in inosine monophosphate (IMP) and ammonia in the intracellular compartment of the muscle. It is unknown if hatching involves anaerobic energy expenditure in trout embryos.

Despite the vast literature available for juvenile (e.g., Goolish 1989; Krumschnabel and Lackner 1993; McDonald et al. 1998) and adult fish (Black et al. 1960; Mommsen and Hochachka 1988; Wang et al. 1994), anaerobic metabolism in embryonic and larval fish has received much less attention (Hinterleitner et al. 1987; Krumschnabel and Lackner 1992; Franklin et al. 1996). Larval fish exhibit several morphological, behavioural, and physiological differences from juvenile and adult fish. Behaviorally, newly hatched trout larvae remain at the bottom of the rearing tray, exhibiting periodic movement consisting mainly of one–two tail flips per minute (M. Ninness, personal observation) and move by tail beating only if disturbed (Nag and Nursall 1972; Proctor et al. 1980). The complete functional differentiation of the red and white fibre types continues well beyond hatching to attain the mature fibre types present in adults (Proctor et al. 1980). Given these differences between larval and adult fish, the balance between anaerobic and aerobic metabolism may be different between early and later life stages.

The first objective of our study was to estimate the overall (aerobic and anaerobic) energy expenditure associated with hatching. We measured the number of movements and oxygen consumption before, during, and after hatching in rainbow trout embryos. Additionally, we measured ATP and ammonia concentration and AMP deaminase activity in embryos that hatched (chorionated) and in embryos that did not hatch (dechorionated) before, during, and after the natural time of hatching. Phosphocreatine (PCr), ATP, and lactate concentrations were measured in embryos immediately after hatching.

The results in the first part of this study indicated that hatching did not involve an increase in anaerobic energy expenditure. We therefore sought to test if this result might be due, in part, to a limited anaerobic capacity at this stage. The objective in the second part of the study, therefore, was to estimate the anaerobic capacity of newly hatched rainbow trout larvae. We predicted that tissue indicators of anaerobic metabolism would be unaltered following a bout of exhaustive exercise in newly hatched rainbow trout larvae. To test this prediction, PCr, ATP, and lactate concentrations were compared in unhatched embryos (at rest) and in newly hatched larvae following a 2 min manual chase. In addition, we predicted that under an alternative condition known to result in anaerobic metabolism (5-day hypoxic exposure), tissue lactate concentration would be unaltered in embryos around the time of hatching.

Materials and methods

Experimental animals

Fertilized rainbow trout (*O. mykiss*) embryos were obtained from Rainbow Springs Trout Farm (Thamesford, Ontario, Canada) from at least three different females. Embryos were maintained in continuous flow incubation trays with mesh bottoms (10 °C; pH 8.1; water hardness 411 $mg \cdot L^{-1}$ as $CaCO_3$; Ca^{2+}, 2.62 $mmol \cdot L^{-1}$; Cl^{-1}, 1.47 $mmol \cdot L^{-1}$; Mg^{2+}, 1.49 $mmol \cdot L^{-1}$; K^+, 0.06 $mmol \cdot L^{-1}$; Na^+, 1.05 $mmol \cdot L^{-1}$) at the Hagen Aqualab, University of Guelph, Ontario, Canada, for the duration of all experiments. Incubation trays were shielded from light during the entire incubation period, unless otherwise specified.

Experimental protocol

There were six series of experiments conducted: Series I, embryo movement during hatch; Series II, oxygen consumption during hatch; Series III, tissue metabolites in chorionated and dechorionated embryos; Series IV, tissue metabolites immediately after hatching; Series V, tissue metabolites after exercise; and Series VI, tissue lactate after hypoxia exposure. Separate batches of embryos were used in each series, and hatching time was consistent between batches of embryos (30–34 days postfertilization (dpf)). In Series III, the chorions of one-half of the embryos were removed (dechorionated) manually using fine forceps under a light microscope prior to the time of hatching (28 dpf). There was no mortality associated with the dechorionating procedure. The chorion remained intact in the remaining half of the embryos (chorionated). Chorionated embryos were manually disturbed under a dissecting microscope to mimic the handling stress incurred by dechorionated embryos. Both groups of embryos were placed into mesh-bottom chambers (~25 embryos per chamber) and returned to the incubation tray. For all other series of experiments, embryos were left undisturbed in the incubation tray until the time of experimentation.

Series I, embryo movement during hatch

To measure the degree of activity or movement during hatching, four intact embryos (27 dpf) were randomly chosen from the incubation tray. Embryos were immediately placed into one of four wells (width 1.2 cm × length 1.8 cm × depth 0.6 cm) in a custom-built Plexiglas chamber (5 cm × 18 cm) supplied with flow-through water. Embryos were kept under a 12 h semi-dark and 12 h dark photoperiod for the duration of the experiment. A video camera mounted above the chamber was used to record movement 24 $h \cdot day^{-1}$ until hatching occurred. Videotapes were later analyzed, and the total number of movements in 5 h was recorded 50 h before and 30 h after the time of hatch. As well, movement was quantified over a smaller time frame (2 h) and recorded in 20 min intervals before (80 min) and after (60 min) hatch. In embryos still encased in the chorion (before hatch), a typical movement consisted of a body flexure into a "C" shape, with the nose and tail being brought into close proximity for a duration of ~1 s. In embryos not encased in the chorion (after hatch), a movement consisted of two body flexions with a duration of ~0.5 s.

Series II, oxygen consumption during hatch

Closed respirometry was used to measure oxygen consumption during hatching. When ~50% of the embryos had hatched, unhatched embryos were removed from the incubation tray and individually placed into one of six temperature-controlled respirometers. Additionally, two respirometers served as controls without any embryos to measure any background signal (negligible). To rule out the possibility that microbes associated with the embryos made a substantial contribution to oxygen consumption, we compared the rates of oxygen consumption in empty respirometers and respirometers containing unfertilized embryos. We found no significant difference ($p > 0.05$) in the slopes from respirometers with unfertilized embryos (–0.0066 ± –0.00086 mg $O_2 \cdot L^{-1} \cdot min^{-1}$) versus the empty respirometers (–0.0058 ± –0.00086 mg $O_2 \cdot L^{-1} \cdot min^{-1}$) and thus are confident that empty respirometers were suitable controls.

The chambers were filled with autoclaved water (~9 mL), and the temperature was maintained at 10 °C. Embryos were left undisturbed in the chambers for about 1 h before sealing each chamber. The chambers were sealed for 2 h, during which time the water oxygen content (>70% saturation) was continuously measured. Measurements were made using automatic, temperature-compensated, dissolved oxygen sensors with built in thermistor and amplifier connected to a LabPro™ serial interface and recorded on a computer using LoggerPro software (Version 3.2, Vernier Software and Technology, Beaverton, Oregon). Oxygen consumption (μmol $O_2 \cdot min^{-1} \cdot g$ dry $mass^{-1}$) was calculated using the following equation:

$$\dot{V}O_2 = \frac{\Delta O_2}{\Delta t} \times \frac{(v - \mathrm{wm})}{m} \times \left(\frac{1\ \mathrm{mmol\ O_2}}{32\ \mathrm{mg\ O_2}}\right) \times \left(\frac{1000\ \mu\mathrm{mol}}{\mathrm{mmol}}\right)$$

where ΔO_2 represents the change in oxygen levels ($mg \cdot L^{-1}$) in the chamber over time, Δt is the change in time (min), v represents the volume of the chamber (L), wm is the volume of water displaced by the embryo (g). It was assumed that the volume of water displaced by the embryo is equal to the wet mass (g) of the whole embryo, as water and the embryo have densities of ~1 $g \cdot mL^{-1}$. Oxygen consumption was adjusted for the dry mass (g) of the separated embryonic body (m). Finally, the rate was adjusted for the number of moles of oxygen in the solution. After 2 h, the chambers were opened, the water was replaced with fresh air-saturated water (10 °C) with minimal disturbance to the embryos, the chambers were re-sealed, and the process repeated. The oxygen probes were calibrated daily.

In preliminary experiments, we estimated the capacity of our system to detect changes in oxygen consumption. To accomplish this, we used three stages of embryos (just-fertilized, eyed, and just-hatched) known to have different rates of oxygen consumption. Just-fertilized embryos consumed 0.46 ± 0.18 mmol $O_2 \cdot min^{-1} \cdot individual^{-1}$. Oxygen consumption increased 3-fold (2.00 ± 0.19 mmol $O_2 \cdot min^{-1} \cdot individual^{-1}$) in eyed embryos compared with fertilized ones and increased 12-fold (5.63 ± 0.46 mmol $O_2 \cdot min^{-1} \cdot individual^{-1}$) in just-hatched embryos compared with just-fertilized ones. Our system easily resolved these differences, and therefore we are confident that we can detect changes in oxygen uptake at different stages and at the same stage if there are metabolic rate changes.

Series III, tissue metabolites in chorionated and dechorionated embryos

To measure tissue metabolites in chorionated and dechorionated embryos, embryos were randomly chosen from the incubation tray, and one-half of the embryos were dechorionated at 28 dpf. Dechorionated and chorionated embryos were randomly separated into three groups for measurements of tissue metabolites: pre-hatch (24 h after dechorionating), during hatch (when ~50% of the chorionated embryos had hatched), and post-hatch (24 h after 100% of embryos had hatched). On their respective day, chorionated and dechorionated embryos were removed from the incubation tray and anaesthetized in 0.15 $g \cdot L^{-1}$ ethyl 3-aminobenzoate methanesulfonate salt (MS-222). The chorion was removed from the intact embryos, and the embryonic body was dissected from the yolk sac in all embryos. The separated embryonic bodies and yolk sacs were individually blotted on a Kimwipe to remove any excess water, frozen in liquid nitrogen, and stored at –80 °C for later analysis (within 1 month).

Series IV, tissue metabolites immediately after hatching

To compare metabolites during complete rest and immediately after hatching, unhatched (control) embryos were removed from the incubation tray and placed individually into water-filled Petri dishes. Embryos that did not move for 10 min were anaesthetized in a lethal dose (2 $g \cdot L^{-1}$) of buffered (1 $g \cdot L^{-1}$ $NaHCO_3$) MS-222. After ~10 s, the chorion was removed, and the embryonic body was dissected from the yolk sac, freeze-clamped between two aluminum plates precooled with liquid nitrogen, and stored as described above. In a second group (hatch), embryos that were observed to be close to hatching (thinning of chorion near the head region) were removed from the incubation tray, placed individually into water-filled Petri dishes, and carefully observed until hatching occurred(defined as when the embryo body was free of the egg case). Immediately after the embryos had hatched, embryos were anaesthetized (as above), left for ~5 s, and treated as described above. The entire sampling procedure took ~0.5–1 min.

Series V, tissue metabolites after a bout of exercise

To measure metabolites in newly hatched trout larvae following a bout of exercise, two groups were used. Unhatched embryos that had not moved for 10 min (control) were treated exactly as described for Series IV control embryos. In a second group (chase), embryos that had hatched <24 h before were individually removed from the incubation tray and manually chased for 2 min around a circular container (diameter 34.5 cm). Immediately following this procedure, embryos were removed from the container, anaesthetized (2 $g \cdot L^{-1}$ MS-222, buffered), and treated as described above.

Series VI, tissue lactate after hypoxia exposure

To further evaluate anaerobic capacity, lactate was measured in embryos exposed to hypoxic conditions. Embryos were removed from the incubation tray at 25 dpf. They were placed into one of two different treatments: normoxia

(10.6 ± 0.0 mg $O_2 \cdot L^{-1}$, 10.1 ± 0.0 °C) or hypoxia (5.2 ± 0.1 mg $O_2 \cdot L^{-1}$, 10.1 ± 0.0 °C). A concentration of 5.2 ± 0.1 mg $O_2 \cdot L^{-1}$ for chronic hypoxia was chosen, as this concentration has been shown to depress growth in both chorionated and dechorionated rainbow trout embryos without having a large effect on mortality (Ciuhandu et al. 2005). Hypoxic water was produced by bubbling nitrogen gas into the water. Oxygen levels were measured with an oxygen meter (YSI model 55, Yellow Springs Instruments Co., Yellow Springs, Ohio) every 12 h over the duration of the experiment. Embryos were maintained under these conditions for 5 days and removed from each treatment at 30 dpf. At this time, embryos were anaesthetized in 0.15 $g \cdot L^{-1}$ MS-222. Embryos were sampled as described for Series III.

Tissue analysis

Lactate, ATP, and phosphocreatine

To measure lactate concentration, tissue (0.1 g) was ground to a fine powder in liquid nitrogen, deproteinized in two volumes of 8% perchloric acid, vortexed, and centrifuged at 18 300*g* for 10 min (4 °C). The supernatant was then used for analysis. For ATP and PCr analysis, ~0.25 g of tissue was treated the same way as described for lactate, except the supernatant was neutralized with 3 $mol \cdot L^{-1}$ K_2CO_3, centrifuged again at 18 300*g* for 5 min (4 °C), and then used for analysis. Lactate, ATP, and PCr concentrations were measured enzymatically according to procedures described by Bergmeyer (1983). All concentrations are expressed as $\mu mol \cdot g^{-1}$.

AMP deaminase

To measure AMP deaminase activity, tissue was prepared according to the procedure described by Raffin (1981). Briefly, tissue samples (0.05–0.1 g) were ground to a fine powder in liquid nitrogen. Powdered tissue was homogenized in a 2% *w/v* solution (50 $mmol \cdot L^{-1}$ imidazole buffer, 100 $mmol \cdot L^{-1}$ KCl, 30% glycerol, pH 6.5). The mixture was centrifuged at 750*g* for 10 min (4 °C), and the supernatant was sonicated (20 kHz, 25 W, 4 × 15 s, Vibracell 50T, Sonics & Materials, Inc., Danbury, Connecticut). AMP deaminase activity was measured enzymatically according to the method described by Passoneau and Lowry (1993) with the following exceptions. The volume of tissue sample or $(NH_4)_2SO_4$ standard was 15 µL, and the first step of the reaction was incubated for 30 min. These modifications resulted in enzyme activity that was linear with respect to time and tissue amount (data not shown). Absorbance was recorded at 340 nm (Ultraspec 3100 pro, Biochrom, Cambridge, UK), and activity was expressed as $\mu mol \cdot g^{-1} \cdot min^{-1}$.

Ammonia

Ammonia concentration was measured in embryonic tissue (0.25–0.4 g) and yolk (0.08–0.1 g) samples. Tissue and yolk samples were ground to a fine powder in liquid nitrogen, deproteinized in two volumes (embryonic tissue) or ten volumes (yolk) of 8% perchloric acid, vortexed, and centrifuged at 18 300*g* for 10 min (4 °C). The supernatant was neutralized with saturated $KHCO_3$ and centrifuged at 18 300*g* for 5 min (4 °C). The final supernatant was analyzed for ammonia concentration using the glutamate dehydrogenase enzymatic assay of Kun and Kearney (1971). Ammonia concentration was expressed as $\mu mol \cdot g^{-1}$.

Statistical analysis

Statistical analysis was performed using the general linear models (GLM) procedure of the SAS system (version 8e; SAS Institute Inc., Cary, North Carolina). Differences in movement and oxygen consumption before, during, and after hatching (Series I and II) were analyzed using a one-way analysis of variance (ANOVA). A Dunnett's test was used to compare time 0 h (control) with all other times. In both Series I and II, the time point immediately preceding hatching was compared with the time point in which hatching occurred using a Student's paired *t* test. Differences in tissue metabolites between chorionated and dechorionated embryos and over time (Series III) were determined using a two-way (treatment and time) ANOVA. Differences in tissue metabolites between control and hatch embryos (Series IV), differences between at rest and chase embryos (Series V), and differences in lactate concentration between normoxia and hypoxia embryos (Series IV) were analyzed using a Student's unpaired *t* test. Statistical differences in all tests were declared at $p < 0.05$. Values are presented as means ± standard error (SE).

Results

Series I

In general, the number of movements in rainbow trout embryos increased dramatically (Fig. 1*a*) over time (~10 movements·5 h^{-1} pre-hatch to ~600 movements·5 h^{-1} by 20 h post-hatch). When the time immediately surrounding hatching was isolated (Fig. 1*b*) and all time points were considered (–60 min to 40 min), there were no significant differences in the number of movements between hatching (0 h) and any of the time points before hatch or after hatch. When the time immediately preceding hatching (–20 min) is compared with the time in which hatching occurred (0 min) (Fig. 1*c*), movement increased by 50% ($p < 0.05$) during hatching.

Series II

Over the entire experimental period (–8 h to 8 h) (Fig. 2*a*), there were no differences in oxygen consumption between hatching (0 h) and any of the time points before or after hatching. When the time immediately preceding hatching (–2 h) was compared with the time in which hatching occurred (0h) (Fig. 2*b*), there was a significant ($p < 0.05$) increase (19%) in oxygen consumption during hatching.

Series III

There were no significant differences in any of the tissue metabolites (Table 1) (ammonia, AMP deaminase, ATP) between chorionated and dechorionated embryos at any of the time points investigated (pre-, during, and post-hatch). In both groups (chorionated and dechorionated), yolk ammonia concentration and AMP deaminase activity increased significantly (~63% and ~82%, respectively; $p < 0.05$) over time (Table 1).

Series IV

The lactate and PCr concentration did not change immediately after hatching (Fig. 3*a*) relative to control rainbow trout embryos. ATP concentration (Fig. 3*a*) was significantly

Fig. 1. Number of movements in 5 h intervals 50 h before hatch (negative times), during hatch (time zero), and 30 h after hatch (positive times) (*a*); number of movements in 20 min intervals 60 min before, during, and 40 min after hatching (*b*); and the number of movements in the 20 min immediately preceding hatching and at the time of hatching (0 h) (*c*) in rainbow trout (*Oncorhynchus mykiss*) embryos. Hatching was defined as the time when the embryo body was completely free of the egg case. An asterisk (*) indicates a significant difference from the –20 min value ($p < 0.05$). Values are expressed as means + standard error (SE) ($n = 4$).

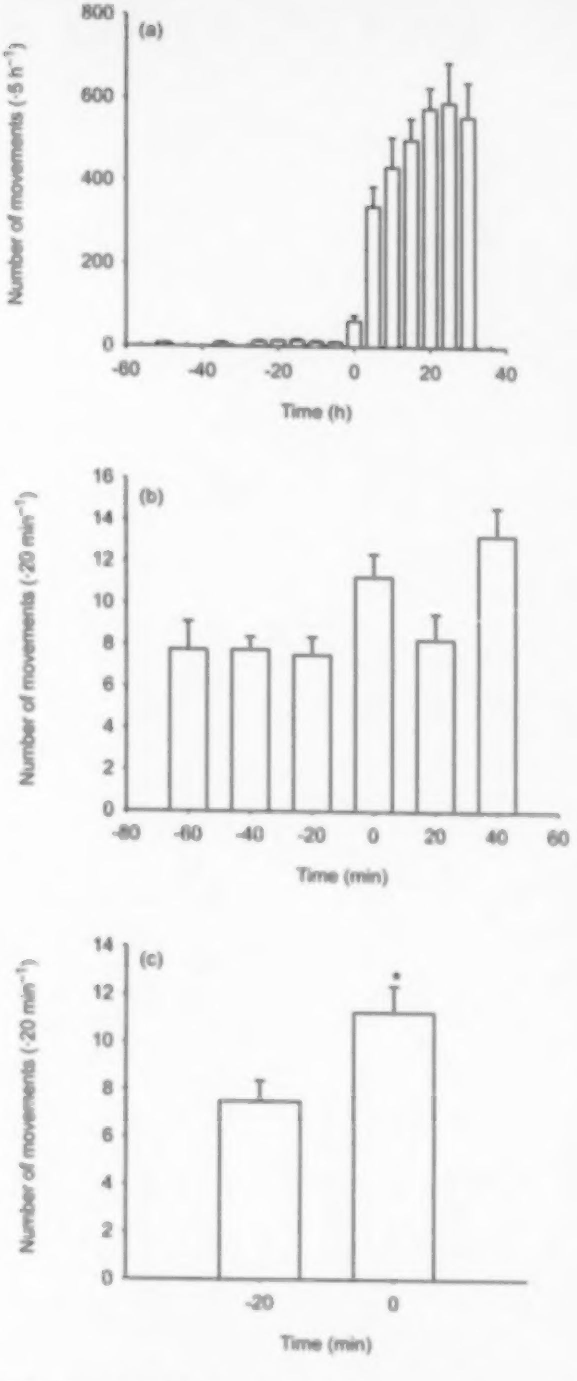

Fig. 2. Oxygen consumption (μmol·min^{-1}·g dry mass^{-1}) over a period of ~20 h (*a*) before (negative times), during (time zero), and after hatching (positive times) and (*b*) in the 2 hours immediately preceding hatching and at the time of hatching (0 h) in rainbow trout (*Oncorhynchus mykiss*) embryos. Hatching was defined as the time when the embryo body was completely free of the egg case. An asterisk (*) indicates a significant difference from the –2 h value ($p < 0.05$). Values are expressed as means ± standard error (SE) ($n = 7$–13).

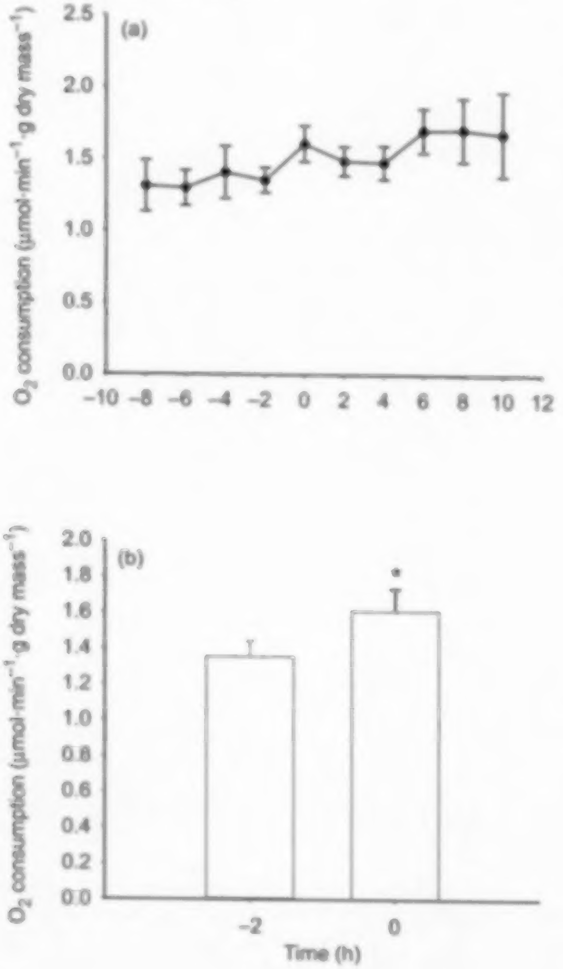

higher ($p < 0.05$) after hatching relative to control embryos, but this difference was small (13%).

Series V

The lactate concentration in newly hatched trout larvae following a 2 min manual chase (Fig. 3*b*) was significantly higher (30%) than that in control embryos ($p < 0.05$). ATP

Table 1. Embryonic body and yolk ammonia concentration, embryonic body adenosine monophosphate (AMP) deaminase activity, and adenosine triphosphate (ATP) concentration in chorionated and dechorionated rainbow trout (*Oncorhynchus mykiss*) embryos pre-, during, and post-hatch.

	Ammonia (µmol·g wet mass^{-1})				AMP deaminase (µmol·min^{-1}·g wet mass^{-1})		ATP (µmol·g wet mass^{-1})	
	Body		Yolk					
	Chorionated	Dechorionated	Chorionated	Dechorionated	Chorionated	Dechorionated	Chorionated	Dechorionated
Pre-hatch	1.10±0.03	0.98±0.09	0.88±0.09	1.23±0.18	0.88±0.09	1.23±0.18	1.90±0.18	1.98±0.14
During hatch	1.25±0.14	1.12±0.07	1.25±0.14	1.12±0.07	1.72±0.14*	1.65±0.19*	2.11±0.11	2.08±0.09
Post-hatch	1.78±0.19	1.55±0.22	1.78±0.19*	1.55±0.22*	1.85±0.12*	1.96±0.24*	2.19±0.15	2.22±0.17

Note: Values are means ± standard error.

*Significantly different from respective pre-hatch value ($p < 0.05$).

Fig. 3. Lactate, adenosine triphosphate (ATP), and phosphocreatine (PCr) concentrations (µmol·g wet mass^{-1}) in control (open bars) rainbow trout (*Oncorhynchus mykiss*) embryos and in embryos immediately after hatching (solid bars) (*a*) and in embryos following a 2 min manual chase shortly after hatch (solid bars) (*b*). Control embryos did not move for 10 min prior to sampling. An asterisk (*) indicates a significant difference from control value ($p < 0.05$). Values are expressed as means + standard error (SE) ($n = 6$).

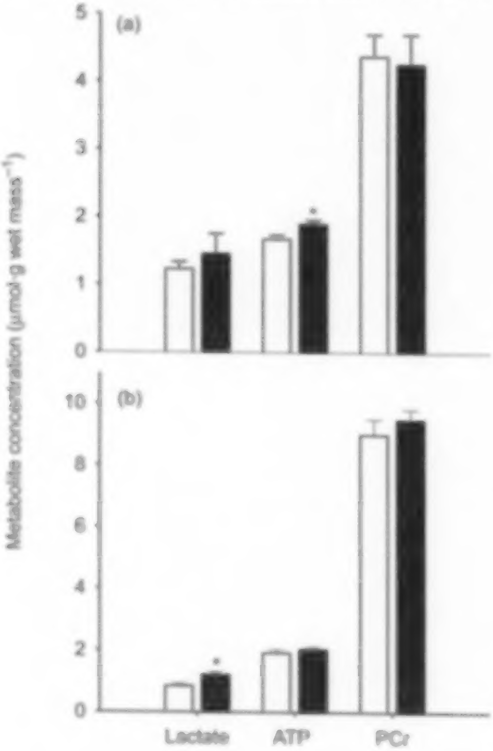

and PCr concentrations were not significantly different in the chased group compared with the control group (Fig. 3*b*).

Series VI

Lactate concentration was significantly higher (2.7-fold; $p < 0.05$) in embryos that had been exposed to 5 days hypoxia compared with control embryos (Fig. 4).

Discussion

Energy expenditure during hatch

Hatching in rainbow trout embryos involved significant increases in movement and oxygen consumption, indicating an increase in overall energy expenditure during hatching. The outer layer of the chorion is not enzymatically digested during hatching (Bell et al. 1969; Schoots et al. 1982), and it was previously assumed that muscular activity or movement is important in assisting the embryo to penetrate this outer, undigested layer (Johnston 1982; Schoots et al. 1982). The 50% and 20% increases in activity and oxygen consumption, respectively, in the present study suggest that although there are not large increases in energy expenditure during hatch-

Fig. 4. Lactate concentration (μmol·g wet mass^{-1}) in rainbow trout (*Oncorhynchus mykiss*) embryos exposed to normoxia (10.6 ± 0.0 mg $O_2·L^{-1}$) or hypoxia (5.2 ± 0.1 mg $O_2·L^{-1}$) for 5 days (25–30 days postfertilization). Values are expressed as means + standard error (SE) ($n = 6$). An asterisk (*) indicates a significant difference from normoxic embryos ($p < 0.05$).

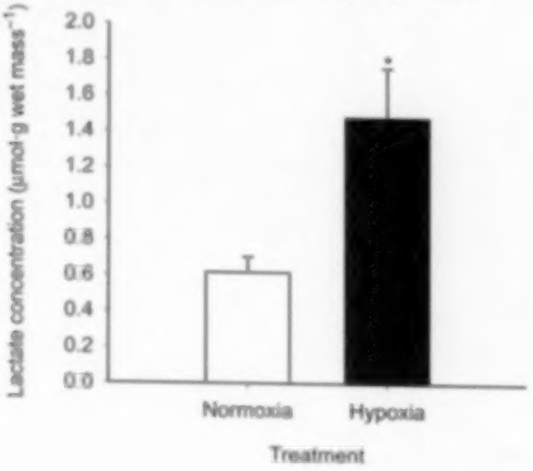

ing, activity does play an important role in the hatching process in rainbow trout embryos. The increase in movement during hatching in rainbow trout in the present study is similar to the increase in movement reported in hatching California grunion (Speer-Blank and Martin 2004). Our results do not, however, agree with the statement made by Peterson and Martin-Robichaud (1983) that hatching in Atlantic salmon required very little mechanical effort by the embryo. However, Peterson and Martin-Robichaud (1983) did not provide any data to support their statement, so it is impossible to compare our results with theirs.

Oxygen consumption in fish typically increases as development proceeds up to and including hatching (e.g., Kaushik et al. 1982; Oliva-Teles and Kaushik 1987; Finn et al. 1991). Increases in oxygen consumption after hatching have been attributed to the fact that the chorion no longer restricts oxygen supply or activity (Rombough 1988). To our knowledge, our study is the first to report oxygen consumption in the hours immediately around hatching. It is likely that the increase in oxygen consumption during hatching is a result of increased movement, as recent evidence indicates that the chorion of rainbow trout embryos is not a barrier to oxygen uptake (Ciuhandu et al. 2005).

It should be pointed out that despite large increases in movement in the hours after hatching (Series I), there were not large increases in oxygen consumption (Series II). This may be due to the fact that embryos behave differently in the respirometry chambers relative to the chamber in which movement was recorded. Indeed, when movement was quantified in the respirometers, the embryos moved about half as much (43.5 ± 5.4 movements·h^{-1}) versus 79.25 ± 8.4 movements·h^{-1} (Series I). The reason for this difference in movement is unknown, but it has been shown that body movements are effective in disrupting boundary layers in aquatic skin breathers (Pinder and Feder 1990), and it is possible that a greater degree of mixing (due to constant stirring) occurred in the respirometers resulting in an overall decrease in the resistance to oxygen uptake by the boundary layer, thus decreasing the need for body movements.

We hypothesized that hatching involves an increase in anaerobic energy expenditure in rainbow trout embryos. There were, however, no differences in anaerobic metabolites between chorionated embryos that hatched and dechorionated embryos that did not hatch (Series III), nor were there any large changes in metabolites immediately after hatching (Series IV). These findings are consistent with the observation that activity increased only slightly during hatching. Taken together, these results suggest that although there is a small increase in energy expenditure during hatching, there is little recruitment of anaerobic metabolism.

Exercise has been linked to an increase in tissue ammonia concentration in mammals and fish (e.g., Meyer et al. 1980; Mommsen and Hochachka 1988; Wang et al. 1994). Ammonia concentrations are elevated at the time of hatch in rainbow trout embryos (Wright et al. 1995), particularly in the yolk sac (Essex-Fraser et al. 2005). This elevated ammonia is clearly not the result of exhaustive muscular activity required to escape the egg capsule at the time of hatching. Ammonia may also be formed aerobically from the catabolism of free amino acids (FAA). The use of FAA as an energy substrate has been well documented in marine (Rønnestad et al. 1993; Sivaloganathan et al. 1998) and freshwater species (Oliva-Teles and Kaushik 1987). It is possible that hatching involves an increase in aerobic energy expenditure given the increases in movement and oxygen consumption during hatching.

It is also possible that the elevation in tissue ammonia concentrations is related to events that occur post-hatch. In the 24 h following hatching, movement by the newly hatched larvae increased dramatically by about 10-fold. It is possible that the increase in activity following hatching relies on an increase in the catabolism of FAA, resulting in the synthesis of ammonia. This idea is consistent with the result that yolk ammonia concentration in the present study was only significantly elevated post-hatch and not during hatching. Furthermore, the yolk sac may be a temporary sink for excess ammonia because the yolk is more acidic than the intra- and extra-cellular pH in trout embryos (Rahaman-Noronha et al. 1996).

It should be pointed out that the values for ammonia concentration in the separated embryonic body and the separated yolk post-hatch from the present study are ~2-fold lower that those values reported by Essex-Fraser et al. (2005). Additionally, the sum of the ammonia concentration in the body and yolk post-hatch in the present study is ~50% lower than the value reported by Wright et al. (1995). Although the source of this variation is unknown, it could be due to differences in the timing of post-hatch measurements, differences in the batches of embryos (e.g., spawning time), or methodological differences.

It is also worth noting that immediately after hatching there was a significant increase in the ATP concentration compared with control fish. Although this was a statistically significant increase, it may not be physiologically relevant. When adult trout are exercised to exhaustion, there is a very large decrease in ATP concentration (~15-fold decrease; Mommsen and Hochachka 1988). Hence, compared with adult trout, the changes we observed in ATP concentration were in the opposite direction (increase) and were comparatively small (13%).

Anaerobic capacity

Anaerobic capacity is low in newly hatched rainbow trout larvae, as demonstrated by a lack of change in anaerobic metabolites (ATP, PCr) following intense activity. Lactate concentration was significantly elevated as a result of intense activity, but this increase (30%) was small compared with the large increases in white muscle lactate reported in adult fish swum to exhaustion (e.g., 8-fold increase, Mommsen and Hochachka 1988). Our results are consistent with Hinterleitner et al. (1987), who reported that the activities of anaerobic enzymes were lowest in the youngest larvae of several different species, including rainbow trout, and increased as the fish grew to adult size, whereas the reverse was true for aerobic enzymes. Furthermore, in cyprinid species, El-Fiky et al. (1987) argued that the functional differentiation of mytomal muscle into slow oxidative (red) and fast glycolytic (white) found in juvenile and adult fish may not occur in larvae.

In contrast with our findings, Franklin et al. (1996) reported significant decreases in whole body PCr and ATP concentrations, as well as a 6-fold increase in lactate concentration in 7-day post-hatch herring larvae after 3 min of repeated stimulation. It is likely that the discrepancies between our study and Franklin et al. (1996) are due to species differences, as well as differences in developmental stage. Herring larvae are pelagic, continually active (Franklin et al. 1996), and start to feed immediately after hatching (Usher et al. 1994). This is in contrast with salmonid larvae that feed endogenously after hatching (Kamler 1992) and are buried in gravel, exhibiting minimal movement (Nag and Nursall 1972; Proctor et al. 1980). It is therefore likely that burst-type swimming, relying primarily on anaerobic metabolism, would be of greater importance in herring larvae, as they would be more vulnerable to predators than trout larvae shortly after hatch.

Intense activity results in very rapid metabolic disturbances in the white muscle. Goolish (1989) reported maximal lactate concentrations after 2 min of activity in adult trout muscle, and Dobson and Hochachka (1987) reported a 2-fold decrease in PCr concentration after one–two tail flips. To achieve exhaustion (i.e., no longer able to sprint), adult fish are typically exercised for 5–10 min (Milligan 1996). Larval fish may not, however, respond to intense activity in the same way as adults. It has been suggested that swimming (including burst swimming) in small fish is powered primarily by aerobic metabolism (Goolish 1991). This idea is consistent with our observation that trout larvae were not fully exhausted and responded to further stimulation after a 2 min chase. These results raise the question of whether anaerobic potential is low at this stage of development or if the experimental protocol was inadequate in achieving exhaustion. To further explore this issue, rainbow trout embryos were exposed to hypoxia (at a concentration known to reduce growth without major mortality) for 5 days. Hypoxic embryos accumulated significantly ($p < 0.05$) more lactate than embryos exposed to normoxia. Although this difference was significant, it was relatively small (~2.5-fold) compared with larger differences reported in juvenile and adult trout (e.g., 22-fold increase in whole body lactate after acute anoxia (0% O_2), Krumschnabel and Lackner 1993; 12-fold increase in plasma lactate after 90 min of hypoxia (25% O_2), Van Raaij et al. 1996). Thus, under circumstances other than exhaustive exercise, the anaerobic capacity of trout larvae appears to be low.

In summary, hatching involved significant increases in movement and oxygen consumption, but did not result in exhaustive exercise relying on anaerobic metabolism. These results suggest that the increase in activity is involved in assisting the embryo in escaping the egg capsule during hatching, but its contribution is relatively small. Furthermore, the results of our study indicate that the anaerobic capacity of newly hatched trout larvae is low compared with juvenile and adult fish.

Acknowledgements

We thank Tammy Rodela for her assistance with the dechorionating and Cosima Ciuhandu for assistance with raising and sampling embryos. We are thankful to Dr. Louise Milligan for helpful discussions. This research was supported by a Natural Sciences and Engineering Research Council of Canada (NSERC) grant to PAW and an NSERC equipment grant to PAW and EDS.

References

Bell, G.R., Hoskins, G.E., and Bagshaw, J.W. 1969. On the structure and enzymatic degradation of the external membrane of the salmon egg. Can. J. Zool. **47**: 146–148.

Bergmeyer, H.U. 1983. Methods of enzymatic analysis. Academic Press, New York.

Black, E.C., Robertson, A.C., Hanslip, A.R., and Chiu, W.G. 1960. Alterations in glycogen, glucose and lactate in rainbow and Kamloops trout (*Salmo gairdneri*) following muscular activity. J. Fish. Res. Board Can. **17**: 487–499.

Ciuhandu, C., Stevens, E.D., and Wright, P.A. 2005. The effect of oxygen on the growth of rainbow trout (*Oncorhynchus mykiss*) with and without a chorion. J. Fish Biol. **67**: 1544.

Dobson, G.P., and Hochachka, P.W. 1987. Role of glycolysis in adenylate depletion and repletion during work and recovery in teleost white muscle. J. Exp. Biol. **129**: 125–140.

El-Fiky, N., Hinterleitner, S., and Weiser, W. 1987. Differentiation of swimming muscles and gills, and development of anaerobic power in the larvae of cyprinid fish (Pisces, Teleostei). Zoomorphology, **107**: 126–132.

Essex-Fraser, P.A., Steele, S., Bernier, N.J., Murray, B.W., Stevens, E.D., and Wright, P.A. 2005. Expression of four glutamine synthetase genes in early stages of development of rainbow trout (*Oncorhynchus mykiss*) in relationship to nitrogen excretion. J. Biol. Chem. **280**: 20268–20273.

Finn, R.N., Fyhn, H.J., and Evjen, M.S. 1991. Respiration and nitrogen metabolism of Atlantic halibut eggs (*Hippoglossus hippoglossus*). Mar. Biol. **108**: 11–19.

Franklin, C.E., Johnston, I.A., Batty, R.S., and Yin, M.C. 1996. Metabolic recovery in herring larvae following strenuous activity. J. Fish Biol. **48**: 207–216.

Goolish, E.M. 1989. The scaling of aerobic and anaerobic muscle power in rainbow trout (*Salmo gairdneri*). J. Exp. Biol. **147**: 493–505.

Goolish, E.M. 1991. Aerobic and anaerobic scaling in fish. Biol. Rev. **66**: 33–56.

Hayes, F.R. 1942. The hatching mechanism of salmon eggs. J. Exp. Zool. **89**: 357–373.

Hinterleitner, S., Platzer, U., and Weiser, W. 1987. Development of the activities of oxidative, glycolytic and muscle enzymes during early larval life in three families of freshwater fish. J. Fish Biol. **30**: 315–326.

Johnston, I.A. 1982. Physiology of muscle in hatchery raised fish. Comp. Biochem. Physiol. B, **73**: 105–124.

Kamler, E. 1992. Early life history of fish: an energetics approach. Chapman and Hall, London, UK.

Kaushik, S.J., Dabrowski, K., and Luquet, P. 1982. Patterns of nitrogen excretion and oxygen consumption during ontogenesis of common carp (*Cyprinus carpio*). Can. J. Fish. Aquat. Sci. **39**: 1095–1105.

Kørsgaard, B., Mommsen, T.P., and Wright, P.A. 1995. Nitrogen excretion in teleostean fish: adaptive relationships to environment, ontogenesis, and viviparity. *In* Nitrogen metabolism and excretion. *Edited by* P.J. Walsh and P.A. Wright. CRC Press, New York. pp. 259–287.

Krumschnabel, G., and Lackner, R. 1992. Metabolic responses of fish larvae (*Rutilus rutilus* L.) to forced activity (Cyprinidae, Teleostei). J. Fish Biol. **41**: 717–724.

Krumschnabel, G., and Lackner, R. 1993. Stress responses in rainbow trout *Oncorhynchus mykiss* alevins. Comp. Biochem. Physiol. A, **104**: 777–783.

Kun, E., and Kearney, E.B. 1971. Ammonia. *In* Methods of enzymatic analysis. Vol. 4. *Edited by* H.U. Bergmeyer. Academic Press, New York. pp. 1802–1806.

McDonald, D.G., McFarlane, W.J., and Milligan, C.L. 1998. Anaerobic capacity and swim performance of juvenile salmonids. Can. J. Fish. Aquat. Sci. **55**: 1198–1207.

Meyer, R.A., Dudley, G.A., and Terjung, R.L. 1980. Ammonia and IMP in different skeletal muscle fibres after exercise in rats. J. Appl. Physiol. **49**: 1037–1041.

Milligan, C.L. 1996. Metabolic recovery from exhaustive exercise in rainbow trout. Comp. Biochem. Physiol. A, **113**: 52–60.

Mommsen, T.P., and Hochachka, P.W. 1988. The purine nucleotide cycle as two temporally separated metabolic units: a study on trout muscle. Metabolism, **37**: 552–556.

Nag, A.C., and Nursall, J.R. 1972. Histogenesis of white and red muscle fibres of trunk muscles of a fish, *Salmo gairdneri*. Cytobios, **6**: 227–246.

Oliva-Teles, A., and Kaushik, S.J. 1987. Nitrogen metabolism during the early ontogeny of diploid and triploid rainbow trout (*Salmo gairdneri* R.). Comp. Biochem. Physiol. A, **87**: 157–160.

Passoneau, J.V., and Lowry, O.H. 1993. Enzymatic analysis. Humana Press, Totowa, N.J.

Peterson, R.H., and Martin-Robichaud, D.J. 1983. Embryo movements of Atlantic salmon (*Salmo salar*) as influenced by pH, temperature and state of development. Can. J. Fish. Aquat. Sci. **40**: 777–782.

Pinder, A.W., and Feder, M.E. 1990. Effect of boundary layers on cutaneous gas exchage. J. Exp. Biol. **143**: 67–80.

Proctor, C., Mosse, P.R.L., and Hudson, R.C.L. 1980. A histochemical and ultrastructural study of the development of the propulsive musculature of the brown trout, *Salmo trutta* L., in relation to its swimming behaviour. J. Fish Biol. **16**: 309–329.

Raffin, J.P. 1981. AMP deaminase from trout gill localization of the activating proteinase. Mol. Physiol. **1**: 223–234.

Rahaman-Noronha, E., O'Donnell, M.J., Pilley, C.M., and Wright, P.A. 1996. Excretion and distribution of ammonia and the influence of boundary layer acidification in embryonic rainbow trout (*Oncorhynchus mykiss*). J. Exp. Biol. **199**: 2713–2723.

Rombough, P.J. 1988. Respiratory gas exchange, aerobic metabolism, and effects of hypoxia during early life. *In* Fish physiology. Vol. 11. *Edited by* W.S. Hoar and D.J. Randall. Academic Press, New York. pp. 1–58.

Rønnestad, I., Groot, E.P., and Fyhn, H.J. 1993. Compartmental distribution of free amino acids and protein in developing yolk-sac larvae of Atlantic halibut (*Hippoglossus hippoglossus*). Mar. Biol. **116**: 349–354.

Schoots, A.F.M., Stikelbroeck, J.J.M., Bekhuis, J.F., and Denucé, J.M. 1982. Hatching in teleostean fishes: fine structural changes in the egg envelope during enzymatic breakdown *in vivo* and *in vitro*. J. Ultrasruct. Res. **80**: 185–196.

Sivaloganathan, B., Walford, J., Ip, Y.K., and Lam, T.J. 1998. Free amino acids and energy metabolism in eggs and larvae of seabass, *Lates calcarifer*. Mar. Biol. **131**: 695–702.

Speer-Blank, T.M., and Martin, K.L.M. 2004. Hatching events in the California grunion, *Leuresthes tenuis*. Copeia, 2004: 21–27.

Usher, M.L., Stickland, N.C., and Thorpe, J.E. 1994. Muscle development in Atlantic salmon (*Salmo salar*) embryos and the effect of temperature on muscle cellularity. J. Fish Biol. **44**: 953–964.

Van Raaij, M.T.M., Van Den Thillart, G.E.E.J.M., Vianen, G.J., Pit, D.S.S., and Balm, P.H.M. 1996. Substrate utilization and hormonal changes in rainbow trout (*Oncorhynchus mykiss*) and common carp (*Cyprinus carpio*) during deep hypoxia and subsequent recovery. J. Comp. Physiol. **166**: 443–452.

Wang, Y., Heigenhauser, G.J.F., and Wood, C.M. 1994. Integrated responses to exhaustive exercise and recovery in rainbow trout white muscle: acid–base, phosphagen, carbohydrate, lipid, ammonia, fluid volume and electrolyte metabolism. J. Exp. Biol. **195**: 227–258.

Wood, C.M. 2001. Influence of feeding, exercise, and temperature on nitrogen excretion and metabolism. *In* Fish physiology. Vol. 20. *Edited by* P.A. Wright and P.M. Anderson. Academic Press, New York. pp. 201–239.

Wright, P.A., and Fyhn, H.J. 2001. Ontogeny of nitrogen metabolism and excretion. *In* Fish physiology. Vol. 20. *Edited by* P.A. Wright and P.M. Anderson. Academic Press, New York. pp. 149–200.

Wright, P.A., Felskie, A., and Anderson, P.M. 1995. Induction of ornithine–urea cycle enzymes and nitrogen metabolism and excretion in rainbow trout (*Oncorhynchus mykiss*) during early life stages. J. Exp. Biol. **198**: 127–135.

Yamagami, K. 1988. Mechanisms of hatching in fish. *In* Fish physiology. Vol. 11. *Edited by* W.S. Hoar and D.J. Randall. Academic Press, New York. pp. 407–446.

Semi-local extraction of ring structures in images of biological hard tissues: application to the Bayesian interpretation of fish otoliths for age and growth estimation

Ronan Fablet

Abstract: This paper deals with the analysis of images of biological tissue that involves ring structures, such as tree trunks, bivalve seashells, or fish otoliths, with a view to automating the acquisition of age and growth data. A bottom-up template-based scheme extracts meaningful ridge and valley curve data using growth-adapted time-frequency filtering. Age and growth estimation is then stated as the Bayesian selection of a subset of ring curves, which combines a measure of curve significativity and an a priori statistical growth model. Experiments on real samples demonstrate the efficiency of the proposed data extraction stage. Our Bayesian framework is shown to significantly outperform previous methods for the interpretation of a data set of 200 plaice otoliths and compares favorably with interexpert agreement rates (88% of agreement to expert interpretations).

Résumé : Cet article traite de l'analyse des images de tissus biologiques à des fins d'automatisation de l'acquisition des données d'âge et de croissance. Nous développons une approche générale pour l'extraction et l'interprétation des structures géométriques concentriques dans les images de tissus biologiques, tels que les troncs d'arbres, les coquilles de bivalves et les otolithes de poissons. La première étape permet d'identifier des courbes signficatives correspondant aux crêtes et aux vallées dans l'image. Elle intègre un filtrage adapté, fonction d'un a priori sur la croissance. Dans un second temps, l'estimation de l'âge et de la croissance est formulée comme un problème de sélection bayésienne d'un sous-ensemble pertinent de courbes parmi l'ensemble des courbes extraites. Des résultats obtenus sur des images de différents tissus démontrent l'efficacité de notre méthode d'extraction des structures d'intérêt. De plus, l'évaluation du schéma bayésien d'interprétation pour un ensemble de 200 otolithes de plie valide notre approche en termes d'amélioration des résultats antérieurs obtenus par des approches automatiques et en termes de comparaison aux taux d'agrément inter-experts de 88 %.

Problem statement and related work

Age and growth data provide key information for a broad range of scientific issues, e.g., the computation of daily temperature series for paleoclimatology from the analysis of daily increments on the shell of sea scallops (Chauvaud et al. 2005), the determination of age–length keys from the interpretation of fish otoliths for marine stock assessments (Panfili et al. 2003), the analysis of fish otolith growth patterns for marine ecology (Hare and Cowen 1997; Panfili et al. 2003), or tree-ring dating for archeology (Baillie 1982). All of these applications initially rely on the interpretation of growth rings observed on biological materials such as tree trunks, corals, shells of seashells, fish otoliths, and fish scales, which will subsequently be referred as biological hard tissues (Fig. 1). The presence of concentric ring structures is due to the variations in chemistry during accretionary formation of these structures. The deposit of the rings is often associated with a biological periodicity (either seasonal or daily, depending on the species and the tissue). Counting growth rings then leads to an estimation of the age of the analyzed tissue, whereas growth increments can be estimated from the distance between successive rings (Fig. 2), although not all observed ring structures are relevant for aging (Campana 2001).

The previously mentioned biological applications require large collections of age and growth data for a consistent analysis. The acquisition of this data is generally performed by expert readers (typically, for marine stock assessment issues, several thousands of fish otoliths per year). The development of digital imaging systems and computer-aided tools brings new solutions to this field (Small and Hirschhorn 1987; Morison et al. 1998). Our work focuses on the automation of age and growth estimation from the analysis of ring structures within the images of biological hard tissues. As detailed below, the key issues lie in the use of growth information to design a ring extraction framework that takes into account growth nonlinearity (Fig. 2*b*) and to discrimi-

Received 8 October 2004. Accepted 14 June 2005. Published on the NRC Research Press Web site at http://cjfas.nrc.ca on 18 May 2006.
J18346

R. Fablet. Laboratoire de Schlérochronologie des Animaux Aquatiques (LASAA), IFREMER Centre de Brest, B.P. 70, F-29280 Plouzané, France (e-mail: rfablet@ifremer.fr).

Can. J. Fish. Aquat. Sci. **63**: 1414–1428 (2006)

doi:10.1139/F06-001

Fig. 1. Examples of images of biological hard tissues involving periodical ring structures exploited for age and growth analysis: (*a*) the shell of a bivalve (spisule), bar = 0.5 cm; (*b*) a plaice otolith, bar = 1 mm; (*c*) the section of a tree trunk, bar = 10 cm.

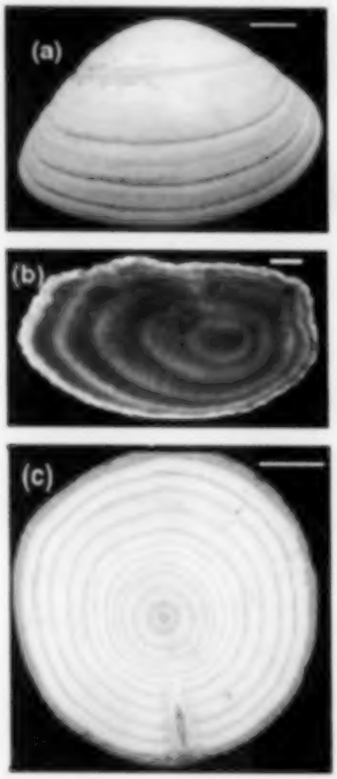

Fig. 2. Illustration of plaice otolith interpretation for a 4-year-old individual. (*a*) Image of a plaice (*Pleuronectes platessa*) otolith acquired under a binocular with transmitted light. The interpretation of the winter translucent rings is displayed by the markers set on the radial drawn on the main reading axis. Bar = 1 mm. (*b*) Associated growth pattern (distance from the otolith center to the last ring as a function of the age).

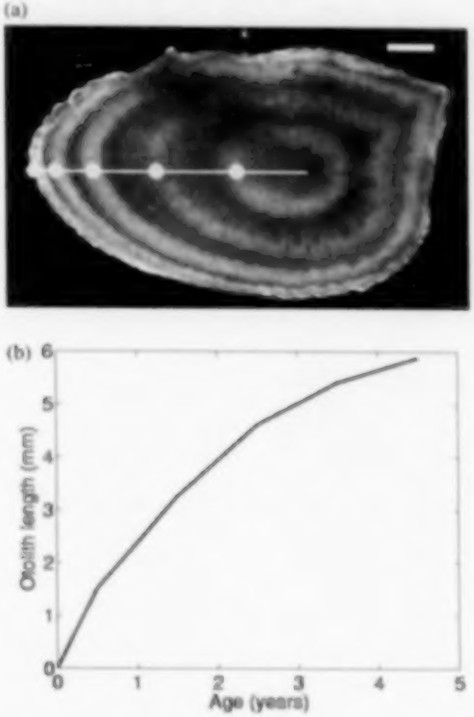

nate actual growth rings from irrelevant ones (Campana 2001). Our approach is tested on fish otoliths, which provide representative samples in terms of complexity of the interpretation task, as well as a mean for quantitative comparisons with previous work (Welleman and Storbeck 1995; Troadec et al. 2000; Guillaud et al. 2002).

There are two broad categories of approaches for the analysis of growth ring structures within the images of biological hard tissues. One the one hand, one-dimensional (1D) methods restrict their analysis to an intensity profile that is extracted along a given reading axis. Different schemes have been proposed using filtering techniques (Welleman and Storbeck 1995) or time-frequency analysis (Lagardère and Troadec 1997; Fablet et al. 2003). The main drawback lies in the absence of two-dimensional (2D) perception of ring continuity, which makes the method sensitive to local artifacts resulting in the low aging performances reported in Guillaud et al. (2002). However, despite the large research effort devoted to the detection of ridges and valleys in generic images (Cohen 1991; McInerney and Terzopoulos 1996; Lindeberg 1998), more efficient algorithms are needed to achieve 2D ring segmentation in the images of biological hard tissues. Two main features need to be further investigated: the geometric properties of concentricity of the growth rings and the irregularity of image features resulting from the underlying nonlinear growth pattern. Several solutions have been developed to tackle these issues: deformable templates deduced from the external shape of the hard tissues (Troadec et al. 2000), a graph framework (Rodin et al. 1996), locally deformable spline-based models (Benzinou et al. 1997), and multi-agent systems (Guillaud et al. 2002). The quantitative evaluation carried out for fish age estimation in Guillaud et al. (2002) points out that important improvements were obtained compared with 1D approaches; however, important difficulties still remain. Whereas different 2D approaches search for closed 2D rings, growth rings are often only partially seen (Fig. 3). In addition, although these 1D and 2D techniques perform age and growth estimation by selecting all the detected rings, for validated ageing protocols, the interpretation step is a complex task (Campana 2001). Two main issues arise: the discrimination of actual growth rings from local artifacts, false rings, or checks (Fig. 3) and the high biological variability in ring appearance and shape, as well as in growth patterns (Fig. 4). The presence of false rings is often due to biological or environmental events (for instance, sexual maturity, environmental stress, etc.). Both ring strength (in terms of image contrast), ring length, and inter-ring distances are implicitly exploited by expert readers. However, using current ageing protocols, it remains difficult to define the objective and quantitative criteria of ring appearance and growth incre-

Fig. 3. Difficulties in otolith ring interpretation: this otolith presents false rings between the first and second rings and between the second and the third ones. Also, because of the nonlinearity of the associated growth pattern, the last rings tend to be closer and hard to distinguish. The positions of validated rings is depicted by markers set on the radial drawn from the otolith center to the edge along the main reading axis. Bar = 1 mm.

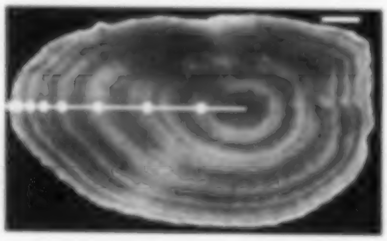

Fig. 4. Illustration of biological growth variability for a set of plaice (*Pleuronectes platessa*) otoliths.

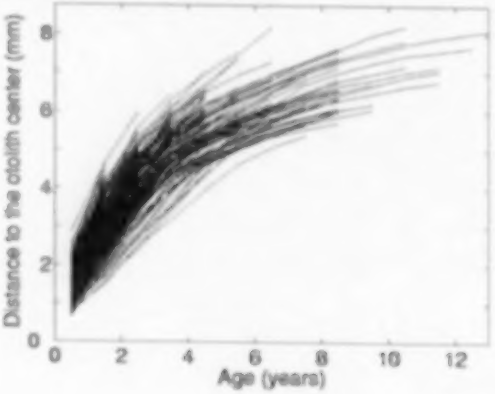

ment that permit actual growth rings to be distinguished from false rings or checks. These important issues demonstrate that only expert readers with a broad experience for given species and stocks can precisely and accurately estimate ages, because they have observed several tens of thousands of otoliths before becoming consistent in their interpretation. The difficulty in defining well-formalized criteria for the interpretation of growth rings has been emphasized by the results of a European workshop on plaice otolith reading held in 2003: inter-reader agreement rates range from 40% to 95% depending on the readers' experience for fish samples from age groups 1 to 6, with between 85% and 95% agreement among expert readers. These results illustrate the complexity of otolith interpretation even for "easy-to-read" samples.

Discriminating realistic growth patterns from irrelevant ones is a crucial step in designing an automated approach for fish age and growth estimation and was recently investigated using statistical learning (Robertson and Morison 1999; Fablet and Josse 2005). In both studies, age estimation is stated as a classification issue that resorts to mapping a vector of features of the content of otolith images (e.g., the vector formed by the Fourier coefficients of a 1D intensity signal along a given axis in Robertson and Morrison (1999)) to an age class. Although promising results have been reported, these schemes only perform age estimation and cannot be extended to growth estimation. In particular, they cannot deliver an iconic interpretation of the image depicting the structures selected as the growth rings (for instance, by drawing markers on the image structures selected as growth rings; Fig. 3).

To bring new solutions to these issues, a novel two-stage approach is developed in this paper. The first stage of this approach aims at extracting 2D growth rings within images of biological hard tissues. This segmentation issue is stated as the detection of concentric ridge and valley structures. Because the assumption that 2D growth rings are closed, as previously considered (Rodin et al. 1996; Troadec et al. 2000; Guillaud et al. 2002), is often violated, a bottom-up strategy, which initially extracts elementary ridge and valley segments, is adopted. To ensure robust detection, a template-based scheme, based on the deformation of local templates issued from the external shape of the hard tissue, is coupled with a growth-adapted filter. Elementary ring segments are then grouped to form meaningful ring curves, exploiting ring concentricity and the alternation of opaque and translucent rings. The second stage of the proposed technique tackles the actual interpretation of growth ring structures. Given candidate ring curves, age and growth estimation resort to the selection of a relevant curve subset. The proposed Bayesian setting formally models the protocols followed by expert readers. Using the MAP (maximum a posteriori) criterion (Geman and Geman 1984), the proposed likelihood function combines both of the significativity measures evaluated for each extracted ring curve, a priori growth information to discriminate realistic growth patterns from irrelevant ones, and hard constraints on the spatial arrangement of the selected ring curves. In particular, an a priori growth model is defined from examples of actual growth patterns. To our knowledge, this work is the first attempt to explicitly rely on experts' protocols and a priori growth information to constrain the automated interpretation of growth rings within images of biological hard tissues. The different steps of our approach for 2D ring segmentation and image interpretation are described and illustrated for a 4-year-old plaice otolith (Fig. 5): the set of detected elementary ridge segments (Fig. 5*b*), the ridge curves resulting from the grouping of the elementary segments (Fig. 5*c*), and the selected subset of ridge curves (Fig. 5*d*). The parameter setting used to process this example is detailed below.

Semi-local extraction of elementary ring segments

Local template based framework

As a result of the accretionary formation of biological hard tissues, the alternated translucent and opaque rings are concentric with respect to the growth center. In addition, ring shapes can be roughly approximated (at least locally) as scaled versions of a given template. This key feature was exploited in Benzinou et al. (1997), where the detection of closed 2D rings is reliant on the scaling of the external shape of the hard tissue relative to the growth center. Although promising, this technique results in poor detection of the rings close to the edge. This is partly due to the sensitivity of this template-based approach to the accuracy of locating

Fig. 5. Illustration of our approach dedicated to the analysis of growth rings within images of biological hard tissues: (*a*) observed hard tissue (here, a plaice (*Pleuronectes platessa*) otolith); (*b*) extracted elementary "ridge" ring segments; (*c*) extracted "ridge" ring curves from the merging of elementary ring segments; and (*d*) subset of the selected ridge ring curves using the developed Bayesian framework. Bar = 1 mm.

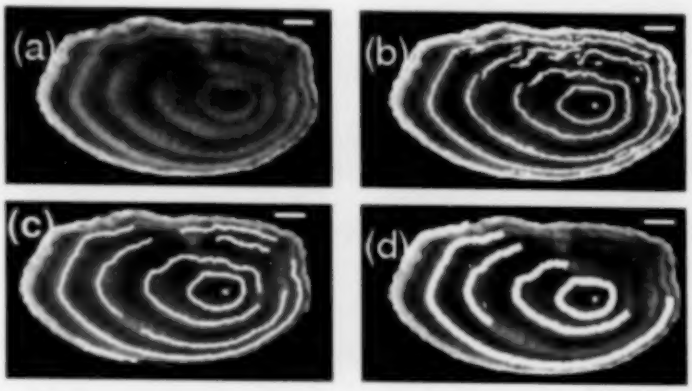

the growth center, as well as to ring discontinuities. On the other hand, purely local techniques for ridge and valley detection (Haralick 1983; Chalmond et al. 1995; Lindeberg 1998) are outperformed by parametric ones if accurate parametric models of ridge and valley shapes within the processed images are available.

Hence, the use of the external shape as the parametric model of ridge and valley structures is further investigated, and the global template approach is extended to a semi-local framework. Within predetermined angular sectors, scaled versions of a semi-local template model are fitted to local ridge or valley image segments (Fig. 6). The semi-local template model is still derived from the external shape. This semi-local parametric framework is a good compromise between the ability to adapt to local ridge and valley shape and the robustness to noise within images. In particular, as shown below, it is more robust to errors in identifying growth centers than the template-based approach described in Troadec et al. (2000), which permits the use of algorithms that perform the automatic detection of the growth center (Guillaud et al. 2002; Cao and Fablet 2004).

More precisely, the extraction of local elementary ridge or valley segments proceeds as follows. Given an image and the position (x_O, y_O) of the growth center O, its external shape is initially extracted. The number of sampling points of the external shape is denoted by N_C and their polar coordinates by $\{(\rho_C^k, \theta_C^k = 2k\pi/N_C)\}_{k\in[1,N_C]}$ in the framework of the two principal axes centered in the growth center. The semi-local detection of ridge and valley structures is performed within N_{SL} overlapping angular sectors, referenced by their angular coordinate $\{\theta_{SL}^n = 2n\pi/N_{SL}\}_{n\in[1,N_{SL}]}$ and their angular width $2\Delta\theta_{SL}$. To ensure overlapping of the angular sectors, $\Delta\theta_{SL}$ is set such that $\Delta\theta_{SL} > \pi/N_{SL}$. Given an angular sector $\theta_{SL}^n \pm \Delta\theta_{SL}$, the associated semi-local template model is defined by its polar coordinates $\{\rho_C^k, \theta_C^k = 2k\pi/N_C)\}_{k\in\kappa^n}$.

Our goal is to determine the scaling factors $\alpha \in [0,1]$ such that the scaled template, defined by the polar coordinates $\{\alpha\rho_C^k, \theta_C^k)\}_{k\in\kappa^n}$ with $\kappa^n = \{[1, N_C]/|\theta_C^k - \theta_{SL}^n| < \Delta\theta_{SL}\,[2\pi]\}$, fit the local ridge and valley segments within the angular sector $\theta_{SL}^n \pm \Delta\theta_{SL}$. Different features computed from the derivatives of the intensity function along and normal to the local template (Lindeberg 1998) can be used as the measure of the strength of local ridges or valleys. However, a simpler and more robust feature is preferred: the median value of the intensity along the scaled local template. It comes to define the following intensity function $s_{SL}^n(\alpha)$ for given angular sector $(\theta_{SL}^n, \Delta\theta_{SL})$ and scaling factor α:

$$(1) \quad s_{SL}^n(\alpha) = \mathrm{med}(\{I(x_0 + \alpha\rho_C^k \cos\theta_C^k, x_0 + \alpha\rho_C^k \sin\theta_C^k)\}_{k\in\kappa^n})$$

where med() is the median estimator and I the image intensity function. The extraction of the elementary ridge and valley segments then resorts to the detection of the extrema of

Fig. 6. Local template based scheme for the detection of elementary ring segments: (*a*) extraction of the external shape using polar coordinates in the framework of the two principal axis of the hard tissue and centered in the growth center O; (*b*) scaling of the local template for a given angular sector $\theta_{SL}^n + \Delta\theta_{SL}$.

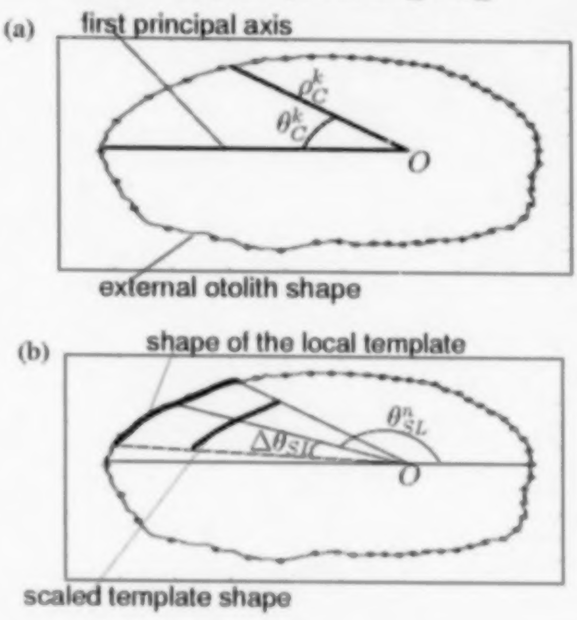

the intensity function s^n_{SL}. Thus, one aims at computing the scaling factors α verifying

$$\frac{ds^n_{SL}(\alpha)}{d\alpha} = 0 \tag{2}$$

Detection of ridges and valleys

Solving for eq. 2 requires computing the derivatives $ds^n_{SL}(\alpha)/d\alpha$ at relevant scales (Lindeberg 1998). In addition, specific time-frequency features of the images of biological hard tissues have to be considered. First, smooth variations of material density (for instance, otolith are usually thicker close to the edge) might result in a continuous evolution of the mean intensity values from the growth center to the edge. Second, the width of translucent and opaque rings is directly related to the underlying growth pattern. Growth patterns are mainly nonlinear. Images of biological hard tissues then involve a frequency modulation applied to the ring structures. The actual growth pattern is obviously unknown, but a mean a priori growth model can be used for demodulation purposes. This idea was first applied to one-dimensional intensity signals using an exponential model (Lagardère and Troadec 1997). Here, a mean growth model is derived from the growth patterns associated with images interpreted by an expert. Mathematically, the mean growth model is defined by the function $L = \Phi(t)$, where L is the distance to the otolith center and t is the time variable in years.

The framework used to solve for eq. 2 then initially demodulates s^n_{SL} with regard to the growth model Φ. The resulting demodulated signal $s^n_{DM}(t)$ is given by

$$s^n_{DM}(t) = s^n_{SL}\left(\frac{\rho^n_C}{\rho^{n^*}_C}\Phi(t)\right) \tag{3}$$

where n^* refers to the point of the external shape on the main reading axis (for instance, $\theta^{n^*}_C = \pi$ for plaice otoliths). Let us point out that $\Phi(t)$ is normalized with regard to $\rho^{n^*}_C$ as the mean growth model is learned along the main reading axis.

To remove the trend s^n_{TDM} from the intensity signal s^n_{DM}, s^n_{TDM} is estimated using a convolution to a Gaussian kernel $g_{\sigma_{TDM}}$ with a large variance σ^2_T: $s^n_{TDM} = g_{\sigma_T} s^n_{DM}$. Then, the detection of the positions of the local ridges and valleys involves the computation of the derivative $d_t s^n_{DM}$ of the intensity function $s^n_{DM} - s^n_{TDM} \cdot d_t s^n_{DM}$ is estimated using a Gaussian kernel g_{σ_D} with a low variance σ^2_D:

$$d_t s^n_{DM} = \frac{d[g_{\sigma_D}(s^n_{DM} - s^n_{TDM})]}{dt} \tag{4}$$

To actually determine the extrema of $s^n_{DM} - s^n_{TDM}$, the zero crossings of its first derivative $d_t s^n_{DM}$ are detected for time values uniformly sampled within $[0, t_{max}]$, with t_{max} computed such that $\Phi(t_{max}) = \rho^{n^*}_C$. The scaling factors solving for eq. 2 are then computed from the inverse transform Φ^{-1}. Typically, the sampling rate is set to 0.01, σ_D to 0.1 and σ_{TDM} to 1.5 (all these values are given in years as they are used in the demodulated domain).

The detection of the elementary ridge and valley segments that arose from the adapted filtering of the semi-local template based function s^n_{SL} is shown (Fig. 7). This example stresses that the growth-adapted demodulation eases the detection of ridge and valley structures close to edge and avoids overdetections close to the center. Applied to the whole set of angular sectors $\{\theta^n_{SL} = 2n\pi/N_{SL}\}_{n\in[1,N_{SL}]}$, the growth-adapted framework finally results in the detection of elementary ridge and valley segments (Fig. 5*b*).

Extraction of two-dimensional ridge and valley curves

Given the set of extracted elementary ridge and valley segments (as depicted in Fig. 5), the aim is to merge these elementary segments to form meaningful curves. Numerous perceptual grouping algorithms have been developed to form segments from candidate points or elementary segments (Guy and Medioni 1996; Jacobs 1996; Cao 2003). These techniques mainly rely on general geometric criteria such as good continuations (Cao 2003) or curve smoothness (Guy and Medioni 1996; Jacobs 1996). When dealing with the analysis of growth rings within hard tissue images, three geometric features are of key interest: the growth rings are concentric, there is an alternation of opaque and translucent rings, and opaque and translucent rings never cross each other.

The proposed grouping procedure exploits these features. More precisely, it proceeds as follows for elementary ridge segments (and, conversely, for valley ring structures). For a given pair of elementary ridge segments associated to two neighboring angular sectors $(\Theta^n_{SL}, \Delta\Theta_{SL})$ and $(\Theta^{n+1}_{SL}, \Delta\Theta_{SL})$, the decision rule used to merge this pair of segments evaluates whether or not elementary valley segments within the neighboring angular sectors $\{(\Theta^k_{SL}, \Delta\Theta_{SL})\}_{k\in[n-1,\ldots,n+2]}$ lie between the pair of tested segments in terms of distance to the growth center. This decision rule is illustrated for two cases: merging is validated and merging is rejected (Fig. 8). A ridge curve is finally formed by the set of elementary ridge segments that can be linked by a path going through merged segments.

An example of the extraction of ridge curves from a set of elementary segments is displayed (Fig. 5*c*). It should be pointed out that the length of resulting curves depends both on the actual length of the rings present in the image and on noise or local occlusions in the image. Depending on these features, the extracted ring curves can be closed curves, as well as only partial ring curves.

Image interpretation for age and growth estimation

From a set of extracted 2D ridge and valley curves, the actual interpretation of the image content in terms of age and growth estimation depends on the selection of a curve subset corresponding to the actual growth rings. Several curve subsets might correspond to the correct interpretation, as an actual growth ring might be covered by several partial curves and some detected curves might not correspond to actual rings, but to false rings, or might be due to noise patterns. The proposed framework relies on the protocols followed by expert readers. Mainly, it involves four different aspects: the focus on an a priori image region around a predefined axis along which the considered images are known to convey

Fig. 7. Detection of elementary ridge segments: (*a*) the processed image with the extracted elementary ridge segments (thick line) within the angular sector $\Theta^{\alpha}_{\mathfrak{M}} = \pi$ (bar = 1 mm); (*b*) the intensity function $s^{\alpha}_{\mathfrak{M}}$; (*c*) the demodulated version (broken line) using the mean growth law, the estimated tendency (dashed–dotted line), the filtered signal (solid line), and the estimated extrema positions (●).

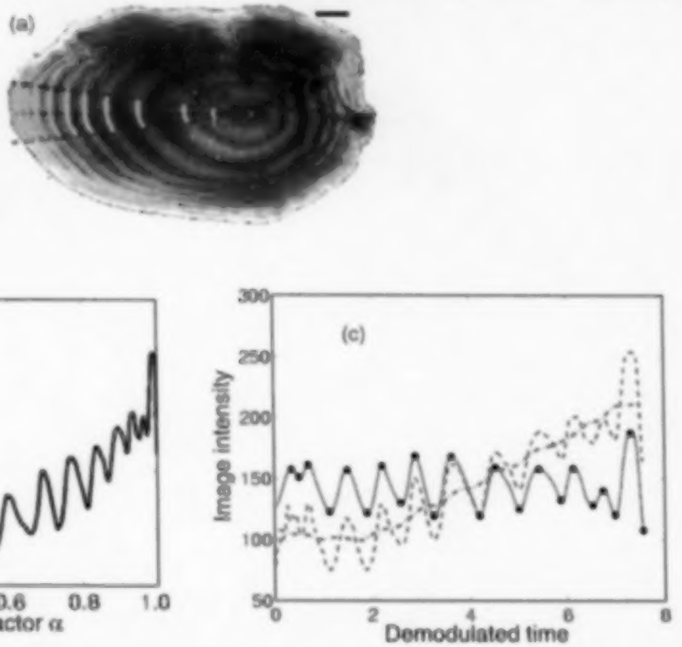

Fig. 8. Decision rule for merging a pair of neighboring elementary ridge segments: (*a*) validated merging; (*b*) rejected merging. The pair of tested segments is displayed by a solid line, and neighboring elementary valley segments are depicted by broken lines.

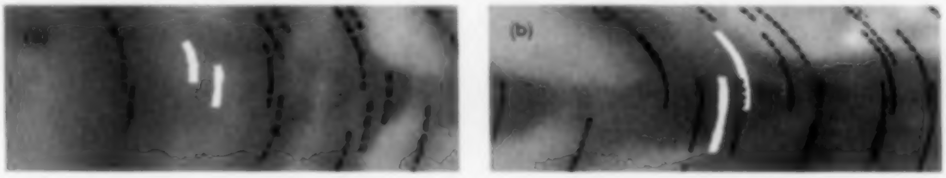

more reliable and more relevant information; the detection of candidate ring-like structures; the evaluation of the significativity of any possible rings with respect to length and contrast information; and the analysis of the spatial arrangement of the selected ring structures, which needs both to correspond to an alternation of translucent and opaque rings and to conform to some a priori growth features.

To satisfy these protocols, a mathematically sound Bayesian framework is developed. The associated data-driven term evaluates the significativity of the extracted candidate ring segments, whereas the a priori model integrates knowledge on growth variability, as well as hard constraints set on the spatial arrangement of the selected rings. As pointed out previously, the discrepancies in disagreement rates in the interpretations of hard tissues for validated ageing protocols prove that it is crucial to benefit from the experience of expert readers (unpublished data; Panfili et al. 2003). The key point is to define a relevant representation of the a priori growth information, which is addressed by deriving our a priori growth model from examples of actual growth patterns estimated by experts.

Our Bayesian setting states the selection of a relevant curve subset as a labeling issue, where each extracted ridge or valley curve is assigned a binary label, "selected" or "rejected". Let $\mathcal{C}$ denote the set of extracted ridge and valley curves as described in the previous section. Let $\mathcal{L}$ be the binary label set {"selected", "rejected"}, $e_{\mathcal{C}}$ the set of labels $\{e_c\}_{c\in\mathcal{C}}$ for a given labeling configuration, $o_{\mathcal{C}} = \{o_c\}_{c\in\mathcal{C}}$ the features computed for all ring curves $c \in \mathcal{C}$ to evaluate their significativity. The selection of the relevant curve subset then comes to retrieve the best labeling configuration $\hat{e}_{\mathcal{C}}$ maximizing the MAP criterion:

$$(5)\qquad \hat{e}_{\mathcal{C}} = \arg\max_{e_{\mathcal{C}}\in\mathcal{L}^{|\mathcal{C}|}} P(e_{\mathcal{C}}|o_{\mathcal{C}}) = \arg\max_{e_{\mathcal{C}}\in\mathcal{L}^{|\mathcal{C}|}} P(o_{\mathcal{C}}|e_{\mathcal{C}})P(e_{\mathcal{C}})$$

where $P(o_{\mathcal{C}}|e_{\mathcal{C}})$ is the data-driven term described subsequently and $P(e_{\mathcal{C}})$ integrates an a priori knowledge on growth variability and on the spatial arrangement of the relevant labeling configurations. Given $g_{e_{\mathcal{C}}}$, the growth pattern associated to the label configuration $e_{\mathcal{C}}$ (i.e., the growth pattern computed for the selected ring curves $S(e_{\mathcal{C}})\{c^* \in \mathcal{C}/e_{c^*} =$ selected}), and $\Theta_{S(e_{\mathcal{C}})}$, the set of angular sectors covered by

Fig. 9. Illustration of the computation of the envelope growth model from a set of examples of plaice (*Pleuronectes platessa*) growth patterns for the year class $k = 4$: (*a*) envelope (bold broken lines) computed from the growth patterns; (*b*) envelope (bold broken lines) computed from their first-order derivative.

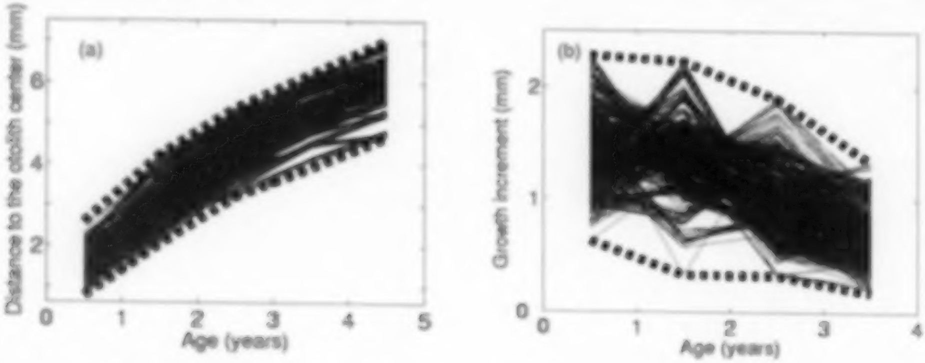

the selected ring curves $S(e_C)$, the a priori model $P(e_C)$ is formally defined by

$$P(e_C) = p(g_{e_C}, \Theta_{S(e_C)}) = P(g_{e_C} | \Theta_{S(e_C)}) P(\Theta_{S(e_C)}) \tag{6}$$

The likelihood $P(g_{e_C} | \Theta_{S(e_C)})$ measures the relevance of the growth pattern g_{e_C} with regard to a priori growth information. Because this model does not depend on direction information, $P(g_{e_C} | \Theta_{S(e_C)})$ simplifies to $P(g_{e_C})$. As a complementary stage, the second term $P(\Theta_{S(e_C)})$ evaluates whether or not the considered labeling configuration conforms to the hard constraints set on the spatial arrangement of the ring curves.

Our Bayesian setting finally comes to solve for

$$\hat{e}_C = \arg \max_{e_C \in E^C} P(o_C | e_C) \cdot (P(g_{e_C}) \cdot P(\Theta_{S(e_C)})) \tag{7}$$

Further details regarding the associated likelihood functions are given subsequently.

Data-driven term

The data-driven likelihood $P(o_C | e_C)$ evaluates the significativity of each ring curve given a labeling configuration e_C:

$$P(o_C | e_C) = \prod_{c \in C} P(o_c | e_c) \tag{8}$$

As previously mentioned, experts mainly rely on the perception of contrast and ring continuity. Because contrast information is already implicitly used to extract ring curves, the likelihood $P(o_c | e_c)$ is defined from the angular length L_c of the curve c. Using an energy setting, $P(o_c | e_c)$ is expressed as $P(o_c | e_c) = \exp[-U_1(L_c, e_c)]$. The energy function U_1 favors the selection of ridge and valley curves with a high length value:

$$\begin{cases} U_1(L_c, e_c) = 1 - s_1(L_c - v_1), & \text{if } e_c = \text{"selected"} \\ U_1(L_c, e_c) = s_1(L_c - v_1), & \text{if } e_c = \text{"rejected"} \end{cases} \tag{9}$$

where $s_1()$ is a smooth step function rescaled between 0 and 1 and v is the length threshold. This parameter value is easy to set as it simply expresses from which length value a ring curve is regarded as visually significant. Typically, this significativity threshold in terms of angular length is set to $\pi/8$ (in radians).

A priori growth information

The interpretation of growth rings on hard tissues implicitly relies on growth information, although expert readers do not generally exploit explicit measurements. As highlighted for plaice otolith samples (Fig. 4), biological growth phenomena usually involve a very high variability. For instance, for this data set, the distance between the first translucent ring and the growth center is between 0.7 and 2.7 mm, whereas this distance for the second translucent ring is between 2.2 and 5 mm. This huge variability and the overlap between successive year classes prevent the use of a mean growth model to predict the position of each translucent ring. More complex representations are therefore required. Besides, in our Bayesian setting, labeling configurations $\{e_C\}$ can correspond either to actual or to erroneous growth patterns. Consequently, rather than determining an accurate representation of the statistical distribution of the growth patterns for each year class, one is interested in designing a decision function that permits discrimination between realistic and irrelevant growth patterns.

An exemplar-based strategy is adopted to tackle this pattern recognition issue. It is assumed that a set of growth patterns representative of the actual biological variability is available. Let us denote by $\{g_i\}_{i \in [1,\dots,n]}$ the set of n examples of growth patterns for the year class k. The a priori growth model is then defined from the lower and upper envelopes of $\{g_i\}_{i \in [1,\dots,n]}$ and of their derivatives. The lower envelope $g^k_{\min}$ is given by

$$g^k_{\min}(t) = \min_{i \in [1,\dots,n]} g_i(t), \text{ for } t \le k \tag{10}$$

and the upper one $g^k_{\max}$ is given by

$$g^k_{\max}(t) = \max_{i \in [1,\dots,n]} g_i(t), \text{ for } t \le k \tag{11}$$

where t is the time variable in years. Similarly, the lower and upper envelopes $\mathrm{d}g^k_{\min}$ and $\mathrm{d}g^k_{\max}$ of the first-order derivative of the growth functions $\{g_i\}$ are computed. The envelope of the first-order derivatives is considered, because growth increments also provide meaningful cues to characterize realistic growth patterns. The computation of these envelopes for a set of examples of plaice growth patterns for the year class $k = 4$ is depicted (Fig. 9). These minimum–maximum fea-

Fig. 10. Illustration of the evaluation of the relevance of growth pattern examples given a variability range set by the envelope $(g^k_{\min}, g^k_{\max})$ for the age class $k = 4$: (*a*) relevant growth pattern; (*b*) irrelevant growth pattern.

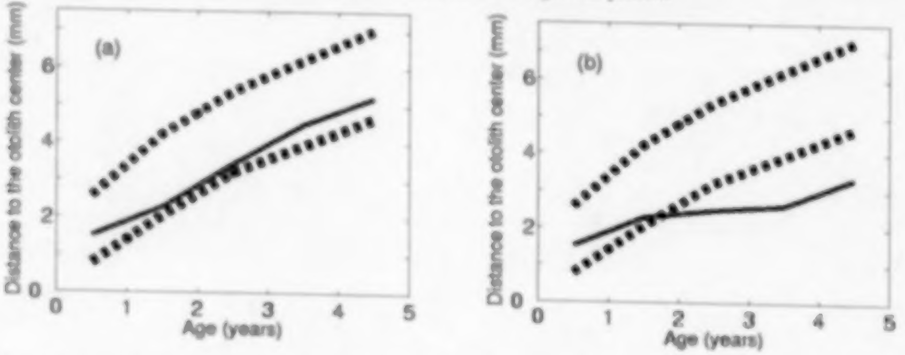

Fig. 11. Constraint on the spatial arrangement of the selected rings curve: relevant (*a*) vs. irrelevant (*b*) configurations. Pair of successive ring curves are required to depict valley and ridge curves because the interpretation of growth rings has to refer to an alternation of opaque and translucent rings.

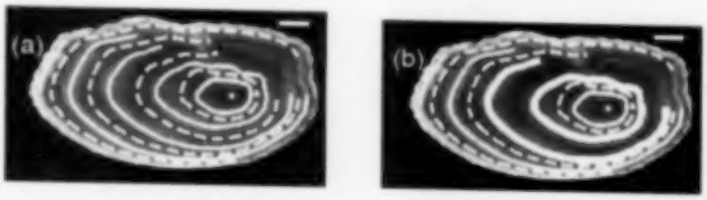

tures are often implicitly used by expert readers to check the reliability of growth increments given their knowledge of growth variability.

From these envelopes, a probabilistic decision function $P(g_{e_C})$ is designed to evaluate whether or not the growth pattern g_{e_C}, associated to a given labeling configuration e_C is relevant. More precisely, the labeling configuration e_C is assumed to refer to a realistic growth sample if g_{e_C} and $\mathrm{d}g_{e_C}$, respectively, remain within the variability range defined by $(g^k_{\min}, g^k_{\max})$ and $(\mathrm{d}g^k_{\min}, \mathrm{d}g^k_{\max})$. An illustration of this statement is provided (Fig. 10). Formally, $P(g_{e_C})$ is written as

$$(12)\quad P(g_{e_C} \text{ is relevant for age class } k) = \min\left(P(g_{e_C}, g^k_{\min}, g^k_{\max}), P(\mathrm{d}g_{e_C}, \mathrm{d}g^k_{\min}, \mathrm{d}g^k_{\max})\right)$$

where $P(g_{e_C}, g^k_{\min}, g^k_{\max})$ is defined by

$$(13)\quad P(g_{e_C}, g^k_{\min}, g^k_{\max}) = \min\left[\min_{0\le t\le k} s_2(g_{e_C}(t) - g^k_{\max}(t)), \min_{0\le t\le k} 1 - s_2(g_{e_C}(t) - g^k_{\min}(t))\right]$$

where s_2 is the opposite of a smooth step function rescaled between 0 and 1. $P(\mathrm{d}g_{e_C}(t), \mathrm{d}g^k_{\min}, \mathrm{d}g^k_{\max})$ is defined in the same way. The introduced growth model can be viewed as a binary classifier (realistic vs. nonrealistic) of growth patterns defined by the probabilistic decision function $P(g_{e_C})$.

The evaluation of the likelihood $P(g_{e_C}$ is relevant for age class $k)$ requires normalizing the growth pattern g_{e_C} with regard to the reference growth axis exploited to estimate $g^k_{\min}$, $\mathrm{d}g^k_{\max}$, $\mathrm{d}g^k_{\min}$, and $g^k_{\max}$. This normalization issue comes to define the normalized positions of the extracted ring curves in C along the reference growth axis. It is iteratively performed as follows. Ring curves in C intersecting the reference axis initially form the set of curves C_{Norm} with known normalized positions. Iteratively, the curve c^* in C/C_{Norm} closest to the reference axis in the direction normal to the axis is selected. The two curves (c_1, c_2) in C_{Norm}, angularly overlapping c^* and the closest to c^*, are then retrieved, and the normalized position of c^* is lineally interpolated from the normalized positions of c_1 and c_2. This normalization procedure does not assume that the reference axis is a straight line or that the growth is angularly isotropic. It can then be applied to complex growth situations, given that the reference growth axis can be automatically extracted for all samples.

Constraints on the spatial arrangement of rings

In addition to a priori growth information, hard constraints on the spatial arrangement of rings are set to help in the minimization of eq. 7. These constraints are introduced in the proposed Bayesian setting through the evaluation of the likelihood $P(\Theta_{S(e_C)})$. The likelihood is set to zero if any of the constraints described below are not verified. The three hard constraints are as follows. As mentioned previously, expert readers perform the interpretation of growth rings along a main reading axis; therefore, the analysis is restricted to a predefined angular sector of interest and selected ring curves $S(e_C)$ are required to intersect this angular sector. Any relevant interpretation $S(e_C)$ must conform to the studied biological structures, which involve an alternation of translucent and opaque growth rings; consequently, $S(e_C)$ is required to depict an alternation of valley and ridge curves. Examples are shown to illustrate this second hard constraint (Fig. 11). Finally, successive ring curves within $S(e_C)$ must angularly overlap, which will lead to visually consistent interpretation.

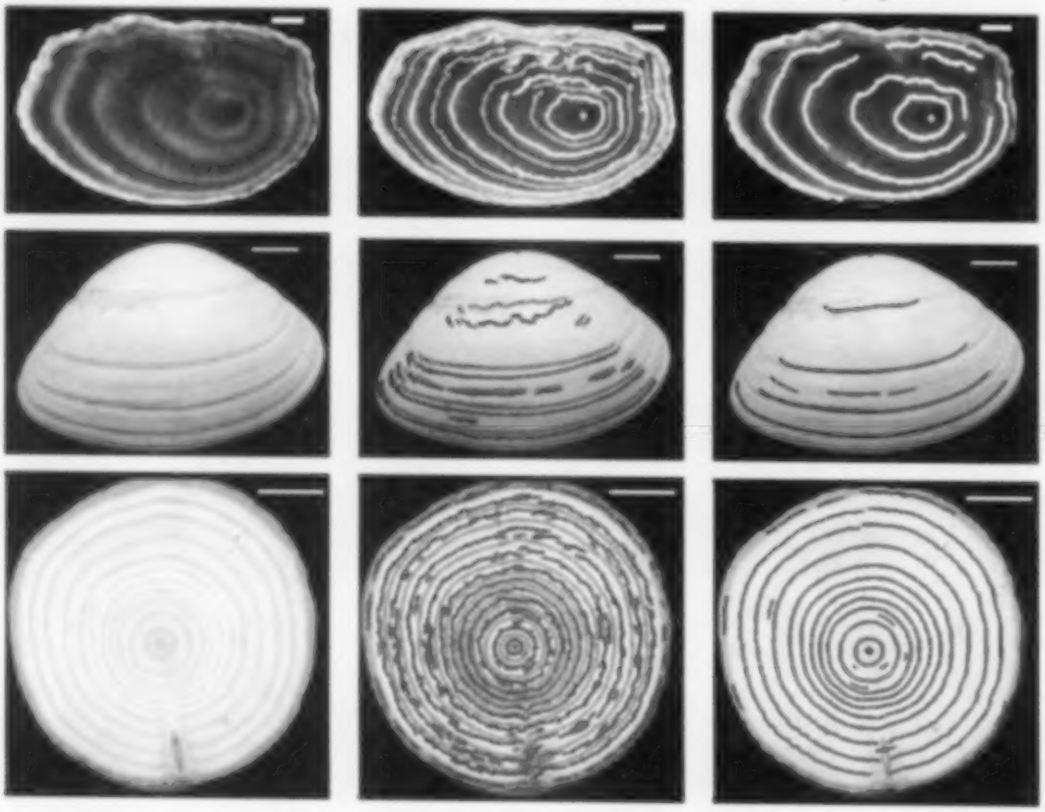

Fig. 12. Extractions of meaningful ring structures within images of biological hard tissues depicting growth ring structures. The first row displays an application to a fish otolith (bar = 1 mm), the second to the shell of a bivalve seashell (bar = 0.5 cm), and the third to the section of a tree trunk (bar = 10 cm). The first column provides the original images, the second the extracted elementary ridge and valley segments, and the third the detected ring curves resulting from the grouping of the elementary segments.

Energy minimization

Given a curve set C, the interpretation comes to solve for eq. 7. Because C typically involves about 50 curves, one cannot test over the whole set of $2^{|C|}$ possible configurations. One might stress that not all of the $2^{|C|}$ configurations are relevant ones. However, the number of relevant configurations cannot be determined analytically from $|C|$, as it depends on the relative positions of the extracted curves. Its evaluation would require testing over all possible configurations. In practice, it has been determined that the total number of relevant configurations was greater than 1000 for about 50 extracted curves.

Consequently, the minimization issue is carried out in a causal manner by introducing one-by-one ring curves $c \in C$ and retaining only the $N_{\max}$ best configurations with regard to likelihood values $P(e_c|o_c)$ (detailed in Appendix A).

Experiments

For all the experiments reported in this section, the same parameter setting is used. The external shape of the hard tissue is represented by $N_C = 500$ points and smoothed by a Gaussian kernel of variance 0.01. The extraction of elementary ring segments is performed for $N_{SL} = 75$ local axes sampled uniformly. The angular sector used for each local template is $\Delta\theta_{SL} = \pi/90$. The growth-adapted filtering is performed with $\sigma_T = 1.5$ and $\sigma_D = 0.05$ (these values are given with regard to time in years or in days depending on the periodicity of the observed ring structures). Concerning the Bayesian labeling of the set of extracted ring curves, the analysis is restricted to an angular sector of $S = \{\theta, |\theta - \pi| \leq \pi/8[2\pi]\}$ around the first principal axis of the otolith. The threshold v_l is set to $\pi/8$ and β is set to 10.

All images used in the experiments have been acquired with a 1000 × 1000 digital video camera under a binocular. A polarized light was used to better separate biological hard tissues from the background. No other preprocessing step was performed.

Extraction of meaningful ring curves

Three examples of the extraction of meaningful ring curves within images of biological hard tissues are first reported (Fig. 12): a plaice otolith, the shell of a bivalve seashell, and the section of a tree trunk. All these images share common characteristics in terms of rather concentric ridge and valley structures associated with a growth-based modulation. As expected, the proposed template-based growth-

Fig. 13. Extractions of meaningful ring structures within images of otolith images depicting ontogenetic changes in the shape of the rings: the first row displays an application to a pollock (*Pollachius pollachius*) otolith, and the second to a cod (*Gadus morhua*) otolith. The first column displays the original images, the second the extracted elementary ridge and valley segments, and the third the detected ring curves resulting from the grouping of the elementary segments. Bar = 1 mm.

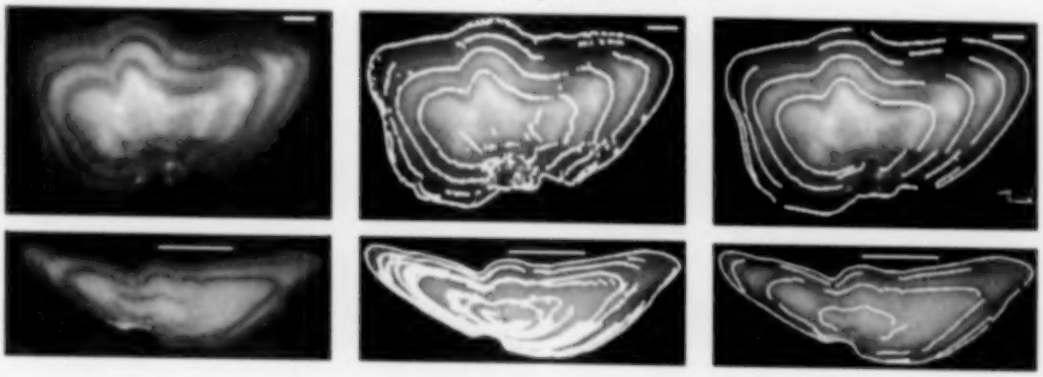

Fig. 14. Extraction of closed ring curves using a global template based scheme (Troadec et al. 2000) for the two images processed using our semi-local template based approach in Fig. 13: (*a*) pollock (*Pollachius pollachius*) otolith; (*b*) cod (*Gadus morhua*) otolith. Bar = 1 mm.

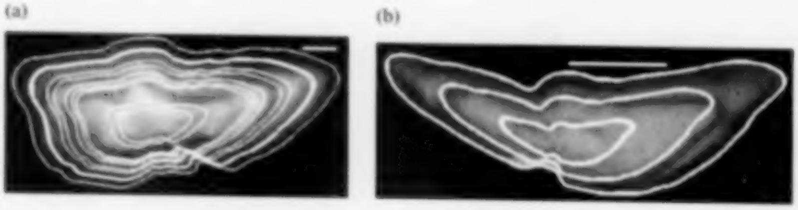

adapted scheme extracts meaningful ring curves mainly corresponding to the actual growth rings.

The extraction scheme is also applied to structures depicting ontogenetic changes in the shape of the rings (Fig. 13). Using a global template approach (Troadec et al. 2000), poor detection results are reported (Fig. 14). In contrast, the proposed local template based approach is able to successfully identify meaningful partial ring curves. It demonstrates first that fitting local scaled versions of the external shape provides a mean to adapt to nonradial growth. Second, it also stresses that growth-adapted detection of ridges and valleys only requires a rough knowledge of the scales relevant to solve for eq. 2. In other words, as used by the proposed demodulation scheme, the distance to the otolith center is a sufficient cue to approximate the width of the structures to be extracted.

Interpretation examples

To evaluate the performance of the proposed Bayesian interpretation scheme, fish otolith analysis is emphasized. The design of the a priori growth model requires building a large growth data collection (typically, several hundreds of samples). Our evaluation set consists of 400 plaice otoliths from the fourth quarter collected by IFREMER at the fish market of Boulogne/Mer in 1993 and 2000. Note that age determination from plaice otoliths has been validated and confirmed (Campana 2001). The processed otolith collection does not contain known-age material but has been interpreted and annotated by an expert from IFREMER according to the agreed-upon and validated plaice-ageing protocol. All the images have been acquired using transmitted light with the same magnification. Half of these interpretations are used to train the a priori growth model, and the other half are used as a control set for the evaluation of our approach.

Three images of plaice otoliths have been chosen to illustrate the behavior of the different stages of our approach (Fig. 15): the first two belong to the age group 6 (seven translucent rings) and the third one to the age group 4 (five translucent rings). For these three examples, the age and growth estimations were performed by an expert reader whose interpretation is used as the control. Reported results include the extracted ridge curves, the selected ridge curve subsets using the Bayesian framework, and the estimated growth pattern compared with the control.

The first example is a 6-year-old plaice otolith (seven translucent rings). Relevant ridge curves are extracted, and the selected interpretation is the same as the expert one. This example was chosen to illustrate the ability of our approach to extract ridge and valley structures close to the otolith edge thanks to the growth-adapted filtering used within the semi-local template framework.

A plaice otolith also assigned to the age group 6 is considered for the second example. It emphasizes the need for an approach capable of extracting nonclosed curves, such as the second translucent ring. The proposed approach extracts meaningful ridge and valley curves for both closed and

Fig. 15. Interpretation of images of plaice (*Pleuronectes platessa*) otoliths for three examples: the first row depicts the otolith images and the associated expert interpretations, the second the extracted ridge curves, the third the curve subsets selected for age and growth estimation, and the fourth the estimated growth patterns (solid line) compared with the ground truth ones (broken line). For each example, the ground truth is provided by the interpretation of an expert in plaice (*P. platessa*) otolith reading. Bar = 1 mm.

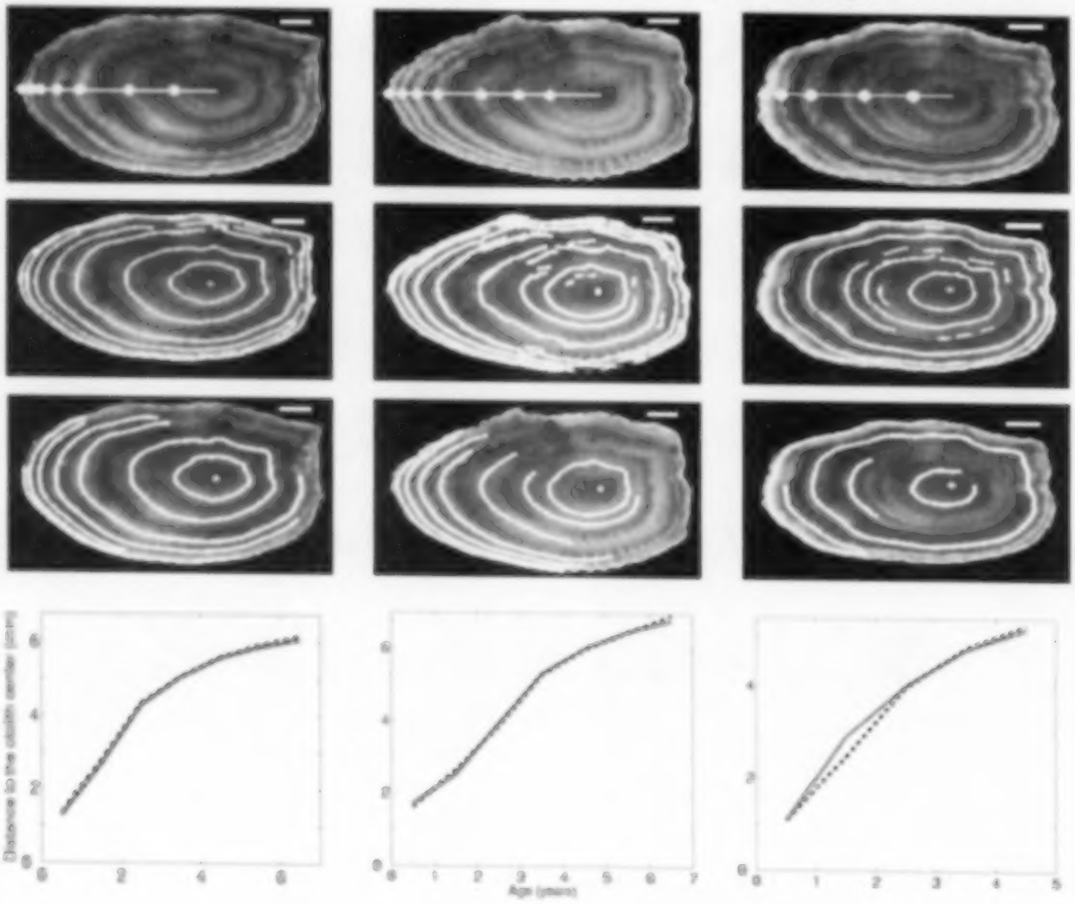

nonclosed seasonal rings and retrieves the correct otolith interpretation.

The third example points out the requirement for formulating the otolith interpretation as a selection–rejection issue of extracted candidate ridge and valley curves. The expert has regarded the second and third translucent rings as belonging to a single translucent area. Given an accurate extraction of ridge and valley curves, the use of a statistical growth model within the introduced Bayesian framework results in discarding configurations that select ridge curves for the two rings of the second translucent area. Compared with the expert interpretation, the selected subset of ridge curves only differ in the position of the second translucent area: the expert has taken the middle of this area, whereas the automated approach has selected a ridge curve associated with the third translucent ring. Therefore, the age is correctly estimated, and the growth patterns just show a minor difference at between years 1 and 2 because of the position chosen for the second translucent ring.

Computational time for our approach under Matlab 7 (The Mathworks Inc. 2004) for the extraction of 2D ring curves runs about 30 s on a 2.4 GHz Pentium IV, whereas the Bayesian labeling needs a few seconds.

Quantitative evaluation

A quantitative evaluation of the proposed approach was carried out using the second half of the collected set of plaice otoliths (i.e., a database of 200 otoliths). The age distribution of this database is reported (Fig. 16*a*). Age groups 1 and 2 are the most frequent, with more than 50 elements, whereas age groups 5 and 6 just comprise 15 and 20 samples, respectively. This age distribution is representative of the estimates from commercial landings, where samples of age group 6 and less usually represent more than 90% of the total. Otoliths older than age group 6 can also be found; however, the number of samples is not sufficient to train a relevant growth model. Consequently, they were not considered during our evaluation.

Fig. 16. Age estimation errors for the test set of 200 images of plaice (*Pleuronectes platessa*) otoliths: (*a*) age composition of the processed otolith data set; (*b*) rates of the age estimation error for age classes 1 to 6; (*c*) mean rate of the age estimation error.

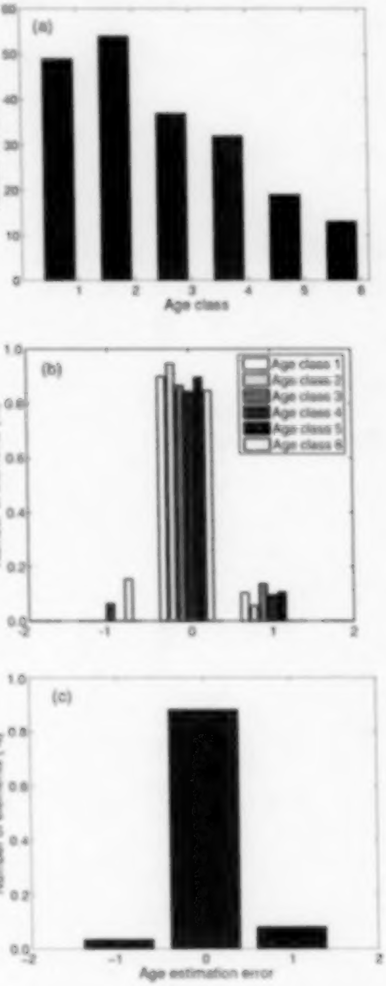

The interpretations provided by the expert are used as the control to compute the class-by-class and overall age estimation errors (results are given in Fig. 16). The agreement rate is between 84% for age group 5 and 94% for age group 2. The overall agreement rate of 89% shows that the proposed approach outperforms previous work, as the maximum overall agreement rate for the different 2D methods evaluated in Guillaud et al. (2002) was below 80% for a similar test set. These results stress the need for the Bayesian interpretation stage to be combined with the extraction of candidate ring curves. For the whole set of 200 otoliths, the estimation error is never greater than one.

The mean values and the associated square-root variances for the distances between the ring positions determined by the automatic scheme and those given by the expert, as a function of the ring number, are reported (Table 1). The analysis is carried out only with the samples for which the two age estimates are equal. The overall accuracy is satisfactory, with mean distance values and square-root variances below 0.15 mm. The discrepancies are more important for the first two rings; in fact, the first rings often involve a wide area presenting several extrema. The expert usually selects the middle of this area to set the ring position, whereas the automatic ring segmentation chooses one of these extrema. Nevertheless, this evaluation shows that the two interpretations almost always agree in terms of both age estimates and estimated growth patterns.

Sensitivity to errors in locating the growth center

Concerning the robustness of the extraction of ring curves to errors in locating the actual growth center, the results of the extraction of ridge curves are reported for two different positions of the nucleus: the actual position of the growth center (Fig. 17*a*) and a position given by the translation of 0.4 mm to the left and 0.25 upward of the actual growth center (Fig. 17*b*). Very few differences are observed in the accuracy of the detection of meaningful ring curves.

To carry out a quantitative evaluation of the robustness to errors in locating the growth center, the effect of using a biased position of the growth center on age estimations has been investigated for the set of 200 plaice otoliths. Fewer than 5% of the images are interpreted differently than with the actual position of the growth center (given the translated position of the growth center). These results stress the robustness of the proposed scheme to errors in locating otolith nucleus, given that the automated techniques for nucleus detection (Guillaud et al. 2002; Cao and Fablet 2004) were shown to perform with a square-root variance below 0.15 mm.

Subjectivity in age reading

Age estimation errors mainly occur with otoliths, the interpretation of which is difficult even for experts. Two representative examples are reported (Fig. 18). The first one involves an otolith aged as two by the expert, whereas the age estimated by the automatic approach is three. These two estimations differ in the interpretation of the area close to the edge: the expert considers only one very large third ring, whereas the automatic approach detects and selects a third ridge curve and a fourth one. Both interpretations are realistic in terms of growth patterns, but the expert has considered that the last ring was not sufficiently contrasted to be selected. The second case is an otolith aged as five by the expert and six by the Bayesian approach. These two interpretations differ in the selection of an additional translucent ring before the first translucent ring selected by the expert. Although this potential translucent ring is slightly less contrasted compared with other translucent rings, its selection results in a more likely growth pattern. Hence, it remains difficult to favor one or the other of these two interpretations.

These two examples of disagreement in otolith interpretations point out the difficulty in balancing between the likelihood of the growth pattern and the perceptibility of translucent and opaque rings. Expert interpretation remains subjective for complex cases. For instance, for routine activities, inter- or intra-expert agreement rates in age reading greater than 90% are considered as satisfactory. In addition,

Table 1. Accuracy of the estimation of the otolith growth pattern for the processed 200 plaice (*Pleuronectes platessa*) otoliths from age classes 1 to 6: the mean values and the associated square-root variances, with respect to the ring number, of the distances between the ring positions determined by the Bayesian scheme and those provided by expert interpretations, when the two age estimates agree, are evaluated.

	Ring number						
	1	2	3	4	5	6	7
Mean value (mm)	0.10	0.09	0.07	0.06	0.07	0.06	0.05
Square-root variance (mm)	0.15	0.11	0.06	0.05	0.05	0.03	0.06

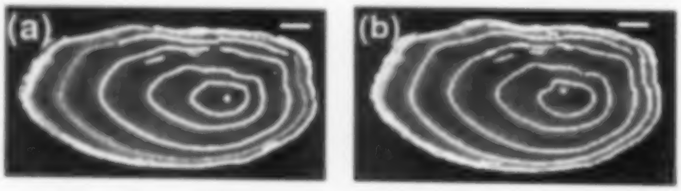

Fig. 17. Influence of errors in locating the actual growth center for the extraction of ridge and valley curves (we only display the extracted ridge curves): on the left, the actual position of the otolith center is used; on the right, the center is translated 30 pixels to the left and 20 to the top with regard to the actual growth center. Bar = 1 mm.

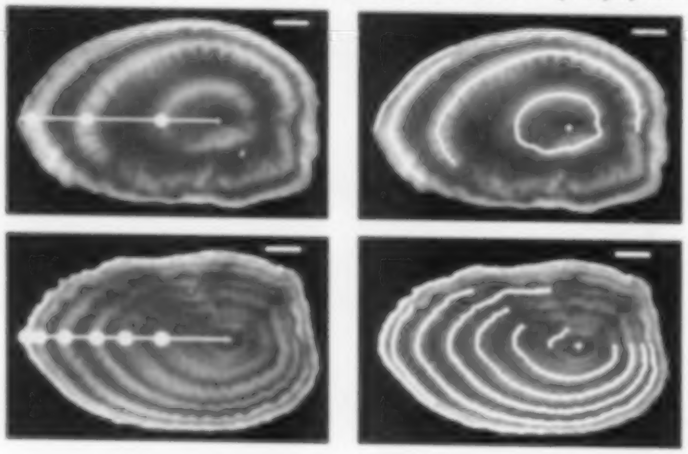

Fig. 18. Examples of two disagreements in age reading between the expert and the proposed approach. The first row displays the processed otolith image with the markers (circles) associated with the expert's interpretation. The second row depicts the otolith interpretation resulting from the Bayesian selection of the extracted ridge and valley curves (we only display the selected ridge curves).

interexpert agreement rates range between 85% and 95%, which demonstrates the relevance of the Bayesian approach for the automated interpretation of growth ring structures. It also demonstrates that this scheme can be used for routine ageing, either as an alternative to expert readings or as a low-cost double reading for verification purposes.

Discussion and future work

In this paper a new technique has been presented for the segmentation of 2D ridge and valley curves applied to the analysis of growth ring structures within images of biological hard tissues. It relies on a semi-local template based scheme using a priori information on ring structures to detect ridges and valleys from an adapted filtering. The Bayesian selection of the extracted ridge and valley curves is proposed to perform the actual interpretation of the growth structures. The considered Bayesian modeling combines a measure of curve significativity and a statistical model of individual growth patterns of the considered species.

Good performances have been reported for the extraction of meaningful ring curves within images of biological hard tissues. Given the emphasis on the interpretation of fish otolith images, the quantitative evaluation carried out for plaice samples stresses that the proposed Bayesian framework significantly outperforms previous work. The agreement rate with regard to expert interpretations can be favorably compared with interexpert agreement rates, which demonstrates the feasibility of using this Bayesian scheme for routine analysis. Different issues then arise. First, a fully automated scheme requires combining the technique proposed in this paper with the automation of the acquisition of otolith images and of the detection of the otolith nucleus as proposed in Cao and Fablet (2004). For routine aging, the cost–benefits analysis of such automated systems needs to balance the accuracy of the system compared with readers vs. the gain in terms of processing time. As stressed by our results, for an "easy-to-read" species such as plaice, the potential gain is huge, as the accuracy levels of the automated system should be in the range of the interexpert agreement rates and greater than those observed for in-training readers. Even if the proposed automated system considers only the youngest age groups (up to 6), they represent more than 90% of the aged data for the considered species and stock. Hence, the use of the proposed scheme for the most important age groups should highly reduce the workload of expert readers. Because the proposed Bayesian scheme exploits an a priori growth model, its robustness in spite of variations in growth patterns should be investigated. The considered minimum–maximum model is potentially more stable over time than a mean model. This aspect is also highly species-dependent as not all species are known to show high dynamics in terms of growth patterns. In any case, the growth model could be trained on a yearly basis on about 100 or 200 samples to reduce the number of samples to be interpreted by the expert (by a factor of two or more).

Apart from routine aging, the proposed approach can be used in a number of different ways to assist the experts in the acquisition of age and growth data. As an illustration, one could use it as a low-cost solution for a second reading of the samples to detect unrealistic interpretation or to evaluate confidence measures of the age estimation (Fablet, unpublished). Such measures are of great interest for assessment models (Reeves 2003). Another potential application consists of helping in the acquisition of the interpretation: given the age estimate provided by the expert, the Bayesian system could detect the most likely ring positions. These examples stress that the proposed system is not strictly limited to the automation of age and growth estimation, but it can bring a wide range of new computer-assisted tools for aging issues in the context of quality assurance and quality control (Morison et al. 1998).

In future work, the application of the proposed scheme to more complex structures and longer-lived species will be investigated. Our approach involves two main steps: the extraction of ring structures and the Bayesian interpretation step. The latter is generic, given that a subset of candidate ring curves is initially extracted. Therefore, it provides a strong basis for an application to more complex situations. Potential improvements mainly concern the statistical growth model. The use of statistical learning techniques (Fablet and Josse 2005) could be investigated. Also, for longer-lived species or microstructure analysis, model training needs to be adapted to deal with a large number of age classes. On the other hand, the extraction step is a challenging task for highly complex structures. The two examples reported for a pollock (*Pollachius pollachius*) and a cod (*Gadus morhua*) otolith stress the ability of our approach to cope with midlevel complexity structures. Improvements could enable the analysis of highly complex samples (e.g., hake (*Merluccius* sp.) or tuna (*Thunnus* sp.) otoliths), for instance, from the estimation of the local direction of the growth rings in the images. As well, although the analysis of annual growth rings usually relies on the analysis of the hard tissue in a single focal plane, the interpretation of daily increments often requires observing the ring structures in several focal planes. To this end, one might rely on the analysis of the sequence of images acquired in successive focal planes. An additional fusion scheme will then be needed either to stack this sequence of images into a single image using the magnitude of the image gradient or to combine the results of the extraction step carried out within each image of the sequence. In both cases, the semi-local template based approach presented in this paper would be a fundamental block.

Acknowledgments

The author wishes to thank André Ogor from IFREMER LASAA for his help in acquiring the image sets, Marie-Line Manten, IFREMER expert, for providing the set of plaice otoliths and the associated their interpretations, and Abdeslamm Benzinou for fruitful discussion on the template based approach.

References

Baillie, M. 1982. Tree-ring dating and archaeology. The University of Chicago Press, Chicago, Illinois.

Benzinou, A., Troadec, H., Bihan, J.L., and Rodin, V. 1997. The locally deformable B-Bubble model: an application to growth ring detection on fish otoliths. *In* Proceedings of the 10th Scandinavian Conference on Image Analysis, SCIA'97, Lappeenranta, Finland. Pattern Recognition Society of Finland, Jampere. pp. 181–187.

Campana, S. 2001. Accuracy, precision and quality control in age determination, including a review of the use and abuse of age validation methods. J. Fish Biol. **59**: 197–242.

Cao, F. 2003. Good continuations in digital image level lines. *In* Proceedings of IEEE Int. Conference on Computer Vision, ICCV'03, Nice, France. IEEE Computer Science Press, Piscataway, N.J. pp. 440–447.

Cao, F., and Fablet, R. 2004. Automatic morphological detection of otolith nucleus. *In* Proceedings of the 17th International Conference on Pattern Recognition, ICPR'04, Cambridge, UK. Vol. 3. IEEE Computer Science Press, Piscataway, N.J. pp. 606–609.

Chalmond, B., Azencott, R., and Colefy, F. 1995. Markov fusion of a pair of noisy images to detect intensity valleys. Int. J. Comp. Vis. **16**: 135–145.

Chauvaud, L., Lorrain, A., Dunbar, R.B., Paulet, Y.-M., Thouzeau, G., Jean, F., Guarini, J.-M., and Mucciarone, D. 2005. The shell of the great scallop *Pecten maximus* as a tool for high frequency paleoenvironmental reconstruction. Geochem. Geophys. Geosyst. **6**: Q08001, doi:10.1029/2004GC000890.

Cohen, L. 1991. On active contour models and balloons. Comp. Vis. Gr. Im. Pr.: Im. Und. **53**(2): 211–218.

Fablet, R., and Josse, N.L. 2005. Automated fish age estimation from otolith images using statistical learning. Fish. Res. **72**(2–3): 279–290.

Fablet, R., Benzinou, A., and Doncarli, C. 2003. Robust time-frequency model estimation in otolith images for fish age and growth analysis. *In* Proceedings of the 10th International Conference on Image Processing, ICIP'03, Barcelona, Spain. Vol. 2. IEEE Computer Science Press, Piscataway, N.J. pp. 593–596.

Geman, S., and Geman, D. 1984. Stochastic relaxation, Gibbs distribution and the Bayesian restoration of images. IEEE Trans. Pat. An. Mach. Int. **6**(6): 721–741.

Guillaud, A., Benzinou, A., Troadec, H., Rodin, V., and Bihan, J.L. 2002. Autonomous agents for edge detection and continuity perception on otolith images. Im. Vis. Comp. **20**(13–14): 955–968.

Guy, G., and Medioni, G. 1996. Inferring global perceptual contours from local features. Int. J. Comp. Vis. **20**(1): 113–133.

Haralick, R. 1983. Ridges and valleys on digital images. Comp. Vis. Gr. Im. Pr. **22**: 28–38.

Hare, J., and Cowen, R. 1997. Effect of age, growth rate, and ontogeny on the otolith size – fish size relationship in bluefish, *Pomatomus saltatrix*, and the implications for back-calculation of size in fish early life history stages. Can. J. Fish. Res. Aquat. Sci. **52**: 1909–1922.

Jacobs, D. 1996. Robust and efficient detection of salient convex groups. IEEE Trans. Pat. An. Mach. Int. **18**(1): 23–37.

Lagardère, F., and Troadec, H. 1997. Age estimation in common sole *Solea solea* larvae: validation of daily increments and evaluation of a pattern recognition technique. Mar. Ecol. Prog. Ser. **155**: 223–237.

Lindeberg, T. 1998. Edge detection and ridge detection with automatic scale selection. Int. J. Comp. Vis. **30**(2): 117–154.

McInerney, T., and Terzopoulos, D. 1996. Deformable models in medical images analysis: a survey. Med. Im. An. **1**(2): 91–108.

Morison, A., Robertson, S., and Smith, D. 1998. An integrated system for production fish aging: image analysis and quality insurance. N. Am. J. Fish. Manag. **18**: 587–598.

Panfili, J., Pontual, H.D., Troadec, H., and Wright, P. 2003. Manual of fish sclerochronology. IFREMER, Paris, France.

Reeves, S. 2003. A simulation study of the implications of age-reading errors for stock assessment and management advice. ICES J. Mar. Sci. **60**: 314–328.

Robertson, S., and Morison, A. 1999. A trial of artificial neural networks for automatically estimating the age of fish. Mar. Freshw. Res. **50**(1): 73–82.

Rodin, V., Troadec, H., Pontual, H.D., Bihan, J.L., Benzinou, A., and Tisseau, J. 1996. Growth ring detection on fish otoliths by a graph construction. *In* Proceedings of the 3rd IEEE International Conference on Image Processing, ICIP'96, Lausanne, Switzerland. Vol. 2. IEEE Computer Science Press, Piscataway, N.J. pp. 685–688.

Small, G., and Hirschhorn, G. 1987. Computer-assisted age and growth pattern recognition of fish scales using a digitizing tablet. *In* Age and growth of fish. *Edited by* R.C. Summerfelt and G.H. Hall. ISU Press, Ames, Iowa. pp. 397–410.

The Mathworks Inc. 2004. Matlab 7 [computer program]. The Mathworks Inc., Natick, Massachussetts.

Troadec, H., Benzinou, A., Rodin, V., and Bihan, J.L. 2000. Use of deformable templates for otolith 2D growth ring detection by digital image processing. Fish. Res. **46**(1–3): 155–163.

Welleman, H., and Storbeck, F. 1995. Automatic ageing of plaice otoliths by means of image analysis. *In* Recent developments in fish otolith research. *Edited by* D. Secor, J. Dean, and S. Campana. University of South Carolina Press, Columbia, South Carolina. pp. 271–282.

Appendix A

The algorithm used to solve for the minimization issue (eq. 7) proceeds as follows.

Step 1

1. $k = 0$
2. Sort curves within $\mathcal{C}$ according to their normalized distance to the nucleus: $\mathcal{C} = \{c_1, \ldots, c_{|\mathcal{C}|}\}$.
3. Initialize the set of current label configurations ε^0 to the empty set.

Step 2

1. $k = k + 1$
2. Define $\mathcal{C}^k = \{c_1, \ldots, c_k\}$.
3. For any $e_{\mathcal{C}^{k-1}}$ within the configuration set ε^{k-1}, add the two new labeling configurations $\{e_{\mathcal{C}^{k-1}}, e_k = \text{“rejected”}\}$ and $\{e_{\mathcal{C}^{k-1}}, e_k = \text{“selected”}\}$ to the set of current configurations ε^k.
4. Compute the likelihood values $P(o_{\mathcal{C}^k} | e_{\mathcal{C}^k}) \cdot P(g_{e_{\mathcal{C}^k}}) \cdot P(\Theta_{S(e_{\mathcal{C}^k})})$ for all the configurations $e_{\mathcal{C}^k} \in \varepsilon^k$.
5. Sort these likelihood values.
6. Keep only the $N_{\max}$ best configurations within ε^k.

Step 3

Repeat step 2 until $k = |\mathcal{C}|$.

The impact of postglacial marine invasions on the genetic diversity of an obligate freshwater fish, the longnose dace (*Rhinichthys cataractae*), on the Quebec peninsula

Philippe Girard and Bernard Angers

Abstract: Postglacial seas are expected to have had significant effects on the genetic structure of populations of obligate freshwater fishes. To assess this influence, mitochondrial DNA variability was evaluated in 32 populations of longnose dace (*Rhinichthys cataractae*) of the Quebec peninsula located within and outside of the maximum extent of marine invasions of the Champlain and Laflamme seas. Three clades of haplotypes diverging from one to two mutations were defined. Despite this low divergence, a clear and significant spatial genetic structure was observed outside of the extent of marine invasions. However, a higher genetic diversity was observed in populations located within the extent of marine invasions because of the admixture of these clades with an additional lineage restricted almost exclusively to those areas. The low genetic divergence between the main haplotypes suggests a single origin, despite the known presence of this species in various refuges. Marine invasions preventing entry to the peninsula, especially from Atlantic refuge, are proposed as a possible explanation to this particular result. This study is a relevant argument for integrating postglacial marine invasions into postglacial colonization models of freshwater species in the northeastern part of North America.

Résumé : Les mers postglaciaires ont possiblement eu les effets significatifs sur la structure génétique des populations des poissons d'eau douce. Afin de vérifier cet effet, la variabilité mitochondriale a été évaluée dans 32 populations de naseux des rapides (*Rhinichthys cataractae*), situées à l'intérieur et à l'extérieur des frontières des mers de Champlain et de Laflamme, qui ont inondé la péninsule québécoise au cours de la dernière déglaciation. Trois clades d'haplotypes divergeant d'une à deux mutations ont été trouvés. Les populations situées à l'extérieur des zones inondées par les invasions marines ont montré une forte structure spatiale. Cependant, une plus grande diversité génétique due au mélange des trois clades et d'une lignée évolutive supplémentaire a été observée à l'intérieur des limites des mers postglaciaires. La faible divergence entre les trois principaux clades suggère une origine commune malgré la présence de cette espèce dans plusieurs des refuges glaciaires connus. Les invasions marines agissant comme barrières à la colonisation, surtout depuis le refuge de l'Atlantique, sont proposées comme explication possible à ce résultat. Cette étude représente ainsi un argument pertinent pour l'intégration des invasions marines dans les modèles décrivant la colonisation postglaciaire des espèces d'eau douce dans le nord-est de l'Amérique du Nord.

Introduction

The spatial genetic structure of populations results from various ecological and demographic causes (Walker and Avise 1998). For species distributed over territories covered by the ice sheet of Pleistocene glaciations, the postglacial dispersal remains one of the major processes that shaped the genetic structure and diversity (Avise et al. 1998; Bernatchez and Wilson 1998; Taberlet et al. 1998). Among potential factors influencing colonization opportunities, the important modifications of the hydrological network that occurred during deglaciation are of prime importance (Rempel and Smith 1998). For instance, the presence of postglacial seas in the northeastern part of North America is expected to have had profound effects on colonization. Both high salinity and size of these seas are believed to act as barriers for a lot of organisms.

A large portion of the Quebec peninsula was covered by postglacial seas about 8000 – 11 000 years BP (Elson 1969). Those seas were formed over territories that were isostatically depressed below sea level after the melting of the ice sheet, allowing the inland invasion of saltwater from the

---

Received 22 August 2005. Accepted 26 January 2006. Published on the NRC Research Press Web site at http://cjfas.nrc.ca on 18 May 2006.
J18854

P. Girard[1] and B. Angers. Département des Sciences Biologiques, Université de Montréal, C.P. 6128, Succ. Centre-Ville, Montréal, QC H3C 3J7, Canada.

[1] Corresponding author (e-mail: philippe.girard@umontreal.ca).

Can. J. Fish. Aquat. Sci. **63**: 1429–1438 (2006) doi:10.1139/F06-047

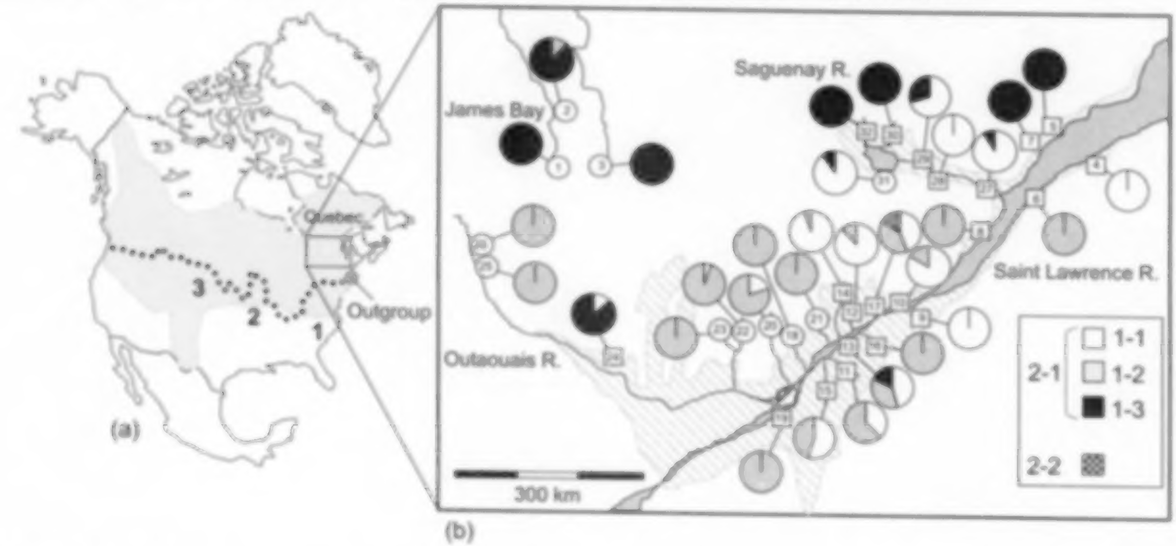

Fig. 1. (*a*) Maximum extent (dotted line) of the last Pleistocene glaciation over North American territory, location of the main glacial refuges that putatively contributed to the colonization of fish on Quebec peninsula (1, Atlantic; 2, Mississippian; 3, Missourian) and actual geographic distribution of longnose dace (*Rhynicthys cataractae*) (shaded region). (*b*) Geographic position of populations combined with their clade composition. Hatched region corresponds to the extension of the Champlain and Laflamme seas (after Occhietti 1989). Sites covered or not by the marine extent are respectively identified by squares or circles. Denomination of clades and lineages is based on the nesting design presented in Fig. 2. Refer to Table 1 for populations and drainages identification.

Atlantic Ocean. Those marine invasions are defined by two main seas. Laflamme Sea inundated a large territory including the actual Lake Saint-Jean and Saguenay River (Elson 1969; Fig. 1). The southwest part of the peninsula was covered by the Champlain Sea, which formed when ocean water invaded the Saint Lawrence lowlands (Occhietti 1989; Fig. 1). Impacts of those seas on the colonization opportunities are expected to be important as both the Saint Lawrence and Saguenay hydrological networks are believed to be major tributaries that allowed the colonization of the eastern and northeastern parts of the peninsula (Legendre and Legendre 1984; Bernatchez 1997). Although these marine invasions at their maximum extent provided dispersal routes inland for marine, estuarine, and salt marsh species (McAllister et al. 1988), they provided a nearly insurmountable barrier for obligate freshwater species, preventing or delaying their colonization to newly deglaciated territory.

Fishes were extensively used as models to understand postglacial colonization (reviewed in Bernatchez and Wilson 1998). As a result, the genetic structure of numerous species was studied over the northeastern part of North America. However, most of the species surveyed over the Quebec peninsula were either anadromous or salt-tolerant Salmonidae (Bernatchez and Dodson 1991; Wilson and Hebert 1996; Turgeon and Bernatchez 2001), and the few surveys of exclusive freshwater species had a limited sampling (Lafontaine and Dodson 1997; Senanan and Kapuscinski 2000). Hence, the hypothesis that Champlain and Laflamme postglacial seas played a significant role on the genetic structure of populations of stenohaline fish species has never been addressed.

The Cyprinidae exhibit many valuable characteristics that allow the evaluation of the potential impacts of marine invasions on the postglacial colonization of fish. As one of the most diversified families, the Cyprinidae colonized almost all of the freshwater habitats available in the Northern Hemisphere (Scott and Crossman 1973) and covered most of the Quebec peninsula, including the areas once inundated by postglacial seas (Legendre and Legendre 1984). Furthermore, both their intolerance to saltwater and their low dispersal capacity across large water bodies (Scott and Crossman 1973) make them especially sensitive to the presence of marine invasions. Finally, the combination of a short reproductive cycle and large population size is expected to result in high genetic diversity, which may increase the accuracy of the dispersal model (Avise et al. 1987).

The objective of this study was to assess the influences of the postglacial Champlain and Laflamme seas on a common Cyprinidae species in North America, the longnose dace (*Rhinichthys cataractae*). In this perspective, the geographic organization of the mitochondrial DNA (mtDNA) diversity was determined from 32 populations located within and outside the extent of those marine invasions. To complement the description of fish dispersal in the northeastern part of North America, arguments are given for the pertinence of integrating postglacial seas into phylogeographic studies of freshwater species in North America in the future.

Materials and methods

Model species and sampling

Longnose dace is typical of turbulent rivers located between the Atlantic and Pacific coasts, from Mexico to the Yukon (Scott and Crossman 1973; Fig. 1). Its present-day distribution overlaps a large fraction of the territory covered by Pleistocene glaciations and results from colonization from

Table 1. The geographic position and genetic diversity of longnose dace (*Rhynicthys cataractae*) populations analysed in this study.

Population	Longitude	Latitude	Altitude (m)	n	h	H_E ($\times 10^{-1}$)	k	π ($\times 10^{-4}$)
James Bay drainage								
1. Martel	77°54′33″	48°31′05″	320	25	2	1.53	1	6.55
2. Coigny	77°57′56″	49°05′43″	200	25	3	2.27	2	4.99
3. Mégiscane	77°07′08″	48°22′43″	320	18	2	4.25	1	18.20
Saint Lawrence River drainage								
4. Mitis	68°04′56″	48°31′15″	100	9	2	2.22	2	4.75
5. Betsiamite	68°57′30″	49°00′40″	15	24	2	4.31	1	18.40
6. Trois-Pistoles	69°12′49″	48°05′39″	15	19	1	0.00	1	0.00
7. Sault-aux-Cochons	69°15′41″	48°47′33″	120	18	2	3.66	1	15.60
8. Malbaie	70°11′49″	47°41′38″	30	24	3	2.36	1	10.40
9. Chaudière	71°12′58″	46°35′16″	120	20	1	0.00	1	0.00
10. Jacques-Cartier	71°44′56″	46°41′35″	40	24	3	3.01	2	19.50
11. St-Francois	72°29′24″	45°53′16″	90	24	2	4.89	2	20.90
12. Des Envies	72°30′13″	46°40′23″	120	26	2	2.12	2	4.54
13. Nicolet	72°32′12″	46°09′16″	20	22	3	6.36	3	27.20
14. Mékinak du Nord	72°38′51″	46°44′52″	170	19	2	1.05	2	6.75
15. Yamaska	72°56′55″	45°37′16″	30	20	3	6.26	2	18.30
16. Bécancour	72°09′27″	46°12′52″	60	25	3	6.60	1	26.10
17. Ste-Anne	72°09′30″	46°38′17″	30	18	4	6.73 (2.12)*	2	145.00 (4.54)*
18. Noire	73°39′14″	46°20′16″	240	19	1	0.00	1	0.00
19. Châteauguay	73°48′00″	45°15′18″	40	22	2	4.55	1	19.40
20. Assomption	73°58′22″	46°25′12″	300	10	2	3.27	2	14.00
21. Du Loup	73°09′01″	46°33′44″	180	17	1	0.00	1	0.00
Outaouais River drainage								
22. Diable	74°30′45″	46°22′17″	330	17	2	1.11	2	2.37
23. Rouge	74°47′36″	46°21′31″	230	13	1	0.00	1	0.00
24. Kazabazua	76°03′04″	45°56′42″	150	15	2	2.48	1	10.60
25. Lavallée	79°21′30″	47°10′17″	200	24	2	0.83	1	3.56
26. Loutre	79°21′04″	47°24′42″	230	23	2	0.83	1	1.78
Saguenay River drainage								
27. Petit-Saguenay	70°03′50″	48°12′10″	30	23	2	1.66	2	7.09
28. À Mars	70°56′06″	48°19′08″	50	22	1	0.00	1	0.00
29. Shipshaw	71°15′11″	48°33′10″	110	21	3	5.14	2	36.20
30. Péribonka	71°45′44″	48°50′32″	150	15	3	3.62	1	13.40
31. Métabetchouane	71°59′55″	48°19′18″	260	20	2	1.90	2	16.20
32. Aux Rats	72°14′36″	48°53′35″	120	19	2	3.51	1	15.00

Note: The longitude (west of the prime meridian) and latitude (north of the equator) of the sample sites, the number of individuals (n), the number of haplotypes (h), the number of clades (k; associated with the nested design presented at Fig. 1) and both gene (H_E) and nucleotide (π) diversities are presented. Numbers next to each population name will be used to identify populations in text and figures.

*Numbers in parentheses are calculated after removing major clade 2-2.

various glacial refuges (McPhail and Lindsey 1970; Fig. 1). Adult longnose dace occupies riffles (Scott and Crossman 1973) and exhibits high site fidelity (Hill and Grossman 1987). This fish has little interaction with humans but is known to be used occasionally as bait by sportfishers. Populations are expected to be almost undisturbed by stocking activities or translocations in Canada (Scott and Crossman 1973).

A total of 640 individuals were sampled by electrofishing (LR-24, Smith-Root Inc., Vancouver, Washington) from 32 rivers of the Quebec peninsula in Canada (Table 1). These rivers are located within four drainage basins (James Bay, Saint Lawrence River, Outaouais River, and Saguenay River) believed to be important colonization routes used by fishes after the deglaciation (Legendre and Legendre 1984). Efforts were made to sample populations both within and outside the maximum extent of marine invasions (Fig. 1). Both Champlain and Laflamme seas rose to an altitude of 200 m (Lasalle and Tremblay 1978; Occhietti 1989). As a result, 21 sampling sites below an altitude of 200 m and located within the inferred maximum extent of these marine invasions (Occhietti 1989) were assumed to be once covered by a postglacial sea. The other populations were considered outside the maximum extent of the marine invasions (Table 1; Fig. 1). To increase the probability of sampling a single panmictic population, each river was sampled only once within a single riffle. Sample sizes ranged from 9 to 26 individuals for each population (Table 1). For each individual, a piece of the caudal fin was removed and stored in 95% ethanol for genetic analysis. A population from the Eight-Mile River (Connecticut, USA), located in the Atlantic watershed (Fig. 1), was analyzed as the outgroup.

Molecular analysis

This study focused on control region and cytochrome *b*, which are expected to display high polymorphism within species (McMillan and Palumbi 1997). Primers were designed on preserved sequences of different fish mtDNA genomes available on GenBank. The primers 5′-GTGACTTGAAAAACCACCGTTG-3′ and 5′-AANNGTTGGTNGKYTCTTACT-3′ successfully amplified, by polymerase chain reaction (PCR), a segment of approximately 1500 bp, covering the cytochrome *b*, tRNA-Thr, tRNA-Pro, and the first 300 bp of the control region. The following reaction conditions were used: a 12.5 μL reaction aliquot containing 1.5 $\text{mmol}\cdot\text{L}^{-1}$ of $MgCl_2$ and 2.5 $\text{nmol}\cdot\text{L}^{-1}$ of each dNTP, 0.2 unit of *Taq* polymerase, 1.25 μL of 10× *Taq* polymerase buffer (Invitrogen Corp., Burlington, Ontario), and approximately 20 ng of DNA. Reaction conditions included an initial denaturation of 30 s at 92 °C, followed by 45 cycles combining 10 s at 92 °C, 15 s at 50 °C, and 2 m at 68 °C, and a final extension of 10 m at 68 °C. Both strands were sequenced with a CEQ 2000XL DNA Analysis System (Beckman Coulter Inc., Fullerton, Calif.) on 20 individuals from 10 distant populations. According to these sequences, primers specific to longnose dace were designed to amplify shorter segments on cytochrome *b* (232 bp; 5′-CATCTGTCGAGACGTTAAC-3′ and 5′-TAATAACGGTAGCGCCTC-3′) and control region (236 bp; 5′-ACCCCTGGCTCCCAAAGC-3′ and 5′-GGTCTATGTACGTCTTAG-3′). PCR reactions that optimize the amplification of those loci contained the same products as above. However, PCR conditions include an initial denaturation of 30 s at 92 °C, followed by 45 cycles combining 10 s at 92 °C, 15 s at 48 °C, and 5 s at 68 °C, and a final extension of 2 m at 68 °C.

The polymorphism of these loci was then screened using the single strand conformation polymorphism (SSCP, Orita et al. 1989). Both loci were conjointly electrophoresed on a 6% nondenaturing gel for 10 h at 20 W in 0.5× TBE (Angers and Bernatchez 1998). The sequence of both loci was determined for individuals showing variation at either cytochrome *b* or control region segments. To confirm the reliability of the SSCP protocol, sequencing of individuals coming from different populations but displaying the same migration pattern was performed. This procedure was performed on six individuals for each of the most frequent haplotypes (I, III, and IX; see Results).

Data analysis

Genetic diversity within population was calculated using the number of haplotypes, haplotype frequencies (Nei 1987), and sequence information (π). Partition of the genetic diversity within and among populations was evaluated with both haplotypes frequencies (F_{ST}) and sequences (ϕ_{ST}) using Arlequin v.2.2 (Schneider et al. 2000). ϕ_{ST} distances were computed using pairwise differences. Significance of both statistics was determined with 1000 permutations.

A minimum spanning network was inferred from the observed haplotypes. Two repeat arrays were observed on the control region locus. Each dinucleotide deletion in these repeats arrays was considered as a single fifth state. Haplotypes were then grouped following the rules used in Templeton et al. (1987) and Templeton and Sing (1993). Accordingly, haplotypes or groups of haplotypes that are one mutation apart on the network are united, producing a hierarchical series of nested clades. This nesting procedure is specifically designed for haplotypes separated by few mutations. However, haplotypes found in this study can be grouped into two highly divergent major clades (hereafter referred as lineages). To counteract this problem, the nesting procedure was done independently in each of these lineages. As an indication of the support of this haplotype grouping, bootstraps (1000) were performed following by a parsimony analysis using SEQBOOT, DNAPARS, and CONSENSE modules of PHYLIP 3.62 (Felsenstein 2004).

Processes defining the population structure

A nested clade analysis (NCA) was conducted to investigate processes that created the spatial organization of the observed genetic variation. The method detects geographic associations of haplotypes and explains them in terms of contributions from either historical or present-day processes that have played a role in defining the patterns of population structure (Templeton et al. 1995; Templeton 1998). The geographical range of each clade (Dc), the distance of each clade from the geographical centre of the next higher level clade (Dn), and contrasts of these distances between tips and interior clades (I–T Dc and I–T Dn) were computed using GeoDis 2.2 (Posada et al. 2000). The significance of these different estimators was evaluated by 1000 permutations.

Geographic organisation

To assess the relative importance of geographical factors in the spatial organisation of genetic diversity among populations, a canonical correspondence analysis (CCA) was performed using Canoco for Windows version 4.02 (ter Braak and Smilauer 1999). This method, designed for relating species composition to different predictive variables (ter Braak 1986), was successfully used to describe relationships between environmental variables and genetic composition (Angers et al. 1999; Costello et al. 2003; Volis et al. 2004). CCA was computed using a matrix **Y** representing frequency of clades in each population and a matrix **X** in which standardized geographical variables associated to the sampling point were compiled. Latitude, longitude, altitude, and three binary variables coding for the four main drainages were used as geographical variables. Test of significance of this CCA was performed using 1000 permutations (detailed procedure described in Angers et al. 1999).

The importance of these geographic factors in shaping the diversity within population was also evaluated. Multiple regressions were performed using either gene or nucleotide diversity computed for each population as the dependant variable versus the geographic matrix **X** described above. Tests of significance of the total regression model and of partial regression coefficients were performed with 1000 permutations of residuals under full model using a program for multiple linear regressions developed by Legendre (2002).

Structuring effects of postglacial seas

The structuring effects of the postglacial seas were evaluated on genetic diversity within and among populations. Populations were separated in relation to whether or not they were covered by a postglacial sea during the deglaciation processes. The structuring effects on the variation among populations were evaluated by comparing the average clade frequencies of the two groups with a *t* statistic tested with

1000 permutations. Each clade was analyzed separately. The structuring effects of those seas on the variation within population were evaluated by comparing the average genetic diversity (haplotype and nucleotide) of those two groups with the same statistical procedure.

Results

Diversity and haplotypes network

A total of 14 haplotypes, characterized by 13 and 17 mutations on cytochrome *b* and control region, respectively (Table 2), was detected in this survey. Sequencing and SSCP results were fully reliable. The haplotype network shows that haplotypes can be assigned to two distinct lineages (2-1 and 2-2; Fig. 2) separated by 21 mutations (4.5% divergence; Table 2). Twelve haplotypes belong to lineage 2-1 and two to lineage 2-2 (Fig. 2). Repeat arrays in the control region show two types of mutation. Single dinucleotide deletion was observed in both arrays but only in lineage 2-1 (haplotypes VII, VIII, and X; Table 2). The two haplotypes of lineage 2-2 show a base substitution in the last repeat of the AC array (position 175; Table 2). Interestingly, the haplotype observed in the population from the Atlantic watershed (outgroup) differed by only two or three mutations from haplotypes of lineage 2-2 (Table 2). Diversity within those lineages is 0.3% and 0.5% for 2-1 and 2-2, respectively. Lineage 2-1 can be divided into three clades characterized by an abundant interior haplotype (I, III, and IX for 1-1, 1-2, and 1-3, respectively) and one to five scarce tip haplotypes (Fig. 2). Bootstrap results showed high support of the differentiation between lineages 2-1 and 2-2 (Fig. 2), suggesting a high separation time between them. However, lack of support was observed within lineage 2-1, in which each clade appeared in less than 25% of the bootstrapped trees (Fig. 2). This result is concordant with a recent differentiation of the three clades, all originating from a single refuge.

Haplotypes from lineage 2-1 were detected in 637 of the 640 individuals (99.5%) from all populations sampled in Quebec, whereas those of lineage 2-2 were restricted to three individuals from population 17 (Fig. 1). The number of clades (i.e., 1-1 to 1-3) observed within populations ranged from 1 to 3, but 18 of the 32 populations exhibited a single clade. Gene diversity and nucleotide diversity ranged from 0 to 0.67 (average 0.27) and from 0 to 0.014 (average 1.5×10^{-3}; Table 1), respectively. Because they strongly inflate the nucleotide diversity of population 17, individuals that shared haplotypes belonging to lineage 2-2 were removed from further analyses. Analysis of molecular variance revealed a significant structure at the population level for both haplotype frequencies ($F_{ST} = 0.67$, $p < 0.001$) and sequences ($\phi_{ST} = 0.61$, $p < 0.001$).

Processes defining the population structure

Below the 1-step level, the nested clade analysis was not very informative because of the presence of unique haplotypes (II, VI, XI, and XII) and those found in a restricted number of populations (IV, V, and VII). According to the geographic scale of this study, the sampling plan can be invoked to explain these inconclusive results. The analysis performed on the 1-step level reveals that the spatial genetic structure conformed to a contiguous range expansion by the clades of lineage 2-1 (Table 3). The 2-step level analysis suggests a past allopatric fragmentation as a possible cause for the divergence of lineages 2-1 and 2-2 (Table 3). This conclusion strengthens the hypothesis of distinct glacial refuge as the origin for those lineages.

Geographic organisation

The CCA revealed that 45% of the genetic variance among populations can be explained with geographic variables. The overall significance test of the two canonical axes showed that the relationship between clade frequencies and geographic variables was highly significant ($F = 3.373$, $p = 0.001$). The correlation biplot (Fig. 3) underlines the nonoverlapping distribution of clades 1-2 and 1-3. Clade 1-2 is closely related to populations sampled in lower latitudes of the Saint Lawrence and Outaouais drainages. An opposing signal can be observed for clade 1-3, exclusively associated with populations in higher latitudes of the James Bay and Saguenay drainages. Clade 1-1 is particular in that it shows a longitudinal association and is negatively correlated to altitude. Populations in which clade 1-1 was detected were almost exclusively in eastern regions (Fig. 1) of the Saint Lawrence and Saguenay drainages. On the other hand, no significant associations were found between geographical factors and both gene ($R^2 = 0.28$, $p = 0.19$) and nucleotide diversities ($R^2 = 0.22$, $p = 0.38$).

Structuring effects of postglacial seas

Interestingly, the genetic structure is not only related to geographic coordinates, because structuring effects of postglacial seas can also be inferred. As pointed out in the correlation biplot (Fig. 3), clade 1-1 is almost exclusively present in populations once covered by postglacial seas ($t = 2.416$, $p = 0.025$). In contrast, clade 1-2 is more abundant in populations outside the extent of the Champlain and Laflamme seas ($t = -2.048$, $p = 0.046$). Finally, no relation was detected for clade 1-3, which is equally frequent in locations within and outside the extent of the postglacial seas ($t = 0.076$, $p = 0.924$). These results, combined with the geographic organisation delineated in the previous section, suggest that the contiguous range expansion was not straightforward, but was constituted by three waves of colonists, each associated with a particular clade.

In contrast to geographic factors, the structuring effects of the postglacial seas can also be observed in the genetic diversity within populations. Populations sampled in locations once covered by postglacial seas showed on average twofold greater haplotype and nucleotide diversity (0.32×10^{-3} and 1.37×10^{-3}, respectively) than populations living outside the maximum extent of the marine invasions (0.15×10^{-3} and 0.62×10^{-3}, respectively). Both of these differences were significant ($p = 0.025$ and 0.033 for haplotype and nucleotide diversity, respectively).

Discussion

Genetic structure of longnose dace populations

Longnose dace populations sampled in Quebec showed a genetic diversity similar to those of other fish species found

Table 2. Variable sites for each haplotype in both mtDNA regions sequenced in this work (Accession Nos. DQ400450–DQ400479).

		Cytb												CR								
		2	2	2	2	2	2	2	3	3	3	3	3	4	1	1	1	1	1	1	1	1
		1	2	3	3	4	5	8	0	5	6	7	8	0	0	2	2	2	3	4	4	5
Lineage	Haplotype	4	6	2	5	1	5	0	7	5	7	3	2	3	0	5	6	9	1	2	8	4
2-1	I	A	T	A	C	G	G	T	G	C	A	A	T	A	A	G	C	G	A	C	G	A
	II	.	.	.	.	.	.	.	.	.	.	.	.	.	.	.	T	.	.	.	.	.
	III	.	.	.	.	.	.	.	.	.	.	.	.	.	.	.	.	.	.	.	.	.
	IV	.	.	.	.	.	.	.	.	.	.	.	.	.	.	.	.	.	.	.	.	G
	V	.	.	.	.	.	.	.	.	.	.	.	.	.	.	.	A	.	.	.	.	.
	VI	.	.	.	.	.	.	C	.	.	.	.	.	.	.	.	.	.	.	.	.	.
	VII	.	.	.	.	.	.	.	.	.	.	.	.	.	.	.	.	.	.	.	.	.
	VIII	.	.	.	.	.	.	.	.	.	.	.	.	.	.	.	.	.	.	.	.	.
	IX	.	C	.	.	.	.	.	.	.	.	.	.	.	.	.	.	.	.	.	.	.
	X	.	C	.	.	.	.	.	.	.	.	.	.	.	.	.	.	.	.	.	.	.
	XI	.	C	.	.	.	.	.	.	.	.	.	.	.	.	.	.	.	.	.	.	.
	XII	.	C	.	.	.	.	.	.	.	.	.	.	.	.	A	.	.	.	.	.	.
2-2	XIII	G	C	G	T	A	A	.	A	T	G	G	C	G	G	.	T	A	G	T	A	.
	XIV	G	C	G	T	A	A	.	A	T	G	G	C	G	G	.	T	A	G	T	A	.
Outgroup		.	C	G	T	A	A	.	A	T	G	G	C	G	G	.	T	A	.	T	A	.

Note: Numbers are associated with site positions of the cytochrome *b* (Cytb) and control region (CR) sequences of the zebrafish (*Danio rerio*; GenBank

Fig. 2. Minimum spanning network based on the mutational steps of mtDNA haplotype sequence observed on longnose dace (*Rhynicthys cataractae*). Nested clades design is also shown. Numbers in parentheses are the percentage of occurrences of each clade after 1000 bootstraps when a maximum parsimony analysis is performed. The diameter of the circle reflects the frequency of the given haplotype observed within all populations surveyed. Shading corresponds to that used in Fig. 1. The solid square represents a haplotype that was not observed in the survey.

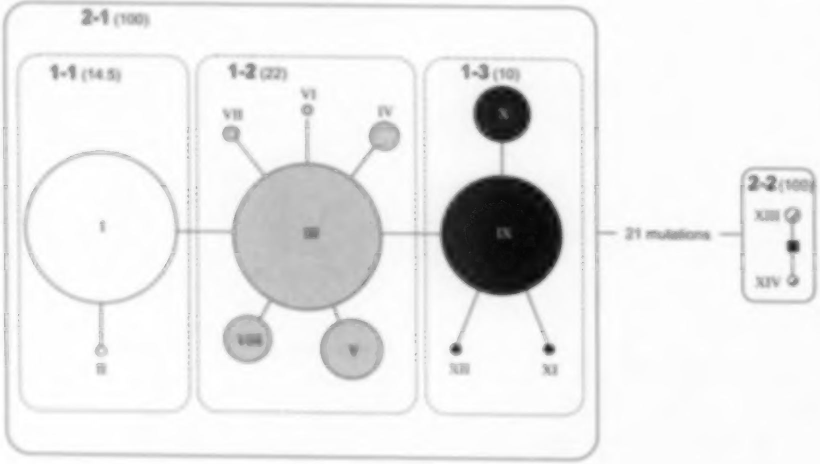

between 45°N and 50°N (Bernatchez and Wilson 1998). The three clades of lineage 2-1 observed on longnose dace differed by no more than 0.3%. This pattern is consistent with northern species that show a genetic structure dominated by few widely dispersed haplotypes diverging from 0.5% to 2% (e.g., Turgeon and Bernatchez 2001).

Longnose dace populations are essentially composed of three closely related clades. Despite the low divergence level between them, a highly significant structure was observed. The geographic organization of this genetic structure is consistent with the idea that the contiguous range expansion was the result of more than one wave of colonists. The opposed distributions of clades 1-2 and 1-3 are consistent with parallel colonization from two distinct entries. Clade 1-2 probably entered the peninsula from the southwest connections via the Great Lakes, whereas a northern entry from the tributaries of James Bay or Ojibway–Barlow Proglacial Lake (8000 – 10 000 years ago) can be proposed for clade 1-3 (e.g., Legendre and Legendre 1984). The colonization of the northern part of the peninsula was made possible readily by headwater interconnections (Legendre and Legendre 1984) and a temporary postglacial drainage system (Gagnon and Angers 2006).

This structure of the genetic variation is higher than what is usually observed on a geographic scale of the same magnitude (Brown et al. 1992; Ferguson et al. 1993; Lafontaine and Dodson 1997). For instance, most of the species for which data are available for the region surveyed in this study

1	1	1	11	22	2	
5	6	6	77	00	4	
6	3	6	45	67	3	Populations
A	C	A	AC	GT	C	4, 9–15, 17, 20, 22, 24, 27–29, 31
.	.	.	.	.	.	4
.	.	G	.	.	.	2, 6, 8, 12, 15–19, 21–23, 25, 26
.	.	G	.	.	.	20
.	.	G	.	.	.	11, 13, 15, 16
.	.	G	.	.	.	26
.	.	G	- -	.	.	8, 10
.	.	G	.	- -	.	8, 10, 14, 16, 19, 25
.	.	G	.	.	.	1–3, 5, 7, 13, 24, 27, 29, 30, 32
.	.	G	.	- -	.	1, 3, 5, 7, 29–32
.	.	.	.	.	.	30
.	.	G	.	.	.	2
T	.	.	.T	.	A	17
.	.	.	.T	.	.	17
T	.	.	.T	.	A	

accession number AC024175).

show an absence of lineage variation (Wilson and Herbert 1996), a nearly complete overlap among lineages (Bernatchez and Dodson 1991; Turgeon and Bernatchez 2001), or an unstructured mitochondrial variability (Lafontaine and Dodson 1997).

Effects of the postglacial seas

Interestingly, the geographic organization of the genetic diversity of longnose dace appeared closely associated with the maximum extents of the marine invasions of Laflamme (Saguenay) and Champlain (Saint Lawrence) seas. The dominance of clade 1-2 in the western regions and clade 1-3 on the north shore of Saguenay River likely resulted from an early colonization. However, the presence of the salted Champlain and Laflamme seas likely acted as temporary barriers to longnose dace dispersion to eastern parts of Quebec. After the retreat of these seas, new habitats appear to have been colonized by the clades already in place (1-2 in the south and 1-3 in the north) and by a new colonist wave composed essentially of clade 1-1. This hypothesis is supported by the nearly complete absence of clade 1-1 above the level of former Champlain and Laflamme seas.

Diversity within populations is not related to geographical factors, including altitude. However, diversity is two times higher in populations located within the marine extents. Because these populations are not expected to have higher effective populations size, the contact zone between genetically distinct founder groups is likely responsible of this high diversity. These results are in accordance with previous studies in which the admixture of different waves of colonists resulted in higher diversity indices (Wilson and Herbert 1998; Turgeon and Bernatchez 2001; Austin et al. 2002).

The distribution of clade 1-1 throughout all regions submerged by postglacial seas and the higher intrapopulation diversity resulting from an admixture of clades are expected to affect the genetic structure. This hypothesis is consistent with the higher genetic structure observed in populations outside the postglacial seas extents ($F_{ST} = 0.79$) as compared with the one covered by postglacial seas ($F_{ST} = 0.55$). Furthermore, clade composition of populations once covered by a postglacial sea appeared more randomly distributed: populations fixed for a clade are next to those fixed for a different clade. The larger diversity associated with several founder groups made stochastic processes such as founder events and (or) genetic drift responsible for such a pattern.

Longnose dace origins

The wide distribution of longnose dace suggests the existence of various refuges that allowed the survival of this species during Pleistocene glaciations (Radforth 1944; McPhail and Lindsey 1970). Among them, three can be proposed as sources of the colonization of the northeastern part of North America, namely the Atlantic, the Missourian, and the Mississipian (Crossman and McAllister 1986). However, as lineage 2-1 is clearly dominant in Quebec populations, the contribution of a single refuge appears as a relevant hypothesis. Assuming 1%–2% divergence per million years (Brown et al. 1979; Wilson et al. 1985), a separation time within the last 75 000 or 150 000 years is expected among clades of this lineage and therefore likely occurred before or during the last glaciation event (75 000 to 10 000 BP). The presence of a few individuals that shared haplotypes from the very divergent lineage 2-2 in a single population seems to be anecdotal such that unintentional translocations could occur via angling.

The low sampling effort in populations located in regions covered by the glacial refuges makes any proposal of the refugial origin of lineage 2-1 rather speculative. However, evidence suggests that this lineage has a Mississippian origin. First, the level of divergence (4.5%) observed between this lineage and the outgroup from Eight-Mile River is expected to be the result of approximately 2 to 4 million years of restricted gene flow. This time lag largely predates the Pleistocene glaciations and suggests different refugial origins. According to the geographical location of Eight-Miles River, lineage 2-2 likely originates from the Atlantic refuge. Second, colonization entries via the Great Lakes or the tributaries of James Bay, as suggested by the spatial organization of mitochondrial diversity observed in this study, are known to be directly connected to the Mississipian refuge (Prest 1970). Third, the importance of this refuge for the postglacial colonization of the northeastern part of North America has been demonstrated in both biogeographical (Bailey and Smith 1981; Crossman and McAllister 1986; Underhill 1986) and phylogeographic (Lu et al. 2001; Gagnon and Angers 2006) studies.

The effective contribution of a single refuge, despite evidence of the presence of longnose dace in all Atlantic, Mississippian, and Missourian refuges, is striking and contrasts with previous studies on other fish species. For instance, current Quebec lake trout (*Salvelinus namaycush*) populations were established with contributions from both Atlantic and Mississipian refuges (Wilson and Hebert 1996). A similar pattern was observed for lake cisco (*Coregonus artedi*; Turgeon and Bernatchez 2001) and brook char (*Salvelinus fontinalis*; Angers and Bernatchez 1998; Danzmann et al. 1998). These comparisons lead to the conclusion that the dispersal connections allowing colonization of Quebec by salt-tolerant species have not been used by longnose dace.

Table 3. Results of the nested clade analysis following the 2004 inference key by Posada et al. (2000).

Haplotypes			1 Step			2 Step		
No.	Dc	Dn	No.	Dc	Dn	No.	Dc	Dn
I	**145^{S}**	**146**						
II	0^{nc}	301						
IT	145^{S}	−156						
1-2-11Yes: RE	1-1	147^{S}	174^{S}					
III	**210^{L}**	**204^{L}**						
IV	0^{S}	22^{S}						
VI	0^{nc}	427						
VIII	122	163						
V	23^{S}	126						
VII	71	253						
IT	158^{L}	70^{L}						
1-2-3-4-9-10 No: FR or IBD?			**1-2**	**147^{S}**	**188^{S}**			
IX	**276^{L}**	**275^{L}**						
X	182^{S}	240^{S}						
XI	0^{nc}	151						
XII	0^{nc}	321						
IT	105^{L}	35^{L}						
1-2-3-4 No: IBD			1-3	267^{L}	307^{L}			
			IT	-54^{S}	-46^{S}			
			1-2-11-12 No: contiguous RE			**2-1**	**211**	**211**
						2-2	0^{S}	97^{S}
						IT	210^{L}	114^{L}
						1-2-3-4-9 No: allopatric FR		

Note: RE, range expansion; FR, fragmentation; IBD, isolation by distances. Superscripts indicate both Dc and Dn statistics that were significantly small (S) or large (L) or that could not be calculated (nc) because of a single occurrence. Shading indicates interior haplotypes and clades.

Fig. 3. Canonical correspondence analysis (CCA) ordination biplot representing clades (broken arrows), sites (dots), and geographic variables (solid arrows for latitude, longitude, and altitude and open triangles for binary variables representing major drainages). Site and major drainage identifiers correspond respectively to numbers and letters in Table 1. The identifiers in bold represent the sites that were putatively covered by Champlain or Laflamme postglacial seas. Proportion of total variance explained by each of the canonical axis is also represented.

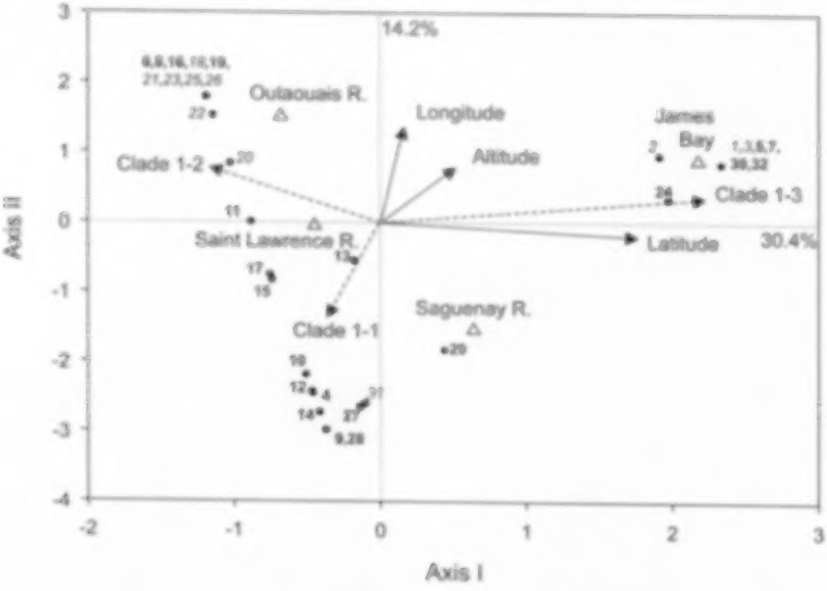

As a result, the barrier caused by marine invasions could be proposed for the observed difference in colonization patterns. This hypothesis is especially relevant in the case of the Atlantic refuge, as southeast connections to the peninsula were temporary blocked by the Champlain Sea and the Gulf of Saint Lawrence.

Postglacial seas appeared to have played a major role in the spatial genetic structure of longnose dace populations. First, a lower genetic structure and a higher diversity within the marine extents were due to the presence of a different founder group restricted to this region. Second, acting as barriers to colonization, the marine extents are likely responsible for the single refuge origin of the longnose dace populations in Quebec. These results present a strong argument for integrating this phenomenon into further phylogeographic studies of freshwater organisms in northeastern North America. We also believe that an increased examination of Cyprinidae species would greatly improve our understanding of fish postglacial dispersal. For instance, longnose dace has the advantage of coupling demographic and ecological characteristics that contribute to high genetic diversity and structure. Combining large population sizes, small-scale site fidelity (Thompson et al. 2001), and a geographic distribution almost unaltered by translocation, longnose dace confirmed its relevance to become a powerful tool in solving specific phylogeographic problems. Examinations of additional Cyprinidae species will no doubt increase the precision of a general hypothetical model describing the spatial genetic structure of fishes established after the Pleistocene glaciations.

Acknowledgments

We thank Pascale Gibeau, Isabelle Bouthillier, and Rolland Vergilino for their assistance in the field and lab. We are also grateful to Roxane Maranger and two anonymous referees for very helpful comments and Eric Shultz for providing samples. This work was supported by a FQRNT (Fonds québécois de la recherche sur la nature et les technologies) scholarship to PG and a Natural Sciences and Engineering Research Council of Canada (NSERC) research grant to BA.

References

Angers, B., and Bernatchez, L. 1998. Combined use of SMM and non-SMM methods to infer fine structure and evolutionary history of closely related brook charr (*Salvelinus fontinalis*, Salmonidae) populations from microsatellites. Mol. Biol. Evol. **15**: 143–159.

Angers, B., Magnan, P., Plante, M., and Bernatchez, L. 1999. Canonical correspondence analysis for estimating spatial and environmental effects on microsatellite gene diversity in brook charr (*Salvelinus fontinalis*). Mol. Ecol. **8**: 1043–1054.

Austin, J.D., Lougheed, S.C., Neidrauer, L., Chek, A.A., and Boag, P.T. 2002. Cryptic lineages in a small frog: the post-glacial history of the spring peeper, *Pseudacris crucifer* (Anura: Hylidae). Mol. Phylogenet. Evol. **25**: 316–329.

Avise, J.C., Arnold, J., Ball, R.M., Bermingham, E., Lamb, T., Neigel, J.E., Reeb, C.A., and Saunders, N.C. 1987. Intraspecific phylogeography: the mitochondrial DNA bridge between population genetics and systematics. Annu. Rev. Ecol. Syst. **18**: 489–522.

Avise, J.C., Walker, D., and Johns, G.C. 1998. Speciation durations and Pleistocene effects on vertebrate phylogeography. Proc. R. Soc. Lond. Ser. B Biol. Sci. **265**: 1707–1712.

Bailey, R.M., and Smith, G.R. 1981. Origin and geography of fish fauna of the Laurentian Great Lakes basin. Can. J. Fish. Aquat. Sci. **38**: 1539–1561.

Bernatchez, L. 1997. Mitochondrial DNA analysis confirms the existence of two glacial races of rainbow smelt (*Osmerus mordax*) and their reproductive isolation in the Saint Lawrence R. Estuary (Québec, Canada). Mol. Ecol. **7**: 73–83.

Bernatchez, L., and Dodson, J.J. 1991. Phylogeographic structure in mitochondrial DNA of the lake whitefish (*Coregonus clupeaformis*) and its relation to Pleistocene glaciations. Evolution, **45**: 1016–1035.

Bernatchez, L., and Wilson, C. 1998. Comparative phylogeography of nearctic and palearctic fishes. Mol. Ecol. **7**: 431–452.

Brown, J.R., Beckenbach, A.T., and Smith, M.J. 1992. Influence of Pleistocene glaciations and human intervention upon mitochondrial DNA diversity in white sturgeon (*Acipenser transmontanus*) populations. Can. J. Fish. Aquat. Sci. **49**: 358–367.

Brown, W.M., George, M., Jr., and Wilson, A.C. 1979. Rapid evolution of animal mitochondrial DNA. Proc. Natl. Acad. Sci. U.S.A. **76**: 1967–1971.

Costello, A.B., Down, T.E., Pollard, S.M., Pacas, C.J., and Taylor, E.B. 2003. The influence of history and contemporary stream hydrology on the evolution of genetic diversity within species: an examination of microsatellite DNA variation in bull trout, *Salvelinus confluentus* (Pisces: Salmonidae). Evolution, **57**(2): 328–344.

Crossman, E.J., and McAllister, D.E. 1986. Zoogeography of freshwater fishes of the Hudson Bay drainage, Ungava Bay and the Arctic Archipelago. *In* The zoogeography of North American freshwater fishes. *Edited by* C.H. Hocutt and E.O. Wiley. John Wiley and Sons, New York. pp. 53–104.

Danzmann, R.G., Morgan, R.P., II, Jones, M.W., Bernatchez, L., and Ihssen, P.E. 1998. A major sextet of mitochondrial DNA phylogenetic assemblages extant in eastern North American brook trout (*Salvelinus fontinalis*): distribution and post-glacial dispersal patterns. Can. J. Zool. **76**: 1300–1318.

Elson, J.A. 1969. Late quaternary marine submergence of Quebec. Rev. Géogr. Montréal, **23**: 247–258.

Felsenstein, J. 2004. PHYLIP (Phylogeny Inference Package). Version 3.6. Distributed by the author. Department of Genome Sciences, University of Washington, Seattle, Washington.

Ferguson, M.M., Bernatchez, L., Gatt, M., Konkle, B., Lee, S., and Malott, M. 1993. Distribution of mitochondrial DNA variation in lake sturgeon (*Acipenser fulvescens*) from the Moose River basin, Ontario. J. Fish Biol. **43**: 91–101.

Gagnon, M.C., and Angers, B. 2006. The determinant role of temporary proglacial drainages on the genetic structure of fishes. Mol. Ecol. **15**: 1051–1065.

Hill, J., and Grossman, G.D. 1987. Home range estimates for three North American stream fishes. Copeia, 1987: 376–380.

Lafontaine, P., and Dodson, J.J. 1997. Intraspecific genetic structure of white sucker (*Catostomus commersoni*) in northeastern North America as revealed by mitochondrial DNA polymorphism. Can. J. Fish. Aquat. Sci. **54**: 555–565.

Lasalle, P., and Tremblay, G. 1978. Dépôts meubles Saguenay lac Saint-Jean. Rapport 191. Ministère des Richesses naturelles, Québec.

Legendre, P. 2002. Program for multiple linear regression (ordinary or through the origin) with permutation test — user's notes. Département de sciences biologiques, Université de Montréal, Montréal, Québec.

Legendre, P., and Legendre, V. 1984. Post-glacial dispersal of freshwater fishes in the Québec peninsula. Can. J. Fish. Aquat. Sci. **41**: 1781–1802.

Lu, G., Basley, D.J., and Bernatchez, L. 2001. Contrasting patterns of mitochondrial DNA and microsatellite introgressive hybridization between lineages of lake whitefish (*Coregonus clupeaformis*): relevance for speciation. Mol. Ecol. **10**: 965–985.

McAllister, D.E., Harington, C.R., Cumbaa, S.L., and Renaud, C.B. 1988. Paleoenvironmental and biogeographic analyses of fossil fishes in the peri-Champlain Sea deposits in Eastern Canada. *In* The Late Quaternary development of the Champlain Sea basin. *Edited by* N.R. Gadd. Geological Association of Canada Special Paper No. 35. pp. 241–258.

McMillan, W.O., and Palumbi, S.R. 1997. Rapid rate of control-region evolution in Pacific butterflyfishes (Chaetodontidae). J. Mol. Evol. **45**(5): 473–484.

McPhail, J.D., and Lindsey, C.C. 1970. Freshwater fishes of northwestern Canada and Alaska. Bull. Fish. Res. Board Can. No. 173.

Nei, M. 1987. Molecular evolutionary genetics. Columbia University Press, New York.

Occhietti, S. 1989. Quaternary geology of Saint-Lawrence Valley and adjacent Appalachian subregion. *In* Quaternary geology of Canada and Greenland. *Edited by* R.J. Fulton. Geological Survey of Canada, Geology of Canada No. 1. pp. 350–389.

Orita, M., Iwahana, H., Kanazawa, H., Hayashi, K., and Sekiya, T. 1989. Detection of polymorphisms of human DNA by gel electrophoresis as single-strand conformation polymorphism. Proc. Natl. Acad. Sci. U.S.A. **86**: 2766–2770.

Posada, D., Crandall, K.A., and Templeton, A.R. 2000. GeoDis: a program for the cladistic nested analysis of the geographical distribution of genetic haplotypes. Mol. Ecol. **9**(4): 487–488.

Prest, V.K. 1970. Quaternary geology of Canada. *In* Geology and economic minerals of Canada. *Edited by* R.J.W. Douglass. Geological Survey of Canada, Ottawa. Econ. Geol. Rep. No. 1. pp. 676–764.

Radforth, I. 1944. Some considerations on the distribution of fishes in Ontario. Contrib. Roy. Ont. Mus. Zool. **25**: 1–116.

Rempel, L.L., and Smith, D.G. 1998. Post-glacial fish dispersal from the Mississippi refuge to Mackenzie River basin. Can. J. Fish. Aquat. Sci. **55**: 893–899.

Schneider, S., Roessli, D., and Excoffier, L. 2000. Arlequin Ver. 2.0: a software for population genetics data analysis. Genetics and Biometry Laboratory, University of Geneva, Switzerland.

Scott, W.B., and Crossman, E.J. 1973. Freshwater fishes of Canada. Bull. Fish. Res. Board Can. No. 184.

Senanan, W., and Kapuscinski, A.R. 2000. Genetic relationships among populations of northern pike (*Esox lucius*). Can. J. Fish. Aquat. Sci. **57**: 391–404.

Taberlet, P., Fumagalli, L., Wust-Saucy, A.G., and Cosson, J.F. 1998. Comparative phylogeography and post-glacial colonization routes in Europe. Mol. Ecol. **7**: 453–464.

Templeton, A.R. 1998. Nested clade analyses of phylogeographic data: testing hypotheses about gene flow and population history. Mol. Ecol. **7**: 381–397.

Templeton, A.R., and Sing, C.F. 1993. A cladistic analysis of phenotypic associations with haplotypes inferred from restriction endonuclease mapping. IV. Nested analyses with cladogram uncertainty and recombination. Genetics, **134**: 659–669.

Templeton, A.R., Crandall, K.A., and Sing, C.F. 1987. A cladistic analysis of phenotypic associations with haplotypes inferred from restriction endonuclease mapping. I. Basic theory and a analysis of alcohol dehydrogenase activiy in Drosophila. Genetics, **117**: 343–351.

Templeton, A.R., Routman, E., and Phillips, C. 1995. Separating population structure from population history: a cladistic analysis of the geographical distribution of mitochondrial DNA haplotypes in the Tiger Salamander, *Ambystoma tigrinum*. Genetics, **140**: 767–782.

ter Braak, C.J.F. 1986. Canonical correspondence analysis: a new eigenvector technique for multivariate direct gradient analysis. Ecology, **67**(5):1167–1179.

ter Braak, C.J.F., and Smilauer, P. 1999. Canoco for Windows 4.02. Centre for Biometry Wageningen, CPRO-DLO, Wageningen, the Netherlands.

Thompson, A.R., Petty, J.T., and Grossman, G.D. 2001. Multiscale effects of resource patchiness on foraging behaviour and habitat use by longnose dace, *Rhynicthys cataractae*. Freshw. Biol. **46**(2): 145–160.

Turgeon, J., and Bernatchez, L. 2001. Mitochondrial DNA phylogeography of lake cisco (*Coregonus artedi*): evidence supporting extensive secondary contacts between two glacial races. Mol. Ecol. **10**: 987–1001.

Underhill, J.C. 1986. The fish fauna of the Laurentian Great Lakes, the Saint-Lawrence Lowlands, Newfoundland and Labrador. *In* The zoogeography of North American freshwater fishes. *Edited by* C.H. Hocutt and E.O. Wiley. John Wiley and Sons, New York. pp. 105–136.

Volis, S., Anikster, Y., Olsvig-Whittaker, L., and Mendlinger, S. 2004. The influence of space in genetic–environmental relationships when environmental heterogeneity and seed dispersal occur at similar scale identifiers. Am. Nat. **163**: 312–327.

Walker, D., and Avise, J.C. 1998. Principles of phylogeography as illustrated by freshwater and terrestrial turtles in the southeastern United States. Annu. Rev. Ecol. Syst. **29**: 23–58.

Wilson, C.C., and Hebert, P.D.N. 1996. Phylogeographic origins of lake trout (*Salvelinus namaycush*) in eastern North America. Can. J. Fish. Aquat. Sci. **53**: 2764–2775.

Wilson, C.C., and Hebert, P.D.N. 1998. Phylogeography and post-glacial dispersal of lake trout (*Salvelinus namaycush*) in North America. Can. J. Fish. Aquat. Sci. **55**: 1010–1024.

Wilson, A.C., Cann, R.L., Carr, S.M., George, M., Jr., Gyllensten, U.B., Helm-Bychowski, K., Higuchi, R.G., Palumbi, S.R., Prager, E.M., Sage, R.D., and Stoneking, M. 1985. Mitochondrial DNA and two perspectives on evolutionary genetics. Biol. J. Linn. Soc. **26**: 375–400.

Contents (concluded) / Table des matières (suite et fin)

Kai Lorenzen, Oriana Almeida, Robert Arthur, Caroline Garaway, and Sophie Nguyen Khoa 1334–1343 Aggregated yield and fishing effort in multispecies fisheries: an empirical analysis

Stephen J. Hall, Jeremy S. Collie, Daniel E. Duplisea, Simon Jennings, Mark Bravington, and Jason Link 1344–1359 A length-based multispecies model for evaluating community responses to fishing

Peter J. Allen, Brian Hodge, Inge Werner, and Joseph J. Cech, Jr. 1360–1369 Effects of ontogeny, season, and temperature on the swimming performance of juvenile green sturgeon (*Acipenser medirostris*)

Daniel D. Heath, J. Mark Shrimpton, Russell I. Hepburn, Sara K. Jamieson, Sarah K. Brode, and Margaret F. Docker 1370–1383 Population structure and divergence using microsatellite and gene locus markers in Chinook salmon (*Oncorhynchus tshawytscha*) populations

M.A. Madej, C. Currens, V. Ozaki, J. Yee, and D.G. Anderson 1384–1396 Assessing possible thermal rearing restrictions for juvenile coho salmon (*Oncorhynchus kisutch*) through thermal infrared imaging and in-stream monitoring, Redwood Creek, California

Ryan A. Thum and Richard S. Stemberger 1397–1404 Pure spatial and spatially structured environmental variables explain *Skistodiaptomus* copepod range limits in the northeastern USA

Marcie M. Ninness, E. Don Stevens, and Patricia A. Wright 1405–1413 Energy expenditure during hatching in rainbow trout (*Oncorhynchus mykiss*) embryos

Ronan Fablet 1414–1428 Semi-local extraction of ring structures in images of biological hard tissues: application to the Bayesian interpretation of fish otoliths for age and growth estimation

Philippe Girard and Bernard Angers 1429–1438 The impact of postglacial marine invasions on the genetic diversity of an obligate freshwater fish, the longnose dace (*Rhinichthys cataractae*), on the Quebec peninsula

National Research Council Canada
Conseil national de recherches Canada

Ottawa, Canada K1A 0R6
Ottawa, Canada K1A 0R6

Postage paid at Ottawa
Publications mail
Registration No. 40062591

Port payé à Ottawa
Poste-publication
Enregistrement n° 40062591

USPS periodical postage paid at Champlain, NY 12919, USA

Canadian Journal of Fisheries and Aquatic Sciences

Journal canadien des sciences halieutiques et aquatiques

Volume 63, Number 6, June 2006

Volume 63, numéro 6, juin 2006

RAPID COMMUNICATION / COMMUNICATION RAPIDE

Simon R. Thorrold, Geoffrey P. Jones, Serge Planes, and Jonathan A. Hare 1193–1197 Transgenerational marking of embryonic otoliths in marine fishes using barium stable isotopes

ARTICLES / ARTICLES

Marion Richard, Philippe Archambault, Gérard Thouzeau, and Gaston Desrosiers 1198–1213 Influence of suspended mussel lines on the biogeochemical fluxes in adjacent water in the Îles-de-la-Madeleine (Quebec, Canada)

Marissa L. Baskett, Mary Yoklavich, and Milton S. Love 1214–1229 Predation, competition, and the recovery of overexploited fish stocks in marine reserves

Shannon M. Claeson, Judith L. Li, Jana E. Compton, and Peter A. Bisson 1230–1241 Response of nutrients, biofilm, and benthic insects to salmon carcass addition

Timothy J. Beechie, Correigh M. Greene, Lisa Holsinger, and Eric M. Beamer 1242–1250 Incorporating parameter uncertainty into evaluation of spawning habitat limitations on Chinook salmon (*Oncorhynchus tshawytscha*) populations

M.P. Lincoln-Smith, K.A. Pitt, J.D. Bell, and B.D. Mapstone 1251–1266 Using impact assessment methods to determine the effects of a marine reserve on abundances and sizes of valuable tropical invertebrates

Nicholas K. Dulvy, Simon Jennings, Stuart I. Rogers, and David L. Maxwell 1267–1275 Threat and decline in fishes: an indicator of marine biodiversity

Sadie K. Rosenthal, Samantha S. Stevens, and David M. Lodge 1276–1285 Whole-lake effects of invasive crayfish (*Orconectes* spp.) and the potential for restoration

Isabelle Larocque, Reinhard Pienitz, and Nicolas Rolland 1286–1297 Factors influencing the distribution of chironomids in lakes distributed along a latitudinal gradient in northwestern Quebec, Canada

Bryce J. Brylawski and Thomas J. Miller 1298–1308 Temperature-dependent growth of the blue crab (*Callinectes sapidus*): a molt process approach

Jan Heggenes, Tore Qvenild, Michael D. Stamford, and Eric B. Taylor 1309–1319 Genetic structure in relation to movements in wild European grayling (*Thymallus thymallus*) in three Norwegian rivers

Henrik Sundberg, Rasha Ishaq, Ulla Tjärnlund, Gun Åkerman, Kerstin Grunder, Cecilia Bandh, Dag Broman, and Lennart Balk 1320–1333 Contribution of commonly analyzed polycyclic aromatic hydrocarbons (PAHs) to potential toxicity in early life stages of rainbow trout (*Oncorhynchus mykiss*)

Continued on inside back cover / Suite au verso

Canada

Printed in Canada by / Imprimé au Canada par
NRC Reprographic Services / Service de reprographie CNRC
Page production by / Mise en page par
NRC Research Press / Presses scientifiques du CNRC

0706-652X(200606)63:6;1-W